



ISMIO

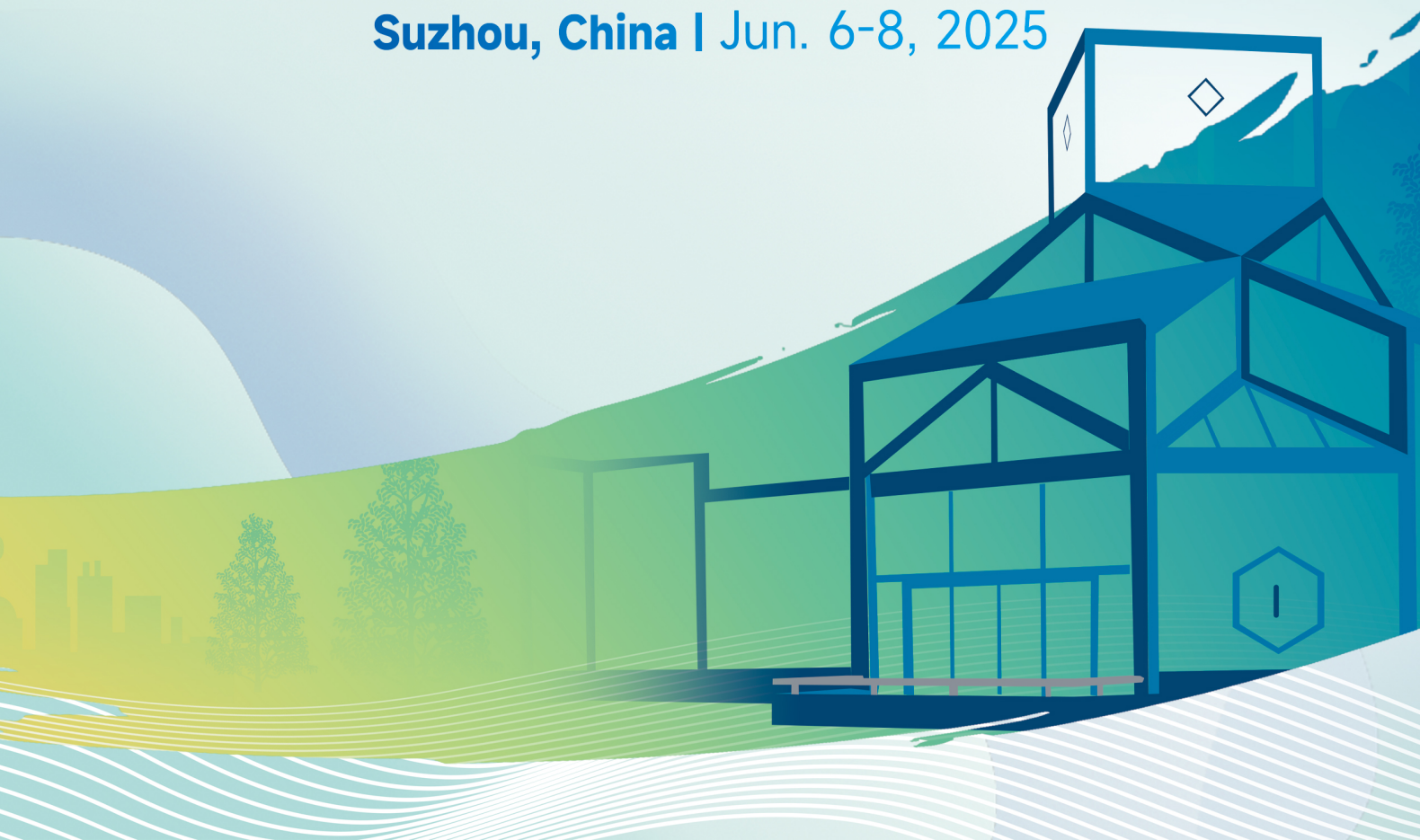
ISMIO 2025

*The Annual Meeting of International Society of
Multidisciplinary Interventional Oncology*

*Interventional Oncology Without Borders:
Embracing Cross-disciplinary Collaboration*

ABSTRACT BOOK

Suzhou, China | Jun. 6-8, 2025



Content

Oral

OR-001 A novel silver nanoparticles-functionalized stent for the treatment of malignant stricture of esophagus.....	1
OR-002 Percutaneous Catheter Drainage (PCD) as Primary Treatment for Necrotizing Pancreatitis: Clinical Outcomes and Comparative Effectiveness	3
OR-003 The Value of 40 keV Virtual Monoenergetic Imaging in Preoperative Assessment for Precision TACE in Hepatocellular Carcinoma.....	4
OR-004 Efficacy and safety of Adebrelimab (a PD-L1 inhibitor) plus Bevacizumab (an VEGF-A-targeting inhibitor) in combination with hepatic artery infusion chemotherapy for advanced stage hepatocellular carcinoma: a retrospective cohort study.....	5
OR-005 A Comparison of Treatment Outcome of Hepatocellular Carcinoma in Caudate Lobe, between Thermal Ablation and Transarterial Chemoembolization: A Retrospective Review	6
OR-006 Percutaneous Transhepatic Cholangiography in Biliary Obstruction: A Retrospective Audit of Outcomes and Complications	7
OR-007 Results of ultrasound guided vacuum assisted breast biopsy treatment for benign breast tumor	8
OR-008 Efficacy of Radiofrequency Ablation for Hepatocellular Carcinoma Adjacent to Gallbladder.	9
OR-009 A nomogram predicting venous thromboembolism risk in primary liver cancer patients ...	10
OR-010 Percutaneous cholangioscopy and fluoroscopy-guided forceps biopsy for pathologically diagnosing highly suspected perihilar malignant diseases: a retrospective cohort study.....	11
OR-011 Mitochondrial-Cytosolic Cascade Metabolic Regulation System: A Robust Strategy to Disrupt Multipath Energy Replenishment in Cancer Therapy.....	12
OR-012 Prevention of acute thrombosis with vascular endothelium antioxidative nanoscavenger ..	13
OR-014 A Prospective, Sing-Arm, Phase 2 Study of Transarterial Embolization Plus Hepatic Arterial Infusion Chemotherapy Combined with Sequential Lenvatinib and Sintilimab in Patients with Infiltrative Hepatocellular Carcinoma.....	14
OR-015 Spatial transcriptomics reveals tryptophan metabolism restricting maturation of intratumoral tertiary lymphoid structures	16
OR-016 Idarubicin-loaded degradable hydrogel for TACE therapy enhances anti-tumor immunity in hepatocellular carcinoma	17
OR-017 Cryoablation enhanced anti-tumor immunity and survival for patients with liver metastatic melanoma receiving PD-1 blockade therapy: Insights from longitudinal RNA-seq data.....	18
OR-018 A real-world survey of 1830 surviving patients with adamantinomatous craniopharyngioma in China	19
OR-019 Response evaluation of liver directed therapies for liver metastasis in NET	20

OR-021 First-in-human study of an artificial intelligence integrated robot for image-guided, trans-thoracic lung biopsy under local anaesthesia	21
OR-022 Analysis of short and medium term clinical effect of prostatic artery embolization on symptomatic prostatic hyperplasia	22
OR-023 Efficacy and safety of TACE combined with TKI against TACE alone for managing intermediate-stage HCC with hypovascular nodules	23
OR-024 First-line durvalumab with arterial chemotherapy in major portal invaded hepatocellular carcinoma: the phase 2 DurHope study with biomolecular analyses.....	24
OR-025 Concomitant Symptomatic Colorectal Cancer and Thoracoabdominal Aortic Aneurysm Treated with staged Endovascular Aneurysm Repair (EVAR) Followed by Anterior Resection	25
OR-026 Drug eluting bead transarterial chemoembolization (DTACE) combined with hepatic arterial infusion chemotherapy versus DTACE alone for hepatocellular carcinoma in Barcelona Clinic Liver Cancer stage C: a prospective, multicenter, analysis	26
OR-027 The role and mechanism of peroxisomes in the response to TACE treatment for hepatocellular carcinoma	27
OR-028 Hepatic Arterial Infusion Chemotherapy with or without Hepatic Artery Chemoembolization for Esophageal Carcinoma patients with Liver Metastasis: A Clinical Retrospective Study.....	28
OR-029 Direct percutaneous embolization of hypervascular renal cell cancer metastasis to the spine.	30
OR-033 CT-guided Percutaneous Cryoablation in Patients with Lung Nodules Mainly Composed of Ground-Glass Opacities	31
OR-034 Long-term outcomes of image-guided ablation and laparoscopic partial nephrectomy for T1 renal cell carcinoma.....	32
OR-035 Global Interest of interventional radiology and interventional oncology: A review of a decade using the google trends platform.....	33
OR-036 The Diversity of Arterial Approaches in Delivering Intra-arterial Chemotherapy for Retinoblastoma: Experiences from Indonesia.....	34
OR-037 Trans-arterial embolisation prior to image-guided ablation for T1b/T2a renal masses – A systematic review and meta-analysis	35
OR-038 MulticentRe rEal World outcomes of IrReversible Electroporation for complex small kiDney cancers (REWired)	36
OR-039 The prognostic value of Neutrophil-to-lymphocyte ratio and platelet-to-lymphocyte ratio for liver tumours after image-guided irreversible electroporation.....	37
OR-040 Integrated machine learning identifies SPP1hi macrophages marker genes for predicting therapeutic response of TACE in HCC.....	38
OR-041 CT-Guided Microwave Ablation with Vertebral Augmentation for Spinal Metastases with Posterior Wall Defects.....	40
OR-042 CT-guided Celiac Plexus Neurolysis in the Management of Visceral Intractable Pain in Patients with Advanced Cancer.....	41

OR-043	Irradiation modulates sEVs-PD-L1 transport in TNBC's tumor immune microenvironment .	42
OR-044	Early Response Evaluation of Hepatocellular Carcinoma After Transarterial Chemoembolization Using Triphasic Computed Tomography	43
OR-045	Retrospective analysis of diagnostic accuracy of image-guided needle biopsy of pancreatic lesions.	44
OR-046	Percutaneous thermal ablation of multiple ground-glass nodules (GGNs) : a retrospective analysis of 36 patients.....	45
OR-047	Role of Sclerotherapy in patients with vascular malformations - A retrospective study.....	46
OR-048	Successful Preoperative Transcatheter Arterial Embolization Significantly Reduces Intraoperative Bleeding in Juvenile Nasopharyngeal Angiofibroma Without the Need for Embolization of Internal Carotid Artery Branches: A Case Report of Two Patients	47
OR-049	Role of interventional radiology in pain management of abdominal cancers	50
OR-050	Transjugular Intrahepatic Portosystemic Shunt Plus Transarterial Chemoembolization of Hepatocellular Carcinoma Patients with Portal Vein Tumour Thrombus-related Variceal Bleeding..	51
OR-051	Health economics analysis of three treatment methods for uterine fibroids	52
OR-052	Transarterial chemoembolization plus radiofrequency ablation and iodine-125 seed implantation for hepatocellular carcinoma in high-risk locations.....	53
OR-053	Hepatic arterial infusion chemotherapy combined with toripalimab and surufatinib in the treatment of advanced intrahepatic cholangiocarcinoma	54
OR-054	TACE combined with immunotherapy plus targeted therapy after 125I irradiation stent placement in HCC with main portal vein tumor thrombosis: A nationwide target trial emulation study (PATENCY II).....	55
OR-055	Development and Validation of Mean Platelet Volume-Based Predictive Model for Early TACE Failure/Refractoriness in Unresectable Hepatocellular Carcinoma: A Real-World Retrospective Cohort Study.....	56
OR-056	AI based analysis of response to first line chemotherapy using radiological reports of epithelial type of ovarian malignancy	58
OR-057	Optimal Thermal Ablation Margin Range Model for Liver Malignancies ≤ 3 cm Based on 979 Cases.....	59
OR-058	Locoregional therapy combined with systemic therapy (LRT + ST) for unresectable and metastatic intrahepatic cholangiocarcinoma: a systematic review and meta-analysis	60
OR-059	Comparing Percutaneous and Endoscopic Biliary Drainage in Inoperable Bismuth III/IV Malignant Hilar Biliary Obstruction: Clinical Outcomes and Prognostic Factors	61
OR-060	Metformin suppress liver cancer metastasis by inhibiting microwave ablation therapy induced EMT through modulation of the TGF- β - Smad2/3 signaling pathway.....	62
OR-061	CCL2 ⁺ Inflammatory Cancer-Associated Fibroblasts Promote Chemoresistance and Tumor Progression in Microsatellite Stable Colorectal Cancer via the CCL2-P4HB-NOTCH-STAT3 Axis ..	63
OR-062	A nomogram predicting venous thromboembolism risk in primary liver cancer patients ...	64

OR-063 Lenvatinib Plus Hepatic Arterial Infusion Chemotherapy of FOLFOX versus Lenvatinib Alone for Advanced Hepatocellular Carcinoma	65
OR-064 Hepatic arterial infusion chemotherapy in hepatocellular carcinoma : A Bibliometric and Knowledge-Map Analysis	66
OR-065 Study on the Role of Pirfenidone in Liver Fibrosis - Hepatocellular Carcinoma.....	67
OR-066 Hyaluronidase additional to transarterial chemoembolization improves efficacy for liver cancer: preclinical evaluation.....	68
OR-067 Revolutionizing Detection and Ablation of Invisible Liver Metastases Post-Chemotherapy in Colorectal Cancer: The Role of Transcatheter CT Hepatic Arteriography	69
OR-068 Celecoxib and cisplatin dual-loaded microspheres synergistically enhance transarterial chemoembolization effect of hepatocellular carcinoma	70
OR-069 Preparation of a Composite Nanozyme and Its Sonodynamic Therapy in Bladder Cancer .	71
OR-070 Transarterial chemoembolisation and tyrosine kinase inhibitors with or without programmed death-1 inhibitors as first-line treatment for unresectable hepatocellular carcinoma: A propensity score matching study	72
OR-071 Real-time MR-guided brain biopsy using 1.0-T open MRI scanner	73
OR-072 3D-printed Versatile Biodegradable Biliary Stent with Zinc/Sirolimus for Anti-bacterial and Anti-hyperplasia in a Rabbit Bile Duct	74
OR-073 Retrospective study to determine diagnostic accuracy of image guided peritoneal biopsies	75
OR-074 Temperature-sensitive Liquid Embolic Agent Transarterial Chemoembolization (TempSLE-TACE) versus D-TACE for Unresectable Hepatocellular Carcinoma(u-HCC): A multicenter retrospective propensity score study in China.....	76
OR-076 The eight mitochondrial metabolism-related genes as diagnostic markers for abdominal aortic aneurysm by integrating machine learning approach	77
OR-077 Superselective ablative chemo-ethanol embolization for recurrent single hepatocellular carcinoma	78
OR-078 Comparison of DEB-TACE Combined with Thermal Ablation versus DEB-TACE alone in the Treatment of Large Hepatocellular Carcinoma and Multinodular Hepatocellular Carcinoma: Efficacy and Prognostic Factors Analysis	79
OR-079 Efficacy and prognostic factors of COVID-19 vaccine in patients with hepatocellular carcinoma: Analysis of data from a prospective cohort study.....	80
OR-080 Conventional Oral Morphine vs. IV Patient-Controlled Analgesia (IPCA) with Hydromorphone (HM) Continuous Infusion plus Rescue Dose (CIRD) or Bolus-Only (BO) for Severe Cancer Pain: A Randomized Phase III study	81
OR-081 Percutaneous core needle biopsy of peripheral lung lesions: A single center experience and analysis of safety and efficacy	82
OR-082 HAIC combined with sindilizumab and bevacizumab for the treatment of advanced HCC: an exploratory clinical study.....	83

OR-083 Fruquintinib combined with sintilimab plus transarterial chemoembolization (TACE) for unresectable hepatocellular carcinoma (uHCC): A single-arm phase II study	84
OR-084 Effect of AFP and PIVKA-II secretion status on prognosis of advanced hepatocellular carcinoma patients receiving TACE combined with systemic therapies	85
OR-085 Safety and Technical Feasibility of Modified Percutaneous Transesophageal Enterostomy (PTEE) in Cancer Patients Ineligible for Conventional Gastrostomy	86
OR-086 Restraining small extracellular vesicles: Dawn of a new era in nanomedicine.....	87
OR-087 Engineered Macrophage Membrane-Mimicking Nanodrugs Activate the cGAS/STING Pathway to Reverse the Immune-Suppressive Microenvironment Induced by RFA.....	88
OR-088 Ablative Therapy for Residual Lesions After First-Line Treatment of Locally Advanced Unresectable Lung Adenocarcinoma: A Prospective, Randomized Controlled Study	89
OR-089 Does needle biopsy immediately after percutaneous microwave and cryoablation of lung neoplasm affect pathological results? A clinical and animal study.....	91
OR-090 Vaginal microbiome and metabolome profiles among HPV positive and HPV negative women based on stratification of vaginitis	92
OR-091 Development and Functional Research of an Irradiation-Cytokine Composite Stent for Modulating Immune Microenvironment Reprogramming.....	93
OR-092 Tailored Liposomal Nanomedicine Suppresses Incomplete Radiofrequency Ablation-Induced Tumor Relapse by Reprogramming Antitumor Immunity.....	94
OR-093 Predictability of the short-term treatment response to Yttrium-90 transarterial radioembolization by pre-treatment cone-beam CT imaging-based radiomics analysis in patients with hepatic malignancy	95
OR-094 The status of cytotoxic lymphocytes indicate therapeutic efficacy and prognosis in patients with advanced hepatocellular carcinoma undergoing transarterial chemoembolization combined with systemic therapies.....	96
OR-095 Comparative Effectiveness of Liquid versus Solid Embolic Agents in Pre-surgical Embolization for Intracranial Tumors: A Systematic Review and Meta-analysis	97
OR-096 A study on the Contribution of LSM11 to the Outcome of Radiotherapy in Hepatocellular Carcinoma Cells.....	98
OR-097 Complications of Interventional Treatment for Vascular Tumors and Vascular Malformations: Mechanisms of Occurrence, Treatment Strategies and Prevention.....	100
OR-099 Whether the choice of location for re-implantation chest port affects the incidence of complications in adult tumor patients undergoing right chest port removal WANG.....	101
OR-100 Radioactive iodine-125 particle implantation combined with transarterial chemoinfusion and synchronous immune checkpoint inhibitors for the management of locally advanced pancreatic cancer: a retrospective single-center analysis.....	102
OR-101 Outcomes of First-Line Microwave Ablation of Treatment-Naive Epidermal Growth Factor Receptor – Mutated Advanced Lung Adenocarcinoma Treated with Tyrosine Kinase Inhibitors ...	103

OR-102 Efficacy Comparison of Liver Venous Deprivation and TACE Combined with Targeted and Immunotherapies in Unresectable Hepatocellular Carcinoma with Insufficient FLR Volume	104
OR-103 Autocatalytic pyroptosis agonists modulate tumor metabolism and enhance TACE efficacy in HCC therapy.....	105
OR-104 Microwave Ablation Versus Lobectomy for Ground-Glass Opacity Nodules in the Hilar Region: A Multicenter Prospective Real-World Study on Efficacy and Safety	106
OR-105 In which tumor burden range does hepatic arterial infusion chemotherapy combined with tyrosine kinase inhibitors and immune checkpoint inhibitors perform better than the combination of tyrosine kinase inhibitors and immune checkpoint inhibitors? A comparative analysis of their efficacy and safety in advanced-stage hepatocellular carcinoma patients with portal vein tumor thrombus, using propensity score matching.....	107
OR-106 Injectable Hydroxyapatite Radiopaque Microspheres: The Next-Generation Material for Cancer Interventional Embolization?	109

Poster

PO-001 Percutaneous transhepatic biliary stenting for bile duct obstruction due to malignancy: efficacy and safety.....	111
PO-002 Successful Treatment of Postoperative Gastric Hemorrhage in a 69-Year-Old Male Using TAE (Transarterial Embolization)	112
PO-003 Transcatheter arterial infusion of anti-programmed cell death 1 antibody combined with nab-paclitaxel in patients with primary anorectal malignant melanoma	113
PO-004 Efficacy analysis of TACE concurrent microwave ablation combined with target-immunotherapy in advanced unresectable liver cancer.....	114
PO-005 Analysis of influencing factors and establishment of clinical prediction model for postoperative complications of PTGD	115
PO-006 Clinical Efficacy of Selective Bladder Artery Embolization with Sequential Transurethral Resection for Bladder Tumor: A Retrospective Comparative Study	117
PO-007 Recurrence scoring system predicting early recurrence for patients with pancreatic ductal adenocarcinoma undergoing pancreatectomy and portomesenteric vein resection	118
PO-008 Successful Management of Gastric Metastasis from Hepatocellular Carcinoma: A Case of Left Gastric Artery Embolization Followed by Total Gastrectomy	119
PO-009 Combination of Particle Embolic Agents and Coils in Total Embolization of Giant Renal Angiomyolipoma with Multiple Aneurysms: A Case Report	120
PO-010 Injectable thermosensitive brachytherapy seed to compete with sealed seed.....	121
PO-011 Self-Regulating Magnetic Thermo-Brachytherapy Overcomes Immunosuppression and Radiotherapy Resistance in Pancreatic Cancer	122
PO-012 Transbrachial TACE for Liver Cancer: A Real-World Study on Safety, Comfort, and Quality of Life in Chinese Patients	123

PO-013 Transarterial chemoembolization with PD-(L)1 inhibitors plus Lenvatinib for MVI of unresectable hepatocellular carcinoma : An exploratory, cohort study	124
PO-014 Complete remission in BCLC stage C hepatocellular carcinoma treated with HAIC combined with PD1 inhibitors and anti-angiogenic therapy.....	125
PO-015 Transarterial chemoembolization combined with percutaneous ethanol injection for the treatment of hepatocellular carcinoma at high-risk areas	126
PO-016 Translational Application of Y90-SIRT Combined with Systemic Therapy in Initially Unresectable Hepatocellular Carcinoma	127
PO-017 Comparing the effectiveness and safety Cancer Imaging Open Access of Sorafenib plus TACE with Apatinib plus TACE for treating patients with unresectable hepatocellular carcinoma: a multicentre propensity score matching study.....	128
PO-018 Prognostic value of acute liver injury in cirrhotic patients after transjugular intrahepatic portosystemic shunt.....	129
PO-019 Development and validation of a prognostic model based on nutritional status after transjugular intrahepatic portosystemic shunt.....	130
PO-020 Study on the effect of a new type of "magnetothermal 125I seed" combined with Flt3-L to promote the "in-situ vaccine" for hepatocellular carcinoma.....	131
PO-021 Genomic feature and potential therapeutic target for cholangiocarcinoma.....	132
PO-022 METTL5 promotes fatty acid metabolism by modulating peroxisome to promote hepatocellular carcinoma recurrence after thermal ablation	133
PO-023 Application research of EqualSpheres embolization microspheres loaded with Idarubicin in VX2 rabbit liver tumor model	134
PO-024 Combination of transnasal ileus tube and local small intestine artery perfusion chemotherapy for late malignant small bowel obstruction.....	135
PO-025 The combination treatment of oncolytic adenovirus H101 with Transcatheter Arterial Embolization Sequential Thermal Ablation for Hepatocellular Carcinoma: A Retrospective Study .	136
PO-026 Predicting Bird-beak Configuration of Stent Graft during Zone 2 Thoracic Endovascular Aortic Repair using Machine Learning Models	137
PO-027 Application of a Question Prompt Checklist in Liver Cancer Surgery Patients: Effects on Patient Engagement, Information Retention, and Communication Satisfaction.....	138
PO-028 Practice and exploration of improving the self-management ability of patients with pancreatic cancer supported by artificial intelligence: taking DeepSeek system as an example	139
PO-029 Retrospective Analysis of The Timing of Radiotherapy Intervention After Induction Chemoimmunotherapy in Unresectable Locally Advanced Lung Squamous Cell Carcinoma.....	140
PO-030 Doxorubicin-Loaded CalliSpheres Microspheres Transcatheter Arterial Chemoembolization Versus Conventional Transcatheter Arterial Chemoembolization: Pharmacokinetics and Antitumor Effect in a VX2 Liver Tumor Model	141
PO-031 Yttrium-90 Ablative-Selective Internal Radiation Therapy for Hepatocellular Carcinoma in Chinese Patients: A Case Series Study	142

PO-032 Diagnostic value of 18F-PSMA-1007 multi-parametric PET/MR imaging in clinically significant for PSA gray area prostate cancer.....	143
PO-033 Long-term Outcomes of Ablation versus Surgery in Patients with Colorectal Lung Oligometastasis: A Retrospective Cohort Study.....	144
PO-034 A Metrology Informatics Investigation of Conversion Therapy in Hepatocellular Carcinoma: 2014-2023.....	145
PO-035 Analysis of short-term clinical efficacy and immune function changes of advanced non-small cell lung cancer after radiotherapy and chemotherapy under CT-guided 125 I seed implantation .	146
PO-036 AI Guided Swift Response: Transforming Stroke Diagnosis.	147
PO-037 Endovascular Management of Post-Transplant Portal Vein Stenosis: A Case Report of Balloon Angioplasty in a Pediatric Living-Donor Liver Recipient	148
PO-038 Growth Pattern of MRI to Predict Tumor Progression for Hepatocellular Carcinoma Response to Systemic and Locoregional Therapies	149
PO-039 Single-cell analysis reveals heterogeneity in the molecular profile of the tumor microenvironment of biliary tract cancers.....	150
PO-040 Efficacy and safety of lenvatinib plus gefitinib in lenvatinibresistant hepatocellular carcinomas: a prospective, single-arm exploratory trial	151
PO-041 Dual-Pathway Interventional Strategy: Addressing Both Venous Obstruction and Neoplastic Burden in Malignant Superior Vena Cava Syndrome in Advanced Non-small Cell Lung Cancer through Combined Stenting and Drug-eluting Beads Transbronchial Arterial Chemoembolization .	152
PO-042 Effect of blood glucose level on prognosis of patients with intermediate and advanced hepatocellular carcinoma treated by transarterial chemoembolization combined with targeted and immune drugs.....	153
PO-043 Precision Targeting of ERK5 Combined with PD-L1 Blockade Remodels the HCC Microenvironment: A Comprehensive Study of Synergistic Antitumor Mechanisms.....	154
PO-045 Mechanism and Application Progress of Nanomedicine Delivery Systems in Inducing Ferroptosis of Tumors.....	155
PO-046 Association between regional lymph node metastasis and survival outcomes in advanced hepatocellular carcinoma receiving transarterial chemoembolization and PD-(L)1 inhibitors-based immunotherapy.....	156
PO-047 TACE combined with Apatinib for Advanced Perihilar Cholangiocarcinoma: A Single-arm, Phase II Study	157
PO-048 Real-world effectiveness and safety of transcatheter arterial chemoembolization with EqualSpheres beads in patients with hepatocellular carcinoma.....	158
PO-049 SLC1A5 Associated with Poor Prognosis and TACE Resistance in Hepatocellular Carcinoma	159
PO-050 TACE combined with DynaCT guided MWA in the treatment of high-risk location liver cancers with ≤ 5 cm tumor size	160

PO-052 Advances in the study of risk factors and precise management of moderate-to-severe abdominal pain after TACE for primary hepatocellular carcinoma.....	161
PO-053 Ablation of pulmonary oligometastasis had influence on intrahepatic tumors response and progression patterns for patients receiving lenvatinib	162
PO-055 Effect of personalized health education on compliance with anticoagulant therapy in patients with deep vein thrombosis of lower extremities.....	163
PO-056 Inhibiting the FGFR4 Signaling Pathway Suppresses Epithelial-to-Mesenchymal Transition in Hepatocellular Carcinoma After Transarterial Chemoembolization	164
PO-057 Chemotherapy plus concurrent irreversible electroporation improved local tumor control in unresectable hilar cholangiocarcinoma compared with chemotherapy alone	165
PO-058 Application of Manchester pain management model combined with targeted psychological intervention in perioperative TACE in patients with liver cancer.....	166
PO-059 Radiological Characteristics Determine the Selection of Intra-arterial Therapy Modality for Intermediate-Stage Hepatocellular Carcinoma	167
PO-060 Proliferative Subtype - based Deep Learning Model for Identifying the Survival Benefit of Patients with Hepatocellular Carcinoma Receiving Intra-arterial Therapies.....	168
PO-061 The construction and preliminary application of a rehabilitation management plan for pancreatic cancer patients after interventional surgery based on goal-setting theory in navigation services	169
PO-063 Investigating the Role of Idarubicin versus Epirubicin in Inducing Immunogenic Cell Death in a Mouse HCC Model of Local Treatment.....	170
PO-064 Radiofrequency Ablation is safe in patients with Hepatocellular Carcinoma and thrombocytopenia	171
PO-065 Berberine induces autophagy and promotes apoptosis in triple-negative breast cancer cells via the PI3K/Akt signaling pathway.....	172
PO-066 Efficacy and safety of TIPS sequential targeted drugs in the treatment of patients with hepatocellular carcinoma with esophagogastric variceal rupture and bleeding	173
PO-067 Efficacy and safety of percutaneous cavity filling in the treatment of type II internal leakage after endovascular repair of abdominal aortic aneurysms.....	174
PO-068 Hippo-TEAD Axis Mediates Adaptive Resistance to Iodine-125 Brachytherapy in NSCLC and Its Therapeutic Exploitation	175
PO-069 To study the factors affecting the outcomes of core needle biopsy in musculoskeletal lesions.	176
PO-070 Efficacy and Safety of TACE Combined with Lenvatinib and PD-1 Inhibitor in Intermediate-Stage HCC exceeding the up-7 Criteria: A Retrospective Cohort Study.....	177
PO-071 Experimental study on inhibition of airway restenosis by novel graphene oxide-loaded rapamycin-coated airway stent	178
PO-072 mFOLFOX6-HAIC with PD-(L)1 inhibitors plus molecular targeted therapies for HBV-related advanced hepatocellular carcinoma	179

PO-073 Early Responses of Serum AFP and PIVKA-II Synergistically Predict Progression in Patients with Unresectable Hepatocellular Carcinoma Receiving Transarterial Chemoembolization Combined with Sintilimab and Bevacizumab	180
PO-074 Evaluation of Percutaneous Microwave Ablation of the Spleen Combined with Splenic Artery Occlusion for Treating Secondary Hypersplenism: A Single-Arm Study.....	181
PO-075 FOLFOX-HAIC plus regorafenib for the treatment of unresectable colorectal liver metastases refractory to first and second-line systemic chemotherapy	183
PO-076 Treatment of femoral artery pseudoaneurysm with intravascular stent and hematoma removal: a case report	184
PO-077 Evaluation of functional magnetic resonance imaging' s effect of transcarotid CA4P infusion therapy on VX2 transplantation tumor model in rabbit brain	185
PO-079 DAP12 Knockdown Suppresses EMT in Colon Cancer Cells by Downregulating AKT and Modulating the Intestinal Microenvironment	186
PO-080 Effects of different doses of X-rays on cGAS-STING signaling pathway and tumor immune microenvironment	187
PO-081 Liver and Liver Tumor Segmentation Based on Swin Transformer	188
PO-082 3D Printed Airway Model-assisted Amplatzer Device for Closure of Gastroairway Fistula After Esophagectomy	189
PO-083 Low-dose CT fluoroscopy-guided interventional minimally invasive robot	190
PO-084 Radiomic Profiling of Tumor Heterogeneity on Pretreatment MRI Stratifies Treatment Outcomes in HCC Patients Undergoing Atezo-Bev Immunotherapy with Adjuvant Locoregional Interventions.....	191
PO-086 Incomplete Thermal Ablation Plus Programmed Cell Death Protein 1 Monoclonal Antibodies Increase The Incidence of Hyperprogressive Disease in Hepatocellular Carcinoma	192
PO-087 Cryoablation Combined with Camrelizumab and Apatinib in Advanced Hepatocellular Carcinoma: A prospective, single-arm, phase II study.....	193
PO-088 Safety and effectiveness of microwave ablation in the treatment of parapleural pulmonary nodules	195
PO-089 Thermosensitive Embolic Agent in the treatment of hepatocellular carcinoma with hepatic arteriportal shunt	196
PO-090 Development and Validation of a Survival Prediction Scoring System in Unresectable Hepatocellular Carcinoma Patients Treated with TACE plus Apatinib and Camrelizumab	197
PO-091 CT-guided 125I brachytherapy for hepatocellular carcinoma in high-risk locations after transarterial chemoembolization combined with microwave ablation: a propensity score-matched study	198
PO-092 Evaluation of models to predict prognosis in patients with advanced hepatocellular carcinoma treated with TACE combined with apatinib.....	199
PO-093 Role of Radiofrequency ablation (RFA) as a salvage treatment in recurrent fibromatosis.	200

PO-095 Investigation of the Efficacy and Safety of Lung Biopsy Plus Microwave Ablation for a Solitary Suspected Malignant Pulmonary Nodule after Radical Mastectomy	201
PO-096 NO-driven self-propelled nanomotors augment chemo-immunotherapy and transcatheter arterial embolization	202
PO-097 Comparative Effectiveness and Safety of Molecular Targeted Therapy Plus PD-(L)1 with or without TACE in Unresectable Hepatocellular Carcinoma: a retrospective study	203
PO-098 Assessing early response to DEB-TACE for unresectable HCC by tumor habitats-based features in contrast-enhanced computed tomography: A retrospective multicenter study	204
PO-099 Multi-modality model predicts Lung Metastasis of Hepatocellular Carcinoma using MRI and pathological: a retrospective multicenter study	205
PO-100 Development and Validation of a Predictive Model for Poor Prognosis in Epithelial Ovarian Cancer	206
PO-101 Evaluating the Role of Large Language Models in Recommending Hepatocellular Carcinoma Patients to Interventional Radiology	207
PO-102 Construction and validation of a predictive model for poor prognosis in epithelial ovarian cancer	208
PO-103 Establishment and validation of a prognostic prediction model for glioma based on key genes and clinical factors	209
PO-104 High risk acute pulmonary embolism after interventional embolization of vaginal hemorrhage in cervical cancer	210
PO-105 The combined model of Clinical and CT radiomics for predicting the efficacy of drug coated balloon therapy in the treatment of femoral- popliteal artery stenosis/occlusion	211
PO-106 Impact of Tumor Burden and Radiation Dose on Survival Outcomes and Treatment Response in Patients with Unresectable Hepatocellular Carcinoma Treat with TARE	213
PO-107 Harmonizing Ancient Wisdom and Modern Technology: Exploring Retrieval-Augmented Generation (RAG) with Large Language Models to Transform Education in Interventional Oncology	214
PO-108 MCTL® Multitarget Individualized Diagnostic and Treatment Technology	215
PO-111 Mineralized supramolecular microspheres with dual phase acid mirco-environment relief and immunoregulating functions for transarterial chemoembolization immunotherapy of hepatocellular carcinoma	216
PO-114 The Efficacy of Combined Treatment with the Anti-fibrotic Drug PFD and TACE in an Animal Model of Liver Cancer	217
PO-117 Value of intratumoral combined with peritumoral radiomics model in the prediction of Ki-67 expression in lung adenocarcinoma: a multi-center study	219
PO-118 CT-guided iodine-125 brachytherapy is an effective palliative treatment for the right lower paratracheal lymph nodes metastasis previously treatment failure	220
PO-119 Engineered microspheres for interventional-magneto-thermal-immunotherapy of tumours	221

PO-122	Endovascular embolisation for life-threatening malignant hemoptysis.....	222
PO-123	Photo-responsive self-expanding catheter with photosensitizer-integrated silicone-covered membrane for minimally invasive local therapy in malignant esophageal cancer	223
PO-124	Risk Factors and Risk Prediction Model for Early Cardiovascular Events After Microwave Ablation for Lung Cancer	224
PO-125	Enhanced Management Strategy of synchronous Percutaneous Biopsy and Microwave Ablation in Patients with Lung Ground-Glass Opacities Undergoing Antithrombotic Treatment: A Clinical Perspective on Our Experience.....	225
PO-126	Anti-inflammatory coupled anti-angiogenic airway stent effectively suppresses tracheal in-stents restenosis	226
PO-127	Pre-operative loco-regional staging of colo-rectal carcinoma by using contrast enhanced computed tomography correlation with histopathology	227
PO-128	Clinical Efficacy of HAIC Combined with TACE in Patients with Unresectable Intrahepatic Cholangiocarcinoma	228
PO-129	Contrast Enhanced T1WI-Based peritumoral Radiomics for Predicting the therapeutic effect of advanced hepatocellular carcinoma after transcatheter arterial chemoembolization	229
PO-130	Study on the predictive effect of sarcopenia on the efficacy of bronchial artery chemoembolization in lung cancer patients.....	230
PO-131	Drug-eluting transarterial chemoembolization combined with anlotinib for non-small cell lung cancer in the elderly: a multicenter retrospective study	231
PO-133	The efficacy and safety of transarterial chemoembolization combined with the different assembly of first-line targeted therapy and immunotherapy for intermediate and advanced hepatocellular carcinoma : a single-center retrospective study	232
PO-134	Efficacy of Compound Pholcodine Syrup and Compound Codeine Phosphate Oral Solution on lung cancer cough	234
PO-135	Berberine's Role in Modulating Gut Microbiota and Endocannabinoid System in Colitis-Associated Colorectal Cancer	235
PO-136	Multi-Center Randomized Controlled Trial of Integrated Early Palliative Care for Non-Small-Cell Lung Cancer Patients in Southwest China: Evaluating Impact and Efficacy	236
PO-138	Knowledge, attitudes, and Current practices toward lung cancer palliative care management in China: a national survey.....	237
PO-139	Establishment of an Extracapsular Chicken Embryo Chorioallantoic Membrane Hepatocellular Carcinoma Model and Magnetic Resonance Imaging Study	238
PO-140	Development and Validation of an Ultrasound Radiomics-Based Prognostic Model for Predicting Short-Term Outcomes After Transcatheter Arterial Chemoembolization in Hepatocellular Carcinoma.....	239
PO-142	Transarterial Chemoembolization plus Donafenib and Immune Checkpoint Inhibitors for Intermediate Hepatocellular Carcinoma (CHANCE2410): A Propensity Score Matching Analysis. .	240

PO-143	Incidence and risk factors exploration for portal vein tumor thrombosis development in patients with hepatocellular carcinoma after transarterial chemotherapy embolization	241
PO-144	Clinical Characteristics and Surgical Treatment Strategies for Primary Intracranial Rosai-Dorfman Disease	244
PO-145	Diagnostic and Therapeutic Strategies for Lhermitte-Duclos Disease.	245
PO-146	Diagnosis and Treatment of Vascular Tumours and Vascular Malformations in the Head and Neck.	246
PO-147	Transarterial chemoembolization for huge hepatocellular carcinoma : to do or not to do, a clinical dilemma	247
PO-148	Development and validation of nomogram including mutations in angiogenesis-related genes as risk factors for HCC patients treated with TACE	248
PO-149	Bibliometric Analysis of Literature on Cancer and Interventional Therapy: A Comprehensive Review.	249
PO-150	Thoracic Radiotherapy: A Game Changer for ES-SCLC Patients on Chemoimmunotherapy.	251
PO-151	Development of a prognostic model for patients with extensive-stage small cell lung cancer undergoing immunotherapy and chemotherapy	252
PO-152	Bioinformatics Analysis of the Invasion-Associated Competing Endogenous RNA Network in Breast Cancer on Single-cell Resolution.....	253
PO-153	Development and validation of a SHAP-based interpretable model for preoperative prediction of microvascular invasion in hepatocellular carcinoma	256
PO-154	Establishment and observation of a tumor transplantation model of shell-less chick embryo chorioallantoic membrane	257
PO-155	Elucidating the Novel Role of RNA-Binding Protein IGF2BP3 in Suppressing HR+/HER2-Breast Cancer Progression via Transcriptional Repression with ESR1	258
PO-156	Advances in the combination of nanomaterials and tumor ablation.....	260
PO-158	Two Decades of Progress in Hepatocellular Carcinoma Research: A Comprehensive Bibliometric and Visualized Analysis (2004 – 2023).....	262
PO-159	Dual-Targeted Microspheres Reshape Metabolic-immune Microenvironment and Reverse Multiple Dilemmas Post-embolization in Hepatocellular Carcinoma	263
PO-160	Prediction model of survival in unresectable HCC with central bile duct invasion receiving TACE after biliary drainage: TEMP Score	264
PO-162	Study of the Mechanism by which CYP2W1 Promotes the Progression of Colorectal Cancer Liver Metastasis through Cholesterol Metabolism	265
PO-163	Efficacy and Safety of Radiofrequency Ablation Combined with Immunotherapy in Advanced Lung Cancer: A Retrospective Study.....	266
PO-164	Efficacy and Safety of Interventional Hemostasis in Massive Hemoptysis Induced by Anti-Tumor Angiogenesis Therapy in Advanced Lung Cancer: A Retrospective Study.....	267

PO-165 The Value and Significance of Health Education in Malignant Tumor Patients Undergoing Radioactive Particle Implantation Therapy.	268
PO-167 Surufatinib plus doublet (FOLFOX/FOLFIRI) or triplet (FOLFOXIRI) chemotherapy as second-line therapy in metastatic colorectal cancer (mCRC): updated results of a randomized, open-label phase II trial.	269
PO-168 Real-world efficacy and safety of TACE plus Lenvatinib with or without programmed death factor 1 (PD-1) inhibitor in huge hepatocellular carcinoma at BCLC stage B-C : a multicenter retrospective study with propensity score matching.	270
PO-169 A Novel Dual Radiosensitizer Reverses Resistance to 125I Brachytherapy and Enhances Antitumor Efficacy.	271
PO-171 Efficacy and safety of transarterial chemoembolization combined with lenvatinib plus programmed death-1 inhibitor for hepatocellular carcinoma with the hepatic vein and/or inferior vena cava tumor thrombus.	272
PO-172 Preliminary Safety and Efficacy of Upfront FOLFOXIRI and Bevacizumab with Cadonilimab in Patients with Proficient Mismatch Repair/Microsatellite Stable (pMMR/MSS) Metastatic Colorectal Cancer: A Multicenter Phase II Study (SYLT-026).	273
PO-174 Tislelizumab (Tisle) combined with POFI (irinotecan, paclitaxel, oxaliplatin, and 5-FU/levoleucovorin) as first-line treatment of advanced gastric/gastroesophageal junction adenocarcinoma (AGC): OS analysis results of the SYLT-023.	274
PO-175 Textbook Outcome in Low Rectal Cancer Patients Undergoing Laparoscopic or Open Surgery: 3-Year Results from the Multicentric LASRE Trial.	275
PO-176 Comparative Oncologic Outcomes of Laparoscopic vs. Open Surgery for Early-Onset Low Rectal Cancer: 3-Year Results from the LASRE Trial.	276
PO-177 Hawthorn Standardized Extract (HSE) Plus Standard Opioid Analgesia to Treat Refractory Cancer Pain: A Single-Arm Phase I Trial (SYLT-024).	277
PO-178 Transdermal fentanyl (TDF) vs immediate-release morphine tablets (IRMT) as opioid titration for opioid-naïve moderate cancer pain (ONMCP): a randomized, open-label, multi-site phase 3 trial.	278
PO-179 HBV reactivation and its management in HBV-related hepatocellular carcinoma patients who underwent HAIC-targeted-immune-antiviral therapy: a multicenter study.	279
PO-180 Molecular mechanism and clinical translational study of remodeling immunosuppressive microenvironment in human lung adenocarcinoma by targeting CHCHD3-cGAS pathway.	280
PO-181 Survival Analysis and Nomogram for Postoperative Pulmonary Sarcomatoid Carcinoma Patients: SEER Database Analysis and External Validation.	281
PO-182 Analysis of the Efficacy of TACE Combined with Fuzhengxiaoliu granules in the Treatment of Stage II Hepatitis B-Related Liver Cancer.	282
PO-183 Highly elastic polyvinyl alcohol embolic microspheres for effective transarterial embolization.	283
PO-184 Comparing the performance of ChatGPT and ERNIE Bot in answering questions regarding liver cancer interventional radiology in Chinese and English contexts: a comparative study.	284

PO-185 Efficacy of antiangiogenic therapy in patients with advanced SMARCA4-deficient thoracic tumor	285
PO-186 Establishment of a Chicken Chorioallantoic Membrane Hepatocellular Carcinoma Model and Magnetic Resonance Imaging Study	286
PO-188 Role of Senescence Escape in Therapeutic Resistance of Cholangiocarcinoma Cells induced by 125I Seed Irradiation.....	287
PO-189 Prognostic Value of Peripheral Blood-Derived Inflammation-Based index in Hepatocellular Carcinoma with Transarterial Chemoembolization Plus PD-(L)1 Inhibitors and Molecular Targeted Agents	289
PO-190 Efficacy and predictive factors of transarterial chemoembolization combined with lenvatinib plus programmed cell death protein-1 inhibition for unresectable hepatocellular carcinoma.	290
PO-191 Risk Stratification in Colorectal Cancer: Nomograms Utilizing Inflammatory Factors and Immunological Hematological Indicators	291
PO-192 Recent advancements in the utilization of nanomaterials for ablative sensitization therapy in the treatment of Hepatocellular carcinoma	292
PO-193 Hepatocellular carcinoma treated with transcatheter arterial chemoembolization followed by radiofrequency ablation: impact of the time interval between the two treatments	293
PO-194 Different body compositions affect the adverse prognosis of hepatocellular carcinoma patients following transarterial chemoembolization combined immunotherapy and target therapy .	294
PO-195 Transarterial Chemoembolization Containing Arsenic Trioxide for the Treatment of Intermediate-stage Hepatocellular Carcinoma: A Randomized, Double-blind, Multicenter Parallel-Controlled Study.....	295
PO-196 C-Reactive Protein Flare: A Promising Prognostic Predictor for Patients with Hepatocellular Carcinoma Treated with TACE Combined with Lenvatinib and Immune Checkpoint Inhibitors	296
PO-197 Predicting progression-free survival with MRI radiomics nomogram for unresectable hepatocellular carcinoma patients treated with transarterial chemoembolization combined with TKI plus PD-1 inhibitors	297
PO-198 TACE-HAIC versus HAIC: Is more always better? Combined with TKIs and ICIs for hepatocellular carcinoma with a high tumor burden—A propensity-score matching comparative study.	299
PO-199 Immune Cells as Potential Targets for Intrahepatic Cholangiocarcinoma: Insights from Mendelian Randomization	300
PO-200 Mechanistic Study of Celiac Sympathetic Denervation in the Treatment of Metabolic Dysfunction-Associated Steatohepatitis (MASH)	301
PO-201 Efficacy and Safety of Radioactive Particle Implantation Combined with Immunotherapy in Advanced Cancer: A Retrospective Study.....	302
PO-202 Clinical Exploration of Arterial Infusion Conversion Therapy for Advanced Gastric Cancer: A Single-Center Long-Term Follow-Up Study of 8 Cases.....	303

PO-203 BCLC Staging-Guided Conversion Therapy for Unresectable Hepatocellular Carcinoma: HAIC Combined with Targeted Therapy and PD-1/L1 Inhibitors	304
PO-204 Multifunctional Nanofiber Patch Integrating Photothermal-Immunomodulatory Trimodel Therapy for Postoperative Hepatocellular Carcinoma Management	305
PO-206 WEE1 combined with radiotherapy affects the regulation of tumor microenvironment through cGAS/STING-STAT3-IRF3 pathway.....	306
PO-208 Combined Therapy of Transhepatic Arterial Chemoembolization and Ablation verse Surgical Resection in the Treatment of Small Liver cancer.....	307
PO-209 A quantitative MRI comparative study of imaging markers for cerebral small vessel disease in the middle-aged and elderly patients with and without hypertension	308
PO-211 Massive hemorrhage after percutaneous liver biopsy in a patient with liver tumour: A successful hepatic vein embolization	309
PO-212 Transarterial chemoembolization combined with lenvatinib plus tislelizumab for unresectable hepatocellular carcinoma: A multicenter cohort study	310
PO-213 Percutaneous transhepatic lymphangiography and embolization treatment for refractory hepatic lymphorrhea: clinical results in 7 patients.....	311
PO-214 Using Neoadjuvant Chemotherapy in combination with Antiangiogenesis and Immune Checkpoint Inhibitors to Treat Locally Advanced Gastric Cancer: A Real-World Retrospective Cohort Study	312
PO-215 Integrative analysis of multi-omics data for constructing an ADME-based risk model in gastric cancer	313
PO-216 Efficacy and safety of CT-guided percutaneous cryoablation for hepatocellular carcinoma at high-risk sites	314
PO-218 Lenvatinib Plus Hepatic Arterial Infusion Chemotherapy of Oxaliplatin, Fluorouracil, and Leucovorin versus Lenvatinib Alone for Advanced Hepatocellular Carcinoma: a multicenter retrospective cohort study.....	315
PO-219 Development and Application of a Whole Transcriptome Sequencing Assay for the Detection of Gene Fusions in Non-Small Cell Lung Cancer Specimens.....	316
PO-220 Experimental Study on EGFR Expression in Hepatocellular Carcinoma Cells and Sensitivity to Gefitinib and Lenvatinib	318
PO-221 ITM2a suppresses proliferation and migration by inhibiting EMT in microvascular invasion-positive hepatocellular carcinoma via the GJA1-MAPK/ERK axes	319
PO-222 Percutaneous MR – guided Thermal Ablation for Recurrent Subcentimeter Hepatocellular Carcinoma.....	320
PO-223 CT-guided percutaneous coaxial cutting needle biopsy of pulmonary lesions using trans-osseous approach	321
PO-224 Tumor acidity-Regulating Lipiodol Pickering Emulsions Stabilized by Iron Nanoparticles Enables transarterial ferro-embolization therapy	322

PO-225 Development and Validation of MRI Radiomics-Based Models for Predicting Overall Survival of Cholangiocarcinoma After Hepatic Arterial Infusion Chemotherapy	323
PO-226 Radioiodine-labeled gel-microspheres for radioembolization combined with photothermal treatment of hepatocellular carcinoma	324
PO-227 Mechanism of action of jujuboside B in regulating the BMAL1-HSP90AA1 pathway to restore the cellular molecular clock to promote the efficacy of TMZ against drug resistance in lung cancer	325
PO-228 Short-term efficacy and safety of novel EqualSpheres® drug-eluting beads bronchial arterial chemoembolization for advanced non-small cell lung cancer: a retrospective cohort study	326
PO-229 The efficacy and safety of TACE combined with systemic therapy in patients with unresectable liver cancer	327
PO-230 Efficacy and Safety of Hepatic Arterial Infusion Chemotherapy(HAIC) Combined with PD-1 Inhibitors for Advanced Hepatocellular Carcinoma with Macrovascular Invasion: A Multicenter Propensity Score Matching Analysis.....	328
PO-232 MRI-Based Radiomics for the Recurrence Prediction of Hepatocellular Carcinoma Treated with Postoperative Adjuvant Transcatheter Arterial Chemoembolization	329
PO-233 Hepatic Arterial Infusion Chemotherapy with mFOLFOX in Advanced Gallbladder Cancer: An Approach with Potential for Conversion and Enhanced Survival	330
PO-234 Personalized Drug Screening of Patient-derived Tumor-like Cell Clusters Based on Specimens Obtained from Percutaneous Transthoracic Needle Biopsy in Patients with Lung Malignancy: A Real-world Study.....	331
PO-235 The Prognostic Nutritional Index (PNI) as a Biomarker for Predicting Survival in Hepatocellular Carcinoma Patients Treated with Transarterial Chemoembolization and Lenvatinib, With or Without PD-1 Inhibitors	332
PO-236 METTL3-mediated m6A Modification of HIF1 α Regulates the TGM2/STAT3 Axis to Promote Chemoresistance in Head and Neck Squamous Cell Carcinoma	333
PO-237 Comparison of the efficacy and safety of HAIC combined with Camrelizumab and Apatinib versus TACE in the treatment of intermediate-advanced HCC	334
PO-238 Copper oxide nanoparticle stents inhibit esophageal carcinoma progression via mitophagy	335
PO-239 Hepatic arterial infusion chemotherapy combined with Lenvatinib and PD-1 inhibitors versus Lenvatinib and PD-1 inhibitors for HCC refractory to TACE	336
PO-240 Hepatic arterial infusion chemotherapy plus lenvatinib and PD-1 inhibitors versus lenvatinib plus PD-1 inhibitors as treatment for unresectable hepatocellular carcinoma, a meta-analysis and trial sequential analysis	337
PO-241 Deep Learning Application of YOLOv8 for Aortic Dissection Screening Using Non-Contrast CT.....	338
PO-242 CT-guided Needle Insertion with an Optical Navigation Robot-assisted Puncture System: Ex Vivo and in Vivo Experimental Studies in the Liver and Kidneys	339

PO-243	Efficacy and Safety Analysis of Transarterial Chemoembolization Combined with Tyrosine Kinase Inhibitors and Immune Checkpoint Inhibitors with or without Microwave Ablation for Unresectable Hepatocellular Carcinoma: A Retrospective, Multicenter, Case-control Study	340
PO-244	Tumor cell-intrinsic MELK augments CCL2-dependent immunosuppression to promote hepatocarcinogenesis and enhance hepatocellular carcinoma radioresistance	342

Published

PU-001	The Role of Interventional Radiology in Hematuria Embolization for Patients with Radiation-Induced Cystitis	343
PU-002	Comparison of efficacy of different sequential radiotherapy combined with TACE in hepatocellular carcinoma with PVTT	344
PU-003	Single-cell transcriptome sequencing reveals SPP1-CD44-mediated macrophage-tumor cell interactions drive chemoresistance in TNBC.	345
PU-004	Skeletal Muscle Mass Predicts Survival Benefit for Hepatocellular Carcinoma Treated with Transarterial Chemoembolization Combining Molecular Targeted Agents and Immune Checkpoint Inhibitors	346
PU-005	A Comparative Study of Gasless Transoral Vestibular Approach Endoscopic and Open Radical Thyroidectomy in a Retrospective Cohort.	347
PU-007	IL11 promotes hepatocellular carcinoma progression through facilitating APOH-mediated fatty acid metabolism to modulate the differentiation of Treg cells.	349
PU-009	Long-Term Outcomes of Transarterial Chemoembolization plus Ablation versus Surgical Resection in Patients with Large BCLC Stage A/B stage HCC	350
PU-010	Analysis of key genes and signaling pathways shared by liver cancer and interventional liver cancer based on bioinformatics methods.	351
PU-011	MNX1-AS1 reduces chemosensitivity by promoting the PI3K/AKT pathway in breast cancer	352
PU-012	2024 Guangzhou consensus of Minimally Invasive and Multidisciplinary Comprehensive Treatment for Hepatocellular Carcinoma	353
PU-014	Treatment strategy for patients with aortic aneurysm complicated with malignant tumors.	354
PU-015	Efficacy and Safety of hydromorphone Patient-controlled Analgesia (PCIA) for analgesia after adjunctive uterine artery embolization in patients with scarred pregnanc	355
PU-017	Application of Percutaneous Transhepatic Cholangioscopy in Diagnosis of Postoperative Biliary Strictures of cholangiocarcinoma patients	356
PU-019	Experimental Study on Drug Delivery System Based on Reprogrammed Macrophages for Hepatocellular Carcinoma Treatment.	357
PU-021	Efficacy of Atezolizumab Plus Bevacizumab Combined with Transarterial Chemoembolization for Unresectable Hepatocellular Carcinoma: A Real-World Study.	358

PU-022	Efficacy and safety of 100-300um and 300-500um drug eluting beads in the treatment of colorectal cancer liver metastasis by TACE.	359
PU-023	Optimizing Imaging Diagnosis Based on Anatomical Complexity of the Inferior Pulmonary Ligament: Dynamic 3D Reconstruction and Interventional-Surgical Decision Support.	360
PU-024	Preoperative T2 MRI radiomics signature in predicting the short - term efficacy of interventional therapy for adenomyosis: a clinical study.	361
PU-025	Value and satisfaction analysis of humanistic care combined with narrative nursing in patients with advanced malignant tumors	362
PU-026	Sustained release hypoxia-activated prodrug-loaded BSA nanoparticles enhance transarterial chemoembolization against hepatocellular carcinoma.	363
PU-027	Lenvatinib Ameliorates the Immunosuppressive Microenvironment of Hepatocellular Carcinoma after Transarterial Chemoembolization	365
PU-028	Prognostic Prediction of Immune Indicator Changing Trend in Unresectable Hepatocellular Carcinoma Undergoing TACE plus ICIs and Anti-VEGF Antibodies/TKIs	366
PU-029	Evaluation of the Radiation Protection Efficacy of a Novel Domestic Lead-Free Protective Glove in a Simulated Direct X-ray Beam	367
PU-030	Radiation dose reduction with modified fluoroscopy during totally implantable venous access port.	368
PU-031	Paradoxical embolism caused by totally implantable venous access port: A case report and literature review	369
PU-032	Intravenous thrombolytic therapy for pancreatic cancer during chemotherapy: a case report and literature review	370
PU-033	Early tumor shrinkage is a prognostic factor for unresectable HCC receiving TACE combined with immune checkpoint inhibitors plus molecular targeted therapies.	371
PU-034	Clinical Observation of Focused Ultrasound Ablation for Aggressive Fibroma	372
PU-035	Focused ultrasound ablation combined with programmed death receptor-1 monoclonal antibody Analysis of Curative Effect on Advanced Pancreatic Cancer	373
PU-036	Short-term efficacy of argon-helium cryoablation for liver metastases Analysis of clinical influencing factors	374
PU-037	Efficacy evaluation and predictive factors analysis of uterine artery embolization in the treatment of adenomyosis	375
PU-038	Clinical efficacy of hepatic arterial infusion chemotherapy (HAIC) in advanced hepatocellular carcinoma complicated with portal vein cancer thrombus	376
PU-039	Transcriptome-wide association study identifies key genes for Follicular lymphoma.	377
PU-040	Study on the application value of transjugular intrahepatic portosystemic shunt in hepatocellular carcinoma complicated with portal hypertension.	378
PU-041	Prognostic Value of Tertiary Lymphoid Structures in Cryoablation Combined Immunotherapy for Soft Tissue Sarcomas	380

PU-042	Short-term Prognostic Value of Ultrasound-based Radiomics Model for Liver Cancer Patients with Radiofrequency Ablation Therapy	381
PU-043	Increment of Skeletal Muscle Mass Predicts Survival Benefit for Hepatocellular Carcinoma Treated with Transarterial Chemoembolization Combining Molecular Targeted Agents and Immune Checkpoint Inhibitors.....	382
PU-044	Clinical study on hepatitis B virus reactivation following transarterial chemoembolization combined with targeted immunotherapy for hepatocellular carcinomas	383
PU-045	Hepatoprotective Effects and Efficacy of Donafenib Combined with Transarterial Chemoembolization in the Treatment of Unresectable Hepatocellular Carcinoma	384
PU-046	TLR-9 Agonist Combined with PD-1 Inhibitor Enhances Cryoablation-Induced Anti-Tumor Immune Response in a Murine Hepatocellular Carcinoma Model	385
PU-047	Multidisciplinary Management of Malignant Carotid Body Tumor with Preoperative Embolization and Adjuvant Radiotherapy: A Case Report	386
PU-048	TACE combined with the intra-arterial infusion of bevacizumab for BCLC-stage B hepatocellular carcinoma beyond up-to-seven Criteria: A prospective, single-arm, phase II study..	387
PU-049	TACE combined with sintilimab and bevacizumab in the treatment of advanced hepatocellular carcinoma: a phase 2 study	388
PU-050	Tumor-Targeted FABP5/STING Cascade Multimodal Nanoreactor Promote Radiofrequency Ablation Induced Ferroptosis and Intratumoral Immune Rewiring in Hepatocellular Carcinoma....	389
PU-051	Association of the pretreatment lung immune prognostic index with immune checkpoint inhibitor outcomes in patients with advanced hepatocellular carcinoma	390
PU-052	Efficacy and safety of chemotherapy combined with iodine-125 seed brachytherapy for intermediate and advanced oncogenic driver gene-negative non-small cell lung cancer.....	391
PU-053	In vitro characteristics of Epirubicin supported thermosensitive liquid embolism	392
PU-054	Comparative analysis of bile culture and blood culture in patients with malignant biliary obstruction complicated with biliary tract infection	393
PU-055	MCM4 in human hepatocellular carcinoma: a potent prognostic factor associated with cell proliferation.....	394
PU-056	In vivo immune response induced by cryoablation of mouse H22 hepatoma cell line	395
PU-057	Analysis of clinicopathological and prognostic factors in 106 patients younger than 55 years of age with prostate cancer: a Chinese single-center study	396
PU-064	Hepatic Adverse Events of Novel Immunotherapy-Based Therapies in Clinical Trials: A Systematic Review and Meta-Analysis.....	397
PU-065	Preoperative Risk Stratification for Early Recurrence of Solitary Hepatocellular Carcinoma by Integrating Clinical, Pathological, and MRI Findings	398
PU-072	Predictive model of unresectable hepatocellular carcinoma treated with TACE-HAIC combined with targeted drugs and immune checkpoint inhibitors.....	399

PU-073 Safety and efficacy of n-butyl α -cyanoacrylate in transcatheter arterial chemoembolization	400
PU-074 Prognostic Nutritional Index Predicts Survival in Intermediate and Advanced Hepatocellular Carcinoma Treated with Hepatic Arterial Infusion Chemotherapy Combined with PD-(L)1 Inhibitors and Molecular Targeted Therapies	401
PU-077 Predicting the risk of radiation enteritis in cervical cancer patients using inflammatory markers through machine learning	402
PU-078 miR-520h Mediates Gemcitabine Resistant Pancreatic Cancer Cell Proliferation, Invasion and Migration via Regulating ABCG2	403
PU-079 Transarterial chemoembolization combined with immunotherapy and targeted therapy as first-line treatment for unresectable and non-metastatic hepatocellular carcinoma	404
PU-080 Interventional treatment of uterine arteriovenous malformation	405
PU-081 Prevention and Treatment of Malignant Gynaecological Tumours Complicated by Pulmonary Embolism	406
PU-082 Interventional embolisation treatment of drug-loaded microspheres for advanced cervical malignancies	407
PU-083 Efficacy of continuous arterial perfusion chemotherapy combined with transarterial chemoembolization regional arterial thermal perfusion in the treatment of pancreatic cancer with liver metastases	408
PU-084 BRPF3 R120H Mutation Enhances TP53-Mediated Tumor Suppression in Advanced Hepatocellular Carcinoma: A Retrospective Study	409
PU-085 The Role of Circ_ANKIB1 in Recurrence and Metastasis of Hepatocellular Carcinoma ...	410
PU-086 The Safety Evaluation of TAE for Ruptured Hepatocellular Carcinoma and Ablation-Related Hemorrhage, and the Clinical Significance of Postoperative Liver Function Changes	411
PU-087 Incidence and factors predictive of recurrent rupture in people with rupture of unresectable hepatocellular carcinoma	412
PU-088 Feasibility, Efficacy, and Safety of Ventral Caudal Artery Access for Transarterial Chemoembolization in a Rat Hepatocellular Carcinoma Model	413
PU-089 Pan-Cancer Analysis Unveils POSTN as a Promising Therapeutic Target for ER+ Breast Cancer	414
PU-091 Clinical Application Value of 1024 Matrix Combined with P3T Technology in Bronchial Artery CTA	416
PU-092 Three anesthesia models during microwave ablation for the treatment of subpleural stage I non-small cell lung cancer:A Prospective,Single-Center Study	417
PU-093 Transcatheter Arterial Embolization: An Alternative for Endoscopically Unmanageable Bleeding Duodenal Ulcer	418
PU-094 Abdominal Aortic Rupture Bleeding with Hemothorax Following Percutaneous Catheter Drainage for Infected Walled-off Pancreatic Necrosis	419

PU-095	Transarterial chemoembolization and hepatic arterial infusion chemotherapy combined with atezolizumab plus bevacizumab for patients with advanced hepatocellular carcinoma	420
PU-096	Clinical efficacy and safety analysis of irreversible electroporation combined with chemotherapy in the treatment of stage IV pancreatic cancer	421
PU-097	MULTISCALE MODELING OF TUMOR-MACROPHAGE INTERACTIONS UNDERLYING IMMUNOTHERAPY RESISTANCE IN GLIOBLASTOMA.....	422
PU-098	Application of Iodine-125 (¹²⁵ I) Seed Implantation in the Treatment of Spinal Metastases	423
PU-099	Using deep learning technology to segment liver tumors on SPECT/CT with MRI	424
PU-101	Therapy-induced Senescent Tumor Cells Modulate Gemcitabine Sensitivity in Intrahepatic Cholangiocarcinoma	425
PU-102	Exploring Yttrium-90 Radioactive Microspheres in Rat Models of Hepatocellular Carcinoma	426
PU-103	Ultrasound guided microwave ablation combined with traditional Chinese medicine in the treatment of benign thyroid nodules	427
PU-106	Variational Attention Fusion Network for Intracranial Aneurysm Segmentation	428
PU-111	A transcriptomic biomarker for predicting the response to TACE correlates with the tumor microenvironment and radiomics features in HCC.....	429
PU-112	Interventional surgery combined with donafenib and anti-PD-1 antibodies as first-line treatment for unresectable hepatocellular carcinoma: A retrospective study	430
PU-113	Drug-eluting beads bronchial arterial chemoembolization in advanced and standard treatment-refractory/ineligible non-small cell lung cancer	431

OR-001

A novel silver nanoparticles-functionalized stent for the treatment of malignant stricture of esophagus

Yan Fu¹, Yuxia Fu¹, Xiaoyu Huang¹, Miao Xing², Wei Jiang¹, Yibo Gao¹, Xiao Li¹

1. National cancer hospital, Beijing, China

2. First Hospital of China Medical University, China

Purpose Stenting is recommended as the primary treatment for malignant esophageal stricture, however, re-stricture caused by tumor growth after stenting remains challenging. This study aimed to develop a novel silver nanoparticles (AgNPs)-functionalized stent to treat malignant esophageal stricture in experimental animal models.

Materials and methods This study was approved by the Institutional Animal and Care and Use Committee and was conducted according to the Guide for the Care and Use of Laboratory Animals. AgNPs-functionalized stents were fabricated via an in-situ chemical reduction method, and the surficial properties of stent were characterized by scanning electron microscope (SEM). Content of silver iron of stent was measured using ICP-MS. The cellular uptake efficiency of AgNPs in human esophageal cancer cells (e.g., KYSE-30, KYSE-150 and KYSE-450) was evaluated, and the anti-cancer activities of AgNPs in human esophageal cancer cells (e.g., KYSE-30, KYSE-150 and KYSE-450) were evaluated via both in vitro assays (e.g., CCK-8 assay, wound healing assay) and subcutaneous xenograft murine models. A total of twenty-four 6-week-old Balb/c nude mice were subcutaneously inoculated with human esophageal cancer cells (e.g., KYSE-150 and KYSE-450), and were randomly allocated to receive sham operation, intertumoral implement of 1 cm segment of control stent, and intertumoral implement of 1 cm segment of AgNPs-functionalized stents, respectively. Tumor weight and tumor cell proliferation were compared among groups on postoperative day 14. Safety of implement of AgNPs-functionalized stents was evaluated in experimental model of esophageal stent in rats. Twenty-four male Sprague–Dawley rats were randomized to receive sham operation, control stent placement and AgNPs-functionalized stents placement. Follow-up fluoroscopy was performed on postoperative day 28, and effect of AgNPs on both stent-related restenosis and hepatorenal impairment were examined. In addition, the concentration of silver iron in esophageal tissue, serum, and digestive juiced in rats were evaluated.

Results Stents functionalized with a low-dose (6mg/ml), median-dose (12mg/ml) and high-dose (12mg/ml) AgNPs were successfully fabricated, respectively. Sizes of AgNPs were $29.1 \pm 13.9\text{nm}$, $31.6 \pm 11.2\text{nm}$ and $29.6 \pm 6.6\text{nm}$ in stents with low-dose, median-dose and high-dose of AgNPs, respectively. AgNPs with small sizes (10nm and 40nm) could be uptake and gathered in the mitochondrial in human esophageal cancer cells, and they could effectively suppress cellular viability and invasion of esophageal cancer cells ($p < 0.05$). Meanwhile, more cellular apoptosis was found in esophageal cancer cells treated by both AgNPs with sizes of 10 nm and 40 nm than in the untreated cells ($p < 0.05$). However, AgNPs with sizes of 100 nm did not significantly inhibit esophageal cancer cell viability and invasion ($p > 0.05$). In subcutaneous xenograft murine models of esophageal cancer, we found that AgNPs-coated stent significantly inhibited tumor growth ($p < 0.05$). In esophageal insertion of AgNPs-coated stent in rattus experimental model. Despite concentrations of silver in esophageal tissue and digestive juice increased postoperatively, concentration of silver in serum did not change ($p > 0.05$). Furthermore, no impairments in histology or biological function of the liver and kidneys were observed following esophageal insertion of AgNPs-coated stents. Besides, AgNPs-coated stent significantly prevented benign tissue hyperplasia after stent insertion ($p < 0.05$).

Conclusion Functionalization of esophageal stent with AgNPs was technically feasible, and this novel stent could be an effective and safe therapeutic option for the treatment of esophageal cancer.

OR-002

Percutaneous Catheter Drainage (PCD) as Primary Treatment for Necrotizing Pancreatitis: Clinical Outcomes and Comparative Effectiveness

Gantulga Vanchinsuren, Purevragchaa Maidar, Baasanjav Narangerel, Erdenebulgan Batmunkh
Second State Center Hospital

Purpose Necrotizing pancreatitis (NP) is a severe form of acute pancreatitis with high morbidity and mortality. Early surgical intervention, although standard practice for infected necrosis, carries significant risks. This study aims to assess the clinical outcomes of using percutaneous catheter drainage (PCD) as a primary treatment approach for NP

Materials and methods A prospective, open-label study was conducted, enrolling 68 patients with acute necrotizing pancreatitis, who underwent ultrasound-guided PCD. The main outcomes were the resolution of organ dysfunction, need for subsequent surgery, and survival at 7 weeks. Data were compared to a control group that received traditional surgical management.

Results In the PCD group, 12 patients (17%) did not require surgery, and 37 (54.4%) exhibited significant improvement in organ failure markers ($p < 0.05$). The 7-week survival rate was 95% for the PCD group compared to 90% for the control group. Two catheter-related complications occurred.

Conclusion PCD is a primary treatment option for necrotizing pancreatitis, improving organ function and survival rates while reducing the need for surgical intervention

OR-003

The Value of 40 keV Virtual Monoenergetic Imaging in Preoperative Assessment for Precision TACE in Hepatocellular Carcinoma

Shuang Li, Yuan-Cheng Wang

Department of Radiology, Zhongda Hospital, Nurturing Center of Jiangsu Province for State Laboratory of AI Imaging & Interventional Radiology, School of Medicine, Southeast University, Nanjing 210009, China

Purpose To comparatively evaluate the efficacy of 40 keV virtual monoenergetic imaging (VMI), digital subtraction angiography (DSA), and conventional single-energy CT (SECT) in preoperative visualization of hepatocellular carcinoma (HCC) tumor-feeding arteries through quantitative and qualitative analyses.

Materials and methods This retrospective single-center study included 22 HCC patients (from 53 screened) undergoing arterial-phase spectral CT (Philips Spectral CT) between October 2023–2024, excluding cases with secondary liver malignancies ($n=14$), hemangiomas ($n=5$), or suboptimal image quality ($n=12$). 40 keV VMI and SECT images were reconstructed for analysis. Two abdominal radiologists independently assessed vascular clarity and overall image quality using Likert 5-point scales. Objective metrics included signal-to-noise ratio (SNR) and contrast-to-noise ratio (CNR). Hepatic arterial systems were semi-automatically segmented using 3D Slicer (v5.6.2) with thresholding and region-growing algorithms, followed by centerline-based vascular topology reconstruction (VMTK plugin) for total vessel length quantification. Interobserver agreement was evaluated via Kappa statistics. Wilcoxon signed-rank tests compared imaging metrics ($p<0.05$ significance).

Results A total of 22 patients with confirmed HCC and good image quality were included in this study. Objective measures showed that 40 keV VMI had significantly higher SNR (48.08 ± 23.37 vs. 19.57 ± 8.71) and CNR (42.50 ± 20.87 vs. 14.79 ± 6.99) compared to traditional SECT. In subjective assessments, radiologists scored the vascular clarity of 40 keV VMI significantly higher than that of SECT ($P < 0.01$), with high inter-rater agreement between the two evaluators. Although 40 keV VMI was more prone to iodine oil deposition artifacts, its image quality was comparable to that of SECT. In terms of vascular recognition sensitivity, among 42 HCC lesions, DSA detected 75 tumor-feeding arteries, 40 keV VMI identified 62, and traditional SECT identified 54. The total hepatic vascular length measurement showed that the median value in the 40 keV VMI group was 102.11 mm (interquartile range: 81.52-116.59), while the median value in the SECT group was 94.79 mm (interquartile range: 73.83-113.30).

Conclusion The results of this study demonstrate that, compared to traditional SECT images, spectral CT reconstructed 40 keV virtual monoenergetic images provide superior image quality, better vascular visibility, and enhanced microvascular display in the preoperative evaluation of HCC feeding arteries. This technology can help operators more accurately identify tumor-feeding arteries preoperatively and is expected to serve as a non-invasive alternative for precise preoperative localization of HCC feeding arteries.

OR-004

Efficacy and safety of Adebrelimab (a PD-L1 inhibitor) plus Bevacizumab (an VEGF-A-targeting inhibitor) in combination with hepatic artery infusion chemotherapy for advanced stage hepatocellular carcinoma: a retrospective cohort study

Wei-Jun Fan, Lujun Shen, Letao Lin, Chen Li
Sun Yat-sen University Cancer Center, China

Purpose In this study, we aim to evaluate the efficacy and safety of combining Adebrelimab (anti-PD-L1 antibody) and Bevacizumab with FOLFOX-HAIC for HCC patients in BCLC stage C.

Materials and methods This retrospective single-arm study enrolled treatment-naïve hepatocellular carcinoma (HCC) patients with BCLC stage C, ECOG 0-1, Child-Pugh score ≤ 7 , and measurable lesions. Treatment comprised FOLFOX-HAIC (oxaliplatin 85 mg/m², leucovorin 400 mg/m², fluorouracil 2500 mg/m²) combined with Adebrelimab (1200 mg) and Bevacizumab (700 mg), administered every 21 days, with Adebrelimab preceding Bevacizumab by >30 minutes. HAIC was delivered via superselective catheterization into tumor-feeding arteries, supplemented by blank microsphere embolization or coil occlusion when necessary. Therapy continued until disease progression, curative conversion, intolerable toxicity, or death. Tumor response was assessed every 3 weeks using contrast-enhanced CT/MRI per RECIST v1.1/mRECIST, with adverse events graded by CTCAE v4.0.

Results From January 14th, 2024 to December 5th, 2024, a total of 32 patients receiving the triplet combination of FOLFOX-HAIC, Adebrelimab and Bevacizumab were reviewed. The primary outcome was objective response rate (ORR) based on the Response Evaluation Criteria in Solid Tumors (RECIST) version 1.1. According to RECIST v1.1 criteria, the confirmed ORR was 77.1% (95% CI: 59.9% to 89.6%), with a disease control rate of 97.1% (95% CI: 85.1% to 99.9%). The median progression-free survival had not yet been reached. Only one case (3.1%) had grade 3/4 treatment-related adverse effect (rash), which could be alleviated after discontinuation of adebrelimab and bevacizumab.

Conclusion The combination of Adebrelimab, Bevacizumab, and FOLFOX-HAIC demonstrated encouraging results and manageable safety concerns for patients with HCC at BCLC stage C.

OR-005

A Comparison of Treatment Outcome of Hepatocellular Carcinoma in Caudate Lobe, between Thermal Ablation and Transarterial Chemoembolization: A Retrospective Review

Sahutchadech Tangisarapap, Somrach Thamtorawat, Jirawadee Yodying
Siriraj Hospital

Purpose Technical challenges are an important factor in the treatment of hepatocellular carcinoma (HCC) in the caudate lobe. As the superior outcome of thermal ablation over transarterial chemoembolization (TACE) has been hypothesized, the purpose of this study was to compare the outcomes of HCC in the caudate lobe between thermal ablation and TACE.

Materials and methods A single-center retrospective, observational study that reviewed data from June 2012 to June 2022. The study included 53 patients who had newly developed HCC in the caudate lobe (size ≤ 3 cm) and had never been treated in this area before, with Barcelona Clinic Liver Cancer (BCLC) stage 0 - A. The patients were treated with either thermal ablation (n=32: RFA=30, MWA=2) or TACE (n=21). The local tumor progression (LTP), disease-free survival (DFS), overall survival (OS) and technical efficacy were compared.

Results The 1-, 3-, and 5-year LTP rates for the thermal ablation group were 10.1%, 14%, and 14%, respectively, while those for the TACE group were 15.6%, 57.8%, and 57.8%, respectively. Thermal ablation was found to be significantly superior to TACE in terms of LTP ($p=0.010$). However, there was no statistically significant difference in DFS or OS between the two groups. The primary and secondary technical efficacy of the thermal ablation group was significantly better than that of the TACE group ($p=0.010$). Neither major complications nor death-related complications in both groups were found.

Conclusion Thermal ablation seems to be superior to TACE for HCC in caudate lobe (< 3 cm) according to better local treatment response and efficacy. Thermal ablation could be considered a more favorable treatment option compared to TACE

OR-006

Percutaneous Transhepatic Cholangiography in Biliary Obstruction: A Retrospective Audit of Outcomes and Complications

Rathna Bhargavi Veerni, Sana Sheykhzadeh, Alexander Valentinov Jordanov, Frank Carey, Mohammad Tariq Ali
Norfolk and Norwich University Hospital

Purpose Biliary obstruction represents a significant clinical challenge with substantial morbidity and mortality, particularly in the setting of malignancy. This retrospective audit aims to evaluate the technical success, clinical outcomes, and complication rates of Percutaneous Transhepatic Cholangiography (PTC) and associated biliary interventions, providing data to inform clinical decision-making and improve patient care.

Materials and methods The study included 38 consecutive patients treated at Norfolk and Norwich University Hospital between September 2023 and December 2024. Methodological parameters were initially established in accordance with the Cardiovascular and Interventional Radiological Society of Europe (CIRSE) Standards of Practice on Percutaneous Transhepatic Cholangiography, Biliary Drainage and Stenting (Das et al., 2021). Once these parameters were defined, patient data were extracted from the local radiological information system (Soliton Radiology+), with imaging reviewed using Synapse®. Biochemical results, were retrieved from the Integrated Clinical Environment (ICE), and additional patient details, were sourced from patient letters.

Results The cohort (mean age 69.6 ± 13.2 years, 55% female) predominantly presented with malignant biliary obstruction (89.5%), with cholangiocarcinoma (36.0%) and pancreatic cancer (30.5%) representing the predominant aetiologies. There were 63.2% proximally located obstructions, with pre-intervention mean serum bilirubin levels of 250.9 ± 98.2 $\mu\text{mol/L}$. Among the patients with cholangiocarcinoma, Bismuth classification revealed 21.4% patients classified as Bismuth Type I, 12.5% as Type II, 4.2% as Type IIIb and 25% as Type IV. Prior to PTC, 58% of patients underwent ERCP, with documented technical failure in 36%, incomplete procedures in 23%, and anatomical unsuitability in 18%. Procedurally, 82% underwent PTC with biliary drainage insertion, while 18% received primary biliary stent placement. Ultrasound guidance was employed in 100% of interventions, with unilateral access preferred (89%)—predominantly left-sided (47%). Technical success was achieved in 92% of procedures. Internal-external biliary drainage was established in 71% of cases, with 8.5 Fr catheters most frequently deployed (71%). Complication analysis revealed intraprocedural events in 16% and early post-procedural complications in 26% of patients. The 30-day mortality rate was 13%, with procedure-related mortality confirmed in 3%. Bilirubin reduction at days 3 and 30 post-procedure averaged $35.9 \pm 29.1\%$ and $77.3 \pm 19.8\%$, respectively. Re-intervention was required in 67.5% of patients (mean time to first re-intervention: 6.0 ± 3.5 days). Among the 28 deceased patients, mean survival post-PTC was 83.8 ± 74.8 days.

Conclusion This audit confirms that PTC effectively manages malignant biliary obstruction, with acceptable complications and significant hepatobiliary improvement despite advanced disease. These findings provide real-world evidence to guide treatment strategies and patient expectations.

OR-007

Results of ultrasound guided vacuum assisted breast biopsy treatment for benign breast tumor

Batmunkh Erdenebulgan
Second state central hospital

Purpose To determine the indications and the diagnostic accuracy of vacuum-assisted breast biopsy (VABB) under ultrasonographic (US) guidance based on a short-term period of clinical use.

Materials and methods This was a retrospective analysis of in 89 consecutive patients who underwent US-guided VABB between January 2020 and October 2023. The proportions of each indication for VABB were analyzed as well as the trend of its use over divided time periods. Histopathological diagnosis and the malignancy rate of the lesions with VABB were analyzed.

Results Palpable lesions (77%), high-risk lesions (9%), and benign lesion (91%) were the most common indications for US-guided VABB. Among 123 therapeutic VABB cases, all of the cases showed no residual or recurrent lesions on long term follow-up US for more than a year. Complications occurred in 1.2% of the patients without need for surgical intervention.

Conclusion US-guided VABB is an accurate and safe method that can help decision-making in the diagnostic process and can be an alternative for excisional surgery in some therapeutic circumstances.

OR-008

Efficacy of Radiofrequency Ablation for Hepatocellular Carcinoma Adjacent to Gallbladder

Batmunkh Erdenebulgan, Vanchinsuren Gantulga, Myagmar Batmunkh, Narangerel Baasanjav, Ganzorig Bat-Amgalan, Gankhuyag Todbayar
Second state central hospital

Purpose Radio Frequency Ablation (RFA) is an alternative therapy for hepatocellular carcinoma and liver metastases when resection cannot be performed or, in the case of hepatocellular carcinoma, when transplant cannot be performed in a timely enough manner to avoid the risk of dropping off the transplant list. However, in some cases there is a very difficult to ablate the tumor in a peripheral and superficial location. To report the technique of hydrodissection of the gallbladder bed, in order to separate the gallbladder wall from the liver surface during radiofrequency ablation of liver malignancies located in segment five.

Materials and methods Between April 2020 and September 2021, percutaneous hydrodissection of the gallbladder fossa was performed in five patients. All treated lesions were located in segment five and abutting the gallbladder. All of patients with hepatocellular carcinoma, classification of Child pugh A and B for patients 2 and 3. Only one had a second treatment for recurrence (mean tumor size, 15 mm \pm 9). Hydrodissection was performed with Chiba needle (20G*20cm) in general anesthesia.

Results Hydrodissection of the gallbladder fossa was technically feasible in all five procedures, and radiofrequency ablation was performed power between 60-140W and used by 5% Dextrose solution for hydrodissection. Minimal distance between the ablation area and the GB increased from virtual to 7 mm on average (range 5-9), with a mean volume of dissection of 35 ml (range 20-50). Technical success was 100%. There was no complication related to the hydrodissection itself, and no acute or delayed gallbladder complication.

Conclusion Hydrodissection of the gallbladder bed is a feasible technique to separate the gallbladder from the liver surface. It's could potentially decrease the risk of thermal injuries to the gallbladder wall when ablating tumor located in segment five.

OR-009

A nomogram predicting venous thromboembolism risk in primary liver cancer patients

Yikun Kang^{1,2}, peng yuan¹

1. Department of VIP Medical Services, National Cancer Centre/National Clinical Research Center for Cancer/Cancer Hospital, Chinese Academy of Medical Sciences and Peking Union Medical College, Beijing 100021, China.

2. Department of Medical Oncology, Beijing Hospital, National Center of Gerontology; Institute of Geriatric Medicine, Chinese Academy of Medical Sciences, P.R. China.

Purpose Currently, de-escalation or escalation of systemic therapy remains to be a controversial topic for HER2-positive early breast cancer. To aid the treatment decisions, here we developed a novel HER2RI prognostic model to predict the risk of recurrence and long-term survival in Asian population with HER2-positive early breast cancer.

Materials and methods The prognostic models based on the 20-gene signature (HER2RIGEP) and combination with nodal stage and progesterone receptor (PR) expression (HER2RIClin) were built using a XGBoost algorithm. Of 482 HER2-positive breast cancer patients, 337 cases were used to train the prognostic risk models, and 145 were used to validate the accuracy of the HER2RI risk score.

Results HER2RIGEP and HER2RIClin models both showed better accuracy in predicting the risk of recurrence whether in the training dataset (81.3% and 80.7%) or in the testing dataset (70.3% and 69.7%). In the training dataset, significant differences were expectedly presented between the low- and high-risk patients stratified by both the HER2RIGEP and HER2RIClin models regarding the 5-year relapse-free survival (RFS) rate. Notably, the 5-year RFS rate of the high-risk patients in the testing dataset was significantly lower than that of the low-risk patients whether using the HER2RIGEP model (80% vs. 93%, $p=0.015$) or using the HER2RIClin model (80% vs. 93%, $p=0.018$).

Conclusion These two novel HER2RI risk models developed in our study are both predictive of the relapse risk in Asian population with HER2-positive early breast cancer and can help the risk stratification of patients to aid the treatment decisions.

OR-010

Percutaneous cholangioscopy and fluoroscopy-guided forceps biopsy for pathologically diagnosing highly suspected perihilar malignant diseases: a retrospective cohort study

Xiangyu Yang, Keyun Liu

Beijing Chao-Yang Hospital, Capital Medical University.

Purpose Pathological evidence determines the diagnosis and therapeutic regimen for patients with highly suspected perihilar malignant diseases (PMDs). This study was conducted to assess the role of percutaneous cholangioscopy (PTCS) in forceps biopsies guiding and mapping to diagnose and stage patients with highly suspected PMDs.

Materials and methods This retrospective observational study included patients diagnosed with highly suspected PMDs who underwent PTCS-assisted forceps biopsies between July 2018 and October 2024 at Beijing Chao-Yang Hospital, Beijing. The technical success, sensitivity, specificity and pathological accuracy were evaluated. The perihilar biliary trees were visually mapped, and staging was recorded.

Results Ninety-one patients who were clinically diagnosed with or highly suspected of having PMDs based on computed tomography and/or magnetic resonance findings and upregulated carbohydrate antigen19-9 participated. The technical success rate was 100%. The accuracy, sensitivity and specificity were 84.6%, 84.3% and 100%, respectively, with a 100% positive predictive value and 12.5% negative predictive value. Multivariate logistic regression analyses showed that total bilirubin significantly affected the accuracy rate of the PTCS-guided forceps biopsies. Wire-guided visual mapping was used to examine 39 surgical candidates, of whom, 21 declined surgery owing to estimated residual tumors, and 18 underwent radical surgical resection. Thirteen patients achieved negative margins. Samples from 51 of 75 patients pathologically diagnosed with malignancy were adequate for next-generation sequencing, and 28 underwent sequencing. No grade III or IV adverse events were observed.

Conclusion PTCS is a good modality for forceps biopsy guiding and biliary mapping of perihilar malignant lesions. Its high diagnostic efficiency, feasibility, success rates, and low complication rates allow definitive diagnoses and therapy for patients with PMDs.

OR-011

Mitochondrial-Cytosolic Cascade Metabolic Regulation System: A Robust Strategy to Disrupt Multipath Energy Replenishment in Cancer Therapy

Tianming Wang¹, Enhua Xiao², Peng Lei¹

1. Xiangya Hospital, Central South University

2. The Second Xiangya Hospital

Purpose This study aims to develop a novel cascade metabolic regulation system by manipulating cancer metabolic reprogramming to disrupt multipath energy replenishment in cancer cells, thereby enhancing antitumor efficacy.

Materials and methods A multi-enzymatic manganese-doped layered double hydroxide (Mn-LDH) nanodisc was synthesized. This nanodisc triggers mitochondrial dysfunction via self-cascade catalysis to impair energy metabolism in mitochondria and blocks compensatory energy metabolism from cellular glycogen. Concurrently, vessel embolization was combined to obstruct carbon sources essential for both cytosolic glycolysis and the mitochondrial tricarboxylic acid (TCA) cycle, while fostering an environment conducive to Mn-LDH catalysis. Comprehensive mechanistic studies were conducted across cellular and animal models to verify the strategy's ability to block multifaceted metabolic adaptations in cancer cells.

Results This dual-pronged regulation strategy induced ATP exhaustion and apoptosis in cancer cells, leading to significantly enhanced antitumor efficacy in orthotopic hepatocarcinoma rabbit models compared to a standard clinical embolization formulation for advanced liver tumors. Mechanistic studies confirmed that the strategy effectively blocked multifaceted metabolic adaptations within both the mitochondria and cytosol of cancer cells.

Conclusion This work provides a promising platform for metabolic intervention and offers important insights into cancer biology and management.

OR-012

Prevention of acute thrombosis with vascular endothelium antioxidative nanoscavenger

Yixin Zhong, Qiankun Ni, Haidong Zhu, Gaojun Teng

Department of Radiology, the Second Affiliated Hospital of Chongqing Medical University, No. 74 Linjiang Rd, Yuzhong District, Chongqing, 400010, P. R. China

Purpose Antiplatelet drugs have been a milestone in treating patients with high risk of thrombosis. However, their clinical use is impeded by bleeding risk and inadequate effect. The excessive reactive oxygen species (ROS) produced by damaged vascular endothelial cells have been shown to be a stimulus for thrombosis.

Materials and methods Herein, a ROS-chemotaxic nanoscavenger, formed by the crosslink between melanin and catalase, is proposed to prevent acute thrombosis by protecting vascular endothelial cells from oxidative stress.

Results We demonstrate that treatment of MDPCP inhibits ROS-induced apoptosis of endothelial cells, contributing to the attenuation of vascular endothelium damage and collagen exposure, which in turn restricts platelet activation and ultimate thrombosis.

Conclusion This MDPCP-based modulation on vascular redox homeostasis provides a promising antithrombotic alternative addressing the bleeding risk of current clinical antithrombotic drugs.

OR-014

A Prospective, Sing-Arm, Phase 2 Study of Transarterial Embolization Plus Hepatic Arterial Infusion Chemotherapy Combined with Sequential Lenvatinib and Sintilimab in Patients with Infiltrative Hepatocellular Carcinoma.

Zhi-Mei Huang, Ying-Wen Hou, Jin-Hua Huang
Sun Yat-sen University Cancer Center

Purpose Hepatocellular carcinoma (HCC) ranks among the leading morbidity and mortality in China, posing a substantial threat to public health. Infiltrative HCC, accounting for 7%-20% of total cases, represents the most aggressive subtype. Surgical resection is often not feasible since infiltrative HCC (iHCC) commonly presents with portal vein invasion or distant metastasis at initial diagnosis. Previous studies have shown limited efficacy of transarterial chemoembolization (TACE) for iHCC. Systemic therapies for advanced HCC achieved low overall responses and survival benefits. HAIC combined with systemic therapies showed promising improvement on ORR in advanced HCC, while the PFS remains constrained. .

Previous studies demonstrated no statistically significant difference in survival benefits between transarterial embolization (TAE) and TACE for HCC. However, conventional chemotherapy dose in TACE may cause hepatotoxicity and liver dysfunction for the patients with iHCC. Furthermore, HAIC may not achieve comprehensive perfusion for all tumor-feeding arteries of large HCC, which usually contain multiple collateral blood supplies. This study is intended to conduct a single-arm prospective phase II clinical trial to evaluate the efficacy and safety of TAE plus HAIC combined with sequential Lenvatinib and Sintilimab in the treatment of patients with iHCC. The anticipated findings are expected to provide high-level evidence for treatment decision making, potentially address the current need of improving synergistic effects for advanced iHCC, and improve the prognosis and the quality of life.

Materials and methods This study is a single-center, single-arm, prospective phase II clinical trial initiated by researchers, to evaluate the efficacy and safety of TAE and HAIC combined with sequential Lenvatinib and Sintilimab in the treatment of patients with iHCC. Patients who underwent initial diagnoses and treatment in Sun Yat-sen University Cancer Center from October 2023 to December 2024 were screened. All patients were diagnosed as HCC by histology or clinical criteria according to the recommendation of American Association for the Study of Liver Diseases, and the infiltrative subtype was confirmed by radiologists. Patients who met the criteria were enrolled in this study and received at least two cycle combination therapy of TAE and HAIC combined with sequential Lenvatinib and Sintilimab. Minor lipiodol and major blank embolic microspheres were applied for TAE and the HAIC regimen was FOLFOX (oxaliplatin, calcium folinate and fluorouracil). Lenvatinib and Sintilimab were applied within 3-7 days after the initial TAE-HAIC procedure. Lenvatinib was managed in a low-dose regimen (<60kg, 4mg/day; ≥60kg, 8mg/day), considering the risk of liver dysfunction in iHCC patients. After 2-cycle approaches, treatment strategy could be translated to other therapies according to the tumor response, such as resection, ablation, radiotherapy or TACE. Follow-up examination was performed after 1 month after treatment, every 3 months for the first 2 years and every 6 months thereafter, including but not limited to enhanced CT or MR. Efficacy was evaluated by the radiologist and competent physician according to the mRECIST criteria. Treatment-related complications and adverse events (AEs) were recorded. The primary endpoint of this study was ORR and the secondary endpoints included PFS, OS and the safety assessment.

Results Of 39 patients screened between October 2023 and December 2024, 30 who met the criteria were enrolled in this study and received at least 2 courses of TAE plus HAIC combined with Lenvatinib and Sintilimab treatment.

1. Efficacy evaluation: Among 30 patients, 12 patients (40.0%) achieved PR (partial response) after the first cycle of treatment, and 22 patients (73.3%) reached PR after 2 cycles. During the study period, 5 patients (16.7%) achieved CR (complete response) after sequent ablation, TACE or radiotherapy, 20 patients (66.7) were evaluated as PR. The overall ORR was 83.3%.

2. The median follow-up time was 7.1 months, and 10 patients died during the period. The median OS was 16.0 months (95%CI: 5.6-26.5 months). The 3-month, 6-month and 12-month rates of OS were 93.3%, 83.0% and 60.2%. The median PFS was 9.5 months (95%CI: 4.9-14.1 months) according to the mRECIST, and the PFS rates at 3-month, 6-months and 12-month were 95.7%, 68.1% and 20.4%, respectively. The median liver-specific PFS was 11.7 months (95%CI: 7.7-15.7 months), and the liver-specific PFS rates at 3-month, 6-months and 12-month were 95.7%, 80.4% and 44.6%, respectively.

3. Safety assessment: the incidence of TAE-HAIC related complications was 90.0% according to SIR (Society of Interventional Radiology) system. The incidences of minor and major complications were 86.7% and 13.3%. The overall incidence of treatment related adverse events was 76.7% according to the CTCAE 5.0 criteria (Common Terminology Criteria for Adverse Events). The incidence of Grade 1-2 AEs was 73.3%, and only one patient experienced Grade 3 AE (severe skin ulcer). Among 30 patients, 10 patients (33.3%) received dose reduction, 9 patients (30.0%) discontinued drug therapy. Among them, 6 patients continued the drug therapies when AEs disappeared or became tolerable after dose reduction. 3 patients discontinued for the persistence of AEs and 6 for personal reasons.

Conclusion This clinical trial investigated the efficacy and safety of TAE and HAIC combined with sequential Lenvatinib and Sintilimab for patients with infiltrative HCCs and reached the primary endpoint. The preliminary results of current study indicates that the combination regimen is safe and effective, and the AEs and complications are controllable and tolerable. This study provides a reference for further phase III clinical research, and a novel treatment option for the advanced HCC.

OR-015

Spatial transcriptomics reveals tryptophan metabolism restricting maturation of intratumoral tertiary lymphoid structures

Shuling Chen, Qianwen Zeng, Jianyu Chen, Tianyi Xu, Ming Kuang
The First Affiliated Hospital, Sun Yat-sen University

Purpose Tertiary lymphoid structures (TLSs) are ectopic lymphoid aggregates that form in nonlymphoid tissues and exhibit a spectrum of maturation states across diverse cancers. Mature TLSs correlate with improved prognosis and immunotherapy response in multiple cancers. In contrast, the clinical relevance of immature TLS remains controversial. However, assessing TLS maturation status remains challenging due to the absence of a standardized classification system. Moreover, factors driving TLS maturation remain incompletely understood. Therefore, we aimed to characterize TLS heterogeneity in hepatocellular carcinoma (HCC) and elucidate key regulators of TLS maturation.

Materials and methods We integrated multi-omics datasets encompassing 46 TLS-positive spatial transcriptomics (Stereo-seq) samples (including samples from treatment-naïve and neoadjuvant ICB-treated HCC patients), 27 scRNA-seq samples, 4 snATAC-seq datasets, and 422 bulk RNA-seq cohorts. Mechanistic validation was conducted through histological staining, *in vitro* culture experiments of B cells and T cells, flow cytometry, and orthotopic HCC murine models.

Results Our proprietary TLS identification pipeline enabled *in situ* detection of 937 TLSs in Stereo-seq data, revealing heterogeneity in spatial gene expression patterns and cell composition within distinct TLSs. We devised a classification schematic distinguishing immature TLSs as conforming TLSs (with potential for maturation) or deviating TLSs (deviating from the maturation process) based on their developmental trajectories. Importantly, conforming TLSs shared mature TLSs' immune niche function and responded to ICB with increased T-cell activity/B-cell interactions, correlating with improved HCC prognosis. Compared to mature/conforming TLSs, tumor cells proximal to deviating TLSs showed upregulated tryptophan metabolism, characterized by upregulation of the rate-limiting enzyme TDO2. snATAC-seq confirmed increased chromatin accessibility at tryptophan metabolism-related loci in these tumor cells. *In vitro* experiments demonstrated that elevated tryptophan/kynurenine levels suppressed T/B cell proliferation, activation, and Tfh differentiation. In orthotopic HCC models, dietary tryptophan supplementation or TDO2 overexpression impaired TLS maturation by reducing GC-B and Tfh, accelerating tumor progression. Conversely, tryptophan restriction or TDO2 inhibition promoted TLS maturation, boosted IgG-mediated antitumor humoral immunity, suppressed tumor growth and synergized with anti-PD-1 therapy.

Conclusion In summary, we present comprehensive profiling of TLSs in an *in-situ* context with cellular resolution in HCC. Our study not only reveals the dynamics of TLS maturation and its modulation by tryptophan metabolism in the tumor microenvironment, but also proposes a potential new strategy to promote TLS maturation and antitumor immunity by modulating this metabolic pathway - addressing a major unmet need in oncology.

OR-016

Idarubicin-loaded degradable hydrogel for TACE therapy enhances anti-tumor immunity in hepatocellular carcinoma

Xiaokai Zhang¹, Jiaping Li²

1. Henan Cancer Hospital/ Affiliated Cancer Hospital of Zhengzhou University

2. The First Affiliated Hospital of Sun Yat-sen University

Purpose We aim to explore the potential of degradable hydrogels for treating HCC, provide more effective treatment options for HCC patients while offering new insights and theoretical foundations for understanding TACE mechanisms and tumor microenvironment regulation.

Materials and methods

Firstly, we prepare the composite hydrogel and test the physicochemical properties. And then, we construct the Animal model for TACE treatment. Materials and methods including CCK-8 cytotoxicity assay, coagulation test, hemolysis assay, magnetic resonance imaging scan, HE staining, immunofluorescence staining, single-cell sequencing/transcriptome sequencing, Western Blotting, biochemical testing.

Results In our research, we developed a composite hydrogel (IF@Gel) made of Poloxamer-407 gel and Fe₃O₄ nanoparticles, loaded with idarubicin, to use as an embolic material for TACE in a rat model of orthotopic HCC. We observed promising therapeutic effects and investigated the impact on the tumor immune microenvironment, focusing on the role of immunogenic cell death (ICD). The composite hydrogel demonstrated excellent potential as an embolic material for TACE, and IF@Gel-based TACE demonstrated significant efficacy in rat HCC. Furthermore, our findings highlight the potential synergistic effects of ICD with anti-PD-L1 therapy, providing new insights into HCC treatment strategies.

Conclusion In conclusion, we employed TACE with a novel Poloxamer-407 composite hydrogel loaded with Idarubicin to evaluate its therapeutic efficacy in an orthotopic HCC model in SD rats, and the alterations in the tumor immune microenvironment following treatment and investigated the potential role of ICD in these processes.

OR-017

Cryoablation enhanced anti-tumor immunity and survival for patients with liver metastatic melanoma receiving PD-1 blockade therapy: Insights from longitudinal RNA-seq data

Lujun Shen, Shuanggang Chen, Dandan Li, Xiaoshi Zhang, Weijun Fan
Sun Yat-sen University Cancer Center/CN

Purpose

Although there are evidences that cryoablation combined with PD-1 blockade therapy have synergistic treatment effect for patients with liver metastatic melanoma, the additive treatment effect of cryoablation and the associated mechanism remain unknown.

Materials and methods A total of 178 patients with liver metastatic melanoma receiving PD-1 blockade therapy or cryoablation combined PD-1 blockade (Cryo-anti-PD1) therapy between August 1st, 2018 to July 31th 2024 in Sun Yat-sen University Cancer Center were enrolled. The overall survival (OS), and progression-free survival (PFS) of the two treatment arms were compared. The bulk RNA sequencing of liver tumor biopsy longitudinally obtained from patients receiving Cryo-anti-PD1 therapy were analyzed to decode the differences between responders and non-responders and identify the patients benefit from combined treatments.

Results Of the patients enrolled, 110 patients (61.8%) received Cryo-anti-PD1 therapy, and 68 (38.2%) received anti-PD1 treatment. The best overall response rates of the Cryo-PD1 and anti-PD1 cohorts were 32.7% and 8.8%, respectively. Multivariate analysis showed patients in Cryo-anti-PD1 group had better OS (HR: 0.62, 95%CI: 0.41-0.96) and PFS (HR: 0.64, 95%CI: 0.64-0.91) rates compared to the anti-PD1 group. For patients in Cryo-anti-PD1 group, combined therapy significantly increased the abundance of DC cells and CD8+ Naive T cells in distal tumors; the responders had significantly superior OS time compared to non-responders (mOS: 29.1 vs 12.0 months). The overall response rate (ORR) of patients with immune activative (IA), immune exclusive (IE) and immune suppressive (IS) tumors were 44.4%, 43.8% and 12.5% respectively. Patients with tumors of IA or IE subtypes had significantly improved OS compared to those with IS subtype ($P < 0.05$).

Conclusion Cryoablation enhances the efficacy of PD-1 blockade therapy and prolong the survival of melanoma patients with liver metastasis; the combination therapy achieved a high response rate for IA and IE tumors, while IS tumors remains a challenge.

OR-018

A real-world survey of 1830 surviving patients with adamantinomatous craniopharyngioma in China

Zhixiong Lin¹, Yanping Deng^{1,2}

1. Department of Neurosurgery, Sanbo Brain Hospital, Capital Medical University

2. School of Pharmacy, Fujian Provincial Key Laboratory of Natural Medicine Pharmacology, Fujian Medical University

Purpose Background: Adamantinomatous craniopharyngioma (ACP) is a rare benign tumor of the central nervous system. Real-world studies on surviving patients in China remain lacking. This study aimed to systematically analyze the demographic characteristics, treatment patterns, complications, recurrence rates, and factors influencing quality of life (QoL) and family economic burden among Chinese ACP survivors through an independent third-party survey.

Materials and methods Methods: In July 2024, a third-party volunteer team conducted a questionnaire survey of 1,830 ACP survivors in Chinese communities. Chi-square tests and multivariate logistic regression analyses (SPSS 21.0) were used to evaluate influencing factors.

Results 72.3% of patients underwent initial surgery at ages 0-10 years, with a male predominance (59.3% vs. 40.7% female). In the initial treatment, 98.6% of patients underwent surgery. Gross total resection (GTR) rates were comparable between transcranial approach (TCA) (84.37%) and endoscopic endonasal surgery (EES) (87.73%), but TCA had significantly higher recurrence rates (26.1% vs. 15.3%; $P < 0.001$) compared to EES. In subtotal resection cases, regrowth rates were higher after TCA (65.26% vs. 40.74% EES; $P = 0.0001$). Among 267 patients with residual tumors, only 108 were recommended radiotherapy (RT), and 56 ultimately received RT. RT recipients required no further treatment significantly more often than non-RT cases (36/56 vs. 77/211; $P = 0.0002$). Among patients with residual tumors after the first operation, only 108 were recommended for RT by doctors, and 56 eventually received it. The proportion of patients who did not require further treatment after radiotherapy was significantly higher than those who did not receive it (36/56 vs. 77/211, $P = 0.0002$). There were differences in the incidence of complications between TCA and EES. Specifically, for gross total resection, TCA associated with higher rates of sinusitis, dyslipidemia, hyperglycemia, flatfoot, and forehead incision suppuration. For subtotal resection, EES was linked to increased incidences of hypothalamic obesity, diabetes insipidus, and scoliosis.

The QoL was significantly affected by the type of surgery (TCA OR = 0.393, $P < 0.001$), absence of hypothalamic obesity (OR = 0.541, $P = 0.001$) and absence of recurrence (OR = 1.923, $P < 0.001$). Family economic burden was significantly associated with age at first operation (OR = 1.020, $P = 0.001$) and impaired QoL (mild OR = 4.427, $P < 0.001$; Moderate OR = 1.825, $P = 0.017$).

Conclusion Conclusions: The treatment of ACP patients in China is predominantly centralized in experienced medical centers. EES offers advantages in reducing recurrence rate, and radiotherapy can provides substantial benefits to patients. CTA is significantly associated with decreased QoL. Therefore, it is necessary to optimize individualized treatment strategies and strengthen postoperative support.

OR-019

Response evaluation of liver directed therapies for liver metastasis in NET

DR VARSHA KEDAR, DR SUYASH KULKARNI, DR NITIN SHETTY, DR KUNAL GALA, DR KAJARI BHATTACHARYA, VARSHA KEDAR
TATA MEMORIAL HOSPITAL, MUMBAI, INDIA

Purpose To know the effect of liver directed therapy on hepatic progression free survival and overall survival.

Materials and methods The records of patients with NET and liver metastasis managed at our institute. Forty-four patients were included in the study. As this was a retrospective observational study, no formal sample size was calculated. Overall survival and hepatic progression free survival (HPFS) from initial liver directed therapy (LDT) by DOTA and FDG-PETCT were identified.

Results Amongst 44 patients, our hepatic progression free survival data ranged from 6-84 months with 2 year HPFS being 48% (21 patients with stable disease at 2 years) with a mean of 26 months. Overall survival ranged from 8-120 months with 3-year overall survival being 53% with a mean of 40 months.

Conclusion Liver directed therapy in the form of ablation or transarterial therapy is an accepted method of treatment of unresectable hepatic metastases from neuroendocrine tumors. Our study shows that long-term palliation is possible using liver directed therapies, especially in those patients who have a predominantly hepatic disease; hence, it could be proposed as first-line non-surgical treatment in this subgroup of patients, and could be associated with somatostatin analogues when unable to control hormone related symptoms alone. In patients presenting with extra-hepatic lesions, it should be initially used in combination with systemic treatments. The need for repeat therapy and the interval between sessions should be tailored according to the patient response, tolerance, and need for palliation, so as to avoid unnecessary sessions.

OR-021

First-in-human study of an artificial intelligence integrated robot for image-guided, trans-thoracic lung biopsy under local anaesthesia

Nadia Andrea Rojas Valenzuela², Jun Kiat Ho², Zehao Tan², Alfred Tan Bingchao², Leong Sum², Arjunana Arjunana Sarupraba², Rehena Ganguly¹, Too Chow Wei², Nadia Rojas

1. Singapore General Hospital

2. Department of Vascular & Interventional Radiology, Singapore General Hospital, Singapore

Purpose To demonstrate the safety and efficacy of a robotic-assisted and artificial intelligence (AI) integrated system for CT-guided trans-thoracic lung biopsy (TTLB) procedure with a prospective, single-centre, single-arm trial.

Materials and methods Patients referred for TTLB during June 2024 to September 2024 were recruited. TTLB was performed under local anesthesia with the trial system on a path (iPath) an interventional radiologist chose. A separate path (nPath) was generated by a proprietary AI software (NDAalyzer) without influence on the procedure. Patient, lesion, procedural details and angular differences between these paths were collected. Technical success was defined as successful completion of TTLB without the need for disengagement of the needle holder for freehand adjustment. Clinical success is defined as obtaining sufficient tissue for histological analysis.

Results Thirty patients were recruited. The median lesion size was 24mm (Interquartile range (IQR), 15.3-32.5mm). Technical success was 93% (28/30). Clinical success was 96% (27/28). Median procedure time and radiation dose were 36.4 minutes (IQR, 27.0-48.3 minutes) and 348.4 mGy·cm (IQR, 267.6-500.1 mGy·cm). The median procedure time was reduced by 30.9 minutes ($p < 0.01$) between the first and last 10 patients. No major complication was encountered. Median angular difference between iPath & nPath was 4.4° (IQR, 3.2-8.7°). No significant correlation between the angular difference and minor complications was demonstrated on univariate & multivariate logistic analysis.

Conclusion The trial system is safe in human use for TTLB with short learning curve, acceptable procedural success and complication rates. AI path prediction software showed satisfactory correlation with operator planned path in a prospective cohort.

OR-022

Analysis of short and medium term clinical effect of prostatic artery embolization on symptomatic prostatic hyperplasia

Shilong Han

Tenth People's Hospital of Tongji University

Purpose This study aimed to retrospectively evaluate the clinical efficacy and safety of prostatic artery embolization (PAE) in treating benign prostatic hyperplasia (BPH), focusing on prostate volume reduction and symptom improvement in patients unsuitable for surgery or refractory to medical therapy

Materials and methods A retrospective analysis was conducted on 45 BPH patients who underwent PAE between January 2020 and December 2023. Inclusion criteria included moderate-to-severe lower urinary tract symptoms (LUTS), failure of conservative management, and contraindications to surgery. All procedures involved selective angiography to identify prostatic arteries (originating from the inferior vesical, internal pudendal, or obturator arteries) followed by embolization using 100–300 μ m Embosphere microspheres and gelatin sponge particles¹². Technical success was defined as successful embolization of at least one prostatic artery. Outcomes assessed pre- and postoperatively (1, 3, 6 months) included International Prostate Symptom Score (IPSS), quality of life (QOL), prostate volume (transrectal ultrasound), maximum urinary flow rate (Qmax), and postvoid residual urine (PVR).

Results Technical success was achieved in 43/45 patients (95.6%). Among 45 patients, 32 (71.1%) exhibited significant prostate volume reduction (mean reduction: $42.3\% \pm 12.1\%$) at 6-month follow-up. IPSS improved from 28.5 ± 4.2 to 8.1 ± 2.3 , QOL scores decreased from 4.9 ± 0.8 to 1.2 ± 0.5 , Qmax increased from 6.8 ± 2.5 mL/s to 16.7 ± 3.1 mL/s, and PVR decreased from 135 ± 45 mL to 25 ± 12 mL (all $P < 0.01$)¹³. Two cases of unilateral PAE also showed symptom relief. Complications included transient pelvic pain (4/45, 8.9%) and self-limited hematuria (3/45, 6.7%), with no major adverse events (e.g., bladder or rectal ischemia)³⁴.

Conclusion PAE is a minimally invasive and effective intervention for BPH, particularly in patients with significant prostate enlargement or surgical contraindications. The procedure demonstrated durable mid-term outcomes in symptom alleviation and prostate volume reduction, with a favorable safety profile³⁴. Further randomized studies are warranted to optimize patient selection and long-term follow-up.

OR-023

Efficacy and safety of TACE combined with TKI against TACE alone for managing intermediate-stage HCC with hypovascular nodules

Jun Yang,Caifang Ni

The First Affiliated Hospital of Soochow University

Purpose This study aimed to compare the safety and efficacy of TACE in combination with TKI against TACE alone for managing intermediate-stage hepatocellular carcinoma (HCC) with hypovascular nodules.

Materials and methods Patients with intermediate-stage HCC who received TACE treatment were investigated and screened. The patients were divided into TACE alone or TACE-TKI group according to whether they used TKI drugs. The safety and toxicity were evaluated by comparing the changes in laboratory values and the incidence of adverse events. The therapeutic effect of the tumor was evaluated according to the Modified Response Evaluation Criteria in Solid Tumors

Results 75 HCC patients with hypovascular nodules were ultimately included in the study cohort, comprising 40 cases treated with TACE combined with TKI and 35 cases receiving TACE monotherapy. The combination therapy group demonstrated significantly higher ORR and DCR than the TACE group ($P<0.05$). In the TACE-TKI group, the median OS was 41.1 months (95% CI, 30.2-52.7 months), compared to 19.7 months (95% CI, 17.0-22.4 months) in the TACE group, with the combination group demonstrating a significantly longer median OS than the TACE group ($P<0.001$). The TACE-TKI group also exhibited a prolonged median PFS of 20.2 months (95% CI, 15.0-25.4 months) versus 9.9 months (95% CI, 3.4-16.4 months) in the TACE group ($P<0.001$). Furthermore, multivariate analysis identified TACE combined with TKI therapy (hazard ratio [HR]=0.300; 95% CI:0.158-0.571; $P<0.001$) and tumor diameter (HR=1.014; 95% CI:1.003-1.025; $P=0.013$) as independent prognostic factors for overall survival. The incidence rates of fever, emesis, abdominal pain, and diarrhea were comparable between the groups. Notably, some patients in the TACE-TKI group experienced adverse reactions such as hypertension, proteinuria, and hand-foot syndrome, with the incidence of proteinuria being significantly higher than that in the TACE group ($P=0.028$). No significant difference was observed in the incidence of severe adverse events between the two groups.

Conclusion This study demonstrated that in patients with intermediate-stage HCC accompanied by hypovascular nodules, the combination therapy of TACE and TKI significantly improved OS and PFS compared to TACE monotherapy.

OR-024

First-line durvalumab with arterial chemotherapy in major portal invaded hepatocellular carcinoma: the phase 2 DurHope study with biomolecular analyses

Ming Zhao, Ning Lyu, Junzhe Yi, Jiongliang Wang, Xintong Wu, Xiongying Jiang, Song Chen, Jie Xu, Jibin Li, Suixing Zhong, Qifeng Chen, Yue Hu, Yimin Zhang, Yujia Song, Genjun Tan, Yunan Zhang
Sun Yat-sen University Cancer Center

Purpose Hepatocellular carcinoma (HCC) patients with Vp4 portal vein tumor thrombus (PVTT) have a poor prognosis and remain underrepresented in global clinical trials. The biomolecular exploratory, phase 2 DurHope study trial was designed to evaluate the efficacy, safety, and biomolecular profile of durvalumab combined with arterial FOLFOX as first-line therapy for advanced HCC with major PVTT.

Materials and methods Thirty patients with major PVTT (Vp4: n = 24, 80.0%; Vp3: n = 6, 20.0%) were enrolled. Treatment consisted of arterial FOLFOX (given on day 1–3 of each 21-day cycle) plus intravenous durvalumab (1120 mg on day 7 ± 2) for up to 8 cycles. Patients with disease control transitioned to maintenance durvalumab (1500 mg every 28 days) until disease progression, unacceptable toxicity, or death. Primary endpoint was 1-year OS rate, and secondary endpoints included progression-free survival (PFS), objective response rate (ORR) per RECIST v1.1, and safety. Single-cell RNA sequencing (scRNA-seq) was performed on baseline tumor biopsies and longitudinally collected peripheral blood mononuclear cells (PBMCs) from responders (CR/PR) and nonresponders (SD/PD).

Results With a median follow-up of 21.6 months, the 1-year OS rate was 63.3%, with a median OS of 13.9 months (95% CI, 10.7–NR) and a median PFS of 9.0 months (95% CI, 4.5–12.2). The ORR was 53.3% (CR: 5/30 [16.7%]; PR: 11/30 [36.7%]), with a median duration of response of 9.1 months (> 6 months: 11/16 [68.8%]; > 12 months: 4/16 [25%]). The combination therapy exhibited an acceptable safety profile, with grade ≥3 TRAEs reported in 43.3% of patients, and no unexpected toxicities beyond those typically associated with either agent. scRNA-seq analysis of tumor biopsies revealed enrichment of chemotherapy resistance and immune escape signatures, and a subcluster of MECOM+ malignant cells associated with reduced clinical benefits in non-responders. In contrast, responders exhibited a tumor microenvironment shift toward immune activation, characterized by increased immune cell infiltration and enhanced immune-malignant cell interaction. Longitudinal scRNA-seq of serial PBMCs demonstrated dynamic expansion of effector T-cell subsets and upregulation of cytotoxicity-associated genes following treatment, which were more pronounced in responders. Additionally, responders exhibited a decrease in nonclassical monocytes and attenuation of anti-inflammatory signaling, suggesting systemic immune modulation. These genomic findings were further validated by in situ immunohistochemistry analysis and in vivo mouse models.

Conclusion Durvalumab plus arterial FOLFOX showed promising efficacy and manageable toxicities in advanced HCC with Vp4 PVTT. Biomolecular exploratory analyses revealed enhanced cellular immune responses triggered by treatment, along with potential predictive biomarkers that could refine patient selection and treatment optimization.

OR-025

Concomitant Symptomatic Colorectal Cancer and Thoracoabdominal Aortic Aneurysm Treated with staged Endovascular Aneurysm Repair (EVAR) Followed by Anterior Resection

Sarrath Sutthipong, Napong Kitpanit, Chanchai Suwannakij
Department of Surgery, Bhumibol Adulyadej Hospital, Bangkok, Thailand

Purpose Colorectal cancer (CRC) is the third most common gastrointestinal cancer in Thailand, primarily affecting older individuals. Thoracoabdominal aortic aneurysm is also age-related conditions, but their concurrent occurrence with CRC is rare. The optimal treatment strategy for concomitant CRC and aortic aneurysm remains debated. We report a case of symptomatic rectosigmoid colon cancer with aneurysms of the supra-aortic trunk, descending aorta and abdominal aorta and its treatment approach.

Materials and methods An 80-year-old male was referred after a colonoscopy and biopsy confirmed rectosigmoid colon cancer, prompted by bowel habit changes. Preoperative abdominal CT revealed segmental bowel wall thickening without distant metastases but incidentally identified an abdominal aortic aneurysm (AAA) measuring 56 mm with severe neck angulation (80 degrees), tortuous iliac arteries, and involved the inferior mesenteric artery. Additional whole-aorta CT angiography showed ectasia of the aortic root and ascending aorta, aortic arch aneurysm (51 mm) and descending thoracic aortic aneurysm (60 mm). No significant lymph node enlargement or tumor invasion of surrounding adipose tissue was noted, leading to a diagnosis of T3N0M0 (cStage II) CRC. Both the thoracic and abdominal aneurysms were unsuitable for endovascular repair and required open surgery. Considering the risks of aneurysm rupture, cancer-related symptoms and the patient's condition, a staged approach was chosen: endovascular aortic repair (EVAR) for the AAA using fixation first and push-up technique, followed by anterior resection for CRC. The supra-aortic trunk aneurysm was left untreated due to high surgical risk.

Results EVAR was performed under general anesthesia, successfully preserving the bilateral renal and all iliac arteries. A minor type 1A endoleak was observed but deemed acceptable due to an adequate sealing zone and proper graft sizing with no migration. Postoperative duplex ultrasound confirmed stent graft patency, thrombosis and shrinkage of the aneurysm sac and no further endoleak. One week after EVAR, the patient underwent anterior resection during the same admission. No significant adhesions around the treated aortic aneurysm were observed and postoperative recovery was uneventful. The pathological report confirmed adenocarcinoma with tumor invasion into pericolic adipose tissue but no malignancy at the proximal, distal or circumferential resection margins. No nodal metastasis was found in 12 examined lymph nodes.

Conclusion A patient with non-urgent concomitant CRC and AAA was successfully treated with EVAR followed by colectomy without complications. Further studies are needed to validate this approach in a larger cohort.

OR-026

Drug eluting bead transarterial chemoembolization (DTACE) combined with hepatic arterial infusion chemotherapy versus DTACE alone for hepatocellular carcinoma in Barcelona Clinic Liver Cancer stage C: a prospective, multicenter, analysis

Shuguang Ju,Xuhua Duan
The First Affiliated Hospital of Zhengzhou University

Purpose To evaluate the performance of drug-eluting bead transarterial chemoembolization (DTACE) combined with hepatic arterial infusion chemotherapy (HAIC) (DTACE-HAIC) compared to DTACE alone in patients with hepatocellular carcinoma (HCC) in Barcelona Clinic Liver Cancer stage C (BCLC C).

Materials and methods This research has been registered on ClinicalTrials.gov under the identifier (NCT05788835). In the prospective study, we enrolled 253 patients diagnosed with advanced HCC and treated at ten hospitals from January 2023 to March 2024. The cohort comprised 110 patients who received DEB-TACE combined with HAIC (DTACE-HAIC group) and 110 patients who received DEB-TACE alone (DTACE group). Progression -free survival (PFS), overall survival (OS), objective response rate (ORR), and disease control rate (DCR) were assessed at an independent review facility according to the modified Response Evaluation Criteria in Solid Tumors (mRECIST).

Results For 220 patients, median PFS was 11.37 months in the D-TACE-HAIC group higher than 7.13 months in DTACE group ($P = 0.014$); median OS was 24.37 months in the DTACE-HAIC group longer than 17.13 months in DEB-TACE group ($P = 0.037$). The ORR in the DTACE-HAIC and DTACE groups was 75.0% and 37.5%, the DCR was 93.8% and 81.3% HAIC respectively. In subgroup analysis, patients with non-smooth tumor margin (median, 20.8 vs 13.0 months; $P < 0.001$), PVTT (median, 15.0 vs 11.0 months; $P = 0.015$), or with enlarged hilar and retroperitoneal lymph nodes (median, 15.0 vs 11.0 months; $P = 0.023$) had significantly longer OS in DTACE-HAIC group than in DEB-TACE group. Most TRAEs were mild and manageable. Myelosuppression after HAIC was more frequent in the DTACE-HAIC group (33.6% vs 8.2%, $P < 0.001$), while hepatic dysfunction was more frequent in the DTACE group (21.8% vs 9.1%, $p = 0.009$).

Conclusion The combination of DTACE and HAIC may lead to improved outcomes in PFS, OS, ORR, and DCR with a comparable safety profile in advanced HCC.

OR-027

The role and mechanism of peroxisomes in the response to TACE treatment for hepatocellular carcinoma

WEN JIE,zhihui wang, Jiaping Li

The First Affiliated Hospital of Sun Yat sen University

Purpose The liver was abundant in peroxisomes, yet the role these organelles played in the progression of hepatocellular carcinoma (HCC) remained largely unknown. This study aimed to investigate the function of peroxisomes in HCC progression, the molecular mechanisms, the role of peroxisomes in response to transarterial chemoembolization (TACE) and the impact on immune microenvironment.

Materials and methods

Firstly, a prognostic model based on peroxisome-related genes would be constructed using bioinformatics and LASSO regression analysis. Patients would be stratified into high-/low-risk groups based on the model, and the molecular pathway alterations will be analyzed. Subsequently, a rat model of TACE would be established to verify changes of genes from the prognostic model before and after TACE. Lastly, spatial transcriptomic sequencing would be employed to analyze the tumor immune microenvironment of HCC patients following TACE.

Results In HCC, we identified 34 overlapping genes between 113 peroxisome-related genes (PRGs) and 5035 clinical prognosis related genes(CPRGs) (Figure 1A). Next, LASSO analysis was performed to select 10 optimal genes to develop a prognostic model with a impressive predictive capabilities (Figure 1B-F). According to the median value, HCC patients were assigned to high-/low-risk group. We screened the different expression genes (DEGs) between high-/low-risk groups and performed GO and KEGG analyses to determine biological pathway alterations (Figure 1G-K). These results provided evidence for the possible regulaiton pathways with regard to peroxisome-function in HCC.

Subsequently, by using a rat model, we discovered that, following TACE, the mRNA levels of certain genes within the prognostic model underwent significant alterations, including PEGR, HSD17B4, RAB8B, UBE2D2 and PPARGC1A (Figure 2A-B).

Finally, we explored the regulation of peroxisomes to immune microenvironment after TACE through spatial transcriptomic sequencing. For PPARGC1A's significant changes after TACE, we categorized PanCK+ HCC cells into PPARGC1A high-/PPARGC1A low-groups (Figure 2C). Significant differences in gene expression profiles were observed between the two groups, with notable disparities in T-cell-related pathways, peroxisome pathways, etc. (Figure 2D-F). PPARGC1A high group exhibited a higher infiltration of CD8+ T cells (PanCK-/CD45+) and a lower infiltration of M2-type macrophages (PanCK-/CD206+) (Figure 2G-H). These results suggested that peroxisomes could indeed remodel the tumor microenvironment of HCC in response to TACE, indicating that peroxisomes may play a crucial role in overcoming TACE resistance in HCC.

Conclusion Peroxisomes may play a significant role in the progression of HCC, particularly in responding to TACE treatment by altering lipid metabolism pathways, ferroptosis pathways, and reshaping the immune microenvironment. Targeting peroxisomes to develop new targeted drugs could offer novel strategies and insights for overcoming TACE resistance.

OR-028

Hepatic Arterial Infusion Chemotherapy with or without Hepatic Artery Chemoembolization for Esophageal Carcinoma patients with Liver Metastasis: A Clinical Retrospective Study

Mingrui Yan^{1,2}, Baojiang Liu¹, Song Gao¹, Jianhai Guo¹, Fuxin Kou¹, Shaoxing Liu¹, Xin Zhang¹, Aiwei Feng¹, Xiaodong Wang¹, Guang Cao¹, Hui Chen¹, Peng Liu¹, Haifeng Xu¹, Qinzong Gao¹, Renjie Yang¹, Liang Xu¹, Xu Zhu¹

1. Peking University Cancer Hospital and Institute

2. Peking University Shougang Hospital

Purpose This study aims to evaluate the efficacy and safety of interventional treatment of liver metastasis in esophageal carcinoma patients with liver metastasis.

Materials and methods This study retrospectively analyzed the clinical data of 47 esophageal carcinoma with liver metastasis (ECLM) patients who received Hepatic arterial infusion chemotherapy (HAIC) with or without Transcatheter arterial chemoembolization (TACE) in the Department of Interventional Therapy in the Peking University Cancer Hospital and Institute between May 2007 and December 2022. Of the 47 patients, 4 were lost to follow-up, and ultimately 43 ECLM patients were included in the final analysis. The primary endpoint was progression-free survival following the first interventional treatment (PFS). The secondary endpoints included overall survival following the first interventional treatment (OS), objective response rate (ORR), disease control rate (DCR) and safety. All treatment responses were evaluated based on the Response Evaluation Criteria In Solid Tumors (RECIST). Treatment-related adverse events were assessed by the Common Terminology Criteria For Adverse Events (CTCAE) version 5.0. Survival analyses for PFS and OS were performed by Kaplan-Meier method. Univariate analysis was performed by the Log-rank test, and multivariate analysis was conducted with the Cox proportional hazards regression model to adjust for potential confounding variables.

Results All of 43 patients, 19 patients (44.2%) received HAIC and 24 patients (55.8%) received HAIC+TACE. The median follow-up time for all patients was 13.0 months. The median progression-free survival (mPFS) following the first HAIC±TACE treatment for all patients was 4.0 months (95%CI: 3.339-4.661). The median overall survival (mOS) following the first HAIC±TACE treatment for all patients was 13.0 months (95%CI: 10.436-15.564). The objective response rate and disease control rate for all patients were 27.9% and 65.1%, respectively. For the patients who received HAIC±TACE after disease progression following first-line systemic therapy, mPFS was 5.0 months (95%CI: 4.035-5.965), and mOS was 16.0 months (95%CI: 12.023-19.977). For the patients who received HAIC±TACE after disease progression following second-line and above systemic therapies, mPFS was 3.0 months (95 % CI: 0.987-5.013), and mOS was 12.0 months (95 % CI: 9.137 -14.863). Patients who received HAIC±TACE after disease progression following first-line systemic therapy demonstrated significantly longer mPFS (5months vs. 3months, $P=0.002$) and mOS (16months vs. 12months, $P=0.044$) compared to those with ≥ 2 prior lines of systemic therapy. The number of prior systemic therapy lines was identified as an independent prognostic factor for both PFS and OS following HAIC±TACE therapy. ORR in HAIC+TACE group was significantly higher than that in HAIC group in different interventional method (41.7% vs. 10.5%, $P=0.024$). DCR in the platinum-containing three-drug group was significantly higher than that in the platinum-containing single-drug/double-drug group

(82.6% vs. 45.0%, $P=0.010$) in different HAIC treatment regimen. When stratified by the number of prior systemic therapy lines, the group which interventional treatment as a second-line treatment exhibited a significantly higher DCR compared to the group which interventional treatment as a third-line and above treatment (82.4% vs. 50.0%, $P = 0.040$). The most common adverse events in patients receiving HAIC \pm TACE were nausea/vomiting, abdominal pain, fever, liver dysfunction, and hematologic toxicity. Grade 3-4 adverse events included hematologic toxicity in 3 cases (3/43, 7.0%) and liver dysfunction in 7 cases (7/43, 16.3%). No new adverse events were observed in the safety analysis.

Conclusion HAIC \pm TACE is safe and effective in the treatment of liver metastasis of esophageal carcinoma, but more studies are needed to further confirm it.

OR-029

Direct percutaneous embolization of hypervascular renal cell cancer metastasis to the spine.

Calvin Cheong, Amos Tan, Rahul Lohan, Anil Gopinathan
National University Hospital, Singapore

Purpose Renal cell carcinoma (RCC) osseous spinal metastasis are usually hypervascular and destructive. This often leads to unstable spinal pathological fractures which are difficult to resect or fix because of their tendency to bleed. Preoperative embolization of these tumours will help reduce intra-operative blood loss, however, there is often difficulty in angioembolization especially in the acute and urgent setting where relatively fast pre-operative embolization of the tumour is required.

Materials and methods We present a case of a patient with a history of RCC and hypervascular metastasis to the spine, presenting to the hospital with acute neurological deficits requiring emergency decompression. Percutaneous direct embolization of the tumour was performed due to difficulty in angioembolization. We will present our techniques, considerations and eventual outcomes of this procedure, eventually achieving minimal intra-operative blood loss.

Results MRI revealed a metastatic osseous lesion at L1.

Right common femoral artery access was obtained in this patient, a 5Fr long sheath was inserted with subsequent interrogation of the T11, T12, L1 and L2 segmental arteries. Tumoral blush seen along the left T12 segmental arteries, however, no dominant/ hypertrophic tumoral feeders seen. Segmental arteries are also severely atherosclerosed with multiple areas of stenoses. Aorta was ectatic making it difficult to cannulate the segmental arteries, as a result, selective embolization was not possible.

Under US guidance, three 22 G spinal needles were placed into different aspect of the L1 metastatic lesion. Needle location confirmed with cone beam CT and contrast injection.

The tumor was embolised with injection of 4.5ml of Glubran (Cyanoacrylate base glue) with Lipiodol (1ml in 4ml) under fluoroscopy.

Patient underwent decompressive surgery the next day with minimal intra-operative blood loss.

Conclusion - Direct embolization can be used as an alternative when identification or cannulation of feeding arteries to the hypervascular tumour is difficult.

- Suitability of direct embolisation depends on tumour factors and (i.e location, type and vascular connections to important arteries) and patient factors (curative, palliative or pre-operative treatment).
- Limited experience and evidence on its efficacy and risks which requires further evaluation.
- Control of embolic material deployment should be assessed under fluoroscopic guidance.
- Patient should proceed for surgery the next day or within 72 hours of embolization.

OR-033

CT-guided Percutaneous Cryoablation in Patients with Lung Nodules Mainly Composed of Ground-Glass Opacities

Lizhi Niu, Shupeng Liu
Guangzhou Fuda Cancer Hospital

Purpose To assess the safety and efficacy of cryoablation in patients with lung nodules mainly composed of ground-glass opacities (GGOs).

Materials and methods In this retrospective study, 50 patients (mean age, 65.0 ± 12.3 ; 28 women) diagnosed with lung GGO nodules who underwent cryoablation were included (from June 2016-June 2021). The local recurrence rate, the incidence of regional metastases to lymph nodes, the incidence of distant metastases, adverse events, and the lung function condition were analyzed.

Results Follow-up computed tomography (CT) was performed an average of 33 months (range, 3-60 months) after the cryoablation procedure. Outcomes were only evaluated in 30 patients. A total of 20 patients were excluded: 10 patients had no cancer detected at histopathological analysis and were diagnosed with CT scan or positron emission tomography-CT (PET/CT), and the other 10 patients had nodules with a diameter of less than 10 mm and a consolidation-to-tumor ratio (CTR) of more than 0.25, and thus histopathological analysis was not performed due to small nodule size and patients were diagnosed with CT or PET/CT. The local recurrence rate was 0% (0 of 30). Evidence of regional metastases of the lymph nodes was not found in any patients (0%; 0 of 30), and the incidence of distant metastases was 0% (0 of 30). No major complications were noted. Lung function recovered to normal within one month after cryoablation in all patients.

Conclusion Cryoablation may serve as a safe and feasible option for the treatment of lung nodules mainly composed of GGOs.

OR-034

Long-term outcomes of image-guided ablation and laparoscopic partial nephrectomy for T1 renal cell carcinoma

Vinson Chan, Filzah Hanis Osman, Jon Cartledge, Walter Gregory, Michael Kimuli, Naveen Vasudev, Christy Ralph, Satinder Jagdev, Selina Bhattarai, Jonathan Smith, James Lenton, Tze Min Wah
University of Leeds

Purpose Image-guided ablation (IGA) is an alternative to surgical management for small renal masses. This study aims to compare long-term outcomes and peri-operative outcomes of image-guided ablation (IGA) and laparoscopic partial nephrectomy (LPN).

Materials and methods This is a retrospective cohort study of localised RCC (T1a/bN0M0) patients undergoing cryoablation (CRYO), radio-frequency ablation (RFA), or LPN at our institution from 2003 to 2016. Oncological outcomes were compared using Cox regression and log-rank analysis. eGFR changes were compared using Kruskal-Wallis and Wilcoxon-rank tests.

Results A total of 296 (238 T1a, 58 T1b) consecutive patients were identified; 103, 100, and 93 patients underwent CRYO, RFA, and LPN, respectively. Median follow-up time was 75, 98, and 71 months, respectively. On univariate analysis, all oncological outcomes were comparable amongst CRYO, RFA, and LPN ($p > 0.05$). On multivariate analysis, T1a patients undergoing RFA had improved local recurrence-free survival (LRFS) (HR 0.002, 95% CI 0.00–0.11, $p = 0.003$) and metastasis-free survival (HR 0.002, 95% CI 0.00–0.52, $p = 0.029$) compared to LPN. In T1a and T1b patients combined, both CRYO (HR 0.07, 95% CI 0.01–0.73, $p = 0.026$) and RFA (HR 0.04, 95% CI 0.03–0.48, $p = 0.011$) had improved LRFS rates. Patients undergoing CRYO and RFA had a significantly smaller median decrease in eGFR post-operatively compared to LPN (T1a: $p < 0.001$; T1b: $p = 0.047$). Limitations include retrospective design and limited statistical power.

Conclusion IGA is potentially as good as LPN in oncological durability. IGA preserves kidney function significantly better than LPN. More studies with larger sample size should be performed to establish IGA as a first-line treatment alongside LPN.

OR-035

Global Interest of interventional radiology and interventional oncology: A review of a decade using the google trends platform

Vinson Chan¹, Helen Hoi-Lam Ng¹, Merlin Kallookkaran¹, Khalil Abdulrauf², Noemi Cinti³, Raghu Lakshminarayan¹, Tze Min Wah¹

1. University of Leeds

2. Pennine care NHS Foundation Trust

3. Hull York Medical School

Purpose Interventional radiology (IR) and interventional oncology (IO) are relatively new specialties that are underrepresented. This study aims to evaluate the global interest in IR utilising online search behaviours on a dominant major search engine.

Materials and methods Google Trends is a tool created by Google to measure the search interest of a particular topic over time. Search terms such as "Interventional Radiology", "Interventional Oncology", and others were investigated on Google Trends from May 2014 to May 2024.

Results Interest in IR worldwide peaked in March 2022, June 2022, and February 2023 on 3 separate occasions and has gradually increased by 30% from 2014 to 2024. Worldwide interest in IO has increased by over 20% in the past decade, with interest peaking in July 2022. Compared to their counterparts of the four pillars of oncology, IO is the least popular, being 36.5, 20, and 12 times less popular on average compared to medical oncology, clinical oncology, and surgical oncology, respectively.

Conclusion Worldwide interest in IR has significantly increased over the past decade but remains significantly less popular compared to surgical specialties. IO is the least popular in terms of public knowledge amongst the four pillars of oncology. Further advocacy by interventional radiologists is needed to increase public awareness.

OR-036

The Diversity of Arterial Approaches in Delivering Intra-arterial Chemotherapy for Retinoblastoma: Experiences from Indonesia

Jason Jason¹, Jacob Pandelaki¹, Sahat Matondang¹, Krishna Pandu Wicaksono¹, Heltara Ramandika¹, Julie Dewi Barliana², Dian Estu Yulia², Rita Sitorus², Ludi Dhyani Rahmartani³, Hikari Ambara Sjakti³

1. Department of Radiology, Faculty of Medicine, Universitas Indonesia - Dr. Cipto Mangunkusumo National General Hospital, Jakarta, Indonesia

2. Department of Ophthalmology, Faculty of Medicine, Universitas Indonesia – Cipto Mangunkusumo National General Hospital, Jakarta, Indonesia

3. Department of Pediatric, Faculty of Medicine, Universitas Indonesia – Cipto Mangunkusumo National General Hospital, Jakarta, Indonesia

Purpose Introduction: Currently, intraarterial Chemotherapy (IAC) is one of the main treatments for retinoblastoma and is considered the most promising rescue treatment method for global salvage. However, because of the common conditions of an inaccessible main arterial route for IAC, it is important to identify alternative routes for IAC delivery. In this study, we presented in-depth techniques and descriptive analyses of alternative IAC routes for retinoblastoma.

Purpose: To review the efficacy and safety of IAC for retinoblastoma administered through alternative routes at our institution in Indonesia, documenting the challenges and outcomes.

Materials and methods A total of 20 patients with retinoblastoma were treated with Intraarterial Chemotherapy (IAC) at Dr. Cipto Mangunkusumo National General Hospital, Jakarta, Indonesia from June 2022 to November 2024. The available regimens comprise melphalan, topotecan, and carboplatin, which are delivered as monotherapy, dual therapy, or triple therapy. The data included consist of demographic characteristics, age at diagnosis, duration of therapy, total IAC session, ICRB group at diagnosis, IAC route, globe salvation rate, and adverse events.

Results Among the 45 IAC sessions received by the 20 patients, 76.1% (n=35) of the IACs were delivered through the ophthalmic artery as the main route, whereas 23.9% (n=11) of the IACs were delivered through the anastomoses from the meningeal media artery, sphenopalatine artery, and zygomatico-orbital artery. Globe salvation was achieved in 90% patients (n=18), while 10% patients (n=2) were enucleated. Adverse events were absent in 52.6% of the sessions (n=30), with pain at the puncture site being the most common adverse event (19.3%; n=11).

Conclusion Our study successfully showed a satisfactory 90% globe salvage rate, delivered through various routes from the internal and external carotid artery branches. When delivering IAC for retinoblastoma, understanding the different arterial routes is mandatory.

OR-037

Trans-arterial embolisation prior to image-guided ablation for T1b/T2a renal masses – A systematic review and meta-analysis

Aisha Ahmed, Hira Zaman, Vinson Wai-Shun Chan, Jim Zhong, Tze Min Wah
University of Leeds

Purpose Image guided ablation (IGA) is an efficacious and safe treatment for small renal cell carcinomas. However, in larger tumours, trans-arterial embolization prior to IGA has been postulated as an adjunctive method to increase the success rates. This systematic review aims to evaluate the evidence for TAE and IGA's safety and efficacy in the literature.

Materials and methods A literature search was performed on 19th October 2023 on Embase, Medline and Cochrane CENTRAL for primary studies evaluating embolisation prior to ablation of T1b/T2a renal masses. Paediatric patients and those with inherited RCCs were excluded. Primary outcome is recurrence free survival. Secondary outcomes include other oncological outcomes, post-operative complications, and renal function.

Results A comprehensive literature search yielded a total of 547 records. Among these, 19 studies, involving 224 patients, were selected for the analysis. Notably, only one study specifically compared TAE and IGA to IGA alone. The sample sizes of the included studies were relatively small, ranging from 2 to 31 patients. Furthermore, only two studies had follow-up periods exceeding two years. At the 3- to 6-year follow-up period, meta-analysis revealed a remarkable 100% cancer-specific survival rate (95% confidence interval: 0.96–1.00). Remarkably, no cancer-specific deaths were reported during this period. Additionally, a pooled recurrence rate of 3% (95% confidence interval: 0.00–0.08) was observed during the follow-up period. Furthermore, the pooled intra-operative complication rate was 3% (95% confidence interval: 0.01–0.05, $I^2 = 0.01\%$). Post-operative complications were reported in 18% (95% confidence interval: 0.08–0.29, $I^2 = 84.59\%$) of the included cases.

Conclusion Embolisation prior to IGA for larger renal tumours appears to be a safe and effective treatment option. However, literature is limited by small sample size and limited follow-up. Further prospective comparative investigation is encouraged.

OR-038

Multicentre Real World outcomes of Irreversible Electroporation for complex small kidney cancers (REWIREd)

Tze Min Wah¹, Vinson Wai-Shun Chan², Helen Hoi-Lam Ng², Ashwin Mahendra³, Govindarajan Narayanan⁴, Jose Maria Abadal⁵

1. Leeds Teaching Hospitals NHS Trust

2. University of Leeds

3. Florida Atlantic University Charles E. Schmidt College of Medicine

4. Herbert Wertheim College of Medicine, Florida International University

5. Hospital Universitario Severo Ochoa

Purpose Irreversible electroporation (IRE) is a novel, non-thermal energy that allows for the precise and complete ablation of complex tumours close to critical structures. This international study on IRE for renal cancer aims to evaluate the efficacy and safety of IRE in RCC treatment.

Materials and methods This is a retrospective multicentre analysis of a prospectively maintained database of all patients from specialist centres in the USA, UK, and Spain who underwent image-guided IRE for renal masses. Cases deemed unsuitable for surgery, or traditional ablation techniques due to proximity to vital structures after local tumour board review were included. All patients received a contrast or non-contrast CT post-operatively. All patients are followed up as per local standard of care using CT or MRI at the discretion of the treating clinician and local protocols. Statistical analyses were performed using STATA/MP 18.0 (STATA Corp). Operative outcomes were reported proportionately and survival outcomes were measured from the time of treatment to time of event and reported by percentages at 1, 3, and 5-years accordingly with respective 95% CIs, alongside Kaplan-Meier Graphs.

Results From May 2015 to September 2023, 58 patients with a mean age of 65.8 years (SD 12.8) were included. The mean tumour size was 3.01cm (SD 1.15), with an average RENAL Nephrometry score of 7.64 (SD 2.13). Primary technical success was achieved in 42 patients (72.4%), with an overall technical success rate of 94.8% (55/58). 2 (3.5%) major complications were observed. No significant change in eGFR was observed pre- to postoperatively ($p=0.08$). Five patients (9.1%) had a >25% reduction in eGFR. The mean follow-up was 52 months (SD 30.2). Local recurrence-free survival was 82.4% (95% CI 67.6-90.9%) at 5 years. The trifecta outcome (defined by <25% decline in eGFR, no major complications, and primary technical success) was achieved in 36 patients (64.3%).

Conclusion IRE is safe and effective in managing complex tumours near vital structures that are less suitable for surgery or other ablative modalities. Studies comparing the efficacy of IRE to other modalities are warranted.

OR-039

The prognostic value of Neutrophil-to-lymphocyte ratio and platelet-to-lymphocyte ratio for liver tumours after image-guided irreversible electroporation

Vinson Wai-Shun Chan, Elias Williams, Krish Gupta, Jim Zhong, Tze Min Wah, Vinson Chan
University of Leeds

Purpose Irreversible electroporation (IRE) had been shown to induce immunomodulation of the tumour microenvironment, leading to a more hostile tumour microenvironment. The neutrophil-to-lymphocyte ratio (NLR) and platelet-to-lymphocyte ratio (PLR) are proposed as cheap and simple biomarkers which may act as a surrogate for successful immunomodulation to predict treatment response in patients undergoing image-guided ablation. This study aims to evaluate the prognostic value of NLR and PLR in liver tumours.

Materials and methods This retrospective analysis examines a prospectively maintained database of all patients undergoing IRE at Leeds Teaching Hospital Trust (LTHT). Pre-operative and post-operative haematology tests are standard of care at LTHT. All laboratory results were collected, and an optimal cut-off value was determined for each outcome and variable using the Cut-off Finder, a validated web application specifically designed for this purpose. The cut-off was derived from a log-rank test and a Cox regression analysis, where the cut-off is defined as the point with the most significant log-rank test split. Subsequently, a univariable Cox regression model was employed to explore the association between the cut-off values of various variables and the outcome.

Results A total of 40 patients with 42 tumours underwent 44 IRE sessions. The patient population consisted of 65% males and 35% females. The mean age (IQR) at the time of treatment was 68.9 (8.5) years.

Of the 40 patients, 85% (34/40) were diagnosed with hepatocellular carcinoma (HCC), 7.5% (3/40) with colorectal liver metastases, 5% (2/40) with cholangiocarcinoma, and 2.5% (1/40) with liver metastases from renal cell carcinoma.

Both peri-operative changes in NLR of > -1.408 and changes in PLR of > 5.27 are associated with significantly worsened local progression-free survival (HR 2.85, 95% CI 1.05-7.76, $p=0.033$; HR 5.03, 1.98-12.77, $p<0.001$). In distant progression free survival, only post-treatment platelet levels of $>145 \times 10^9/L$ are associated with worsened outcomes (HR 9.77, 95% CI 1.01-94.76, $p=0.016$). Peri-operative change of NLR > -1.052 is associated with improved cancer-specific survival (HR 0.32; 95% CI 0.11-0.95; $p=0.032$), however, a peri-operative change of PLR > 36.7 is associated with a worsened cancer-specific survival (HR 3.68; 95% CI 1.15-11.74; $p=0.019$). In overall survival, a peri-operative change in NLR of > -0.2041 is associated with improved overall survival (HR 0.21; 95% CI 0.06-0.7, $p=0.005$). However, both pre- and post-treatment PLR of >97.73 and >89.82 are associated with worsened overall survival (HR 2.15, 95% CI 1.01-4.57, $p=0.042$; HR 4.53, 95% CI 1.35-15.17, $p=0.007$).

Conclusion IRE may stimulate immunomodulation of the tumour microenvironment. NLR and PLR is a possible surrogate for immunomodulation and hence prediction of treatment outcomes.

OR-040

Integrated machine learning identifies SPP1hi macrophages marker genes for predicting therapeutic response of TACE in HCC

Zilin Wang¹, Liu Meiling², Minjiang Chen², Yang Yang², Ji Jiansong²

1. Zhejiang University School of Medicine/ Zhejiang University Lishui Hospital

2. Zhejiang University Lishui Hospital

Purpose Transcatheter arterial chemoembolization (TACE) is a crucial treatment modality for hepatocellular carcinoma (HCC), which remains a leading cause of cancer-related mortality worldwide. As a minimally invasive locoregional therapy, TACE aims to induce tumor ischemia and enhance cytotoxic effects by selectively delivering chemotherapeutic agents while simultaneously blocking the tumor's arterial blood supply. Despite its widespread use and demonstrated efficacy in improving survival, the clinical outcomes of TACE vary significantly among patients. This variability is largely attributed to the molecular and cellular heterogeneity within the tumor microenvironment (TME) of HCC, which plays a pivotal role in shaping therapeutic responses. Among the diverse cellular components of the TME, macrophages are particularly influential, as they exhibit plasticity in response to environmental cues, potentially contributing to either anti-tumor immunity or tumor progression. The differential polarization of macrophage subsets—ranging from pro-inflammatory, anti-tumorigenic M1-like macrophages to immunosuppressive, tumor-promoting M2-like macrophages—can significantly impact the efficacy of TACE by modulating inflammation, angiogenesis, and immune surveillance. Understanding these complex interactions within the TME is critical for refining TACE strategies, exploiting combination therapies to enhance treatment efficacy and developing multiple machine learning models for predicting response of TACE accurately.

Materials and methods Leveraging single-cell sequencing data from PRJNA793914, which provides a high-resolution transcriptomic landscape of HCC after TACE, offers a unique opportunity to investigate the role of macrophages in shaping therapeutic responses. After preprocessing alignment, Quantification quality control, normalization, dimensionality reduction, clustering, cell type annotation. We select macrophages subsets for further analysis. reclustering, reannotation pseudo-time analysis and interaction between different type of cells were clarified. By using marker genes of SPP1 macrophages, we developed 101 type of machine learning methods for predicting response of TACE with GSE104580 database. Finally, we identified the function of SPP1hi macrophages through coculture between SPP1hi macrophages and CD8⁺ T cells.

Results We observed significant alterations in immune cell populations following TACE in HCC. Notably, the proportions of CD8⁺ T cells and NK cells were markedly reduced, whereas macrophage levels were significantly elevated post-TACE. To further investigate changes in cellular abundance and transcriptional dynamics, we employed MiloR and Augur algorithms, which revealed distinct differences in NK cells, CD4⁺ T cells, CD8⁺ T cells, macrophages, and dendritic cells between primary tumors and post-TACE samples, indicating a robust immunological response to treatment.

We observed significant alterations in immune cell populations following TACE in HCC. Notably, the proportions of CD8⁺ T cells and NK cells were markedly reduced, whereas macrophage levels were significantly elevated post-TACE. To further investigate changes in cellular abundance and transcriptional dynamics, we employed MiloR and Augur algorithms, which revealed distinct differences in NK cells, CD4⁺ T cells, CD8⁺ T cells, macrophages, and dendritic

cells between primary tumors and post-TACE samples, indicating a robust immunological response to treatment.

Specifically, the abundance of macrophages and dendritic cells increased, while that of NK cells, CD8⁺ T cells, and CD4⁺ T cells decreased following TACE. Functional enrichment analysis of macrophages highlighted a significant upregulation of inflammatory pathways, including inflammatory response, TNF α signaling via NF κ B, and interferon- γ response, suggesting that macrophage-driven inflammation plays a crucial role in shaping the post-TACE immune microenvironment. The increased macrophage infiltration may contribute to an immunosuppressive tumor microenvironment (TME) after TACE, potentially impacting treatment efficacy and disease progression.

By reclustering macrophages, we identify 10 subcelltypes, including Macrophages_CXCL10, Macrophages_Cycling, Macrophages_HSPA1A, Macrophages_IL32, Macrophages_LGALS2, Macrophages_LGALS3, Macrophages_MT1G, Macrophages_RNASE1, Macrophages_SLC40A1, Macrophages_SPP1. Among these subsets, Macrophages_SPP1 particularly increased after TACE treatment. What's more, pseudotime analysis revealed that Macrophages_SPP1 subcelltype increased through cell development. And by development, Macrophages developed immunosuppressive tumor microenvironment and promotion of angiogenesis function.

Given the central role of macrophages in the post-TACE immune landscape, we conducted a comprehensive analysis to identify macrophage marker genes (MMGs). To further explore their prognostic significance, we performed integrative modeling using 101 machine learning models across 10 different algorithms on the GSE104580 cohort. Through this extensive computational approach, we developed and validated an optimal prognostic signature, termed the SPP1hi Macrophage Marker Gene Prognostic Signature (SMMGPS), which serves as a potential biomarker for predicting patient outcomes post-TACE. This work provides valuable insights into the immunological remodeling induced by TACE and underscores the importance of macrophage-related pathways in shaping therapeutic responses in HCC.

Conclusion SPP1hi Macrophages plays a significant role in immunosuppressive tumor microenvironment and promotion of angiogenesis. SPP1hi macrophages mediate the immune response of CD8⁺ T cells through SPP1-CD44 pairs and furtherly could suppress cytotoxicity ability of CD8⁺ T cells. Our findings underscore the SMMGPS as a potent tool for enhancing the response of HCC patients to TACE, providing a robust conceptual framework for a deeper exploration of the complexities associated with response of TACE among hepatocellular carcinoma patients. Simultaneously, our study holds the potential to identify a novel macrophages subset after TACE and develop a novel approach for precision therapy in HCC.

OR-041

CT-Guided Microwave Ablation with Vertebral Augmentation for Spinal Metastases with Posterior Wall Defects

Kaixian Zhang,Xusheng Zhang
Tengzhou Central People's Hospital

Purpose To evaluate the efficacy and safety of combined microwave ablation (MWA) and vertebral augmentation (VA) in the treatment of spinal metastases with posterior wall defects.

Materials and methods A retrospective review was conducted for 67 patients (42 men, 25 women) with painful spine metastases with posterior wall defects who underwent MWA combined with VA. Among these patients, 52 vertebrae had no epidural invasion and 33 had mild invasion but did not compress the spinal cord. Procedural effectiveness was determined by comparing visual analog scale (VAS) scores and Oswestry disability index (ODI) scores before the procedure and during the follow-up period.

Results The procedure was technically successful in all patients. The mean VAS score declined significantly from 6.85 ± 1.81 before the procedure to 3.27 ± 1.97 at 24 h, 1.96 ± 1.56 at 1 week, 1.84 ± 1.50 at 4 weeks, 1.73 ± 1.45 at 12 weeks, and 1.71 ± 1.52 at 24 weeks post-procedure ($p < 0.01$). The mean ODI score was lower post-procedure than before the procedure ($p < 0.001$). Transient nerve injury occurred in two patients (SIR classification D), and the incidence of asymptomatic bone cement (SIR classification A) was 43.5% (37/85).

Conclusion MWA combined with VA is an effective and safe treatment for painful spine metastases with posterior wall defects.

OR-042

CT-guided Celiac Plexus Neurolysis in the Management of Visceral Intractable Pain in Patients with Advanced Cancer

Tai Tan Nguyen
Nhan Dan Gia Dinh Hospital

Purpose Celiac plexus neurolysis (CPN) is a well-established palliative intervention for managing severe, intractable visceral pain in patients with advanced abdominal malignancies, particularly pancreatic, gastric, and hepatobiliary cancers. It offers a targeted, minimally invasive approach to manage this pain by disrupting the celiac plexus, a central hub for visceral nociceptive transmission. This study aims to evaluate the efficacy, safety, and clinical outcomes of computed tomography (CT)-guided CPN in alleviating pain severity and opioid dependence, thereby improving the quality of life in patients with advanced cancer.

Materials and methods A retrospective analysis was conducted on patients with advanced abdominal cancer who underwent CT-guided CPN for intractable visceral pain. Patient selection was based on refractory pain despite optimal medical management. The procedure was performed using either a posterior or an anterior percutaneous approach under CT guidance for precise needle placement and neurolytic agent distribution. Pain intensity was assessed using the Visual Analogue Scale (VAS) score before the procedure and at multiple follow-up intervals (24 hours, 1 week, 1 month, and 3 months post-procedure). Additional parameters included changes in opioid consumption, procedural complications, and overall patient satisfaction.

Results Clinical evidence demonstrates that CT-guided CPN achieves substantial pain relief in 75-90% of patients, with effects lasting from weeks to months. The procedure enhances quality of life and reduces opioid reliance. Complications, including transient hypotension or diarrhea, occur in less than 10% of cases, affirming its favorable safety profile.

Conclusion CT-guided CPN is a highly effective and safe procedure for alleviating intractable visceral pain in patients with advanced abdominal malignancies. The precise imaging guidance provided by CT enhances procedural accuracy, optimizing pain relief while minimizing complications. This technique significantly reduces pain scores, reduces opioid reliance, and improves quality of life, making it a valuable palliative intervention for patients with advanced cancer. Further prospective studies are warranted to refine patient selection criteria and optimize long-term outcomes.

OR-043

Irradiation modulates sEVs-PD-L1 transport in TNBC's tumor immune microenvironment

Yubin Wei¹, Wei Zhao²

1. Guangxi Medical University

2. Wuming Hospital of Guangxi Medical University

Purpose To elucidate the mechanisms underlying irradiation's remodeling of the tumor immune microenvironment (TIME) in triple-negative breast cancer (TNBC) by regulating the transport of PD-L1 in small extracellular vesicles (sEVs) derived from tumor cells (sEVs-PD-L1), ultimately enhancing the efficacy of TNBC immunotherapy and providing a scientific rationale for clinical interventions.

Materials and methods Bioinformatics analysis identified PD-L1 expression in breast cancer, which was further validated using RT-qPCR and western blot. MDA-MB-231 cells were treated with chloroquine, rapamycin, and MG132 to ascertain the primary degradation pathway of PD-L1. Irradiation's effects on PD-L1 expression, cellular localization, and sEVs were examined using cellular immunofluorescence, transmission electron microscopy (TEM), and nanoparticle tracking analysis (NTA). Western blot assessed sEVs-PD-L1 expression before and after irradiation. Bioinformatics analysis correlated ATG7 with the STAT3 signaling pathway. Lentivirus-mediated ATG7 knockdown, combined with western blot, evaluated the impacts of irradiation, autophagy, and sEVs activity on PD-L1 and STAT3 expression. A co-culture system assessed sEVs' influence on T-cell activity post-irradiation and the efficacy of Sintilimab combined with irradiation on MDA-MB-231 cells.

Results TNBC cell lines and tissues exhibited high PD-L1 expression, primarily regulated by the autophagy-lysosome pathway. Irradiation upregulated PD-L1 expression and facilitated its cytoplasmic translocation. While irradiation enhanced sEVs production, it downregulated sEVs-PD-L1 expression. This may involve sEVs-PD-L1 transport and STAT3 activation. Post-irradiation, sEVs exhibited anti-tumor immune effects. Combined irradiation and Sintilimab significantly inhibited tumor cell activity and activated T-cell cytotoxicity.

Conclusion Irradiation promotes the endocytosis of sEVs-PD-L1 in TNBC's TME, leading to their degradation via the autophagy-lysosome pathway and reducing sEVs-PD-L1 expression. This ameliorates TNBC's immunosuppressive microenvironment, enhancing immunotherapy efficacy.

OR-044

Early Response Evaluation of Hepatocellular Carcinoma After Transarterial Chemoembolization Using Triphasic Computed Tomography

Nasr ullah Yaqoob

INDUS HOSPITAL KARACHI PAKISTAN

Purpose The aim of this study was to evaluate early response of hepatocellular carcinoma (HCC) to transarterial chemoembolization (TACE) with triphasic computed tomography (CT).

Materials and methods We retrospectively reviewed 102 patients who underwent TACE treating unresectable HCC, who had pre- and post-procedure CT imaging. Response to TACE was assessed 6 weeks post-TACE by modified RECIST criteria: CR, PR, SD, or PD. The diagnostic in vivo accuracy of triphasic CT, as well as inter rater agreement between radiologists and the diagnostic accuracy of triphasic CT in identifying viable tumor tissue was analyzed. This study was performed from January 2023 to December 2023 in Indus Hospital & health network.

Results CR was observed in 36% and PR in 32% patients, giving an overall response rate (CR + PR) of 68%. In 20% of patients we noted SD; in 12% we noted PD; and all patients had tangle degree 1% (0.5–12.5 tangles innervated); There was substantial inter rater agreement of response assessment ($\kappa = 0.82$, $p < 0.001$) of triphasic CT indicating reproducibility of this measurement. Triphasic CT showed diagnostic accuracy of 88% for biologically viable tumor detection with a sensitivity of 85% and a specificity of 90%. A subgroup analysis indicated higher response rates in patients with better liver function (Child-Pugh A; 76%) than in those with poorer liver function (Child Pugh B; 50%), no statistically significant difference ($p = 0.09$).

Conclusion Triphasic CT is an effective, reproducible imaging modality to assess early tumor response to TACE in HCC, with high diagnostic accuracy and substantial inter-rater agreement. It supports its use in early treatment evaluation for potential use in aiding clinical decisions and redirection of subsequent patient management. Additional imaging biomarkers need to be evaluated to refine response assessment and a further research should probe the effects of liver function on treatment outcomes.

OR-045

Retrospective analysis of diagnostic accuracy of image-guided needle biopsy of pancreatic lesions.

Antariksh Vijan, Suyash Kulkarni, Nitin Shetty, Kunal Gala, Kajari Bhattacharya, Akshay Rafaliya
Tata Memorial Hospital, Mumbai, India

Purpose The aim of the study is to determine the diagnostic accuracy of image-guided pancreatic biopsy and various factors affecting the yield of pancreatic biopsy. To evaluate the diagnostic yield of biopsy and safety of the procedure.

Materials and methods Patients who underwent image-guided pancreatic biopsy from 2015-2021, with the availability of post-biopsy histopathological reports were analysed in this study. The total number of patients with post-biopsy HPR reports suggestive of malignancy, benign and infective were calculated and the total numbers of patients whose results came as an insufficient, non-diagnostic, inflammatory, haemorrhagic and non-representative were calculated. PPV, NPV, sensitivity and specificity were evaluated for the same. Standard used in this study was post operative surgical HPR if patient was operated. In case patient was not operated, follow up imaging to see the response or clinical response of patient after one year of follow up was considered.

Results A total of 181 biopsies were studied. Of these, 166 showed diagnostic post biopsy histopathological reports, while 15 were non-diagnostic. These cases were further evaluated with either repeat biopsy, or post-surgical HPR (if operated), or follow up imaging/ clinical response after one year if the patient is not operated. In this retrospective study, we have found high diagnostic accuracy of 91.7%, diagnostic yield 82.87%, sensitivity 90.91 %, specificity 100%, PPV 100% and NPV 51.6 %.

Conclusion Image-guided pancreatic biopsy has a low rate of major complications and it is a useful method for obtaining samples of tissue for pathological evaluations of pancreatic conditions.

OR-046

Percutaneous thermal ablation of multiple ground-glass nodules (GGNs) : a retrospective analysis of 36 patients

Xin Zhang,YUEYONG XIAO

the first medical center of Chinese PLA General Hospital

Purpose Multiple ground glass nodule (GGN) is a special type of simultaneous multiple primary lung cancer. Thermal ablation is one of the preferred treatment methods for multiple GGN-like lung cancer or an important supplement to surgical resection. This paper aims to explore the thermal ablation strategy for multiple ground glass nodule.

Materials and methods A retrospective analysis was conducted on 96 patients with multiple ground-glass nodules who received radiofrequency ablation treatment in our hospital from July 2017 to July 2019. The analysis was summarized from aspects such as preoperative diagnosis, ablation methods, pathological data and prognosis. The basic principles of ablation: individualized treatment plans were formulated in the preoperative stage using the MDT model; the main lesions were confirmed based on the size of the nodules, solid components, imaging morphology (including lobulation, spiculation, pleural indentation, vacuole sign, bronchial air sign, vascular convergence sign or vascular distortion and dilation within the lesion, and cystic type, etc. malignant signs), and changes in the lesions during the follow-up period; the ablation plan prioritized the main lesions while taking into account the secondary lesions; lesions located in the same pulmonary segment or lobe could be ablated simultaneously; for main lesions larger than 1 cm, without communication with the bronchus, and without obvious blood vessels, combined with biopsy during ablation; for lesions close to the pleura or interlobar fissure and patients with normal coagulation and renal function, argon-helium knife cryoablation was used; for lesions rich in blood vessels, radiofrequency ablation or microwave ablation was adopted.

Results All patients underwent thin-slice CT examination before ablation, and a total of 152 ablation operations were performed on 235 ground glass lesions. There were no death cases, of which 52 lesions were pathologically confirmed to be malignant. Thermal ablations were performed at the same time for patients with multiple lesions located in the same lung lobe, and ablations were performed in stages for other patients in different lobes on both sides or the same side with a time interval of 1-2 months. The median follow-up was 32.6 months, and the 3-year progression-free survival was 98.3%.

Conclusion Multiple ground glass nodules have different locations, and the main lesions can be predicted by analyzing the image characteristics such as size, morphology and density of lesions by thin-slice CT scanning. Percutaneous thermal ablation of GGN has the characteristics of less trauma, high safety, low cost, light damage to lung tissue, and can be performed multiple times, etc. The thermal ablation of major lesions is effective, and the ablation of different lung lobe lesions can be completed in stages. The secondary lesions should be followed up dynamically, and elective thermal ablation has a good prognosis. Puncture biopsy at the same time as ablation of ground glass nodules is safe.

OR-047

Role of Sclerotherapy in patients with vascular malformations - A retrospective study

Anand Agrawal, Suyash Kulkarni, Nitin Shetty, Kunal Gala, Kajari Bhattacharya
Tata Memorial Hospital

Purpose The aim of the study is to evaluate the clinical and radiological response of vascular malformations to sclerotherapy.

Materials and methods A retrospective observational study included 100 patients of ISSVA grade 2 and 3 venous malformations which were accessible to percutaneous sclerotherapy. All patients had undergone baseline MRI and USG of the affected area and were followed up after 1 month with imaging to assess the presence of residual lesion. Clinical response was evaluated as per EORTC QLQ-C30 Score (European Organization for Research and Treatment of Cancer). The volume of the lesions was assessed in follow-up visits and compared to baseline.

Results The mean pre and post procedure lesion size of patients was 167.27 cm³ and 56.18 cm³ respectively with significant difference in lesion size as per Student t-test ($p < 0.05$). The mean pre and post procedure VAS score was 7.05 and 2.61 respectively with significant difference in VAS score as per Student t-test ($p < 0.05$). The mean pre and post procedure EORTC QLQ-C30 score was 7.01 and 3.43 respectively with significant difference in EORTC QLQ-C30 score as per Student t-test ($p < 0.05$). The mean number of sessions of sclerotherapy were 5. The mean dose of sclerosant used was 27.14 ml.

Conclusion Sclerotherapy is a well-tolerated method in the treatment of VMs. Smaller lesions have a more favourable response. Sclerotherapy is a cost-effective procedure with low complications, significant clinical improvement and a high success rate offering an effective and cheap treatment option to the majority of patients suffering from vascular malformations.

OR-048

Successful Preoperative Transcatheter Arterial Embolization Significantly Reduces Intraoperative Bleeding in Juvenile Nasopharyngeal Angiofibroma Without the Need for Embolization of Internal Carotid Artery Branches: A Case Report of Two Patients

Stephen Kurniawan¹, Jacob Pandelaki¹, Heltara Ramandika¹, Kevin Julius Tanady², Febian Sandra², Prijo Sidipratomo¹

1. Department of Radiology, Dr. Cipto Mangunkusumo Hospital-Faculty of Medicine Universitas Indonesia

2. Indonesian Society of Interventional Radiology, Jakarta, Indonesia.

Purpose Juvenile nasopharyngeal angiofibroma (JNA) is a benign yet highly vascular tumor located in the nasopharynx, predominantly affecting males aged 9 to 19. With an incidence of approximately 1 in 150,000, it accounts for roughly 0.5% of all head and neck tumors. Patients commonly present with symptoms such as nosebleeds and nasal obstruction, and in more advanced cases, facial deformity, exophthalmos, double vision, headaches, and ear problems due to aggressive local tumor extension into adjacent areas such as the nasal cavity, ethmoid and sphenoid sinuses, maxillary sinus, lateral pterygoid region, infratemporal fossa, skull base, or superior orbit. The exact cause of JNA remains unclear, with some experts suggesting a neoplastic origin influenced by hormonal and genetic factors, while others propose it stems from a vascular malformation related to the nonresorption of an arterial remnant of the first branchial arch. Surgery is the primary treatment for JNA, with radiotherapy being reserved for rare cases involving unresectable or recurrent tumors with intracranial invasion. A key challenge in surgical management is the tumor's vascularity, which can lead to severe bleeding. Preoperative transcatheter arterial embolization provides a valuable, minimally invasive approach to reduce intraoperative blood loss, shorten surgery duration, and ultimately lower both morbidity and mortality rates.

Materials and methods This study included two male patients diagnosed with juvenile nasopharyngeal angiofibroma (JNA), both of whom underwent preoperative transcatheter arterial embolization before endoscopic tumor removal.

Patient 1: A 17-year-old male presented with a one-year history of predominantly left-sided nasal obstruction and five months of recurrent nosebleeds. The patient reported no symptoms of double vision, headaches, or ear problems. A contrast-enhanced CT scan revealed a lobulated, homogeneously enhancing mass in the sphenopalatine foramen extending into the left nasal cavity, with no invasion of the pterygopalatine fossa or sinus wall destruction. These imaging findings were consistent with a Fisch grade I JNA diagnosis.

For preoperative preparation, the patient was referred to the interventional radiology department for digital subtraction angiography (DSA) and transcatheter arterial embolization. Under local anesthesia, the right common femoral artery was accessed using a 6-Fr introducer sheath. A 5-Fr vertebral angiographic catheter (Glidecath, Terumo, Tokyo, Japan) was employed for DSA of the left common carotid artery (CCA), which demonstrated a highly vascular lesion in the left nasopharyngeal area. Selective DSA of the left internal and external carotid arteries (ECA) revealed the left internal maxillary artery as the main feeder of the tumor, with minimal contribution from the artery of the pterygoid canal, a branch of the internal carotid artery (ICA).

A 2.7-Fr microcatheter (Progreat, Terumo, Tokyo, Japan) was advanced into the left internal maxillary artery, followed by embolization using 500-700 μ m polyvinyl alcohol (PVA) particles (Bearing, MeritMedica, Jordan, USA) and gelatin foam slurry. A post-embolization arteriogram showed minimal blood flow from the embolized left internal maxillary artery and slight residual tumor blush from the left artery of the pterygoid canal. Given the associated risks, embolization of the artery of the pterygoid canal was not performed. The tumor was successfully removed endoscopically the next day, with intraoperative blood loss totaling around 1100 mL, and no postoperative complications were observed.

Patient 2:

A 14-year-old male presented with bilateral nasal obstruction, frequent epistaxis occurring twice a week, and stridor for 1 year. The patient reported no dizziness, headaches, or ear-related issues. Contrast-enhanced magnetic resonance imaging (MRI) revealed a well-defined, lobulated mass exhibiting flow-void signals with homogeneous enhancement, originating from the sphenopalatine foramen and extending into the pterygopalatine fossa, nasal cavity, and nasopharyngeal cavity. These findings were consistent with a diagnosis of JNA, classified as Fisch grade II.

Similar to the first patient, the second patient underwent preoperative digital subtraction angiography (DSA) and transcatheter arterial embolization. A 6-Fr introducer sheath was placed into the right common femoral artery under local anesthesia. DSA of the left common carotid artery (CCA) revealed a highly vascular lesion in the left nasopharyngeal region. Selective DSA of the left internal and external carotid arteries (ECA) identified the left internal maxillary artery and left ascending pharyngeal artery as the primary tumor feeders, with the artery of the pterygoid canal from the internal carotid artery (ICA) acting as a secondary feeder.

The same embolization procedures were conducted on the left and right internal maxillary arteries and the left and right ascending pharyngeal arteries, using a 2.7-Fr microcatheter, along with 500-700 μ m polyvinyl alcohol (PVA) particles and gelatin foam slurry. Follow-up arteriograms showed insignificant flow from the embolized arteries and minimal tumor blush from the arteries of the pterygoid canal.

The tumor was successfully resected endoscopically the day after embolization, with an estimated intraoperative blood loss of approximately 1300 mL. No complications were reported during or after the procedure.

Both cases were managed using standard angiographic techniques under local anesthesia. Digital subtraction angiography (DSA) was utilized to delineate the vascular supply of the tumors and identify both primary and secondary feeding arteries. Embolization was performed using polyvinyl alcohol (PVA) particles and gelatin foam slurry to occlude the arterial supply, significantly reducing intraoperative blood loss. Follow-up arteriograms were obtained post-embolization to verify the procedure's success. Endoscopic tumor resection was conducted within 24 hours of the embolization.

Results Both patients underwent successful embolization, resulting in reduced intraoperative blood loss. Patient 1, a 17-year-old male with a Fisch grade I tumor, experienced an intraoperative blood loss of 1100 mL. Patient 2, a 14-year-old male with a Fisch grade II tumor, had an intraoperative blood loss of 1300 mL. These values are notably lower than the reported average of 1428 mL for patients who received embolization involving both internal and external carotid artery branches.

Conclusion Preoperative transcatheter arterial embolization proves to be an effective method for reducing intraoperative blood loss in surgeries for juvenile nasopharyngeal angiofibroma (JNA). Embolizing branches of the external carotid artery alone is sufficient to significantly decrease blood loss without the need to embolize branches of the internal carotid artery, thereby reducing

the associated risks. This approach offers a minimally invasive strategy that enhances surgical outcomes in JNA patients.

OR-049

Role of interventional radiology in pain management of abdominal cancers

Shahzad Bhatti

Mayo Hospital/King Edward Medical University, Lahore, Pakistan

Purpose The study aims to highlight the effectiveness of Interventional radiology in pain management under image guidance in abdominal cancer patients showing increased accuracy with decreased complications as compared to a routine approach.

Materials and methods The study was done in Interventional radiology department of Mayo Hospital, Lahore, using ultrasound, angiofloro suite and 168 slice CT scanner.

Study type was descriptive. Sample size of 148 patients was estimated by using 95% confidence level, 8% absolute precision with expected percentage pain control on 56 %.³ Study duration was 18 months after ethical approval. Pain was assessed on VRS (Verbal rating scale) with increasing intensity of pain range from 0 to 10.⁴

Results Out of 148 patients, 78 were female and 70 were male. 70 % patients were referred mostly from oncology department. 30% from surgery and allied departments and from different hospitals. 85% percent patients had significant pain reduction. 10% has moderate reduction in pain and 5% showed mild decrease in pain intensity. No serious complication was faced. Only 7 patients experienced orthostatic hypotension that resolved after IV fluids.

Conclusion Image guided pain management procedures are targeted and very precise since every movement of the needle is being observed visually resulting in minimal chances of soft-tissue or vascular injury. Interventional pain management can be a useful companion in palliative as well as curative treatment in cancer patients.

OR-050

Transjugular Intrahepatic Portosystemic Shunt Plus Transarterial Chemoembolization of Hepatocellular Carcinoma Patients with Portal Vein Tumour Thrombus-related Variceal Bleeding

Wei-Zhong Zhou, Zhu-Yu Feng, Wei Yang, Hai-Bin Shi, Sheng Liu
The first affiliated hospital of Nanjing medical university, China

Purpose The study aims to assess the safety and efficacy of TIPS combined with transarterial chemoembolization (TACE) for treating HCC patients who have variceal hemorrhage and PVTT.

Materials and methods This retrospective study analysed 29 patients with HCC and PVTT who experienced variceal bleeding were treated with TIPS combined with TACE from June 2018 to February 2025. The evaluated outcomes included the overall survival (OS), technical success, complications, portosystemic pressure gradient, symptom relief, the recurrence of variceal bleeding, the incidence of overt hepatic encephalopathy (HE) and the adverse events related to treatments for HCC.

Results The technical success rate of TIPS was 100 %. There are no significant procedure-related complications. Variceal hemorrhage was successfully controlled in all patients, with a recurrence rate of 24.1% in 12 months. The subsequent treatment following TIPS included TACE alone in 22 patients. Furthermore, 5 patients underwent a combined regimen of TACE and immunotherapy, while 2 patients received an integrated treatment protocol that combined TACE with targeted immunotherapy. The median OS was 11.4 (95% CI: 3.1 – 19.7) months and the cumulative survival rates at 1, 3, 6, 12, and 24 months was 93.1%, 75.9%, 51.9%, 34.9%, and 31.8%, respectively.

Conclusion TIPS combined with TACE appears to be safe and effective for patients who had HCC and PVTT complicated with variceal bleeding.

OR-051

Health economics analysis of three treatment methods for uterine fibroids

Yong Jin

The Second Affiliated Hospital of Soochow University, China

Purpose Uterine fibroids are common benign tumors that significantly impact women's health. With advancements in medical technology, Uterine Artery Embolization (UAE), Laparoscopic Myomectomy (LM), and Abdominal Myomectomy (AM) have become the main surgical options for treating uterine fibroids. This study aims to compare the health economics of these three surgical approaches in the management of uterine fibroids.

Materials and methods This study included 349 women with uterine fibroids who received UAE, LM, or AM at the Second Affiliated Hospital of Suzhou University, Lianyungang First People's Hospital, and Lianyungang Maternal and Child Health Hospital between 2019 and 2023. Data were collected from hospital cost records, telephone follow-ups, and patient quality of life questionnaires. Cost analysis and health outcome analysis were performed to conduct a health economic evaluation of the three surgical approaches.

Results The study involved 349 women treated with UAE, LM, or AM for uterine fibroids. The cost analysis revealed that the direct medical costs in the UAE group were significantly higher than in the AM group ($p < 0.001$). In terms of direct non-medical costs, productivity loss costs were significantly lower in the UAE group compared to the LM and AM groups ($p < 0.001$). Work loss, caregiving, and nutritional costs were also significantly lower in the UAE group compared to the LM and AM groups, with statistically significant differences ($p < 0.001$). The utility cost analysis indicated that Quality-Adjusted Life Years (QALYs) were significantly higher in the UAE and LM groups compared to the AM group ($p < 0.001$). The QALY indices for the UAE, LM, and AM groups were 0.20 ± 0.21 , 0.19 ± 0.22 , and 0.09 ± 0.13 , respectively. Linear regression analysis demonstrated that the UAE group had the best cost-effectiveness, followed by the LM group and the AM group. Sensitivity analysis showed that the cost of consumables had the greatest impact on the main results, while nutritional costs had the least impact.

Conclusion Considering the surgical treatment effects, economic costs, and cost-effectiveness, UAE and LM procedures exhibit better cost-effectiveness and treatment outcomes compared to the AM procedure in treating uterine fibroids. Despite the higher direct medical costs associated with UAE and LM, their lower complication rates and faster recovery suggest that they may be more cost-effective treatment options in the long term.

OR-052

Transarterial chemoembolization plus radiofrequency ablation and iodine-125 seed implantation for hepatocellular carcinoma in high-risk locations

Guilin Zhang, Yanqiao Ren, Xuefeng Kan

Wuhan Union Hospital, Tongji Medical College, Huazhong University of Science and Technology

Purpose The effect of transarterial chemoembolization (TACE) plus radiofrequency ablation (RFA) (TACE-RFA) for hepatocellular carcinoma (HCC) in high-risk locations is not satisfactory. The aim of this study was to compare the clinical outcomes of TACE-RFA plus iodine-125 (125I) seed implantation (TACE-RFA-125I) therapy with those of TACE-RFA for unresectable HCC (≤ 5 cm) in high-risk locations.

Materials and methods From January 2010 to June 2023, the clinical data of 126 patients with unresectable HCC (≤ 5 cm) in high-risk locations who received TACE-RFA-125I or TACE-RFA treatment were retrospectively analyzed. The clinical outcomes between the two groups were compared after propensity score matching (PSM) analysis.

Results Forty-six pairs of patients were matched. The local progression-free survival rates at 1-, 2-, 3-, 4-, and 5-years were 100%, 82.4%, 74.8%, 63.5%, and 54% in the TACE-RFA-125I group, which were significantly higher than 91.3%, 69.4%, 50.7%, 29.4%, and 26.7% in the TACE-RFA group, respectively ($p = 0.004$). The median progression-free survival in the TACE-RFA-125I group was significantly longer than that in the TACE-RFA group ($p = 0.002$). The overall survival rates at 1-, 2-, 3-, 4-, and 5-years were 100%, 93.4%, 80.7%, 74.9%, and 64.7% in the TACE-RFA-125I group, which were significantly higher than 97.8%, 78%, 68.6%, 51.1%, and 45.3% in the TACE-RFA group, respectively ($p = 0.011$). There was no occurrence of major complications or procedure-related deaths in the two groups.

Conclusion Compared with the TACE-RFA treatment, TACE-RFA-125I should be a more effective treatment strategy for patients with unresectable HCC (≤ 5 cm) in high-risk locations.

OR-053

Hepatic arterial infusion chemotherapy combined with toripalimab and surufatinib in the treatment of advanced intrahepatic cholangiocarcinoma

Songlin Song, Chuansheng Zheng, Bin Liang

Department of Interventional Radiology, Union Hospital, Tongji Medical College, Huazhong University of Science and Technology, Wuhan, 430022, China.

Purpose The aim of the present study was to report the clinical results of advanced intrahepatic cholangiocarcinoma (ICC) patients who received hepatic arterial infusion chemotherapy (HAIC) and toripalimab chemotherapy, followed by surufatinib maintenance therapy.

Materials and methods The study cohort comprised 28 advanced ICC patients treated with the above schedule and regimens. The baseline characteristics of the study cohort were obtained. The tumor response and drug-associated toxicity were assessed and reported.

Results During the follow-up period (median follow-up time: 11.3 months; range 4–19 months), four patients died of tumor progression. The objective response rate (ORR) and disease control rate (DCR) were 58% and 79%, respectively. The median progression-free survival (mPFS) was 9.5 months, and the OS% was 85%. The most frequent adverse events were nausea and vomiting (100%), and abdominal pain (85.7%). Serious complications that related deaths were not observed.

Conclusion The combination treatment schedule for advanced ICC seems to offer good efficacy and safety.

OR-054

TACE combined with immunotherapy plus targeted therapy after 125I irradiation stent placement in HCC with main portal vein tumor thrombosis: A nationwide target trial emulation study (PATENCY II)

Jun-Hao Mei, Kai-Zhi Jia, Jian Lu, Gao-Jun Teng
zhongda hospital

Purpose To evaluate the safety and efficacy of combining transcatheter arterial chemoembolization (TACE) with immune checkpoint inhibitors (ICIs) and molecular targeted therapy (MTT) after irradiation stent placement (ISP) as a first-line treatment for HCC patients with Vp4 portal vein tumor thrombosis (PVTT).

Materials and methods This multicenter retrospective cohort study enrolled 444 patients with HCC and Vp4 PVTT treated with either ISP, TACE, ICIs, and MTT (ISP-containing quadruple group, n = 131) or with ICIs and MTT (ICIs-MTT group, n = 313) between January 2020 and May 2023. Target trial emulation balanced the observed confounder. The primary endpoint was overall survival (OS), with secondary endpoints including progression-free survival (PFS), objective response rate (ORR), PVTT response, portal vein patency, and safety.

Results Among 444 patients with HCC and Vp4 PVTT, 127 patients from the ISP-containing quadruple group were matched with 220 patients from the ICIs-MTT group. The median OS (11.9 months vs. 8.6 months; $P < 0.001$), PFS (5.1 months vs. 3.1 months; $P < 0.001$), and ORR was also higher in the ISP group (52.8% vs. 27.7% with RECIST1.1; 58.3% vs. 29.1% with mRECIST). Moreover, the ISP group had a higher PVTT positive response rate (64.6% vs. 20.5%). Median stent patency was 10.4 months (IQR: 8.2-12.7), and grade ≥ 3 adverse events occurred in 29.1% of the ISP group and 25.5% of the ICIs-MTT group ($P = 0.456$).

Conclusion Following ISP, treatment combining TACE with ICIs plus MTT can significantly prolong OS and PFS in patients with HCC and Vp4 PVTT and is generally well-tolerated.

OR-055

Development and Validation of Mean Platelet Volume-Based Predictive Model for Early TACE Failure/Refractoriness in Unresectable Hepatocellular Carcinoma: A Real-World Retrospective Cohort Study

Hairui Wang

Shengjing Hospital of China Medical University

Purpose Transarterial chemoembolization (TACE) is a primary locoregional therapy for unresectable hepatocellular carcinoma (uHCC). However, a significant subset of patients develop TACE failure/refractoriness (TACEFR), which is associated with poor prognosis and limited therapeutic options. Elevated mean platelet volume (MPV) has also been closely linked to adverse outcomes in HCC. This study aimed to investigate the correlation between MPV and TACEFR and to develop a nomogram to predict the likelihood of TACEFR, thereby refining treatment protocols and improving patient outcomes.

Materials and methods This retrospective study included 1,837 treatment-naïve patients with uHCC who underwent TACE at our center from January 2010 to December 2020. Patients receiving antiplatelet therapy or with incomplete data were excluded. TACE procedures were performed by experienced interventional radiologists, with therapeutic response assessed by enhanced CT/MRI according to modified RECIST (mRECIST) criteria. TACEFR was defined based on the Japan Society of Hepatology criteria, with early TACEFR identified after the initial two TACE sessions. Follow-up continued until December 2024, with time to progression (TTP) and overall survival (OS) calculated. Statistical analysis included machine learning methods, specifically Support Vector Machine (SVM) and Random Forest (RF), to identify key risk factors associated with TACEFR. The intersection of risk factors highlighted by both SVM and RF was subjected to logistic regression analysis to determine independent predictors of TACEFR. Based on the outcomes of this logistic regression analysis, a nomogram was developed to predict the risk of TACEFR. The model's predictive performance was evaluated using the concordance index (C-index), calibration plots, and decision curve analyses (DCA), and Receiver Operating Characteristic (ROC) curves, ensuring its reliability and clinical utility.

Results Among the 1,837 uHCC patients who underwent initial TACE, 709 (38.6%) developed TACEFR. Machine learning algorithms, SVM and RF, prioritized MPV and platelet count, platelet-to-lymphocyte ratio (PLR), AFP, and tumor size as key risk factors, confirmed by a Venn diagram showing common selections. Logistic regression analyses substantiated MPV, platelet count, PLR, AFP, and tumor size as independent predictors of TACEFR. A nomogram integrating these predictors exhibited a C-index of 0.82, with calibration plots and DCA attesting its reliability and clinical utility. The ROC curve confirmed its discriminative power with an AUC of 0.82. The median TTP was 8.2 months in the TACEFR group versus 14.7 months in the non-resistance group ($p < 0.001$). The 1-year OS rates were 76.3% and 85.5%, respectively ($p < 0.001$), with 3-year OS rates at 45.2% and 64.7% ($p < 0.001$).

Conclusion Our study identified key risk factors for TACEFR in uHCC using machine learning techniques. Independent predictors of TACEFR included MPV, platelet count, PLR, AFP, and tumor size. A predictive nomogram was developed and demonstrated strong discriminative ability and clinical utility. The findings underscore the importance of personalized risk assessment in HCC management, potentially improving patient outcomes by guiding tailored treatment strategies.

OR-056

AI based analysis of response to first line chemotherapy using radiological reports of epithelial type of ovarian malignancy

Chirag Kurane,Suyash Kulkarni,Nitin Shetty,Nilesh Sable,Jaya Ghosh,Kedhar Deodhar,Palak Popat,Akshay Baheti
Tata Memorial Centre

Purpose The main objective is to read the radiological report automatically using Natural Language Processing (NLP) and analyse the response to first line chemotherapy using baseline CT and post chemotherapy CT scan reports in treatment naive cases.

Materials and methods This research is a retrospective analysis study aimed to read the radiological report automatically using Natural Language Processing (NLP) and analyse the response to first line chemotherapy using baseline CT and post chemotherapy CT scan reports in treatment naive cases. Secondary objective is to classify the above cases based on type of epithelial carcinoma ovary using NLP. Then the Diagnosed baseline and post chemotherapy CT reports and the AI based features selected through NLP system are fed into the AI model to predict the response and classify the scan reports of the patients based on the HPR type using AI model.

Results Patient's mean age at diagnosis for epithelial ovarian cancer in our study is 52.6 years and median age is 51.5 years.Serous adenocarcinoma (91.3%) was the most common type of histopathology followed by endometrioid (3.7%), mucinous (2.1%) and clear cell (0.8%).Combination of taxane and platin was most commonly used first line regimen in baseline patients of serous carcinoma ovary and other types as well. The study was done in two phases.In the first phase,all the cases were selected for experimentation, while in the second phase only a specific histopathological type of epithelial type of carcinoma ovary i.e. serous adenocarcinoma cases were selected. In the first phase, the overall classification accuracy came out to be 59 % which shows that the overall system is providing suboptimal results for response prediction if all histopathological types of epithelial carcinoma ovary are taken together. In the second phase, the overall classification accuracy came out to be 72.1 % which is promising as prototype experimentation. The possibility of correlating response prediction with the NLP parameters of the baseline CT report is evident from this phase of the study. The suboptimal results during phase I of the study with improved results in phase II of the study indicate that the CT report parameters of the histopathological subtypes of the epithelial carcinoma ovary differ and need to be experimented separately.

Conclusion This study served as a pilot study in predicting the response to first line chemotherapy in patients of epithelial type of carcinoma ovary using NLP algorithms from primary and first post chemotherapy CECT reports. With the best possible results of overall accuracy of 72.1% with serous type of epithelial carcinoma ovary, this study has shown good outcome in response prediction using NLP based analysis of baseline and post first line chemotherapy CT scan reports and further studies can be commenced for the development of better algorithms with improved precision.

OR-057

Optimal Thermal Ablation Margin Range Model for Liver Malignancies ≤ 3 cm Based on 979 Cases

Zhenkang Qiu, Fei Gao
Sun Yat-sen University Cancer Center

Purpose This study aimed to evaluate the influencing factors of technical success in thermal ablation for liver malignancies ≤ 3 cm and to develop a recommended model for the optimal ablation margin range.

Materials and methods We delineated and calculated the tumor size and ablation margin range of 979 cases who received computed tomography-guided thermal ablation by the treatment planning system. Basic characteristics were compared using t-test or Pearson χ^2 test. Univariate and multivariate logistic analyses were performed to identify factors associated with ablation's technical effects. The nomogram for the predictive probability of residual was established and evaluated using Harrell's concordance index.

Results Tumor diameter >2 cm was an independent factor associated with ablation failure ($p=0.002$). Volume ratio (3.73 ± 2.04 vs. 2.81 ± 1.12 , $p<0.001$) of the no-residual group was significantly higher than that of the residual group. Multivariate logistic analysis showed that adjacent large vessel (odd ratio=1.97, $p=0.015$), preoperative maximum tumor area (odd ratio=1.44, $p=0.014$), and volume ratio (odd ratio=0.77, $p=0.009$) were significant predictive factors for the technical effect of ablation. A nomogram was made to predict the probability of residual tumor occurrence and was validated by an ROC curve with an AUC of 0.685. The optimal ablation margin for tumors with a diameter of 1.0, 2.0, and 3.0 cm were 0.3, 0.8, and 1.6 cm, respectively.

Conclusion We developed a model to calculate the optimal ablation margin range for liver malignancies ≤ 3 cm, which will be employed as a practical guide in clinical.

OR-058

Locoregional therapy combined with systemic therapy (LRT + ST) for unresectable and metastatic intrahepatic cholangiocarcinoma: a systematic review and meta-analysis

Zhenkang Qiu, Fei Gao
Sun Yat-sen University Cancer Center

Purpose The outcome of systemic therapy (ST) for unresectable and metastatic intrahepatic cholangiocarcinoma (iCCA) is poor. This study aims to further evaluate the efficacy and safety of locoregional therapy combined with systemic therapy (LRT + ST) compared with only ST in unresectable and metastatic iCCA by performing a systematic literature review and meta-analysis.

Materials and methods A comprehensive search was performed in PubMed, Web of Science, EMBASE, and the Cochrane Library up to November 3, 2022. The primary outcome was overall survival (OS), and the secondary outcomes were progression-free survival (PFS), objective response rate (ORR), and adverse events (AEs).

Results Ten retrospective cohort studies with 3,791 unresectable or metastatic iCCA patients were enrolled in this study, including 1,120 who received ablation, arterially directed therapy (ADT), or external beam radiation therapy (EBRT) combined with ST. The meta-analysis showed that the LRT + ST group had a better OS (HR = 0.51; 95% CI = 0.41–0.64; p value < 0.001), PFS (HR = 0.40, 95% CI = 0.22–0.71, p value = 0.002) and ORR (RR = 1.68; 95% CI = 1.17–2.42; p value = 0.005). Subgroup analysis showed that both ST combined with ADT (HR = 0.42, 95% CI = 0.31–0.56, p value < 0.001) and EBRT (HR = 0.67, 95% CI = 0.63–0.72, p value < 0.001) could improve OS. Neutropenia, thrombocytopenia, anemia, anorexia, and vomiting did not show significant differences between the groups (p value > 0.05).

Conclusion Compared with only ST, LRT + ST improved survival outcomes for unresectable and metastatic iCCA patients without increasing severe AEs, which can further provide a basis for guidelines.

OR-059

Comparing Percutaneous and Endoscopic Biliary Drainage in Inoperable Bismuth III/IV Malignant Hilar Biliary Obstruction: Clinical Outcomes and Prognostic Factors

XIAOBO FU, Maoyuan Mu, Zixiong Chen, Yuzhe Cao, Lijie Qiu, Fei Gao
Sun Yat-sen University Cancer Center

Purpose This study aimed to evaluate the short- and long-term clinical outcomes of percutaneous and endoscopic biliary decompression in patients with unresectable Bismuth type III and IV malignant hilar biliary obstruction (MHBO). While biliary drainage is the preferred palliative approach for inoperable cases with malignant obstructive jaundice, the optimal drainage method for advanced MHBO remains uncertain. Endoscopic drainage is commonly used for Bismuth type I and II cases due to its minimally invasive nature, whereas percutaneous drainage may offer more effective outcomes in complex cases. However, existing studies primarily focus on type II MHBO, with limited data on type III and IV. By addressing this clinical gap, our study seeks to provide insights into the efficacy and safety of both drainage approaches in this patient population.

Materials and methods A comprehensive database search was conducted from January 1, 2014, to October 31, 2021. A total of 365 inoperable cancer patients with biliary obstruction who underwent biliary stent implantation via either percutaneous or endoscopic retrograde cholangiopancreatography (ERCP) as the primary intervention were reviewed. Ultimately, 66 patients with unresectable Bismuth type III and IV MHBO were retrospectively analyzed. Clinical outcomes, including drainage effectiveness and complications, were compared between the two approaches. Additionally, clinical and treatment factors influencing median overall survival (mOS) were evaluated.

Results Successful biliary drainage was achieved in 44 patients (66.7%), with a significantly higher success rate in the percutaneous group compared to the endoscopic group (80% vs. 55.5%, $p = 0.036$). Patients with successful drainage had a longer mOS than those with unsuccessful drainage (8.9 months vs. 2.3 months, $p = 0.025$). Moreover, patients who received sequential anticancer therapy had a significantly prolonged mOS compared to those receiving only best supportive care (11.6 months vs. 2.3 months, $p < 0.001$). Multivariate analysis identified successful biliary drainage ($p = 0.023$) and anticancer treatment ($p < 0.001$) as significant favorable prognostic factors for survival.

Conclusion For inoperable cancer patients with Bismuth type III or IV MHBO, the percutaneous approach demonstrated safety and effectiveness in reducing bilirubin levels. However, while promising, this study alone does not establish percutaneous stent implantation as the preferred first-line intervention for these patients. Effective biliary drainage may enable patients to receive anticancer treatments, potentially prolonging survival. Further well-designed, randomized controlled trials are needed to validate these findings and optimize treatment strategies.

OR-060

Metformin suppress liver cancer metastasis by inhibiting microwave ablation therapy induced EMT through modulation of the TGF- β - Smad2/3 signaling pathway

Xianmei Liu, Lan Liu, Min Xu, Shuai Zhang, Tianpeng Jiang, Shi Zhou
Affiliated Hospital of Guizhou Medical University,

Purpose To investigate the effects of metformin on epithelial-mesenchymal transition (EMT) in liver cancer cells and assess its potential as an adjuvant therapy following microwave ablation for liver cancer.

Materials and methods A subcutaneous liver cancer model in mice was established and treated with microwave ablation combined with metformin. The inhibitory effects of metformin on the EMT of residual liver cancer cells, extracellular matrix (ECM) deposition and tumor stiffness were analyzed. Simultaneously, using cellular and molecular biology techniques to investigate the effects of metformin on the EMT of liver cancer cells in vitro, including alterations in cells molecular phenotypes (E-cadherin, N-cadherin and Vimentin) and their migration abilities, and furtherly explore the underlying molecular mechanisms.

Results It was observed that microwave ablation treatment for subcutaneous liver cancer in mice resulted in progressive ECM deposition and increased stiffness in the surrounding tissues; the expression levels of N-Cadherin and Vimentin in the residual liver cancer cells was upregulated, whereas the level of E-Cadherin was downregulated. Metformin administration could significantly reverse these changes. In vitro, the results showed that metformin could significantly inhibit the EMT process in liver cancer cells, which characterized by a reduction in the expression of N-Cadherin and Vimentin, an upregulation of E-Cadherin expression, and a suppression of the migratory capabilities of liver cancer cells. Mechanistically, transcriptome sequencing and validation results showed that metformin exerts an inhibitory effect on the TGF- β - Smad2/3 signaling pathway in liver cancer cells.

Conclusion Metformin can mitigate microwave ablation therapy induced ECM deposition and tissue stiffness in liver cancer, and restrict the EMT process of liver cancer cells by inhibiting the TGF- β - Smad2/3 signaling pathway, thereby suppressing liver cancer metastasis. These findings suggest that metformin may serve as an effective adjuvant therapy to prevent the recurrence of liver cancer post-microwave ablation.

OR-061

CCL2⁺ Inflammatory Cancer-Associated Fibroblasts Promote Chemoresistance and Tumor Progression in Microsatellite Stable Colorectal Cancer via the CCL2-P4HB-NOTCH-STAT3 Axis

Siyuan Weng¹, Zhengqiang Yang¹, Zaoqu Liu², Xinwei Han²

1. National Cancer Center/National Clinical Research Center for Cancer/Cancer Hospital, Chinese Academy of Medical Sciences and Peking Union Medical College

2. The First Affiliated Hospital of Zhengzhou University

Purpose Colorectal cancer (CRC) remains a leading cause of cancer-related morbidity and mortality worldwide, with chemotherapy resistance contributing significantly to treatment failure. The tumor microenvironment (TME), particularly cancer-associated fibroblasts (CAFs), plays a critical role in modulating the response of tumors to chemotherapy. This study investigates the role of CAFs in chemoresistance and tumor progression in microsatellite stable (MSS) CRC.

Materials and methods Using single-cell RNA sequencing (scRNA-seq) and spatial transcriptomics, we identified the CCL2⁺ iCAF subpopulation in untreated MSS CRC tissues. Immunohistochemistry and multiplex immunofluorescence staining were performed to assess CAF infiltration and its correlation with chemotherapy resistance. In vitro and in vivo experiments were conducted to explore the molecular mechanisms underlying the interaction between CCL2⁺ iCAFs and tumor cells.

Results Our analysis revealed that CCL2⁺ iCAFs were enriched in chemotherapy-resistant MSS CRC tumors and correlated with poor prognosis. JUNB, a key transcription factor, regulates the CCL2⁺ iCAF phenotype, linking it to cellular senescence and tumor progression. CCL2 secreted by iCAFs activated the NOTCH-STAT3 signaling pathway in tumor cells, enhancing tumor stemness and chemoresistance. Targeting the CCL2-P4HB interaction significantly suppressed tumor growth and improved chemotherapy sensitivity.

Conclusion The CCL2⁺ iCAF subpopulation plays a critical role in promoting chemoresistance in MSS CRC through the CCL2-P4HB axis, which activates the NOTCH-STAT3 signaling pathway. These findings provide new insights into CAF-mediated therapy resistance and highlight the potential of targeting P4HB as a therapeutic strategy to improve CRC treatment outcomes.

OR-062

A nomogram predicting venous thromboembolism risk in primary liver cancer patients

Jing Xiao

Chongqing University Cancer Hospital, China

Purpose This study aimed to develop a nomogram chart model capable of accurately predicting the probability of venous thromboembolism (VTE) in patients diagnosed with primary liver cancer (PLC) within the general population.

Materials and methods Using data collected from patients diagnosed with PLC at Chongqing University Cancer Hospital in China, logistic regression and multivariate analysis techniques were employed to identify independent risk factors associated with VTE. An integrated nomogram was constructed for internal validation. The effectiveness of the nomogram prediction was assessed using the receiver operating characteristic (ROC) curve, calibration curve, decision curve analysis (DCA), and clinical impact curve (CIC).

Results A total of 1,565 patients diagnosed with PLC were analyzed. The nomogram integrated eight risk factors for VTE: activated partial thromboplastin time (APTT) ($P=0.007$), D-dimer ($P=0.019$), lymphocyte count (LYM) ($P=0.012$), monocyte count (MONO) ($P=0.002$), transarterial chemoembolization (TACE) ($P<0.001$), surgical intervention ($P=0.010$), immunotherapy ($P=0.010$), and β 2-microglobulin ($P=0.053$). The nomogram model demonstrated strong discriminatory ability, with C indices of 0.753 and 0.710 in the training and validation cohorts, respectively. The calibration chart for the nomogram showed a strong correlation between the estimated and actual probabilities. Both decision curve analysis (DCA) and clinical impact curves (CIC) demonstrated favorable clinical utility within the cohorts designated for training and validation.

Conclusion We developed a nomogram model to precisely estimate the likelihood of VTE risk in patients with PLC. This model enables doctors to effectively identify at-risk patients and implement timely preventive measures and therapeutic approaches to minimize the occurrence of thrombosis.

OR-063

Lenvatinib Plus Hepatic Arterial Infusion Chemotherapy of FOLFOX versus Lenvatinib Alone for Advanced Hepatocellular Carcinoma

Qicong Mai, Feng Shi, Xiaoming Chen
Guangdong Provincial People's Hospital

Purpose Lenvatinib stands out as a first-line therapy for individuals with advanced hepatocellular carcinoma (HCC). Concurrently, hepatic arterial infusion chemotherapy comprising oxaliplatin, fluorouracil, and leucovorin (FOLFOX-HAIC) has emerged as a potential option for those with advanced HCC. It is necessary to investigate the efficacy and safety of lenvatinib plus FOLFOX-HAIC (lenvaHAIC) for advanced HCC in real-world situations.

Materials and methods In this retrospective analysis, 127 consecutive patients underwent lenvaHAIC, while 184 patients received lenvatinib alone as first-line treatment at six Chinese academic centers between January 2019 and June 2022. Following 1:1 propensity-score matching, we established paired cohorts (113 patients in each group) for evaluating survival. Overall survival (OS), progression-free survival (PFS), objective response rate (ORR), and safety profiles were compared between the two groups.

Results The lenvaHAIC group exhibited significantly prolonged median PFS and OS than the lenvatinib group (PFS: 12.3 vs. 6.2 months; OS: 25.6 vs. 12.3 months; $P < .001$ for each). In the propensity-score matched cohorts (113 pairs), both PFS and OS were notably extended in the lenvaHAIC group compared with those in the lenvatinib group ($P < .001$). Multivariate analysis identified lenvaHAIC treatment as an independent factor for improved PFS (hazard ratio [HR] 0.45; $P < .001$) and OS (HR 0.38; $P < .001$). Grade 3-4 adverse events, including nausea, vomiting, diarrhea, thrombocytopenia, and neutropenia, were more prevalent in the lenvaHAIC group.

Conclusion LenvaHAIC may be a promising treatment in patients with advanced hepatocellular carcinoma, demonstrating enhanced OS, PFS, and ORR and an acceptable safety profile.

OR-064

Hepatic arterial infusion chemotherapy in hepatocellular carcinoma : A Bibliometric and Knowledge-Map Analysis

Yuqing Xu^{1,2,3}, Haipeng Yu^{1,2,3}, Li Wang^{1,2,3}, Hao Qin^{1,2,3}, Mei Li^{1,2,3}

1. Tianjin Medical University Cancer Institute & Hospital, National Clinical Research Center for Cancer

2. Tianjin's Clinical Research Center for Cancer

3. Tianjin Key Laboratory of Digestive Cancer

Purpose In recent years, hepatic arterial infusion chemotherapy (HAIC) has gained popularity in the treatment of hepatocellular carcinoma. Although several studies have been published, no bibliometric analysis have been conducted on this topic. Objectives: To understand the development status and future trends in the application of HAIC, we conducted bibliometric analysis to examine the cooperation and influence among countries, institutions, authors, and journals.

Materials and methods All relevant articles and reviews on the use of HAIC in HCC treatment were retrieved from the Web of Science database. A bibliometric analysis of countries, institutions, journals, authors, and keywords related to this field was performed using R and VOSviewer software. The main aspects analyzed were the research status and key fields of HAIC in HCC treatment.

Results A total of 1026 articles published in 292 journals by 4937 authors from 959 institutions between 1974 and 2021 were retrieved. A rapid increase in articles published after 1990 was observed, which reached the peak in 2021. Japan had the most publications and citations. Yonsei University, Sun Yat-sen University, and Hiroshima University were the three leading institutions in research on this topic. Kwang-Hyub Han and Masatoshi Kudo have the greatest academic influence in this field. Most publications were made in the Hepato-Gastroenterology, whereas cancer had the most citations. The main aspects of HAIC treatment of HCC include HAIC and TACE, chemotherapy drug selection, HAIC and targeted therapy and immunotherapy, HAIC and surgery, and hepatotoxicity. Keywords such as FOLFOX, lenvatinib, hepatic arterial infusion chemotherapy are hot words in this field in recent years.

Conclusion The research on the use of HAIC in the treatment of HCC has been on the rise. Currently, HAIC combined with targeted therapy or immunotherapy has attracted significant attention.

OR-065

Study on the Role of Pirfenidone in Liver Fibrosis - Hepatocellular Carcinoma

Shuai Zhang, Zhimei Cheng, Yi Lei

Department of Interventional Radiology, the Affiliated Hospital of Guizhou Medical

Purpose Transarterial chemoembolization (TACE) is considered the main treatment for intermediate and advanced liver cancer. Nevertheless, TACE may aggravate liver fibrosis in these patients, which could affect the therapeutic effect after TACE. Pirfenidone (PFD) exhibits significant antifibrotic effects in the liver, primarily via inhibition of hepatic stellate cells (HSCs) activation. However, owing to the high dose required for effective treatment, oral administration of PFD is associated with several side effects. This study introduces an oral folic acid (FA)-modified protein-polysaccharide PFD nanoemulsion designed to treat post-TACE liver fibrosis via liver targeting.

Materials and methods We synthesized the ZP-DEX conjugate (ZD) using the green and safe Maillard reaction, and then conjugated with FA by esterification reaction to obtain ZD-FA. It was used to prepare PFD-loaded nanoemulsion (PFD@ZD-FA) through microjet high-pressure homogenization method, which was used for the treatment of liver fibrosis after TACE in the rabbit tumor model via oral administration.

Results The findings indicate that PFD@ZD-FA significantly improved the stability of PFD both in vivo and in vitro, facilitated its penetration through the mucus layer and Caco-2 monolayer, and prolonged its retention in the gastrointestinal tract, thereby improving oral absorption. PFD@ZD-FA effectively increased the accumulation of PFD in the liver and targeted delivery to activated HSCs via FA-mediated endocytosis, leading to the successful inhibition of liver fibrosis in rats. Moreover, in the rabbit model of fibrosis after TACE for liver cancer, PFD@ZD-FA treatment demonstrated superior antifibrotic effects compared to other PFD formulations, outperforming even high-dose free PFD.

Conclusion Overall, this research thoroughly evaluated the physicochemical properties and antifibrotic efficacy of orally administered PFD nanoemulsions and PFD@ZD-FA showed promising potential in the treatment of fibrosis after TACE for liver cancer.

OR-066

Hyaluronidase additional to transarterial chemoembolization improves efficacy for liver cancer: preclinical evaluation

Dan Zhao^{1,2,3}, Chuansheng Zheng^{1,2,3}, Bin Liang¹

1. Department of Radiology, Union Hospital, Tongji Medical College, Huazhong University of Science and Technology

2. Hubei Provincial Clinical Research Center for Precision Radiology & Interventional Medicine

3. Hubei Province Key Laboratory of Molecular Imaging

Purpose To evaluate whether hyaluronidase (HYAL), an enzyme that degrades hyaluronan (HA) in the extracellular matrix, enhances drug delivery and therapeutic efficacy when combined with TACE in preclinical models of HCC.

Materials and methods In vitro experiments were performed using HepG2 multicellular tumor spheroids (MCTS) treated with doxorubicin (160 μ M) \pm HYAL (160 μ M), aiming to assess drug penetration via fluorescence microscopy. For in vivo studies, a rabbit VX2 liver tumor model was utilized, where HYAL (10 mg/kg) was administered intra-arterially or intravenously, followed by TACE (doxorubicin + Lipiodol embolization). Tumor IFP, HA expression, doxorubicin concentration (LC-MS), and penetration (immunofluorescence) were measured. Efficacy was evaluated via tumor necrosis rates (histopathology) and animal survival. Safety was assessed through liver/renal function tests and histopathology of non-tumorous tissues.

Results In vitro experiments demonstrated that HYAL treatment reduced HA expression in HepG2 multicellular tumor spheroids (MCTS) by 61.3% ($P < 0.001$) and significantly increased doxorubicin penetration distance by 225% ($34.1 \pm 4.1 \mu\text{m}$ vs. $10.5 \pm 2.7 \mu\text{m}$, $P < 0.001$). In vivo, intra-arterial administration of HYAL reduced tumor HA expression ($2.4 \pm 1.8\%$ vs. $26.2 \pm 6.7\%$ in controls, $P < 0.001$) and decreased tumor interstitial fluid pressure (IFP) by $47.2 \pm 11.7\%$ compared to a reduction of $8.6 \pm 2.45\%$ in the control group ($P < 0.001$). Combination therapy with HYAL + TACE resulted in a significantly higher intratumoral doxorubicin concentration ($11,526 \pm 4,811.4 \text{ ng/g}$ vs. $3,802.8 \pm 1,290.2 \text{ ng/g}$, $P = 0.021$) and greater doxorubicin penetration distance ($38.1 \pm 8.7 \mu\text{m}$ vs. $29.5 \pm 4.8 \mu\text{m}$, $P = 0.021$) compared to TACE alone. Furthermore, HYAL + TACE led to increased tumor necrosis ($90.61 \pm 5.38\%$ vs. $77.49 \pm 7.11\%$ with TACE alone, $P < 0.001$) and extended median survival (46.0 ± 8.4 days vs. 40.9 ± 6.8 days, $P < 0.05$). No significant differences in liver/renal function or metastasis risk were observed between the combination therapy and TACE alone.

Conclusion HYAL enhances TACE efficacy by degrading HA, reducing tumor IFP, and improving doxorubicin penetration and distribution. The combination demonstrates superior tumor necrosis, prolonged survival, and a favorable safety profile in preclinical models. These findings support further clinical evaluation of HYAL as an adjunct to TACE for advanced HCC.

OR-067

Revolutionizing Detection and Ablation of Invisible Liver Metastases Post-Chemotherapy in Colorectal Cancer: The Role of Transcatheter CT Hepatic Arteriography

Hang Yuan¹, Hong-Tao Hu¹, Xiao-Hui Zhao², Ho-Young Song¹, Wei-Jun Fan⁴, Xiao Li³

1. Henan Cancer Hospital

2. Tianjin Medical University Cancer Institute & Hospital

3. National Cancer Center/National Clinical Research Center for Cancer/Cancer Hospital

4. Sun Yat sen University Cancer Center

Purpose To investigate whether transcatheter CT hepatic arteriography (CTHA) can reveal liver metastatic cancer lesions that have disappeared after chemotherapy, and then to accurately locate these lesions for ablation or preoperative treatment.

Materials and methods A total of 138 patients with liver metastasis from colorectal cancer, who underwent liver metastasis ablation treatment between December 2018 and January 2021, were continuously observed, and their data were analyzed. All these patients were either unwilling or unable to undergo surgical resection but met the criteria for ablation treatment. Prior to ablation, all patients underwent hepatic artery angiography and then were transported to the CT room. To detect the tumor before ablation, a double diluted contrast agent was injected into the hepatic artery at an injection rate of 4ml/second for 4 seconds. CT scan was performed with a delay of 2 seconds following the end of the contrast agent injection. These images were compared with previous MR images to determine whether lesions that had disappeared on MR were visible on CTHA images, and to observe the imaging characteristics of the lesions. Once the lesions were confirmed, CT-guided ablation was performed.

Results Twenty-one patients (15.2%, 21/138) experienced partial disappearance of intrahepatic lesions after chemotherapy (not shown on MR before ablation). Among these 21 patients, there were a total of 75 metastatic lesions before starting chemotherapy. Of these, 26 out of 27 disappeared lesions became visible on CT hepatic arteriography (CTHA) images (96.3%, 26/27). Of the 26 disappeared lesions, 21 lesions (80.8%) exhibited circular enhancement of the tumor, while five lesions (19.2%) showed atypical semicircular enhancement. These were determined as disappearing lesions after comparison with the enhanced MR images at the initial diagnosis. All 74 lesions underwent percutaneous ablation treatment with complete ablation achieved. Three patients experienced a small amount of subcapsular bleeding, which did not increase. These patients were observed without the need for special treatment. There were no instances of bile duct or vascular damage, nor any deaths within 30 days post-treatment. All 21 patients survived, and no residual or recurrent lesions were found in all ablation lesions until the end of follow up.

Conclusion Liver metastases from colorectal cancer that disappear after chemotherapy can be re-visualized by CTHA. In the ablation procedure, CTHA can provide precise guided ablation and immediate evaluation of ablation efficacy without damaging renal function and acceptable radiation.

OR-068

Celecoxib and cisplatin dual-loaded microspheres synergistically enhance transarterial chemoembolization effect of hepatocellular carcinoma

Xin-Wei Han, Jianzhuang Ren, Kewei Ren, Dechao Jiao, Yanan Zhao, Kunpeng Wu
The First Affiliated Hospital of Zhengzhou University, China

Purpose The purpose of this study was to explore a potential therapeutic approach for refractory hepatocellular carcinoma. The research aimed to develop and evaluate a novel material, specifically microspheres with dual-drug loading, for its effectiveness in treating hepatocellular carcinoma.

Materials and methods Polyvinyl alcohol (PVA), celecoxib (CXB), cisplatin (DDP), and various reagents were utilized in this study. Human liver cancer cell lines MHCC-97H and human hepatocellular carcinoma cells SMMC-7721, as well as Balb/c mice and New Zealand rabbits, served as experimental models. PVA microspheres were fabricated using an emulsion crosslinking technique. Polydopamine-coated CXB and DDP-loaded microspheres (PCDMS) were synthesized via dopamine modification. Characterization of the microspheres was performed using scanning electron microscopy (SEM), energy-dispersive X-ray spectroscopy (EDS), and Fourier transform infrared spectroscopy (FTIR). The loading and release profiles were assessed using ultraviolet-visible spectrophotometry. The impact of PCDMS on cellular proliferation, migration, and invasion was evaluated through CCK-8 assays, live/dead cell staining, cell cycle analysis, wound healing assays, and Transwell invasion assays. In vivo studies involved constructing subcutaneous H22 xenograft tumor models in Balb/c mice and VX2 hepatocellular carcinoma models in New Zealand rabbits. Following treatment, changes in body weight and tumor volume were monitored, biochemical analyses and histological staining were conducted, hematological parameters and liver and kidney function indices were measured, and the therapeutic efficacy and safety of PCDMS were comprehensively evaluated.

Results Regarding the physical and chemical properties, the surface roughness of dopamine-modified microspheres was enhanced, and CXB and DDP were successfully encapsulated. In vitro cellular assays demonstrated that the PCDMS significantly inhibited the proliferation and migration of MHCC-97H and SMMC-7721. In vivo studies using a subcutaneous H22 liver cancer model in Balb/c mice and an intrahepatic VX2 tumor model in New Zealand rabbits revealed that PCDMS exhibited remarkable tumor growth inhibition, effectively remodeling the tumor microenvironment and demonstrating a synergistic anti-tumor effect exceeding the sum of individual components. In summary, the dual-loaded microspheres exhibit promising potential for the treatment of liver cancer.

Conclusion This work provides a potential therapeutic approach for the treatment of refractory hepatocellular carcinoma and holds significant translational potential.

OR-069

Preparation of a Composite Nanozyme and Its Sonodynamic Therapy in Bladder Cancer

Jiajia Zheng, Jun Chen

Zhejiang Provincial People's Hospital (Affiliated People's Hospital), Hangzhou Medical College

Purpose Bladder cancer is the second most common malignant tumor in the urinary system. 75% of patients diagnosed early belong to non - muscle - invasive bladder cancer (NMIBC). To treat NMIBC patients, we prepared a new type of nanozyme particle loaded with the photosensitizer chlorin e6 (Ce6). It can catalyze the endogenous hydrogen peroxide in the tumor to produce oxygen to support sonodynamic therapy.

Materials and methods Prussian blue nanoparticles and cerium oxide nanoparticles were connected through amide reaction. Ce6 was loaded onto HPB-CeO₂ NPs by electrostatic adsorption. The hydrodynamic particle size and zeta potential of the synthesized nano - particles were detected by dynamic light scattering. The cytotoxicity of HPB-CeO₂@Ce6 NPs was tested in two bladder cancer cell lines (T24 and 5637) and a normal bladder epithelial cell line (SV-HUC-1) using the CCK8 kit. After determining the safe concentration, 6 - well plates coated with two cancer cell lines were incubated under hypoxia for 24 hours, and HPB-CeO₂@Ce6 NPs were added for 12 hours. Proteins were extracted for WB detection of hypoxia proteins. 12 - well plates coated with two cancer cell lines were treated with HPB-CeO₂@Ce6 NPs for 12 hours, followed by ultrasound treatment with a handheld ultrasonicator. Cell apoptosis rate was detected with an apoptosis kit, intracellular ROS levels with a ROS kit, and mitochondrial membrane potential with a JC-1 kit. Also, confocal dishes coated with two cancer cell lines were stained with a live/dead cell kit after the same treatment to observe cell viability.

Results The composite nanozyme HPB-CeO₂@Ce6 NPs loaded with Ce6 was successfully prepared, with an average size of 163.4 nm and a negative surface charge. In the absence of ultrasound stimulation, it showed low toxicity to T24 and 5637 bladder cancer cells and normal SV-HUC-1 bladder epithelial cells, with cell viability maintained at around 80% even at a concentration of 6 µg/ml. WB results showed a significant reduction in intracellular hypoxia protein levels in cells treated with HPB-CeO₂@Ce6 NPs. After ultrasound stimulation, intracellular ROS levels in cancer cells were significantly increased, mitochondrial membrane potential was markedly decreased, and cell apoptosis rate was significantly increased to about 55%. Live/dead cell staining also showed an increase in red fluorescence representing dead cells and a significant decrease in green fluorescence representing live cells.

Conclusion We synthesized a composite nano - particle that can relieve tumor cell hypoxia, with low biotoxicity. After SDT, it can produce a large amount of ROS to induce cancer cell apoptosis and treat bladder cancer.

OR-070

Transarterial chemoembolisation and tyrosine kinase inhibitors with or without programmed death-1 inhibitors as first-line treatment for unresectable hepatocellular carcinoma: A propensity score matching study

Xuegang Yang¹, Guo Wei², Yi Ren³, Lei Cao⁴, Guohui Xu¹

1. Sichuan Cancer Hospital & Institute

2. Chengdu Public Health Clinical Medical Center

3. Chengdu Second People's Hospital

4. Chengdu Qingbaijiang District People's Hospital

Purpose This research aimed to evaluate the therapeutic effects of combining transarterial chemoembolisation (TACE) and tyrosine kinase inhibitors (TKIs), with or without programmed death-1 (PD-1) inhibitors, as first-line treatment for unresectable hepatocellular carcinoma (uHCC).

Materials and methods This multicentre retrospective cohort study involved 514 patients with uHCC who underwent treatment with either TACE combined with TKIs and PD-1 inhibitors (TACE-TKI-ICI) or TACE with TKIs (TACE-TKI) from January 2019 to December 2023. The two groups were evaluated for differences in progression-free survival (PFS), overall survival (OS), objective response rate (ORR), and safety. Propensity score matching (PSM) was employed to decrease bias between two groups.

Results A total of 241 patient pairs with uHCC were included after PSM. In comparison to the TACE-TKI group, the TACE-TKI-ICI group demonstrated a significantly longer median PFS of 13.8 months (95% CI: 10.3-17.4) versus 10.8 months (95% CI: 9.3-12.4) ($P = 0.005$), and a hazard ratio (HR) of 0.73 (95% CI: 0.58-0.91). Additionally, the median OS was extended to 22.6 months (95% CI: 18.1-27.1) compared to 16.7 months (95% CI: 14.1-19.2) ($P = 0.006$), and an HR of 0.71 (95% CI: 0.56-0.91). The ORR was also higher (58.9% vs. 41.5%, $P < 0.001$). Grade 3/4 adverse events occurred in 10.8% of the TACE-TKI-ICI group and 8.3% of the TACE-TKI group ($P = 0.352$).

Conclusion In comparison to TACE combined with TKIs, the addition of PD-1 inhibitors to TACE and TKIs can significantly improve PFS, OS, and ORR as a first-line treatment for uHCC, while being well tolerated.

OR-071

Real-time MR-guided brain biopsy using 1.0-T open MRI scanner

Cheng-Li Li

Shandong Provincial Hospital Affiliated to Shandong First Medical University, China

Purpose To evaluate the safety, feasibility and diagnostic performance of real-time MR-guided brain biopsy using a 1.0-T open MRI scanner.

Materials and methods Medical records of 86 consecutive participants who underwent brain biopsy under the guidance of a 1.0-T open MRI scanner with real-time and MR fluoroscopy techniques were evaluated retrospectively. All procedures were performed under local anaesthesia and intravenous conscious sedation. Diagnostic yield, diagnostic accuracy, complication rate and procedure duration were assessed. The lesions were divided into two groups according to maximum diameters: ≤ 1.5 cm ($n = 16$) and > 1.5 cm ($n = 70$). The two groups were compared using Fisher's exact test.

Results Diagnostic yield and diagnostic accuracy were 95.3% and 94.2%, respectively. The diagnostic yield of lesions ≤ 1.5 cm and > 1.5 cm were 93.8% and 95.7%, respectively. There was no significant difference in diagnostic yield between the two groups ($p > 0.05$). Mean procedure duration was 41 ± 5 min (range 33–49 min). All biopsy needles were placed with one pass. Complication rate was 3.5% (3/86). Minor complications included three cases of a small amount of haemorrhage. No serious complications were observed.

Conclusion Real-time MR-guided brain biopsy using a 1.0-T open MRI scanner is a safe, feasible and accurate diagnostic technique for pathological diagnosis of brain lesions. The procedure duration is shortened and biopsy work flow is simplified. It could be considered as an alternative for brain biopsy.

OR-072

3D-printed Versatile Biodegradable Biliary Stent with Zinc/Sirolimus for Anti-bacterial and Anti-hyperplasia in a Rabbit Bile Duct

Jung-Hoon Park, Dong-Sung Won, Yubeen Park
Asan Medical Center

Purpose Biodegradable biliary stents (BDBSs) have emerged as a potential alternative to relieve the burden of re-intervention in patients with unresectable malignant biliary obstruction (MBO). Single therapeutic agent-coated BDBS such as silver nanoparticles, sirolimus (SRL), or paclitaxel has been demonstrated a great potential to prevent stent-induced tissue hyperplasia or biofilm formations. However, a multifunctional approach is required to simultaneously achieve both anti-proliferative and antimicrobial effects. This study aims to investigate the efficacy and safety of zinc (Zn)-SRL-coated BDBS for inhibition of tissue hyperplasia and bacterial activity in the rabbit common bile duct (CBD).

Materials and methods Polycaprolactone (PCL) composites with silica (fPCL) to improve mechanical properties were fabricated via 3D printing and the BDBS was 3 mm in diameter and 8 mm in length. The SRL or Zn-SRL was coated onto the surface of BDBS. All BDBSs were crimped onto a 3-mm-diameter and 12-mm-long balloon catheter. Twenty male New Zealand White rabbits were divided into four groups: PCL, fPCL, SRL@fPCL, and Zn-SRL@fPCL. The efficacy and safety of the Zn-SRL-coated BDBS were evaluated and compared by cholangiography, hematological, histological, and immunohistochemistry analysis between the study groups.

Results BDBS placement was successful in all rabbits without procedure-related complications. All rabbits survived until the end of the study, but jaundice was observed at 10–18 d in six rabbits in the PCL ($n = 3$), fPCL ($n = 2$), and SRL@fPCL ($n = 1$) groups. Follow-up cholangiography showed the dilated CBD and intrahepatic duct caused by luminal narrowing at the stented CBD in the PCL and fPCL groups; however, stent patency was relatively preserved in the Zn-SRL@PCL and SRL@PCL groups. In gross findings, the sludge formation was considerably reduced in the Zn-SRL@PCL group. Hepatobiliary function levels and in-stent restenosis related variables were significantly lower in SRL@fPCL and Zn-SRL@PCL groups than those in the PCL and fPCL groups (all, $p < 0.05$).

Conclusion The Zn-SRL coated BDBS was effective and safe to inhibit stent-induced tissue hyperplasia and biofilm formation, resulting in prolonged stent patency without hepatobiliary dysfunction in the rabbit CBD. Multi-functionalized BDBSs present a therapeutic potential for preventing stent-related complications and reducing re-intervention in patients with unresectable MBO.

OR-073

Retrospective study to determine diagnostic accuracy of image guided peritoneal biopsies

Arun Gopalakrishnapillai
Tata Memorial Hospital

Purpose In the realm of diagnostic medicine, the accuracy of procedures is paramount. In this retrospective study, we analyze the diagnostic accuracy of image-guided peritoneal biopsy. By examining past cases, we aim to evaluate the reliability of this technique in diagnosing peritoneal conditions, providing valuable insights into its clinical effectiveness.

Aims/objectives: To determine the safety and diagnostic accuracy of image guided peritoneal biopsy as well as factors affecting the yield of peritoneal biopsy.

Materials and methods Retrospective review of 200 image guided percutaneous peritoneal biopsies were performed from 2016-2023. Biopsy results were compared with subsequent surgical pathology when available or with subsequent radiological or clinical response. Sensitivity, Specificity, Positive and negative predictive value and diagnostic accuracy were calculated. Chi square test was used to determine the statistical significance of various variables.

Results Out of 200 patients, histopathology was positive in 169 (84.5%) patients for malignancy and positive for infective/inflammatory etiology in 12 patients (6%). The outcome parameters were as follows: Diagnostic accuracy 92.5%, diagnostic yield 84.5%, sensitivity 91.8%, specificity 100 %, positive predictive value 100% and negative predictive value 51.6%. The diagnostic yield of biopsy improves with increasing core size, increasing throw of needle , with properly targeting the lesion. The diagnostic yield was higher for USG than CT and higher for age group ≥ 40 years, and for malignant lesions as compared to benign/ inflammatory lesions. Yield was higher for those patients in whom ascitic fluid cytology was positive for malignant cells. Yield was higher for peritoneal mass than peritoneal caking or nodularity. No major complications were observed.

Conclusion Image guided peritoneal biopsy is a safe and cost effective method with minimum complication rate for diagnosing the peritoneal lesions.

OR-074

Temperature-sensitive Liquid Embolic Agent Transarterial Chemoembolization (TempSLE-TACE) versus D-TACE for Unresectable Hepatocellular Carcinoma(u-HCC): A multicenter retrospective propensity score study in China

Qingyun Xie¹, Ying Yang¹, Chang Liu², Hong Wu¹

1. Liver Transplantation Center, State Key Laboratory of Biotherapy and Cancer Center, West China Hospital, Sichuan University and Collaborative Innovation Center of Biotherapy.

2. Division of Abdominal Tumor Multimodality Treatment, Cancer Center, West China Hospital, Sichuan University

Purpose Hepatocellular carcinoma (HCC) is a leading cause of cancer-related mortality in China, with approximately 70% of patients diagnosed at unresectable stages (u-HCC). Conventional drug-eluting TACE (D-TACE) faces limitations such as incomplete embolization and unpredictable drug release. Temperature-sensitive liquid embolic agent (TempSLE), with its phase-transition controllability and precision embolization, may enhance local tumor control, yet its clinical efficacy and safety require systematic validation.

Materials and methods This multicenter retrospective cohort study included u-HCC patients treated with T-TACE (n=101) or D-TACE (n=186) between 2020-2022. Propensity score matching (PSM) balanced baseline characteristics. Outcomes included objective response rate (ORR, mRECIST criteria), adverse events (CTCAE v5.0), and survival analysis (Kaplan-Meier method, Cox regression).

Results After propensity score matching (90 pairs), T-TACE demonstrated superior objective response rate (ORR 56.67% vs 41.11%, $P=0.037$) and reduced incidence of abdominal pain (44.79% vs 63.74%, $P=0.003$) and fever (23.96% vs 56.98%, $P<0.001$) compared to D-TACE. Histopathological analysis of postoperative specimens (H&E staining) revealed more complete embolization of tumor-feeding arteries in the T-TACE group (Figure 4). While pre-PSM analysis showed significant survival benefits for T-TACE (median OS: 21 vs 16 months, $P=0.006$; median PFS: 12 vs 8 months, $P<0.001$), post-PSM survival differences attenuated, retaining significance only for PFS (12 vs 8 months, $P=0.008$). Cox models identified advanced CNLC stages (IIb–IIIb) as independent predictors of poor OS ($HR=10.80-16.61$, $P\leq 0.004$) and PFS ($HR=4.64-7.42$, $P\leq 0.002$), while BCLC-C paradoxically reduced PFS risk ($HR=0.45$, $P=0.027$). AFP 200–400 ng/mL conferred OS protection ($HR=0.19$, $P=0.003$).

Conclusion T-TACE achieved superior local tumor control through enhanced vascular occlusion, supported by histopathological evidence of complete embolization. Despite attenuated OS benefits post-PSM, T-TACE maintained prolonged PFS with improved safety, positioning it as a promising locoregional therapy for u-HCC.

OR-076

The eight mitochondrial metabolism-related genes as diagnostic markers for abdominal aortic aneurysm by integrating machine learning approach

Yang Zheng
Chongqing University Cancer Hospital

Purpose Approximately 13,000 people die of an abdominal aortic aneurysm (AAA) every year. A growing number of studies suggests that mitochondrial metabolism plays an important role in the processes of AAA. This study aimed to identify the mitochondrial metabolism-related genes (MMRGs) that could be used as diagnostic markers for AAA.

Materials and methods The three gene expression datasets including GSE57691, GSE47472 and GSE165470 were downloaded from GEO database. We conducted differential expression analysis on a select list of 1234 candidate MMRGs. Subsequently, an integrated machine learning approach were applied to identify key hub genes and assess the diagnostic efficacy for AAA. Finally, the potential compounds for AAA treatment were screened according above key genes by CMap database and the oncoPredict algorithm.

Results The three gene expression datasets including GSE57691, GSE47472 and GSE165470 were obtained with a total of 73 AAA samples and 18 normal samples. 652 AAA-related genes (283 up-regulated and 369 down-regulated) were observed to participate in multiple mitochondrial metabolism pathways. By overlapping with 1234 mitochondrial metabolism-related genes (MMRGs), we further identified 8 hub AAA-MMRGs could be used as diagnostic markers for AAA using an integrated machine learning approach, including AHR, OSBPL10, POLG, PTGS2, ASS1, NDUFS3, PIP4K2C and POLG2. At same time, Gene-TFs, Gene-miRNAs and Protein-Drugs regulatory network of the eight diagnostic markers were constructed by NetworkAnalyst. In addition, the immune infiltration landscape affected by AAA were also delineated. Pearson's correlation analysis showed that M2 macrophages had the strongest negative correlation with AHR, OSBPL10 and PTGS2, while OSBPL10 had the strongest positive correlation with activated NK cells. Finally, the potential compounds for AAA treatment were screened according above key genes by CMap database and the oncoPredict algorithm, the expression of OSBPL10 showed a significant positive correlation with selumetinib, while the expression of ASS1 and PD0325901 showed a significant positive correlation.

Conclusion In summary, mitochondrial metabolism was involved in the processes of AAA. Eight genes, AHR, OSBPL10, POLG, PTGS2, ASS1, NDUFS3, PIP4K2C and POLG2, may play important roles in the development, diagnosis, and treatment of AAA.

OR-077

Superselective ablative chemo-ethanol embolization for recurrent single hepatocellular carcinoma

Kun Yung Kim, Jae Hwan Lee
Seoul National University Bundang Hospital, Korea

Purpose To evaluate the safety and effectiveness of superselective ablative chemo-ethanol embolization (SACE) for the treatment of patients with recurrent single hepatocellular carcinoma (rHCC).

Materials and methods This retrospective study included 22 patients (19 men; median age, 63 years [range, 38-86]) with Child-Pugh class of A/ B/C (16/3/3) that underwent SACE between January and June 2023 for recurrent single HCCs measuring ≤ 5 cm in diameter using a mixture of 99% ethanol and ethiodized oil/doxorubicin emulsion. The primary endpoint was the 6-month tumor response, and the secondary endpoints were the 1-month tumor response and treatment-related safety. This study was approved by our institutional review board, and the requirement for informed consent was waived.

Results SACE was successfully performed in 22 patients (95.2%). The complete response rates at 1-month and 6-month after treatment were 100.0% and 83.3%, respectively. At 6-month, local tumor progression occurred in one patient and intrahepatic distant metastasis was found in six patients (30.0%). No 6-month mortalities were reported. No adverse events greater than grade 2 or laboratory deteriorations were observed. Biliary complications or liver abscesses were not observed.

Conclusion SACE for a single rHCC was highly effective in achieving a favorable 6-month tumor response and showed acceptable adverse events. However, further prospective studies are required to verify these findings.

OR-078

Comparison of DEB-TACE Combined with Thermal Ablation versus DEB-TACE alone in the Treatment of Large Hepatocellular Carcinoma and Multinodular Hepatocellular Carcinoma: Efficacy and Prognostic Factors Analysis

Lin Zheng

The Affiliated Cancer Hospital of Zhengzhou University, China

Purpose To explore the efficacy and prognostic factors of DEB-TACE combined with thermal ablation compared to DEB-TACE alone in the treatment of large hepatocellular carcinoma and multinodular hepatocellular carcinoma.

Materials and methods A retrospective analysis was conducted on 111 patients with CNLC I b-II b stage large HCC and multinodular HCC diagnosed and treated in our Department of Interventional Radiology from July 2020 to June 2023. All patients underwent DEB-TACE treatment for the first time and were divided into two groups: the DEB-TACE alone group (n=69) and the DEB-TACE combined with thermal ablation group (n=42). After 2 cycles of treatment, the complete response (CR) rate, objective response rate (ORR), and disease control rate (DCR) were evaluated by magnetic resonance imaging (mRECIST criteria), the progression free survival (PFS) and overall survival (OS) were calculated. treatment-related adverse events were recorded, and the prognostic factors affecting PFS and OS were analyzed.

Results The CR rates of the simple group and the combined group were 14.5% and 54.8%, respectively ($\chi^2=20.266$, $P<0.001$); the ORR were 65.2% and 82.6%, respectively ($\chi^2=4.257$, $P=0.039$); the DCR were 89.9% and 93.5%, respectively ($\chi^2=1.015$, $P=0.314$); the mPFS were 7.0 months and 12.0 months, respectively ($\chi^2=15.966$, $P<0.001$); the mOS were 23.0 months and 29.0 months, respectively ($\chi^2=7.954$, $P=0.005$). Multivariate analysis showed that different groups (simple/combined), ECOG score (0/1), and sum of tumor diameters (≤ 8.0 / >8.0 cm) were independent prognostic factors affecting PFS of patients with large HCC and multinodular HCC, and different groups (simple/combined) and sum of tumor diameters (≤ 8.0 / >8.0 cm) were independent prognostic factors affecting OS of patients with large HCC and multinodular HCC. The incidence of adverse events caused by treatment in both groups was controllable, with no significant difference in occurrence rates.

Conclusion DEB-TACE combined with thermal ablation demonstrates greater advantages over DEB-TACE alone in the treatment of large HCC and multinodular HCC, and can significantly improve short-term efficacy and long-term survival. Whether DEB-TACE is combined with thermal ablation, sum of tumor diameters, and ECOG score are independent predictive factors for PFS of patients with large HCC and multinodular HCC; whether DEB-TACE is combined with thermal ablation and sum of tumor diameters are independent predictive factors for OS. The adverse reactions caused by DEB-TACE combined with thermal ablation in the treatment of large HCC and multinodular HCC are controllable with good safety.

OR-079

Efficacy and prognostic factors of COVID-19 vaccine in patients with hepatocellular carcinoma: Analysis of data from a prospective cohort study

He Zhao

National Cancer Center/National Clinical Research Center for Cancer/Cancer Hospital, Chinese Academy of Medical Sciences and Peking Union Medical College, Beijing, China

Purpose The purpose of the article is to explore the efficacy of COVID-19 vaccines in preventing SARS-CoV-2 infection among patients with hepatocellular carcinoma (HCC) and to identify the prognostic factors, with the aim of informing future strategies for the prevention and management of global infectious diseases.

Materials and methods Methods: From January 2022 to October 2022, patients diagnosed with HCC in a prospective, multicenter, observational cohort were analyzed.

Results Results: One hundred and forty-one patients with (n=107) or without COVID-19 vaccination (n=34) were included. The number of patients with severe or very severe infection was relatively lower in the vaccinated group (3.7% vs. 11.8%, $p=0.096$). Median infection-free survival in the vaccinated group (14.0 vs. 8.3 months, $p=0.010$) was significantly longer than that in the unvaccinated group. COVID-19 vaccination (hazard ratio (HR) HR=0.47), European Cooperative Oncology Group performance score=0 (HR=2.06), and extrahepatic spread (HR=0.28) were found to be the independent predictive factors for infection-free survival.

Conclusion COVID-19 vaccines could effectively reduce the SARS-Cov-2 infection in patients with HCC.

OR-080

Conventional Oral Morphine vs. IV Patient-Controlled Analgesia (IPCA) with Hydromorphone (HM) Continuous Infusion plus Rescue Dose (CIRD) or Bolus-Only (BO) for Severe Cancer Pain: A Randomized Phase III study

Liyu Su¹, Shen Zhao¹, Yingquan Ye¹, Yanhong Meng², Rongbo Lin¹

1. Fujian Cancer Hospital

2. Nanping Jianyang First Hospital

Purpose Our phase II study (Lin, JNCCN 2022) reported that IPCA with HM CIRD or BO was superior to conventional oral extended-release (ER) morphine around the clock (ATC) plus immediate-release (IR) for rescue dose in patients with severe cancer pain (≥ 7 at rest on the 11-point NRS). Although the phase II study suggested comparable efficacy between CIRD or BO, the sample size was insufficient to test noninferiority. This phase III study aims to validate these preliminary findings in a larger cohort.

Materials and methods A 6 days, open-label, randomized controlled phase III study was conducted at 48 cancer centers across China. Patients aged 18 to 80 years diagnosed with malignant solid tumors experiencing severe cancer pain were enrolled and after successful opioid titration were randomly assigned in a 2:2:1 ratio to one of three arms: (A1) IPCA HM with BO as needed (PRN); (A2) IPCA HM with continuous infusion (akin to ATC) plus bolus (rescue dose); or (B) oral ER morphine plus IR morphine. The primary endpoint was average NRS over days 1-3 (3DNRS, sum of previous 24-hour average pain scores for days 1–3 divided by 3).

Results A total of 1,349 subjects underwent randomization: 542 to Arm A1, 540 to Arm A2, and 267 to Arm B. The mean of 3DNRS (SD) were significantly lower in Arm A1 (2.36 [0.89], $P_{\text{superiority}} < 0.001$) and Arm A2 (2.26 [0.87], $P_{\text{superiority}} < 0.001$) compared to Arm B (2.94 [1.16]). The mean difference in 3DNRS between Arm A1 and Arm A2 was 0.099 (95% CI, -0.005, 0.204). The upper limit of the 95% CI is below the predefined non-inferiority margin of 0.3 ($P_{\text{noninferiority}} < 0.001$). Daily NRS and patient satisfaction scores on Day 3 and Day 6 were no significant differences between Arms A1 and A2, albeit inferior to Arm B. The daily equivalent morphine consumption was highest in Arm B, followed by A2, and lowest in Arm A1. Opioid-related adverse events were significantly more frequent in Arm B compared to both Arm A1 and A2.

Conclusion IPCA HM regardless of with or without continuous infusion offers superior pain control compared to conventional oral morphine in severe cancer pain management. Furthermore, IPCA HM with BO demonstrates non-inferiority to CIRD, suggesting that a PRN approach with IPCA is an effective alteration for managing severe cancer pain.

OR-081

Percutaneous core needle biopsy of peripheral lung lesions: A single center experience and analysis of safety and efficacy

Suyoung Park

Department of Radiology, Gil Medical Center, Gachon University College of Medicine

Purpose To evaluate the accuracy and complications of percutaneous transthoracic core needle biopsy (TTNB) for peripheral lung lesions, and to identify factors associated with diagnostic failure and occurrence of significant pneumothorax.

Materials and methods Data from 566 TTNB procedures on lung lesions in contact with or adjacent to the visceral pleura at a distance less than 1 cm, performed at a single center between March 2019 and December 2021, were retrospectively reviewed. Technical and diagnostic success rates were calculated. Procedure details and lesion(s) characteristics were analyzed using univariate and multivariate logistic regression analyses to identify factors associated with diagnostic failure and postprocedural pneumothorax.

Results The technical and diagnostic success rates were 100% and 90.1% (510/566), respectively. Postprocedural pneumothorax occurred in 19.4% (110/566) of patients. Univariate and multivariate analyses revealed that lesion diameter less than 10 mm ($p < 0.001$) was associated with diagnostic failure, and the transfissural route ($p = 0.042$) and longer tract length ($p = 0.018$) were associated with the occurrence of postprocedural pneumothorax.

Conclusion TTNB was an effective and safe diagnostic method for peripheral lung lesions, with a high diagnostic success rate and low incidence of postprocedural pneumothorax.

OR-082

HAIC combined with sintilizumab and bevacizumab for the treatment of advanced HCC: an exploratory clinical study

Zizhuo Wang, Chuansheng Zheng, Bin Liang
Wuhan Union Hospital

Purpose Although systemic therapy is currently the standard treatment for advanced hepatocellular carcinoma (HCC), its therapeutic efficacy remains unsatisfactory. Recently, hepatic arterial infusion chemotherapy (HAIC), either alone or in combination with systemic therapies, has achieved encouraging outcomes against HCC. Meanwhile, sintilimab plus bevacizumab, a combination of an immune checkpoint inhibitor and an antiangiogenetic targeted agent, has been approved as the first-line systemic therapy for advanced HCC in China. HAIC combined with sintilimab and bevacizumab may represent a potential combination of local and systemic therapies, yet prospective clinical evidence supporting the combination therapy is lacking. This study aims to evaluate the efficacy and safety of HAIC combined with sintilimab and bevacizumab in the treatment of advanced HCC patients.

Materials and methods This single-center, prospective Phase II clinical study recruited patients diagnosed with BCLC stage C HCC between November 2022 and March 2024. Eligible patients, who had not previously received systemic therapy, were scheduled to undergo FOLFOX-HAIC combined with sintilimab and bevacizumab. The FOLFOX-HAIC regimen consisted of oxaliplatin (85 mg/m², from hour 0 to 2 on day 1), leucovorin (200 mg/m², from hour 2 to 3 on day 1) and fluorouracil (400 mg/m², bolus at hour 3; and 2400 mg/m² over 46 hours on days 1 and 2) on a 3-week cycle for the usual 6 cycles or as adjusted for tumor response and patient tolerance. The sintilimab (200 mg, on day 3) and bevacizumab (7.5 mg/kg, on day 3) were intravenously administered every 3 weeks for a maximum of 24 months unless there was any evidence of disease progression or unacceptable toxicity. The primary endpoint was progression-free survival (PFS) as assessed by Response Evaluation Criteria in Solid Tumors (RECIST) version 1.1. The secondary endpoints included PFS as assessed by modified RECIST (mRECIST), and objective response rate (ORR), disease control rate (DCR), time to response (TTR), and duration of response (DOR) based on RECIST 1.1 and mRECIST, as well as inter-subgroup variability in ORR, overall survival (OS), and treatment-emergent adverse events (TEAEs).

Results Up to January 2025, a total of 37 eligible patients were included, with a median follow-up of 18.9 months (range: 5.7–26.2). The median PFS was 11.3 months (95% CI: 3.5–19.0) by RECIST 1.1 and 11.7 months (95% CI: 1.4–21.9) by mRECIST. The median TTR was 1.9 months (95% CI: 1.4–2.4) by RECIST 1.1 and 1.7 months (95% CI: 1.7–1.8) by mRECIST. The median DOR was not reached by RECIST 1.1 (95% CI: not reached) and was 15.2 months (95% CI: 5.9–24.5) by mRECIST. The confirmed ORR was 67.6% (95% CI: 50.2%–82.0%) by RECIST 1.1 and 73.0% (95% CI: 55.9%–86.2%) by mRECIST. The DCR was 97.3% (95% CI: 85.8%–99.9%) for both RECIST 1.1 and mRECIST. ORR was not statistically different between subgroups. The median OS has not yet been reached (95% CI: not reached). Safety analysis revealed a high incidence of TEAEs, with the most common Grade 3–4 TEAEs being lymphopenia (40.5%) and neutropenia (18.9%). The TEAEs were relieved after symptomatic treatment, and no treatment-related deaths occurred.

Conclusion The combination of HAIC with sintilimab and bevacizumab achieves superior therapeutic efficacy with a manageable safety profile in patients with advanced HCC.

OR-083

Fruquintinib combined with sintilimab plus transarterial chemoembolization (TACE) for unresectable hepatocellular carcinoma (uHCC): A single-arm phase II study

Hui Zeng, Zhewei Zhang, Dinghu Zhang, Jiaping Zheng, Jun Luo, Liwen Guo, Zheng Yao
Zhejiang Cancer Hospital

Purpose Tyrosine kinase inhibitor combined with immune checkpoint inhibitor has been reported a synergetic survival benefit in patients with uHCC. TACE induced tumor necrosis and tumor antigen release was believed to increase immune responses of anticancer immunotherapies. This study aimed to evaluate the safety and efficacy of fruquintinib combined with sintilimab plus TACE for uHCC.

Materials and methods This study was a single-arm, open-label phase II exploratory clinical study (NCT05971199). Eligible patients were China liver cancer stage (CNLC) II b-IIIa and not candidates for surgical resection or ablation, or liver transplantation, at least one target lesion evaluable, ECOG performance status of 0-1, and Child-Pugh score ≤ 7 . Enrolled patients would receive treatment with TACE (TACE was repeated on demand, but < 5 times) followed by sintilimab 200 mg every 3 weeks and fruquintinib (5 mg QD, 2w on/1w off) until intolerable toxicity or disease progression. The primary endpoint was progression free survival (PFS). The secondary endpoints included adverse events (AEs), overall survival (OS), objective response rate (ORR) and disease control rate (DCR) per mRECIST.

Results As of January 8, 2025, 27 enrolled patients with uHCC were treated. Median follow-up time is 19.4 months. The median age is 61.0 years. At present, 24 patients were included for efficacy and safety evaluation. Number of patients with CNLC stage II b and IIIa was 1 (4 %) and 23 (96 %), respectively. The median PFS was 9.1 months (95% CI 6.2-21.8) and OS data was not yet mature. The ORR and DCR were 92.6 % and 100 % respectively based on mRECIST (4 CR, 16.7 %; 18 PR, 75.0 %; 2 SD, 8.3 %). The most common TRAEs (\geq Grade 3) were elevated glutamic oxaloacetic transaminase, hypertension, proteinuria. No unexpected toxicity or treatment-related deaths occurred.

Conclusion Fruquintinib combined with sintilimab and TACE is a promising and tolerable therapeutic regimen for patients with CNLC II b-IIIa uHCC.

OR-084

Effect of AFP and PIVKA-II secretion status on prognosis of advanced hepatocellular carcinoma patients receiving TACE combined with systemic therapies

Jinfeng Bai, Rong Ding
Yunnan Cancer Hospital

Purpose Few biomarkers can predict the efficiency of transcatheter arterial chemoembolization (TACE) combined with systemic therapies in patients with advanced hepatocellular carcinoma (HCC). This study aimed to investigate the prognostic values of changing trends in alpha-fetoprotein (AFP) and prothrombin induced by vitamin K absence-II (PIVKA-II) and their clinical usefulness for patient receiving TACE combined with immune checkpoint inhibitors (ICIs) and tyrosine kinase inhibitors (TKIs).

Materials and methods This was a retrospective cohort study of advanced HCC patients who underwent TACE combined with ICIs and TKIs obtained from the third affiliated Hospital of Kunming Medical University between May, 2021 and March, 2024. Based on serum AFP and PIVKA-II levels before and after treatments, patients were divided into four statuses: AFP (↑) PIVKA-II (↑) (status 1), AFP (↑) PIVKA-II (↓) (status 2), AFP (↓) PIVKA-II (↑) (status 3) and AFP (↓) PIVKA-II (↓) (status 4). Kaplan-Meier analyses were employed to compare overall survival (OS) and progression-free survival (PFS) of the four groups. Univariate and multivariate Cox analysis were performed to identify the potential prognostic factors of OS and PFS.

Results A total of 187 patients were enrolled. The obvious differences of OS and PFS among different AFP-PIV status were observed ($P < 0.001$). Patients with AFP (↑) and PIVKA-II (↑) showed the poorest OS and PFS comparing to the other statuses. Whether elevated AFP alone or elevated PIVKA-II alone, increases the risk of disease progression or death. Those with reduced expression of both the AFP and PIVKA-II mean were associated with better prognosis. The AFP-PIV secretion status was an independent risk factor for OS and PFS in advanced HCC patients.

Conclusion The AFP-PIV status demonstrated significant prognostic value as independent predictors of OS and PFS in advanced HCC patients receiving TACE combined with systemic therapies.

OR-085

Safety and Technical Feasibility of Modified Percutaneous Transesophageal Enterostomy (PTEE) in Cancer Patients Ineligible for Conventional Gastrostomy

Ji Hoon Shin

Asan Medical Center, University of Ulsan College of Medicine, Korea

Purpose To describe the safety and technical feasibility of modified percutaneous transesophageal enterostomy (PTEE) in patients with cancer for whom conventional gastrostomy is not feasible.

Materials and methods A retrospective review was conducted on 17 consecutive patients (M:F=16:1, mean age 71.3 years, range 42-85 years) with feeding problems who were treated with modified PTEE, which involves puncture of an 18-mm diameter esophageal balloon with inserting the feeding tube tip from the stomach to the jejunum. Patient baseline characteristics, underlying conditions requiring PTEE, time from balloon puncture to feeding tube insertion, final position of the feeding tube tip, and complications were evaluated.

Results Underlying cancers included stomach cancer (n=7), esophageal cancer (n=6), both esophageal and stomach cancers (n=1), common bile duct cancer (n=1), pancreatic cancer (n=1), and lung cancer (n=1). The reasons for requesting PTEE were subtotal or total gastrectomy (n=6), esophagectomy (n=1), both esophagectomy and gastrectomy (n=1), extensive stomach involvement by esophageal or stomach cancer (n=3), high-lying stomach (n=3), pancreas-preserving pancreaticoduodenectomy (n=1), peritoneal seeding with small bowel dilatation preventing gastric access (n=1), and refusal of gastrostomy (n=1). PTEE was successfully achieved in 16 patients (94.1% technical success, 16/17). The median time from balloon puncture to feeding tube insertion was 15 minutes (range: 8-52 minutes). The final position of the feeding tube tip was in the jejunum (n=9), duodenum (n=6), and stomach (n=1). No procedure-related complications occurred.

Conclusion Modified PTEE is a safe and technically feasible option for providing feeding support in cancer patients for whom conventional gastrostomy is not feasible. The tube tip was successfully positioned in the duodenum or jejunum in most patients.

OR-086

Restraining small extracellular vesicles: Dawn of a new era in nanomedicine

Ming Yang, Linzhu Zhang, Haidong Zhu
Zhongda Hospital, Southeast University

Purpose In the past 30 years, research in the field of cancer nanomedicine has seen tremendous expansion. But achieving high concentrations of nanomedicine at the tumor site remains a critical research focus in the field. In a recent paper published in *Nature Materials*, Gong et al. identified the tumor cell-derived small extracellular vesicles (sEVs) as a defense system that impedes selective delivery of nanoparticles to tumors. The authors also discovered that this defense system could be a prospective target for enhancing the efficacy of nanoparticle-based tumor therapies.

Materials and methods To overcome the complex microenvironment constituted by the dense extracellular matrix of tumors, solid stress, and abnormal vascular structures, the authors initially utilized CRISPR-Cas9 technology to knock out the key gene Rab27a, which regulates sEVs secretion, in a mouse model. They found Rab27a knockout can significantly reduce the secretion of sEVs in mouse tumor cells and greatly increase the accumulation of lipid nanoparticles (LNPs) in the tumors. Further investigation found that, through interactions such as van der Waals forces, sEVs can bind to nanoparticles and physically transport them to the Kupffer cells in the liver for degradation, consequently diminishing the accumulation of nanoparticles in the tumors. Similarly, relevant in vitro cell experiments have shown that sEVs can influence the cellular uptake of LNPs. By blocking the adhesion molecules, intercellular cell adhesion molecule-1 (ICAM-1), on the surface of sEVs with corresponding antibodies, the uptake of LNPs by Kupffer cells was greatly decreased. Moreover, Kupffer cells expressed higher levels of macrophage-1 antigen (Mac-1, the receptor for ICAM-1) compared to other cell subsets in the liver. This finding elucidates the mechanism behind the uptake of LNPs by Kupffer cells: LNP binds to tumor-derived sEVs, forming an lipid nanoparticles-small extracellular vesicles (LNP-sEV) complex, which is then specifically taken up via the ICAM-1-Mac-1 interaction.

Results This study revealed that Rab27a knockout (KO) enhances nanoparticle accumulation in tumors by reducing lipid nanoparticle (LNP) uptake by Kupffer cells and improving LNP delivery to tumor cells. Further investigation demonstrated that small extracellular vesicles (sEVs) can bind to nanoparticles through interactions such as van der Waals forces and physically transport them to Kupffer cells in the liver for degradation. This process reduces nanoparticle accumulation in tumors, indicating that sEV binding to LNPs facilitates their trafficking to liver Kupffer cells. Additionally, the study found that Rab27a KO significantly increased LNP uptake by tumor cells, while sEV supplementation markedly decreased LNP uptake across multiple tumor cell lines. Moreover, inhibiting sEVs enhanced the in vivo delivery of both Pten mRNA and Sting mRNA, suggesting that sEV suppression can improve the therapeutic efficacy of nanoparticle-based mRNA delivery.

Conclusion This study offers a potential strategy to enhance nanoparticle-based cancer therapies by overcoming the defense mechanisms of tumor cell sEVs. The findings not only deepen the understanding of sEVs' role in the tumor microenvironment but also provide valuable insights for developing new cancer treatment strategies.

OR-087

Engineered Macrophage Membrane-Mimicking Nanodrugs Activate the cGAS/STING Pathway to Reverse the Immune-Suppressive Microenvironment Induced by RFA

Weihua Zhang
Southeast university

Purpose Radiofrequency ablation (RFA) is a commonly used radical treatment for tumors, but its recurrence rate increases with larger tumor diameters. After sublethal thermal ablation, tumors often become more malignant and more resistant to conventional therapies. Our study aims to investigate the biological changes in tumors following sublethal thermal damage and the mechanisms behind their resistance, while developing a nanodrug to enhance treatment efficacy.

Materials and methods We developed a nanodrug composed of copper-doped ZIF-8 as a carrier, encapsulating TH-302 and β -lapachone within CCR2-overexpressing M1 macrophage membranes. We evaluated the drug's accumulation efficiency in tumors and its impact on macrophages. The activation of the HSP70/NRF2/NQO1 pathway, CCL2 secretion, and macrophage polarization were analyzed to assess tumor changes after sublethal thermal ablation.

Results Our findings demonstrated that tumors subjected to sublethal thermal damage showed significantly enhanced proliferation and migration abilities. The activation of the HSP70/NRF2/NQO1 pathway increased the antioxidant capacity of tumors, further contributing to their resistance against conventional therapies. Additionally, tumors secreted higher levels of CCL2, recruiting more macrophages and promoting their polarization to the M2 phenotype. Nanodrugs encapsulated within CCR2-overexpressing M1 macrophage membranes showed improved accumulation in tumors and reduced macrophage aggregation. Tumor-induced hypoxia, combined with oxygen consumption by β -lapachone, effectively activated the hypoxia-activated prodrug TH-302. This synergistically induced the production of reactive oxygen species (ROS), triggering the release of DAMPs and activation of the cGAS-STING pathway. The activation of this pathway recruited cDC1 to present tumor-associated antigens, promoting CD8⁺ T cell activation, reversing the immune microenvironment after ablation, and inhibiting the growth of residual cancer cells.

Conclusion The combination of β -lapachone and copper-doped ZIF-8 nanodrugs, activated by tumor-induced hypoxia, promotes ROS production and triggers the cGAS-STING pathway. This activation enhances CD8⁺ T cell responses, reverses the immune microenvironment post-ablation, and inhibits the growth of residual cancer cells

OR-088

Ablative Therapy for Residual Lesions After First-Line Treatment of Locally Advanced Unresectable Lung Adenocarcinoma: A Prospective, Randomized Controlled Study

Feng Xian, Guohui Xu
Sichuan Cancer Hospital

Purpose Residual lesions are frequently observed in patients with locally advanced unresectable lung adenocarcinoma after first-line treatment, with chemotherapy and targeted therapy being the main treatment options. However, recurrence rates remain high. This study aims to evaluate the efficacy and safety of combining ablative therapy with standard treatments for managing residual lesions.

Materials and methods Lung adenocarcinoma patients meeting the inclusion criteria and treated at Sichuan Cancer Hospital and Nanchong Central Hospital between October 2022 and December 2024 will be enrolled in this study. Patients without gene mutations will be randomly assigned to either the chemotherapy group or the chemotherapy combined with ablation group. Patients with gene mutations will be randomly assigned to either the targeted therapy group or the targeted therapy combined with ablation group. For gene-mutated patients who refuse or cannot tolerate targeted therapy, they will be assigned following the same method as patients without gene mutations. The primary endpoints will include overall survival (OS) and progression-free survival (PFS) rates at 6 months, 1 year, and 2 years, as well as complication rates. OS and PFS between groups will be compared using hazard ratios (HR) with 95% confidence intervals (CI), while the incidence of adverse events will be compared using risk ratios (RR) with 95% CI.

Results As of now, a total of 112 eligible patients with lung adenocarcinoma have been enrolled in this study. Among them, 71 patients had no gene mutations: 36 were assigned to the chemotherapy group (median age 55.7) and 35 to the chemotherapy combined with ablation group (median age 56). Forty-one patients had gene mutations: 22 were assigned to the targeted therapy group (median age 57.2) and 19 to the targeted therapy combined with ablation group (median age 55.7). In patients without gene mutations, the 1- and 2-year progression-free survival (PFS) rates were 62% and 59%, respectively, in the chemotherapy group, compared to 80% and 71% in the chemotherapy combined with ablation group. The hazard ratios (HR) for these groups were 0.44 (95% CI: 0.25-0.77, $p < 0.05$) and 0.30 (95% CI: 0.18-0.50, $p < 0.01$), respectively. In patients with gene mutations, the 1- and 2-year PFS rates were 77% and 63%, respectively, in the targeted therapy group, compared to 89% and 79% in the targeted therapy combined with ablation group. The HRs for these groups were 0.50 (95% CI: 0.42-0.60, $p < 0.01$) and 0.37 (95% CI: 0.31-0.45, $p < 0.01$), respectively. Additionally, one patient in the chemotherapy combined with ablation group experienced mild bleeding related to ablation, and two patients in the targeted therapy combined with ablation group developed mild coughing related to ablation, both of which resolved after treatment. The incidence of other adverse events did not differ significantly from the chemotherapy or targeted therapy groups ($p > 0.05$). Due to the limited number of cases, subgroup analysis based on whether patients received radiotherapy and the type of radiotherapy has not yet been performed. OS data has not yet been reached.

Conclusion The addition of ablative therapy significantly improves PFS in patients with locally advanced unresectable lung adenocarcinoma and residual lesions following first-line treatment, without increasing the incidence of adverse events.

OR-089

Does needle biopsy immediately after percutaneous microwave and cryoablation of lung neoplasm affect pathological results? A clinical and animal study

Junting Ma, Xudan Wang, Haibo Shao
First Hospital of China Medical University

Purpose To investigate whether needle biopsy immediately after percutaneous ablation of lung neoplasms affects pathological results.

Materials and methods A retrospective analysis was performed on patients who underwent single-procedure sequential ablation therapy and needle core biopsy for lung neoplasms. Differences in the pathological results of ablation and biopsy sequence and different ablation modalities were compared between groups to identify the factors affecting the pathological results. Animal experiments were performed to further verify the differences in tumor pathology before and immediately after ablation.

Results Sixty-nine patients who underwent intraprocedural percutaneous ablation and biopsy were divided into biopsy before ablation ($n = 28$), biopsy after microwave ablation (MWA, $n = 21$), and biopsy after cryoablation (CA, $n = 20$) groups, which had pathological diagnosis rates of 96.4%, 85.7%, and 85.0%, respectively ($p = 0.281$). The only factor affecting the pathological diagnosis was insufficient sample size ($p < 0.01$). Animal experiments showed that CK7, P63, and TTF-1 expression in the biopsy sample was reduced after MWA ($p = 0.025$, $p = 0.046$, and $p = 0.025$, respectively), while no significant difference in immunohistochemical results was found before and after CA. Epidermal growth factor receptor (EGFR) gene mutation was accurately detected in all samples biopsied after MWA and CA.

Conclusion Needle biopsy immediately post-ablation was accurate and dependable for the pathological diagnosis of lung neoplasm. Samples obtained by this method could still be used for genetic testing.

OR-090

Vaginal microbiome and metabolome profiles among HPV positive and HPV negative women based on stratification of vaginitis

Shuang Zhao, Aiming Lv, Sichen Zhang, Ying Hui, Weihong Qi, Xin Wang

Beijing Hospital, National Center of Gerontology, Institute of Geriatric Medicine, Chinese Academy of Medical Sciences

Purpose This study aimed to investigate the differences in vaginal microbiota and metabolism between HPV positive and HPV negative women based on the stratification of vaginitis.

Materials and methods This was a case-control study. A total of 164 women were included in this study analysis with a ratio of 1:3 for HPV positive and HPV negative women. The V3-V4 region of the 16S rRNA gene was amplified by polymerase chain reaction (PCR) followed by sequencing with Illumina. Untargeted metabolomic sequencing was conducted by the liquid chromatography-mass spectrometry (LC-MS) system. Specific microbial species and differentially expressed metabolites associated with these differences were explored.

Results We found that a statistically significant difference existed in the bacterial structure between HPV positive and HPV negative women ($R=0.2177$, $P=0.001$), and HPV positivity was associated with the enrichment of *Lactobacillus iners* among women diagnosed with vaginitis. However, this difference was not observed in women without vaginitis. Regarding metabolic differences, HPV positive women with vaginitis displayed elevated levels of organic acids and their derivatives, accompanied by decreased lipid levels in their vaginal secretions. Conversely, HPV positive women without vaginitis showed higher lipid levels and lower concentrations of organic acids and their derivatives. Among women with vaginitis, *Lactobacillus iners* was positively correlated with biogenic amine, organic acids and derivatives and negatively correlated with kessyl glycol. Among women without vaginitis, *Lactobacillus iners* was negatively correlated with pelargonic acid.

Conclusion The disparity in the abundance and metabolites of vaginal microbiota between HPV positive and HPV negative women could be affected by whether the woman has been diagnosed with vaginitis. Metabolic differences indicated that antioxidant therapy holds promising prospects for potential application in the management and treatment of HPV infections. Further in-depth research into the molecular mechanisms is crucial for clarifying the precise role that vaginal microbiota and metabolites play in HPV infection.

OR-091

Development and Functional Research of an Irradiation-Cytokine Composite Stent for Modulating Immune Microenvironment Reprogramming

Juan Qin, Duo Wang, Hai-Dong Zhu, Gao-Jun Teng
Zhongda Hospital, Medical School, Southeast University

Purpose Intraluminal irradiation stents utilizing ^{125}I seeds as a radiation source have been widely used for treating malignant luminal stenosis. While these irradiation stents have been shown to significantly reduce the incidence of stent restenosis in malignant luminal obstruction, tumor metastasis and recurrence remain major challenges in follow-up treatment. This is largely due to the formation of an immunosuppressive microenvironment in cancer patients, which weakens their anti-tumor immune response. To overcome these immunosuppressive barriers and enhance the therapeutic efficacy of radiotherapy, additional or combination immunotherapy is necessary.

Materials and methods This study utilized PLGA and PEO in varying ratios to develop a bilayer biodegradable polylactic acid-based drug delivery coating loaded with IL-12 cytokine, which was then applied to the surface of a ^{125}I seed-loaded stent. The coating's biocompatibility, tunable degradation, and drug release stability were systematically evaluated. Through in vitro and animal experiments, the safety and feasibility of ^{125}I irradiation therapy combined with in situ, sustained, low-dose IL-12 delivery were validated at molecular, cellular, and systemic levels. Additionally, in vivo experiments were conducted to assess the therapeutic efficacy of the composite stent in local tumor control, recurrence prevention, and metastasis inhibition.

Results The sequential degradation of the bilayer coating enabled localized IL-12 release, rapidly reaching an effective drug concentration and therapeutic window within 4 hours while maintaining a sustained and stable release over 14 days, ensuring IL-12 levels remained within the therapeutic range. Further characterization and testing, along with in vivo experiments, confirmed that the cytokine-internal radiation composite stent ($^{125}\text{I}@IL-12$), which integrates iodine-125 seed brachytherapy with localized low-dose cytokine immunotherapy, not only delivers targeted internal radiation to tumor cells but also facilitates the controlled release of IL-12. Acting as an adjuvant, IL-12 enhances the presentation of tumor cells and tumor antigen-derived peptides, stimulating an adaptive anti-tumor immune response. This induces an "in situ tumor vaccination" effect, generating both local and systemic anti-tumor immunity, increasing CD8⁺ T cell infiltration, reducing immunosuppressive cell populations, and effectively reversing tumor-induced immune suppression.

Conclusion This approach offers a new, effective, and safe treatment option for malignant luminal obstructions, such as esophageal cancer, extrahepatic cholangiocarcinoma, and portal vein tumor thrombus in liver cancer.

OR-092

Tailored Liposomal Nanomedicine Suppresses Incomplete Radiofrequency Ablation-Induced Tumor Relapse by Reprogramming Antitumor Immunity

Duo Wang

Zhongda Hospital, Southeast University

Purpose Radiofrequency ablation (RFA), a thermoablative treatment for small hepatocellular carcinoma (HCC), has limited therapeutic benefit for advanced HCC patients with large, multiple, and/or irregular tumors owing to incomplete RFA (iRFA) of the tumor mass.

Materials and methods It is first identified that iRFA-treated tumors exhibited increased pyruvate kinase M2 (PKM2) expression, exacerbated tumor immunosuppression featured with increased tumor infiltration of suppressive immune cells and increased proliferation, and programmed cell death ligand 1 expression of cancer cell and ultimately a poor prognosis.

Results Herein, a multifunctional nanomedicine is fabricated by encapsulating nanoassemblies of anti-PD-L1 and spermidine-grafted oxidized dextran with shikonin-containing lipid bilayers to reverse iRFA-induced treatment failure. Shikonin, a PKM2 inhibitor, is used to suppress glycolysis in cancer cells, while anti-PD-L1 and spermidine are introduced to collectively reprogram the proliferation and functions of infiltrated CD8⁺ T lymphocytes. Combined with iRFA, which promoted the exposure of tumor antigens, the intravenous injection of liposomal SPS-NPs effectively stimulated dendritic cell maturation and reversed tumor immunosuppression, thus eliciting potent antitumor immunity to synergistically suppress the growth of residual tumor masses and lung metastasis.

Conclusion The as-prepared liposomal nanomedicine is promising for potentiating the therapeutic benefits of RFA toward advanced HCC patients through reprogramming iRFA-induced tumor immunosuppression.

OR-093

Predictability of the short-term treatment response to Yttrium-90 transarterial radioembolization by pre-treatment cone-beam CT imaging-based radiomics analysis in patients with hepatic malignancy

Mingjie Tang¹, Haidong Zhu²

1. Southeast University

2. Center of Interventional Radiology & Vascular Surgery, Department of Radiology, Basic Medicine Research and Innovation Center of Ministry of Education, Zhongda Hospital, Medical School, Southeast University

Purpose To explore the feasibility of the application of pre-treatment cone-beam CT imaging-based radiomics in the prediction of short-term treatment response to transarterial radioembolization (TARE) in patients with hepatic malignancy, and to compare the efficacy of the traditional radiomics model, tumor habitat-derived radiomics model and combined model built on radiomics features and and clinical features

Materials and methods In this IRB-approved retrospective single-center study 48 patients with a total of 85 malignant hepatic tumors (40 HCC and 45 liver metastases) underwent CBCT prior to TARE and follow-up imaging after therapy. Treatment response was evaluated according to mRECIST version 1.1(for HCC) and RECIST version 1.1(for liver metastases) and dichotomized into responders (complete response/partial response) versus non-responders (stable disease/progressive disease). Subsequently, traditional radiomics model, tumor habitat-derived radiomics model and a combined model of the radiomics score (rad-score) and clinical features for each sequence were generated and compared between the groups.

Results For HCC, the radiomics models showed good discriminatory ability with an area under the curve (AUC) of 0.824 [95% confidence interval (CI), 0.684–0.927] for the traditional radiomics model, AUC of 0.867 (95% CI, 0.716–0.968 for the tumor habitat-derived radiomics model, and AUC of 0.883 (95% CI, 0.750-0.975) for the combined model.

For liver metastases, the radiomics models showed good discriminatory ability with an area under the curve (AUC) of 0.805 (95% CI, 0.704-0.918) for the traditional radiomics model, AUC of 0.884 (95% CI, 0.803–0.975 for the tumor habitat-derived radiomics model, and AUC of 0.914 (95% CI, 0.823-0.993) for the combined model.

Conclusion Traditional radiomics models created by pre-treatment CBCT can predict the short-term response to Yttrium-90 TARE in hepatic malignancy patients with good accuracy. Habitat-derived radiomics models outperforms traditional radiomics models, as evidenced by higher accuracy and statistically significant improvements. In this study, combining radiomics with clinical features couldn't increase the power of the test. Large-scale studies of pre-treatment CBCT with internal and external validations are needed to determine the clinical value of radiomics in hepatic malignancy patients.

OR-094

The status of cytotoxic lymphocytes indicate therapeutic efficacy and prognosis in patients with advanced hepatocellular carcinoma undergoing transarterial chemoembolization combined with systemic therapies

Hai-Feng Zhou, Zhi-Hui Hong, Fei-Da Wu, Wei Yang, Wei-Zhong Zhou, Sheng Liu, Hai-Bin Shi
The First Affiliated Hospital of Nanjing Medical University

Purpose To identify key cellular statuses and easily accessible biomarkers prior to transarterial chemoembolization (TACE) combined with tyrosine kinase inhibitors (TKIs) and immune checkpoint inhibitors (ICIs) in patients with advanced hepatocellular carcinoma (aHCC) for predicting therapeutic efficacy and prognosis.

Materials and methods In patients with aHCC, we analyzed the cellular components in both tumor and peritumoral tissues prior to TACE combined with TKIs and ICIs, aiming to identify key cellular statuses associated with favorable treatment responses. The Cox regression analyses were conducted on peripheral lymphocyte subsets to determine predictors of overall survival (OS). The area under the curves (AUCs) was utilized to evaluate the predictive performance of OS at 12, 18, and 24 months.

Results Among two patients with aHCC who exhibited favorable responses to TACE plus the TKI (apatinib) and the ICI (carlizumab), we observed that tumor tissues contained a higher frequency of CD8⁺ effector T cells, and a lower frequency of CD4⁺ regulatory T cells and CD8⁺ exhausted T cells compared to peritumoral tissues. In a cohort of 41 patients with aHCC undergoing TACE combined with TKIs and ICIs, the Cox regression analyses indicated that the total T cell percentage, the percentages of cytotoxic T cells, the natural killer (NK) cell percentage, and the CD4⁺/CD8⁺ T cell ratio were significant predictors of OS. Notably, the AUCs for total T cell percentage and NK cell percentage exceeded 0.75 for predicting OS at 12, 18, and 24 months.

Conclusion The activation of CD8⁺ T cells within HCC tumor tissues is indicative of favorable treatment responses in patients with aHCC undergoing TACE plus TKIs and ICIs. Furthermore, the total T cell percentage and NK cell percentage in peripheral blood demonstrate strong predictive capabilities for medium- and long-term prognosis.

OR-095

Comparative Effectiveness of Liquid versus Solid Embolic Agents in Pre-surgical Embolization for Intracranial Tumors: A Systematic Review and Meta-analysis

Yi Zhang

Southeast University Affiliated Zhongda Hospital

Purpose To compare the impacts of the selection of solid embolization materials and the selection of liquid embolization materials during the preoperative embolization of intracranial tumors.

Materials and methods This meta-analysis collects relevant articles from January 1975 to September 2024 were included. Meta-analysis was conducted using the average operation duration and estimated blood loss. Heterogeneity was also evaluated.

Results A total of 7 retrospective studies were included, in which a total of 361 patients met the criteria and were thus included. There were 220 female patients, accounting for 60.9%. The patients were divided into the liquid embolization group and the solid embolization group. We discovered that during the preoperative embolization of intracranial tumors, the selection of liquid embolization materials, as compared with that of solid materials, did not have a significant influence on the intraoperative blood loss (MD = -5.30, 95% confidence interval [CI] -54.78 — 44.18). Additionally, in terms of the impact on surgical operation time, no significant statistical difference was observed between the two groups either (MD = -98.49, 95% confidence interval [CI] -289.75 — 92.76).

Conclusion The current meta-analysis reveals that, in patients undergoing preoperative embolization of intracranial tumors, there is no significant statistical difference in the surgical resection of intracranial tumors among different preoperative embolization materials during subsequent tumor resection procedures. The selection of preoperative embolization materials for intracranial tumors cannot serve as a determinant factor influencing the expected degree of blood loss and surgical duration. The decision regarding preoperative embolization still necessitates individualized diagnosis and treatment.

OR-096

A study on the Contribution of LSM11 to the Outcome of Radiotherapy in Hepatocellular Carcinoma Cells

Wenyi Jiang, Weihu Wang
Peking University Cancer Hospital

Purpose This study aims to deeply explore how the LSM11 gene regulates the cellular stress response in hepatocellular carcinoma cells upon radiation stimulation, and the potential molecular mechanisms by which this regulation affects the radiotherapy effect.

Materials and methods Firstly, the CRISPR technology was utilized to construct a genome-wide knockout hepatocellular carcinoma cell line. These cells were inoculated subcutaneously in nu/nu mice to establish a tumor-bearing mouse model, which was then divided into a radiation group and a non-radiation group. One week later, the tumor tissues were excised, and the genomes were extracted for high-throughput sequencing. Through data analysis, the key gene LSM11, which showed significantly differential expression under radiation conditions, was successfully screened out. To further clarify the function of LSM11, LSM11 gene knockdown and overexpression hepatocellular carcinoma cell lines were constructed. A variety of cell biology techniques such as the MTT assay, cell apoptosis detection, cell cycle analysis, scratch assay, and Transwell assay were used to systematically detect the effects of LSM11 on the phenotypes of hepatocellular carcinoma cells, including proliferation, apoptosis, cell cycle progression, migration, and invasion ability. Meanwhile, by means of the single-hit multi-target model, micronucleus assay, comet assay, etc., the regulatory effects of LSM11 on the proliferation ability, apoptosis level, and chromatin stability of hepatocellular carcinoma cells after radiation treatment were deeply explored. In terms of mechanism research, the Western blot technique was used to detect the expression levels of related proteins, and combined with the ROS flow cytometry detection technique, the signal pathways and molecular mechanisms by which LSM11 participates in regulating the radiation stress response of hepatocellular carcinoma cells were analyzed. In addition, in vivo animal experiments were carried out to verify the effect of LSM11 on the radiation stress response of hepatocellular carcinoma cells at the whole animal level. Finally, using the organoid model, an LSM11 siRNA transient transfection experiment was carried out to evaluate the regulatory effect of LSM11 on the radiation stress response at the level of hepatocellular carcinoma tissue and explore the possibility of its clinical translation and application.

Results The experimental results showed that LSM11 gene knockdown significantly inhibited the proliferation, migration, invasion, and colony formation ability of hepatocellular carcinoma cells, and at the same time promoted cell apoptosis, resulting in cell cycle arrest in the G2/M phase, and causing increased chromatin instability and DNA damage. In contrast, LSM11 gene overexpression had no significant effect on the above phenotypes of hepatocellular carcinoma cells. Further research found that LSM11 gene knockdown could upregulate the expression of PMP70 protein, prompting peroxisomes in hepatocellular carcinoma cells to generate more reactive oxygen species (ROS), weakening the radiation stress regulation ability of hepatocellular carcinoma cells, and thus enhancing the killing effect of radiotherapy on hepatocellular carcinoma cells. The results of in vivo animal experiments were highly consistent with those of in vitro cell experiments, further verifying the important role of LSM11 in the radiotherapy of hepatocellular carcinoma. The organoid model experiment provided strong evidence for the transformation from basic research to clinical application of LSM11.

Conclusion This study for the first time reveals the key role of LSM11 in the radiation stress regulation of hepatocellular carcinoma cells. LSM11 promotes the stress regulation response of hepatocellular carcinoma cells under radiation conditions by negatively regulating the expression of PMP70 and reducing the generation of ROS by peroxisomes. It is worth noting that LSM11 is not a traditional oncogene, and its high expression does not enhance the radiotherapy resistance of hepatocellular carcinoma cells. The results of this study indicate that LSM11 is an important node gene in the stress regulation network of hepatocellular carcinoma cells and is expected to become a new potential therapeutic target for the clinical radiotherapy of hepatocellular carcinoma, providing a new theoretical basis and research ideas for the optimization of radiotherapy strategies for hepatocellular carcinoma.

OR-097

Complications of Interventional Treatment for Vascular Tumors and Vascular Malformations: Mechanisms of Occurrence, Treatment Strategies and Prevention

Qi Wang

Department of Interventional Radiology, Guangdong Provincial People's Hospital (Guangdong Academy of Medical Sciences), Southern Medical University, Guangzhou 510080, China

Purpose This study aimed to evaluate the incidence, mechanisms, and clinical management of complications following interventional therapy for vascular anomalies including vascular tumors and malformations, with a focus on establishing preventive strategies to enhance procedural safety.

Materials and methods A retrospective cohort analysis was conducted on 1,592 consecutive interventional procedures performed between January 2021 and December 2024. The cohort included three categories: infantile hemangiomas treated with arterial embolization using pingyangmycin-lipiodol-particle emulsion (163 cases), venous malformations (VM) managed by ethanol or foam sclerotherapy (1,016 cases), and arteriovenous malformation (AVM) treated with embolization and ethanol sclerotherapy (413 cases). Complications were categorized as skin injury or tissue/organ necrosis. Data on procedural techniques, imaging guidance, and clinical outcomes were systematically analyzed.

Results Complications occurred in 3.07% (5/163) of vascular tumors, primarily attributed to reflux of the pingyangmycin-lipiodol emulsion into normal arteries. Skin injury (4 cases) resolved with conservative wound care, while one case of extensive tissue necrosis necessitated plastic surgical.

Skin injury was observed in 8.07% (82/1,016) of sclerotherapy procedures of venous VM. Tissue necrosis occurred in 0.89% (9/1,016), with two distinct etiologies: wet gangrene secondary to ethanol extravasation into interstitial tissues (6 cases) and dry gangrene due to accidental arterial injection or ethanol reflux through arteriovenous shunts (3 cases). Three out of the nine patients with tissue necrotic lesions required plastic surgical intervention.

The complication rate reached 6.05% (25/413) for skin injury and 2.18% (9/413) for tissue/organ necrosis of AVMs. Necrosis associated with sclerosing agents (7 cases) predominantly resulted from overdosage or extra-arterial leakage, with two cases requiring plastic surgical intervention.

Super-selective embolization combined with strict emulsion dosage control reduced complications in vascular tumors. The double needle technique can significantly reduce the incidence of wet gangrene in VM. Prior to the injection of sclerosing agents, it is necessary to make sure the puncture needle is not located within the arterial lumen. For AVMs, real-time fluoroscopic monitoring and staged therapy with limited ethanol dosage (<1 mL/kg/session) mitigated toxicity risks.

Conclusion The principal factor leading to complications is the infiltration of embolic or sclerosing agents into normal tissues or the feeding arteries to normal tissue. Standardized treatment protocols, along with the judicious selection of appropriate sclerosing and embolic agents is crucial. Notably, AVMs exhibit a markedly higher incidence of treatment related complications. Consequently, there is an even greater need to promote and implement standardized treatment approaches to enhance the safety and effectiveness of treatment for this condition.

OR-099

Whether the choice of location for re-implantation chest port affects the incidence of complications in adult tumor patients undergoing right chest port removal WANG

Caoye Wang

Changzhou First People's Hospital

Purpose To compare the choice of re-implantation chest port and the incidence of complications in adult tumor patients who had undergone right chest port removal.

Materials and methods 180 adult patients with right chest port extraction history were retrospectively analyzed. Of these, 120 patients were re-implanted on the right side (right group) and 60 patients were re-implanted on the left side (left group). The median time between removal of the first port and placement of the second port was 235 days (range 0-3612 days). Body-related complications include infection (port implant site and/or blood flow), mechanical damage, thrombosis, and skin complications at port site. The incidence of complications was compared between the two groups. PSHREG was used to determine whether the location of port replanting was an independent risk factor for port-related complications.

Results The cumulative follow-up period was 31187 catheter days (median follow-up period 253 days). There were 22 patients (18.3%) in the right group and 4 patients (6.7%) in the left group ($P=0.24$), accounting for 0.6 and 0.3/1000 catheter days of the overall complication rate, respectively ($P=0.23$). There was no significant difference in the incidence of infection between the two groups (18/120 vs 2/60, $P=0.17$), mechanical damage (0/120 vs. 2/60, $P=0.35$), thrombosis (2/120 vs. 0/60, $P=1.1$), and skin-related complications (2/120 vs. 0/60, $P=1.1$). In multivariate PSHREG, the lateral position of replanting ($HR=3.12$, $95\%CI=0.85-12.16$, $P=0.13$) was not a significant risk factor for the occurrence of port-related complications.

Conclusion There is no significant difference in the incidence of complications between left and right side re-implantation in adult tumor patients who have received right side port removal.

OR-100

Radioactive iodine-125 particle implantation combined with transarterial chemoinfusion and synchronous immune checkpoint inhibitors for the management of locally advanced pancreatic cancer: a retrospective single-center analysis

Bin Li
Beijing Hospital

Purpose The aim of this study was to evaluate the clinical efficacy of radioactive iodine-125 particle implantation in combination with transarterial chemoinfusion (TAI) and synchronous immune checkpoint inhibitors (ICIs) for the management of locally advanced pancreatic cancer (LAPC).

Materials and methods We conducted a retrospective analysis of 10 LAPC patients treated with radioactive iodine-125 particle implantation and TAI synchronous ICIs from January 2021 to January 2024. Local tumor response was evaluated according to the mRECIST criteria. The study recorded the technical success rate, adverse events (AEs) and complications during treatment, objective response rate (ORR), disease control rate (DCR), and patient survival.

Results All patients successfully underwent CT-guided percutaneous radioactive iodine-125 particle implantation with a prescribed dose of 110-130 Gy, achieving a technical success rate of 100%. Following implantation, all patients received TAI and synchronous ICIs one week later. Chemotherapy regimens included gemcitabine plus raltitrexed in six cases, albumin-bound paclitaxel in four cases, and immunotherapy regimens included tilibulinumab in five cases, sintilimab in three cases, and davunilibab in one case. Follow-up duration ranged from 6 to 12 months, with a median survival period of 9.5 months. According to mRECIST criteria, the ORR was 60% and 50% at 3- and 6-months post-procedure, the DCR was 80% and 70%, respectively. AEs and complications were manageable and resolved with symptomatic treatment, and no treatment-related mortality occurred.

Conclusion Radioactive iodine-125 particle implantation in combination with TAI and synchronous ICIs represents a safe and efficacious integrated treatment approach for LAPC. While the findings are promising, they are derived from a retrospective analysis with a limited patient cohort. Future studies involving larger, prospective, and multicenter trials are warranted to validate these results and further explore the potential of this treatment strategy in LAPC management.

OR-101

Outcomes of First-Line Microwave Ablation of Treatment-Naive Epidermal Growth Factor Receptor–Mutated Advanced Lung Adenocarcinoma Treated with Tyrosine Kinase Inhibitors

Xu Sheng

Beijing Hospital, National Center of Gerontology

Purpose To investigate the outcomes of first-line image-guided microwave ablation (MWA) plus tyrosine kinase inhibitors (TKIs) in untreated epidermal growth factor receptor (EGFR)–mutant advanced lung adenocarcinoma (LUAD) and to compare with TKIs alone.

Materials and methods This retrospective cohort study included patients between December 2015 and December 2021 and was divided into 2 groups (Group A: first-line MWA+TKIs; Group B: TKIs alone). Progression-free survival (PFS) was the primary end point, whereas overall survival (OS) was the secondary end point and were compared via the Kaplan–Meier methods. Univariate and multivariate analyses were used to investigate the predictors of PFS and OS. Propensity score matching (1:1 ratio) was applied between Group B and the subgroup of complete ablation in Group A.

Results A total of 117 patients were included (Group A: $n = 43$; Group B: $n = 74$). In a mean follow-up of 47.0 months ($SD \pm 19.4$), Group A had significantly longer median PFS (19.0 vs 10.0 months; $P < .001$) and OS (41.0 vs 25.0 months; $P = .044$) than Group B. Predictors of PFS included first-line MWA ($P < .001$) and tumor stage ($P = .020$), while that of OS included first-line MWA ($P = 0.039$), tumor stage ($P = 0.014$), and usage of third-generation TKIs ($P = 0.001$). There were 23 pairs of patients obtained after propensity score matching (Group A1: complete ablation+TKIs; Group B1: TKIs alone). Group A1 had significantly longer median PFS (24.0 vs 10.0 months; $P < .001$) and OS (48.0 vs 24.0 months; $P = .012$) than Group B1.

Conclusion First-line MWA significantly improved the outcomes of patients with untreated EGFR-mutant advanced LUAD treated with TKIs. Complete ablation predicted a better prognosis.

OR-102

Efficacy Comparison of Liver Venous Deprivation and TACE Combined with Targeted and Immunotherapies in Unresectable Hepatocellular Carcinoma with Insufficient FLR Volume

Ying Yang, Chang Liu, Hong Wu

Department of General Surgery, West China Hospital, Sichuan University, Chengdu 610041, China; Liver Transplant Center, Transplant Center, West China Hospital, Sichuan University

Purpose To compare the efficacy of liver venous deprivation (LVD) with transcatheter arterial chemoembolization (TACE) combined with targeted and immunotherapies (TACE+T+I) in patients with unresectable hepatocellular carcinoma (HCC) due to insufficient future liver remnant (FLR) volume.

Materials and methods This single-institution retrospective study included 92 patients with unresectable HCC due to insufficient FLR volume who underwent LVD or TACE+T+I between December 2019 and December 2022. Propensity score matching (PSM) was used to balance baseline characteristics. The primary outcomes were conversion resection rates and time from intervention to surgical resection. Secondary outcomes included surgical treatment outcomes and postoperative complications.

Results Before PSM, the successful conversion hepatectomy rate was significantly higher in the LVD group (75.00%) compared to the TACE+T+I group (48.33%) ($p = 0.014$). After PSM, the conversion rate remained higher in the LVD group but the difference was not statistically significant (75.00% vs. 56.25%, $p = 0.114$). The median time from intervention to hepatectomy was significantly shorter in the LVD group (39 days) compared to the TACE+T+I group (122 days) ($P < 0.001$). Intraoperative blood loss was significantly lower in the LVD group (250 mL vs. 550 mL; $P = 0.005$). No significant differences were observed in operation duration, intraoperative blood transfusion, surgical type, postoperative stay, R0 resection rate, postoperative complications, or severe postoperative complications between the two groups.

Conclusion LVD demonstrated a higher conversion rate and shorter time to surgery compared to TACE+T+I in patients with unresectable HCC due to insufficient FLR volume. Both treatments had comparable safety profiles. Further prospective studies are needed to confirm these findings.

OR-103

Autocatalytic pyroptosis agonists modulate tumor metabolism and enhance TACE efficacy in HCC therapy

Lin-Zhu Zhang, Hai-Dong Zhu
Zhongda Hospital, Southeast University

Purpose Hepatocellular carcinoma (HCC) is characterized by an immunosuppressive tumor microenvironment (TME) that limits therapeutic efficacy [1]. Pyroptosis, a novel form of programmed cell death, has been shown to enhance anti-tumor immunity. However, inducing effective pyroptosis to reverse the immunosuppressive TME remains challenging [2]. Metabolic modulation therapy offers significant therapeutic benefits with minimal side effects. Glycolysis, the predominant form of glucose metabolism in tumors, can enhance the efficacy of immune checkpoint inhibitors when its activity is increased [3]. Here, we developed a glucose oxidase (GOx)-loaded CoF₂ nanoparticles (NPs) enzyme-activated pyroptosis inducer (GOCO₂) to modulate hepatic glucose metabolism and synergistically induce pyroptosis. This agent was combined with lipiodol to form a Pickering emulsion, thereby enhancing the therapeutic outcomes of transarterial chemoembolization (TACE) in HCC.

Materials and methods CoF₂ NPs were synthesized by thermal decomposition and a high-temperature oil-phase method, and were self-assembled with Gox to form GOCO₂ after modification with DSPE-PEG2000-NH₂. The chemical composition and crystal structure of the samples were characterized by X-ray diffraction (XRD). Flow cytometry was used to detect reactive oxygen species (ROS), cell death, and immune response, and laser confocal microscopy was used to observe the morphology of pyroptotic cells. RNA-seq was used to analyze potential therapeutic mechanisms. Glucose content in cells was assessed using a commercial glucose assay kit. SD rats and BALB/c mice were used as model animals, and small animal magnetic resonance imaging and in vivo imaging were performed to observe the tumor inhibitory effect of GOCO₂.

Results GOCO₂ NPs, synthesized via high-temperature thermal decomposition, effectively induced pyroptosis in H22 cells by depleting glucose and generating ROS. This mechanism was validated through XRD, flow cytometry, and western blot analysis (Fig. A-G). In vivo studies using H22 tumor-bearing mice demonstrated that GOCO₂ treatment significantly inhibited tumor growth, outperforming the effects of GOx or CoF₂ alone (Fig. H&I). Furthermore, GOCO₂ promoted dendritic cell (DC) maturation and enhanced CD8⁺ T cell infiltration within the tumor microenvironment, thereby bolstering antitumor immunity (Fig. J&K). RNA transcriptome analysis revealed significant enrichment of inflammatory and metabolic pathways, indicating the induction of tumor pyroptosis and metabolic reprogramming following treatment (Fig. L). Additionally, GOCO₂ augmented the therapeutic efficacy of TACE in a rat orthotopic liver cancer model, underscoring its potential for interventional therapy (Fig. M). These findings underscore the dual role of GOCO₂ in modulating tumor metabolism and immune responses, offering a promising strategy for enhancing cancer treatment.

Conclusion This study proposes an innovative inorganic nanozyme strategy to regulate tumor glucose metabolism, inducing cancer cell pyroptosis and enhancing immunotherapy. GOCO₂, a pyroptosis inducer, reverses the immunosuppressive tumor microenvironment by inhibiting glucose metabolism, offering a novel approach to bioactive material design. Additionally, GOCO₂ demonstrates potential in TACE therapy for liver cancer, providing an alternative to traditional TAE or TACE treatments, thus advancing cancer therapeutic strategies.

OR-104

Microwave Ablation Versus Lobectomy for Ground-Glass Opacity Nodules in the Hilar Region: A Multicenter Prospective Real-World Study on Efficacy and Safety

Jiachang Chi, Wangrui Liu
Thoracic Surgery

Purpose Ground-glass opacities (GGOs) in the lung, particularly in the hilar region, are increasingly detected and present unique management challenges. While lobectomy remains the standard treatment, microwave ablation (MWA) has emerged as a minimally invasive alternative for high-risk patients. This multicenter, prospective study compared the efficacy and safety of MWA and lobectomy in treating hilar GGOs

Materials and methods A total of 100 patients with GGOs ($\leq 50\%$ solid components) were enrolled across five tertiary centers and allocated to MWA ($n=50$) or lobectomy ($n=50$) based on clinical evaluation and patient preference. The primary endpoint was 3-year recurrence-free survival (RFS). Secondary endpoints included complication rates, postoperative recovery, hospital stay, costs, and quality of life (QoL). Kaplan-Meier analysis was performed for survival outcomes, and Cox regression adjusted for confounders.

Results At 36 months, the 3-year RFS was 88% in the MWA group and 90% in the lobectomy group (HR: 1.10, 95% CI: 0.72–1.45; $P = 0.68$), demonstrating non-inferiority. Subgroup analysis showed comparable RFS for GGOs ≤ 2 cm (90% vs. 92%; $P = 0.77$). Among high-risk patients (age >65 or with comorbidities), MWA demonstrated superior outcomes (3-year RFS: 85% vs. 78%).

MWA had significantly fewer complications (12% vs. 30%; $P < 0.01$), including lower rates of pneumothorax (6% vs. 20%) and infections (2% vs. 10%). Recovery was faster with MWA (7 vs. 20 days; $P < 0.01$), with shorter hospital stays (2.5 vs. 7.5 days; $P < 0.01$) and 30% lower treatment costs. QoL scores 1 month post-treatment were higher in the MWA group (85/100 vs. 72/100), with less long-term respiratory impairment (2% vs. 15%).

Conclusion MWA is a safe and effective alternative to lobectomy for hilar GGOs, achieving comparable 3-year RFS with fewer complications, faster recovery, and lower costs. These findings highlight MWA as a minimally invasive strategy for early-stage lung cancer, particularly for high-risk patients, and support its broader adoption in clinical practice.

OR-105

In which tumor burden range does hepatic arterial infusion chemotherapy combined with tyrosine kinase inhibitors and immune checkpoint inhibitors perform better than the combination of tyrosine kinase inhibitors and immune checkpoint inhibitors? A comparative analysis of their efficacy and safety in advanced-stage hepatocellular carcinoma patients with portal vein tumor thrombus, using propensity score matching

Jiaxi Liu, Haibo Shao
The First Hospital of China Medical University

Purpose Advanced-stage hepatocellular carcinoma (HCC) is typically linked to unfavorable survival rates. Rapid tumor control typically enhances long-term outcomes, which is challenging to attain by systematic targeted therapy and immunotherapy alone, as per current guidelines. In this study, a propensity score matching (PSM) was performed to compare the survival outcomes, efficacy, and safety of hepatic arterial infusion chemotherapy (HAIC) combined with tyrosine kinase inhibitors (TKIs) and immune checkpoint inhibitors (ICIs) (H+T+I) versus TKIs combined with ICIs alone (T+I) in various tumor burden ranges in advanced HCC patients with portal vein tumor thrombus (PVTT).

Materials and methods This retrospective multicenter study screened advanced HCC patients who received T+I combination therapy with or without HAIC treatment at three centers from January 2021 to December 2023. The inclusion criteria included PVTT, no extrahepatic metastasis, and liver function of Child-Pugh B7 or better. Antitumor efficacy was evaluated by comparing overall survival (OS), progression-free survival (PFS), and objective response rate (ORR) between the two groups across different tumor burden populations divided by up to eleven criteria and tumor burden score (TBS). Safety was assessed by comparing adverse events (AEs) between the groups. PSM was performed to balance baseline characteristics between the two groups.

Results A total of 97 patients were included in this analysis; among them, 51 patients were treated with H+T+I, while 46 patients were treated with T+I. After PSM, 36 patients were included in each group. In the primary cohort, H+T+I significantly extended overall OS (23.4 vs. 10.8 months, HR = 0.46, P = 0.005), as well as OS in patients with tumor burdens up to 11 out (25.0 vs. 7.0 months, HR = 0.34, P = 0.001) and those classified as low and medium TBS (25.0 vs. 14.4 months, HR = 0.46, P = 0.024). Furthermore, H+T+I significantly prolonged overall PFS (10.0 vs. 5.2 months, HR = 0.58, P = 0.018), PFS for intra-hepatic lesions (11.4 vs. 5.7 months, HR = 0.57, P = 0.019), PVTT (23.4 vs. 9.3 months, HR = 0.40, P < 0.001), and extrahepatic lesions (12.9 vs. 8.0 months, HR = 0.55, P = 0.016). Compared to T+I, H+T+I significantly improved the ORR for intra-hepatic lesions (62.7% vs. 26.1%, P = 0.001), PVTT (64.7% vs. 15.2%, P < 0.001), and overall (60.8% vs. 21.7%, P < 0.001). In the propensity score-matched (PSM) cohort, H+T+I also significantly extended overall OS, as well as OS in patients with tumor burdens up to 11 out and those classified as low and medium TBS (see figure). Additionally, H+T+I significantly prolonged overall PFS (10.8 vs. 3.3 months, HR = 0.50, P = 0.008), PFS for intrahepatic lesions (11.4 vs. 4.8 months, HR = 0.51, P = 0.013), PVTT (23.4 vs. 7.7 months, HR

= 0.39, $P = 0.003$), and extrahepatic lesions (12.7 vs. 8.0 months, $HR = 0.47$, $P = 0.006$). Compared to T+I, H+T+I significantly increased ORR for intra-hepatic lesions (55.6% vs. 22.2%, $P = 0.004$), PVTT (61.1% vs. 11.1%, $P < 0.001$), and overall (55.6% vs. 22.2%, $P = 0.004$). Multivariate analysis indicated that treatment regimen, AFP levels, and the number of intra-hepatic lesions were independent factors influencing both PFS and OS, while direct bilirubin was an independent factor influencing PFS. Regarding AEs, only leukopenia and thrombocytopenia occurred more frequently in the H+T+I group than in the T+I group; overall, adverse events were manageable.

Conclusion In comparison to T+I treatment, H+T+I significantly prolongs both PFS and OS while also improving the ORR, without significantly increasing the incidence of AEs. In advanced HCC patients with PVTT and tumor burden up to 11 out, H+T+I provides greater clinical benefit than T+I. Therefore, further investigation is necessary to determine the efficacy and safety of HAIC in combination with TKIs and ICIs for patients with high tumor burden.

Injectable Hydroxyapatite Radiopaque Microspheres: The Next-Generation Material for Cancer Interventional Embolization?

Yinan Ding¹, Yi Jiang¹, Chao-Yi Qian¹, Bin-yan Zhong¹, Peng-tao Chen², Xiao-xia Wu¹, Chuan Hu¹, Kun Chen¹, Jia-ping Zheng¹, Xu-feng Ni³, Jun Ling³

1. Zhejiang Cancer Hospital

2. Wenzhou Medical University

3. Zhejiang University

Purpose To develop and evaluate $\text{HA}_\text{H}\text{-HAP}_\text{I}@\text{HA}_\text{L}$, a novel visual embolization microsphere, this study used HAP as the core, coated with two layers of HA of different MWs. $\text{HA}_\text{H}\text{-HAP}_\text{I}@\text{HA}_\text{L}$ aims to overcome limitations of current embolization microspheres by enhancing biocompatibility and X-ray imaging. Additionally, TXA incorporation promotes local autologous thrombus formation, enhancing embolization and reducing recanalization risk.

Materials and methods The preparation of injectable HAP microspheres includes dissolving HA_H , loading HAP with iopromide (HAP_I), adsorbing HA_H onto HAP_I ($\text{HA}_\text{H}\text{-HAP}_\text{I}$), mixing with HA_L to form a dry powder, and reconstituting it with water ($\text{HA}_\text{H}\text{-HAP}_\text{I}@\text{HA}_\text{L}$). Characterization involved optical microscopy, SEM, and EDS for morphology, size, and chemical composition. LSCM confirmed HA_H adsorption. Settling time and iodine concentration were monitored by ICP-MS. Degradation of HA was assessed by outflow time and viscosity number measurement. CT and DSA evaluated X-ray visualization, with DSA confirming imaging stability. Renal embolization was validated by DSA, CT, and DSA reassessment post-surgery, followed by dissection and microscopic observation. Biosafety was verified by measuring serum levels and plasma parameters, and microscopic examination of rabbit organs.

Results Characterization of $\text{HA}_\text{H}\text{-HAP}_\text{I}@\text{HA}_\text{L}$

Research designed visualizable embolization microspheres based on hydroxyapatite (HAP) (Figure 1A) and tested their characteristics. Figure 1B shows minimal changes in shape and size (80-120 μm) before and after modification. Figure 1C demonstrates FITC-labeled hyaluronic acid coated on HAP microspheres. SEM observation confirmed similar shapes and sizes (Figure 1D). EDS testing found iodine in $\text{HA}_\text{H}\text{-HAP}_\text{I}$, indirectly confirming successful encapsulation (Figure 1E). ICP-MS revealed iodine mass fraction in $\text{HA}_\text{H}\text{-HAP}_\text{I}$ as 3.7wt%. Sedimentation rates compared: HAP stratified rapidly, $\text{HA}_\text{H}\text{-HAP}_\text{I}$ within 1 minute, $\text{HA}_\text{H}\text{-HAP}_\text{I}@\text{HA}_\text{L}$ after 10 minutes (Figure 1F), facilitating uniform accumulation in target blood vessels. Figure 1G and 1H show $\text{HA}_\text{H}\text{-HAP}_\text{I}@\text{HA}_\text{L}$ passing smoothly through needles and microcatheters, paving the way for in vivo experiments. Figure 1I shows stable viscosity of HA_H but significant decrease and stabilization of HA_L within 7 days, indicating rapid degradation.

The visualization effect of $\text{HA}_\text{H}\text{-HAP}_\text{I}@\text{HA}_\text{L}$

The visualization of microspheres is crucial and urgently needs addressing. Figure 2A showed iodine-free $\text{HA}_\text{H}\text{-HAP}_\text{I}@\text{HA}_\text{L}$'s DSA effect was slightly better than pure water. To enhance this, 3.7wt% iodine contrast agent was attached to HAP, significantly improving DSA visualization of 30% iodine $\text{HA}_\text{H}\text{-HAP}_\text{I}@\text{HA}_\text{L}$ (Figure 2B). Large-volume (800 μL) $\text{HA}_\text{H}\text{-HAP}_\text{I}@\text{HA}_\text{L}$ showed significant DSA effect in a syringe. Liver visualization was simulated by injecting $\text{HA}_\text{H}\text{-HAP}_\text{I}@\text{HA}_\text{L}$ into an excised pig liver (Figure 2C). Good visualization stability over seven days was evaluated (Figure 2D). Comparable CT visualization effects among different mass fractions of $\text{HA}_\text{H}\text{-HAP}_\text{I}@\text{HA}_\text{L}$ were observed in vitro (Figure 2E). In vivo experiments showed clear DSA visualization after injecting $\text{HA}_\text{H}\text{-HAP}_\text{I}@\text{HA}_\text{L}$ into rabbit kidneys (Figure 2F). One week post-

surgery, CT imaging revealed high-density shadows, proving long-term embolization and CT visualization (Figure 2G). These results confirm $\text{HA}_\text{H}\text{-HAP}_\text{I}@\text{HA}_\text{L}$'s X-ray visualization, addressing issues with current embolization microspheres.

Evaluation of Embolization Effectiveness and Safety of Visualizable Embolization Microspheres Based on Hydroxyapatite Combined with TXA ($\text{HA}_\text{H}\text{-HAP}_\text{I}@\text{HA}_\text{L}@\text{TXA}$):

The embolization effect of $\text{HA}_\text{H}\text{-HAP}_\text{I}@\text{HA}_\text{L}@\text{TXA}$ is crucial. We first applied to the kidney. Post-injection dissection revealed microspheres only in the embolized right renal artery (Figure 3A). One week later, the embolized right kidney showed necrosis, contrasting with the healthy left kidney (Figure 3B). CT imaging showed high-density casting in embolized vessels of the $\text{HA}_\text{H}\text{-HAP}_\text{I}@\text{HA}_\text{L}$ and $\text{HA}_\text{H}\text{-HAP}_\text{I}@\text{HA}_\text{L}@\text{TXA}$ groups, confirming microsphere presence (Figure 3C). TXA addition in $\text{HA}_\text{H}\text{-HAP}_\text{I}@\text{HA}_\text{L}@\text{TXA}$ kept embolization proximal, preventing recanalization seen in the $\text{HA}_\text{H}\text{-HAP}_\text{I}@\text{HA}_\text{L}$ group (Figure 3D). HE staining showed more necrosis and thrombus in the $\text{HA}_\text{H}\text{-HAP}_\text{I}@\text{HA}_\text{L}@\text{TXA}$ group (Figure 3E). Biosafety of $\text{HA}_\text{H}\text{-HAP}_\text{I}@\text{HA}_\text{L}@\text{TXA}$ was confirmed, not damaging organs (Figure 3F), affecting coagulation (Figure 3G), or causing liver/kidney side effects (Figure 3H). Renal function was partially preserved and compensated by the left kidney.

Conclusion We have successfully developed a novel radiopaque embolization microsphere, whose biosafety, radiopacity under DSA/CT, and embolization effectiveness have all been thoroughly verified. This innovative achievement is expected to offer a new option for future tumor embolization therapy.

PO-001

Percutaneous transhepatic biliary stenting for bile duct obstruction due to malignancy: efficacy and safety

Tai Tan Nguyen
Nhan Dan Gia Dinh Hospital

Purpose To evaluate the efficacy and safety of percutaneous transhepatic biliary stenting (PTBS) in patients with malignant bile duct obstruction, assessing its impact on biliary drainage, symptom relief, and complication rates.

Materials and methods A retrospective analysis was conducted on patients who underwent PTBS for malignant biliary obstruction. Clinical and radiological data were reviewed, including technical success, functional success (bilirubin reduction), procedure-related complications, and overall survival. Technical success was defined as successful stent placement with bile duct decompression, while functional success was measured by a significant decrease in serum bilirubin levels post-procedure.

Results PTBS was successfully performed in the majority of patients, achieving a high rate of technical success. Functional success was observed in a significant proportion of cases, with notable reductions in bilirubin levels post-stenting. Common complications included mild post-procedural pain, infection, and, in a few cases, stent occlusion or migration. However, severe complications were rare, including hemobilia. The procedure provided effective palliation, improving patients' quality of life and facilitating further oncologic treatment.

Conclusion PTBS is a safe and effective palliative intervention for malignant biliary obstruction, offering high technical and functional success rates with manageable complications. It remains a valuable option for patients who are not candidates for surgical or endoscopic intervention, significantly improving biliary drainage and symptom control. Further studies are needed to optimize patient selection and long-term outcomes.

PO-002

Successful Treatment of Postoperative Gastric Hemorrhage in a 69-Year-Old Male Using TAE (Transarterial Embolization)

Gantulga Vanchinsuren, Erdene Orgodol, Baasanjav Narangerel, Erdenebulgan Batmunkh
Second State Center Hospital

Purpose Surgical resection is one of the primary treatments for gastric cancer, but postoperative hemorrhage is not an uncommon complication. Angiographic techniques and transarterial embolization (TAE) play a critical role in diagnosing and managing such bleeding. This case report highlights the effective use of TAE to control postoperative hemorrhage following surgery for gastric cancer

Materials and methods Patient Information:

Age and Gender: 69-year-old male

Medical History: Diagnosed with primary gastric cancer and underwent radical gastrectomy (partial stomach resection).

Symptoms: On postoperative day 3, the patient experienced a drop in blood pressure and a significant decrease in hemoglobin levels (7.0 g/dL), indicating severe hemorrhage.

Diagnosis:

Clinical Examination:

- Symptoms of anemia, including weakness and shortness of breath.
- No visible signs of bleeding from the surgical site.

Imaging Studies:

- Contrast-enhanced computed tomography (CT) revealed a focal point of intragastric bleeding. (Fig.1)

Angiographic evaluation identified the left gastric artery as the feeder vessel responsible for the bleeding

Results The patient's hemodynamic stability was restored after TAE. No recurrent bleeding occurred during the 7-day postoperative period, and hemoglobin levels stabilized (10 g/dL). Follow-up CT confirmed the success of the procedure

Conclusion This case illustrates the potential of angiographic techniques and TAE in diagnosing and treating postoperative gastric hemorrhage. The combination of skilled medical intervention and imaging support ensured the successful resolution of this case.

PO-003

Transcatheter arterial infusion of anti-programmed cell death 1 antibody combined with nab-paclitaxel in patients with primary anorectal malignant melanoma

Wei-Jun Fan,Xiaoshi Zhang,Lujun Shen,Dandan Li,Chen Li,Letao Lin
Sun Yat-sen University Cancer Center, China

Purpose This retrospective study aims at analysing the outcome in patients with ARMM treated with transcatheter arterial infusion (TAI) of antiprogrammed cell death 1 antibody combined with nab-paclitaxel.

Materials and methods This is a retrospective study of 20 patients with anorectal malignant melanoma treated with transcatheter arterial infusion of anti-programmed cell death 1 antibody combined with nab-paclitaxel. The primary endpoint was the progression-free survival (PFS).

We retrospectively identified patients with primary anorectal malignant melanoma treated with transcatheter arterial infusion of anti-programmed cell death 1 antibody combined with nab-paclitaxel between 2019 and 2024 at Sun Yat-Sen University Cancer Center. Data regarding patient demographics, treatments and related parameters, and outcomes were obtained from the medical records, including sex; age, stage, Eastern Cooperative Oncology Group (ECOG) performance status; tumor size; tumor location; presence of BRAF, NRAS, and KIT mutations; number and characteristics of prior and subsequent systemic therapies; treatment-related variables (anti-PD-1 agent used, duration of treatment, reason for discontinuation, toxicities), and survival status. The inclusion criteria were as follows: a) pathologically confirmed malignant melanoma, b) at least one cycle of treatment with transcatheter arterial infusion of anti-programmed cell death 1 antibody combined with nab-paclitaxel.

Results Twenty individuals were enrolled, ten (50.0%) patients had received prior therapy, including immunotherapy, chemotherapy, radiotherapy and surgical resection. All patients received targeted TAI into the tumor-feeding artery with anti-PD-1 antibody and nab-paclitaxel administered every 3 weeks. The overall PFS was 8.2 months, with 11 partial responses, 4 stable diseases and 5 progressive diseases. Among them, 10 patients initially received arterial infusion therapy, and 10 patients received arterial infusion therapy after the failure of first-line treatment, with PFS of 21.6 months and 16.5 months, respectively.

Conclusion transcatheter arterial infusion(TAI) with anti-PD-1 antibody and nab-paclitaxel was well tolerated and provided clinically meaningful antitumor activity as first-line therapy in patients with primary anorectal malignant melanoma.

PO-004

Efficacy analysis of TACE concurrent microwave ablation combined with target-immunotherapy in advanced unresectable liver cancer

Jian Li

Affiliated Hospital of Qingdao University

Purpose To explore the clinical efficacy and safety of microwave ablation (MWA) combined with synchronous transarterial chemoembolization (TACE) and targeted immunotherapy in unresectable liver cancer

Materials and methods We conducted a retrospective analysis of patient records from January 2021 to September 2024, 17 patients with large hepatocellular carcinoma who received MWA combined with synchronous TACE and targeted and immunotherapeutic drugs in our hospital, with Child-Pugh class A or B liver function, were followed up to analyze the efficacy and safety.

Results This technique was successfully applied in all patients. Among the 17 patients, 3 cases (3/17, 17.6%) achieved complete remission (CR), 11 cases (11/17, 64.7%) achieved partial remission (PR), 1 case (accounting for 1/17, or 5.8%) presented with stable disease (SD), while 2 cases (2/17, equivalent to 11.8%) had progressive disease (PD). The objective response rate (ORR), calculated as the sum of complete response (CR) and partial response (PR), reached 82.3%. The disease control rate (DCR) was 88.2%. Moreover, the median progression - free survival (PFS) was not reached. The median OS was not reached. The survival rates at 6 months, 12 months, 24 months were 100%, 93.8%, 66.8%, respectively. Among the 10 patients with BCLC stage C, the median overall survival (OS) was 20 months. There were no bleeding or other related complications. In the safety assessment during the treatment with targeted and immunotherapeutic drugs, the overall incidence of adverse events was 100.0% (17/17). Among them, 3 cases (17.6%) had grade 3 adverse events, and grade 1 - 3 adverse events could be relieved after symptomatic treatment.

Conclusion MWA combined with synchronous TACE and targeted immunotherapy is safe and effective for the treatment of large hepatocellular carcinoma.

PO-005

Analysis of influencing factors and establishment of clinical prediction model for postoperative complications of PTGD

Yijun Jin, Dongniang Lei, Lizhou Wang
Guizhou Medical University

Purpose Explore the influencing factors of complications in percutaneous transhepatic gallbladder drainage (PTGD), and then construct a clinical prediction model for PTGD postoperative complications based on logistic regression, providing a basis for risk prediction and benefit assessment of PTGD postoperative complications.

Materials and methods Collect clinical data of patients with acute cholecystitis who received PTGD treatment at the Affiliated Hospital of Guizhou Medical University from June 2020 to October 2024. Patients receiving PTGD treatment were divided into a complication group (Cg) and a non complication group (Ncg), and their clinical data were statistically analyzed to compare the postoperative complications between the two groups. Complications include: abdominal infection, bacteremia, gallbladder perforation, and death.

Collect clinical data of possible complications after PTGD in patients with acute cholecystitis, mainly including age, gender, whether they have a history of drinking, whether they have a history of hypertension, whether they have a history of diabetes, whether they have a history of coronary heart disease, whether they have a history of cerebral infarction, whether they use antibiotics before surgery, hand operation duration, anesthesia method, body mass index (BMI), preoperative white blood cell (WBC), preoperative neutrophil percentage (NEU%), preoperative hemoglobin (HGB), preoperative platelet (PLT), and preoperative total bile Total Bilirubin (TBil), preoperative direct bilirubin (DBil), preoperative indirect bilirubin (IBIL), preoperative glutamic pyruvic transaminase (ALT) Preoperative aspartate aminotransferase (AST), preoperative alkaline phosphatase (ALP), preoperative total protein (TP), preoperative albumin (ALB), preoperative prothrombin time (PT), preoperative international normalized ratio (INR), preoperative prothrombin time activity (PTA), preoperative activated partial thromboplastin time (APTT), preoperative fibrinogen (Fg), preoperative thrombin time (TT).

Perform univariate and multivariate logistic regression analysis on the influencing factors of postoperative complications in PTGD. Construct a clinical prediction model for postoperative complications of PTGD based on the selected influencing factors. And present the prediction model in the form of a column chart. At the same time, the clinical efficacy of the predictive model for postoperative complications of PTGD was evaluated by plotting the Receiver Operating Characteristic (ROC) curve and calculating the Area Under Curve (AUC).

Results 1. 105 cases were ultimately selected through inclusion and exclusion criteria, including 39 cases in the Cg group and 66 cases in the Ncg group. Age, gender, whether there is a history of drinking, hypertension, diabetes, coronary heart disease, cerebral infarction, whether antibiotics are used before surgery, duration of surgery, mode of anesthesia, body mass index (BMI) of the two groups of patients. Laboratory examinations before surgery are as follows: WBC、NEU%、HGB、PLT、TBil、DBil、IBIL、ALT、AST、ALP、TP、ALB、PT、INR、PTA、APTT、Fg There is no significant statistical difference, indicating comparability.

2. The results of univariate analysis showed that preoperative complication of diabetes, preoperative HGB level, preoperative PLT level, preoperative ALT level, preoperative AST level, preoperative PT level were the influencing factors of postoperative complications of PTGD;

Further multivariate logistic regression analysis showed that preoperative HGB level, preoperative AST level, preoperative PT level, preoperative complication with diabetes were independent influencing factors of postoperative complications of PTGD.

3. The clinical prediction model of PTGD postoperative complications was constructed. The results of multi factor logistic regression analysis: preoperative HGB level, preoperative AST level, preoperative PT level, preoperative factors combined with diabetes were used to construct the clinical prediction model of PTGD postoperative complications, and the prediction model was displayed in the form of nomogram. Draw the Receiver Operating Characteristic (ROC) curve and calculate the area under the curve (AUC=0.84).

Conclusion 1. The preoperative HGB level, preoperative AST level, preoperative PT level, preoperative complications with diabetes and other factors are related to the postoperative complications of PTGD.

2. A risk prediction model for postoperative complications of PTGD in patients with acute cholecystitis was established based on the influencing factors obtained from univariate and multivariate analysis. The ROC curve results showed that the model had good predictive efficiency.

PO-006

Clinical Efficacy of Selective Bladder Artery Embolization with Sequential Transurethral Resection for Bladder Tumor: A Retrospective Comparative Study

Hao Zheng, Long Cheng, ChengTao Gu, ShaoChen Wang, ZiLong Zhang, Hao Xu
The Fourth Affiliated Hospital of Soochow University

Purpose To evaluate the therapeutic and safety profile of preoperative selective bladder artery embolization (SBAE) followed by transurethral resection of bladder tumor (TURBT) in patients with bladder cancer.

Materials and methods A retrospective cohort study was conducted involving 104 histologically confirmed bladder cancer patients (excluding 25 cases due to incomplete data or non-compliance with inclusion criteria). Patients were divided into two groups: Group A (n = 61): TURBT alone, Group B (n = 43): SBAE performed 24 hours prior to TURBT. Baseline characteristics including age, sex, tumor size and clinical staging show no statistically significant differences between two groups ($P > 0.05$, independent t-test/ χ^2 test). Primary endpoints include operative duration, intraoperative blood loss, postoperative hospitalization, catheterization duration, and adverse event incidence. Statistical analysis was performed using SPSS with $\alpha = 0.05$.

Results Operation time for Group A was 67.9 ± 14.2 min, blood loss was 80.7 ± 24.7 ml, postoperative hospital stay was 8.5 ± 1.6 days, and duration of catheterization was 6.9 ± 1.1 days. Operation time for Group B was 54.0 ± 12.6 min, blood loss was 58.6 ± 27.3 ml, postoperative hospital stay was 7.3 ± 1.4 days, and duration of catheterization was 6.4 ± 0.9 days. The results in Group B were significantly lower than those in Group A ($P < 0.05$). No statistically significant difference was identified between the two groups in the incidence of postoperative adverse reactions ($P > 0.05$).

Conclusion SBAE prior to TURBT significantly reduces intraoperative hemorrhage and accelerates postoperative recovery without increasing perioperative morbidity. This benefit establishes SBAE as a clinically advantageous neoadjuvant strategy in bladder cancer management.

PO-007

Recurrence scoring system predicting early recurrence for patients with pancreatic ductal adenocarcinoma undergoing pancreatectomy and portomesenteric vein resection

Hang He, Caifeng Zou, Deliang Fu
Huashan Hospital, Shanghai Medical College, Fudan University

Purpose Pancreatectomy with concomitant portomesenteric vein resection (PVR) enables patients with portomesenteric vein (PV) involvement to achieve radical resection of pancreatic ductal adenocarcinoma, however, early recurrence (ER) is frequently observed. We aim to predict ER and identify patients at high risk of ER for individualized therapy.

Materials and methods Totally 238 patients undergoing pancreatectomy and PVR were retrospectively enrolled and were allocated to the training or validating cohort. Univariate Cox and LASSO regression analyses were performed to construct serum recurrence score (SRS) based on 26 serum-derived parameters. Uni- and multivariate Cox regression analyses of SRS and 18 clinicopathological variables were performed to establish a Nomogram. Receiver operating characteristic curve analysis was used to evaluate the predictive accuracy. Survival analysis was performed using Kaplan-Meier method and log-rank test.

Results Independent serum-derived recurrence-relevant factors of LASSO regression model, including postoperative carbohydrate antigen 19-9, postoperative carcinoembryonic antigen, postoperative carbohydrate antigen 125, preoperative albumin (ALB), preoperative platelet to ALB ratio, and postoperative platelets to lymphocytes ratio, were used to construct SRS [area under the curve (AUC): 0.855, 95%CI: 0.786–0.924]. Independent risk factors of recurrence, including SRS [hazard ratio (HR): 1.688, 95%CI: 1.075-2.652], pain (HR: 1.653, 95%CI: 1.052-2.598), perineural invasion (HR: 2.070, 95%CI: 0.827-5.182), and PV invasion (HR: 1.603, 95%CI: 1.063-2.417), were used to establish the recurrence nomogram (AUC: 0.869, 95%CI: 0.803-0.934). Patients with either SRS > 0.53 or recurrence nomogram score > 4.23 were considered at high risk for ER, and had poor long-term outcomes.

Conclusion The recurrence scoring system unique for pancreatectomy and PVR, will help clinicians in predicting recurrence efficiently and identifying patients at high risk of ER for individualized therapy.

PO-008

Successful Management of Gastric Metastasis from Hepatocellular Carcinoma: A Case of Left Gastric Artery Embolization Followed by Total Gastrectomy

Baasanjav Narangerel, Gantulga Vanchinsuren, Batmunkh Myagmar, Bat-Amgalan Ganzorig, Erdenebulgan Batmunkh
Second State Central Hospital

Purpose Gastric metastasis from hepatocellular carcinoma (HCC) is rare and presents significant management challenges. This case highlights the successful use of left gastric artery transcatheter arterial embolization (TAE) to control bleeding, followed by total gastrectomy for definitive treatment.

Materials and methods A 65-year-old man with hepatitis B virus (HBV)-induced HCC was diagnosed in 2017 and had undergone eight sessions of transcatheter arterial chemoembolization (TACE). He presented to our emergency department with severe abdominal pain and nausea. He developed anemia. Upper gastrointestinal endoscopy revealed irregularly elevated tumors in the lower anterior gastric body, which were diagnosed to be metastasis from HCC. Urgent esophagoscopy and abdominal CT revealed a 6.8 cm × 7.5 cm mass in the gastric cardia and small mesentery, causing significant luminal changes.

Results Due to worsening anemia, urgent TAE was performed via the left gastric artery, successfully stabilizing hemodynamics. Following embolization, a total gastrectomy was performed, and the patient recovered without complications.

Conclusion TAE of the left gastric artery effectively controlled hemorrhage, allowing for a successful total gastrectomy. This case underscores the importance of interventional radiology in stabilizing patients with rare gastric metastases from HCC, enabling optimal surgical outcomes.

Combination of Particle Embolic Agents and Coils in Total Embolization of Giant Renal Angiomyolipoma with Multiple Aneurysms: A Case Report

Anthony Yusuf^{1,3}, Jacob Pandelaki², Prijo Sidipratomo², Kevin Trigono², Jason Jason², Raymond Sudarma⁴

1. Intern, Department of Radiology, Dr. Cipto Mangunkusumo National General Hospital, Faculty of Medicine, Universitas Indonesia

2. Department of Radiology, Dr. Cipto Mangunkusumo National General Hospital, Faculty of Medicine, Universitas Indonesia, Jakarta, Indonesia

3. Faculty of Medicine, Pelita Harapan University, Tangerang, Indonesia

4. Mitra Keluarga Kelapa Gading Hospital, Jakarta, Indonesia

Purpose This study aims to present a case of giant renal angiomyolipoma effectively treated using a combination of coils and particle embolants. Additionally, it also reviews endovascular therapy for angiomyolipoma and addressing the choice of embolants for the treatment.

Materials and methods We report a 55-year-old female presented with a chief complaint of epigastric pain. Abdominal CT scan with contrast showed findings consistent with cholelithiasis, but also revealed a giant angiomyolipoma in the left kidney. Vascular access was achieved via right common femoral artery. Diagnostic angiography showed tortuous arterial structures within the mass, feeding arteries at upper and lower poles, and multiple aneurysms. Embolic agents used as materials for the embolization consisted of particle embolants (Embosphere Microsphere 700-900 micron) and coils (Penumbra SMART coils and Optima Complex-10 coils). Embolization of the upper and lower poles were done differently with combinations of microspheres and four detachable coils for the upper pole, and five detachable coils for the lower pole.

Results Combination of microspheres and coils successfully managed the mass, as post-embolization angiography of the left renal artery confirmed that the lesion was fully embolized. Renal ultrasound (at 3-month follow-up) showed absence of hypervascularity in the left renal mass, with normal morphology of the left kidney and normal doppler spectrum. Abdominal CT scan with contrast (at 6-month follow-up) revealed regression of the mass with no post-contrast enhancement. Selective angiographic embolization is the preferred treatment option for angiomyolipoma due to its minimally invasive nature, proven efficacy in reducing tumor size, and low complication risk. Common embolic agents utilized in treatment include coils, particle embolants, and liquid embolants. Prior studies stated that coils effectively treat aneurysms and prevent reperfusion, while particle embolants are used to occlude distal vessels, further reducing blood flow. In contrast, another study found that particle-coils combination have similar efficacy and safety profiles to particle-only embolization in angiomyolipoma. Other embolic agents reported for the embolization of angiomyolipoma include polyvinyl alcohol, NBCA-lipiodol, and ethylene vinyl alcohol copolymers, although specific guidelines for the selection of embolic agents are lacking.

Conclusion Combinations of particle embolants and coils proved effective in treating giant angiomyolipoma, evidenced by total lesion embolization on post-treatment angiography and notable mass regression on follow-up imaging, while preserving normal renal morphology and function. This case supports the utility of combined embolic agents in managing complex angiomyolipoma, although further studies are needed to find the most optimal embolant for the management.

PO-010

Injectable thermosensitive brachytherapy seed to compete with sealed seed

Wenge Liu, Qin Wang
Zonsen PepLib Biotech inc

Purpose Brachytherapy (BT) uses a radioactive pellet or seed placed inside the tumor or surrounding area to seal radionuclide within a tumor to irradiate the tumor mass while minimizing systemic toxicity selectively. Although permanent seed brachytherapy (titanium-sealed I-125 seed), also known as low-dose-rate brachytherapy has demonstrated significant therapeutic effects, it still has some drawbacks that must be improved to achieve more success, such as a need for complex implantation, requiring general anesthesia, the seeds migration to other organs, permanent alien existing and fixed-dose (per seed) as a terminal treatment. To improve the applicability of BT and overcome these disadvantages, an injectable, thermal responsive, and more stable and degradable BT seed has been developed by using elastin-like polypeptides (ELPs), a thermally responsive biopolymers derived from natural elastin labeled with ^{131}I and ^{125}I .

Materials and methods Through genetic engineering, ELPs were designed by adjusting the amino acid sequence and length. The suitable ELP was testified with a sharp thermal sensitivity, and high in vitro and in vivo stability. Then the ELPs were labeled with ^{131}I or ^{125}I , making two iodine-labeled ELP BTs. Finally, the anticancer efficacy, toxicity, and tumor retention of radioactivity after a single intratumoral injection were evaluated in mice bearing cancer xenograft.

Results The formation of these injectable and biodegradable ELP BT seeds led to a high in vitro stability after thermal transition at 37°C and prolonged in vivo retention ($\sim 80\%$ ID/tumor at 7 days post-injection subcutaneously). ELP BT seeds achieved 100% tumor regression in all treated with either ^{131}I -ELP or ^{125}I -ELP in human xenografts (FaDu) and cured more than 67% of tumor-bearing animals after a single administration of ELP BT seed. The in situ stability of ELP BT was confirmed by the BT seed retaining the ^{131}I radioactivity within the tumor over 60 days, matching the biological decay with the physical one. The ELP BT seed was demonstrated safe in these trials by finding no body weight loss in any animal treated with ELP BT (Fig.1)

Conclusion We developed an alternative modality to the I-125 seed, which consists of a biodegradable, genetically engineered polypeptide conjugated to a therapeutic radioisotope that spontaneously transitions from an easily infusible liquid into a seed-like depot upon injection into a solid tumor. These results demonstrated that ELP brachytherapy could provide a valuable alternative to improve upon the current I-125 seed. Thus, ELP BT seed will be another choice of cancer brachytherapy for both early-stage and advanced cancers due to its injectable, dose-adjustable, and seed-degradable properties (table 1). Similarly, it is necessary to complete two key studies, a treatment plan program, and injection advice to translate the ELP seed to clinical application.

Self-Regulating Magnetic Thermo-Brachytherapy Overcomes Immunosuppression and Radiotherapy Resistance in Pancreatic Cancer

Haifeng Li, Peng Zeng, Zeqian Yu, Jiahua Zhou
Zhongda Hospital Southeast University

Purpose Pancreatic cancer (PC) remains one of the most lethal malignancies due to its dense stromal barrier, immunosuppressive tumor microenvironment (TME), and resistance to conventional therapies. While ^{125}I brachytherapy provides localized radiation, it inadvertently promotes PD-L1⁺ neutrophil infiltration that exacerbates immunosuppression. Magnetic hyperthermia (MH) has shown potential to sensitize tumors to radiotherapy but faces clinical limitations in precise temperature control. To address these challenges, we developed a self-regulating magnetic thermos-brachytherapy seed ($^{125}\text{I}@MH$) designed to synergistically deliver controlled radiation and hyperthermia while reversing immunosuppressive TME dynamics.

Materials and methods The $^{125}\text{I}@MH$ seed was engineered by coupling ^{125}I -impregnated silver rods (6 × 0.8 mm) with Fe₃O₄-based magnetic nanoparticles (MNPs) exhibiting a Curie temperature (T_{C}) tuned to 42°C via cobalt doping. Structural stability and thermal self-regulation were validated using TEM, XRD, and alternating magnetic field (AMF) exposure (150 kHz, 30 kA/m). Orthotopic PC models were established in C57BL/6 mice using Panc02-H7 cells. Treatment groups included: 1) Untreated controls, 2) ^{125}I seeds (7.4 MBq), 3) MH alone (AMF cycles: 15 min ON/12 h OFF), and 4) $^{125}\text{I}@MH$ combination. Tumor progression was monitored via bioluminescence imaging. Immune profiling employed 18-parameter flow cytometry (CD45⁺/CD11b⁺/Ly6G⁺/PD-L1⁺ neutrophils, IFN- γ ⁺CD8⁺ T cells) and multiplex immunohistochemistry (α -SMA, HIF-1 α , CD31).

Results The $^{125}\text{I}@MH$ platform demonstrated stable radiation emission (dose variation <2.1% over 60 days) and precise thermal regulation (42.0 ± 0.3°C) under AMF. In contrast to ^{125}I monotherapy—which increased PD-L1⁺ neutrophil infiltration by 3.2-fold ($p < 0.001$) and reduced IFN- γ ⁺ CD8⁺ T cells to 18% of total lymphocytes—the $^{125}\text{I}@MH$ combination suppressed PD-L1⁺ neutrophils by 68% ($p = 0.002$) and restored cytotoxic T-cell populations to 41% ($p < 0.001$). This immunomodulation correlated with 72% tumor volume reduction (vs. 42% for radiation alone, $p = 0.007$) and stromal normalization (α -SMA⁺ CAFs decreased by 54%, $p = 0.01$). Mechanistically, hyperthermia disrupted HIF-1 α -mediated PD-L1 upregulation in neutrophils while enhancing radiation-induced DNA damage (γ -H2AX foci increased 2.7-fold vs. monotherapy). No systemic toxicity was observed (ALT/AST levels < 1.2× baseline).

Conclusion This study presents the first dual-modality brachytherapy system that concurrently addresses PC's physical and immunological resistance mechanisms. By integrating self-regulated hyperthermia with ^{125}I radiation, the $^{125}\text{I}@MH$ seed achieves: 1) Enhanced radiosensitization through thermal disruption of hypoxic niches, 2) Reprogramming of immunosuppressive neutrophils via PD-L1 inhibition, and 3) Preservation of antitumor T-cell immunity. The temperature-controlled design resolves historical challenges in clinical hyperthermia application, positioning this platform as a translatable strategy for overcoming therapy-resistant PC.

PO-012

Transbrachial TACE for Liver Cancer: A Real-World Study on Safety, Comfort, and Quality of Life in Chinese Patients

Miaomiao Yang, Ying Liu, Wenjing Gong

Yantai Yuhuangding Hospital, Affiliated to Medical College of Qingdao University

Purpose Transarterial chemoembolization (TACE) is widely utilized for the treatment of intermediate to advanced primary liver cancer. Although the traditional transfemoral access (TFA) is effective, it presents several disadvantages, including patient discomfort due to prolonged immobilization and increased complication rates. While transradial access (TRA) reduces immobilization time, it is limited by anatomical variants and a higher probability of vasospasm. Consequently, the transbrachial approach (TBA) has emerged as a promising strategy, offering larger diameter access and lower spasm rates, potentially improving procedural success and reducing complications. However, few studies have evaluated the comfort and safety of TBA for TACE.

Materials and methods This retrospective study assessed the safety and comfort of TACE via TBA in 530 patients with intermediate-advanced liver cancer, undergoing a total of 1056 TACE procedures at Yantai Yuhuangding Hospital from January 2022 to July 2024. Key metrics included technical success rate, complication rate, and patient-reported comfort. Health-related quality of life (HRQoL) was measured using post-catheterization questionnaires and EORTC QLQ-30 questionnaires at 1 day and 7 days post-treatment, respectively. Radial and ulnar arterial patency following brachial artery compression was evaluated by Doppler ultrasound.

Results TBA demonstrated a technical success rate of 99.15%, with an average procedure time of 34.43 ± 8.74 minutes. The crossover rate, referring to the conversion of the procedure to an alternative arterial site, was minimal at 0.85%. Patient feedback indicated minimal discomfort and a positive quality of life, as reflected in post-catheterization questionnaires and HRQoL surveys. The incidence rate of complications was low (2.37%), including pseudoaneurysm (0.19%), arterial thrombosis (0.09%), puncture site oozing (0.85%), nerve injury (0.19%), and subcutaneous hematoma (1.14%). No instances of arterial spasm or vascular occlusion were reported. Fluoroscopy time was reported to be lower than that for TFA and TRA in previous studies. Compression of the brachial artery did not influence the blood supply to the forearm.

Conclusion TACE via TBA demonstrated high technical success rates, low crossover rates, and minimal drawbacks, significantly enhancing patient comfort and quality of life. These results suggest that TBA is a viable alternative to conventional vascular access routes. Despite the absence of a comparison group in this study, these findings highlight the potential of TBA in improving outcomes and quality of life for liver cancer patients. Future prospective studies with comparative analyses are necessary to validate these results.

PO-013

Transarterial chemoembolization with PD-(L)1 inhibitors plus Lenvatinib for MVI of unresectable hepatocellular carcinoma : An exploratory, cohort study

Chao An, PEIHONG WU
Chinese PLA General Hospital

Purpose This study aimed to evaluate the efficacy and safety of transarterial chemoembolisation (TACE) combined with lenvatinib and programmed cell death protein-1 (PD-1) inhibitors compared to TACE monotherapy in treating large hepatocellular carcinoma (HCC) with microvascular invasion (MVI).

Materials and methods A total of 516 patients with single large HCC who underwent either TACE monotherapy (n = 392) or TACE combined with PD-1 inhibitors and lenvatinib (n = 271) between April 2009 and September 2022 were retrospectively analysed. Propensity score matching (PSM) was employed to minimise selection bias, yielding two matched groups of 186 patients each. Overall survival (OS) and recurrence-free survival (RFS) were analysed using the Kaplan–Meier method with log-rank tests. Independent risk factors for MVI were identified through multivariable analyses using forward stepwise regression.

Results TACE combination therapy significantly improved rates of MVI clearance and pathological complete response compared to TACE monotherapy (both $P < 0.001$). The 5-year OS rate was comparable between combination group and monotherapy group (69.9% vs. 60.7%; $P = 0.544$). However, the 5-year RFS rate was significantly lower in the combination group compared to the monotherapy group (26.7% vs. 55.0%; $P < 0.001$). Multivariate analysis identified several protective factors against MVI, including a reduction in alpha-fetoprotein levels by more than 50% (hazard ratio [HR]: 3.33; 95% confidence interval [CI]: 1.82–8.16; $P < 0.001$), absence of intratumoral arterial enhancement (HR: 3.71; 95% CI: 1.83–7.51; $P < 0.001$), objective response to TACE (HR: 0.23; 95% CI: 0.15–0.35; $P < 0.001$) and TACE combined with PD-1 inhibitors and lenvatinib (HR: 0.27; 95% CI: 0.18–0.41; $P < 0.001$).

Conclusion TACE combined with lenvatinib and PD-1 inhibitors offers significant benefits in the SR management of patients with large HCC.

PO-014

Complete remission in BCLC stage C hepatocellular carcinoma treated with HAIC combined with PD1 inhibitors and anti-angiogenic therapy

Shi-Tao Lu

First Affiliated Hospital of Suzhou University

Purpose Hepatocellular carcinoma (HCC) at BCLC stage C poses substantial therapeutic challenges and is typically associated with a poor survival prognosis. The triple therapy regimen, comprising hepatic artery infusion chemotherapy (HAIC), programmed death receptor-1(PD-1) inhibitors, and anti-angiogenic therapy, is currently under investigation for this stage of HCC.

Materials and methods In our study, we observed 9 advanced cases that achieved complete response (CR) through this triple combination therapy. The criteria for CR were defined as the complete disappearance of all lesions or no enhancement on arterial phase CT/MR imaging, the absence of new lesions, and the normalization of alpha-fetoprotein (AFP) levels. We analyzed the time to CR, changes in AFP levels during follow-up, and recurrence rates.

Results Among the 214 HCC patients treated with this triple therapy in our center from January 2021 to December 2023, 9(4.2%) achieved CR. The time to CR ranged from 2 to 10 months, with an average of 5.3 months. The duration for AFP levels to normalize varied from 79 to 259 days, with a median of 118 days.

Conclusion This indicates that the triple combination therapy of HAIC, PD-1 inhibitors, and anti-angiogenic agents has a modest probability of inducing CR in advanced HCC, with the occurrence of this response being relatively rapid.

PO-015

Transarterial chemoembolization combined with percutaneous ethanol injection for the treatment of hepatocellular carcinoma at high-risk areas

Wencong Feng

Department of Interventional Radiology, The First Affiliated Hospital of Soochow University

Purpose To analyze the efficacy and safety of the combination of transarterial chemoembolization (TACE) with percutaneous ethanol injection (PEI) in the treatment of hepatocellular carcinoma (HCC) at high-risk areas.

Materials and methods Data from cases involving TACE combined with PEI for HCC treatment in high-risk regions were analyzed from January 2016 to December 2023 at three medical centers. High-risk areas were defined as those less than 10 mm from the diaphragm, gallbladder, gastrointestinal tract, or secondary branches of the portal vein or bile duct. The guidance modalities for PEI were computed tomograph (CT) and cone beam computed tomograph (CBCT). Each lesion received only one session of TACE combined with PEI. Treatment efficacy was assessed by complete ablation rate of target lesions at the 2-month follow-up. Factors affecting the efficacy were determined by binary logistic regression analysis. The difference in efficacy between CT-guided and CBCT-guided PEI was analyzed by Chi-square test.

Results About 62 patients with 67 target lesions were included in the analysis. The overall complete ablation rate lesion-based was 80.6% (54/67). Lesion diameter was significantly associated with the probability of achieving complete ablation (OR = 6.89, 95% CI: 1.57–30.234, $P = 0.011$). There was no significant difference in the complete ablation rates between CT- and CBCT-guided approaches (83.3% vs. 80%, $P = 0.867$). No severe complications occurred during treatment or follow-up.

Conclusion The combination of TACE with a single PEI proves to be a safe and effective treatment for HCC in high-risk areas. There was no difference between CBCT-guided and CT-guided outcomes.

PO-016

Translational Application of Y90-SIRT Combined with Systemic Therapy in Initially Unresectable Hepatocellular Carcinoma

Tianming Wang¹, Enhua Xiao²

1. Xiangya Hospital, Central South University

2. The Second Xiangya Hospital

Purpose To evaluate the clinical efficacy and long-term survival benefits of Y90 resin microsphere selective internal radiation therapy (Y90-SIRT) combined with systemic therapy in patients with initially unresectable massive hepatocellular carcinoma (HCC) with portal vein tumor thrombosis (PVTT).

Materials and methods A retrospective analysis was conducted on a case of initially unresectable HCC with portal vein tumor thrombosis treated with Y90-SIRT combined with targeted and immune therapy, leading to complete remission and radical resection. Relevant literature was also reviewed.

Results A 62-year-old male patient with a 20-year history of hepatitis was retrospectively recruited to have a massive HCC in the right liver (10.2 cm in diameter, BCLC C stage) invading the main branch of the right portal vein. Imaging suggested liver cirrhosis, and laboratory tests indicated Child-Pugh A grade. The treatment plan included Y90-SIRT (administration of resin microspheres (SIR-Spheres®) via the right hepatic artery, radiation dose: 120 Gy, injection activity: 1.6±0.1 GBq), with adjuvant therapy using lenvatinib and sintilimab. Enhanced MRI at 6 months post-treatment showed minimal tumor and thrombus activity. Seven months after Y90-SIRT, imaging confirmed near-complete tumor necrosis (>95%) and thrombus reduction, enabling laparoscopic right hepatectomy and thrombectomy. Pathological results showed near-complete tumor necrosis. The patient continued the original systemic therapy for 1 year post-surgery. After 16 months of follow-up, no local recurrence or distant metastasis was observed.

Conclusion Y90-SIRT can serve as an effective neoadjuvant therapy for patients with massive HCC and PVTT, enabling R0 resection through complete tumor necrosis and significantly prolonging recurrence-free survival. This combined approach offers a novel treatment strategy for advanced HCC patients, particularly those with high tumor burden and vascular invasion who are not candidates for direct surgery.

PO-017

Comparing the effectiveness and safety Cancer Imaging Open Access of Sorafenib plus TACE with Apatinib plus TACE for treating patients with unresectable hepatocellular carcinoma: a multicentre propensity score matching study

Liang Yin

Department of Interventional Radiology, The First Affiliated Hospital of USTC, Division of Life Sciences and Medicine, University of Science and Technology of China, Hefei, 230000, People's Republic of China

Purpose Local combined systemic therapy has been an important method for the treatment of unresectable hepatocellular carcinoma (HCC). The purpose of this study was to compare the effectiveness and safety of transarterial chemoembolization (TACE) plus Sorafenib versus TACE plus Apatinib for treating patients with unresectable HCC.

Materials and methods The clinical data of patients with unresectable HCC who were treated with TACE plus Sorafenib or TACE plus Apatinib at 5 Chinese medical centers between January 2016 and December 2020 were retrospectively analyzed. Propensity score matching (PSM) was applied to reduce the bias from confounding factors.

Results total of 380 patients were enrolled, of whom 129 cases were treated with TACE plus Sorafenib and 251 cases with TACE plus Apatinib. After the 1:1 PSM, 116 pairs of patients were involved in this study. The results showed that the PFS and OS in the TACE-Sorafenib group were significantly longer than those in the TACE-Apatinib group (PFS: 16.79 ± 6.45 vs. 14.76 ± 6.98 months, $P = 0.049$; OS: 20.66 ± 6.98 vs. 17.69 ± 6.72 months, $P = 0.013$). However, the ORR in the TACE-Apatinib group was markedly higher than that in the TACE-Sorafenib group (70.69% vs. 56.03%, $P = 0.021$). There were more patients with adverse events (AEs) in the TACE-Apatinib group than those in the TACE-Sorafenib group before dose adjustment (87 vs. 63, $P = 0.001$); however, the number of patients who suffered from AEs was not significantly different between the two groups after the dose adjustment (62 vs. 55, $P = 0.148$). No treatment-related death was found in the two groups. Subgroup analysis revealed that patients with unresectable HCC could better benefit from regular doses than reduced doses (Sorafenib, 22.59 vs. 18.02, $P < 0.001$; Apatinib, 19.75 vs. 16.86, $P = 0.005$).

Conclusion TACE plus either Sorafenib or Apatinib could effectively treat patients with unresectable HCC, the safety of TACE plus Sorafenib was better. and the ORR of TACE plus Apatinib was higher.

PO-018

Prognostic value of acute liver injury in cirrhotic patients after transjugular intrahepatic portosystemic shunt

Liang Yin

Department of Interventional Radiology, The First Affiliated Hospital of USTC, Division of Life Sciences and Medicine, University of Science and Technology of China, Hefei, 230000, People's Republic of China

Purpose Acute liver injury (ALI) following a transjugular intrahepatic portosystemic shunt (TIPS) procedure may negatively impact clinical outcome. The incidence, risk factors, and prognostic value for survival concerning TIPS procedure-related ALI in patients with liver cirrhosis were investigated.

Materials and methods Between January 2016 and March 2022, data from 346 patients with liver cirrhosis who underwent a TIPS procedure were reviewed for analysis of ALI, defined by alanine transaminase ≥ 3 -fold the upper limit of normal at 72 hours after TIPS. Kaplan-Meier curves and log-rank tests were performed to analyze the rates of overt hepatic encephalopathy (HE) and overall survival (OS) between patients with or without ALI. Risk factors associated with ALI and mortality were analyzed using logistic regression and Cox proportional hazards regression model. A nomogram was established based on the Cox regression results. The discrimination capacity, calibration, and clinical value of the model were evaluated.

Results Seventy-four patients (21.4%, 74/346) developed ALI at 72 hours after TIPS. The patients with ALI had higher overt HE and lower OS compared to patients without ALI after TIPS. Serum creatinine was independently associated with ALI. Age, Model for End-Stage Liver Disease (MELD) score, sarcopenia, and post-TIPS ALI were independent predictors of mortality. Finally, a nomogram with good performance for survival prediction was established (C-index 0.743).

Conclusion Post-TIPS ALI is a potentially serious complication in cirrhotic patients, and may be used as a predictor of adverse postoperative outcomes.

PO-019

Development and validation of a prognostic model based on nutritional status after transjugular intrahepatic portosystemic shunt

Liang Yin

Department of Interventional Radiology, The First Affiliated Hospital of USTC, Division of Life Sciences and Medicine, University of Science and Technology of China, Hefei, 230000, People's Republic of China

Purpose Malnutrition commonly occurs in cirrhotic patients scheduled for transjugular intrahepatic portosystemic shunt (TIPS). Prognostic prediction based on Psoas muscle thickness per height (PMTH) and prognostic nutritional index (PNI) after TIPS in cirrhotic patients may contribute to better therapeutic response.

The aim of this study was to assess the predictive value of nutritional status using PMTH and PNI in cirrhotic patients who underwent TIPS.

Materials and methods A total of 356 cirrhotic patients who had undergone TIPS were retrospectively evaluated. Kaplan-Meier and Cox regression techniques were applied for survival analyses. A prognostic nomogram was formulated, focusing on nutritional status, and its performance was assessed based on discrimination, calibration, and clinical usefulness.

Results Patients with nutritional status grade 3 (low-PMTH and low-PNI) showed the lowest overall survival (OS) rate; grade 2 (high-PMTH and low-PNI, or low-PMTH and high-PNI) following; and grade 1 (high-PMTH and high-PNI) presenting the highest OS rate. A multivariate Cox regression analysis pinpointed nutritional status grade, age, total bilirubin, and creatinine as independent prognostic indicators for OS. These factors were harnessed to construct the prognostic nomogram model (C-indices were 0.793 and 0.707 in the training and validation groups). Furthermore, the nutritional status grade consistently outperformed existing scoring systems.

Conclusion The novel nutritional status-based model could furnish a more refined approach for forecasting survival in cirrhotic patients after TIPS.

PO-020

Study on the effect of a new type of "magnetothermal 125I seed" combined with Flt3-L to promote the "in-situ vaccine" for hepatocellular carcinoma

Peng Zeng
Zhongda Hospital, Southeast University

Purpose The immunosuppressive tumor microenvironment in hepatocellular carcinoma (HCC) significantly limits the therapeutic efficacy of immune checkpoint inhibitors. To enhance immunotherapy response rates, we developed a novel composite system combining magnetic nanoparticles with 125I particles (125I-MNPs). This integrated approach synergistically improves tumor hypoxia through magnetothermal therapy, enhances radiosensitivity, and combines with Fms-related tyrosine kinase 3 ligand (Flt3-L) to promote dendritic cell (DC)-mediated antigen presentation, thereby reversing immunosuppression and activating an in situ vaccination effect.

Materials and methods Thermoregulated magnetic nanoparticles (MNPs) were synthesized and conjugated with 125I particles to form 125I-MNP composites, with Flt3-L employed as a DC maturation inducer. In vitro experiments evaluated the magnetothermal properties (temperature uniformity and self-regulating capability) and radiosensitizing effects on HCC cells. For in vivo studies, an HCC mouse model was established with treatment groups: 125I-MNPs ± magnetothermal therapy ± Flt3-L. Tumor microenvironment alterations were analyzed through immunohistochemistry (CD8+ T cell infiltration, MDSC reduction) and flow cytometry (DC maturation markers CD80/CD86 and memory T cell formation). ELISA quantified hypoxia markers (HIF-1α) and T cell activation molecules (IFN-γ, Granzyme B).

Results 1. The 125I-MNPs achieved precise hyperthermia ($42\pm1^{\circ}\text{C}$), reducing HIF-1α expression by 50% and significantly improving tumor hypoxia, while enhancing radiotherapy efficacy with 60% greater tumor volume reduction compared to monotherapy.

2. Flow cytometry revealed that Flt3-L combination therapy tripled the proportion of mature DCs (CD80+/CD86+), enhanced antigen presentation efficiency, increased CD8+ T cell infiltration by 2.5-fold, and significantly decreased immunosuppressive cells (MDSCs and Tregs).

3. The triple-modality therapy (125I-MNPs + magnetothermal therapy + Flt3-L) elevated memory effector T cell (TEM) populations, achieving 70% growth inhibition in untreated distal tumors and extending survival by 40%, demonstrating potent in situ vaccination effects.

Conclusion The 125I-MNPs/Flt3-L combination synergistically modulates the HCC immunosuppressive microenvironment through: (1) magnetothermal therapy-mediated hypoxia alleviation and radiosensitization; (2) Flt3-L-enhanced DC maturation and antigen presentation; and (3) systemic antitumor immune activation. This innovative strategy provides a promising solution to overcome HCC immunotherapy resistance.

PO-021

Genomic feature and potential therapeutic target for cholangiocarcinoma

Bohao Zheng, Sheng Shen, Xiaojian Ni, Xiaoling Ni, Houbao Liu, Yuan Ji
Zhongshan Hospital

Purpose The genomic feature of biliary tract carcinoma (BTC) has been characterized, but limited studies focus on the potential therapeutic target for cholangiocarcinoma patients. In this study, we conducted a comprehensive analysis of genome profiles of 43 cholangiocarcinoma patients, systematically analyzed the gene alternation in cholangiocarcinoma patients, and investigated the clinicopathological significance of these genomic features, thus providing clues to explore potential therapeutic targets for cholangiocarcinoma.

Materials and methods 43 BTC patients were enrolled in this retrospective study. Genomic characteristics including genomic alterations and mutational signatures were detected and analyzed. Then, the correlation between the genomic characteristics and clinicopathologic features was investigated. Next, the prognostic significance of these altered genes was evaluated. Besides, personalized targeted therapies for patients harboring potentially actionable targets (PATs) were investigated.

Results Among 43 patients, the genomic mutation was detected in 38 patients. Among these mutations, KRAS (44.2%), TP53(37.2%), ARID1A (18.6%), SMAD4(18.6%), BRCA2, CDKN2A (11.6%), and VEGFA (11.6%) are the most frequently altered cancer-related genes. Besides, germline mutations mainly occurred in ERBB, PI3K/AKT, MAPK, and RAS signaling. Among detected mutations, we found that TP53, STK11, MYC, and ERBB3 are gene alternations with significant prognostic values. In terms of potentially actionable target (PAT) analysis, 19 genes were proposed to be PATs in BTCs. and we found out that 79.1% of patients have Tier II somatic mutation in our cohort.

Conclusion The molecular feature is closely related to clinical characteristics in cholangiocarcinoma patients. In this study, we identified several commonly altered genes in cholangiocarcinoma patients and determined potential prognostic biomarkers and therapeutic targets for cholangiocarcinoma patients.

PO-022

METTL5 promotes fatty acid metabolism by modulating peroxisome to promote hepatocellular carcinoma recurrence after thermal ablation

Xie Zonglin, Yifan Wu, Lina Wang, Zihao Dai, Shuling Chen
The First Affiliated Hospital of Sun Yat-sen University,

Purpose Thermal ablation (e.g. radiofrequency ablation, RFA) is a critical curative therapy for hepatocellular carcinoma (HCC). However, high recurrence rate after ablation remains a major clinical challenge. Hyperactive RNA translation mediated by aberrant RNA modifications is critical for tumor heat stress adaption. 18S rRNA m6A modification catalyzed by Methyltransferase 5 (METTL5) is one of the most prevalent rRNA modifications, however, the role of METTL5-mediated rRNA modification in HCC recurrence after RFA remains unknown.

Materials and methods We analyzed the gene expression profiles of recurrent HCC after RFA and constructed insufficient RFA (iRFA) models in vivo and in vitro under heat stress to verified the functions of METTL5 in regulation of HCC malignant biological behavior. Mechanically, we performed the RNC-sequencing and Ribo-sequencing assays to explore potential downstream targets regulated by METTL5.

Results We found that the levels of METTL5 and 18S rRNA m6A modification were significantly upregulated in post-RFA recurrent HCC. Further experiments showed that METTL5 was able to promoted HCC proliferation and metastasis under heat stress. Mechanically, heat-mediated METTL5 upregulation enhanced the PEX16 mRNA translation that promoted peroxisomal biogenesis and β -oxidation of very long-chain fatty acid (VLCFA), which promoted mitochondrial respiration to mediate HCC progression. Knockdown of METTL5 or PEX16 significantly mitigated tumor progression and metastasis induced by iRFA.

Conclusion Our study uncovers the novel mechanistic insights in HCC recurrence after iRFA through hyperactive peroxisome function in promoting VLCFA β -oxidation regulated by METTL5, thus providing a new target to prevent and treat HCC recurrence after thermal ablation.

PO-023

Application research of EqualSpheres embolization microspheres loaded with Idarubicin in VX2 rabbit liver tumor model

Chuntao Wang
GuiZhou Medical University

Purpose Explore the pharmacokinetic parameters of EqualSpheres uniform particle size embolization microspheres, CalliSpheres non-uniform particle size embolization microspheres, and iodized oil loaded chemotherapy drug Idarubicin for arterial chemoembolization treatment of VX2 rabbit liver cancer model within 24 hours, as well as the drug concentration in liver tumor tissue and normal liver tissue after 24 hours, and analyze the expected therapeutic effects of each embolization material.

Materials and methods Twelve New Zealand white rabbits were randomly selected for ultrasound-guided percutaneous puncture to establish a rabbit VX2 liver cancer model. They were randomly divided into EqualSpheres group, CalliSpheres group, and iodized oil group using a random number table method, with four rabbits in each group. EqualSpheres microspheres, CalliSpheres microspheres, and iodized oil were used as embolic materials to carry Idarubicin for embolization treatment in each group. Peripheral blood was centrifuged at 5 min, 0.5 h, 1 h, 4 h, 12 h, and 24 h after surgery to obtain serum, and the experimental and control groups were euthanized at 24 h after TACE treatment. Liver cancer tissue and normal liver tissue were taken, and UPLC-MS/MS was used to measure the levels of peripheral blood and tissue. The concentration of idarubicin in peripheral blood was fitted with Graphpad software to observe the changes in concentration over time. Using independent sample t-test to compare the drug concentration and pharmacokinetic indicators at different sites 24 hours after TACE with different embolic materials.

Results The average drug concentration in liver cancer tissues of the EqualSpheres group was 920.06 ng/ml, significantly higher than that of the CalliSpheres group at 79.47 ng/ml and the iodized oil group at 118.71 ng/ml. However, the average drug concentration in normal liver tissues of all three groups was lower, with no significant difference. The peripheral blood drug concentrations of the three groups decreased at 5 minutes and then rebounded within 24 hours. The average blood drug concentration curve of the EqualSpheres group increased relatively steadily compared to the CalliSpheres group and the iodized oil group. The iodized oil group reached C_{max} 11.54 ng/ml at 0.5 hours, while the CalliSpheres group and EqualSpheres group both reached C_{max} at 5 minutes, which were 7.82 ng/ml and 8.36 ng/ml, respectively.

Conclusion EqualSpheres drug loaded microspheres loaded with Idarubicin TACE for the treatment of VX2 liver cancer model have higher drug concentration at the tumor site under the same conditions, maintain lower concentration in peripheral blood within 24 hours, and have good pharmacokinetic curves, verifying the stable drug release performance of EqualSpheres drug loaded microspheres.

PO-024

Combination of transnasal ileus tube and local small intestine artery perfusion chemotherapy for late malignant small bowel obstruction

Er-Sheng Li

The First Affiliated Hospital, Xingtai Medical College, Xingtai, Hebei Province, China

Purpose Malignant bowel obstruction (MBO) caused by peritoneal carcinomatosis is a common complication of advanced abdominal malignancies, and surgical treatment provides little benefit. To investigate the decompression efficacy of transnasal ileus tube combined with local arterial infusion chemotherapy in the treatment of advanced malignant small intestine obstruction.

Materials and methods 109 patients diagnosed with malignant intestinal obstruction between January 2016 and December 2022 in our hospital were divided into the ileus tube + local infusion chemotherapy group (test group, n=51) and the ileus tube group (control group, n =58). The control group only received catheter decompression therapy, while the test group used ileus tube combined with local arterial infusion chemotherapy. The data on the technical success, initial and final angiographic results, GPS scores, KPS scores and the final clinical outcome were collected and follow-up was performed at 1-, 3-, 6-, 12-months, and yearly after the procedures.

Results All patients had successful placement of the ileus tube and local infusion chemotherapy without complications. The average catheter duration in the test group was significantly lower than that of the control group ($P<0.05$). The final clinical follow-up showed that the remission rate of intestinal obstruction symptoms in the test group was significantly higher than that of the control group ($P<0.05$, 84.3% vs 22%), and the survival time of patients in the test group was significantly longer than that of the control group ($P<0.05$). Finally, although the GPS and KPS scores of both groups decreased significantly after surgery, compared with the control group, the test group had a more significant decrease and significant differences at each follow-up period ($P<0.05$).

Conclusion Compared with ileus tube group, the ileus tube combined with local small bowel arterial infusion chemotherapy can effectively alleviate clinical symptoms of malignant small intestinal obstruction and prolong patients' survival time, which is worth promoting clinically.

PO-025

The combination treatment of oncolytic adenovirus H101 with Transcatheter Arterial Embolization Sequential Thermal Ablation for Hepatocellular Carcinoma: A Retrospective Study

Jianjun Li, CHANGYOU JING, TONG ZHU, YONGHONG ZHANG
Beijing Youan Hospital, Capital Medical University

Purpose This study aims to analyze the efficacy and safety of oncolytic adenovirus H101 combined with transcatheter arterial embolization (TAE) sequential thermal ablation in hepatocellular carcinoma (HCC).

Materials and methods This single-center retrospective study evaluated the progression-free survival (PFS) and overall survival (OS) of HCC patients who received H101 combined with TAE sequential thermal ablation therapy from July 2015 to January 2022, and recorded adverse reactions during treatment.

Results A total of 55 HCC patients were included, with a median follow-up of 37 months (range: 10-106 months). According to the Barcelona Clinic Cancer (BCLC) staging, there were 32 patients with early-stage HCC (BCLC stage 0/A) and 23 patients with intermediate-stage HCC (BCLC stage B). The median PFS of early- and intermediate-stage HCC patients were 16 and 10 months, respectively. The one-year PFS among patients with early- and intermediate-stage HCC was 69% and 39%, respectively. The three-year PFS among patients with early- and intermediate-stage HCC was 25% and 14%, respectively. The median OS of early- and intermediate-stage HCC patients were 87 months and 54 months, respectively. The one-year OS among patients with early- and intermediate-stage HCC was 96.9% and 90.9%, respectively. The three-year OS among patients with early- and intermediate-stage HCC was 82.3% and 70.0%, respectively. No patient had a serious adverse event, or a fatal or disabling event, due to the injection of oncolytic virus.

Conclusion This study suggests that H101 combined with TAE sequential thermal ablation is safe and effective for HCC, and further validation of efficacy in prospective randomized controlled trials is warranted.

PO-026

Predicting Bird-beak Configuration of Stent Graft during Zone 2 Thoracic Endovascular Aortic Repair using Machine Learning Models

Haiyang Chang, Yuliang Li, Bowen Lin
the Second Hospital of Shandong University

Purpose Bird-beak configuration (BBC) is responsible for reducing the effective proximal landing zone and increasing the risk of type Ia endoleak. We aim to develop a machine learning-based baseline framework (MLBF) for geometric modeling of thoracic aorta and risk prediction of BBC during zone 2 thoracic endovascular aortic repair (TEVAR).

Materials and methods From October 2019 to March 2022, 201 patients with acute type B aortic dissections (TBADs) who underwent zone 2 TEVAR were enrolled retrospectively. 131 patients were used as the derivation and internal validation cohorts, and 70 patients were selected as the external validation cohort.

Results In the 5-fold cross-validation experiments on 131 cases, the averages of the four metrics (accuracy, precision, sensitivity, and area under the curve [AUC]) were 80.88%, 84.43%, 82.67%, and 74.51% for the neural network (NN) in the multiparameter model, and 88.52%, 90.64%, 89.42%, and 88.71% for the NN in the 64-points-centerline-curvature model. In the external dataset, the averages of the four metrics for the NN in the 64-points-centerline-curvature model were 75.71%, 79.48%, 77.5%, and 76.83%, respectively. In addition, we retrained six ML models with 131 patients as training data. NN still performed the best on the external dataset.

Conclusion Among the constructed multiparameter and 64-point-centreline-curvature models, the NN classifier had the best overall performance in predicting the risk of BBC occurrence, followed by random forest and decision tree. The MLBF developed in this study is efficient and effective for risk stratification and planning TEVAR, and is easy to update for optimization.

PO-027

Application of a Question Prompt Checklist in Liver Cancer Surgery Patients: Effects on Patient Engagement, Information Retention, and Communication Satisfaction

Hongxia Song, Hongxia Song

Department of Hepatobiliary and Pancreatic Surgery, Henan Provincial People's Hospital

Purpose To explore the application of a question prompt checklist in liver cancer surgery patients and evaluate its effects on patient engagement, information retention, psychological well-being, and overall satisfaction with healthcare communication.

Materials and methods A prospective interventional study will be conducted involving 80 liver cancer surgery patients at Henan Provincial People's Hospital. Participants will be randomly assigned to either a control group receiving standard preoperative and postoperative counseling or an intervention group using a structured question prompt checklist during consultations. Data will be collected using pre- and post-intervention surveys measuring patient satisfaction, anxiety levels, perceived understanding of their condition and treatment plan, and recall of provided information.

Results It is anticipated that patients in the intervention group will demonstrate higher levels of engagement, greater understanding of their treatment plans, and lower anxiety levels compared to the control group. Additionally, increased satisfaction with healthcare communication is expected.

Conclusion Implementing a question prompt checklist can enhance patient-centered communication in liver cancer surgical care. This tool may empower patients to actively participate in their care, leading to improved psychological outcomes and overall satisfaction. The findings could provide a practical framework for integrating question prompt checklists into routine clinical practice for liver cancer patients.

PO-028

Practice and exploration of improving the self-management ability of patients with pancreatic cancer supported by artificial intelligence: taking DeepSeek system as an example

Zhiyu Ren

Department of Hepatobiliary and Pancreatic Surgery, Henan Provincial People's Hospital

Purpose To explore the practical effects of AI-supported, DeepSeek system-based interventions on improving self-management abilities in pancreatic cancer patients, and to analyze the system's impact on health management, care compliance, health behavior changes, and mental health.

Materials and methods This prospective interventional study selected 40 pancreatic cancer patients who received treatment at Henan Provincial People's Hospital from February to March 2025. Patients were randomly divided into a control group and an observation group, with 20 patients in each group. The control group received conventional health management, while the observation group received personalized health management interventions using the DeepSeek system. Health behavior assessments, the General Self-Efficacy Scale (GSES), care compliance scores, and mental health evaluations were used to compare the two groups in terms of disease management, self-management abilities, health behavior changes, and mental health levels.

Results After the intervention, the observation group showed significant improvements in health management behaviors, particularly in areas such as nutritional management, blood glucose monitoring, and pain management, with significantly higher self-management ability scores than the control group ($P < 0.05$). At 2 weeks post-intervention, the observation group's GSES score was (29.14 ± 3.56) points, and at 4 weeks it was (35.42 ± 2.33) points, both significantly higher than those of the control group ($P < 0.05$). Mental health scores in the observation group at 2 and 4 weeks post-intervention were (77.39 ± 9.14) and (84.22 ± 6.76) points, respectively, which were significantly better than those of the control group ($P < 0.05$). Additionally, the observation group demonstrated significantly higher care compliance, with increased patient motivation and confidence in self-health management.

Conclusion Personalized health management interventions based on the DeepSeek system have a significant effect on enhancing self-management abilities in pancreatic cancer patients. The system effectively improves patients' health behaviors, increases care compliance, and enhances mental health. This study provides strong empirical support for the application of AI in oncology nursing, laying a foundation for the intelligent and personalized development of cancer care.

PO-029

Retrospective Analysis of The Timing of Radiotherapy Intervention After Induction Chemoimmunotherapy in Unresectable Locally Advanced Lung Squamous Cell Carcinoma

Li Zeng,Daiyuan Ma

Department of Oncology, Affiliated Hospital of North Sichuan Medical College

Purpose In the era of immunotherapy, the best combination of immune checkpoint inhibitors (ICIs) and radiotherapy and chemotherapy (CRT) in the treatment of unresectable locally advanced non-small cell lung cancer (LA-NSCLC) has not been determined. The purpose of this study was to evaluate the efficacy and safety of induction chemoimmunotherapy followed by radiotherapy in patients with unresectable locally advanced lung squamous cell carcinoma (LA-LUSC), and to explore the effect of intervention timing of radiotherapy on the efficacy.

Materials and methods The clinical data of 54 patients with unresectable LA-LUSC who received induction chemoimmunotherapy followed by radiotherapy were analyzed retrospectively. According to radiotherapy after 2-3 and 4-6 cycles of induction chemoimmunotherapy, the patients were divided into early radiotherapy group (n=18) and late radiotherapy group (n=36). Kaplan-Meier method was used for survival analysis, and Log-rank test was used to test the differences between groups. Progression-free survival (PFS), local progression-free survival (LPFS), distant metastasis-free survival (DMFS), overall survival (OS) and safety were compared between the two groups, and the prognostic factors affecting PFS and OS were explored.

Results The median follow-up time was 30.7 months (10.5-51.8 months). The median PFS of all patients was 21.9 months. The PFS (HR=0.43, P=0.024) and LPFS (HR=0.36, P=0.038) in the early radiotherapy group were significantly longer than those in the late radiotherapy group. Prognostic analysis showed that interventional radiotherapy after 2-3 induction cycles was an independent predictor of PFS (P=0.040). The overall treatment tolerance of the whole group was good, and the incidence of \geq grade 3 pneumonia was 5.56%. Subgroup analysis showed that the OS of patients receiving induction combined with consolidation ICIs was significantly longer than that of patients who only received induction ICIs (HR=0.51, P=0.038).

Conclusion For patients with unresectable LA-LUSC, induction chemoimmunotherapy followed by radiotherapy shows a good curative effect and its safety is controllable. Interventional radiotherapy as early as possible after 2-3 cycles of induction chemoimmunotherapy may help to prolong PFS and LPFS. Consolidation ICIs after induction ICIs may still be necessary.

PO-030

Doxorubicin-Loaded CalliSpheres Microspheres Transcatheter Arterial Chemoembolization Versus Conventional Transcatheter Arterial Chemoembolization: Pharmacokinetics and Antitumor Effect in a VX2 Liver Tumor Model

Delei Cheng
The First Affiliated Hospital of USTC

Purpose We aimed to investigate the aspects of plasma pharmacokinetic profiles and antitumor effect for doxorubicin (DOX)-loaded CalliSpheres® microspheres (CSM, 100–300 μm) by transcatheter arterial chemoembolization (TACE) in rabbits with VX2 liver tumors

Materials and methods A total of 30 VX2 liver tumor rabbits were randomly and equally divided them into three groups (N = 10 for each group), which received DOX-loaded CSM by TACE (CSM-DOX group), DOX by conventional TACE (cTACE-DOX group), hepatic arterial infusion DOX (HAIC group). Tumor volume were monitored at 7 days by magnetic resonance imaging. DOX concentration was analyzed at 5 min, 6 h, 12 h, 24 h, 3 days, 5 days, and 7 days after the treatment using the LC–MS/MS method. Tumor necrosis, tumor proliferation and apoptosis were subjected to histological analysis.

Results 28 rabbits were successfully treated with TACE. The plasma DOX concentration in the three groups peaked at 5 min and in the CSM-DOX group was significantly lower than that in cTACE-DOX and HAIC groups. The tumor volume was significantly suppressed in the CSM–DOX group compared to cTACE–DOX group and HAIC group. Pathological results revealed that tumor necrosis and apoptosis was promoted while proliferation was suppressed in the CSM-DOX group compared to the cTACE-DOX and HAIC groups.

Conclusion Systemic drug concentrations were relatively low in the CSM–DOX group, suggesting fewer chemotherapy-related adverse effects. DOX-loaded CSM by TACE suppressed tumor growth and promoted tumor apoptosis, which showed a better antitumor effect than cTACE–DOX and HAIC groups.

PO-031

Yttrium-90 Ablative-Selective Internal Radiation Therapy for Hepatocellular Carcinoma in Chinese Patients: A Case Series Study

Yuelin Zhang

The First Affiliated Hospital, Zhejiang University School of Medicine

Purpose Hepatocellular carcinoma (HCC) stands as the predominant primary liver malignancy globally. Ablative-selective internal radiation therapy (A-SIRT) using yttrium-90 (90Y) radioactive microspheres, which delivers focused high-dose radiation directly to tumors via hepatic arterial injection aiming to induce tumor ablation with minimal damage to normal liver, has emerged as a promising treatment option for patients with HCC. Despite its potential, comprehensive evaluations of effectiveness, safety profile, and sustained outcomes of A-SIRT in HCC patients are scarce, especially in Chinese patient population.

Materials and methods This is a retrospective case series study of ten consecutive HCC patients who were treated with 90Y A-SIRT at our institution. Clinical parameters and outcomes of A-SIRT procedures, tumor responses (assessed by mRECIST criteria), subsequent treatments, and adverse events were meticulously documented.

Results All patients were male with a median age of 66.5 years. Half had previously undergone transarterial chemoembolization, and the average tumor diameter prior to A-SIRT was 5.37 cm. The mean 90Y administered activity was 1.15 GBq, with median target tumor absorbed doses of 325 Gy and 50 Gy in the normal liver. The objective response rate and complete response rate were 90% and 60%, respectively. No serious adverse events were observed and all patients were still alive at the time of manuscript submission.

Conclusion This is the first case series reporting the efficacy, safety and sustained outcomes of A-SIRT for HCC from China. A-SIRT showed a high response rate and manageable side effects, making it a potentially suitable option for HCC patients at various stages. The study provides a promising outlook for future treatment approaches.

PO-032

Diagnostic value of 18F-PSMA-1007 multi-parametric PET/MR imaging in clinically significant for PSA gray area prostate cancer

Lei Wang
JiLin Cancer Hospital

Purpose To evaluate the diagnostic value of 18F-PSMA-1007 PET/MR imaging in clinically significant prostate cancer (csPCa) at prostate-specific antigen (PSA) 4-10ng/mL. This reduces unnecessary biopsies in patients with PSA gray zone.

Materials and methods A retrospective analysis was performed for 40 patients with suspected prostate cancer (PSA 4-10ng/mL) from January 2023 to March 2024 in Jilin Provincial Cancer Hospital, aged (68.5±8.5) years. 18F-PSMA-1007 PET/MR imaging was performed within 2 weeks. The patient's clinical and imaging data were recorded. Histopathology with rectal ultrasound-guided biopsy (referred to as biopsy) or histopathological findings after prostatectomy is used as the "gold standard". Lesions with a Gleason score (GS) of ≥ 3 and 4 were diagnosed as csPCa, and lesions with negative pathological results or GS score less than 6 were diagnosed as non-csPCa. PET/MR imaging was performed using the uPMR 790 from Shanghai United Imaging Medical Technology Co., Ltd. Prostate PET/MR scans were performed 60 minutes after injection of 18F-PSMA-1007, and single-bed scanning time was 20 minutes. T1w FSE sequence, T2w FSE sequence and DWI sequence were used for MRI image acquisition ($b=50, 800, 1400$ s/mm²). The PRIMARY Score was used to evaluate the degree of imaging agent uptake of prostate lesions. MRI images were evaluated using the Prostate Imaging Reporting and Data System (PI-RADS) version 2.1.

Results The PRIMARY Score score ≥ 3 or PI-RADS ≥ 3 , and the diagnosis of CSPCa was made by PET/MR. Among all the enrolled patients, there were 28 patients with csPCa and 12 non-csPCa patients with a pathological Gleason score (GS \geq) score of 3 and 4 points. 18F-PSMA-1007 PET/MR imaging SUVmax was 5.0, and 22 cases were diagnosed with CSPCa by PET, 20 cases were diagnosed by MRI, and 24 cases were diagnosed by PET/MR. The accuracy, sensitivity, specificity, positive predictive value and negative predictive value of 18F-PSMA-1007 PET/MR imaging for the diagnosis of csPCa were 85.00%, 85.71%, 75.00%, 85.71% and 75.00%, respectively. The sensitivity, specificity, positive predictive value of 78.57%, and negative predictive value of 66.67% were higher than those of MRI alone.

Conclusion 18F-PSMA-1007PET/MR imaging has high accuracy and specificity in prostate tumor screening. 18F-PSMA-1007 PET/MR imaging significantly improved the detection of csPCa, mainly to improve the diagnostic value of prostate-specific antigen (PSA) at 4-10ng/mL for clinically significant prostate cancer (csPCa), which helped to reduce unnecessary prostate biopsy.

PO-033

Long-term Outcomes of Ablation versus Surgery in Patients with Colorectal Lung Oligometastasis: A Retrospective Cohort Study

Tian-Qi Zhang, Yu-Zhe Cao, Pei-Hong Wu, Jin-Hua Huang
Sun Yat-sen University Cancer center

Purpose Lung is the common metastatic site of colorectal carcinoma. Treatment of colorectal lung oligometastasis (CLOM) by surgical and ablative procedures has been proved to prolong survival and palliate symptoms. We aimed to analyze the long-term outcomes of patients with CLOM treated with surgery or ablation.

Materials and methods •From January 2012 to October 2018, patients diagnosed with CLOM that underwent surgery or ablation at the Sun Yat-sen University Cancer Center were retrospectively analyzed. •To ascertain the nuances between these treatment modalities, statistical comparisons were conducted utilizing the Chi-square test, t-test, or Wilcoxon test, depending on the nature of the variables under consideration. •The survival analyses on overall survival and progression-free survival were meticulously calculated using the Kaplan-Meier method and the disparities in survival rates between the two treatment groups were rigorously examined employing the log-rank test.

Results The study included 96 patients with 134 lesions, including 25 females (26.0%) and 71 males (74.0%). All the patients had received the primary colorectal lesion resection before treatment of metastasis. There were 41 patients with 75 lesions receiving ablation and 55 patients with 59 lesions receiving surgery. The median follow-up time was 58.3 months (IQR: 38.6-73.7). The median overall survivals (mOS), 3- and 5-year survival rates between the two groups showed no significant difference (Ablation vs. Surgery, mOS: 73.3 months vs 70.4 months, $P=0.64$; 3-year survival rate: 82.6% vs. 79.8%; 5-year survival rate: 59.9% vs. 58.7%. The median progression-free survivals (mPFS) were 12.1 months in the ablation group and 11.5 months in the surgery group ($P=0.48$), respectively. Local rates of recurrence per lesion were 26.7% and 22.0% ($P=0.68$). And the pulmonary mPFS were 14.5 months vs. 14.1 months ($P=0.95$).

Conclusion Our retrospective cohort data showed that there was no significant difference between surgery and ablation in long-term survival benefit to CLOM patients.

PO-034

A Metrology Informatics Investigation of Conversion Therapy in Hepatocellular Carcinoma: 2014-2023

Qi-Feng Chen, Ming Zhao
SYSUCC

Purpose With advancements in drug therapy, local treatments, and evolving concepts, conversion therapy has shown benefits for patients initially diagnosed with unresectable hepatocellular carcinoma (HCC). Over past ten years, the conversion therapy field has accumulated a vast amount of underutilized data, necessitating in-depth bibliometric evaluation.

Materials and methods This cross-sectional retrospective study collected a substantial amount of research on conversion therapy published between 2014 and 2023, adhering to strict search criteria. The primary outcomes were publication volume, citation count, and inter-study relationships. Comprehensive analysis was conducted using unsupervised hierarchical clustering, spatiotemporal analysis, regression model, and the Walktrap algorithm.

Results Over the past decade, conversion therapy has demonstrated significant progress, with an annual growth rate of 23.0%. Post-2020, these metrics saw a marked increase, reaching 116 publications and 1,943 citations by 2023. Cluster analysis grouped 244 authors into 17 clusters, highlighting early and sustained contributions from Western authors compared to later-emerging Eastern authors. Research characteristics in HCC conversion therapy were classified into five clusters, with Cluster 2 (Target Therapy and Immunotherapy) emerging as a new focus. Thematic analysis categorized research characteristics into four quadrants, identifying "immune checkpoint inhibitor" and "combination therapy" as highly relevant and rapidly developing themes, while "hepatic arterial infusion chemotherapy" and "radioembolization" show high potential for future research.

Conclusion This study highlights key contributors and emerging trends and provides important predictions for future research directions. To achieve effective conversion therapy for HCC, researchers may prioritize immunotherapy and locoregional treatments such as hepatic arterial infusion chemotherapy or radioembolization.

PO-035

Analysis of short-term clinical efficacy and immune function changes of advanced non-small cell lung cancer after radiotherapy and chemotherapy under CT-guided ¹²⁵I seed implantation

Yunfeng Kou, Chuang Li
Zhongshan Hospital of Dalian University

Purpose To assess the clinical efficacy, safety, and immune status of advanced NSCLC patients after radiotherapy and chemotherapy with CT-guided ¹²⁵I particles.

Materials and methods From January 2016 to June 2022, 34 NSCLC patients who progressed after radiotherapy and chemotherapy were studied retrospectively. There were 34 evaluable lesions, and ¹²⁵I seeds were implanted into the lesions under CT guidance. The study's endpoints were as follows: Short-term clinical efficacy, quality of life score, and adverse reaction status assessment, with patients being collected from January 2020 to January 2022 for immune status assessment.

Results The average postoperative follow-up period was 16.58 ± 7.41 months. The one-year postoperative survival rate was 76.47%, the two-year postoperative survival rate was 58.82%, and the median overall survival was 16 (6–24) months; one-year PFS after operation The rate was 61.76%, the two-year PFS rate was 41.18%, and the median PFS was 12.5 (1–24) months. The percentage of CD3+ and CD4+T lymphocytes in the treatment group increased after surgery, and the percentage of NK cells increased. Positive immune factor levels of IL-2 and TNF- α , γ -IFN levels were increased after surgery, IL-4 levels were decreased after surgery, and IL-10 levels were decreased after surgery. TH17 (IL-17) levels decreased after surgery.

Conclusion ¹²⁵I particle therapy is an effective treatment for NSCLC that has progressed following radiotherapy and chemotherapy. Local treatments improve patients' quality of life and reduce tumor burden, ¹²⁵I particle therapy can improve the immune status of patients.

PO-036

AI Guided Swift Response: Transforming Stroke Diagnosis.

Ruqqayia Adil

NUST School of Health Sciences NSHS, National University of Sciences and Technology NUST, Islamabad, PAKISTAN

Purpose

To mitigate stroke diagnosis challenges, we propose an AI-guided stroke diagnosis system that leverages advanced AI approaches, such as deep learning frameworks, to provide timely and precise stroke diagnosis and efficient treatment planning.

- To collect brain CT scan data from local radiology centres.

- To perform annotation and manual segmentation of CT scan images to identify stroke affected regions.

- To develop a stroke diagnosis model utilizing CT scans by using deep neural networks.

- To design and develop a digital user-friendly interface for deploying of model.

Materials and methods This diagnostic system utilizes local computerized tomography CT brain scan data collected from different hospitals in Pakistan (around 5000 images to train the model) within a deep learning framework for timely and precise diagnosis. Moreover, these techniques will be incorporated into the digital system in GUI to support physicians in decision making, for efficient stroke treatment.

Results ongoing study. results end of April

Conclusion In conclusion, the delay in seeking medical attention, misdiagnosis, delayed diagnosis, and limited accessibility of diagnostic services worsens the stroke's timely treatment. Timely initiation of the treatment upon the hospital's arrival is crucial to ensure optimal recovery. AI technologies have the potential to revolutionize stroke detection and treatment by increasing diagnostic accuracy and streamlining patient care, benefiting affected individuals.

PO-037

Endovascular Management of Post-Transplant Portal Vein Stenosis: A Case Report of Balloon Angioplasty in a Pediatric Living-Donor Liver Recipient

Dayanara Prama Iswari, Stefani Stascia, Sahat Matondang, Krishna Pandu Wicaksono
Department of Radiology, University of Indonesia

Purpose We report a case of a 2-year-old patient with elevated liver enzyme and had abnormal findings on Doppler ultrasonography and developed portal venous stenosis seven months after LDLT.

Materials and methods The procedure was performed under general anesthesia. A 7 Fr introducer sheath was placed percutaneously into the right ileocolic vein followed by 5 Fr Cobra diagnostic catheter over a 0.035" guidewire and advanced into the main portal vein. Diagnostic venography revealed a stenosis at the portal hilum, with the narrowest segment measuring 2 mm in diameter, with normal proximal portal vein diameter of 6 mm.

Initial guidewire was exchanged for a 0.035" 260 cm exchange wire, followed by a 12 mm × 40 mm Mustang balloon catheter at the site of stenosis. Serial inflations were performed in a controlled manner, at 4 atm, 6 atm and 8 atm. Each inflation was followed by a 2-minute interval. Post-dilation venography was performed to assess procedural success.

Results Post-ballooning venography demonstrated complete resolution of the stenosis, with the portal vein lumen at the hilar region fully restored to 6 mm. No evidence of vascular dissection, thrombus formation, or extravasation was observed. The catheter, wire, and sheath were then removed and followed by reconstruction of right ileocolic vein.

Doppler ultrasound was done the next day confirming normal hepatic vascular flow, with improved peak velocity indicating successful restoration of portal flow. The patient remained stable, clinically well and was discharged in stable condition two days post-procedure.

Conclusion Portal vein balloon angioplasty proved to be an effective and minimally invasive intervention for post-transplant portal vein stenosis in a pediatric LDLT recipient. This case highlights the role of endovascular techniques in managing vascular complications after liver transplantation, offering a safe and viable alternative to surgical revision.

PO-038

Growth Pattern of MRI to Predict Tumor Progression for Hepatocellular Carcinoma Response to Systemic and Locoregional Therapies

Langlang Tang², Zhuting Fang¹

1. Clinical Oncology School of Fujian Medical University, Fujian Cancer Hospital (Fujian Branch of Fudan University Shanghai

2. Longyan First Affiliated Hospital of Fujian Medical University

Purpose Hepatocellular carcinoma (HCC) is common in East and Southeast Asia and is usually diagnosed at intermediate or late stages, complicating treatment that involves both local and systemic approaches. As the best examination method for the liver, MRI is considered as one of the markers for evaluating treatment response. To investigate the value of pre-treatment MRI tumor growth patterns in hepatocellular carcinoma (HCC) and early progress.

Materials and methods This study retrospectively analyzed MRI data from patients diagnosed with hepatocellular carcinoma. Tumors were classified according to four distinct growth patterns: rough, smooth, focal extraocular protuberant(FEP), and nodular confluent(NC). Patient progression-free survival (PFS) was evaluated in relation to these growth patterns. Cox regression analyses, both univariate and multivariate, were employed to identify independent risk factors associated with PFS. Furthermore, Kaplan-Meier methods and log-rank tests were utilized to assess the statistical differences across various risk groups.

Results A total of 161 patients from 2 independent centers were enrolled. In the primary cohort(n=86), 18.60% were classified as rough type, 46.51% as smooth type, 27.91% as focal extraocular protuberant(FEP) type, and 6.98% as nodular confluent(NC) type. Patients with smooth and FEP growth patterns experienced longer progression-free survival (PFS), whereas those with rough and NC types had shorter PFS ($P<0.001$). In multivariate Cox analysis, primary cohort showed rough- and NC-growth patterns (hazard ratio [HR]:3.87, 95% confidence interval [CI]: 1.59-9.42, $P=0.003$) and multiple lesions(HR:0.34, 95%CI: 0.14-0.83, $P=0.018$) were independent risk factors for PFS. In validation cohort(n=75), the PFS of the high-risk growth patterns was shorter than that of the low-risk ($P<0.05$). Furthermore, low-risk groups exhibited favorable pathological characteristics, such as fewer lesions and lower histological grades, underscoring the clinical relevance of growth pattern assessment.

Conclusion In HCC, both NC and rough growth patterns observed in pre-treatment MRI are linked to disease progression, even in unresectable cases, and may inform treatment decisions.

PO-039

Single-cell analysis reveals heterogeneity in the molecular profile of the tumor microenvironment of biliary tract cancers

Qing GOU

Guangdong Provincial People's Hospital

Purpose To identify potential transcriptomic changes of clinical significance in BTCs and explore the impact of these changes and heterogeneity on immunotherapy.

Materials and methods We integrated single-cell RNA sequencing data from BTC patients (iCCA, GBC, and eCCA) and RNA sequencing data from cholangiocarcinoma samples to construct a cellular molecular atlas of BTCs. Through enrichment analysis, we explored signaling pathways in tumor and TME cells, identified developmental trajectories and characterized transcription factors regulating different cell subpopulations via pseudotime analysis and gene regulatory network analysis. Moreover, we analyzed the intercellular communication between tumor cells and TME cells in different BTCs and developed a prognostic model.

Results Malignant cells in different BTCs displayed significant heterogeneity, with variations in immune cell composition, biological functions, and metabolic pathways. Notably, the iCCA subpopulation presented increased invasive potential, whereas the eCCA and GBC subpopulations presented significant activation of energy metabolism-related pathways. The carcinoma-associated fibroblast subpopulations in eCCA and GBC may regulate tumor cell metabolism through metabolic reprogramming, thereby facilitating tumor proliferation. GBC specifically exhibited enrichment of CXCL13⁺ tumor-reactive CD8⁺ T cells, indicating a potentially favorable response to immune checkpoint blockade therapy. Additionally, as tumor progression occurred, the macrophage subpopulations in all three BTCs displayed M1/M2 dichotomous polarization, and the antigen-presenting ability of monocyte-derived dendritic cells gradually decreased.

Conclusion This study analyzed single-cell landscape heterogeneity across BTC subtypes, revealing complex intercellular communication within the TME. A prognostic model was developed, providing insights for personalized precision medicine.

PO-040

Efficacy and safety of lenvatinib plus gefitinib in lenvatinibresistant hepatocellular carcinomas: a prospective, single-arm exploratory trial

Yaoping Shi, Dan Cui, Lei Xia, Wenxin Qin, Rene Benards, Haojie Jie, Bo Zhai
Renji Hospital, Shanghai Jiao Tong University School of Medicine

Purpose Lenvatinib, a multi - kinase inhibitor, is approved as first - line treatment for advanced hepatocellular carcinomas (HCC), yet its efficacy is restricted. Previous work demonstrated that the combination of lenvatinib and EGFR TKI can overcome lenvatinib resistance in EGFR high HCC. This study aims to explore the effect of the combination of lenvatinib and the EGFR-TKI gefitinib in patients with HCC resistant to lenvatinib.

Materials and methods A single - arm, open - label, exploratory study (NCT04642547, n = 30) was conducted. Only patients with EGFRhigh HCC who had progressive disease after lenvatinib treatment were recruited and received the combination of lenvatinib and gefitinib. Gefitinib was initially administered at half of the normal clinical dose, that is, 125 mg per day. If the patient could tolerate well after 1 week, then the dose was adjusted to 250 mg per day. Lenvatinib was administered at the normal clinical dose (body weight <60 kg, 8mg per day; body weight ≥60 kg, 12 mg per day). The primary end point was ORR, and the secondary end points was PFS, DCR and OS. The overall response was assessed by means of RECIST1.1 and mRECIST, respectively. All AEs were documented and evaluated in accordance with the National Cancer Institute Common Terminology Criteria for Adverse Events version 3.0.

Results The most common all - grade adverse events were fatigue (27 patients, 90%), followed by rash (25 patients, 83.3%), diarrhea (24 patients, 80%), and anorexia (12 patients, 40%). According to mRECIST criteria, 9 out of 30 patients (30%) achieved a confirmed partial response and 14 (46.7%) had stable disease. Based on RECIST1.1, 5 patients (16.7%) achieved a confirmed partial response and 18 (60%) had stable disease. The estimated median progression free survival (PFS) was 4.4 months (95% CI: 2.5 - 5.9) and the overall survival (OS) was 13.7 months (95% CI: 9.0 - NA). The objective response rate (ORR) of this study was more favorable compared to the two approved second - line treatments for HCC (cabozantinib ORR 4%; regorafenib ORR 11%).

Conclusion The combination of lenvatinib and gefitinib was well - tolerated. Thus, further clinical studies of this combination are needed.

PO-041

Dual-Pathway Interventional Strategy: Addressing Both Venous Obstruction and Neoplastic Burden in Malignant Superior Vena Cava Syndrome in Advanced Non-small Cell Lung Cancer through Combined Stenting and Drug-eluting Beads Transbronchial Arterial Chemoembolization

Yi Deng¹, Wei Cui²

1. Kunming University of Science and Technology

2. Department of Interventional Radiology, Guangdong Provincial People's Hospital (Guangdong Academy of Medical Sciences), Southern Medical University.

Purpose The technical feasibility and clinical safety of endovascular stenting combined with DEB-BACE for the treatment of patients with advanced NSCLC combined with malignant SVCS need to be demonstrated.

Materials and methods Twelve patients who underwent treatment of malignant SVCS in advanced NSCLC with endovascular stenting combined with DEB-BACE from May 2022 to October 2024. All patients were primarily reassessed within 72h after operation to evaluate technical success, clinical symptom, Kishi score, SVCS grade, and potential postprocedural complications. Patients were contacted by telephone for secondary follow-up, and tumor response outcome, stent patency, OS and treatment-related complications were evaluated between 1 to 29 months after procedure.

Results Baseline characteristics of endovascular stenting combined with DEB-BACE for treating malignant SVCS in 12 patients with advanced NSCLC were summarized in Table 1. Within 72h postoperatively, 11 patients (91.7%) achieved clinical success compared to the preoperative period. One patient (8.3%, case 4) experienced clinical symptoms relief but still had dyspnea, and most patients still had a mild cough. The Kishi score ranged from 0 to 3, with a mean value of 0.8. It demonstrated statistically significant differences preoperatively and 72h postoperatively ($Z=-3.084$, $p=0.002$, Fig 3a). Except for one patient (case 4) who had a postoperative SVCS grade of 1, the SVCS grade was reduced to 0 in remaining patients ($p=0.001$). Only one (case 5) of the 12 patients had transient chest pain within 72h after the operation, which was a minor complication and was relieved after symptomatic treatment, and the rest of the patients did not have any complication. There were no cases of death caused by SVCS stenting or DEB-BACE. There was no significant difference in blood routine and liver and kidney function before and 1 month after operation (all $p>0.05$). The tumor responses were PR (3 of 12 patients [25%]), SD (8 of 12 patients [66.7%]), PD (1 of 12 patients [8.3%]), and no CR. The median follow-up duration was 17.0 months (range 0.8-28.4 months). At the end of follow-up, the stents of all patients were unobstructed, and the stent patency was 11.2 ± 9.2 months. The percentage of patients who died during follow-up was 41.7% (5 of 12). Median OS was not reached. The mean OS was 17.6 months (95% CI: 10.3-24.8) (Fig 5b). The estimated OS rates at 1 month and 8 months were 83.3% and 56.3%, respectively.

Conclusion Endovascular stenting combined with DEB-BACE is a feasible, safe, and effective treatment option for patients with malignant SVCS with advanced NSCLC

PO-042

Effect of blood glucose level on prognosis of patients with intermediate and advanced hepatocellular carcinoma treated by transarterial chemoembolization combined with targeted and immune drugs

Haodong Wu,Chenyou Liu,Nan Jiang,Ruizhe Chen,Wanci Li,Shuai Zhang,Xiaoli Zhu,Jian Shen
The First Affiliated Hospital of Soochow University

Purpose To investigate the effect of fasting glucose level on the prognosis of patients with intermediate-advanced hepatocellular carcinoma (HCC) treated by transarterial chemoembolization (TACE) combined with PD-1/PD-L1 inhibitors and molecular targeted drugs.

Materials and methods The clinical data of patients with intermediate-advanced HCC who received TACE combined with targeted immunotherapy in our hospital from February 2019 to November 2023 were retrospectively analyzed, and the patients meeting the inclusion criteria were screened and divided into hyperglycemic group(HG group) and normal blood glucose group(NG group) according to the fasting blood glucose level before treatment. Survival curves were plotted by Kaplan-Meier method, and differences between groups were evaluated by Log-Rank method. Median progression-free survival (mPFS) and median overall survival (mOS) were compared between the two groups. Cox proportional hazard regression was used to analyze the prognostic factors of patients with intermediate-advanced HCC. The incidence of adverse reactions (AEs) was compared between the two groups.

Results A total of 82 HCC patients were included in this study, including 37 in the HG group and 45 in the NG group. The median PFS of HG group and NG group were 8.17 (95%CI: 6.78-9.56) months and 9.53 (95%CI: 7.56-11.50) months, respectively, and the difference was statistically significant ($P=0.007$). The median OS of HG group and NG group were 10.93 (95%CI: 9.30~12.56) months and 17.43 (95%CI: 15.54~19.32) months, with a statistically significant difference($P<0.001$). Multivariate Cox proportional risk regression analysis showed that the history of diabetes and vascular invasion were independent risk factors for the long term prognosis of HCC patients. There was no significant difference in the incidence of treatment-related adverse reactions between the two groups.

Conclusion High blood glucose level is an adverse factor affecting the prognosis of patients with intermediate-advanced HCC who receive TACE combined with PD-1/PD-L1 inhibitors and molecule-targeted drugs.

PO-043

Precision Targeting of ERK5 Combined with PD-L1 Blockade Remodels the HCC Microenvironment: A Comprehensive Study of Synergistic Antitumor Mechanisms

Qiaoting Hu, Yundan You, Xiaojie Wang, Zengqing Guo
Clinical Oncology School of Fujian Medical University

Purpose To delineate the expression patterns of MAPK subtypes and immune checkpoints within the HCC microenvironment, explore the interplay between MAPK signaling and immune modulation, and identify synergistic therapeutic targets specifically targeting a MAPK subtype and an immune checkpoint.

Materials and methods Integrated analyses including single-cell RNA sequencing, multiplex immunofluorescence, and flow cytometry were performed to examine ERK5 and PD-L1 expression patterns. In vitro mechanistic studies utilized ERK5 knockdown via siRNA and pharmacological inhibition, along with functional assays for CD8⁺ T cell cytotoxicity. In vivo experiments were conducted using murine HCC models treated with ERK5 inhibitor, anti-PD-L1 antibody, or combination therapy.

Results ERK5 and PD-L1 showed significant co-localization with high expression predominantly in tumor cells and immunosuppressive cell populations (TAMs and Tregs). ERK5 activation upregulated PD-L1 expression via the NF- κ B/AP-1 signaling axis, impairing CD8⁺ T cell function. ERK5 inhibition decreased PD-L1 levels and restored CD8⁺ T cell cytotoxicity. Combined ERK5 inhibitor and anti-PD-L1 antibody treatment synergistically suppressed tumor growth, remodeled immune cell composition within the tumor microenvironment, and enhanced T cell-mediated antitumor responses.

Conclusion Dual targeting of ERK5 and PD-L1 synergistically remodels the HCC microenvironment and activates antitumor immunity, representing a promising strategy for precision immunotherapy in HCC with valuable insights for clinical translation.

PO-045

Mechanism and Application Progress of Nanomedicine Delivery Systems in Inducing Ferroptosis of Tumors

Jiaqi You

The First Affiliated Hospital of China Medical University

Purpose This article aims to systematically review the research progress on inducing ferroptosis in tumor cells based on nanomedicine delivery systems, explore its potential in anti-tumor therapy, and analyze the combined application of nanomedicines with other therapeutic approaches.

Materials and methods Through literature review, this paper summarized the molecular mechanism of iron death and its application in cancer therapy. The role of nanomedical drug delivery systems in promoting iron death was analyzed, including the design and application of iron-based and non-iron-based nanomaterials. In addition, the combined application of nanomedicine with chemotherapy, photothermal therapy, photodynamic therapy, sonodynamic therapy and immunotherapy was also discussed.

Results Iron death, as a new type of cell death, has significant anti-tumor potential. Nano drug delivery system can effectively induce iron death of tumor cells by promoting Fenton/Fenton-like reaction, inhibiting antioxidant defense system and regulating lipid metabolism. The combination therapy strategy further enhanced the anti-tumor effect of nanomedicine, especially in refractory cancers such as liver cancer and lung cancer.

Conclusion The iron death induction strategy based on nanomaterial drug delivery system provides a new direction for tumor therapy. Future studies should further optimize the design of nanomedicine, explore its potential for clinical application, and address its potential toxicity and targeting. The combination treatment of iron death nanomedicine is expected to be an important breakthrough in cancer treatment.

PO-046

Association between regional lymph node metastasis and survival outcomes in advanced hepatocellular carcinoma receiving transarterial chemoembolization and PD-(L)1 inhibitors-based immunotherapy

Qian Chen, Longwang Lin, Zhicheng Jin, Gaojun Teng
Southeast University, Zhongda Hospital

Purpose Tumor-draining lymph nodes play an important role in anti-tumor immune responses. In patients with hepatocellular carcinoma (HCC), however, the relationship between regional lymph node metastasis (LNM) and immunotherapy-based efficacy is unclear. We aimed to evaluate whether extrahepatic LNM is associated with worse survival outcomes as compared to other metastatic sites.

Materials and methods From May 2019 to August 2023, this retrospective, multicenter study enrolled 129 patients with metastatic HCC receiving first-line PD-(L)1 inhibitors plus molecular targeted agents (MTAs) and transarterial chemoembolization (TACE). Patients with only LNM were matched 1:1 with metastatic HCC without LNM, using nearest neighbor matching with a caliper of 0.2 to balance out baseline confounders (i.e., performance status, liver function, AFP level, tumor burden, portal vein tumor thrombus and number of metastases). Overall survival (OS) and progression-free survival (PFS) were compared between the two groups using Kaplan-Meier curves and log-rank test, and the magnitude of the differences was estimated by Cox proportional hazards model.

Results Extrahepatic LNM occurred in 54 (41.9%) patients, of which 45 (83.3%) involved hilar lymph nodes. Other metastatic sites included lung (37.2%), bone (11.6%), adrenal gland (7.0%), peritoneum (6.2%), and the others (4.6%). A total of 42 patients with LNM were matched correspondingly. The median OS (11.6 months [95% CI 9.7-16.0] vs 23.0 months [15.2-NA]; hazard ratio (HR) 2.25 [1.31-3.89]; $p = 0.003$) and PFS (6.2 months [95% CI 4.7-8.9] vs 8.9 months [5.7-13.5]; HR 1.74 [95% CI 1.07-2.81]; $p = 0.023$) in LNM patients were significantly shorter compared to those metastatic HCC without LNM. Besides, the number of LNM (> 4) and hilar involvement were both associated with significantly worse PFS and OS (all $p < 0.05$). According to RECIST version 1.1, objective response rate was numerically lower for LNM group (21.4% vs 26.2%).

Conclusion In patients with metastatic HCC treated with TACE plus PD-(L)1 inhibitors and MTAs, LNM is associated with significant deterioration in OS and PFS, compared with non-LNM. These findings suggest a negative impact of regional LNM on the efficacy of immunotherapy, and additional extrahepatic treatment strategies may be warranted for these targeted patients.

PO-047

TACE combined with Apatinib for Advanced Perihilar Cholangiocarcinoma: A Single-arm, Phase II Study

Hao Li,Xuhua Duan

The First Affiliated Hospital of Zhengzhou University

Purpose To confirm combination of TACE-delivered albumin paclitaxel and gemcitabine with apatinib for advanced PCC is effective and safe.

Materials and methods A comprehensive treatment plan involving TACE combined with targeted therapy was implemented for the patients with pathologically diagnosed advanced PCC, where TACE was performed every 4-6 weeks to deliver albumin paclitaxel and gemcitabine for a maximum of six times. Oral apatinib was administered in between TACE cycles. The main endpoint of this study was the objective response rate (ORR), and the secondary endpoints were progression free survival (PFS), overall survival (OS), and adverse events. Kaplan-Meier method was used to assess survival risk factors. From November 2019 to October 2020, a total of 41 patients were enrolled with perihilar cholangiocarcinoma who were pathologically diagnosed. All underwent TACE treatment and received at least two treatment cycles.

Results As of October 2022, the median follow-up period of this study was 28.3 months, the ORR of this study reached 56.1% (95% CI: 39.7-71.5%); DCR reached 90.2% (95% CI: 76.9-97.3%), and the median PFS was 9.7 months (95% CI: 7.6-11.8 months), the median OS was 16.5 months (95% CI: 13.6-19.3 months). The treatment-related adverse events (AEs) in this study were mild, mainly Grade 1 or 2. Among the most common AEs were bone marrow suppression and hand-foot syndrome, while no patient had Grade 4 AE.

Conclusion Comprehensive treatment combining TACE-delivered albumin paclitaxel and gemcitabine with apatinib for advanced PCC had favorable therapeutic effects, and no major safety issue was observed in the patients enrolled.

PO-048

Real-world effectiveness and safety of transcatheter arterial chemoembolization with EqualSpheres beads in patients with hepatocellular carcinoma

Shuguang Ju,Xuhua Duan
The First Affiliated Hospital of Zhengzhou University

Purpose This retrospective study aimed to investigate the short-term efficacy and safety and outcomes of HCC patients treated by transarterial chemoembolization (TACE) using EqualSpheres beads (ETACE) with layered embolization strategy.

Materials and methods Eligible patients were given 3-4 cycles ETACE with layered embolization strategy, until either disease progression or intolerable toxicities emerged. Toxicity was assessed using NCI CTCAE v5.0. Response was assessed using mRECIST criteria. Objective response rates (ORR) and progression-free survival (PFS) was the primary endpoint. Disease control rates (DCR), and treatment-related adverse events (TRAEs) were secondary endpoints.

Results Total, 310 patients with HCC were were successfully enrolled. Overall, the best objective response rate (ORR) was 71.0% (220/310) and DCR was 89.0% (276/310). Median follow-up lasted 14.5 months (95% CI: 11.8–20.5 months). Median PFS was 11.2 months (95% CI: 7.2–24.6 months). Majority of TRAEs were mild and manageable. ETACE-related adverse events (AEs) was commonly embolism syndrome such as fever, pain, gastrointestinal reactions, nausea, vomiting, new ascites, and abscess. Controllable liver abscess was special phenomena in the study. The ten patients with uncontrollable liver abscess were successfully control by intubation and drainage.

Conclusion In this prospective study, high ORR and long PFS were observed after ETACE with layered embolization strategy with encouraging results and manageable safety.

PO-049

SLC1A5 Associated with Poor Prognosis and TACE Resistance in Hepatocellular Carcinoma

Guixiong Zhang, Jiaping Li

The First Affiliated Hospital, Sun Yat-Sen University

Purpose Hepatocellular carcinoma (HCC) is a common malignant tumor, and glutamine is vital for tumor cells. The role of glutamine transporter SLC1A5 in tumor progression and transarterial chemoembolization (TACE) efficacy is under study. This research seeks to determine the impact of SLC1A5 expression on the prognosis and TACE efficacy of HCC and elucidate its mechanisms.

Materials and methods SLC1A5 expression in HCC, correlation with patient outcomes, and response to TACE were studied in an open access liver cancer dataset and confirmed in our cohort. Additionally, the correlation between SLC1A5 expression and hypoxia, angiogenesis and immune infiltration was analyzed and verified by immunohistochemistry, immunofluorescence and transcriptome sequencing. Liver cancer cell lines with SLC1A5 expression knockdown or overexpression were constructed, and cell proliferation, colony formation, apoptosis, migration and drug sensitivity as well as in vivo xenograft tumor were measured. A gene set enrichment analysis was conducted to determine the signaling pathway influenced by SLC1A5, and a western blot analysis was performed to detect protein expression alterations.

Results SLC1A5 expression was higher in HCC tissue and associated with poor survival and TACE resistance. Hypoxia could stimulate the upregulation of glutamine transport, angiogenesis and SLC1A5 expression. The SLC1A5 expression was positively correlated with hypoxia and angiogenesis-related genes, immune checkpoint pathways, macrophage, Tregs, and other immunosuppressive cells infiltration. Knockdown of SLC1A5 decreased proliferation, colony formation, and migration, but increased apoptosis and increased sensitivity to chemotherapy drugs. Downregulation of SLC1A5 resulted in a decrease in Vimentin and N-cadherin expression, yet an increase in E-cadherin expression. Upregulation of SLC1A5 increased Vimentin and N-cadherin expression, while decreasing E-cadherin. Overexpression of β -catenin in SLC1A5-knockdown HCC cell lines could augment Vimentin and N-cadherin expression, suppress E-cadherin expression, and increase the migration and drug resistance.

Conclusion Elevated SLC1A5 was linked to TACE resistance and survival shortening in HCC patients. SLC1A5 was positively correlated with hypoxia, angiogenesis, and immunosuppression. SLC1A5 may mediate HCC cell migration and drug resistance via Epithelial-mesenchymal transition (EMT) pathway.

PO-050

TACE combined with DynaCT guided MWA in the treatment of high-risk location liver cancers with ≤ 5 cm tumor size

Xuhua Duan, Daqian Han

The First Affiliated Hospital of Zhengzhou University

Purpose To evaluate the safety and effectiveness of transcatheter arterial chemoembolization (TACE) combined with DynaCT guided microwave ablation (MWA) in the treatment of ≤ 5 cm high-risk location liver cancers.

Materials and methods Clinical materials of 55 newly diagnosed liver cancer patients with ≤ 5 cm unifocal lesion admitted in our department from September 2019 to January 2021 were collected. Liver function change, adverse reaction, tumor control rate, cumulative survival rate, overall survival (OS) and progression-free survival (PFS) of the group were compared.

Results All patients successfully completed the treatment of TACE combined with MWA. According to Common Terminology Criteria for Adverse Events (CTCAE), adverse reactions and complications are mainly Grade 1 or 2 (mild symptoms, no or local/noninvasive intervention indicated). The average OS in high-risk location group were 39.938 months (95% CI: 39.763, 40.113). The average PFS in high-risk location group were 32.219 months (95% CI: 31.976, 32.462). The objective response rates (ORR) one month after the first combinational treatment in high-risk location group were 96.4%, and disease control rates (DCR) were 98.2%. The cumulative survival rates of 6, 12, 24, 36 months in high-risk location group were 100%, 92.8%, 82.1% and 67.9%.

Conclusion TACE combined with MWA is equally safe and effective for ≤ 5 cm high-risk location liver cancers.

PO-052

Advances in the study of risk factors and precise management of moderate-to-severe abdominal pain after TACE for primary hepatocellular carcinoma

Nian nian Weng
Chongqing University Cancer Hospital

Purpose Primary hepatocellular carcinoma (HCC) is the second leading cause of cancer-related deaths in China, and most patients have lost the opportunity for surgery at the time of diagnosis, so hepatic artery chemoembolisation (TACE) has become the core treatment for intermediate and advanced hepatocellular carcinoma. However, the incidence of moderate-to-severe abdominal pain after TACE is as high as 38.6%, which significantly affects patients' recovery and treatment compliance.

Materials and methods In this study, we systematically searched 48 high-quality studies (including 12 RCTs and 26 cohort studies) in PubMed, Web of Science and other databases from 2018-2023, and performed Meta-analysis using RevMan 5.4 software, integrating the clinical data with the application of emerging technologies, to systematically investigate the post-TACE abdominal pain. The epidemiological characteristics, risk factors and management strategies of post-TACE abdominal pain were systematically investigated.

Results The results showed that: i) the incidence of moderate-to-severe abdominal pain was significantly different between conventional TACE (45.2%) and drug-loaded microsphere TACE (29.8%) ($P < 0.01$), and the peak of pain was mostly concentrated in the 6 hours after the procedure; ii) age < 50 years ($OR = 2.31$), non-super-selective embolism ($OR = 4.05$), and portal cancer embolism ($OR = 2.78$) were the key independent risk factors (all $P < 0.01$); (iii) the combination of an intelligent assessment system based on facial expression analysis (FaceScale) and serum substance P ($SP > 45 \text{ pg/ml}$) improved the sensitivity of pain recognition to 89.3% ($AUC = 0.86$); (iv) the constructed risk prediction model of TACE-PAIN ($C\text{-index} = 0.81$) and XGBoost machine learning model ($AUC = 0.87$) both showed good clinical efficacy; ⑤ the multimodal analgesic regimen improved pain control satisfaction to 78.5% ($P < 0.001$).

Conclusion This study confirms that the management of abdominal pain after TACE needs to be combined with individual patient characteristics, technological innovation and accurate prediction, and that imaging models and intelligent management systems should be further developed in the future in order to promote a paradigm shift towards a 'patient experience-centred' approach to interventional therapy for hepatocellular carcinoma.

PO-053

Ablation of pulmonary oligometastasis had influence on intrahepatic tumors response and progression patterns for patients receiving lenvatinib

Qunfang Zhou, Feng Duan
Chinese PLA General Hospital

Purpose For advanced hepatocellular carcinoma (HCC), the lung is the most common metastatic organ. Systemic therapy is the standard treatment for advanced HCC with pulmonary metastasis. Aggressive interventions such as surgery or ablation for oligometastasis can lead to better outcomes. For HCC with pulmonary oligometastasis, ablation of metastases improved patients' survival. This study aimed to explore the efficacy of ablation of metastases combined with lenvatinib (Ablation+Len) improved the survival and the influence on intrahepatic tumor response and progression patterns compared with Lenvatinib alone (Len).

Materials and methods This study included patients diagnosed with advanced HCC and pulmonary oligometastasis between January 2018 and June 2022 from six hospitals. The follow-up period concluded on June 30, 2024. 202 patients in the Len group and 182 patients in the Ablation+Len group were included. Propensity score-matching (PSM) analyses were used to balance baseline variables between the two groups. The primary endpoint was progression-free survival (PFS), defined as the time from the initiation of systemic therapy to tumor progression according to RECIST v 1.1 or the last follow-up. All tumors response and intrahepatic tumor response, overall survival (OS) and progression patterns were compared between the two groups.

Results The status of intrahepatic tumors was evaluated at 3 months according to mRECIST. The proportions of PR and SD in intrahepatic tumor responses were not significantly different between the two groups across the entire ($P = 0.184$), PSM ($P = 0.715$). At the 6-month evaluation, pulmonary oligometastasis in the Ablation+Len group were completely ablated. The proportions of CR, PR, SD, and PD were also significantly different between the two groups in the entire ($P = 0.002$), PSM ($P = 0.037$) cohorts. The median PFS was 11.0 ± 0.3 and 14.1 ± 0.5 months in the Len and Ablation+Len groups, respectively. The 6-, 12-, and 24-month PFS rates were 85.6%, 38.4%, and 5.4% in the Len group and 89.0%, 56.4%, and 18.1% in the Ablation+Len group, respectively. Compared with the Len group, the Ablation+Len group had significantly better PFS ($P < 0.001$). The median OS was 23.0 ± 1.2 months and 31.3 ± 1.2 months in the Len and Ablation+Len groups, respectively. The 1-, 2-, and 3-year OS rates were 89.8%, 55.8%, and 8.2% in the Len group and 97.4%, 64.2%, and 27.7% in the Ablation+Len group, respectively. The Ablation+Len group had better OS than the Len group in the entire ($P = 0.001$) and PSM ($P = 0.006$). Subgroup analysis revealed that Ablation+Len treatment improved the intrahepatic response ($P = 0.023$). In addition, the progression patterns between Len and Ablation+Len groups were obviously significant ($P = 0.017$).

Conclusion The ablation of pulmonary oligometastasis with lenvatinib resulted in longer PFS and OS than lenvatinib alone. Intratumor response was improved by the ablation of metastases, and Ablation+Len treatment had higher proportion of liver-only progression patterns.

PO-055

Effect of personalized health education on compliance with anticoagulant therapy in patients with deep vein thrombosis of lower extremities

Ping Hu
Cancer Hospital Chongqing University

Purpose To explore the effect of personalized health education nursing intervention on the compliance of anticoagulant treatment in patients with deep vein thrombosis of lower limbs.

Materials and methods A total of 80 patients with deep venous thrombosis of lower limbs who received anticoagulant and thrombolytic therapy in our hospital from January 2023 to January 2024 were selected as study objects and randomly divided into control group (n=40) and observation group (n=40), and the control group was given routine care; The observation group was given personalized health education nursing intervention on the basis of routine nursing, and targeted health education programs were developed according to the diagnosis and treatment plan of patients, the precautions of anticoagulant drugs used, the education level of patients and their families, occupational status, family environment, physical and mental status, etc. Anticoagulation files shall be established in duplicate, with one copy placed at the end of the bed during the patient's hospitalization and updated dynamically by the responsible nurse; one copy shall be handed over to the patient after discharge, and the date of blood monitoring shall be arranged; the other copy shall be kept by a special person in the department. After discharge, the patient shall be followed up once every two weeks, and the patient shall be followed up again in the afternoon of the day of blood monitoring, and the monitoring results shall be informed to the doctor in charge. Adjust the drug dose, update the anticoagulant file in time, and give medication guidance to patients again. After 3 months of intervention, the scores of anticoagulation knowledge and the compliance of anticoagulation treatment were compared between the two groups.

Results After 3 months of personalized health education intervention, the median score of anticoagulation knowledge was 10 points in the observation group and 6 points in the control group, and the difference between the two groups was statistically significant ($Z=-8.397$, $P < 0.01$). 77.5% of patients in the observation group and 40% in the control group had good compliance with anticoagulant therapy, and the difference was statistically significant ($\chi^2=13.254$, $P < 0.05$).

Conclusion Personalized health education nursing intervention can increase the anticoagulation knowledge of patients with deep vein thrombosis of lower limbs, improve the compliance and satisfaction of patients with anticoagulation treatment, provide patients with individualized anticoagulation management, enhance patients' confidence in self-management, strengthen patients' self-monitoring behavior, and improve the prognosis.

PO-056

Inhibiting the FGFR4 Signaling Pathway Suppresses Epithelial-to-Mesenchymal Transition in Hepatocellular Carcinoma After Transarterial Chemoembolization

Shen Zhang,Xiao li Zhu

First Affiliated Hospital of Soochow University

Purpose To investigate the mechanism of Lenvatinib inhibiting epithelial-mesenchymal transition(EMT) in hepatocellular carcinoma after transarterial chemoembolization(TACE).

Materials and methods HCC rats were categorized into either TACE alone or TACE combined with Lenvatinib group. EMT-associated proteins were analyzed using bioinformatic databases and validated in vitro using HCC cell lines(Huh7 and SNU-449) and in vivo through nude mouse. Statistical significance was set at $P<0.05$ using ANOVA and Pearson correlation.

Results Immunohistochemistry analysis post-TACE demonstrated EMT enhancement and PD-L1 upregulation, both attenuated by lenvatinib ($P<0.05$). Bioinformatic analysis found a closed correlation between PD-L1 and Snail-1, which is the crucial transcription factor of EMT($P<0.001$). In vitro Transwell assays exhibited that lenvatinib restrained the migration and invasion abilities in Huh7 and SNU-449 cells under hypoxic/starvation condition. PD-L1 overexpression facilitated HCC cells invasion, which lenvatinib suppressed. FGFR4 inhibitor reduced Huh7 migration and invasion. In nude mouse, PD-L1 overexpression decreased E-cadherin, increased Snail-1 expression in HCC tissue, and promoted lung metastasis ($P<0.01$), which was reversed by lenvatinib administration or FGFR4 knockdown($P<0.01$).

Conclusion Inhibiting the FGFR4 signaling pathway suppresses EMT in HCC after TACE.

PO-057

Chemotherapy plus concurrent irreversible electroporation improved local tumor control in unresectable hilar cholangiocarcinoma compared with chemotherapy alone

Lizhi Niu, Yangyang Ma
Guangzhou Fuda Cancer Hospital

Purpose To compare the curative effect for UHC, chemotherapy plus concurrent IRE and chemotherapy alone were set up.

Materials and methods From July 2015 to May 2019, 47 patients with UHC were analysed to chemotherapy+IRE group (n=23) or chemotherapy alone group (n=24) in this study. Treatment response was assessed with computed tomography (CT) or magnetic resonance imaging (MRI) 1 month after treatment and every 3 months thereafter. Local tumor progression (LTP), time to LTP, overall survival (OS) and procedure-related complications were compared between the two groups.

Results Chemotherapy plus concurrent IRE group showed a tendency toward a decreased rate of LTP (16.7% vs. 39.5%; $p=0.039$) and an increased complete response rate (52.2% vs. 12.5%; $p=0.011$) compared with chemotherapy alone group. Time to LTP was significantly longer in the chemotherapy plus concurrent IRE group compared to chemotherapy alone group (11.2 months vs. 4.2 months; $p=0.001$). Median OS was significantly longer in the chemotherapy plus concurrent IRE group compared to chemotherapy alone group (19.6 months vs. 10.2 months; $p=0.001$).

Conclusion Chemotherapy plus concurrent IRE improved local control and prolonged time to LTP and OS in patients with UHC.

PO-058

Application of Manchester pain management model combined with targeted psychological intervention in perioperative TACE in patients with liver cancer

Rong Zhou
Chongqing University Cancer Hospital

Purpose To explore the application of Manchester pain management model combined with targeted psychological counseling in the perioperative TACE of liver cancer patients, improve the painless interventional management program and build a specialty brand.

Materials and methods A total of 90 patients with malignant liver tumors who underwent transcatheter chemoembolization treatment from January 1, 2024 to August 16, 2024 were selected as the study objects, and were divided into the observation group and the control group by random number table method, 45 cases in each group. The control group received routine perioperative nursing for interventional patients, and the observation group received Manchester pain management model combined with targeted psychological counseling. In the observation group, the Manchester pain management model was introduced, and a multidisciplinary cooperative management team (including head nurse, attending physician, nurse, technician, pain management members, and psychological team members) was set up. Pain and psychological assessment and intervention were carried out in three stages according to the context of time: preoperative 1d, intraoperative, and postoperative (1h, 6h, 24h, 48h, 72h). The effective rate of pain control (NRS), patient satisfaction with analgesia, psychological status (DMSM), and comfort (Kolcaba's Comfort Status Scale (GCQ) were compared between the two groups.

Results The effective rate of pain control in the control group was 80% (NRS \leq 3 was classified as up to the standard and 9 people were not up to the standard), and the effective rate of pain control in the observation group was 93.3% (3 people were not up to the standard). The NRS scores in the observation group were lower than those in the control group at 1h, 6h, 24h, 48h and 72h after surgery ($P<0.01$). In the control group, the analgesic satisfaction of patients in the control group was 97.2% (40 patients were very satisfied with pain control, 5 patients were relatively satisfied), and the analgesic satisfaction of patients in the observation group was 98.8% (43 patients were very satisfied, 2 patients were relatively satisfied), with no statistical significance. Patients with positive mental state (7 in the observation group and 13 in the control group) could actively accept treatment, expressed confidence in the treatment plan and treatment effect, and had no incidents of suicide and self-injury. At 4 days after operation, GCQ scores and total scores in the observation group were higher than those in the control group ($P<0.05$).

Conclusion Manchester pain management model combined with targeted psychological intervention can effectively relieve patients' intraoperative and postoperative pain and correct adverse psychological states, which is of great significance to improve the efficiency of pain control, patient comfort, and patient medical experience, so as to build a perfect painless intervention management program and build a specialty brand.

PO-059

Radiological Characteristics Determine the Selection of Intra-arterial Therapy Modality for Intermediate-Stage Hepatocellular Carcinoma

Mengxuan Zuo, Weijun Fan
Sun-yat sen university cancer center

Purpose Radiologic pattern is a key factor for preoperative selection between hepatic arterial infusion chemotherapy (HAIC) and transarterial chemoembolization (TACE) for intermediate-stage hepatocellular carcinoma (HCC), but clinical evidence is required. We aimed to compare the effectiveness and safety between TACE and HAIC according to different radiologic pattern.

Materials and methods Between January 2009 and December 2022, 3,060 consecutive patients with intermediate-stage HCC underwent initial TACE or HAIC were identified retrospectively. The radiological features of HCC were classified into pseudo-capsulated type, pseudocapsule breakthrough type, confluent multinodular type and infiltrative type. Propensity score matching (PSM) method was used to reduce the selective bias. The progression-free survival (PFS) was compared using the Kaplan–Meier method with log-rank test. Multivariable analyses of independent prognostic factors were evaluated by means of the forward stepwise Cox regression model.

Results After PSM, 237 patients per group was included in the infiltrative HCC cohort and 262 in the non-infiltrative HCC cohort, respectively. Notably, radiologic patterns were highly associated with tumor burden (six-to-twelve criteria). Pseudo-capsulated type was dominant (55.6%) in < 6 cohorts and infiltrative type was dominant (49.5%) in >12 cohorts. A higher PFS were observed in HAIC group than that in TACE group in the infiltrative HCC cohort ($P<0.001$), but comparable PFS was found between two groups in the non-infiltrative HCC cohort ($P=0.532$). Tumor burden and radiologic morphology were significantly associated with PFS in the multivariate analysis.

Conclusion HAIC present a safe and effective treatment for infiltrative intermediate-stage HCC that provided power evidence for supplement in updated BCLC guideline.

PO-060

Proliferative Subtype–based Deep Learning Model for Identifying the Survival Benefit of Patients with Hepatocellular Carcinoma Receiving Intra-arterial Therapies

Mengxuan Zuo, Fei Gao
Sun-yat sen university cancer center

Purpose Hepatocellular carcinoma (HCC) is a leading cause of cancer-related mortality. The proliferative subtype, characterized by aggressive behavior, accounts for 30%–50% of all cases. However, A biopsy to identify proliferative HCC is not routinely performed before therapy. This study aims to develop a multitasking transformer model capable of identifying patients with proliferative HCC and predicting survival benefits following intra-arterial therapies (IATs), including transarterial chemoembolization (TACE) and hepatic arterial infusion chemotherapy (HAIC).

Materials and methods This retrospective study included 398 patients with HCC who had undergone surgical resection with a pathological diagnosis of proliferative or nonproliferative HCC (cohort 1) and 1749 unresectable HCC (uHCC) patients who had received initial TACE or HAIC as first-line therapy (cohort 2). All patients underwent standard dynamic contrast-enhanced computed tomography (CECT) within 2 weeks before initial treatment. A pretrained nnUNet model automatically delineated the entire liver and tumor regions in the arterial and venous phases. Prototype Mamba Net (PMN) models were constructed to identify proliferative HCCs in cohort 1 to obtain the deep learning (DL) risk score. Then, nomograms were developed by a new Cox-proportional-hazards model integrating the CECT imaging features and clinical data to identify proliferative HCCs and predict overall survival (OS) after IATs. Additionally, the predictive accuracy of tumor stages and DL models were compared.

Results The DL model achieved high accuracy in identifying proliferative HCCs, with an area under curve (AUC) of 0.825 (95% confidence interval [CI], 0.781–0.884) in the training set and 0.792 (95% CI, 0.732–0.841) in the testing set. The TACE- and HAIC-nomograms provided superior prognostic prediction ability, with time-dependent AUC (td-AUC) values of 0.83 and 0.87, respectively, and lower integrated Brier scores (IBS) than common staging systems (all $P < 0.001$). Additionally, high-risk patients who underwent HAIC exhibited better cumulative OS than those who underwent TACE in both the training set ($P < 0.001$) and the test set ($P < 0.001$).

Conclusion Our study presents a novel DL model approach to identifying patients with proliferative HCC and predicting survival after IATs. The developed models offer a clinically useful tool for personalized treatment decision-making in uHCC, potentially improving patient outcomes and guiding the selection of IATs.

PO-061

The construction and preliminary application of a rehabilitation management plan for pancreatic cancer patients after interventional surgery based on goal-setting theory in navigation services

Rong Zhou, Jing Xiao

Affiliated Tumor Hospital of Chongqing University

Purpose Based on Goal Setting Theory (GST), a personalized navigation service scheme for patients with pancreatic cancer after interventional surgery was constructed and its application effect was preliminarily evaluated.

Materials and methods Based on the core principles of GST (clarity, challenge, attainability, feedback and time-bound), a rehabilitation management framework was designed, which covers goal setting, task decomposition, dynamic feedback and adjustment optimization. This framework was implemented through a digital platform to enable real-time interaction and monitoring between patients and medical teams.

A total of 90 patients with pancreatic cancer who received interventional therapy in a tertiary hospital from July 2023 to September 2024 were randomly divided into an intervention group (n=45) and a control group (n=45). The intervention group received GST-based navigation service scheme, and the control group received routine rehabilitation management. The main outcome measures included postoperative complication rate, quality of life (assessed by EORTC QLQ-C30 scale), psychological status (assessed by HADS scale), and treatment compliance.

Results The results showed that the quality of life score of the intervention group was significantly higher than that of the control group at 1 and 3 months after surgery ($P<0.01$), and the anxiety and depression scores were significantly reduced ($P<0.05$). In addition, the incidence of postoperative complications in the intervention group was significantly lower than that in the control group ($P<0.05$), and the treatment compliance was significantly improved ($P<0.01$).

Conclusion Navigation services based on goal setting theory can effectively improve the quality of life of pancreatic cancer patients after interventional surgery, relieve psychological burden, reduce the incidence of complications, and improve treatment compliance. This scheme provides a scientific and personalized new model for the rehabilitation management of pancreatic cancer patients, and has high clinical application value. Future studies can further expand the sample size and extend the follow-up time to verify the long-term effect and feasibility of popularization.

Investigating the Role of Idarubicin versus Epirubicin in Inducing Immunogenic Cell Death in a Mouse HCC Model of Local Treatment

Haikuan Liu, Jiaping Li

First Affiliated Hospital of Sun Yat-sen University

Purpose This study aimed to establish a subcutaneous tumor-bearing mouse model to compare the differences in molecular mechanism between Idarubicin (IDA) and Epirubicin (EPI) loaded on DEB respectively in inducing immunogenic cell death (ICD) and activating immune responses.

Materials and methods Cultured HCC cells were injected subcutaneously into mouse to establish tumor models. DEB loaded with IDA or EPI respectively was injected intratumorally into the mouse model, dividing them into four groups: CTRL, DCB, EPI, and IDA group. HE staining and histopathological examination of the tumor samples were performed. RNA-sequence, Western blot (WB) and immunohistochemical (IHC) staining were used to assess changes in hypoxia and angiogenesis pathways, the degree of ICD, and changes of the immune response and the immune microenvironment among the groups.

Results The mouse subcutaneous tumor models were successfully established, with baseline tumor volumes being comparable among the groups. Tumor growth varied significantly after treatment among the groups, with rapidly growth in the CTRL group, slowly growth in the DCB group, tumor shrinkage in the EPI group, and the most pronounced tumor regression in the IDA group. HE staining revealed disorganized tumor cell structures in the CTRL group, with large, irregularly shaped nuclei and prominent mitotic figures. In contrast, the IDA group showed more orderly cell arrangements, smaller nuclei, and fewer cells in the differentiation phase. All three treatment groups exhibited DEB deposits surrounded by necrotic areas, with clear demarcation between necrotic and viable tumor cells. The CTRL group had the highest expression of Ki-67, indicating the most active tumor cell proliferation, while Ki-67 expression decreased progressively in the treatment groups, with the lowest levels observed in the IDA group, means the most slowly tumor cell proliferation. RNA-sequence revealed that samples within each group clustered together, with clear distinctions between groups. Differentially expressed genes between groups indicated significant molecular changes induced by treatment. Genes and proteins associated with hypoxia and angiogenesis, such as HIF-1a and VEGF, were significantly upregulated in the DCB, EPI, and IDA groups, which means that the HCC model in this study can mimic changes after TACE treatment to some extent. Among the top 10 upregulated genes in the IDA group compared to the EPI group, four were related to DDR or ICD. WB and IHC results showed increased expression of ICD markers HMGB1 and CRT in the IDA and EPI groups, with higher levels in the IDA group, confirming that IDA induced a more significant ICD response than EPI. RNA-sequence revealed upregulation of genes related to T-cell exhaustion, chemokine, T/NK cell activation, Fc activation and cytokine receptor signaling in the IDA and EPI groups. IHC confirmed that PD-1 and PD-L1 expression increased significantly, especially in the IDA group, indicating a more robust immune response induced by IDA.

Conclusion The mouse subcutaneous tumor model with intratumoral DEB injection simulated changes in the tumor microenvironment similar to those observed after TACE. DEB loaded with IDA released chemotherapeutic agents slowly, exerting cytotoxic effects on tumor cells while inducing ICD, recruiting DCs to present tumor antigens, and activating CTLs to enhance anti-tumor immunity. This mechanism may explain IDA's superior efficacy compared to other anthracyclines like EPI in treating HCC.

PO-064

Radiofrequency Ablation is safe in patients with Hepatocellular Carcinoma and thrombocytopenia

Songchi Xiao

West China hospital of Sichuan University

Purpose This study aims to evaluate the efficacy and safety of radiofrequency ablation (RFA) in cirrhotic patients with hepatocellular carcinoma (HCC) and severe thrombocytopenia (platelet count $< 50 \times 10^9/L$).

Materials and methods A retrospective analysis was conducted on 166 cirrhotic HCC patients who underwent RFA at West China Hospital from January 2017 to January 2024. Patients were categorized into two groups based on preoperative platelet counts: Group A ($< 50 \times 10^9/L$) and Group B ($\geq 50 \times 10^9/L$). The primary outcome was perioperative major hemorrhage. Secondary outcomes included overall survival (OS), tumor response, and postoperative complications.

Results Perioperative major hemorrhage occurred in 2.4% of patients, all of whom were in Group B. Postoperative complications were observed at similar rates in both groups (Group A: 13.6%, Group B: 10.5%), with no significant differences ($p = 0.725$). There were no statistically significant differences in overall survival (OS) between the groups ($p = 0.633$), with 1-year OS rates of 97.6% in Group A and 96.6% in Group B, and 3-year OS rates of 86.3% in Group A and 94.6% in Group B. Tumor response rates were comparable between the groups.

Conclusion RFA is an effective and safe treatment for cirrhotic patients with HCC, even with severe thrombocytopenia. A platelet count below $50 \times 10^9/L$ should not contraindicate RFA.

PO-065

Berberine induces autophagy and promotes apoptosis in triple-negative breast cancer cells via the PI3K/Akt signaling pathway

Yuqin Wei¹, Wei Zhao²

1. Guangxi Medical University

2. Wuming Hospital of Guangxi Medical University

Purpose To elucidate the molecular mechanisms and therapeutic potential of Berberine (BBR) in triple-negative breast cancer (TNBC), leveraging an integrated approach of network pharmacology, molecular docking, and experimental validation.

Materials and methods Active compounds and their targets were identified from multiple databases, while disease targets for TNBC were retrieved from GeneCards, OMIM, and other sources. Protein-protein interaction (PPI) networks were constructed and analyzed, followed by functional enrichment analysis using GO and KEGG to identify key pathways. Molecular docking was employed to evaluate the binding affinity of BBR with high-degree targets. In vitro experiments assessed BBR's effects on TNBC cell proliferation, apoptosis, and autophagy, while in vivo studies utilized a nude mouse xenograft model to validate its antitumor efficacy.

Results A total of 273 BBR targets and 808 TNBC-related proteins were identified, with TP53, AKT1, EGFR, CASP3, HIF1A, and CTNNB1 emerging as key targets. Functional enrichment analysis revealed that BBR primarily modulates protein phosphorylation, gene expression, and the PI3K/Akt signaling pathway. Molecular docking demonstrated strong binding of BBR to these targets through hydrogen bonds and hydrophobic interactions. In vitro experiments showed that BBR inhibited TNBC cell proliferation by inducing cell cycle arrest, apoptosis, and autophagy via PI3K/Akt signaling. In vivo studies confirmed its antitumor efficacy in a nude mouse xenograft model, with significant tumor growth inhibition.

Conclusion This study elucidates the molecular mechanisms and therapeutic potential of BBR in TNBC, highlighting its ability to modulate key signaling pathways and induce antitumor effects. These findings provide a scientific basis for the use of BBR in traditional Chinese medicine and support its development as a promising treatment strategy for TNBC, a challenging and aggressive cancer subtype.

PO-066

Efficacy and safety of TIPS sequential targeted drugs in the treatment of patients with hepatocellular carcinoma with esophagogastric variceal rupture and bleeding

Chunlin Li
Chongqing University Cancer Hospital

Purpose The use of targeted drugs and immune drugs in patients with liver cancer significantly prolongates the survival time of patients with liver cancer. However, many patients with liver cancer often have esophageal and gastric fundus variceal rupture and bleeding in the later stage or during treatment, and the risk of bleeding again in the later stage is significantly increased, and some targeted drugs may increase the risk of bleeding, which makes the anti-tumor treatment of such patients unable to continue. The survival time and quality of life of these patients were seriously affected. Transjugular portal shunt can effectively relieve portal hypertension, treat esophageal and gastric varices, reduce the risk of rebleeding, save the lives of such patients, continue anti-tumor therapy, extend the survival time of patients, and improve life treatment. This study aims to explore the efficacy and safety of TIPS sequential targeted therapy in patients with hepatocellular carcinoma accompanied by esophageal variceal hemorrhage.

Materials and methods The data of patients with liver cancer with esophageal variceal hemorrhage treated with TIPS in the Affiliated Cancer Hospital of Chongqing University from November 2019 to November 2023 were retrospectively analyzed. The success rate of TIPS technique and the changes of PPG before and after operation were recorded, and perioperative adverse reactions and complications were observed. A telephone follow-up was conducted every 2 weeks after the operation to evaluate the relief of portal hypertension-related symptoms and screen for hepatic encephalopathy. Abdominal enhanced CT/MRI plain scan + enhancement, blood routine, biochemical and liver tumor markers were reviewed every 1 to 3 months after surgery to evaluate stent function and tumor progression. The follow-up period ended on November 1, 2023. The main end point of the study was all-cause death. The follow-up included relief of symptoms related to portal hypertension, stent patency, hepatic encephalopathy, gastrointestinal bleeding, and survival.

Results TIPS surgery was successfully performed in all patients, and the technical success rate was 100% (8/8). The PPG before and after surgery was (31.73 ±5.48) mmHg(1 mmHg= 0.133kPa) and (17.60 ±3.66) mmHg, respectively, with statistical significance ($t=13.57, P<0.001$). None of the 8 cases had perioperative death, hepatic artery/bile duct injury, acute liver failure and other complications. Compared with before TIPS, the physical status score of patients 1 month after TIPS was decreased [0(0) score vs. 3(3) score, $z=-3.57, P<0.001$], and the Child-Pugh score was also decreased [6(5,8) score vs. 9(8,10) score, $z=-3.44, P=0.001$]. The differences were statistically significant.

Conclusion TIPS combined with sequential systemic targeted therapy is safe and effective in the treatment of advanced HCC complicated with esophagogastric variceal rupture and bleeding, and may be an effective supplement to the current treatment of advanced HCC.

PO-067

Efficacy and safety of percutaneous cavity filling in the treatment of type II internal leakage after endovascular repair of abdominal aortic aneurysms

Xin Zhang, Yueyong Xiao
the first medical center of Chinese PLA General Hospital

Purpose Type II internal leakage is a common complication after endovascular repair of abdominal aortic aneurysm (EVAR), which seriously affects the long-term outcome of EVAR. However, there are no unified guidelines and consensus on the treatment of type II internal leakage. With the continuous development of embolic materials, percutaneous puncture cavity filling technology has more and more advantages. This paper discusses the efficacy and safety of percutaneous cavity filling technique in the treatment of type II internal leakage after endovascular repair of abdominal aortic aneurysm, in order to select a simple and effective treatment plan for clinicians.

Materials and methods 3 patients with type II internal leakage after intracavity repair of abdominal aortic aneurysm were treated with percutaneous cavity filling technique, and fibrin glue and gelatin sponge mixture were inserted into the cavity accurately.

Results All operations were successful, and there were no complications such as ectopic embolism, intestinal ischemia and tumor rupture. CT three-dimensional vascular reconstruction showed no residual type II internal leakage, and the diameter and volume of tumor cavity were reduced at 6 months after the operation.

Conclusion The mixture of fibrin glue and gelatin sponge has high viscosity and fast coagulation, and the direct injection of the tumor through percutaneous puncture can avoid the damage to the vascular wall, and the treatment of type II internal leakage after EVAR is safe and effective, and the operation is simple and feasible. The key points for the successful implementation of this technique are the preparation of embolic agent and the effective sealing of leakage.

PO-068

Hippo-TEAD Axis Mediates Adaptive Resistance to Iodine-125 Brachytherapy in NSCLC and Its Therapeutic Exploitation

Shuhui Tian, Bin Liu

The Second Hospital of Shandong University

Purpose To investigate the role of TEAD family genes in the brachytherapy of non-small cell lung cancer (NSCLC) and their association with the Hippo signaling pathway.

Materials and methods An iodine-125 brachytherapy model was established in H1299 and H1975 cells. RNA sequencing identified differentially expressed genes, followed by GO/KEGG pathway analysis. TEAD was silenced via siRNA, and functional assays, including CCK-8, flow cytometry (apoptosis/cell cycle), wound healing, and Transwell assays, were performed to assess the effects of radiotherapy, TEAD knockdown, and their combination.

Results TEAD inhibition significantly enhanced the anti-tumor effects of radiotherapy, increasing proliferation suppression to 56.7% compared to monotherapies (siRNA: 23.5%, radiotherapy: 29.4%, $P < 0.05$). Migration inhibition in Transwell assays reached 85.4%, exceeding radiotherapy alone by 32.1% ($P < 0.01$), and wound healing assays confirmed a synergistic effect (68.7% vs. 33.5% in monotherapy). Mechanistically, TEAD knockdown reversed radiotherapy-induced Hippo pathway activation, suggesting a potential radiosensitization mechanism.

Conclusion TEAD inhibition enhances the efficacy of iodine-125 radiotherapy in NSCLC by suppressing proliferation and migration, potentially through Hippo pathway modulation. Targeting TEAD may represent a novel strategy to improve brachytherapy outcomes.

PO-069

To study the factors affecting the outcomes of core needle biopsy in musculoskeletal lesions.

Vivek Khandelwal
Tata Memorial Hospital, Parel

Purpose Delve into the intricate landscape of musculoskeletal lesion diagnostics as we examine the influencing factors of core needle biopsy. This study investigates variables that impact the accuracy and efficacy of this diagnostic procedure, offering valuable insights for clinicians and researchers in the field of orthopedic and musculoskeletal medicine

Materials and methods Patients who had undergone percutaneous core needle biopsy of musculoskeletal lesions were included in the study. Lack of pre-procedure imaging and records on PACS and loss to follow up were the exclusion criteria. A total of 180 patients who had undergone percutaneous needle biopsy for musculoskeletal lesions were included in the study, and a total of 209 biopsy procedure performed.

Results A total of 209 consecutive core needle biopsy of the musculoskeletal system were performed on 180 patients (64 females and 116 males). There were 75 (41.7%) patients with lytic lesion in the bone, 31(17.2%) patients with lytic with soft tissue component, 14(7.8%) patients with sclerotic lesions and 40(22.2%) patients with mixed lytic and sclerotic lesions and 20 with only soft tissue (11.1%). Lytic lesions had diagnostic accuracy of 97.3% (73/75), lytic with soft tissue had 96.8% (30/31) while that of mixed lesions was 75% (30/40) and sclerotic lesions was 57.1% (8/14). This was statically significant with p value of 0.001. The diagnostic accuracy of the biopsy according to the lesion size was 100% (7/7) for lesions < 10 mm, 85.4% (41/48) for 10-25 mm lesions, 88.6% (78/88) for 25-50 mm lesions and 94.6% (35/37) for larger than 50 mm lesions. This was not statically significant with p=0.2. The diagnostic accuracy in respect to needle size was as follows: 11G had 82.1% (55/67), 13 G had 100% (2/2), 18G had 93.9% (93/99), 11+18G had 90.9% (10/11) and 13+18G had 100% (1/1).

Conclusion The current study shows that CT guided percutaneous biopsy of musculoskeletal lesions is a safe, easy and effective outpatient procedure. The diagnostic yield correlated with the type of lesion (lytic vs sclerotic) whereas size of lesion and size of needle used did not significantly affect the outcome. Lower success was noted in the benign or inflammatory disease and also with vertebral lesions.

PO-070

Efficacy and Safety of TACE Combined with Lenvatinib and PD-1 Inhibitor in Intermediate-Stage HCC exceeding the up-7 Criteria: A Retrospective Cohort Study

Miao Xue, Jiaping Li

The First Affiliated Hospital of Sun Yat-Sen University

Purpose This study aimed to assess the efficacy and safety of combining transarterial chemoembolization (TACE) with lenvatinib and a PD-1 inhibitor (TACE+LEN+PD-1) compared to TACE with lenvatinib alone (TACE+LEN) in intermediate-stage hepatocellular carcinoma (HCC) patients exceeding the up-to-7 criteria. In the abstract, "were prospectively collected and retrospectively analyzed" contains a contradiction and should be revised. If referring to the time until MVI/EHS occurrence, it is recommended to write: "Time to MVI or EHS was significantly prolonged..."

Materials and methods Data from 115 patients with intermediate-stage HCC exceeding the up-to-7 criteria, treated between January 2015 and December 2023, were prospectively collected and retrospectively analyzed. Key clinical outcomes, including overall survival (OS), progression-free survival (PFS), tumor response rates based on modified Response Evaluation Criteria in Solid Tumors (mRECIST), and adverse events (AEs), were evaluated and compared between the two treatment groups. Univariate and multivariate analyses were performed to identify factors affecting OS and PFS.

Results Among the patients, 35 received TACE+LEN+PD-1, and 80 underwent TACE+LEN. The TACE+LEN+PD-1 group achieved a longer median PFS (10.0 months vs. 5.7 months; $P=0.002$) and a median OS of 21.0 months, compared to 16.2 months in the TACE+LEN group, though the OS difference was not statistically significant ($P=0.096$). Progression to macrovascular invasion (MVI) or extrahepatic spread (EHS) was delayed in the TACE+LEN+PD-1 group compared to the TACE+LEN group (12.0 months vs. 7.5 months; $P=0.007$). Multivariate analysis identified treatment modality and tumor burden score (TBS) as independent prognostic factors for OS and PFS. Subgroup analyses showed that patients with an Eastern Cooperative Oncology Group (ECOG) performance status (PS) of 0 or HBV positivity derived greater benefits from TACE+LEN+PD-1, while those with high TBS or a Child-Pugh score of 7 did not show similar advantages. The rates and severity of AEs were comparable between groups (any grade: 88.6% vs. 91.3%, $P=0.733$; grade 3 or 4: 48.6% vs. 42.5%, $P=0.546$).

Conclusion TACE+LEN+PD-1 significantly improved PFS, particularly by delaying progression to MVI or EHS after the first TACE session in intermediate-stage HCC patients exceeding the up-to-7 criteria, compared to TACE+LEN. Subgroup analysis indicated superior survival benefits for patients with a PS of 0 or HBV positivity, but not in those with high TBS or a Child-Pugh score of 7. The safety profile of TACE+LEN+PD-1 was comparable to TACE+LEN. However, the OS benefit between the two groups was not statistically significant.

PO-071

Experimental study on inhibition of airway restenosis by novel graphene oxide-loaded rapamycin-coated airway stent

Zongming Li, Kewei Ren, Kunpeng Wu, Yahua Li, Zihou Zhou, Yifan Li, Xinwei Han
The First Affiliated Hospital of Zhengzhou University, China

Purpose Experimental study on inhibition of airway restenosis by novel graphene oxide-loaded rapamycin-coated airway stent

Materials and methods The dip coating method was used to develop a GO@RAPA-SEMS and a poly(lactic-co-glycolic)-acid loaded rapamycin coated self-expandable metallic airway stent (PLGA@RAPA-SEMS). The surface structure was evaluated using a scanning electronic microscope. The in vitro drug-release profiles of the 2 stents were explored and compared. In the animal study, a total of 45 rabbits were randomly divided into 3 groups and underwent 3 kinds of stent placements. Computed tomography was performed to evaluate the degree of stenosis at 1, 2 and 3 months after the stent operation. Five rabbits in each group were sacrificed after the computed tomography scan. The stented trachea and blood were collected for further pathological analysis and laboratory testing.

Results The in vitro drug-release study revealed that GO@RAPA-SEMS exhibited a sudden release on the first day and maintained a certain release rate on the 14th day. The PLGA@RAPA-SEMS exhibited a longer sustained release time. All 45 rabbits underwent successful stent placement. Pathological results indicated that the granulation tissue thickness in the GO@RAPA-SEMS group was less than that in the PLGA@RAPA-SEMS group. The TUNEL and hypoxia-inducible factor-1 α staining results support the fact that the granulation inhibition effect in the GO@RAPA-SEMS group was greater than that in the PLGA@RAPA-SEMS group.

Conclusion GO@RAPA-SEMS effectively inhibited stent-related granulation tissue hyperplasia.

PO-072

mFOLFOX6-HAIC with PD-(L)1 inhibitors plus molecular targeted therapies for HBV-related advanced hepatocellular carcinoma

Fengchen Jiang, Shouzhong Fu

Department of Interventional Angiology, Affiliated Nantong Hospital 3 of Nantong University

Purpose To investigate the efficacy and safety of mFOLFOX6-HAIC with PD-(L)1 inhibitors plus molecular targeted therapies for HBV-related advanced HCC.

Materials and methods The clinical data of 34 HBV-related BCLC III stage HCC patients, who were contraindicated to or refractory to transcatheter arterial chemoembolization (TACE) and treated with mFOLFOX6-HAIC combined with PD-(L)1 inhibitors plus molecular targeted therapies in Nantong Third People's Hospital between January 2020 and December 2023, were retrospectively analyzed. Follow-up ended on December 31, 2024. The modified Response Evaluation Criteria in Solid Tumors (mRECIST) was used to statistically analyze the clinical efficacy, the Common Terminology Criteria For Adverse Events version 5.0 (CTCAE 5.0) was adopted to record and evaluate the treatment-related adverse events (TRAEs). The primary endpoints were overall survival (OS) and progression-free survival (PFS), the secondary endpoints were objective response rate (ORR), disease control rate (DCR), conversion therapy rate, and safety.

Results The median OS was 17.6 months (95%CI: 12.836-22.364 months), the median PFS was 7.6 months (95%CI: 3.443-11.824 months), the ORR was 41.2%, and the DCR was 73.5%. 13 patients are still alive, 11 patients were subsequently treated with TACE, and 1 patient underwent surgical resection. The most common TRAE was elevated alanine aminotransferase (11.7%), and the most common TRAE of grade 3/4 was upper gastrointestinal hemorrhage (8.8%). Two patients (5.8%) with the main portal vein tumor thrombus died of upper gastrointestinal hemorrhage.

Conclusion For the treatment of HBV-related BCLC III stage HCC patients, mFOLFOX6-HAIC combined with PD-(L)1 inhibitors plus molecular targeted therapies is clinically safe and effective. It provides a new option for the treatment of advanced HCC, but long-term survival benefits need to be confirmed in larger cohort clinical studies.

PO-073

Early Responses of Serum AFP and PIVKA-II Synergistically Predict Progression in Patients with Unresectable Hepatocellular Carcinoma Receiving Transarterial Chemoembolization Combined with Sintilimab and Bevacizumab

Chenyou Liu, Mengfan Wang, Xiaoyang Xu, Ze Wang, Xiaoli Zhu
The First Affiliated Hospital of Soochow University

Purpose This study aimed to assess the synergistic predictive value of early changes in serum alpha-fetoprotein (AFP) and protein induced by vitamin K absence-II (PIVKA-II) for progression in patients with unresectable hepatocellular carcinoma (HCC) treated with transarterial chemoembolization (TACE) combined with sintilimab and bevacizumab.

Materials and methods Patients with unresectable HCC who received TACE combined with sintilimab and bevacizumab were retrospectively enrolled. Serum biomarkers were measured at the first radiological assessment after the initiation of combination therapy. Optimal thresholds for variations in AFP and PIVKA-II were determined using receiver operating characteristic curves and the Youden index, and their prognostic value for progression-free survival (PFS) was evaluated through univariate and multivariate analyses.

Results A total of 30 patients with baseline AFP >20 ng/mL and PIVKA-II >40 mAU/mL were included. Of these, 80% were male, with a median age of 61 years. 73% patients had hepatitis B virus infection, 53% had cirrhosis, and HCC stages were classified as BCLC stage B (46.7%) or stage C (53.3%). Early responses, defined as a decrease in AFP by $\geq 20\%$ and PIVKA-II by $\geq 40\%$ from baseline, independently predicted reduced risk of progression (AFP: HR, 0.17; 95% CI, 0.06–0.50; $p=0.001$; PIVKA-II: HR, 0.21; 95% CI, 0.07–0.66; $p=0.007$). Furthermore, the combination of early response of AFP and PIVKA-II stratified patients into distinct progression-risk categories: double-responders (median PFS 20.6 months, 95%CI 19.37-NR), single-responders (12.8 months, 95%CI 10.57-NR), and non-responders (3.6 months, 95%CI 1.73-NR) ($p=0.0003$).

Conclusion Early combined responses in serum AFP and PIVKA-II refines progression risk discrimination in patients with unresectable HCC receiving TACE combined with sintilimab and bevacizumab.

Evaluation of Percutaneous Microwave Ablation of the Spleen Combined with Splenic Artery Occlusion for Treating Secondary Hypersplenism: A Single-Arm Study

Xing Li^{1,2}, Huilai Li^{1,2}, Yong Xu^{1,2}, Tongguo Si^{1,2}, Rui Xia^{1,2}, Mao Yang¹, Rentao Li^{1,2}, Yang Liu¹

1. Tianjin Medical University Cancer Institute and Hospital

2. Tianjin Cancer Hospital Airport Hospital

Purpose Portal hypertension, often caused by cirrhosis, is a common complication in liver cancer patients, leading to obstruction of splenic vein outflow, increased splenic pressure, splenomegaly, and secondary hypersplenism. As the spleen enlarges, platelet and white blood cell counts decrease, raising the risk of esophageal and gastric variceal bleeding, which may compromise anti-tumor therapies. Traditional surgical treatments for hypersplenism are highly invasive, and many patients are not suitable candidates. Splenic artery embolization, while effective, may carry significant side effects. This study aims to evaluate the safety and efficacy of percutaneous microwave ablation as a less invasive treatment option.

Materials and methods This study collected data from 40 patients with cirrhosis-induced secondary hypersplenism who underwent percutaneous microwave ablation of the spleen. Preoperative assessments included complete blood count, liver and kidney function tests, coagulation studies, and abdominal imaging (CT, MRI, or ultrasound). The ablation procedure involved splenic artery balloon occlusion, artificial pleural effusion, evaluation of splenic artery blood flow velocity, moving-shot and fixed-needle microwave techniques, and contrast-enhanced ultrasound to assess ablation volume. The primary endpoint was to evaluate the safety and efficacy of microwave ablation combined with splenic artery occlusion, while the secondary endpoint was to assess the therapeutic outcomes with varying ablation ranges.

Results From August 2023 to October 2024, a total of 40 patients were treated, with a mean age of 58.0 years (range: 37-72 years), including 24 males (60%) and 16 females (40%). Among them, 28 patients (70%) had Child-Pugh Class A liver function, while 12 (30%) were classified as Child-Pugh Class B.

Preoperative blood tests showed:

- White blood cell count: $(7.85 \pm 6.92) \times 10^9/L$
- Red blood cell count: $(2.88 \pm 0.68) \times 10^{12}/L$
- Platelet count: $(51.55 \pm 16.86) \times 10^9/L$

Changes in Platelet Counts Post-Ablation:

- At 7 days: increased to $(77.33 \pm 37.25) \times 10^9/L$
- At 1 month: increased further to $(113.7 \pm 81.44) \times 10^9/L$
- At 3 months: peaked at $(215.53 \pm 147.88) \times 10^9/L$
- At 6 months: decreased to $(159.47 \pm 118.46) \times 10^9/L$

Although platelet counts peaked at 3 months, they remained significantly higher than pre-ablation levels at all time points ($P < 0.05$). White blood cell counts initially increased post-ablation but returned to baseline levels by 6 months, showing no significant difference from pre-ablation levels ($P > 0.05$). Red blood cell counts showed minimal changes throughout the study period ($P > 0.05$).

Immediate ultrasound and MRI evaluations post-ablation indicated that the average ablated volume accounted for $(78.30 \pm 12.45)\%$ of the total spleen. MRI follow-ups at 1-3 months showed that the ablated volume averaged $(79.65 \pm 18.22)\%$ of the spleen in 6 patients.

No ablation-related deaths were reported among the 40 patients; however, 5 patients (12.5%) experienced complications: 3 cases of bleeding, 1 case of renal failure, and 1 case of splenic vein thrombosis.

Conclusion Percutaneous microwave ablation of the spleen combined with splenic artery occlusion significantly increases the ablated volume, reduces procedure time, and demonstrates a high safety profile. This minimally invasive treatment shows promising short-term efficacy and has the potential to be an effective alternative for patients with hypersplenism. Further studies are warranted to evaluate long-term outcomes.

PO-075

FOLFOX-HAIC plus regorafenib for the treatment of unresectable colorectal liver metastases refractory to first and second-line systemic chemotherapy

Jiacheng Liu, Chuansheng Zheng, Bin Liang
Wuhan Union Hospital

Purpose Hepatic arterial infusion chemotherapy (HAIC) is a potentially attractive locoregional therapy for patients with unresectable colorectal liver metastases (CRLM). This study aimed to evaluate the safety and efficacy of FOLFOX-HAIC plus regorafenib in the treatment of unresectable CRLM refractory to first and second-line systemic chemotherapy.

Materials and methods A total of 35 patients with unresectable CRLM who underwent FOLFOX-HAIC plus regorafenib between July 2020 and January 2023 were included in this retrospective study. The objective response rate (ORR), disease-controlled rate (DCR), progression-free survival (PFS), overall survival (OS) and adverse event were assessed. Factors affecting OS were analyzed.

Results Kaplan–Meier curves showed that the median OS1 (measured from the time of diagnosis), OS2 (measured from the time of the first HAIC treatment) and PFS (measured from the time of the first HAIC treatment) were 29.0 (95%CI, 18.9-39.1) months, 21.0 (95%CI, 14.9-27.1) months and 13.0 (95%CI, 9.3-16.7) months, respectively. The ORRs at 3 months, 6 months and 12 months after HAIC were 57.1%, 45.7% and 22.9%, respectively, and the DCRs were 88.6%, 80.0% and 51.4%, respectively. No grade 5 adverse events (AEs) (death) were observed. Common Regorafenib-related AEs were hand-foot skin reaction (n = 18, 51.4%) and fatigue (n = 15, 42.9%). Common HAIC-related AEs were weight loss (n = 28, 80.0%), abdominal pain (n = 19, 54.3%) and nausea (n = 15, 42.9%).

Conclusion FOLFOX-HAIC plus regorafenib was beneficial and tolerable in the treatment of unresectable CRLM refractory to first and second-line systemic chemotherapy.

PO-076

Treatment of femoral artery pseudoaneurysm with intravascular stent and hematoma removal: a case report

Yang Zheng
Chongqing University Cancer Hospital

Purpose To explore the feasibility and challenge of endocaval stent implantation combined with surgical hematoma removal in the treatment of femoral artery false aneurysm (FAP) in drug addicts, and analyze its clinical effect and special management points.

Materials and methods A 38-year-old male drug user was admitted to hospital due to "right groin pulsating mass with pain for 7 months, aggravated for 1 day". Physical examination showed a mass of 6 cm×8 cm, and CTA confirmed a femoral artery pseudoaneurysm with local hematoma formation and superficial signs of infection. The patient had a long history of injecting drug use and poor vascular condition. In the emergency department, the closed tumor neck was implanted with a covered stent (Gore Viabahn), and the infectious hematoma was removed by incision at the same time. After surgery, broad-spectrum antibiotics and individualized anticoagulant therapy were given. Follow-up for 6 months was performed to evaluate the efficacy and complications.

Results The surgery successfully isolated the tumor cavity and the hematoma was completely removed. Three days after surgery, the body temperature and inflammatory indexes were normal, and the incision healed well. After 6 months of follow-up, the stent was unobstructed, no recurrence of infection, thrombosis or aneurysm occurred, and the blood flow and function of the affected limb were completely recovered. The patient had poor compliance with postoperative detoxification and still had intraoperative pain, but no treatment-related adverse events occurred.

Conclusion Treatment of drug users is complicated due to vascular damage, high risk of infection and poor compliance. Intracavitary combined open surgery can quickly control bleeding, remove the source of infection, and reduce the risk of long-term recurrence. However, perioperative anti-infection, individualized anticoagulation and multidisciplinary collaboration (such as drug withdrawal intervention) should be strengthened to optimize the efficacy and prognosis of this high-risk population. This case suggests that combined surgery can be used as a salvage treatment for drug-related FAP under strict indication control.

PO-077

Evaluation of functional magnetic resonance imaging's effect of transcatheter CA4P infusion therapy on VX2 transplantation tumor model in rabbit brain

Junting Ma, Xudan Wang, Haibo Shao
First Hospital of China Medical University

Purpose To evaluate the efficacy of carotid artery infusion of the precursor of cobustatin A4 (CA4P) in the treatment of VX2 transplanted tumor in rabbit brain by functional magnetic resonance imaging (fMRI).

Materials and methods The rabbit brain VX2 transplanted tumor model was constructed, and CA4P was infused into the carotid artery for treatment. The tumor growth was evaluated by functional MRI before and 24 hours after administration; It was also verified with pathological vascular related indexes VEGF and CD31.

Results After intra-arterial perfusion of CA4P, the parameters of DWI and PWI sequences of tumor in experimental group (group A) were significantly changed compared with those in control group (group B). After administration, the ADC value of tumor margin in group A was higher than that in group B (1.19 ± 0.14 , 0.98 ± 0.11 , $P=0.04$); The rCBV and rCBF of PWI sequence (0.97 ± 0.08 , 0.96 ± 0.11) were significantly lower than those of group B (1.88 ± 0.13 , 2.01 ± 0.10) ($P<0.01$, $P<0.001$), and the rMTT was significantly higher than that of group B ($P<0.05$). MVD of group A was lower than that of group B (15.83 ± 4.26 , 27.00 ± 6.10 , $P<0.01$); VEGF score decreased significantly (1.17 ± 1.17 , 9.00 ± 3.79 , $P<0.01$); The pathological changes were consistent with PWI parameters.

Conclusion Functional magnetic resonance imaging verified that the effect of carotid artery perfusion of CA4P on the treatment of VX2 transplanted tumor in rabbit brain was reliable, and the changes of tumor blood supply could be observed earlier.

PO-079

DAP12 Knockdown Suppresses EMT in Colon Cancer Cells by Downregulating AKT and Modulating the Intestinal Microenvironment

Lihao Shi, Guangxi Zhou
Shandong University

Purpose DNAX-activating protein 12 (DAP12, also known as TYROBP) is a transmembrane signaling protein containing an immunoreceptor tyrosine-based activation motif (ITAM). It is primarily expressed in immune cells but has also been detected in certain tumor cells, where it may influence cancer progression through NF- κ B, PI3K/AKT, and TGF- β signaling pathways. This study aims to elucidate the role and molecular mechanisms of DAP12 in epithelial-mesenchymal transition (EMT) in colon cancer cells.

Materials and methods 1. In Vitro Cellular Assays

Colon cancer cell lines (HCT116 and SW480) were used to assess the effects of DAP12 manipulation through three approaches: DAP12 overexpression (plasmid transfection), DAP12 knockdown (siRNA), and DAP12 inhibition (pharmacological inhibitors). EMT marker expression (E-cadherin, N-cadherin, and Vimentin) was evaluated via Western blot and qPCR. Additionally, cell migration and invasion assays were performed to assess EMT-related functional changes.

2. AOM/DSS-Induced Colon Cancer Mouse Model

A murine model of spontaneous colon carcinogenesis was established using azoxymethane (AOM) and dextran sulfate sodium (DSS). DAP12 knockout (DAP12^{-/-}) mice were compared to wild-type (WT) controls. Tumor burden (tumor count and size), EMT marker expression in tumor tissues (Western blot/qPCR), and immune microenvironment parameters (flow cytometry analysis of myeloid-derived suppressor cells [MDSCs] and T-cell infiltration) were assessed. Additionally, 16S rRNA sequencing was performed to analyze gut microbiota alterations following DAP12 knockdown.

Results DAP12 overexpression promoted EMT in colon cancer cells, as evidenced by decreased E-cadherin and increased Vimentin/N-cadherin expression. These changes correlated with enhanced cell migration and invasion, along with activation of the PI3K/AKT signaling pathway. Conversely, DAP12 knockdown or inhibition reversed these effects. In the AOM/DSS-induced colon cancer model, DAP12 knockout mice exhibited reduced tumor burden, lower mortality, beneficial alterations in gut microbiota composition, and a more favorable immune microenvironment, characterized by altered distributions of MDSCs and T cells.

Conclusion This study identifies DAP12 as a key regulator of EMT in colon cancer cells and provides mechanistic insights into its role in tumor progression. DAP12 promotes EMT, targeting DAP12 could represent a novel therapeutic strategy to prevent colon cancer metastasis. The AOM/DSS-induced colon cancer model provides a clinically relevant tumor microenvironment, further supporting the role of DAP12 in colorectal cancer progression.

PO-080

Effects of different doses of X-rays on cGAS-STING signaling pathway and tumor immune microenvironment

Lei Xiao, Mingyan Xu, Xian Chen, Hua Zhang, Yiliyaer Nu'erula
The First Affiliated Hospital of Xinjiang Medical University

Purpose To study the effects of different doses of X-ray irradiation on the immune microenvironment and cGAS-STING signaling pathway of hepatocellular carcinoma cells.

Materials and methods C57BL/C mice were subcutaneously injected with Hepa 1-6 hepatocellular carcinoma cells in the right axilla to establish a subcutaneous tumor-forming hepatocellular carcinoma model, and were randomly divided into 0, 4, 8, and 12 Gy irradiation groups, with 10 mice in each group, and body weights and tumor volumes were monitored. Specimens were collected 28 d after irradiation, and the ELLSA method was used to compare the macrophage-associated cytokines tumor necrosis factor- α (TNF- α), interferon- γ (IFN- γ), interleukin-6 (IL-6), chemokine ligand 5 (CCL5), interleukin-10 (IL-10), interleukin-13 (IL-13), transforming growth factor- β (TGF- β), interleukin-4 (IL-4) and macrophage M1, M2 phenotype ratio (M1/M2); real-time fluorescence quantitative polymerase chain reaction (qRT-PCR) and immunoblotting assay were used to detect the expression of genes and proteins related to the cGAS-STING signaling pathway in hepatoma cells.

Results With the increase of irradiation dose, the tumor volume was significantly reduced ($F=8.42$, $P<0.05$), the proportion of cell necrosis increased ($F=3.89$, $P<0.05$), the content of macrophage-associated cytokines other than IL-4 increased ($F=6.32-15.50$, $P<0.05$), and the proportion of M1 and M2 types of macrophage in the immune microenvironment of hepatocellular carcinoma tumors was elevated ($F=5.46, 5.14$, $P<0.05$). The gene expression and protein expression levels of cGAS-STING signaling pathway were elevated in hepatocellular carcinoma cells (mRNA expression of cGAS and STING: $F=6.35, 16.10$, $P<0.05$; protein expression of cGAS and STING: $F=71.31, 37.15$, $P<0.05$).

Conclusion X-ray irradiation activates the cGAS-STING signaling pathway in hepatocellular carcinoma cells and contributes to the remodeling of the tumor immune microenvironment.

Liver and Liver Tumor Segmentation Based on Swin Transformer

Jianwei Yang¹, Gao-Jun Teng²

1. Jiangsu Key Laboratory of Intelligent Medical Image Computing, School of Future Technology, Nanjing University of Information Science and Technology

2. Center of Interventional Radiology & Vascular Surgery, Department of Radiology, Zhongda Hospital Affiliated to Southeast University

Purpose Accurate segmentation of the liver and liver tumors is crucial in interventional oncology. It is a prerequisite for cancer diagnosis, treatment planning, and treatment response monitoring. To enhance segmentation precision and efficiency, a novel AI-based segmentation model has been developed.

Materials and methods LiTS¹ is a publicly available, large-scale liver tumor segmentation dataset collected from seven clinical sites worldwide, serving as a benchmark for our research. A Swin Transformer-based segmentation framework, which contains a Swin Transformer encoder, a multi-level feature fusion module and an image decoder, is proposed. The Swin Transformer encoder employs a hierarchical window attention mechanism that divides the 3D medical images into non-overlapping windows, computing self-attention within each window to effectively capture long-range dependencies. Multi-level feature fusion leverages the feature information from each encoder layer, combining shallow detail features with deep semantic features through skip connections, thereby improving segmentation boundary accuracy. The decoder progressively restores spatial resolution through up-sampling and feature fusion, ultimately producing the segmentation output. During the training phase, a composite loss function combining Dice loss and cross-entropy loss is utilized. The learning rate is gradually reduced via cosine annealing to enhance model convergence stability.

Results A total of 123 CT scans are divided into the training set (n=101) and test set (n=22), with 5-fold cross-validation applied. The proposed method achieves a Dice Similarity Coefficient (DSC) of 0.96 and a Normalized Surface Distance (NSD) of 0.89 in the liver segmentation task, and a DSC of 0.53 and an NSD of 0.57 in the tumor segmentation task, both outperforming the competitive methods. Meanwhile, a detailed analysis of the parameter count and computational complexity is conducted. The model has a total of 120 million parameters, with an inference speed of 3.2 samples per second on a single V100 GPU. The reduction in model size and the increase in inference speed lay a solid foundation for practical clinical applications.

Conclusion Our method represents a significant advancement toward creating more reliable and robust AI-driven diagnostic tools for liver tumor intervention.

PO-082

3D Printed Airway Model-assisted Amplatzer Device for Closure of Gastroairway Fistula After Esophagectomy

Yahua Li, Kewei Ren, Zongming Li, Xinwei Han
the first affiliated hospital of zhengzhou university

Purpose Gastroairway fistula (GAF) after esophagectomy is a rare but life-threatening complication. We aim to share our experiences with 3D-printed airway models that can assist with the choice of AD to close the GAF.

Materials and methods The data of 14 patients who received 3D-printed airway model-assisted AD for GAF closure after esophagectomy from January 2020 to January 2023 were retrospectively analyzed. The quality of life (QoL) score and the results of chest CT, bronchoscopy and gastroscopy before and after AD placement were collected and analyzed.

Results A total of 14 patients successfully received 15 ADs, and one patient received two consecutive ADs. The technique success rate was 100%. Ten of the cases involved GBFs, and 4 involved GTFs. Five patients received ASD placement, and 9 received VSD placement. After AD placement, the QoL score significantly improved ($P < 0.0001$). The first follow-up CT examination revealed that the total infection lung volume decreased from 213.57 ± 167.01 ml to 103.03 ± 79.08 ml ($P = 0.0053$). The durations of AD in GTF and GBF were 95.8 ± 32.7 and 259.8 ± 185.9 days, respectively ($P = 0.021$).

Conclusion The application of AD in the GAF produces good short-term results. However, the long-term results of the GBF are better than those of the GTF.

PO-083

Low-dose CT fluoroscopy-guided interventional minimally invasive robot

Xiaofeng He, Yueyong Xiao
Chinese PLA General Hospital

Purpose This study aimed to assess the feasibility, safety, and accuracy of a low-dose CT fluoroscopy-guided remote-controlled robotic real-time puncture procedure.

Materials and methods The study involved two control groups with Taguchi method: Group A, which underwent low-dose traditional CT-guided manual puncture (blank control), and Group B, which underwent conditional control puncture. Additionally, an experimental group, Group C, underwent CT fluoroscopy-guided remote-controlled robotic real-time puncture. In a phantom experiment, various simulated targets were punctured, while in an animal experiment, attempts were made to puncture targets in different organs of four pigs. The number of needle adjustments, puncture time, total puncture operation time, and radiation dose were analyzed to evaluate the robot system.

Results Successful punctures were achieved for each target, and no complications were observed. Data were calculated for all parameters using Taguchi method.

Conclusion The low-dose CT fluoroscopy-guided puncture robot system is a safe, feasible, and equally accurate alternative to traditional manual puncture procedures.

PO-084

Radiomic Profiling of Tumor Heterogeneity on Pretreatment MRI Stratifies Treatment Outcomes in HCC Patients Undergoing Atezo-Bev Immunotherapy with Adjuvant Locoregional Interventions

Jinxing Zhang

Department of Interventional Radiology, The First Affiliated Hospital with Nanjing Medical University

Purpose To quantify intratumoral heterogeneity (ITH) based on magnetic resonance imaging (MRI) and evaluate its predictive performance for treatment response to triple therapy in unresectable HCC.

Materials and methods To quantify ITH based on magnetic resonance imaging (MRI) and evaluate its predictive performance for treatment response to triple therapy in unresectable HCC. Methods: Patients with unresectable HCC who received triple therapy at multiple centers were enrolled between January 2019 and January 2024. Conventional and habitat radiomic features were extracted from MRI to construct the ITH score. Predictive models based on clinical variables, radiomic features, and the ITH score were developed and were evaluated using the area under the receiver operating characteristic curve (AUC).

Results A total of 151 patients were enrolled in this study. Seventy-six patients (42.5%) showed a response to the triple therapy. The combined model based on the ITH score achieved the highest accuracy in predicting treatment response to triple therapy with an AUC of 0.991, 0.973 and 0.868 in the training, validation, and testing cohort, respectively. Furthermore, the combined model can categorize patients into high-risk and low-risk groups for progression-free survival (PFS) and overall survival (OS) in the training ($p < 0.001$ for PFS and OS), validation ($p < 0.001$ for PFS and OS) and testing cohort ($P = 0.005$ for PFS; $p < 0.001$ for OS).

Conclusion A model based on the ITH score derived from MRI demonstrated strong performance in predicting treatment response to triple therapy in patients with HCC.

Incomplete Thermal Ablation Plus Programmed Cell Death Protein 1 Monoclonal Antibodies Increase The Incidence of Hyperprogressive Disease in Hepatocellular Carcinoma

Yu-Zhe Cao^{1,2,3}, Guang-Lei Zheng^{1,2,3}, Meng-Xuan Zuo^{1,2,3}, Wang Li^{1,2,3}, Fei Gao^{1,2,3}

1. Sun Yat-Sen University Cancer Center

2. State Key Laboratory of Oncology in South China

3. Guangdong Provincial Clinical Research Center for Cancer

Purpose Hepatocellular carcinoma (HCC) is the most common type of liver cancer. Reports of hyperprogressive disease (HPD) following administration of programmed cell death protein 1 (PD-1) monoclonal antibodies (mabs) triggered clinical concern. Though mechanism still not clear, HPD was hypothesized related to interaction between the fragment crystalline (Fc) of PD-1 mabs and Fc γ receptors (Fc γ R) on macrophages. Thermal ablation is recommended as the first-line choice for early stage patients. However, incomplete ablation (IA) is not rare when the tumors are large, multiple or adjacent to vessels. To deal with metastases or residual lesions, a regimen consist of ablation and PD-1 mabs has raised concern due to synergy between PD-1 mabs and tumor-related antigen release caused by ablation. Nonetheless, ablation could induce macrophage infiltration, which may interact with Fc of PD-1 mabs and result in HPD. So we conducted a retrospective clinical study to explore whether the IA plus PD-1 mabs increase the incidence of HPD than PD-1 mabs in HCC patients. And the animal experiment was also performed to validate the clinical findings, study the underlying mechanism of HPD and explore the potential precautions.

Materials and methods This study retrospectively enrolled immunotherapy-naïve HCC patients with Child - Pugh score ≤ 7 who underwent IA plus PD-1 mabs (IAP) or PD-1 mabs alone (P) from January 2018 to December 2022. Each patient had at least 2 times image data available for baseline tumor growth rate (TGR) assessment before administration of PD-1 mabs. The diagnostic criteria of HPD was: 1) Time to progression < 2 months; 2) $\geq 50\%$ increase of sum of target lesions major diameters; 3) Two-fold increase in TGR or at least 10 new lesions after treatment. C57/BL6 mice with subcutaneous tumor were randomly assigned to P (sham ablation + PD-1 mab, $n = 4$), IAP (IA + PD-1 mab, $n = 3$) and IAMP (IA + modified PD-1 mab with D265A mutation on Fc, $n = 3$). The tumor volume is calculated according to the modified ellipsoidal volume formula. And the TGR is the ratio between logarithm of tumor volume and interval time. The difference between pre- and post-treatment TGR was recorded as Δ TGR.

Results In total, 55 patients met the criteria and were included in the present study (IAP group: $n=12$, P group: $n=43$), the incidence of HPD in the IAP group was significantly higher than that in the P group (58.3% vs. 20.9%, $P = 0.028$). The animal study verified that IAP could accelerate the tumor growth (Δ TGR: IAP vs. P, 0.047 ± 0.0030 vs. -0.0031 ± 0.0080 , $P < 0.001$), and suggested that the blocking the interaction between Fc and Fc γ R receptors could interfere with the phenomenon (Δ TGR: IAMP vs. P, -0.0033 ± 0.0068 vs. -0.0031 ± 0.0080 , $P = 0.96$).

Conclusion IAP is likely to induce the high incidence of HPD. And the Fc-modified PD-1 mabs without the ability to bind to Fc γ R may block the process of HPD.

PO-087

Cryoablation Combined with Camrelizumab and Apatinib in Advanced Hepatocellular Carcinoma: A prospective, single-arm, phase II study

Yu-Zhe Cao^{1,2,3}, Fei Gao^{1,2,3}, Li-Jie Qiu^{1,2,3}, Zi-Xiong Chen^{1,2,3}, Mao-Yuan Mu^{1,2,3}, Xiao-Bo Fu^{1,2,3}, Han Qi^{1,2,3}

1. Sun Yat-Sen University Cancer Center

2. State Key Laboratory of Oncology in South China

3. Guangdong Provincial Clinical Research Center for Cancer

Purpose Anti-angiogenesis agents plus immune checkpoint inhibitors (ICIs) have been established as the first-line systemic therapy for advanced hepatocellular carcinoma (HCC). However, a relatively high proportion of advanced HCC patients haven shown resistance to these treatment regimens. Tumor ablation, particularly cryoablation, may inactivate tumor tissue locally, releasing the tumor-related proteins and potentially inducing an abscopal effect. Few studies have explored whether cryoablation can enhance the efficacy of these agents in advanced HCC. Therefore, this prospective study aimed to evaluate the efficacy and safety of combining cryoablation with apatinib and camrelizumab in patients with advanced HCC.

Materials and methods This study aimed to recruit 27 patients with advanced HCC, and 7 patients have been enrolled thus far. The main inclusion criteria are as follows: aged 18-70 years; pathologically confirmed diagnosis of HCC; CT/MRI diagnosed portal vein tumor thrombus (PVTT); the sum of the number and maximum diameter of intrahepatic lesions not exceeding 7 cm; no previous systemic or locoregional anticancer treatment; Child-Pugh grade A; ECOG PS 0-1. Patients were treated with cryoablation to inactivate lesions as much as possible. Within 48 hours of cryoablation, they received camrelizumab (200mg, intravenous infusion, d1, q3w) and apatinib (250mg, orally, qd) for a maximum duration of 2 years, disease progression or unacceptable adverse events occurred. The primary endpoint was the objective response rate (ORR), assessed using mRECIST v1.1/mRECIST criteria). The secondary endpoints included progression-free survival (PFS), overall survival (OS), and safety. Drug safety was evaluated according to CTCAE v5.0.

Results All patients in the study were male, and all were infected with hepatitis viruses (HBV 7/7, 100%, HCV 1/7, 14.3%). Vp3/4 PVTT was present in 57.1% (4/7) of patients. Three patients were diagnosed with extrahepatic metastasis (1 with lymph node metastasis, 1 with lung metastasis, and 1 with metastasis). Five patients reached the study endpoint (3 patients due to disease progression, 1 due to withdraw of informed consent, and 1 due to intolerable adverse effects). Among these, 6 patients (38%) had extrahepatic metastasis. 14 (88%) patients were classified as Child-Pugh A class. With a median follow-up of 15.6 months (IQR: 6.33-18.8), the ORRs were 71.4% (95%CI, 29.0%-96.3%) with 5 patients achieving partial responses (PR) according to mRECIST, and 14.3% (95%CI, 0.00%-57.9%) with 1 patient achieving PR according to RECISTv1.1. The median PFS (mRECIST) and OS were 4.63 months (95%CI: 3.97-Not reached) and 19.0 months (95%: 18.5-Not reached), respectively. The most common adverse events were hypertension (3/7, 42.9%), proteinuria (3/7, 42.9%), elevated aminotransferase (2/7, 28.6%), and pituitary dysfunction (2, 28.6%). No treatment-related serious adverse events were observed.

Conclusion Cryoablation combined with apatinib and camrelizumab as a first-line strategy for advanced HCC patients with PVTT, following the up-to-7 criteria, demonstrated promising results by improving ORR and OS, with acceptable side effects.

Clinical trial information: NCT04724226, URL: <https://clinicaltrials.gov/>

PO-088

Safety and effectiveness of microwave ablation in the treatment of parapleural pulmonary nodules

Mingqing Zhang
the Second Affiliated Hospital of Soochow University

Purpose To evaluate the safety and effectiveness of CT-guided microwave ablation in the treatment of parapleural pulmonary nodules.

Materials and methods From December 2018 to December 2023, a total of 67 parapleural nodules were treated with percutaneous lung microwave ablation under CT guidance. The clinical data, technical success rate, complications and efficacy of patients were analyzed to evaluate the safety and effectiveness of microwave ablation in the treatment of parapleural pulmonary nodules.

Results The success rate of microwave ablation in the treatment of parapleural nodules was 100%. Only one patient showed progress after surgery, and all patients survived. The incidence of small pneumothorax after surgery was 38.1%, the incidence of medium-mass pneumothorax was: 4.8%; the incidence of subcutaneous emphysema: 4.8%; the incidence of pleural effusion was 11.1%; the main adverse reaction was pain, with an incidence of 15.9%. No serious complications such as bleeding and death.

Conclusion Microwave ablation under CT is safe and effective in treating parapleural nodules.

PO-089

Thermosensitive Embolic Agent in the treatment of hepatocellular carcinoma with hepatic arterioportal shunt

Tong-Guo Si, Yong-Fei Guo

Tianjin Medical University Cancer Hospital and Institute, China

Purpose To investigate the safety and efficacy of using thermosensitive embolic agents (TempSLE) in the treatment of hepatocellular carcinoma (HCC) combined with hepatic arterioportal shunt (HAPS)

Materials and methods A retrospective analysis was performed on the clinical data of 36 patients who were admitted to Tianjin Cancer Hospital Airport Hospital between June 2022 and July 2023 for treatment of HCC with HAPS using thermosensitive embolic agents. The liver function levels, including preoperative serum albumin levels, ascites, and Child-Pugh classification, were evaluated. Digital subtraction angiography (DSA) imaging characteristics of HAPS were collected. The initial success rate of fistula occlusion, recanalization rates at 1m, 3m post-procedure, changes in liver function according to Child-Pugh classification before and after the procedure, tumor response rates (DCR, ORR), and survival times were recorded. HAPS severity was classified into four grades. Cumulative survival rates were calculated using the Kaplan-Meier method, prognostic factors were analyzed using the Cox proportional hazards model, and tumor response was assessed based on the modified Response Evaluation Criteria in Solid Tumors (mRECIST)

Results The initial occlusion success rate for HAPVF was 86.1% (with 100% success rate for grade 1-2 HAPVF and 50% for grade 3). The recanalization rate was 5% at one month (0% for grade 1-2 and 25% for grade 3) and 0% at three months (0% for both grade 1-2 and grade 3). There was no statistically significant difference in liver function as indicated by Child-Pugh classification pre- and post-operation ($P=0.053$). Median overall survival was 351 days, with 432 days for grade 1, 348 days for grade 2, and 268 days for grade 3. Survival analysis showed a significant difference among the three groups ($P=0.035$). Preoperative serum albumin levels ($P=0.005$, hazard ratio [HR]=0.735, 95% confidence interval [CI] 0.660, 0.916), presence or absence of ascites ($P=0.026$, HR=8.528, 95% CI 1.322, 65.233), and preoperative Child-Pugh classification ($P=0.030$, HR=0.078, 95% CI 0.011, 0.712) were identified as potential prognostic factors for HCC with HAPS.

Conclusion Thermosensitive embolic agents represent a novel, safe, and effective approach for treating HCC combined with HAPS.

PO-090

Development and Validation of a Survival Prediction Scoring System in Unresectable Hepatocellular Carcinoma Patients Treated with TACE plus Apatinib and Camrelizumab

Fang Sun, Wei Fu Lv

Department of Radiology, The First Affiliated Hospital of University of Science and Technology of China

Purpose Hepatocellular carcinoma (HCC) is a malignancy that severely threatens human health worldwide. About 75%–85% of HCC patients are diagnosed at the locally advanced or late stages, losing the opportunity for surgical intervention. Transcatheter arterial chemoembolization (TACE) combined with targeted therapy and immunotherapy has further improved the prognosis of these patients. This regimen has shown significant efficacy through synergistic anti-tumor effects, but due to tumor heterogeneity, the patient population that benefits remains unclear. Currently, the choice of clinical treatment regimens largely depends on guidelines and clinical experience. This study aims to construct and validate a prognostic scoring system for patients receiving this triple therapy to identify potential benefit populations and guide precise clinical decision-making.

Materials and methods This study employed a retrospective cohort design, including patients with unresectable hepatocellular carcinoma who first received TACE combined with apatinib and camrelizumab from January 2019 to June 2022 at the First Affiliated Hospital of the University of Science and Technology of China. After applying inclusion and exclusion criteria, 154 patients were enrolled, with an additional 50 patients treated with the same regimen from July 2022 to June 2023 as an external validation group. Baseline data were collected, and short-term efficacy was assessed. Cox regression analysis was used to identify independent prognostic factors and construct a score. Risk stratification was performed using the optimal cutoff value, and internal and external validation groups were used for validation.

Results The objective response rate exceeded 50% in all three groups, and the disease control rate exceeded 80%. Cox regression analysis identified portal vein tumor thrombus, alpha-fetoprotein levels, and the systemic immune-inflammation index as independent risk factors. The prognostic model based on these factors effectively distinguished survival differences among low, medium, and high-risk patients in the training group, validation group, and external validation group, with Kaplan-Meier survival curves showing significant differences (log-rank test $P < 0.05$).

Conclusion Portal vein tumor thrombus, alpha-fetoprotein levels, and the systemic immune-inflammation index are independent risk factors affecting the prognosis of patients with unresectable hepatocellular carcinoma receiving triple therapy. The prognostic scoring model constructed in this study has good predictive performance and can provide a scientific basis for individualized treatment decisions, helping to identify potential benefit populations and optimize clinical resource allocation.

PO-091

CT-guided 125I brachytherapy for hepatocellular carcinoma in high-risk locations after transarterial chemoembolization combined with microwave ablation: a propensity score-matched study

Zi-Xiong Chen, Fu Xiao-Bo, Qiu Zhen-Kang, Mu Mao-Yuan, Jiang Wei-Wei, Wang Gui-Song, Zhong Zhi-Hui, Qi Han, Gao Fei, Zixiong Chen
Sun Yat-sen University Cancer Center

Purpose This study aimed to evaluate the safety and efficacy of 125I brachytherapy combined with transarterial chemoembolization (TACE) and microwave ablation (MWA) for unresectable hepatocellular carcinoma (HCC) in high-risk locations.

Materials and methods After 1:2 propensity score matching (PSM), this retrospectively study analyzed 49 patients who underwent TACE +MWA+125I brachytherapy (group A) and 98 patients who only received TACE +MWA (group B). The evaluated outcomes were progression-free survival (PFS), overall survival (OS), and treatment complications. Cox proportional hazards regression analysis survival was used to compare the two groups.

Results The patients in group A showed a longer PFS than group B (7.9 vs. 3.3 months, $P = 0.007$). No significant differences were observed in median OS between the two groups ($P = 0.928$). The objective response rate (ORR), disease control rate of tumors in high-risk locations, and the ORR of intrahepatic tumors were 67.3%, 93.9%, and 51.0%, respectively, in group A, and 38.8%, 79.6% and 29.6%, respectively, in group B ($P < 0.001$, $P = 0.025$ and $P = 0.011$, respectively). TACE-MWA-125I ($HR = 0.479$, $P < 0.001$) was a significant favorable prognostic factor that affected PFS. The presence of portal vein tumor thrombosis was an independent prognostic factor for PFS ($HR = 1.625$, $P = 0.040$). The Barcelona clinic liver cancer (BCLC) stage (BCLC C vs. B) was an independent factor affecting OS ($HR = 1.941$, $P = 0.038$). The incidence of complications was similar between the two groups, except that the incidence of abdominal pain was reduced in the group A ($P = 0.007$).

Conclusion TACE-MWA-125I resulted in longer PFS and better tumor control than did TACE-MWA in patients with unresectable hepatocellular carcinoma in high-risk locations.

PO-092

Evaluation of models to predict prognosis in patients with advanced hepatocellular carcinoma treated with TACE combined with apatinib

Fang Sun, Wei Fu Lv

Department of Radiology, The First Affiliated Hospital of University of Science and Technology of China

Purpose The HAP, Six-and-Twelve, Up to Seven, and ALBI scores have been substantiated as reliable prognostic markers in patients presenting with intermediate and advanced hepatocellular carcinoma (HCC) undergoing transarterial chemoembolization (TACE) treatment. Given this premise, our research aims to assess the predictive efficacy of these models in patients with intermediate and advanced HCC receiving a combination of TACE and Apatinib. Additionally, we have conducted a meticulous comparative analysis of these four scoring systems to discern their respective predictive capacities and efficacies in combined therapy.

Materials and methods Performing a retrospective analysis on the clinical data from 200 patients with intermediate and advanced HCC, we studied those who received TACE combined with Apatinib at the First Affiliated Hospital of the University of Science and Technology of China between June 2018 and December 2022. To identify the factors affecting survival, the study performed univariate and multivariate Cox regression analyses, with calculations of four different scores: HAP, Six-and-Twelve, Up to Seven, and ALBI. Lastly, Harrell's C-index was employed to compare the prognostic abilities of these scores.

Results Cox proportional hazards model results revealed that the ALBI score, presence of portal vein tumor thrombus (PVTT), and tumor size are independent determinants of prognostic survival. The Kaplan-Meier analyses showed significant differences in survival rates among patients classified by the HAP, Six-and-Twelve, Up to Seven, and ALBI scoring methods. Of the evaluated systems, the HAP scoring demonstrated greater prognostic precision, with a Harrell's C-index of 0.742, surpassing the alternative models ($P < 0.05$). In addition, an analysis of the area under the AU-ROC curve confirms the remarkable superiority of the HAP score in predicting short-term survival outcomes.

Conclusion Our study confirms the predictive value of HAP, Six-and-Twelve, Up to Seven, and ALBI scores in intermediate to advanced Hepatocellular Carcinoma (HCC) patients receiving combined Transarterial Chemoembolization (TACE) and Apatinib therapy. Notably, the HAP model excels in predicting outcomes for this specific HCC subgroup.

PO-093

Role of Radiofrequency ablation (RFA) as a salvage treatment in recurrent fibromatosis.

Rajas Thaker, Dr Suyash Kulkarni, Dr Nitin Shetty, Dr kunal Gala
Tata Memorial Hospital

Purpose This study explores the role of radiofrequency ablation (RFA) as a salvage treatment option for recurrent fibromatosis. by investigating its effectiveness in managing this challenging condition, we aim to provide insights into the potential of RFA as an alternative therapeutic approach when conventional treatments prove inadequate.

To evaluate the safety and efficacy of percutaneous Radiofrequency Ablation (RFA) in managing recurrent fibromatosis.

Materials and methods The patients with recurrent fibromatosis who underwent RFA after the failure of at least one form of treatment

(medical/surgical/radiotherapy) were included in this retrospective study. Forty patients (18 males and 22 females) with a median age of 29 years (range, 6 – 68 years, mean- 30.8 years) underwent 109 sessions of RFA. The clinical and imaging evaluation was done before RFA and 1, 6, 12 and 24 months post RFA. The clinical evaluation was done by Visual Analogue Score (VAS) for pain assessment, Musculoskeletal Tumor Society (MSTS) score for functional assessment and imaging response was evaluated by CE-MRI using RECIST criteria.

Results All 40 patients were evaluated till 12 months, out of which 27 patients were followed upto 24 months and mean duration of follow-up was 38.5 months (5-110 months). There was a significant improvement in pain score at 12 months (VAS:3, $p<0.001$) and 24 months (VAS:2.45, $p<0.001$) compared to pre-procedure VAS of 4.94. The MSTS score improved from a pre-procedure score of 21 to 25 at 12 months ($p<0.001$) and 26.5 at 24 months ($p<0.001$). There was statistically significant reduction in the volume of the lesions after RFA at 12 months (mean vol:144cc, $p<0.001$) and 24 months (mean vol:92cc, $p<0.001$) from a baseline mean volume of 168 cc. There were five complications seen out of 109 sessions (4.5%) of RFA.

Conclusion Radiofrequency ablation is a safe and effective treatment modality in the treatment of recurrent fibromatosis. It reduces the size of the tumor, helps in pain palliation and improves functional outcomes.

PO-095

Investigation of the Efficacy and Safety of Lung Biopsy Plus Microwave Ablation for a Solitary Suspected Malignant Pulmonary Nodule after Radical Mastectomy

Peishun Li,Chao Xing,Sen Yang,Linlin Wu,Qirong Man,Xusheng Zhang,Miaomiao Hu,Yunling Bai,Kaixian Zhang
Tengzhou Central People's Hospital

Purpose To investigate the efficacy and safety of CT-guided lung biopsy combined with microwave ablation for a solitary suspected malignant pulmonary nodule in breast cancer patients after radical surgery.

Materials and methods From January 2014 to December 2018, 37 breast cancer patients who underwent radical surgery and had a solitary suspected malignant pulmonary nodule received CT-guided lung biopsy combined with microwave ablation. The study was approved by the local institutional review board. The clinical efficacy and complications of lung biopsy and microwave ablation were examined.

Results Among the 37 patients, 5 cases (5/37, 13.5%) were pathologically diagnosed as primary lung cancer, and 30 cases (30/37, 81.1%) cases were diagnosed as invasive ductal carcinoma. The major complications were pneumothorax, chest pain and hemoptysis. The 2-year, 3-year and 5-year survival rates of patients with lung metastases from breast cancer were 86.2%, 58.3% and 35.3% respectively. The median time from microwave ablation of lung metastases to disease progression was 35 months (ranging from 4 to 72 months, 95% confidence interval 24.53–46.48). The median OS time in the lung metastases subgroup was 44 months (95% confidence interval 32.55–55.45).

Conclusion CT-guided lung biopsy combined with microwave ablation is safe and effective in the treatment of a solitary suspected malignant pulmonary nodule in breast cancer patients after radical surgery.

PO-096

NO-driven self-propelled nanomotors augment chemo-immunotherapy and transcatheter arterial embolization

Lei Chen, Chuansheng Zheng
Wuhan Union Hospital

Purpose Chemo - immunotherapy is a first - line treatment for clinical cancer patients, but there are major challenges such as poor tumor penetration, multidrug resistance (MDR), and T cell - related immune escape in clinical translation. The purpose is to develop a solution to address these challenges.

Materials and methods The researchers describe a nitric oxide (NO) - driven nanomotor that integrates bio - inspired self - propulsion and immunosuppression alleviation for augmented chemo - immunotherapy.

Results In two types of mouse tumor models, this nanomotor can be excited in response to the tumor microenvironment. It allows for enhanced drug penetration, sustained NO release, and immune cell infiltration within the tumor, resulting in significant tumor growth inhibition and synergistic immune checkpoint blockade. In a VX2 orthotopic rabbit liver cancer model, the nanomotor achieves interventional transcatheter arterial embolization therapy and boosted immunity.

Conclusion The versatility and potency of the nanomotor validate its future application in translational anticancer nanomedicine.

PO-097

Comparative Effectiveness and Safety of Molecular Targeted Therapy Plus PD-(L)1 with or without TACE in Unresectable Hepatocellular Carcinoma: a retrospective study

Li Cui¹, Jiangtao Liu², Yan Wang¹, Feng Duan¹

1. PLA General Hospital

2. Hainan hospital of Chinese PLA General Hospital

Purpose This study aims to compare the effectiveness and safety of TACE combined with molecular targeted therapy (MTT) plus Programmed death-ligand 1 (PD-(L)1) antibodies versus MTT plus PD-(L)1 antibodies for HCC patients.

Materials and methods Data from HCC patients who received either MTT plus PD-(L)1 (systemic therapy group) or TACE combined with MTT plus PD-(L)1 (combination therapy group) were retrospectively analyzed. The primary outcome was the objective reaction rate (ORR) at the initial assessment post-treatment initiation. Secondary outcomes included progressive free survival (PFS), overall survival (OS) and grade-3 or higher adverse events.

Results A total of 222 HCC patients were included (109 in the systemic therapy group, 113 in the combination therapy group). Propensity score matching yielded 80 patients per group. The odds ratio for ORR in the combination therapy group was 1.29 (95% CI: 0.64–2.60; $p=0.479$). Subgroup analysis revealed significantly higher ORR for patients with $\text{AFP} \leq 200$ ng/mL in the combination therapy group ($\text{OR}=3.54$, $p=0.016$). For patients without PVTT, the ORR odds were slightly higher with combination therapy ($\text{OR}=5.33$, $p=0.068$). Multivariate Cox regression analysis showed no significant differences in PFS ($\text{HR}=0.68$, $p=0.131$) or OS ($\text{HR}=0.86$, $p=0.674$) between the two groups. Higher baseline AFP (>200 ng/mL) was associated with worse PFS ($\text{HR}=1.68$, $p=0.012$) and OS ($\text{HR}=2.33$, $p=0.021$). Surgical resection improved PFS ($\text{HR}=0.42$, $p<0.001$) and OS ($\text{HR}=0.31$, $p=0.004$). Grade 3 or higher adverse events were more common in the combination therapy group (52% vs. 15%, $p<0.0001$).

Conclusion No significant benefits were observed for combining TACE with MTT and PD-(L)1 in unresectable HCC patients. However, TACE may offer advantages for patients with $\text{AFP} \leq 200$ ng/mL or without PVTT.

PO-098

Assessing early response to DEB-TACE for unresectable HCC by tumor habitats-based features in contrast-enhanced computed tomography : A retrospective multicenter study

Kaikai Liu, Wanyin Shi, Xingwang Wu, Kai-cai Liu
The First Affiliated Hospital of Anhui Medical University

Purpose The early response to drug-eluting beads transcatheter arterial chemoembolization (DEB-TACE) in patients with unresectable hepatocellular carcinoma (HCC) is closely linked to prognosis. This study aims to predict the early response to DEB-TACE in unresectable HCC by developing a combined model that integrates sub-regional radiomic features from contrast-enhanced CT and clinical factors.

Materials and methods This retrospective study collected data on patients with unresectable HCC treated with DEB-TACE, who were then divided into the training, internal validation, and external validation cohorts. Based on tumor response to DEB-TACE, clinical information was used to build a clinical prediction model. Radiomic features from the entire tumor region of interest (ROI) were extracted to construct a radiomics prediction model, while sub-regional Habitats features were utilized to build an intra-tumor heterogeneity Habitat prediction model. Logistic regression analysis was employed to integrate clinical and radiomics features, clinical and heterogeneity Habitats features to form Rad-clinical and Hab-clinical combined models, respectively. Model performance was evaluated using area under the receiver operating characteristic curve (AUC), accuracy, specificity, sensitivity, positive predictive value (PPV), and negative predictive value (NPV).

Results A total of 193 patients with unresectable HCC were included in the analysis. 145 patients randomly divided in a 7:3 ratio into 101 patients for training and 44 for internal validation, while the external validation cohort included 48 patients. Among all patients, 14 achieved CR, 109 achieved PR, 65 had SD, and 5 showed PD. The objective response rate (ORR) was 63.73%, with a disease control rate (DCR) of 97.41%. Across all cohorts, the Hab-clinical model showed the highest predictive performance (AUC(95% CI) of 0.954(0.914-0.994), 0.942(0.878-1), and 0.954(0.896-1) for the training, internal validation, and external validation groups, respectively), outperforming the Rad-clinical model and other single models. Furthermore, Kaplan-Meier analysis revealed that patients predicted as responders by the Hab-clinical model had significantly longer progression-free survival (PFS) across all datasets [all $P < 0.001$].

Conclusion The model combining tumor Habitats features and clinical factors demonstrated superior performance in predicting early response to DEB-TACE in patients with unresectable HCC.

PO-099

Multi-modality model predicts Lung Metastasis of Hepatocellular Carcinoma using MRI and pathological: a retrospective multicenter study

Kaikai Liu, Wanyin Shi, Xingwang Wu
The First Affiliated Hospital of Anhui Medical University

Purpose Lung metastasis directly affects the prognosis of patients with hepatocellular carcinoma, How to predict the occurrence of lung metastasis and assist in advance can improve the efficacy of surgical treatment for hepatocellular carcinoma. This study aimed to develop and validate a model for predicting future lung metastasis of hepatocellular carcinoma (HCC) to assist in timely intervention.

Materials and methods A retrospective analysis of 700 HCC cases from three hospitals in China between January 2018 and June 2022 was conducted. A total of 395 patients were included from one hospital in the training and internal validation cohort, and 210 patients from two other hospitals in the external validation cohort. MRI (T2W, CE-T1W, and DWI) images of liver tumors and their full slide images of H&E-stained biopsy sections were collected for annotation and feature extraction. The Multi-modality model comprehensive prediction model was established based on three feature sets related to lung metastasis: Radiological features, Radiomics features and Pathomics features. The accuracy of the model in predicting lung metastasis in hepatocellular carcinoma was validated in the validation cohorts, using area under curve (AUC), sensitivity, specificity, positive predictive value (PPV), and negative predictive value (NPV).

Results The Multi-modality model had favorable accuracy for the prediction of lung metastasis in the training cohort (AUC:0.877[95%CI0.832-0.921], Sensitivity:0.885(0.830-0.923), Specificity:0.755(0.659-0.831), NPV:0.926(0.891-0.982), PPV:0.654(0.524-0.73)), and internal validation cohort (AUC:0.839(0.765-0.913), Sensitivity:0.853(0.781-0.851), Specificity:0.909(0.788-0.964), NPV:0.906(0.867-0.957), PPV:0.841(0.752-0.896)) and external validation cohort (AUC:0.835(0.779-0.890), Sensitivity:0.876(0.751-0.886), Specificity:0.868(0.753-0.911), NPV:0.903(0.852-0.942), PPV:0.845(0.761-0.902)). The Multi-modality model also significantly outperformed any single-modality prediction models: AUC of 0.608 [0.538-0.679] for the MR model, 0.759 [0.699-0.818] for the radiomics model, and 0.808 [0.755-0.862] for the pathomics model.

Conclusion The Multi-modality model proposed in our study could predict the risk of lung metastasis in hepatocellular carcinoma with high accuracy, and may be served as a predictive tool to guide patients in early systematic treatment.

Development and Validation of a Predictive Model for Poor Prognosis in Epithelial Ovarian Cancer

Yueyue Ma¹, Zhiyu Tian³, Songquan Wen², Weihong Zhao²

1. Shanxi Medical University

2. Department of Obstetrics and Gynecology, the Second Hospital of Shanxi Medical University

3. Department of Epidemiology, School of Public Health, Shanxi Medical University

Purpose To analyze the epidemiological characteristics and identify independent risk factors affecting the prognosis of epithelial ovarian cancer (EOC), and to develop and validate a nomogram model for individualized prediction of 3-year and 5-year overall survival (OS) in postoperative patients.

Materials and methods A total of 3,286 epithelial ovarian cancer (EOC) patients who received standardized treatment were included from the SEER database (2016–2019). These patients were randomly divided into a modeling group (n=2,300) and an internal validation group (n=986) in a 7:3 ratio. Additionally, 184 patients from the Second Hospital of Shanxi Medical University were enrolled as an external validation group. Independent prognostic factors were identified using univariate and multivariate Cox regression analyses, and a nomogram model was developed. The predictive accuracy, discriminative ability, and clinical utility of the model were evaluated using the concordance index (C-index), calibration curves, area under the receiver operating characteristic curve (AUC), and decision curve analysis (DCA).

Results Univariate and multivariate Cox regression analyses demonstrated that age, CA125 levels, AJCC stage, distant metastasis, single tumor, bilateral tumor, and the pathological type of serous carcinoma were independent risk factors for poor prognosis in postoperative EOC patients (all $P < 0.05$). Based on these findings, a nomogram model was developed. The concordance index (C-index) of this model in the modeling group, internal validation group, and external validation group were 0.718, 0.700, and 0.681, respectively. The area under the receiver operating characteristic curve (AUC) ranges for 3-year and 5-year survival rates were 0.693–0.736 and 0.670–0.754, respectively, indicating that the model exhibited moderate discriminative ability. The calibration curves showed good agreement between the predicted and observed survival rates, and the decision curve analysis (DCA) confirmed the model's strong clinical utility.

Conclusion This study integrated seven independent risk factors, including age, CA125 levels, and AJCC stage, to develop a nomogram model for predicting survival in postoperative EOC patients. Through internal and external validation, the model demonstrated high accuracy and strong clinical applicability in predicting 3-year and 5-year OS, offering a reliable tool for individualized prognosis assessment and treatment decision-making.

PO-101

Evaluating the Role of Large Language Models in Recommending Hepatocellular Carcinoma Patients to Interventional Radiology

Zibo Gong

Shenjing Hospital of China Medical University

Purpose The purpose of this study is to evaluate the performance of multiple large language models (LLMs) in recommending hepatocellular carcinoma (HCC) patients to Interventional Radiology (IR). By analyzing how these models suggest IR as a treatment option, we aim to understand their potential impact on public awareness of IR and patient referral patterns.

Materials and methods HCC was selected as the focus disease, and a standardized prompt, "I have hepatocellular carcinoma. What kinds of doctors can treat this disease?" was designed. Each prompt was repeated three times to ensure consistency. The study evaluated the following LLMs: ChatGPT4o, ChatGPTo1, Claude 3.7, Deepseek R1, Kimi k1.5, ERNIE Bot, Tongyi Qianwen, Zidong Taichu, and Doubao. Responses from each model were recorded, and whether IR was recommended (1 = recommended, 0 = not recommended) and its ranking in the recommendation list were annotated. Statistical analysis, including one-way ANOVA and chi-square tests, was performed to compare the differences among models in recommending IR, with a significance level set at $p < 0.05$.

Results The results showed that mainstream models such as ChatGPT 4o and Deepseek R1 had a high frequency of recommending IR, with IR being suggested in 73.9% and 60.9% of responses, respectively. The average ranking of IR in the recommendation list was 3-4 across all models, indicating that IR is recognized as a viable treatment option but is not always the first recommendation. International models generally outperformed domestic models in recommending IR, although domestic models demonstrated better performance in Chinese-language contexts. Statistical analysis revealed significant differences in the frequency and ranking of IR recommendations among the models ($p < 0.05$).

Conclusion This study highlights the potential of LLMs in recommending HCC patients to IR, reflecting a growing recognition of IR's role in HCC treatment. However, the lower ranking of IR in recommendations suggests that public awareness of IR still needs improvement. The differences in performance between international and domestic models may be attributed to variations in training data and algorithms. Future research should focus on leveraging LLMs to enhance public awareness of IR and improve patient referral rates, particularly in regions where IR is underutilized.

Construction and validation of a predictive model for poor prognosis in epithelial ovarian cancer

Yueyue Ma¹, Zhiyu Tian², Songquan Wen³, Weihong Zhao³

1. Shanxi Medical University

2. Department of Epidemiology, School of Public Health, Shanxi Medical University

3. Department of Obstetrics and Gynecology, the Second Hospital of Shanxi Medical University

Purpose To analyze the epidemiological characteristics and identify independent risk factors affecting the prognosis of epithelial ovarian cancer (EOC), and to develop and validate a nomogram model for individualized prediction of 3-year and 5-year overall survival (OS) in postoperative patients.

Materials and methods A total of 3,286 EOC patients who underwent surgery combined with chemotherapy from the SEER database (2016–2019) were included and randomly divided into a modeling group (n=2,300) and an internal validation group (n=986) in a 7:3 ratio. Additionally, 184 patients from the Second Hospital of Shanxi Medical University were enrolled as an external validation group. Independent prognostic factors were identified using univariate and multivariate Cox regression analyses, and a nomogram model was developed. The predictive accuracy, discriminative ability, and clinical utility of the model were evaluated using the concordance index (C-index), calibration curves, area under the receiver operating characteristic curve (AUC), and decision curve analysis (DCA).

Results Univariate and multivariate Cox regression analyses demonstrated that age, CA125 levels, AJCC stage, distant metastasis, single tumor, bilateral tumor, and the pathological type of serous carcinoma were independent risk factors for poor prognosis in postoperative EOC patients (all $P < 0.05$). Based on these findings, a nomogram model was developed. The concordance index (C-index) of this model in the modeling group, internal validation group, and external validation group were 0.718, 0.700, and 0.681, respectively. The area under the receiver operating characteristic curve (AUC) ranges for 3-year and 5-year survival rates were 0.693–0.736 and 0.670–0.754, respectively, indicating that the model exhibited moderate discriminative ability. The calibration curves showed good agreement between the predicted and observed survival rates, and the decision curve analysis (DCA) confirmed the model's strong clinical utility.

Conclusion This study integrated seven independent risk factors, including age, CA125 levels, and AJCC stage, to develop a nomogram model for predicting survival in postoperative EOC patients. Through internal and external validation, the model demonstrated high accuracy and strong clinical applicability in predicting 3-year and 5-year OS, offering a reliable tool for individualized prognosis assessment and treatment decision-making.

PO-103

Establishment and validation of a prognostic prediction model for glioma based on key genes and clinical factors

Dan Hua

Tianjin Medical University General Hospital

Purpose Glioma is a common brain tumour that is associated with poor prognosis. Immunotherapy has shown significant potential in the treatment of gliomas. Herein, we proposed a new prognostic risk model based on immune- and mitochondrial energy metabolism-related differentially expressed genes (IR&MEMRDEGs) to enhance the accuracy of prognostic assessment in patients with glioma.

Materials and methods Data from samples from 671 glioma patients and 5 normal controls with available follow-up data and prognostic outcomes were downloaded from the Gene Expression Omnibus (GEO) and The Cancer Genome Atlas (TCGA) databases. All data were downloaded on 13 November 2023. IR&MEMRDEGs were screened from the GeneCards website and published literature. Prognostic prediction models were constructed and analysed using Cox and Least Absolute Shrinkage and Selection Operator (LASSO) regression, Kaplan-Meier (KM) curve, and receiver operating characteristic (ROC) curve analyses. Single_x0002_sample gene set enrichment analysis (ssGSEA) was further performed to ascertain the percentage of immune cell infiltration in the glioma specimens.

Results Bioinformatics analysis of the GEO and TCGA databases identified eleven MEMRDEGs with dysregulated expression in gliomas: EIF4EBP1, TP53, IDH1, PRKCZ, CD200, GPI, PGM2, PKLR, AK2, ATP4A, and ALDH3B1. Further analysis identified EIF4EBP1, TP53, IDH1, PRKCZ, CD200, GPI, PGM2, AK2, and ALDH3B1 as separate predictive factors for glioma, among which PGM2 and AK2 exhibited superior accuracy [area under the ROC curve (AUC) >0.9], while EIF4EBP1, TP53, IDH1, PRKCZ, GPI, and ALDH3B1 demonstrated slightly lower accuracy ($0.7 < \text{AUC} < 0.9$), and CD200 displayed poor accuracy ($0.5 < \text{AUC} < 0.7$). Among these genes, the levels of AK2, ALDH3B1, EIF4EBP1, GPI, IDH1, PGM2, and TP53 were significantly higher in the high-risk group (HRG) compared with the low-risk group (LRG) ($P < 0.001$), indicating a negative association with patient prognosis. In contrast, CD200 and PRKCZ were significantly downregulated in the HRG compared to the LRG ($P < 0.05$), indicating a potential correlation with patient outcomes. Subsequently, prognostic models were constructed based on IR&MEMRDEG and MEMRDEGs to anticipate the outcomes of glioma patients, while the predictive efficacy of the model was validated via KM and ROC curve analysis. The results revealed that EIF4EBP1, TP53, IDH1, PRKCZ, GPI, PGM2, ALDH3B1, and AK2 had superior accuracy in predicting glioma prognosis. The ssGSEA results showed that only IDH1 was negatively linked to the amount of immune cell infiltration in the LRG, while displaying a positive connection in the HRG ($r \text{ value} > 0$), indicating that the expression levels of IDH1 may have a distinct influence on the tumour immune microenvironment.

Conclusion The present study confirmed the significant predictive value of IDH1 for glioma prognosis, which may guide immunotherapy for glioma treatment.

PO-104

High risk acute pulmonary embolism after interventional embolization of vaginal hemorrhage in cervical cancer

Jing Xiao

Chongqing University Cancer Hospital, China

Purpose This article aims to explore the clinical efficacy of interventional embolization in patients with cervical cancer experiencing massive vaginal bleeding and to analyze the diagnosis, treatment, and prevention strategies for high-risk acute pulmonary embolism (APE) postoperatively, providing references and guidance for clinical practice.

Materials and methods This article details the case of a cervical cancer patient who underwent bilateral uterine artery embolization for massive vaginal bleeding. The procedure involved the use of gelatin sponge, polyvinyl alcohol (PVA) particles, and coils for embolization. Postoperatively, the patient developed acute pulmonary embolism, which was managed through pulmonary angiography, thrombectomy/thrombolysis, and anticoagulation therapy guided by digital subtraction angiography (DSA). Additionally, a four-character guideline of “drain, suture, prevent, and mobilize” was proposed to reduce the incidence of postoperative pulmonary embolism.

Results Following interventional embolization, the patient’s active vaginal bleeding was effectively controlled. Acute pulmonary embolism was successfully managed through timely diagnosis and intervention, leading to stable patient conditions and successful extubation. Subsequently, the patient received standardized anti-tumor therapy, and follow-up examinations showed near-complete resolution of the mass, assessed as complete remission (CR), with no significant abnormalities observed during follow-up.

Conclusion Interventional embolization demonstrates significant hemostatic efficacy in cervical cancer patients with massive bleeding, providing a foundation for subsequent treatment. Postoperative acute pulmonary embolism is a severe complication, but timely diagnosis and effective management can save lives. The adoption of the “drain, suture, prevent, and mobilize” preventive measures can significantly reduce the incidence of pulmonary embolism. This article offers valuable insights into the clinical management of massive bleeding in cervical cancer and its postoperative complications.

PO-105

The combined model of Clinical and CT radiomics for predicting the efficacy of drug coated balloon therapy in the treatment of femoral-popliteal artery stenosis/occlusion

Yuxin Hang

The First Affiliated Hospital of China Medical University

Purpose Drug-coated balloon (DCB) angioplasty has been widely adopted for treating lower extremity arteriosclerosis obliterans (ASO), particularly in femoropopliteal artery stenosis/occlusion. Preoperative prediction of DCB efficacy remains crucial. This study aims to identify factors influencing symptom relief duration post-DCB intervention, and establish a clinical-radiomics integrated model for preoperative prediction of symptom recurrence risk and therapeutic outcomes, and the indirect prediction of efficacy.

Materials and methods According to the inclusion and exclusion criteria, A total of 130 patients with femoral-popliteal ASO treated with DCB at Center 1 (Interventional Therapy Department, First Affiliated Hospital of China Medical University) between June 2019 and December 2022, and 56 patients from Center 2 (Radiology Interventional Ward, Shengjing Hospital, China Medical University) between June 2018 and December 2022, were retrospectively enrolled. Clinical data and symptom relief duration were collected. Survival analysis of symptom relief time was performed to evaluate long-term efficacy and identify independent prognostic predictors. Patients were stratified based on symptom relief duration, with Center 1 designated as the training group and Center 2 as the test group. Classification prediction models (clinical model, radiomics model and the combined model of clinical-radiomics) were constructed to predict symptom recurrence risk and indirectly evaluate DCB efficacy.

Results In the survival analysis of symptom relief time, the median symptom relief time for all patients (n=186) was 24.0 months (95% CI: 20.2–27.8). Lesion calcification (HR=1.996, 95% CI: 1.348–2.955, P=0.001) and post-treatment residual stenosis rate (HR=1.706, 95% CI: 1.062–2.739, P=0.027) significantly influenced symptom relief duration. In classification models, after excluding non-significant clinical features and redundant radiomics features, calcification (OR=4.741, 95% CI: 1.703–13.201, P=0.003), residual stenosis rate (OR=3.920, 95% CI: 1.552–9.900, P=0.004), and 13 radiomics features (including 1 first-order feature, 2 shape-based features and 10 texture/higher-order features) showed significant associations with symptom relief time classification. The clinical model, radiomics model and the combined model of clinical-radiomics all demonstrated strong predictive performance. After comparing the potency of the three constructed models, the combined model of clinical-radiomics outperformed other models: training group AUC=0.844 (95% CI: 0.777–0.910); test group AUC=0.827 (95% CI: 0.718–0.936). In the training group, the combined model's AUC was higher than the clinical model (0.844 vs. 0.768) and radiomics model (0.844 vs. 0.789), and the difference was statistically significant (DeLong $P_{\text{the combined model-clinical model}}=0.0158<0.05$; DeLong $P_{\text{the combined model-radiomics model}}=0.0416<0.05$). In the test group, though the combined model's AUC was numerically higher than the clinical (0.827 vs. 0.756) and radiomics models (0.827 vs. 0.700), the differences were non-significant (DeLong $P_{\text{the combined model-clinical model}}=0.1639>0.05$; DeLong $P_{\text{the combined model-radiomics model}}=0.0549>0.055$).

Conclusion The Symptom relief duration after DCB treatment for femoral-popliteal artery ASO closely correlates with lesion calcification and post-treatment residual stenosis rate. The

combined model of clinical-radiomics effectively predicts DCB efficacy, outperforming standalone clinical or radiomics models.

Impact of Tumor Burden and Radiation Dose on Survival Outcomes and Treatment Response in Patients with Unresectable Hepatocellular Carcinoma Treat with TARE

Xiaoyong Liu, Yuxing Yu, Zhangxian Chen, Mingzhi Hao, Wenchang Yu, Zhuting Fang, Yubin Hu
Fujian Cancer Hospital

Purpose Hepatocellular carcinoma (HCC) is a leading cause of cancer-related mortality. Transarterial radioembolization (TARE) shows promise for treating unresectable HCC. However, interpatient variability underscores the need for effective patient stratification and optimized protocols.

Materials and methods This retrospective study analyzed 33 HCC patients treated with resin-based TARE. Treatment efficacy was evaluated based on the objective response rate (ORR) and disease control rate (DCR). Survival outcomes, including median overall survival (OS) and progression-free survival (PFS), were assessed using Kaplan-Meier analysis. Tumor burden, tumor absorbed dose (TAD), and tumor-to-normal liver ratio (TNR) were analyzed as potential predictive factors for treatment response.

Results TARE achieved an ORR of 66.7% and a DCR of 87.9%. The median OS was 16.69 months, with the median PFS significantly higher for patients with target lesions (16.69 months) compared to those with lesions of totality (4.86 months). For patients with target liver lesions, the ORR reached 71.9% at 1 month and 78.6% at 3 months. High-risk patients, characterized by tumor burden score >24.8 or the presence of ≥ 6 scattered lesions, exhibited significantly poorer PFS (HR = 3.355, 95% CI: 1.25–9.00, $p = 0.016$). Multivariate analysis further indicated that higher TNR values were associated with improved therapeutic responses, while a TAD exceeding 160 Gy correlated with reduced efficacy, potentially due to uneven radiation delivery.

Conclusion TARE is an effective treatment option for controlling intrahepatic lesions and improving survival outcomes in patients with unresectable HCC. However, treatment planning should carefully account for tumor burden, tumor count, lesion distribution, and radiation dose distribution to optimize clinical outcomes. These findings provide a foundation for integrating TARE into clinical practice, and further large-scale studies are warranted to validate and refine personalized treatment strategies for improved patient management.

PO-107

Harmonizing Ancient Wisdom and Modern Technology: Exploring Retrieval-Augmented Generation (RAG) with Large Language Models to Transform Education in Interventional Oncology

Hassan Magdy, Mohamed Ahmed
Gastrointestinal Surgery Center, Mansoura University, Egypt

Purpose Just as the ancient Silk Road once connected civilizations, modern technology can bridge gaps in medical knowledge. This abstract proposes a pioneering educational study utilizing Retrieval-Augmented Generation (RAG)—a powerful integration of Large Language Models (LLMs) with continuously updated evidence—to enhance clinical reasoning and decision-making skills among interventional oncology trainees. We aim to explore whether this innovative educational approach can foster deeper understanding, efficiency, and harmony among future interventional oncology specialists.

Materials and methods This prospective educational study will recruit 30 interventional oncology trainees, equally divided into two groups. While one group engages with traditional educational methods (standard case-based teaching and textbooks), the other will experience training enriched by RAG-enhanced AI platforms. By seamlessly embedding the latest interventional oncology guidelines, state-of-the-art research, and clinical wisdom into dynamic and interactive educational modules, trainees will experience learning akin to an expert mentor guiding each decision step-by-step. The study will quantitatively assess the impact through structured clinical assessments, and qualitatively through trainee satisfaction surveys and self-assessments.

Results We anticipate trainees using the AI-enhanced RAG educational platform to exhibit substantial improvement in clinical accuracy, decision-making confidence, and critical thinking speed, reflecting the harmony between human intuition and AI-driven precision. Moreover, we foresee enhanced trainee satisfaction due to personalized, culturally-sensitive learning experiences, aligned with the Chinese philosophy of continuous self-improvement and collaborative excellence.

Conclusion This study proposes that the thoughtful integration of Retrieval-Augmented Generation with Large Language Models not only modernizes education but also echoes traditional Chinese values of wisdom-sharing, cross-disciplinary harmony, and lifelong learning. Success in this approach would inspire global collaboration, elevating interventional oncology training and setting the foundation for educational excellence without borders.

PO-108

MCTL® Multitarget Individualized Diagnostic and Treatment Technology

Zhi Huang

Affiliated Hospital of Guizhou Medical University

Purpose The development of MCTL® technology is designed to address significant challenges in cancer treatment, such as immune evasion, drug resistance, and tumor heterogeneity. Faced with the limitations of traditional treatment methods (including surgery, chemotherapy, radiation therapy, and targeted therapy) in certain cases, there is an urgent need for new strategies to enhance treatment effectiveness, reduce recurrence, and extend patient survival. MCTL® aims to revolutionize cancer treatment strategies through a multitarget individualized approach, improving precision and effectiveness in treating tumors that are highly heterogeneous and resistant to standard treatments.

Materials and methods Materials and Methods: Target Selection and Confirmation: Using BoHai Bio's tumor tissue microarray screening library, 300,000 clinical biopsy samples are screened to identify specific tumor targets based on their expression levels and heterogeneity among different patients within the same tumor type. Target Synthesis and Cell Culture: Once positive targets are confirmed, they are synthesized ex vivo using peptide synthesis technology. Subsequently, blood samples are collected from patients, and dendritic cells (DC cells) and T cells are isolated and cultured. These cells are trained in vitro against specific targets to enhance their ability to recognize and attack tumor cells. Cell Reinfusion and Immune Activation: Trained DC cells and T cells are reinfused into the patient. DC cells activate T cells through antigen presentation, while T cells directly engage in attacking tumor cells. This process not only initiates an active immune response but also enhances the patient's passive immunity, thereby strengthening overall immune surveillance and tumor control.

Results Results: Clinical trials included patients with advanced non-small cell lung cancer who had failed first and second-line treatments. The treatment regimen involved MCTL® technology combined with PD-1 inhibitors. Recent evaluations of 23 enrolled patients showed an objective response rate of 33.3%, a disease control rate of 85.7%, a progression-free survival of 8.5 months, and a median survival time of 26 months, significantly outperforming other second-line cancer drugs. Additionally, no Grade III adverse reactions were observed during the treatment, indicating good safety.

Conclusion Conclusion: The application of MCTL® technology in the treatment of solid tumors has shown significant advantages in terms of safety and efficacy. The multitarget and individualized treatment strategy offers new possibilities for treating complex and heterogeneous tumors, showcasing broad prospects as an adjunct therapy for cancer. This innovative treatment method is expected to be a significant advancement in the field of oncology, providing patients with more durable and effective treatment outcomes. MCTL® Multitarget Individualized Diagnostic and Treatment Technology.

PO-111

Mineralized supramolecular microspheres with dual phase acid mirco-environment relief and immunoregulating functions for transarterial chemoembolization immunotherapy of hepatocellular carcinoma.

Xiangyu Yang

Beijing Chao-Yang Hospital, Capital Medical University.

Purpose Transcatheter arterial chemoembolization (TACE) is a pivotal therapeutic option for hepatocellular carcinoma (HCC) at intermediate or advanced stage. Current microspheres face some limitations including a tedious treatment process, low versatility and suboptimal therapeutic outcome. The aim of the study is to develop a β -cyclodextrin (β -CD) based mineralized supramolecular microspheres (Mn-DCA-VB124-MS) with dual phase acid mirco-environment relief and immunoregulating functions to provides a novel strategy for improving the therapeutic outcome of advanced HCC treatment by combining TACE with multiple TME modulations.

Materials and methods VB124, a monocarboxylate transporter 4 (MCT-4)inhibitor, is loaded in the porous microspheres through cyclodextrin-based host-guest recognition, which are further mineralized by manganese ion (Mn^{2+}) and dichloroacetate (DCA). The mineralized Mn^{2+} were to activate the cyclic GMP-AMP synthase (cGAS)-stimulator of interferon genes (STING) pathway, and DCA and VB124 were aimed to inhibit lactate production in TME. The NMR spectra, SEM and TEM were employed for characterization of Mn-DCA-VB124-MS. The IL-6, $INF\beta$ and STING proteins were examined by western blot and ELLSA to detect the activation of cCAS-STING in vitro and in a mouse subcutaneous liver cancer model. The extracellular lactate amount was tested in vitro and in vivo. The flow cytometry and propidium iodide staining were performed to access the apoptosis of treated liver cells. The Mn-DCA-VB-MS were locally administrated to an Hepa1-6 subcutaneous mouse model, and the growth of the tumors were recorded. The VX2 orthotopic liver cancer model was developed in rabbits. Catheteration was performed and the Mn-DCA-VB124-MS was administrated i.a. into the tumor. The tumor growth and remote migration were recorded and analyzed.

Results The Mn-DCA-VB124-MS microsphere was successfully synthesized and characterized. In vitro, the Mn-DCA-VB124-MS activated the cCAS-STING pathway and restricted the lactate amount. The synergistic anti-tumor effect was observed in vitro and in vivo. in the mouse model intensive cCAS-STING pathway activation was observed. The VX2 tumor growth rate treated by Mn-DCA-VB124-MS TACE was significantly lower than control groups. Surprisingly, the peritoneal and lung metastases in the Mn-DCA-VB-MS were also lower than control groups, showing promising systematic immune response.

Conclusion Overall, this study successfully integrates the effects of TACE with chemotherapy and TME modulation to effectively inhibit tumor growth and metastasis, providing a novel approach of microsphere-based embolization for advanced HCC.

PO-114

The Efficacy of Combined Treatment with the Anti-fibrotic Drug PFD and TACE in an Animal Model of Liver Cancer

Zhimei Cheng

Affiliated Hospital of Guizhou Medical University

Purpose Explore whether the anti-fibrotic drug pirfenidone (PFD) can enhance the efficacy of liver cancer TACE treatment by inhibiting the activation of hepatic stellate cells (HSCs) and reducing peritumoral fibrosis.

Materials and methods

(1) To further validate how post-TACE peritumoral fibrosis affects the efficacy of TACE in liver cancer, DEN-induced liver cancer in SD rats was treated with TACE, and tissue samples were collected 14 days postoperatively. Flow cytometry was used to detect the percentages of CD3, CD4, CD8, and Foxp3 immune cells in blood, spleen, liver, boundary, and tumor. (2) Subsequently, rabbits with VX2 liver cancer and DEN-induced liver cancer in SD rats were treated with a combination of the anti-fibrotic drug pirfenidone (PFD) and TACE. Animals were randomly divided into Model, TACE, and TACE + PFD groups, with 3 animals per group. PFD administration via gastric gavage started on the first day after TACE treatment at a dose of 250 mg/kg, based on the animal's weight, and continued for 14 days. Liver and tumor tissue samples were collected at the end of the experiment. Masson's trichrome and Sirius red staining were performed to detect peritumoral fibrosis, and immunohistochemistry was used to evaluate the expression of α -SMA, FAP α , HK2, PKM2, LDHA, and MCT1 proteins. (3) LX2 and HSC T6 cells were treated with 4 mmol/L PFD for 48 hours. RT-qPCR was performed to detect α -SMA gene expression, while Western blotting and immunofluorescence were used to assess α -SMA protein expression. (4) To evaluate the synergistic enhancement of liver cancer TACE efficacy by PFD, DEN-induced SD rats were randomly divided into Model, TACE, and TACE + PFD groups ($n = 10$). PFD was administered via gastric gavage at 250 mg/kg daily for 1 to 14 days after TACE. Tumor size was measured by ultrasound at the end of the experiment. Survival time of the rats was recorded from the first day after TACE until death. (5) Independent sample t-tests were used for between-group comparisons, one-way analysis of variance was used for multi-group comparisons, and LSD was used for post hoc multiple comparisons. GraphPad Prism was used to plot survival curves, and Log Rank was used to assess survival rates. A significance level of $P < 0.05$ was considered statistically significant.

Results (1) Tissue samples collected from DEN-induced SD rats with liver cancer after TACE treatment showed, via flow cytometry, an increased proportion of CD8+ T cells in the blood, spleen, and peritumoral liver tissues compared to the untreated group (all $P < 0.05$). (2) In the PFD combined with TACE treatment group, compared to the TACE group, immunohistochemistry results showed reduced expression of α -SMA and FAP α in the peritumoral area (both $P < 0.05$); Masson's trichrome and Sirius red staining demonstrated reduced peritumoral fibrosis (both $P < 0.05$). Additionally, immunohistochemistry detected decreased expression of glycolytic metabolism key enzymes HK2 and PKM2 in the peritumoral residual viable tumor tissue (both $P < 0.05$). Furthermore, there was a decreasing trend in the expression of LDHA and MCT1 (both $P < 0.05$). Flow cytometry also revealed an increased percentage of CD8+ T cells and a decreased proportion of Foxp3 in the tumor in the TACE + PFD group (both $P < 0.05$). (3) In vitro RT-qPCR, Western blot, and immunofluorescence experiments showed that the mRNA and protein expression of α -SMA in LX2 and HSC T6 cells

decreased after PFD treatment (all $P < 0.05$). (4) Compared to the untreated group, the tumor volume was smallest in the TACE + PFD group, and survival analysis indicated an extended survival time in the TACE + PFD group ($P < 0.05$).

Conclusion PFD attenuates peritumoral fibrosis by inhibiting HSCs activation, promoting infiltration of CD8⁺ T cells into the tumor, and synergistically enhancing the efficacy of TACE in SD rat liver cancer models.

PO-117

Value of intratumoral combined with peritumoral radiomics model in the prediction of Ki-67 expression in lung adenocarcinoma: a multi-center study

Ye Feng

Wenzhou Medical University Affiliated Fifth Hospital

Purpose To assess the role played by intratumoral and peritumoral radiomics together with radiomics nomogram in Ki-67 expression prediction in lung adenocarcinoma (LUAD).

Materials and methods A cohort of 388 individuals diagnosed with LUAD at the Fifth Affiliated Hospital of Wenzhou Medical University (WMU) fell into a training cohort (TC, n = 272) and an internal validation cohort (IVC, n = 116). Furthermore, 176 and 221 patients from the First Affiliated Hospital of Jiaxing University and the Sixth Affiliated Hospital of WMU constituted external validation cohort 1 (EVC1) and 2 (EVC2), respectively. We extracted 1,688 CT-based radiomics features from the gross tumor volume (GTV) encompassing peritumoral areas of 3, 6, and 9 mm (GPTV3, GPTV6, GPTV9). The study constructed a radiomics nomogram, which combined independent predictors in clinical practice with the radiomics score (Rad-score) generated by the most effective radiomics model.

Results The GPTV6 radiomics model with AUC values of 0.896, 0.844, 0.784, and 0.835 in the TC, IVC, EVC1 and EVC2, respectively. The delong test shows that it outperformed the GTV, GPTV3, and GPTV9 models in relevant prediction. In the clinical model, independent predictors included nodule size, spicule sign, and nodule density. The combined nomogram, incorporating these predictors and the GPTV6-Radscore, demonstrated significant clinical utility, achieving AUCs of 0.905, 0.871, 0.806, and 0.882 across the respective cohorts.

Conclusion CT-based radiomics nomogram excels in Ki-67 expression prediction in patients suffering from LUAD, providing reference for the personalized treatment of these patients.

PO-118

CT-guided iodine-125 brachytherapy is an effective palliative treatment for the right lower paratracheal lymph nodes metastasis previously treatment failure

Hang Yuan, Hong-Tao Hu, Ho-Young Song
Henan Cancer Hospital

Purpose This study aimed to evaluate the effectiveness and safety of iodine-125 brachytherapy as a treatment for right lower paratracheal lymph node metastasis following unsuccessful prior therapies.

Materials and methods A retrospective review of patients who underwent iodine-125 brachytherapy for right lower paratracheal lymph node metastasis was conducted. The study included 24 patients who met the predefined criteria. Iodine-125 seeds were implanted under CT guidance, and treatment planning was performed using a treatment planning system. The primary endpoint was the objective response rate (ORR), while overall survival (OS) and complications were secondary endpoints.

Results The ORR was 87.5%, with 4 patients achieving complete response (CR) and 17 patients achieving partial response (PR). The mean diameter of metastatic lymph nodes significantly reduced from 40.21 ± 6.66 mm before treatment to 12.25 ± 9.27 mm at the last follow-up ($p < 0.001$). The median OS was 14.70 months, with 1-year and 2-year survival rates of 78.9% and 20.9%, respectively. Clinical symptoms significantly improved, as indicated by increased Karnofsky Performance Score (KPS) scores. Complications were manageable, with no procedure-related deaths.

Conclusion Iodine-125 brachytherapy demonstrated promising efficacy and safety as an alternative treatment for right lower paratracheal lymph node metastasis after unsuccessful prior therapies.

Engineered microspheres for interventional-magneto-thermal-immunotherapy of tumours

Yong Jin, Di Wang, Xingwei Sun

Department of Interventional Radiology, The Second Affiliated Hospital of Soochow University, Suzhou, 215004, People's Republic of China

Purpose Aiming at the bottleneck of the single function of embolic microspheres (only blocking the tumour blood supply) and the insufficient regulation of the immunosuppressive microenvironment in hepatocellular carcinoma in traditional transcatheter arterial chemoembolisation (TACE), the present study aims to develop a novel multifunctional embolic microsphere system, which improves the tumour microenvironment and enhances anti-tumour efficacy through the synergistic immune regulation by the magneto-thermal effect.

Materials and methods Zn/Co bimetallic gradient-doped ZnCo-Fe₃O₄ core-shell nanocrystals (CSNCs) were synthesised by high-temperature thermal decomposition, and magnetic gelatin microspheres with adjustable sizes (20-200 µm) were prepared by microfluidic technique. The structure and magneto-thermal properties of the materials were characterised by transmission electron microscopy (TEM), X-ray diffraction (XRD), and vibrating sample magnetometer (VSM); the magneto-thermal response, ion-release properties, anti-tumour effect, and immunomodulatory mechanism of the microspheres were evaluated using in vitro cellular experiments (HSP expression, mitochondrial membrane potential, and pyroptosis pathway) and the H22-loaded mice and rabbit VX2 hepatocarcinoma models; and the arterial embolism assays (rabbit ear/renal artery) and PET-CT imaging to verify its clinical translational potential.

Results ZnCo-Fe₃O₄ CSNCs exhibited excellent magnetothermal properties ($M_s = 92.3$ emu/g, SAR = 412 W/g) with 4 mg/mL microspheres for 300 s up to 86.9°C. Zn²⁺/Fe²⁺ synergistic mild hyperthermia (42°C) was shown to be effective through inhibition of HSP70/HSP90 (52.1%/42% reduction in expression), inducing mitochondrial membrane potential collapse (63% decrease in $\Delta\Psi_m$) and activating GSDMD-mediated pyroptosis (85% release of LDH), significantly killing tumour cells (21.0% survival). In vivo experiments showed that AMF-driven microsphere treatment inhibited H22 tumour growth (>80% volume reduction) and promoted dendritic cell maturation (3.8-fold increase in CD8⁺ T-cell infiltration) and M1 macrophage polarisation (64% reduction in MDSC) through the release of DAMPs (150% increase in ATP release and a decrease in HMGB1) and reversal of the immunosuppressive microenvironment. Combined anti-PD-1 therapy resulted in 60% primary tumour elimination and inhibited distal tumour growth. Arterial embolisation experiments confirmed that microspheres can precisely block the tumour blood supply, and in the rabbit VX2 hepatocellular carcinoma model, the efficacy of magnetothermal embolisation (MTA) was significantly better than that of conventional microwave ablation (PET-CT showed a 78% decrease in tumour metabolic activity).

Conclusion In this study, a novel interventional magnetothermal immunotherapy microsphere system was successfully constructed, which breaks through the functional limitations of traditional TACE microspheres and achieves the synergistic effect of 'embolisation-magnetothermia-immunomodulation'. It induces focal death and reshapes the immune microenvironment through magnetic heat-triggered ion release, and enhances the systemic anti-tumour response by combining with immune checkpoint inhibitors, which provides an innovative strategy for interventional therapy of hepatocellular carcinoma.

PO-122

Endovascular embolisation for life-threatening malignant hemoptysis

Stephanie Woo, Lik Fai Cheng, Fung Him Ng, Sun Yu Lam, Ka Hon, Stephen Wong, Ka Fai, Johnny Ma
Princess Margaret Hospital

Purpose Advanced lung tumors often invade into the airways and can bleed profusely, causing life threatening situations including significant airway obstruction, significant abnormal gas exchange, or hemodynamic instability.

Traditionally, different bronchoscopic techniques are used to control pulmonary hemorrhage and eventually surgery may be needed.

Bronchial artery embolization (BAE) has a well-established role in benign causes of hemoptysis such as bronchiectasis¹.

Malignancy-related hemoptysis from primary or metastatic lung cancer has received less attention comparatively.

Little published regarding BAE specifically for malignancy-related hemoptysis^{2,3}

Aim of this study is to evaluate the safety and efficacy in endovascular embolization for the treatment of life-threatening hemoptysis in patients with lung tumours.

Materials and methods Endovascular embolization done for malignant hemoptysis from 2013 to 2023 in a single centre were retrospectively examined.

The data on baseline characteristics, procedural and clinical outcomes was collected and analysed.

Results A total of six patients with lung malignancy underwent embolization for hemoptysis. All of the cases (100%) were male patients, with a mean age of 74 (range, 51-86). All of the cases had primary lung malignancies, 83% (4/6) of them had a histological diagnosis while 17% (1/6) had only radiological diagnosis. Technical success, defined as the ability to selectively embolize the abnormal vessel, was achieved in all cases. • Clinical success rate³, defined as resolved hemoptysis without recurrence within 30 days, was 83% (5/6). None of them required re-intervention. Different embolic agents were used, as shown in chart. Single vessel embolization was performed in 83% (5/6) of cases, while multi-vessel embolization were performed in 17% (1/6) cases. No complications were recorded. Mean follow-up period was 4.3 months (range, 2-9 months). None of the patient had clinically significant re-bleeding events within 6 months.

Conclusion In our experience endovascular embolization can be considered as an effective and safe technique for the treatment of malignant hemoptysis. Further prospective studies with a larger number of patients are necessary.

PO-123

Photo-responsive self-expanding catheter with photosensitizer-integrated silicone-covered membrane for minimally invasive local therapy in malignant esophageal cancer

Jung-Hoon Park, Seung Jin Eo, Dae Sung Ryu, Do Hoon Kim
Asan Medical Center

Purpose Photodynamic therapy (PDT) using photosensitizer (PS)-integrated covered self-expandable metallic stents (SEMS) is newly suggested as a new therapeutic approach for the treatment of palliative malignancies. However, the current hydrophobic PS reduces the photoreactive effect, which leads to aggregation due to low water solubility. Thus, this study aimed to investigate the efficacy and safety of PDT using hydrophilic PS (aluminum (III) phthalocyanine chloride tetrasulfonic acid; Al-PcS4)-integrated silicone-covered self-expanding catheter in a rabbit esophagus model.

Materials and methods The photodynamic activity of the Al-PcS4-integrated silicone membrane was evaluated through laser exposure on membrane-layered tumor cell lines and tumor xenograft-bearing mice. Localized PDT using the Al-PcS4-integrated silicone-covered self-expanding catheter was conducted in a rabbit esophagus model. Follow-up endoscopy and esophagography were performed before and immediately after the PDT procedure and before sacrifice at 1, 7, 14, and 28 days following the procedure. Histological analysis was performed to evaluate the thickness of the epithelial and submucosal layer, degree of inflammatory cell infiltration, collagen, terminal deoxynucleotidyl transferase-mediated dUTP nick and labeling (TUNEL)-, caspase-3-, heat shock protein (HSP70)-, and fibroblast growth factor receptor 1 (FGFR1)-positive deposition.

Results PDT with the Al-PcS4-integrated membrane successfully generated sufficient cytotoxic singlet oxygen, inducing cell death in the esophageal cancer cell lines. PDT-treated tumor xenograft-bearing mice undergo apoptotic cell death and showed significant tumor regression. Localized PDT using an Al-PcS4-integrated silicone-covered self-expanding catheter was technically successful in the rabbit esophagus without procedure-related complications. Based on the endoscopy, esophagography, histology, and immunohistochemistry, our study verified that localized PDT using the Al-PcS4-integrated silicone-covered self-expanding catheter safely induced apoptotic cell death evenly.

Conclusion Al-PcS4-integrated silicone-covered self-expanding catheter has substantial potential for minimally invasive local therapy in malignant esophageal cancer. Further, it may represent a promising approach for treating endoluminal malignancies in non-vascular organs.

PO-124

Risk Factors and Risk Prediction Model for Early Cardiovascular Events After Microwave Ablation for Lung Cancer

Nan Wang,Xin Ye

Shandong University of Traditional Chinese Medicine, Shandong Provincial Qianfoshan Hospital

Purpose Objective: This study aims to identify and predict risk factors for cardiovascular events in lung cancer patients following microwave ablation (MWA) and to construct a risk prediction model to provide personalized guidance for clinical treatment.

Materials and methods Methods: A retrospective analysis was conducted on 131 patients with primary lung cancer who underwent CT-guided percutaneous MWA at Q Hospital between May 2020 and December 2023. Among them, 30 patients experienced cardiovascular events postoperatively, while 101 did not. Univariate analysis and multivariate logistic regression models were used to screen for risk factors, and ROC curves were employed to evaluate the accuracy and discriminative ability of the prediction model.

Results Results: Multivariate analysis revealed that a history of coronary heart disease (HR = 4.263, $p = 0.024$), preoperative use of anticoagulants (HR = 4.409, $p = 0.022$), and intraoperative use of hemostatic drugs (HR = 9.377, $p = 0.014$) were significant independent risk factors for cardiovascular events. The established prediction model had an overall accuracy of 86.26% and demonstrated good discriminative ability in external validation (AUC = 0.797, 95% CI: 0.692-0.901), showing high sensitivity and specificity, indicating promising clinical application prospects.

Conclusion Conclusion: A history of coronary heart disease, preoperative use of anticoagulants, and intraoperative use of hemostatic drugs are independent risk factors for new-onset cardiovascular events in lung cancer patients after MWA. The constructed prediction model can provide strong support for preoperative assessment and personalized management, thereby reducing the risk of perioperative cardiovascular complications in lung cancer patients undergoing MWA.

PO-125

Enhanced Management Strategy of synchronous Percutaneous Biopsy and Microwave Ablation in Patients with Lung Ground-Glass Opacities Undergoing Antithrombotic Treatment: A Clinical Perspective on Our Experience

Nan Wang, Xin Ye

Shandong University of Traditional Chinese Medicine, Shandong Provincial Qianfoshan Hospital

Purpose This retrospective study was conducted to delineate our experience in managing perioperative antithrombotic agents in patients receiving antithrombotic therapy underwent percutaneous biopsy and microwave ablation (B+MWA) for lung ground-glass opacities (GGOs).

Materials and methods The study comprised 67 patients with GGOs who receiving antithrombotic therapy underwent B+MWA sessions from January 1, 2020, to May 31, 2022. During the perioperative period, patients who received rivaroxaban as a bridging drug were assigned to Group A, and who interrupted the antithrombotic therapy were assigned to Group B. Information about the technical success rate, positive biopsy rate, local control rates, and major bleeding and thrombotic complications were collected and analyzed.

Results Group A comprised 36 patients (19 males; mean age, 67.97 ± 8.49 years), while Group B comprised 31 patients (12 males; mean age, 65.48 ± 4.32 years). The technical success rate was 100%. The positive biopsy rates were 94.44% and 96.77%, respectively. In group A and B, the overall local control rates at 6, 18, and 24 months were 100.0% vs. 100.0%, 94.44% (34/36) vs. 96.77% (30/31), and 86.11% (31/36) vs. 87.10% (27/31), with no significant difference between the two groups ($p = 0.2156$). During the perioperative period, a single case of lower extremity venous thrombosis was identified in Group A, while three cases of lower extremity venous thrombosis, one case of new-onset cerebral infarction, and one case of new-onset pulmonary embolism were identified in Group B, with no statistically significant difference in the overall incidence of bleeding and thrombotic complications between the two groups.

Conclusion In conclusion, for patients with pulmonary GGOs who are on antithrombotic therapy, the use of oral rivaroxaban as a bridging strategy during perioperative period for simultaneous CT-guided percutaneous B+MWA is both safe and effective. This approach can lower the incidence of severe thrombotic complications during the perioperative period, compared to the abrupt discontinuation of antithrombotic therapy during this time.

Anti-inflammatory coupled anti-angiogenic airway stent effectively suppresses tracheal in-stents restenosis

Yanan Zhao, Yiming Liu, Jiheng Shan, Chengzhi Zhang, Kewei Ren, Dechao Jiao, Jianzhuang Ren, Yong Jiang, Xinwei Han
First Affiliated Hospital of Zhengzhou University

Purpose Excessive vascularization during tracheal in-stent restenosis (TISR) is a significant but frequently overlooked issue. We developed an anti-inflammatory coupled anti-angiogenic airway stent (PAGL) incorporating erlotinib and silver nanoparticles using advanced electrospinning technology.

Materials and methods The physicochemical characteristics of the stent were assessed using transmission electron microscopy, Fourier-transform infrared spectroscopy, scanning electron microscopy, water contact angle measurements, and drug release profiling. The antibacterial efficacy was evaluated through live/dead bacterial staining and plate colony counting. The anti-angiogenic and anti-proliferative effects were examined via CCK-8 assays, cell migration assays, cell cycle, and live/dead cell staining. Finally, the in vivo performance of the stent was evaluated using computed tomography scans, immunohistochemical staining, and reverse transcription polymerase chain reaction.

Results PAGL exhibited hydrophobic surface properties, exceptional mechanical strength, and appropriate drug-release kinetics. Moreover, it demonstrated a remarkable eradication effect against methicillin-resistant *Staphylococcus aureus*. It also displayed anti-proliferative and anti-angiogenic properties on human umbilical vein endothelial cells and lung fibroblasts. PAGL was implanted into the tracheae of New Zealand rabbits to evaluate its potential for inhibiting bacterial infection, suppressing the inflammatory response, reducing angiogenesis, and attenuating excessive fibroblast activation. RNA sequencing analysis revealed a significant downregulation of genes associated with fibrosis, intimal hyperplasia, and cell migration following PAGL treatment.

Conclusion This study provides insight into the development of airway stents that target angiogenesis and inflammation to address problems associated with TISR effectively and have the potential for clinical translation.

PO-127

Pre-operative loco-regional staging of colo-rectal carcinoma by using contrast enhanced computed tomography correlation with histopathology

Yussra Khattri
Liaquat national hospital

Purpose : To determine the correlation of contrast enhanced computed tomography in TNM staging system of colo-rectal carcinoma with histopathology in preoperative patients for establishing the treatment and predicting the prognosis.

Materials and methods Total 50 patients were included in our study. All patients were underwent the contrast enhanced multi-detector CT scan with rectal contrast, Colonoscopy, biopsy and histopathology. All patients were also underwent the CT chest and bone scan turn out to be negative for distant metastasis that is stage IV disease. Data was retrospectively reached through the electronical medical record. We have evaluate the accuracy of Multi-detector CT scan in comparison with histopathology.

Results Total number of 50 patients were included with age range from 01-85 years. Mean age of patient was 51.54 years. Majority of patients 18 (36%) were between 46-60 years of age. Out of these 50 patients, 32 (64%) were male and 18 (36%) were female. On conclusion 39 (78%) were diagnosed as same stage on multi-detector CT scan in association with histopathology and 11 (22%) were not corresponding to the stage of colorectal carcinoma on histopathology.

Conclusion Multi-detector CT scan with rectal oral and IV contrast has good accuracy in diagnosis of colorectal carcinoma beyond the bowel wall with loco regional extension. It has good accuracy in diagnosis of T3 and T4 that is stage II and III, however low accuracy to evaluate the T1 and T2 that is Stage I.

PO-128

Clinical Efficacy of HAIC Combined with TACE in Patients with Unresectable Intrahepatic Cholangiocarcinoma

Juncheng Wan, Chaoqiao Jin, Caihong Yu, Zihan Zhang, Changyu Li, Zhuoyang Fan, Yongjie Zhou, Wei Zhang, Xudong Qu
Zhongshan Hospital Fudan University

Purpose To evaluate the efficacy and safety of combined treatment based on hepatic arterial infusion chemotherapy (HAIC) and transarterial chemoembolization (TACE) in the treatment of unresectable intrahepatic cholangiocarcinoma (ICC).

Materials and methods A total of 82 patients with unresectable ICC were retrospectively included in this study. Of these, 40 patients received HAIC combined with TACE treatment (HAIC+TACE group) and 42 received intravenous chemotherapy (Chemo group). Propensity score matching (PSM) was performed to reduce selection bias between the HAIC+TACE group and the Chemo groups. Efficacy was evaluated using the modified Response Evaluation Criteria in Solid Tumors (mRECIST) 1.1. Differences in tumor response, progression-free survival (PFS), overall survival (OS), and adverse events were compared between the two groups.

Results The HAIC+TACE group had a higher disease control rate (97.5% vs. 81.0%, $P = 0.030$) compared to the Chemo group. The objective response rate was similar between the groups (65.0% vs. 64.3%). The median OS was 14.00 months (95% CI 9.11-18.89) in the HAIC+TACE group and 12.70 months (95% CI 10.53-14.87) in the Chemo group. The PFS in the HAIC+TACE group was significantly longer in the Chemo group (8.40 months vs. 6.50 months, $P = 0.036$). No significant difference in adverse events was observed between the two groups.

Conclusion HAIC combined with TACE demonstrates a higher DCR and PFS in the treatment of unresectable ICC, with manageable adverse reactions. Although no significant difference in OS was observed, HAIC combined with TACE may serve as an effective treatment option to improve disease control and delay disease progression when compared to standard chemotherapy.

PO-129

Contrast Enhanced T1WI-Based peritumoral Radiomics for Predicting the therapeutic effect of advanced hepatocellular carcinoma after transcatheter arterial chemoembolization

Diwen Zhu, Han Yang, Weixin Ren

The First Affiliated Hospital of Xinjiang Medical University

Purpose To evaluate and predict the feasibility and value of peritumoral radiomics model based on T1-enhanced imaging in predicting the therapeutic effect in patients with advanced hepatocellular carcinoma after TACE.

Materials and methods One hundred and nine patients with advanced HCC who underwent TACE were retrospectively analyzed. And randomly divided into a training dataset (n=85) and a validation dataset (n=24) at the ratio of 8:2. Using 3D-Slicer software in axial T1WI enhanced arterial-phase sequences to manually outline areas of interest in the larger three dimensions of the lesion, and then isometric outreach of 5mm and 10mm to generate purely peritumoural regions of interest (ROI). A total of 107 texture features were extracted from each peri-tumour ROI respectively. Univariate analysis, correlation analysis and least absolute shrinkage and selection operator (LASSO) algorithm were employed for feature selection, and the prediction model was finally constructed based on peritumour alone, clinical combined peritumour. Receiver operating characteristic curve analysis was performed to evaluate the performance of the model.

Results Compared with the response group, in the TACE-Refractoriness group the percentage of Child-Pugh grade B (OR=1.58, 95%CI 1.18~2.41, $P<0.01$), tumor number [$n\geq 3$, (OR=2.32, 95%CI 1.59~2.39, $P<0.01$)] and the ALP ≥ 200 U/L (OR=1.32, 95%CI 1.17~2.25, $P<0.01$) was remarkably elevated, were the independent risk factors for tumor non-response. The clinical combined peri-tumour 5mm imaging model had the best predictive efficacy, with an AUC of 0.835 (95%CI 0.791-0.927) in the training group, and an AUC of 0.801 (95%CI 0.725-0.885) in the validation group.

Conclusion The radiomics model based on clinical combined peri-tumour 5mm imaging can effectively evaluate and predict the characteristics of early curative effect after TACE of advanced hepatocellular carcinoma.

PO-130

Study on the predictive effect of sarcopenia on the efficacy of bronchial artery chemoembolization in lung cancer patients

Jianfei Tu, Jinying Wu

The Fifth Affiliated Hospital of Wenzhou Medical University

Purpose The aim of this study was to investigate the value of sarcopenia in predicting the outcome of lung cancer patients treated with bronchial artery chemoembolization (BACE).

Materials and methods There 160 lung cancer patients who received BACE treatment in Lishui Central Hospital between December 2012 to August 2021, and applied CT to measure and calculate skeletal muscle index (SMI) at the fourth thoracic vertebral level, and divided the patients into Sarcopenia group and non-sarcopenia group according to the lower quartile of the gender-specific group. Differences in overall survival and progression-free survival between the two groups after BACE were analyzed by Kaplan-Meier analysis, and risk factors affecting overall survival and progression-free survival were determined using COX regression analysis.

Results The median progression-free survival was 5.6 months and 3.0 months in the non-sarcopenia group and the Sarcopenia group, respectively, and the 14-month progression-free survival rate was 16.7% and 5%, respectively. There was a significant difference in progression-free survival between the two groups ($\chi^2=5.141$, $P=0.023$). The COX regression analysis showed that sarcopenic disorder was an independent risk factor for progression-free survival after BACE in lung cancer patients.

Conclusion Sarcopenia is an independent risk factor affecting the efficacy of BACE in lung cancer patients, and can be used as a predictor of the efficacy of BACE.

PO-131

Drug-eluting transarterial chemoembolization combined with anlotinib for non-small cell lung cancer in the elderly: a multicenter retrospective study

Jianfei Tu, Linqiang Lai, Dengke Zhang, Yonghui Wang, Jie Chen
The Fifth Affiliated Hospital of Wenzhou Medical University

Purpose To investigate the safety and effectiveness of drug-eluting transarterial chemoembolization combined with anlotinib of non-small cell lung cancer in the elderly.

Materials and methods Patients with at least 75 years old, refusal or unresectable, driver gene-negative, refusal or inability to tolerate radiotherapy, chemotherapy and immunotherapy, non-small cell lung cancer, were enrolled in this retrospective, multicenter study. (January 2018–December 2023). DE-TACE consisted cisplatin (75 mg/m²) and gemcitabine (600 mg/m²) via feeding arteries and then embolization using drug-eluting beads carrying gemcitabine (400 mg). Anlotinib was administered at a 12 mg/day dose for two consecutive weeks, with a one-week cessation period in-between, forming a single 21-day treatment cycle. The primary objectives were overall survival (OS) and safety. Overall survival (OS) was analyzed using multivariate COX proportional hazards regression, as well as Kaplan-Meier analysis.

Results The final analysis included 90 patients (median age, 80 years, 74 men). The technical success rate of intratumoral drug delivery was 100%. The median OS was 25.6 months (95% CI 21.1-29.7) and the median PFS was 8.6 months (95% CI 7.8-9.3). In multivariate Cox regression analysis, DE-TACE combined with anlotinib was associated with lower risk of death (HR 1.94, 95% CI 1.04-3.61; log rank test P = 0.037) and lower risk of disease progression (HR 1.87, 95% CI 1.07-3.25; log rank test P = 0.028). Grade 3 or higher treatment-emergent adverse events was 2.2% (2/90). Procedure-related complications included post-embolization syndrome (27.8%; 25/90), chest pain (15.6%; 14/90), access site complication (3.3%; 3/90). No spinal cord injury and cerebral embolism was observed.

Conclusion DE-TACE combined with anlotinib was a technically successful and effective treatment for non-small cell lung cancer in the elderly, with no severe adverse events.

PO-133

The efficacy and safety of transarterial chemoembolization combined with the different assembly of first-line targeted therapy and immunotherapy for intermediate and advanced hepatocellular carcinoma : a single-center retrospective study

Hao Yang,Xiaoli Zhu

The First Affiliated Hospital of Soochow University

Purpose To investigate the efficacy and safety of transarterial chemoembolization (TACE) combined with the first-line targeted therapy and immunotherapy for intermediate and advanced hepatocellular carcinoma(HCC).

Materials and methods The clinical data of a total of 82 patients with intermediate and advanced HCC, who were admitted to the First Affiliated Hospital of Soochow University between July 2019 and March 2024, were retrospectively analyzed. The patients were divided into TACE+D+D group(n=47, receiving TACE combined with sintilimab and bevacizumab), TACE+A+T group(n=13, receiving TACE combined with atezolizumab and bevacizumab) and TACE+A+A group(n=19, receiving TACE combined with camrelizumab and apatinib). Survival curves were drawn by Kaplan-Meier method, the median overall survival (mOS)and median progression-free survival (mPFS) were compared between the three groups. According to mRECIST criterion, the objective response rate (ORR) and disease control rate (DCR) were compared between each of the three groups. The occurrences of adverse events in the three groups were recorded. Following up was completed on August 31, 2024.

Results As far as the review of data from our center is concerned, the mOS and mPFS of the TACE+D+D group, the TACE+A+T group and TACE+A+A group were 19.5 months, not reached, 26.1 months, and 12.2 months, 11.3 months, and 11.1 months, respectively, with no statistically significant difference ($P>0.05$). The ORR and the DCR were 63.8%, 76.9%, 89.5%, and 95.7%, 92.3%, 94.7%, respectively, with no statistically significant difference ($P>0.05$). No statistically significant difference in the incidence of severe adverse events existed between the three groups ($P=0.403$). TACE combined with first-line systemic therapy has prolonged the mPFS of intermediate and advanced hepatocellular carcinoma to 11.1 months. Among the three regimens, the TACE+A+T group or the TACE+D+D group was superior in controlling the disease (12.2 months vs. 11.3 months vs. 11.1 months), but the data did not show a statistically significant difference in terms of the median PFS ($P=0.928$). On the one hand, this may be due to the small sample size, and on the other hand the inherently progression-prone nature of intermediate and advanced HCC. The average enrollment time of the TACE+A+A group patients was two years earlier than that of the TACE+T+A group and the TACE+D+D group patients, which may have contributed to the longer OS of the camrelizumab-apatinib regimen.

Conclusion From our initial study, TACE combined with the different assembly of the first-line targeted therapy and immunotherapy had marked efficacy and controllable adverse events in the treatment of intermediate and advanced HCC, which provides a potential new option for treatment of intermediate and advanced HCC. More real-world studies with larger samples will be conducted in the future to confirm the advantages and disadvantages of regimens, thus bringing better and more objective choices to patients.

PO-134

Efficacy of Compound Pholcodine Syrup and Compound Codeine Phosphate Oral Solution on lung cancer cough

Mengting Chen

Chongqing University Cancer Hospital, Nanyang Technological University

Purpose To assess the therapeutic effect of compound pholcodine syrup and compound codeine phosphate oral solution on lung cancer cough.

Materials and methods A total of 60 patients from department of geriatric oncology, Chongqing University Cancer Hospital with diagnosed middle-advanced stage lung cancer accompanied with lung cancer cough from Jan, 2022 to May, 2022 were enrolled and investigated with prospective study. According to the method of random number table, the patients were divided into two groups: observation group and control group. Observation group [n=30, 21 male and 9 female, age 62.3 ± 10.4 years] received compound pholcodine syrup treatment, while control group [n=30, 21 male and 9 female, age 62.0 ± 8.1 years] received compound codeine phosphate oral solution treatment. The dosage of the two drugs was 15 ml each time, 3 times a day, and the treatment course was 5 days. The antitussive effectiveness, cough severity and quality of life [Leicester Cough Questionnaire in Mandarin-Chinese scale], were observed and compared between the two groups before and after the 3 days and 5 days treatment, respectively.

Results All 60 patients completed the treatment. Both two groups were effective in controlling lung cancer cough. After the 3 days treatment, the antitussive effective rates of the observation group and the control group were 83.3% (25/30) and 73.3% (22/30), respectively, with no statistical significance ($P=0.347$). After the 5 days treatment, the antitussive effective rates of observation group and control group were 90.0% (27/30) and 86.6% (26/30), respectively, with no statistical significance ($P=0.687$). There was no significant difference in the composition of patient cough severity between observation group [moderate and severe cough, 56.7% (17/30)] and control group [moderate and severe cough, 67.7% (20/30)]. After 3 days treatment, cough symptoms were relieved in both groups. Patients with mild cough accounted for 73.3% (22/30) in the observation group and 56.7% (17/30) in the control group, the difference was not statistically significant ($P=0.331$). What's more, after 5 days treatment, there was also no significant difference ($P=0.067$) between observation group [mild cough, 86.7% (26/30)] and control group [mild cough, 66.7% (20/30)]. In the meantime, there were no significant differences in the physiological score, psychological score, social score and total score of the Leicester Cough Questionnaire in Mandarin-Chinese scale before the treatment, after 3 days and 5 days treatment between the two groups (all $P > 0.05$). Patients in the observation group had a lower incidence of xerostomia (0.0% vs 20.0%, $P=0.024$) and constipation (0.0% vs 20.0%, $P=0.024$) than control group.

Conclusion Compound pholcodine syrup and compound codeine phosphate oral solution are effective in treating lung cancer cough with similar antitussive effectiveness. Compound pholcodine syrup has a lower incidence of xerostomia and constipation than control group, which indicates that the security may be better.

PO-135

Berberine's Role in Modulating Gut Microbiota and Endocannabinoid System in Colitis-Associated Colorectal Cancer

Mengting Chen

Chongqing University Cancer Hospital, Nanyang Technological University

Purpose This study aimed to investigate the effects of BRR on gut microbiota and the ECS in a mouse model of colitis-associated CRC.

Materials and methods The CRC model in mice was induced by azoxymethane (AOM) and dextran sulfate sodium (DSS). Berberine was administered daily at doses of 50 and 100 mg/kg. The effect of berberine on colitis-associated colorectal tumorigenesis was assessed by general imaging, tumor counting, and H&E staining. Intestinal flora changes were detected by 16S rDNA sequencing technology. Additionally, interventions involving the CB2 antagonist (AM630) and GPR55 agonist (O-1602) were performed to examine the influence of the ECS on CRC, particularly in relation to the modulation of the gut barrier and intestinal inflammatory responses. Furthermore, a cocktail of antibiotics was employed to investigate the role of intestinal microbiota in mediating the inhibitory effects of BBR on inflammatory cancer transformation.

Results BRR significantly inhibited tumor development. This was demonstrated by a dose-dependent increase in body weight and a notable decrease in both the number and size of tumors. Histopathological examinations showed a reduction in aberrant crypt foci and inflammation. Additionally, BRR treatment led to lower levels of pro-inflammatory cytokines, including TNF- α , IL-1 β , and IL-6, while increasing the levels of the anti-inflammatory cytokine IL-10, indicating a modulation of immune responses. Importantly, BRR altered gut microbial communities by promoting beneficial bacteria such as *Akkermansia muciniphila*, *Bacteroides*, *Lachnospirillum*, *Blautia*, and *Prevotellaceae_UCG-001*, while reducing harmful species. We also observed improvements in intestinal barrier integrity, characterized by decreased permeability and lower levels of plasma lipopolysaccharides. Furthermore, BRR restored the expression of cannabinoid receptors CB2 and GPR55, suggesting that the ECS plays a role in mediating its effects.

Conclusion In summary, BRR shows significant promise in alleviating colitis-associated CRC through various mechanisms, including the modulation of gut microbiota, regulation of immune responses, and enhancement of intestinal barrier function. Future studies should aim to validate these findings clinically and further explore the efficacy of BRR in the prevention and treatment of CRC.

PO-136

Multi-Center Randomized Controlled Trial of Integrated Early Palliative Care for Non-Small-Cell Lung Cancer Patients in Southwest China: Evaluating Impact and Efficacy

Mengting Chen

Chongqing University Cancer Hospital, Nanyang Technological University

Purpose Effective interventions to improve prognosis in non-small-cell lung cancer (NSCLC) are urgently needed. We assessed the effect of the early integration of interdisciplinary palliative care (based on Ewarm model) for patients with NSCLC on the quality of life (QoL), psychological state, cancer pain and nutritional status.

Materials and methods In this multi-centric randomised controlled trial, 332 newly diagnosed NSCLC patients were enrolled and randomly assigned (1:1) to the combined early palliative care (CEPC) group integrated with standard oncologic care or standard oncological care (SC) group. QoL and psychological state were assessed at baseline and at 24 weeks by Functional Assessment of Cancer Therapy-Lung (FACT-L) scale, the Hospital Anxiety and Depression Scale (HADS) and Patient Health Questionnaire-9 (PHQ-9), respectively. Cancer nutritional and pain status were assessed with the use of the Patient-Generated Subjective Global Assessment (PG-SGA) and Numerical Rating Scale (NRS), respectively. The primary end point was overall survival (OS). The second end point was the change in the quality of life, psychological state, pain and nutritional status at 24 weeks. Analysis was by intention to treat.

Results 332 patients were enrolled: 166 in CEPC group (120 completed) and 166 in the SC group (97 completed). CEPC group had a better QoL than SC group (all $P < 0.05$). In addition, fewer patients in the CEPC group than in the SC group had depressive ($P < 0.05$) symptoms. Furthermore, patients in CEPC group had a better nutritional status and pain than SC group ($P = 0.007$ and $P = 0.003$). Patients in the CEPC group had significantly longer survival than those in the SC group (median OS, 24.6 vs. 20.4 months; $P = 0.042$) (HR, 0.19; 95% CI, 0.04 to 0.85; $P = 0.029$).

Conclusion Among patients with non-small-cell lung cancer, early palliative care led to significant improvements in longer survival, quality of life, psychological state, pain and nutritional status.

PO-138

Knowledge, attitudes, and Current practices toward lung cancer palliative care management in China: a national survey

Mengting Chen

Chongqing University Cancer Hospital, Nanyang Technological University

Purpose To demonstrate the status and differences in knowledge, attitudes, and practices (KAP) of lung cancer palliative care (LCPC) management, and to measure patient controlled analgesia (PCA) in cancer pain management in of China.

Materials and methods A questionnaire on LCPC management was used in this study, which involved a total of 2093 participants from 706 hospitals in China. Seven major components make up the questionnaire, including chi-square tests or Fisher exact probabilities to measure the differences in KAP between hospitals grades. Comparing distributions of ordered data between groups was done using the Kruskal-Wallis H test or the Mann-Whitney U test. Multiple choice questions use multiple response cross analysis. Correlation was evaluated by the Spearman correlation coefficient.

Results 84.2% participants believed that anti-tumor therapy is equally important as palliative care. The satisfaction rate of participants from grade 3 hospitals, which was significantly higher than that of grade 2 and grade 1 hospitals ($\chi^2=27.402$, $P=0.002$). The most common symptoms requiring LCPC was pain. The major barriers toward to LCPC were "Patients and families are concerned about the safety of long-term use of palliative care related drugs". The most common reasons for the use of PCA treatment were 31.1% participants thought "Patients with systemic application of large doses of opioids or adverse reactions to opioids that cannot be tolerated". The top three barriers toward PCA treatment of cancer pain were (i) worry about adverse reactions of drug overdose, (ii) worry about opioid addiction, and (iii) increase of patients' economic burden. In the past 24 months, 33.9% of the participants had not participated in online or offline training related to palliative care of lung cancer.

Conclusion Chinese healthcare workers are in need of training for lung cancer palliative care and, in particular, for controlling cancer pain symptoms.

PO-139

Establishment of an Extracapsular Chicken Embryo Chorioallantoic Membrane Hepatocellular Carcinoma Model and Magnetic Resonance Imaging Study

Xiaoshu Zhu, Weili Peng
Zhejiang Provincial People's Hospital

Purpose This study aims to explore the establishment of a hepatocellular carcinoma (HCC) model on the chorioallantoic membrane (CAM) outside the eggshell and conduct in - vivo magnetic resonance imaging (MRI) observations.

Materials and methods Thirty fertilized chicken eggs were selected. The chicken embryos were transferred to a self - made container for extracapsular culture at 3 days of age. On the 7th day, HEPG2 cells were implanted onto the CAM. The growth of the transplanted tumor was observed, and the maximum diameter of the tumor was measured by daily photography. Eight chicken embryos were randomly selected on the 3rd, 5th, 7th, and 9th days after transplantation for multi - sequence MRI. The size of the lesions, apparent diffusion coefficient (ADC) values, and T1 mapping values at different time points were analyzed. Western blot (WB) was used to analyze the expression levels of the biomarker epidermal growth factor receptor (EGFR) in HEPG2 cells and HEPG2 - HCC - CAM tumor tissues respectively.

Results Among the 30 fertilized chicken embryos, 2 died on the second day of model establishment, and 1 died on the fifth day due to yolk rupture. The remaining 27 survived. Tumor specimens were obtained after MRI examination and sacrifice on the 3rd (7 embryos), 5th (7 embryos), 7th (7 embryos), and 9th (6 embryos) days. The success rate of model establishment was 90%. On the 9th day, the tumor volumes measured by in - vivo MRI and tumor specimens were (28.67 ± 18.63) and (28.78 ± 18.09) respectively ($P < 0.05$), and there was no significant difference between the two measurement methods. The ADC values of tumor tissues and peritumoral tissues were (1.254 ± 0.131) and (0.633 ± 0.265) respectively ($P < 0.05$). The T1 mapping values were (3345.517 ± 92.011) and (2474.318 ± 935.582) respectively ($P < 0.05$). Immunohistochemistry (IHC) and WB assays demonstrated that HEPG2 - HCC - CAM tumor tissues retained the biomarker characteristics of HEPG2 cells.

Conclusion The HEPG2 - HCC - CAM model can be established in a self - made container outside the eggshell. The tumor tissues can retain the biomarker characteristics of HEPG2 cells. Conventional MRI can dynamically observe the growth of tumors in vivo, and functional MRI can quantitatively analyze tumors with multiple parameters.

PO-140

Development and Validation of an Ultrasound Radiomics-Based Prognostic Model for Predicting Short-Term Outcomes After Transcatheter Arterial Chemoembolization in Hepatocellular Carcinoma

Xushuang Qin, Weili Peng, Jiajia Zheng, Jiaqi Zhang, Houhui Shi, Jun Chen, Yang Liu
Hangzhou Normal University

Purpose To investigate the feasibility of constructing a prognostic model based on ultrasound radiomics for predicting short-term treatment responses in patients with hepatocellular carcinoma (HCC) undergoing transarterial chemoembolization (TACE).

Materials and methods This retrospective study included 135 HCC patients (112 males, 23 females; age 44–83 years, mean \pm SD 58 ± 10) who underwent TACE at Zhejiang Provincial People's Hospital between June 2018 and July 2023. All patients were histologically confirmed with HCC and underwent preoperative and postoperative ultrasound imaging. Based on mRECIST criteria, patients were classified into effective (complete remission + partial remission) and ineffective groups (stable disease + progressive disease). Patients were randomly divided into training ($n=95$) and validation sets ($n=40$). Clinical parameters were compared using χ^2 -test and independent t-test. Ultrasound radiomics features were extracted using AK software (Volume of Interest, VOI segmentation) from preoperative images. Texture parameters were analyzed using R language, and LASSO regression combined with 10-fold cross-validation was applied to select significant features. A logistic regression model incorporating selected radiomic features was constructed to predict treatment response. Model performance was evaluated using ROC analysis (AUC), sensitivity, specificity, and calibration curves.

Results In the training set ($n=95$), 52 patients were effective and 43 were ineffective. In the validation set ($n=40$), 21 were effective and 19 were ineffective. No significant differences were observed between groups in baseline characteristics. A total of 396 texture features were extracted from each ultrasound image, and LASSO regression identified four key features: ClusterProminence_angle135_offset4, Correlation_angle135_offset4, Inertia_angle135_offset4, and InverseDifferenceMoment_angle45_offset4. The radiomics model achieved an AUC of 0.87 (95% CI: 0.722–0.901) with sensitivity 0.83 and specificity 0.69 in the training set, and an AUC of 0.80 (95% CI: 0.65–0.95) with sensitivity 0.89 and specificity 0.63 in the validation set. Calibration curves confirmed good model fit.

Conclusion This study demonstrates that ultrasound-based radiomics can effectively predict short-term outcomes after TACE in HCC patients. The developed model exhibits stable performance and potential clinical utility for optimizing individualized treatment strategies.

PO-142

Transarterial Chemoembolization plus Donafenib and Immune Checkpoint Inhibitors for Intermediate Hepatocellular Carcinoma (CHANCE2410): A Propensity Score Matching Analysis

Bin-Yan Zhong

Department of Interventional Radiology, Zhejiang Cancer Hospital, Hangzhou Institute of Medicine (HIM), Chinese Academy of Sciences, Hangzhou 310022, China

Purpose To compare the efficacy and safety between the combination therapy of transarterial chemoembolization (TACE) plus donafenib and immune checkpoint inhibitors (ICIs) (combination therapy) and TACE monotherapy for intermediate hepatocellular carcinoma (HCC).

Materials and methods This nationwide, multicenter, retrospective cohort study included patients with intermediate HCC receiving either combination therapy or TACE monotherapy between January 2021 and May 2024 in China. The primary outcome was progression-free survival (PFS). The secondary outcomes included overall survival (OS) rate, objective response rate (ORR) and safety. Tumor response was evaluated according to the mRECIST criteria. 1:1 propensity score matching (PSM) analysis was employed to minimize bias. Cox proportional-hazards regression model was used to analyze factors affecting PFS and OS.

Results A total of 364 patients were enrolled, with 192 receiving combination therapy and 172 receiving TACE monotherapy. After PSM, 127 patients from each group were included for analysis.

The median PFS were significantly longer in the combination therapy group than it in the TACE monotherapy group (19.6 months [95% CI, 14.9-24.4] vs. 15.3 months [95% CI, 12.8-17.8], HR 0.647 [95% CI, 0.464-0.903], $p = 0.010$). The OS rate was higher in the combination therapy group (94.8% vs. 83.5%, 1-year OS rate; 76.4% vs. 64.8%, 2-year OS rate; HR 0.542 [95% CI, 0.327-0.989], $p = 0.016$). The ORR was also higher in the combination therapy group (78.9% vs. 62.5%, $p = 0.002$). Grade 3 or 4 adverse events from any cause were observed at a rate of 12.5% and 5.5% in the combination and monotherapy groups, respectively. Multivariate analysis identified combination therapy as an independent prognostic factor for both longer PFS and OS.

Conclusion Compared to TACE monotherapy, TACE plus donafenib and ICIs offers superior PFS and OS, which demonstrates as an alternative for the treatment of intermediate HCC.

Incidence and risk factors exploration for portal vein tumor thrombosis development in patients with hepatocellular carcinoma after transarterial chemotherapy embolization

Wenchang Yu, Weifu Liu, Kongzhi Zhang, Xiaolong Wang
Fujian Cancer Hospital & Fujian Medical University Cancer Hospital

Purpose In clinical practice, transarterial chemoembolization (TACE) is the most widely applied treatment for unresectable hepatocellular carcinoma (HCC). According to previous studies, it is widely used not only for Barcelona Clinic Liver Cancer (BCLC) intermediate-stage HCC but also for selected cases of early-stage. Owing to HCC's complex biological characteristics, most patients experience disease progression in the form of macrovascular invasion or others over time varying from 3.1 to 13.5 months, even after the initial TACE treatment has effectively controlled the disease. Portal vein tumor thrombosis (PVTT), a form of macrovascular invasion, causes hepatic hypofunction, portal hypertension, and ascites, often culminating in disease progression and fatality. Although treatments such as surgical resection, TACE, radioembolization, stereotactic body radiotherapy, and systemic treatment offer the potential for improved survival outcomes, options are limited once PVTT has developed, and overall survival rates remain low. Hence, it is important to identify the risk factors for PVTT events in patients with HCC who have not yet developed PVTT. The early identification of these risk factors is crucial for timely intervention and improved patient outcomes. However, to our knowledge, few studies have focused on exploring the incidence and risk factors for PVTT development in patients with unresectable HCC after TACE treatment. The present study aimed to investigate the incidence and risk factors for PVTT development during longitudinal follow-up imaging in patients with HCC after TACE treatment.

Materials and methods Between March 2013 and July 2023, consecutive patients diagnosed with unresectable HCC who received TACE therapy from our treatment team were included in this retrospective study. This study was conducted in compliance with the ethical guidelines of the Declaration of Helsinki and approved by the institutional review board of our hospital. Written informed consent was obtained from all included patients at the final follow-up. The diagnosis of HCC was confirmed by histopathological or non-invasive criteria, defined by the American Association for the Study of Liver Disease based on specific imaging features. Characteristics considered diagnostic of PVTT include thrombus enhancement in the arterial phase on computed tomography (CT), magnetic resonance imaging (MRI), or ultrasound with contrast; expansion of the portal vein; and a clear relationship between the thrombus and neoplasm[19]. The choice of TACE treatment was determined through a multidisciplinary team discussion. The inclusion criteria were: (1) age ≥ 18 years, (2) patients with unresectable BCLC stage A/B HCC, receiving TACE therapy as initial treatment, (3) patients with Eastern Cooperative Oncology Group (ECOG) performance status 0-2, (4) patients with newly diagnosis or recurrent HCC after previous curative hepatectomy or ablation therapy, (5) Child-Pugh class A or B7, (6) patients with adequate organ function (i.e., white blood cell count $\geq 3.5 \times 10^9 / L$; platelet count $\geq 75 \times 10^9 / L$; aspartate transaminase and alanine transaminase ≤ 5 -time or less of the upper limit of the normal; serum creatinine ≤ 2.0 mg/dL), and (7) patients with at least one measurable lesion in accordance with the modified Response Evaluation Criteria in Solid Tumors (mRECIST). The exclusion criteria were as follows: patients with (1) previous locoregional or systematic treatment; (2) with other malignancies; (3) serious medical comorbidities, including severe dysfunction of the heart or lungs; (4) lack of >3 months of regular follow-up data; and (5) human immunodeficiency virus infection and hematological diseases. All the patients in our study underwent conventional TACE or TACE with drug-eluting beads. Subse

quent TACE procedures were performed “on demand”; if a residual tumor or new intrahepatic lesions were observed, the patient was evaluated for repeated TACE treatment. Tumor response was evaluated as complete response (CR), partial response (PR), stable disease (SD), or progressive disease (PD), based on contrast-enhanced CT or MRI findings according to mRECIST. PVT development was the primary endpoint and PVTT-free survival (PVFS) was defined as the time interval between TACE initiation and PVTT development. The secondary study endpoint was the ORR. The cutoff date for the data was December 31, 2023. Continuous variables were expressed as mean \pm standard deviations (SD) or median (interquartile range, IQR) and were compared using the Student t-test or Mann–Whitney U test based on the underlying distribution of the data. Categorical variables were summarized as numbers with percentages and compared using chi-square or Wilcoxon rank-sum tests. PVFS was investigated using Kaplan–Meier curves, and differences between subgroups were compared using the log-rank test. Variables with P values < 0.2 in univariate analysis were included in a multivariable Cox proportional hazards model with backward stepwise selection to identify the independent risk factors of PVTT.

Results A total of 180 patients with unresectable HCC who underwent TACE between March 2013 and July 2023 were included in this study (Fig.1). During the follow-up period, 109 patients did not develop PVTT (non-PVTT development cohort), while 71 developed PVTT (PVTT development cohort). All laboratory data were obtained within 3 days before the first TACE session. Statistical differences in baseline characteristics between the two cohorts are shown. No significant differences were observed in age, maximal tumor size, tumor number, tumor distribution, number of TACE sessions, albumin, total bilirubin, aspartate transaminase, HBV infection, ECOG-PS score, AFP, or BCLC stage between the two cohorts. Following mRECIST[20], 16 (14.7%) vs. 11 (15.5%) patients achieved CR, 45 (41.3%) vs. 27 (38.0%) achieved PR, 26 (23.9%) vs. 13 (18.3%) had SD, and 22 (20.1%) vs. 20 (28.2%) had PD in the non-PVTT and PVTT development cohorts, respectively. The best ORRs were 56.0% and 53.5% in the non-PVTT and PVTT development cohorts, respectively, which were not significantly different between the two cohorts ($P=0.748$). During the follow-up period of 19.3 months (median) [10.3(P25), 35.9(P75)], 71 patients developed PVTT with an incidence rate of 39.4% (71/180). Based on the PVTT classification defined by the Liver Cancer Study Group of Japan, 19 (26.8%), 27 (38.0%), and 25 (35.2%) patients developed Vp2-, Vp3-, and Vp4-type PVTT in the PVTT development cohort ($n=71$). The median PVTT diameter was 1.4 cm (median) [1.0(P25), 1.7(P75)]. The median PVFS was 34.8 months (95% CI, 22.9–46.7 months), and the 1-, 3-, and 5-year PVFS rates were 85.7%, 49.7%, and 34.2% respectively (Fig. 2). The cumulative 1-, 3-, and 5-year PVTT event rates for the entire cohort were 14.3%, 50.3%, and 65.2%, respectively. (Fig.3)

The independent predictive factors for PVTT based on the univariate and multivariate Cox proportional hazards models are shown in Table 3. In multivariate analyses, tumor response (non-responder vs. responder), AFP (≥ 400 vs. < 400 ng/mL), and tumor distribution (two halves of the liver vs. the right or left half of the liver) were identified as significant influencing factors of PVFS (all P value < 0.05). Specifically, compared with the responder, AFP < 400 ng/mL, and tumor distribution of the right or left half of the liver; non-responder, AFP ≥ 400 ng/mL, and tumor distribution of the two halves of the liver significantly negatively influenced PVFS of patients with a HR of 1.99 (95% confidence interval [CI]: 1.19–3.33), 2.13 (95% CI: 1.27–3.58), 1.88 (95% CI: 1.06–3.34), respectively (all P value < 0.05). Considering that the β coefficients and HR values of the above three variables were close in COX multivariate analysis, we assigned 0 point to AFP < 400 ng/mL, CR or PR treatment response, and the distribution of lesions within the right or left half of the liver; correspondingly, the AFP ≥ 400 ng/mL, SD or PD treatment response, and the distribution of tumors within the two halves of the liver were assigned 1 point. The risk of PVTT development was stratified into low-risk (0 point), moderate-risk (1 point), and high-risk (2–3 points) groups according to the score (Table 4). The cumulative risk rate of PVTT was significantly different among the three gr

roups (log-rank test, $P=0.001$). The high-risk group exhibited a significantly higher incidence of PVTT formation, while the low-risk group tended to have the lowest incidence of PVTT (Fig.4).

Conclusion In conclusion, patients with unresectable HCC have a high probability of developing PVTT after TACE. The score and risk stratification criteria comprising AFP level, tumor distribution, and response to TACE can better distinguish the risk of PVTT formation after treatment, help identify high-risk patients, and promote clinical follow-up management.

PO-144

Clinical Characteristics and Surgical Treatment Strategies for Primary Intracranial Rosai-Dorfman Disease

Ouyang Hui,Ziyang Chen

Guangdong Sanjiu Brain Hospital Institute of Brain Science and Rehabilitation Medicine, South China Normal University Affiliated Brain Hospital of Jinan University

Purpose This study aims to explore the clinical characteristics and surgical efficacy of primary intracranial Rosai-Dorfman Disease (RDD) diagnosed through clear pathological examination at Guangdong Sanjiu Brain Hospital from 2017 to 2023.

Materials and methods We conducted a retrospective analysis of three patients treated in the Neurosurgery Department from August 2017 to November 2023. We reviewed their clinical features, imaging data, comorbidities, tumor location, size, invasion extent, signal intensity, presence of cystic enhancement, surgical treatment methods, extent of resection, postoperative recovery, and prognosis.

Results Among 17 RDD patients, ages ranged from 18 to 64 years, with a mean age of 41 years. There were 9 males and 8 females, resulting in a male-to-female ratio of 1.125:1. Tumors were located as follows: 5 in the frontal sinus area, 5 in the cerebellopontine angle, 4 in the parietal sinus area, 2 in the spinal canal, and 1 in the lateral ventricle, with lesions involving the dura mater. Fourteen patients underwent total resection, while three had subtotal resection. All 17 patients had good postoperative recovery without neurological deficits. Histologically, RDD showed significant proliferation of tissue cells, with abundant plasma cell and lymphocyte infiltration. The distribution of tissue cells and lymphoplasmacytic cells exhibited an alternating pattern of "dark" and "light." Inflammatory cell "infiltration" was observed in the cytoplasm of the pathological tissue cells, which were positive for CD68, Cyclin D1, and S-100.

Conclusion Primary intracranial Rosai-Dorfman Disease (RDD) is a rare non-Langerhans cell histiocytosis with an unclear etiology and pathogenesis. Its clinical presentation is highly heterogeneous, leading to frequent misdiagnosis and missed diagnoses. Currently, there is no standardized treatment protocol, and diagnosis requires pathological examination of the affected meninges. Surgical resection of the affected meninges is the preferred treatment method.

PO-145

Diagnostic and Therapeutic Strategies for Lhermitte-Duclos Disease

Fan Yanfeng, Ziyang Chen

Guangdong Sanjiu Brain Hospital, Institute of Brain Science and Rehabilitation Medicine, South China Normal University; Affiliated Brain Hospital of Jinan University

Purpose This study aims to explore the clinical characteristics and surgical outcomes of patients diagnosed with Lhermitte-Duclos disease (LDD) at Guangdong Sanjiu Brain Hospital over the past four years.

Materials and methods We conducted a retrospective analysis of three patients with confirmed pathological diagnoses of LDD treated at our institution from August 2006 to November 2023. We reviewed their clinical features, imaging data, comorbidities, and relevant clinical information, including tumor location, size, invasion extent, signal intensity, presence of cystic enhancement, surgical approach, extent of resection, postoperative recovery, and prognosis.

Results Among the three LDD patients, one had a tumor located in the left cerebellar hemisphere, another involved both the left cerebellar hemisphere and the left cerebellar peduncle, and the third affected the left cerebellar hemisphere and brainstem, extending into the spinal canal. All patients exhibited the characteristic "tiger stripe" sign on imaging, significant peritumoral edema, and no notable enhancement. One patient underwent total resection, while two had subtotal resections. One patient required reoperation for severe postoperative cerebellar edema, while the other two had good postoperative recoveries without significant neurological deficits. One patient presented with multiple thyroid nodules, skin cysts, and a Thornwaldt cyst at the posterior wall of the nasopharynx, suggesting the possibility of Cowden syndrome (hamartoma syndrome), with pathological examination revealing a 60% loss of PTEN expression in tumor cells.

Conclusion LDD has distinct MRI characteristics that allow for preoperative diagnosis in most cases. The unique imaging findings (low signal on T1-weighted images, high signal on T2-weighted images, and the typical "tiger stripe" sign, along with significant mass effect) are crucial for preoperative diagnosis and determining the extent of the tumor. Treatment for LDD includes both surgical and conservative approaches, with total resection being the optimal treatment method. Most patients with subtotal or partial resections can maintain long-term stability of residual disease with regular follow-ups. For patients with complex tumor growth patterns where complete resection is not feasible, the surgical goal should focus on alleviating symptomatic mass effects.

PO-146

Diagnosis and Treatment of Vascular Tumours and Vascular Malformations in the Head and Neck

Teng Hui Zhan, Rong Zhang
Fujian Maternity and Child Health Hospital

Purpose This research aims to investigate the clinical characteristics, imaging manifestations, and treatment outcomes of head and neck vascular tumours and vascular malformations, with the goal of optimising diagnostic and therapeutic strategies. The lesions of head and neck vascular tumours and malformations are diverse and complex, and accurate diagnosis and appropriate treatment plans are crucial for improving patient prognosis.

Materials and methods This study conducted a retrospective analysis of 65 patients with vascular tumours and vascular malformations of the head and neck who received diagnosis and treatment at our hospital from January 2022 to December 2024. All patients underwent detailed clinical assessments and imaging examinations prior to treatment, including ultrasound, magnetic resonance imaging (MRI), and computed tomography (CT). Based on the type of lesions and the characteristics of the condition, patients received personalised treatment, which included β -blocker therapy (propranolol), sclerotherapy, interventional embolisation, laser treatment, and surgical procedures. Follow-up assessments were conducted post-treatment to evaluate efficacy and the occurrence of complications.

Results In this study involving 65 patients, 35 were diagnosed with haemangiomas and 30 with vascular malformations. Among the patients with haemangiomas, the efficacy rate of propranolol treatment reached 91.4%, with no serious adverse reactions reported. For patients with vascular malformations, the combination of sclerosing agent injection and interventional embolisation achieved an efficacy rate of 86.7%. Some patients experienced mild swelling and pain following treatment, but these were managed effectively with symptomatic treatment, and no severe complications were observed. The accuracy of imaging examinations in diagnosing and assessing the extent of lesions was 98%, providing important support for treatment decisions.

Conclusion The diagnosis of vascular tumours and vascular malformations in the head and neck should rely on a detailed clinical assessment and high-quality imaging examinations to ensure accurate diagnosis and precise evaluation of the extent of the lesions. Employing individualised treatment plans based on the different types of lesions can significantly improve the clinical prognosis for patients. Propranolol has demonstrated good efficacy and safety in the treatment of vascular tumours, while the injection of sclerosing agents combined with interventional embolisation represents an effective strategy for treating vascular malformations. This study provides robust evidence to support the clinical treatment of vascular tumours and malformations in the head and neck, and offers a basis for optimising future diagnostic and therapeutic approaches.

PO-147

Transarterial chemoembolization for huge hepatocellular carcinoma : to do or not to do, a clinical dilemma

Hong-Jian Shi, Liang Zhou, Tao Chen, Zhen Gan

The Second Affiliated Hospital of Nanjing Medical University, Nanjing, China

Purpose Background: The difference of transarterial chemoembolization (TACE) indications for hepatocellular carcinoma (HCC) between Eastern and Western world is existed. The Chinese National Liver Cancer diagnosis and treatment guideline recommends some advanced stage HCC with good liver function should be selected for TACE or TACE plus systemic therapy.

Purpose: To re-evaluate the indications of transarterial chemoembolization for huge hepatocellular carcinoma (HCC) with good performance status.

Materials and methods Three cases of huge hepatocellular carcinoma (at least one lesion's diameter large than 10 cm) with Child-Pugh score A performed transarterial chemoembolization were included in this retrospective study, with literature review. Two cases had multi-nodule lesions, and all cases had some degree portal vein invasion. Mean age is 67.3 ± 6.8 years, ranged from 57 to 73 years. Mean diameter of the largest lesion of HCCs is 12.3 ± 1.3 cm. Clinical outcomes including overall survival, peri-procedure complications were analyzed.

Results In our study, post embolization syndrome was encountered in each case. There were no serious complications peri-procedure. The mean overall survival is 139.7 ± 64.9 days, ranged from 74 to 204 days. The causes of death are hepatic failure in two cases and gastrointestinal hemorrhage in one case. One large retrospective study included 511 patients with huge HCC who underwent serial TACE reported median overall survival 6.5 months. During the follow-up period, 160 (31.3 %) died from tumor progression, 59 (11.5 %) died from hepatic encephalopathy, 24 (5.8 %) died from gastrointestinal hemorrhage, and 4 (0.8 %) died from rupture of the tumor.

Conclusion The indications of TACE for huge HCC should be carefully chosen. Patient with large tumor burden even with good performance status might avoid invasive treatment. Systemic therapy might be the first line therapy for most huge HCC.

PO-148

Development and validation of nomogram including mutations in angiogenesis-related genes as risk factors for HCC patients treated with TACE

Wanqing Shen, Jiaping Li
the first affiliated hospital of sun yat-sen university

Purpose This study explores the relationship between angiogenesis-related genes and transarterial chemoembolization (TACE) failure in patients with hepatocellular carcinoma (HCC) and develops a predictive model for assessing treatment outcomes.

Materials and methods Somatic mutation profiles of 165 patients with HCC treated with TACE were analyzed using whole-exome sequencing (WES). Multivariate Cox regression analysis was performed to calculate the genetic risk score (GRS) for angiogenesis-related gene mutations. The participants were randomly divided into training and validation groups. In the training set, independent prognostic factors of TACE-treated patients with HCC were screened using univariate Cox-LASSO-stepwise Cox regression, and a nomogram was established and evaluated using the receiver operating characteristic curve, calibration curve, and decision curve analysis of the two sets.

Results Among 165 patients, significant genetic alterations were identified, with TP53 being the most frequently mutated gene. Mutations in FGFR4, MST1R, and RECK were associated with the treatment efficacy of patients receiving TACE treatment, and the constructed GRS was associated with poor prognosis. Furthermore, AFP, ALT, AST, PLR, PD-L1 immune drug treatment, and GRS were confirmed as independent factors affecting the prognosis of patients with HCC treated with TACE. A nomogram was constructed, which demonstrated excellent discrimination, calibration, and clinical benefits in both the training and validation sets.

Conclusion These findings highlight the critical role of angiogenesis-related genes in predicting TACE outcomes in patients with HCC and indicate that the developed prognostic model and nomogram can serve as valuable tools to predict prognosis based on the GRS of angiogenesis-associated gene mutations.

Bibliometric Analysis of Literature on Cancer and Interventional Therapy: A Comprehensive Review

Xiaohan Sun

the First Affiliated Hospital of China Medical University

Purpose Cancer, as a highly prevalent and high-risk disease, poses a severe threat to global public health. In recent years, its incidence and mortality rates have been continuously rising, imposing a heavy burden on individuals, families, and society. Interventional therapy has emerged as an effective treatment for cancer, boasting advantages such as minimal invasiveness, precision, and rapid recovery. Despite numerous studies on cancer interventional therapy, the existing research lacks systematic collation and integration, making it difficult to comprehensively grasp the current situation and potential research directions in this field. Bibliometrics, as a powerful tool for the quantitative analysis of scientific literature, can effectively address this issue. By applying bibliometric methods to the literature related to cancer interventional therapy, it is possible to systematically evaluate the research achievements, citation patterns, collaboration networks, and research hotspots in this field. This not only helps researchers gain a comprehensive understanding of the research status quo and trends in cancer interventional therapy but also provides valuable references for future research planning and resource allocation.

Materials and methods This study conducted a search using the Web of Science Core Database. With the search formula $TS=((\text{cancer or tumor or carcinoma}) \text{ AND } ("Interventional therapy" \text{ OR } "Interventional radiology"))$, all relevant literature from 2000 to the present was collected. To ensure the quality and relevance of the data, article types other than original research papers and review articles were excluded, and non-English literature was also removed. Subsequently, the obtained data were analyzed using VOSviewer software. Analyses such as co-citation analysis, author collaboration analysis, and keyword co-occurrence analysis were carried out to explore the potential correlations among different research elements and identify the most influential studies, core researchers, and major research themes in this field.

Results The research results show that as of March 2025, a total of 2,329 relevant articles have been published. In terms of the number of relevant articles published, the United States ranks first with 787 articles, and it also has the highest number of citations, reaching 18,505 times. Among research institutions, Memorial Sloan-Kettering Cancer Center has published the largest number of articles, which is 69, while Northwestern University has the highest number of citations, amounting to 2,087 times. Among researchers, De baere, Thierry and Deschamps, Frederic have published the most articles, both with 30 articles each, and Salem, Riad has the highest number of citations, reaching 2,320 times. Regarding journals, Seminars in interventional radiology has published the most relevant articles, with 154 articles. The article with the highest number of citations is percutaneous radiofrequency ablation for hepatocellular carcinoma - an analysis of 1000 cases, which was published in the journal Cancer in 2005, and the author is Tateishi, R. The keyword analysis is divided into four clusters, among which liver cancer, radiofrequency ablation, interventional therapy, and risk are the keywords mentioned most frequently.

Conclusion Through this bibliometric-based study, we have comprehensively reviewed the literature in the field of cancer interventional therapy from 2000 to the present. The study has identified the leading position of the United States in terms of research output and influence in this field. Meanwhile, it has revealed the important roles of core research institutions such as Memorial Sloan-Kettering Cancer Center, key researchers like De baere, Thierry, and important journals such as Seminars in interventional radiology in promoting the development of this field. The keyword cl

uster analysis has highlighted core research themes such as liver cancer and radiofrequency ablation. This study provides a systematic perspective for a deep understanding of the academic landscape in the field of cancer interventional therapy, helps researchers grasp research hotspots and development trends, provides a powerful reference for the selection of future research directions and the rational allocation of resources, and promotes more efficient and in-depth research in this field.

PO-150

Thoracic Radiotherapy: A Game Changer for ES-SCLC Patients on Chemoimmunotherapy

Yunbin Gao, Lujun Zhao, meng yan, Xingyue Li
Tianjin Medical University Cancer Institute and Hospital

Purpose Thoracic radiation therapy (TRT) is known to enhance the prognosis of patients with extensive-stage small-cell lung cancer (ES-SCLC) following chemotherapy. This research aimed to explore how TRT impacts ES-SCLC patients in the context of immunotherapy.

Materials and methods We conducted a retrospective study at our institute from October 2018 to March 2022 on ES-SCLC cases confirmed by histopathology as receiving chemoimmunotherapy with or without TRT. We minimized selection bias by using propensity score matching. Kaplan-Meier analysis was used to assess progression-free survival (PFS) and overall survival (OS) from the initiation of first-line therapy. A Log-rank test was utilized to examine survival rates among different groups, and a Cox proportional hazards model was used to determine the factors linked to survival. Subgroup analyses were used to determine the influencing factors on TRT.

Results The study examined 172 patients with a median follow-up of 20.1 months. Patients receiving TRT had median OS and PFS of 24.2 and 11.3 months, compared to 15.9 and 6.6 months for those without TRT ($p = 0.006$ and $p < 0.001$, respectively). The multivariate Cox regression analysis showed that TRT was a favorable factor for both OS and PFS. In addition, patients in all subgroups may benefit from TRT for OS.

Conclusion TRT might enhance OS and PFS in ES-SCLC patients receiving chemoimmunotherapy. It is necessary to conduct randomized controlled trials in order to confirm this.

PO-151

Development of a prognostic model for patients with extensive-stage small cell lung cancer undergoing immunotherapy and chemotherapy

Yunbin Gao, meng yan, Lujun Zhao
Tianjin Medical University Cancer Institute and Hospital

Purpose

In this study, we aimed to develop a predictive model for patients receiving chemotherapy and immunotherapy for extensive-stage small cell lung cancer

Materials and methods We retrospectively analyzed 112 extensive-stage small cell lung cancer patients treated with first-line immunotherapy and chemotherapy. The relevant clinical data were collected to evaluate the changes during the treatment. The best subset regression, univariate analysis, and LASSO regression with cross-validation were applied for variable selection and model establishment. The nomograms for 1- and 2-year survival probabilities were established, and the calibration curve was utilized to evaluate the correspondence between actual and predicted survival. The model prediction capacity was assessed using decision curve analysis, calibration curves, and receiver operating characteristic curves. Moreover, five-fold cross-validation was conducted for internal validation. According to risk score, the patients were assigned to high- and low-risk groups, and survival curves were generated for each group.

Results The LASSO regression model was established based on the variables such as age, ECOG, metastatic sites, NLR, and immunotherapy cycles. This predictive model displayed robust performance, evidenced by the Area Under the Curve of 0.887 and concordance index of 0.759. The nomogram effectively predicted 1- and 2-year survival probabilities and demonstrated a high degree of calibration. The decision curve analysis displayed that the model possessed superior predictive capability. The risk stratification for patients with high- and low-risk categories facilitated more individualized survival assessment.

Conclusion The study successfully developed a prognostic model for extensive-stage small cell lung cancer patients undergoing immunotherapy and chemotherapy, demonstrating the good accuracy and predictability.

Bioinformatics Analysis of the Invasion-Associated Competing Endogenous RNA Network in Breast Cancer on Single-cell Resolution.

Haowei Deng, Wenjia Guo
Xinjiang Medical University Affiliated Tumor Hospital

Purpose Breast cancer is the most common neoplasm among females. The fact that most breast cancers are invasive makes it vitally important to elucidate the role and mechanism of invasion in breast cancer. This study aims to probe the relationship between invasion and long non-coding RNAs (lncRNAs) and to establish an invasion-related competing endogenous RNA (ceRNA) network in breast cancer.

Materials and methods CancerSEA (<http://biocc.hrbmu.edu.cn/CancerSEA/home.jsp>) is the first dedicated database that aims to comprehensively decode distinct functional states of cancer cells at single-cell resolution (Yuan et al., 2019). In this study, CancerSEA database was employed to identify invasion-related lncRNAs and genes in breast cancer. Only those lncRNAs and genes that were significantly associated with invasion in breast cancer were included. Two databases, including GEPIA (<http://gepia.cancer-pku.cn/>) and starBase (<http://starbase.sysu.edu.cn/>), were used to analyze the expression of lncRNAs in breast cancer (Li et al., 2014; Tang et al., 2017). Only lncRNAs that were significantly upregulated or downregulated in both two databases were selected for subsequent analysis. StarBase was also used to conduct expression correlation analysis. The prognostic values of RAMP2-AS1, hsa-miR-1301-3p and KMT2A in breast cancer were determined using Kaplan-Meier plotter (<http://kmplot.com/analysis/>), which is an online database capable of accessing the effects of genes or miRNAs on survival in more than 20 cancer types including breast cancer (Lou et al., 2021). miRNet (<http://www.mirnet.ca>), a database for miRNA functional analysis and systems biology, was used to predict the binding miRNAs of RAMP2-AS1 and the downstream target genes of hsa-miR-1301-3p (Chang et al., 2020). Venn (<https://jvenn.toulouse.inrae.fr/app/index.html>) was employed to perform intersection analysis for target genes of miRNAs and invasion-related genes in breast cancer. Only the genes that commonly appeared in both two gene sets were included for subsequent analysis. The statistical analyses were directly performed using online databases or tools as mentioned above.

Results Identification of RAMP2-AS1 as an invasion-Related Long Non-Coding RNA in BRCA and a Potential Therapeutic Target in Pan-cancer.

To elucidate the underlying molecular mechanism of the invasion in BRCA, four BRCA-associated scRNA-seq studies were gathered (Braune et al., 2016, Jordan et al., 2016, Chung et al., 2017, Aceto et al., 2018). Consequently, a total of 2412 lncRNAs that were significantly associated with invasion in BRCA were screened out. Among these lncRNAs, 45 of them appear in more than one scRNA-seq studies (Supplementary Table 1,2) and 22 of them significantly showed difference between cancer and normal tissues in starBase. Next, we successively determined the expression levels of these lncRNAs in BRCA by GEPIA database (Table 1). Turns out only RAMP2-AS1 expression was markedly decreased in both two databases, when compared with normal controls in BRCA (Figure 1A). We further performed survival analysis for invasion-related RAMP2-AS1 in BRCA, OS and RFS results showed it might be a potential BRCA suppressor (Figure 1B). These findings suggested that RAMP2-AS1 might be the most potential invasion-related lncRNA in BRCA.

Next, we conducted survival analysis of RAMP2-AS1 in pan-cancers and 3 types of immunological therapies. OS result in pan-cancer indicated that patients with high RAMP2-AS1 expression ha

d a more satisfying prognosis and more pleasing response to anti-PDL1 therapy, but vice versa in anti-PD1 and anti-CTLA4 treatment (Figure 1C). We also found that in addition to the invasive phenotype in BRCA, RAMP2-AS1 is highly correlated with many other tumor phenotypes, such as angiogenesis, EMT, hypoxia, inflammation, which has been previously reported (Aceto et al., 2018), and stemness. At the same time, various tumor phenotypes associated with RAMP2-AS1 were also discovered in other tumors.(Figure 1D).

Prediction and Analysis of Downstream Potential miRNAs of RAMP2-AS1 in BRCA

For closer exploration and of downstream action mechanism of invasion-related RAMP2-AS1 in BRCA and more accurate prediction of the miRNAs that potentially bind to RAMP2-AS1, miRNet was employed. A total of 13 miRNAs were identified (Figure 2A), 5 of them were significantly downregulated in BRCA and 3 of them were significantly overexpressed in BRCA (Figure 2B,C). According to ceRNA hypothesis, there should be a negative correlation between lncRNA and miRNA. Therefore, correlation of RAMP2-AS1 with these miRNAs was clarified using starBase. 8 of predicted miRNAs were significantly negatively related with RAMP2-AS1 in BRCA, while only 3 of them, hsa-mir-1301-3p, hsa-mir-2277-5p and hsa-mir-660-5p, were overexpressed in BRCA (Table 2, Figure 2D). We then performed prognostic analysis using the Kaplan-Meier plotter, results showed that in MATEBRIC database, patients with high expression of hsa-mir-1301-3p had a poor prognosis (Figure 2E), we double-checked it in TCGA database, hsa-mir-1301-3p also stood out (Figure 3C). By combination of correlation analysis, expression analysis and survival analysis, hsa-mir-1301-3p might be the most potential downstream binding miRNAs of RAMP2-AS1 in BRCA. Survival analysis for RAMP2-AS1 and hsa-mir-1301-3p in HER2+/- BRCA .

Kaplan-Meier plotter was employed to further discover the relationship between the RNA network we currently demonstrated, RAMP2-AS1/hsa-mir-1301-3p, and HER2 status. In PAM50 and StGallen subtypes, RAMP2-AS1 turned out to be a risk factor in HER2+ (Figure 3A), while on the contrary, hsa-mir-1301-3p was a protective factor (Figure 3D). We then conducted survival analysis in HER2 positive and HER2 negative patients, RAMP2-AS1 (Figure 3B) and hsa-mir-1301-3p (Figure 3E) showed the same remarkable results. Combined with the diametrically opposed outcomes of RAMP2-AS1 in immunological therapy, the RNA network we found might be a good indication of prognosis in HER2+ patients.

Identification of Downstream invasion-Related Targets of RAMP2-AS1-miRNA Pathways in BRCA

2,528 invasion-related genes that were significantly associated with invasion in BRCA were obtained by analyzing the four scRNA-seq studies as mentioned above (Supplementary Table 3). 696 hsa-miR-1301-3p target genes were forecasted by miRNet and 51 of them were found in both miRbase and tarbase (Figure 4A, Supplementary Table 4). By intersected with invasion-related genes and hsa-miR-1301-3p target genes, 4 genes (KMT2A, SYNJ2, COPE and SLAIN2) were selected (Figure 4B) and their expression correlation analysis with RAMP2-AS1 (Figure 4C) and hsa-mir-1301-3p (Figure 4D) was conducted. KMT2A, SYNJ2 and SLAIN2 turned out to be significantly inversely correlated with hsa-miR-1301-3p and positively correlated with RAMP2-AS1 in BRCA (Table 3). The prognostic values of KMT2A, SYNJ2 and SLAIN2 in BRCA were evaluated using Kaplan-Meier plotter database. As presented in Figure 4E, high expression of KMT2A significantly indicated unsatisfactory prognosis in breast. Finally, an invasion-related ceRNA network in BRCA at the single cell level was established based on lncRNA RAMP2-AS1, hsa-miR-1301-3p and KMT2A mRNAs.

Expression and Survival Analysis of KMT2A in pan-cancer Level

After establishing the RNA network, we performed a pan-cancer analyses of KMT2A. The mRNA expression of KMT2A was increased in various tumor tissues, such as bladder urothelial carcinoma (BLCA), breast invasive carcinoma (BRCA), lung squamous cell carcinoma (LUSC), uterine c

corpus endometrial carcinoma (UCEC) ($p < 0.001$), endocervical adenocarcinoma (CESC), glioblastoma multiforme (GBM), thyroid carcinoma (THCA) ($p < 0.01$), kidney chromophobe (KICH), prostate adenocarcinoma (PRAD) ($p < 0.05$) when compared to corresponding normal tissue (Figure 5A). Tumor tissues of cholangiocarcinoma (CHOL), head and neck squamous cell carcinoma (HNSC), liver hepatocellular carcinoma (LIHC) ($p < 0.001$), esophageal carcinoma (ESCA) ($p < 0.01$), kidney Papillary Cell Carcinoma (KIRC) ($p < 0.05$), had significantly higher KMT2A expression when compared to corresponding normal tissue (Figure 5A). Significantly higher KMT2A expression was also observed in HPV-positive head and neck squamous cell tumor tissues compared with HPV-negative tissues ($p < 0.001$) (Figure 5A). In addition to transcription, we also assessed KMT2A at a protein level using the large-scale proteome data available through the National Cancer Institute's CPTAC dataset. We found that the total protein expression of KMT2A was significantly higher in ccRCC and GBM, and significantly lower in UCEC tissues compared to normal tissues (Figure 5B). We also employed OS and DFS analysis of KMT2A in 33 tumors in GEPIA2, KMT2A was confirmed to be a risk prognosis factor (Figure 5C). We found that in addition to the invasive phenotype in BRCA, KMT2A was also correlated with many other tumor phenotypes, which were fairly consistent with RAMP2-AS1, such as angiogenesis, hypoxia, inflammation and stemness. At the same time, various tumor phenotypes associated with KMT2A were also discovered in other tumors. (Figure 5D).

Conclusion At the end, a novel inflammation-related lncRNA-miRNA-mRNA regulatory network in BRCA was successively established based on ceRNA hypothesis and scRNA-seq data. There were several limitations in this study. For example, the miRNAs in this network were not identified using scRNA-seq data; the results from this study were only based on *in silico* analysis. However, this is the first study to comprehensively explore invasion-related lncRNA-miRNA-mRNA network in BRCA. All these findings need to be further validated using basic experiments and clinical trials in the future.

PO-153

Development and validation of a SHAP-based interpretable model for preoperative prediction of microvascular invasion in hepatocellular carcinoma

Jianxi Guo
Shenzhen People's Hospital

Purpose To develop an interpretable machine learning model for preoperative noninvasive prediction of microvascular invasion (MVI) in hepatocellular carcinoma (HCC).

Materials and methods This retrospective study included 308 HCC patients who underwent curative hepatectomy at our institution from January 2020 to December 2023 (MVI-positive: 132; MVI-negative: 176), randomly allocated into training (n=216) and validation (n=92) sets at a 7:3 ratio. Univariate and multivariate logistic regression identified independent risk factors for MVI. Least absolute shrinkage and selection operator (LASSO) regression screened predictive features. Ten machine learning models were constructed, including Logistic Regression (LR), Naive Bayes (NB), Decision Tree (DT), Random Forest (RF), k-Nearest Neighbors (KNN), Support Vector Machine (SVM), Extreme Gradient Boosting (XGBoost), Gradient Boosting, Adaptive Boosting (AdaBoost), and Multilayer Perceptron (MLP). Model performance was evaluated using the areas under receiver operating characteristic curve (AUC), accuracy, sensitivity, specificity, and F1-score. Model interpretability was analyzed through the SHapley Additive exPlanations (SHAP) framework.

Results Multivariate analysis identified hepatitis virus load, alpha-fetoprotein (AFP), gamma-glutamyl transferase (GGT), tumor size, and radiologic venous invasion (RVI) as independent risk factors for MVI ($P < 0.05$). LASSO regression selected 12 key predictive features, including hepatitis virus load, AFP, GGT, Child-Pugh grade, pseudocapsule integrity, RVI, arterial phase peritumoral hypodensity. The XGBoost model demonstrated optimal performance, with a training set AUC of 0.852 (95% CI: 0.756–0.947), accuracy of 0.792, sensitivity of 0.852, specificity of 0.775, and F1-score of 0.776. In the validation set, the model achieved an AUC of 0.815 (95% CI: 0.719–0.912), accuracy of 0.750, sensitivity of 0.677, specificity of 0.805, and F1-score of 0.700. Calibration curve and decision curve analysis (DCA) show that the model has accurate risk stratification ability and high clinical practicability. SHAP analysis revealed that viral load, RVI, pseudoenvelope integrity, AFP and tumor size were the five most important variables affecting the prediction ability of XGBoost model. Hepatitis viral load, AFP, RVI, and tumor size were positive predictors of MVI, while pseudoenvelope integrity was protective.

Conclusion The XGBoost model based on multi-dimensional clinical-imaging features can accurately predict MVI in HCC patients before surgery, and its interpretable framework provides a reliable basis for individualized surgical decision-making.

PO-154

Establishment and observation of a tumor transplantation model of shell-less chick embryo chorioallantoic membrane

Jiaqi Zhang, Jun Chen

Zhejiang Provincial People's Hospital (Affiliated People's Hospital), Hangzhou Medical College

Purpose The aim of this study was to establish and observe a modified Chick Embryo Chorioallantoic Membrane (CAM) tumor transplantation model to overcome the limitations of the traditional in-shell observation method, and to provide a more efficient and visual experimental platform for the study of tumorigenesis, progression and its molecular mechanisms. With the improved off-shell modeling method, we hope to improve the convenience of experimental manipulation, enhance the visualization of tumor growth, and provide an economical and efficient animal model for oncology research.

Materials and methods Fertilized eggs and human gastric cancer cell lines were used as experimental materials in this study. Firstly, the eggs were incubated in the incubator, and then transferred to out-of-shell incubation on the third day (EDD3). Tumor cell transplantation was performed on the fourth day (EDD7) of off-shell incubation. Cell processing consisted of culturing gastric cancer cells using RPMI 1640 medium, digesting them, mixing them with matrix gel, and inoculating them onto the CAM surface. Tumor growth was monitored by various means including visual observation and magnetic resonance imaging (MRI). At the end of the experiment, the harvested tumor tissues were subjected to pathological and molecular biological tests to verify the molecular characteristics of the tumor tissues.

Results We successfully established a reproducible and high-throughput chicken CAM tumor transplantation model through a modified off-shell modeling method. Tumor cells grew rapidly on CAM, and solid tumor formation was observed several days after inoculation. Pathological assays confirmed that the harvested tissues had the heterogeneous and invasive characteristics of tumor tissues and were consistent with the biological behavior of tumors. Molecular biology assays showed that the tumor tissues retained the molecular characteristics of the original cell lines, indicating that the model was able to reliably reproduce the molecular characteristics of human tumors. In addition, the application of multiple imaging techniques made it possible to monitor tumor growth and angiogenesis in real time, which further improved the practicality and accuracy of the model.

Conclusion The modified chicken CAM ex vivo modeling method proposed in this study significantly improved the operability and visualization of the experiment while retaining the advantages of the traditional CAM model. The model not only can efficiently and economically simulate the growth and metastasis process of tumors, but also provides a reliable experimental platform for molecular mechanism studies of tumors and drug development. Through pathological and molecular biological validation, we confirmed the reliability and consistency of the model, demonstrating its potential for wide application in precision tumor therapy and preclinical research.

Elucidating the Novel Role of RNA-Binding Protein IGF2BP3 in Suppressing HR+/HER2- Breast Cancer Progression via Transcriptional Repression with ESR1

Ziwen Wang, Xu Zhang, Liang Shi, Ji-Fu Wei, Qiang Ding
The First Affiliated Hospital of Nanjing Medical University

Purpose As the most common type of breast cancer, HR+/HER2- breast cancer accounts for 2/3 of all breast cancers, and despite effective control by endocrine therapy, 20% of patients still face recurrence, and some patients even have distant metastasis at the time of the first diagnosis, i.e., primary stage IV breast cancer; the high heterogeneity of the tumor and resistance to hormone therapy are closely related to the risk of long-term recurrence, which poses a great challenge to the HR+/HER2- breast cancer patients a great challenge. With the continuous development of targeted therapies such as PARP inhibitors and CDK4/6 inhibitors, the survival rate of HR+/HER2- breast cancer patients has been improved; however, the limitations in the use of drug targets and the complex uncertainties in the molecular mechanisms still pose a great obstacle to clinical treatment. Therefore, continuing to search for effective therapeutic targets and refining their mechanisms of action is of great clinical significance for improving the prognosis of HR+/HER2- breast cancer patients and realizing the precision treatment of breast cancer.

Materials and methods Immunohistochemical (IHC) staining and Kaplan-Meier survival analysis of breast cancer cohorts stratified by molecular subtypes (luminal A/B, HER2+, TNBC) revealed divergent IGF2BP3 expression patterns and prognostic associations (pro-tumorigenic vs. tumor-suppressive roles). RNA sequencing of IGF2BP3-knockdown/overexpression models identified subtype-specific transcriptional networks modulated by IGF2BP3. Nuclear-cytoplasmic fractionation and immunofluorescence (IF) localization assays demonstrated subtype-dependent spatial redistribution of IGF2BP3. RNA immunoprecipitation sequencing (RIP-seq) in cytoplasmic extracts and CUT&Tag sequencing in nuclear extracts were integrated to define compartment-specific regulatory targets. Co-immunoprecipitation (co-IP) coupled with LC-MS/MS in nuclear/cytoplasmic fractions identified IGF2BP3-binding partners. Truncated variant pull-down assays mapped functional domains mediating protein-RNA/DNA interactions. Methylation-specific PCR (MSP) and bisulfite sequencing quantified IGF2BP3 promoter methylation levels across subtypes. Structure-based molecular docking and pharmacophore modeling prioritized small-molecule inhibitors targeting the DNMT3B/IGF2BP3 axis, validated by surface plasmon resonance (SPR) and dose-response assays.

Results Our investigations revealed a paradoxical role of IGF2BP3 in breast cancer pathogenesis: IGF2BP3 overexpression drives oncogenesis in TNBC, while IGF2BP3 exhibits low expression and tumor-suppressive functions in HR+/HER2- breast cancer. Mechanistically, spatial redistribution leads to this duality—in TNBC, cytoplasmic IGF2BP3 acts as an m6A-binding protein to promote mRNA stability/translation, whereas in HR+/HER2- tumors, nuclear-localized IGF2BP3 functions as a transcriptional repressor that attenuates ESR1 transactivation activity, thereby suppressing oncogenic transcriptional programs. Considering that the tumor suppressor effect of IGF2BP3 in HR+/HER2- breast cancer is limited by its low expression, we found DNMT3B as the DNA methyltransferase responsible for silencing IGF2BP3 and will design small molecule inhibitors to block.

Conclusion This project using molecular/cell biology technologies, combined with clinical sample analysis, PDX model, gene editing technology, etc., proposes to elucidate the reasons for the low expression of IGF2BP3 in HR+/HER2- breast cancer and its novel function as a transcription

al repressor with a key role in cancer suppression, thereby designing small molecule inhibitors to target DNMT3B/IGF2BP3 in the treatment of HR+/HER2- breast cancer.

Advances in the combination of nanomaterials and tumor ablation

Duo Yu

Department of Interventional Radiology, the First Hospital of China Medical University

Purpose Percutaneous tumor ablation is a minimally invasive treatment for tumors. The release of tumor neoantigens after ablation not only remodels the local tumor microenvironment, but also achieves distant effects by mediating local and systemic immune effects. However, studies have shown that a single ablation technique is not sufficient to achieve the desired anti-tumor immune effect. Numerous studies have shown that the combination of nanomaterials and tumor ablation can transform immunologically "cold" tumors into "hot" tumors, significantly improving the suppressive anti-tumor immune properties of the local microenvironment, while enhancing systemic anti-tumor immunity and the distant effect. The great advances in nanotechnology are expected to further enhance the synergistic anti-tumor efficiency and immune effects. This paper reviews the anti-tumor responses induced by different ablation techniques, including thermal ablation, cryoablation, high-frequency focused ultrasound, photodynamic therapy (PDT), magnetic heat therapy (MHT) and irreversible electroporation. The research progress in recent years on the combination of nanomaterials and ablation techniques in improving anti-tumor efficiency and enhancing immune effects is reviewed, mainly including materials based on engineered nano/micrometre platforms, such as tumor ablation in-situ vaccines, nano-metallic organic frameworks, polylactic acid-hydroxyacetic acid copolymers (PLGA), hydrogels and other nanomaterials. This paper discusses recent research advances in the use of nanomaterials in combination with ablation, demonstrating the immense immune effects of this synergistic therapy and its promising application in clinical oncology treatment.

Materials and methods This article focuses on metal-organic frameworks (MOFs), poly(lactic-co-glycolic acid) (PLGA), liposomes, and other nanomaterials such as carbon nanotubes and quantum dots. Metal-organic frameworks (MOFs) possess a high specific surface area and adjustable pore structures. They can not only load chemotherapeutic drugs or photosensitizers for chemotherapy and photodynamic therapy but also enhance the tumor ablation effect synergistically through responses to external stimuli. Poly(lactic-co-glycolic acid) (PLGA) nanoparticles, owing to their degradability and excellent drug encapsulation ability, are used for the sustained release of chemotherapeutic drugs in tumor ablation, effectively improving the drug efficacy and reducing systemic toxicity. Tumor in-situ vaccines, by activating the body's immune response and combining with ablation therapy, use nanomaterial carriers to deliver tumor antigens and immune adjuvants to the tumor site, triggering a specific immune response against tumor cells, thereby preventing tumor recurrence and metastasis. Liposomes, as classic nanocarriers, can encapsulate chemotherapeutic drugs, gene drugs, or hyperthermia agents and accumulate in tumor tissues through passive or active targeting, achieving efficient tumor ablation therapy. In addition, other nanomaterials such as carbon nanotubes and quantum dots also exhibit unique application potential in tumor ablation. For example, carbon nanotubes can be used for photothermal therapy, and quantum dots can be used for precise ablation under the guidance of tumor imaging. The application methods of these nanomaterials in tumor ablation cover physical ablation (photothermal, cryoablation, etc.), chemical ablation (release of chemotherapeutic drugs), biological ablation (immune activation), and the combined treatment of multiple ablation methods.

Results I. Therapeutic Efficacy

Nanomaterials significantly boost tumor ablation. Hydrogels as drug carriers raise tumor - site drug concentration by 2 - 3 - fold and extend drug residence from hours to days, with a 20% - 30% higher growth inhibition. MOFs in chemodynamic and photodynamic therapies show high cell apoptosis rates (50% - 60% in chemo - and enhanced ablation with external stimuli in photo -). PLGA nanoparticles sustain drug release for 1 - 2 weeks, reducing blood - drug fluctuations and shrinking tumors by 40% - 50%. Tumor in - situ vaccines, combined with ablation, cut recurrence by 40% - 50% and double - triple CD8+ T - cell infiltration. Liposomes, through EPR, increase tumor - tissue drug uptake by 3 - 4 times and achieve 70% - 80% local control in hyperthermia. Carbon nanotubes for photothermal therapy kill 70% - 80% of tumor cells, and quantum dots improve ablation accuracy, raising the complete remission rate by 15% - 20%.

II. Safety

Hydrogels, PLGA, and liposomes have good biocompatibility with no severe side effects. Their degradation products are non - toxic and can be metabolized. Nanomaterials also reduce chemotherapeutic drug toxicity, with liposome - encapsulated drugs cutting hematological and gastrointestinal toxicity incidence by 30% - 40%.

III. Tumor Microenvironment Regulation

Tumor in - situ vaccines and MOFs modulate immune cells, switching macrophages from M2 to M1. MOF - loaded adjuvants enhance dendritic - cell function. Hydrogels with angiogenesis inhibitors lower vascular density by 30% - 40% and boost oxygenation by 2 - 3 times. In summary, these nanomaterials show great promise in tumor treatment.

Conclusion Nanomaterials like hydrogels, MOFs, etc., offer distinct advantages in tumor ablation. Hydrogels can slowly release drugs, while MOFs are great at drug - loading and stimulus - responsive therapy. Their combined use shows broad prospects. However, challenges exist, such as difficult synthesis, unclear in - vivo safety, and obstacles in clinical translation. In the future, efforts should focus on optimizing material design, exploring combined - treatment strategies, promoting clinical translation through large - scale trials, and enhancing interdisciplinary integration. Nanomaterials hold great potential. Overcoming these challenges may improve tumor ablation efficacy, benefiting patients.

PO-158

Two Decades of Progress in Hepatocellular Carcinoma Research: A Comprehensive Bibliometric and Visualized Analysis (2004–2023)

Liqi Shang

The First Affiliated Hospital of China Medical University

Purpose This study conducts a comprehensive bibliometric analysis of hepatocellular carcinoma (HCC) research spanning 2004 to 2023, utilizing VOSviewer to map the evolving landscape of this field. As one of the most prevalent malignant tumors globally, HCC has attracted substantial scientific interest over the past two decades, generating an extensive corpus of literature.

Materials and methods Our analysis encompasses 93,987 publications extracted from the Science Citation Index Expanded Database of the Web of Science Core Collection, enabling the identification of key research hotspots and the projection of future directions.

Results The annual publication output demonstrated a fluctuating yet upward trajectory, with 65,583 articles (69.78%) published in the most recent decade (2014–2023). Geographically, China, the United States, and Japan emerged as the leading contributors. Among journals, PLOS One published the largest volume of studies, while Gastroenterology achieved the highest average citation rate, reflecting its significant academic impact. Institutionally, Fudan University stood out as the most prolific contributor. Thematic analysis revealed five major research clusters: molecular mechanisms, therapeutic strategies, prognosis and immunology, risk factors, and diagnostic approaches.

Conclusion These findings not only elucidate publication trends and collaborative networks but also highlight potential avenues for advancing HCC research. Notably, further exploration of HCC immune mechanisms is poised to drive transformative progress in diagnostic and therapeutic strategies, offering promising opportunities for improving patient outcomes.

PO-159

Dual-Targeted Microspheres Reshape Metabolic-immune Microenvironment and Reverse Multiple Dilemmas Post-embolization in Hepatocellular Carcinoma

Nan Jiang¹, Caifang Ni¹, Zifan Pei², Jiachen Xu³, Liang Cheng²

1. The first affiliated hospital of Soochow University

2. Soochow University

3. The fourth affiliated hospital of Soochow University

Purpose Transarterial embolization (TAE) is a cornerstone treatment for hepatocellular carcinoma (HCC), but its efficacy is often limited by post-embolization hypoxia-driven angiogenesis and metabolic reprogramming. This study aimed to develop a dual-functional embolic agent, ZnS-loaded gelatin microspheres (ZnS@GMs), to simultaneously target angiogenesis and glycolysis, reshape the tumor microenvironment, and enhance therapeutic outcomes.

Materials and methods Bioinformatics analysis and rat N1S1 liver tumor models were used to identify angiogenesis and glycolysis as key therapeutic targets. ZnS@GMs were synthesized to co-deliver H₂S and Zn²⁺, leveraging H₂S to inhibit mitochondrial respiration and destabilize HIF-1 α , and Zn²⁺ to directly target glycolytic enzymes. In vitro and in vivo experiments, including subcutaneous H22, orthotopic N1S1, and rabbit VX2 liver cancer models, were conducted to evaluate tumor suppression, vascular normalization, and immune activation. RNA sequencing, histopathological analysis, and flow cytometry were employed to assess molecular and cellular changes.

Results ZnS@GMs significantly suppressed tumor growth by inhibiting HIF-1 α /VEGF signaling and glycolytic metabolism. They induced immunogenic cell death, promoting dendritic cell maturation, cytotoxic T cell infiltration, and macrophage polarization toward an anti-tumor phenotype. In rodent and rabbit models, ZnS@GMs demonstrated robust embolic efficacy, vascular normalization, and enhanced immune infiltration. Combination with anti-PD-1 therapy elicited a potent abscopal effect, controlling both treated and distant tumors. RNA sequencing confirmed downregulation of angiogenesis- and glycolysis-related genes, alongside upregulation of immune activation pathways.

Conclusion This study demonstrates that ZnS@GMs effectively overcome post-embolization tumor adaptation by integrating metabolic modulation with immune activation. The dual-functional design of ZnS@GMs addresses the root causes of treatment resistance, offering a promising strategy for improving HCC therapy.

PO-160

Prediction model of survival in unresectable HCC with central bile duct invasion receiving TACE after biliary drainage: TEMP Score

Xinlin Zheng, Wenzhe Fan

The First Affiliated Hospital of Sun Yat-Sen University

Purpose Central bile duct invasion (BDI) by hepatocellular carcinoma (HCC) is rare and associated with poor prognosis, lacking treatment guidelines. While transarterial chemoembolization (TACE) is often used for unresectable cases, determining optimal candidates post-biliary drainage is controversial. We aim to develop a prognostic prediction model for unresectable HCC (uHCC) patients with central BDI receiving sequential TACE after successful biliary drainage.

Materials and methods We retrospectively analyzed 267 uHCC patients with central BDI receiving successful biliary drainage and sequential TACE from seven tertiary centers (2015-2021), divided into training (n=187) and validation (n=80) sets. Using Cox proportional-hazards regression model, we identified key prognostic indicators for overall survival (OS) and constructed a prediction model.

Results Pre-TACE total bilirubin (TBil) values, extrahepatic spread (EHS), multiple intrahepatic tumors (MIT), and portal vein tumor thrombus (PVTT) were identified as the significant clinical indicators for OS. These four parameters were included in a novel prediction model, named TEMP score, which could successfully categorize patients in the training set into three distinct risk grades with median OS of 26.9, 9.4, and 5.8 months, respectively. The TEMP score predicted the time-dependent areas under the receiver operating characteristic curves for OS at 6 months, 1 year, and 2 years of 0.813/0.907, 0.833/0.782, and 0.838/0.811 in the training and validation sets, with corresponding C-indices of 0.812/0.929, 0.829/0.761, and 0.818/0.791, respectively, outperforming other currently available models in both cohorts. The calibration curve of the model for predicting OS presented good consistency between observations and predictions in both the training set and validation set.

Conclusion The TEMP score effectively stratifies the prognosis of uHCC patients with central BDI who have undergone successful bile drainage and sequential TACE, helping to identify those who may benefit from TACE treatment.

PO-162

Study of the Mechanism by which CYP2W1 Promotes the Progression of Colorectal Cancer Liver Metastasis through Cholesterol Metabolism

Hui Zhang

Clinical Oncology School of Fujian Medical University, Fujian Cancer Hospital

Purpose Better understanding the molecular mechanisms of CRC liver metastasis to support early and targeted intervention measures can reduce the incidence of liver metastasis in patients and improve survival rates.

Materials and methods We obtained the expression profiles of CYP2W1 in primary and liver metastatic lesions using data from CRC patients in the GEO database and validated them using data from the GEPIA database and TIMER 2.0 database. We then silenced the expression of CYP2W1 in CT26 and HCT116 cells and assessed the biological functions of these cells in vitro through CCK8, colony formation, wound healing, and Transwell assays. We measured the expression of different mRNAs and proteins in CRC cells via RT-qPCR and Western blot experiments. Immunohistochemistry was used to determine the localization and expression of different proteins. We established subcutaneous xenograft mouse tumour models and spleen injection models to test the effects of CYP2W1 on the progression of mouse colon cancer and liver metastasis, as well as to investigate the underlying mechanisms.

Results Bioinformatics analysis revealed that CYP2W1 expression was significantly higher in liver metastatic lesions than in primary CRC tissues, identifying CYP2W1 as a potential therapeutic target for CRC liver metastasis. Our study demonstrated that CYP2W1 can promote the proliferation, migration, and invasion of CRC cells. In vivo animal experiments also confirmed that CYP2W1 can promote the progression of mouse colon cancer and liver metastasis. Mechanistic studies indicated that CYP2W1 can activate the cholesterol metabolic pathway and that cholesterol supplementation in the culture medium of CRC cells can reverse the growth inhibition caused by silencing CYP2W1.

Conclusion CYP2W1 can promote the occurrence and development of CRC and promote CRC liver metastasis through cholesterol metabolism. Targeting CYP2W1 is a potential new strategy to prevent the development of CRC liver metastasis.

PO-163

Efficacy and Safety of Radiofrequency Ablation Combined with Immunotherapy in Advanced Lung Cancer: A Retrospective Study.

Yong Li¹, Xiaobing Li²

1. Hanyang Hospital Affiliated to Wuhan University of Science and Technology

2. Hubei Cancer Hospital, Tongji Medical College, Huazhong University of Science and Technology

Purpose This retrospective study aims to evaluate the efficacy and safety of radiofrequency ablation (RFA) combined with immunotherapy in patients with advanced lung cancer.

Materials and methods We reviewed the clinical data of advanced lung cancer patients who received RFA combined with immunotherapy. The primary outcomes assessed were the overall survival (OS), progression-free survival (PFS), and the incidence of treatment-related adverse events. Additionally, the response rate to the combination therapy was analyzed.

Results A total of 60 patients were included in this study. The combination therapy showed a significant improvement in both OS and PFS compared to standard treatments. The median OS for patients receiving RFA combined with immunotherapy was 18 months, while the median PFS was 10 months. The overall response rate was 65%, with partial response observed in 50% and stable disease in 15%. The treatment was well-tolerated, with only 10% of patients experiencing grade 3 or higher adverse events, including mild to moderate pain and transient fever.

Conclusion The combination of radiofrequency ablation and immunotherapy demonstrates promising efficacy and an acceptable safety profile in the treatment of advanced lung cancer. This approach could provide an effective therapeutic option for patients with limited treatment options. Further prospective studies are necessary to confirm these findings and optimize treatment protocols.

PO-164

Efficacy and Safety of Interventional Hemostasis in Massive Hemoptysis Induced by Anti-Tumor Angiogenesis Therapy in Advanced Lung Cancer: A Retrospective Study.

Jinbo Liang¹, Xiaobing Li²

1. Yicheng People's Hospital

2. Hubei Cancer Hospital, Tongji Medical College, Huazhong University of Science and Technology

Purpose This retrospective study aims to evaluate the efficacy and safety of interventional hemostasis in patients with advanced lung cancer who develop massive hemoptysis following anti-tumor angiogenesis therapy.

Materials and methods We reviewed the medical records of advanced lung cancer patients who underwent interventional hemostasis after experiencing massive hemoptysis induced by anti-angiogenesis treatment. The primary outcomes assessed were the control of bleeding, the survival rate post-intervention, and any complications associated with the procedure.

Results A total of 45 patients were included in the study. The success rate of bleeding control through interventional hemostasis was 93%, with 10% of patients experiencing recurrence of hemoptysis. The overall survival rate for patients following the procedure was significantly improved compared to those who did not undergo the intervention. Complications were minimal, with only 5% of patients reporting minor adverse events, including infection and temporary respiratory distress.

Conclusion Interventional hemostasis demonstrates high efficacy and an acceptable safety profile in controlling massive hemoptysis in advanced lung cancer patients treated with anti-angiogenesis therapy. This approach should be considered an effective and safe management strategy for these patients to prevent life-threatening bleeding and improve prognosis. Further prospective studies are needed to confirm these findings.

PO-165

The Value and Significance of Health Education in Malignant Tumor Patients Undergoing Radioactive Particle Implantation Therapy.

Aoli Zhang,Xiaobing Li

Hubei Cancer Hospital, Tongji Medical College, Huazhong University of Science and Technology

Purpose Health education plays a crucial role in the treatment of malignant tumor patients undergoing radioactive particle implantation therapy. This study explores the value and significance of health education in improving patient outcomes during and after this specific treatment.

Materials and methods Radioactive particle implantation is a minimally invasive procedure that requires careful planning, precise execution, and post-treatment management.

Results Health education provides patients with essential information about the procedure, potential side effects, and necessary precautions, which enhances their understanding and cooperation. It also helps to reduce anxiety and fear, leading to better psychological well-being and treatment adherence. By equipping patients with knowledge, health education can facilitate early detection of complications, promote proper post-treatment care, and improve the overall quality of life. Furthermore, effective health education strengthens the communication between healthcare providers and patients, leading to better patient satisfaction and treatment compliance.

Conclusion In conclusion, integrating health education into the treatment process for malignant tumor patients receiving radioactive particle implantation therapy not only optimizes treatment outcomes but also empowers patients to actively participate in their care, promoting long-term health benefits.

PO-167

Surufatinib plus doublet (FOLFOX/FOLFIRI) or triplet (FOLFOXIRI) chemotherapy as second-line therapy in metastatic colorectal cancer (mCRC): updated results of a randomized, open-label phase II trial

Liyu Su, Shen Zhao, Yingquan Ye, Rongbo Lin
Fujian Cancer Hospital

Purpose The three active agents (oxaliplatin, irinotecan, and 5-FU/leucovorin) have demonstrated synergistic antitumor effects and may overcome resistance to standard doublet chemotherapy (FOLFOX/FOLFIRI) in metastatic colorectal cancer (mCRC). FOLFOXIRI as a second-line treatment for mCRC has shown promising outcomes (ORR 25%, DCR 71%, mPFS 5.7 months) in our previous phase II study, compared to doublet chemotherapy (ORR 4-15%, mPFS 2.5-4.2 months) as reported in the V308 study (Tournigand C, J Clin Oncol 2004). Additionally, surufatinib, a small-molecule kinase inhibitor targeting VEGFR1-3, FGFR, and CSF-1R, has been approved for neuroendocrine tumors (NET) in China. Preclinical studies suggest that surufatinib enhances the antitumor effects of chemotherapy by modulating the tumor microenvironment. This study aimed to evaluate the efficacy and safety of surufatinib combined with chemotherapy and to explore the differences between doublet (FOLFOX/FOLFIRI) and triplet (FOLFOXIRI) chemotherapy regimens in mCRC.

Materials and methods This open-label, 2-arm, phase II trial enrolled patients with mCRC who had progressed after standard first-line doublet chemotherapy. Patients were randomized (1:1) to receive surufatinib (250 mg, once daily) in combination with mFOLFOX6/FOLFIRI (arm A) or FOLFOXIRI (arm B), administered every 2 weeks until disease progression or unacceptable toxicity. The primary endpoint was objective response rate (ORR) per RECIST 1.1. Secondary endpoints included progression-free survival (PFS), disease control rate (DCR), overall survival (OS), and safety. A Simon 2-stage design was used, with each arm planning to enroll 28 patients in stages 1 and 2. If $\geq 7/28$ patients achieved a partial or complete response (PR/CR), the arm was deemed worthy of further investigation.

Results As of the data cutoff date of March 31, 2024, both arms completed enrollment (29 patients in arm A, 27 evaluable for efficacy; 27 patients in arm B, 23 evaluable for efficacy). The median age was 63/60 years, 67/80% were male, 40/47% had an ECOG PS of 1, and 73/60% had ≥ 2 metastatic sites. The ORR was 25.93% (7/27; 1 CR and 6 PR) in arm A and 34.78% (8/23; 8 PR) in arm B, with DCRs of 81.5% and 82.6%, respectively. Median PFS was 5.52 months (95% CI: 3.49-7.55) in arm A and 5.95 months (95% CI: 5.63-6.27) in arm B. All patients were evaluable for safety. The most common treatment-emergent adverse events (TEAEs; total; grade ≥ 3) in arm A were anemia (55.17%; 0%), neutropenia (44.83%; 13.79%), and leukopenia (41.38%; 3.4%); in arm B, they were leukopenia (66.67%; 22.22%), anemia (62.96%; 14.81%), and neutropenia (62.96%; 40.74%).

Conclusion Surufatinib combined with either mFOLFOX6/FOLFIRI or FOLFOXIRI as a second-line treatment for mCRC achieved its primary endpoint with an acceptable safety profile. These promising results warrant further investigation in larger mCRC cohorts.

PO-168

Real-world efficacy and safety of TACE plus Lenvatinib with or without programmed death factor 1 (PD-1) inhibitor in huge hepatocellular carcinoma at BCLC stage B-C : a multicenter retrospective study with propensity score matching

Ye Liang

Interventional Radiology at Chinese PLA General Hospital

Purpose To compare the efficacy and safety of transarterial chemoembolization (TACE) combined with lenvatinib and programmed death receptor-1 (PD-1) inhibitor (TACE+Len+PD-1) versus TACE combined with lenvatinib (TACE+Len) in the treatment of huge HCC ($\geq 10\text{cm}$) at BCLC stage B-C.

Materials and methods A total of 147 patients in TACE+Len group and 241 patients in TACE+Len+PD-1 group were analysed. Propensity score matching (PSM), inverse probability treatment weighting (IPTW), and coarsened exact matching (CEM) analyses were used to balance the bias between two groups. Mediation analysis was performed to assess the impact of treatment type on survival.

Results The median progression-free survival (PFS) was 6.03 months (95% CI, 4.47-10.73) in TACE+Len group and 8.30 month (95%CI, 5.07-13.3) in TACE+Len+PD-1 group. The TACE+Len+PD-1 group had better PFS than the TACE+Len group in the entire cohort (hazard ratio [HR], 0.669; 95% CI, 0.539–0.830; $P < 0.001$). This advantage in PFS was sustained in the PSM, IPTW, and CEM cohorts. TACE+Len+PD-1 group also showed better overall survival (OS) than the TACE+Len group (HR, 0.659; 95% CI, 0.565–0.828; $P < 0.001$). The OS was also superior in the PSM, IPTW, and CEM cohorts. The objective response rate (ORR) in TACE+Len+PD-1 group was higher than TACE+Len group. Further mediation analysis indicated that tumor responses at three and six months had different mediation effects on survival.

Conclusion TACE combined with lenvatinib and PD-1 inhibitor showed improved better OS and PFS than TACE plus lenvatinib. This triple therapy could be recommended as a first-line treatment for huge HCC at BCLC stage B-C.

PO-169

A Novel Dual Radiosensitizer Reverses Resistance to ¹²⁵I Brachytherapy and Enhances Antitumor Efficacy

Zhongkai Wang^{1,2}, Cheng Feng^{1,2}, Jian Lu^{1,2}, Jinhe Guo^{1,2}

1. Center of Interventional Radiology & Vascular Surgery, Department of Radiology, Zhongda Hospital, Medical School, Southeast University

2. Basic Medicine Research and Innovation Center of Ministry of Education, Zhongda Hospital, Southeast University

Purpose Iodine-125 (¹²⁵I) brachytherapy is a pivotal treatment for advanced hepatocellular carcinoma (HCC), delivering high-dose radiation directly to tumors while sparing surrounding healthy tissues. Despite its widespread clinical use, a substantial subset of HCC patients develops resistance to ¹²⁵I brachytherapy, primarily due to the hypoxic tumor microenvironment. Additionally, dysregulation of apoptotic pathways further contributes to radioresistance. These resistance mechanisms compromise treatment efficacy, necessitating strategies that address both hypoxia and alternative cell death pathways to enhance ¹²⁵I brachytherapy outcomes.

Materials and methods We developed a MnO_x-CaO₂@Ma nanoparticle system by incorporating CaO₂ nanoparticles into MnO_x nanoflowers and coating them with macrophage membranes to prolong circulation time. This system simultaneously generates H₂O₂ and O₂, effectively alleviating tumor hypoxia. The MnO_x nanoflowers not only deplete glutathione (GSH) and downregulate GPX4 but also catalyze the conversion of H₂O₂ into reactive oxygen species (ROS), thereby inducing lipid peroxidation and ferroptosis. To evaluate the therapeutic potential, we systematically assessed the system's oxygen-generating capacity, hypoxia-reversing efficacy, and radiosensitizing effects on ¹²⁵I brachytherapy in HCC.

Results The MnO_x-CaO₂@Ma system demonstrated a remarkable enhancement in radiosensitivity, increasing the response of Hepa 1-6 cells to ¹²⁵I brachytherapy. Through dual modulation of tumor hypoxia and apoptotic resistance pathways, this nanoplateform significantly improved the therapeutic outcomes of ¹²⁵I brachytherapy in orthotopic Hepa 1-6 tumor-bearing C57BL/6 mice.

Conclusion The MnO_x-CaO₂@Ma nanoparticle platform offers a promising strategy for overcoming radioresistance in HCC. By addressing hypoxic conditions and evading apoptosis, this approach provides valuable insights for developing advanced radiosensitizers that integrate apoptotic and non-apoptotic cell death pathways to optimize cancer treatment outcomes.

PO-171

Efficacy and safety of transarterial chemoembolization combined with lenvatinib plus programmed death-1 inhibitor for hepatocellular carcinoma with the hepatic vein and/or inferior vena cava tumor thrombus

Long-Wang Lin

Zhongda Hospital Affiliated to Southeast University

Purpose The aim of this study was to assess the safety and effectiveness of transarterial chemoembolization (TACE) plus lenvatinib with a programmed death-1 (PD-1) inhibitor compared with TACE plus lenvatinib and TACE alone for hepatocellular carcinoma (HCC) with hepatic vein and/or inferior vena cava tumor thrombus (HVTT and IVCTT).

Materials and methods Data on HCC accompanied by HVTT and IVCTT from June 2015 to August 2022 were analyzed in this single-center retrospective study. Drug-eluting bead TACE (DEB-TACE) or conventional TACE (cTACE) was used. The primary study outcomes were overall survival (OS) and progression-free survival (PFS). Univariate and multivariate Cox analyses were performed to determine the predictive factors for OS and PFS. A subgroup analysis was conducted.

Results Overall, 214 patients were enrolled. Among them, 60 received triple therapy consisting of TACE, lenvatinib, and PD-1 inhibitors (TACE+L+P), 72 received dual therapy consisting of TACE and lenvatinib (TACE+L), and 82 received TACE alone. The TACE+L+P group (16.2; 95% confidence interval [CI]: 12.8~19.5 months) had a significantly longer median OS compared with the TACE+L group (11.2; 95% CI: 10.0~12.3 months) ($P = 0.001$) and the TACE group (8.3; 95% CI: 7.7~8.5 months) ($P < 0.001$); the TACE+L+P group (12.3; 95% CI: 10.9~13.7 months) had a significantly longer median PFS compared with the TACE+L group (8.5; 95% CI: 7.7~9.2 months) ($P < 0.001$) and the TACE group (6.2; 95% CI: 5.8~6.3 months) ($P < 0.001$). Multivariate Cox analysis demonstrated that treatment strategy was a significant factor for OS and PFS. Skin rash was more common in the triple therapy group and might be attributed to PD-1 ligand inhibitor therapy (33.33% vs. 16.66%, $P = 0.026$).

Conclusion Triple therapy consisting of TACE plus lenvatinib with a PD-1 inhibitor showed promising efficacy for advanced HCC patients with HVTT and IVCTT, with manageable safety profiles.

PO-172

Preliminary Safety and Efficacy of Upfront FOLFOXIRI and Bevacizumab with Cadonilimab in Patients with Proficient Mismatch Repair/Microsatellite Stable (pMMR/MSS) Metastatic Colorectal Cancer: A Multicenter Phase II Study (SYLT-026)

Liyu Su¹, Shen Zhao¹, Yingquan Ye¹, Yanhong Meng², Rongbo Lin¹

1. Fujian Cancer Hospital

2. Nanping Jianyang First Hospital

Purpose The AtezoTRIBE phase II trial demonstrated that adding Atezolizumab to upfront FOLFOXIRI plus Bevacizumab significantly improved overall survival (OS) in patients with metastatic colorectal cancer (mCRC). However, the improvement in OS was modest within the pMMR/MSS subgroup (HR, 0.80 [80% CI, 0.63–1.02]; $P = 0.117$) [Antoniotti, et al, J Clin Oncol, 2024]. Cadonilimab, a humanized bispecific antibody targeting both PD-1 and CTLA-4, may offer enhanced therapeutic benefits. Therefore, this study aims to investigate whether the addition of Cadonilimab to upfront FOLFOXIRI plus Bevacizumab improves efficacy while maintaining safety in patients with pMMR/MSS mCRC.

Materials and methods This multicenter, single-arm phase II study enrolled treatment-naïve patients with pMMR/MSS mCRC, aged 18–75, who had at least one measurable lesion according to RECIST 1.1, an ECOG performance status (PS) of 0–2, and adequate organ function. Patients with dMMR/MSI-H tumors or prior immunotherapy were excluded. Eligible participants received FOLFOXIRI (irinotecan 165 mg/m², oxaliplatin 85 mg/m², leucovorin 200 mg/m², and fluorouracil 2400 mg/m² as a 48-hour infusion), along with Bevacizumab (5 mg/kg), and Cadonilimab (6 mg/kg). Treatment was administered for up to twelve 14-day cycles, followed by maintenance therapy with fluoropyrimidine and Bevacizumab plus Cadonilimab for up to 52 weeks, or until disease progression, unacceptable toxicity, or withdrawal of consent. Patients were equally enrolled, with 10 having liver metastases and 10 without. The primary endpoint was objective response rate (ORR) per RECIST 1.1.

Results As of August 30, 2024, 20 patients were enrolled, with a median age of 65.5 years (range: 33–74). Of these, 40% had an ECOG PS of 1 or 2, 55% had three or more metastatic organs, and 7 patients (35%) had RAS or BRAF mutations. The median follow-up was 5.0 months. Fifteen patients underwent at least two imaging assessments, revealing a confirmed ORR of 100% (15/15) and a disease control rate (DCR) of 100%. The median progression-free survival (PFS) and OS data were not yet mature. All 20 patients experienced treatment-emergent adverse events, most of which were grade 1 or 2. One patient (5%) discontinued treatment due to immune-mediated colitis. The most common grade 3/4 adverse events included neutropenia (55%), leukopenia (15%), infusion reactions (5%), dermatitis (5%), colitis (5%), anemia (5%), elevated ALT (5%), and diarrhea (5%). No new safety signals were identified.

Conclusion In conclusion, Cadonilimab in combination with FOLFOXIRI and Bevacizumab demonstrated promising efficacy and a manageable safety profile as a first-line treatment for patients with pMMR/MSS mCRC. Further investigation in larger trials is warranted.

PO-174

Tislelizumab (Tisle) combined with POFI (irinotecan, paclitaxel, oxaliplatin, and 5-FU/levoleucovorin) as first-line treatment of advanced gastric/gastroesophageal junction adenocarcinoma (AGC): OS analysis results of the SYLT-023

Liyu Su, Shen Zhao, Yingquan Ye, Rongbo Lin
Fujian Cancer Hospital

Purpose Tisle is an anti-PD-1 antibody. The combination of Tisle + XELOX/FP is a first-line treatment for AGC in China. Both irinotecan and paclitaxel have also demonstrated antitumor activity in AGC. In this phase II study, we explored the safety, tolerability, and efficacy of Tisle + POFI as a first-line treatment for HER-2 negative, pMMR AGC.

Materials and methods In a phase I dose-finding study using a standard 3+3 design, subjects received four escalating dose levels (DL) of irinotecan/paclitaxel (mg/m^2): 135/45 (DL #1), 150/45 (DL #2), 135/67.5 (DL #3), and 135/90 (DL #4) in combination with Tisle 200 mg, oxaliplatin $85 \text{ mg}/\text{m}^2$, levoleucovorin $200 \text{ mg}/\text{m}^2$, and 5-FU $2400 \text{ mg}/\text{m}^2$ over 46 hours every 2 weeks. Primary endpoints were safety, tolerability, and RP2D.

Results Fifteen treatment-naïve AGC subjects were enrolled (3 each in DL #1, DL #2, and DL #3, and 6 in DL #4). The median age was 65 years (range 36-72); 80% were male. Two subjects (13.3%) were diagnosed with GE junction cancer, 11 (73.3%) had undifferentiated disease, and 5 (33.3%) had liver metastasis. PD-L1 CPS scores were 5 ($n = 5$); 1 ($n = 1$); and 0 ($n = 9$). All subjects were evaluated for DLT. One DLT (grade 4 neutropenia) occurred within 28 days in DL #4. No maximum tolerated dose was reached; the RP2D was DL #4. As of September 18, 2024, the confirmed objective response rate in 15 subjects with measurable disease was 100% (1 CR, 12 PR) per RECIST 1.1. Of the 2 subjects with non-measurable disease, one was a CR and the other was non-CR/non-PD. The median PFS was 10.51 months (95% CI: 7.44, 13.58) (versus 6.9 [5.7-7.2] months for the ITT population in RATIONALE 305, ESMO 2023), the median DOR was 7.39 months (95% CI: 5.34, 9.44), and the median OS was 14.75 months (95% CI: 5.48, 24.02). The OS showed no significant differences between CPS ≥ 1 and CPS < 1 . All subjects (100%) experienced AEs. Seven subjects ($n = 7$, 46.67%) reported grade ≥ 3 AEs, including neutropenia ($n = 7$; 46.67%), leukopenia ($n = 3$; 20%), and anemia ($n = 2$; 13.33%).

Conclusion Tisle + POFI was well-tolerated and demonstrated preliminary antitumor activity in AGC. A phase II study is ongoing.

PO-175

Textbook Outcome in Low Rectal Cancer Patients Undergoing Laparoscopic or Open Surgery: 3-Year Results from the Multicentric LASRE Trial

Yanwu Sun, Zihan Tang, Xiaojie Wang, Zhenyu Xu, Weizhong Jiang, Ying Huang, Pan Chi
Fujian Medical University Union Hospital

Purpose The textbook outcome has emerged as a valuable metric for quality assessment in oncological surgery. However, its application within randomized controlled trials involving low rectal cancer remain underexplored. This study aimed to investigate the incidence and predictors of textbook outcome in patients with low rectal cancer undergoing laparoscopic or open resection.

Materials and methods This post-hoc analysis included patients from the prospective, multicentric LASRE trial. Eligible patients had clinically staged I-III rectal cancer located within 5 cm of the dentate line, with a tumor diameter less than 6 cm, and they underwent radical laparoscopic or open surgery. A textbook outcome was defined by multiple criteria, such as no 30-day postoperative mortality, absence of intraoperative and postoperative complications, achievement of an R0 resection (negative margins: circumferential resection margin >1 mm, proximal resection margin >1 mm, and distal resection margin >1 mm), and good total mesorectal excision (TME) quality (complete or nearly complete TME).

Results A textbook outcome was achieved in 74.9% of patients, with a higher rate in the laparoscopic group (71.2%) than in the open group (76.7%). Multivariate analysis identified independent predictors of non-textbook outcome, including BMI >24 kg/m², surgical type (abdominoperineal resection), and operative time >200 minutes. Achievement of a textbook outcome was associated with improved DFS.

Conclusion Achieving a textbook outcome is significantly associated with improved DFS in patients with low rectal cancer. These findings highlight the importance of optimizing perioperative and intraoperative care to enhance surgical outcomes, particularly within the context of randomized controlled trials.

Comparative Oncologic Outcomes of Laparoscopic vs. Open Surgery for Early-Onset Low Rectal Cancer: 3-Year Results from the LASRE Trial

Yanwu Sun, Zhenyu Xu, Xiaojie Wang, Zihan Tang, Weizhong Jiang, Ying Huang, Pan Chi
Fujian Medical University Union Hospital

Purpose Low rectal cancer, due to its anatomical location, presents unique surgical challenges. Early-onset low rectal cancer (EO-LRC), diagnosed in patients younger than 50 years, may have distinct biological and clinical characteristics. This study aims to evaluate and contrast the oncologic outcomes of laparoscopic and open surgery in EO-LRC patients.

Materials and methods In this post-hoc analysis of the LASRE trial, 1039 patients aged 18 - 75 years, diagnosed with rectal adenocarcinoma located within 5 cm of the dentate line, were randomly assigned to either the open or laparoscopic resection group. The primary endpoints of this analysis were the 3-year overall survival (OS) and disease-free survival (DFS).

Results Patients with EO-LRC exhibited better ECOG performance status and lower ASA scores; however, they presented with more advanced disease. Preoperative therapy was more prevalent in EO-LRC patients. Laparoscopic surgery was more conducive to low anterior resection and sphincter preservation. The operative time and blood loss were comparable. EO-LRC patients had a higher proportion of pN2 stage disease and poorly differentiated tumors. The quality of total mesorectal excision (TME) and the achievement of negative margins were similar. The 3-year OS and DFS rates were equivalent between groups. Multivariate analysis identified preoperative therapy and pN classification as significant prognostic factors for DFS. No significant differences in oncologic outcomes were observed between groups.

Conclusion Laparoscopic TME provides non-inferior oncologic control in EO-LRC despite aggressive tumor biology. These results emphasize the necessity for personalized treatment strategies that take into account the unique biological and clinical characteristics of EO-LRC.

PO-177

Hawthorn Standardized Extract (HSE) Plus Standard Opioid Analgesia to Treat Refractory Cancer Pain: A Single-Arm Phase I Trial (SYLT-024)

Liyu Su, Shen Zhao, Yingquan Ye, Rongbo Lin
Fujian Cancer Hospital

Purpose Refractory cancer pain does not respond adequately to standard pain management treatment. In vitro and in vivo studies have shown that HSE confers central and peripheral analgesic effects. This study explored the safety, tolerability, and efficacy of adding HSE to standard opioid analgesia in patients with refractory cancer pain.

Materials and methods Patients with an average NRS score (0=no pain and 10=excruciating pain) of 3-6 who reported unsatisfactory pain control after 1-2 weeks of opioid treatment were enrolled into a phase 1 dose-finding study using a standard 3+3 design. In combination with a stable dose of standard opioid analgesia given over 7 days, subjects received five escalating dose levels of HSE: 8.0 g BID, 12.0 g BID, 16.0 g BID, 16.0 g TID, or 24.0 g TID. Primary objectives were safety, tolerability, and recommended phase 2 dose (RP2D).

Results Fifteen subjects were enrolled (3 at each dose level). Median age was 58 (range 29-73) years; 8 pts (53.3%) were female. Primary cancer sites included: colorectal (n=10); stomach (n=4); and pancreatic (n=1). Metastatic sites included: lymphatics (n=10); liver (n=6); bone (n=5); peritoneum (n=4); lung (n=3); and other (n=3). The median average NRS score at baseline was 4 (IQR: 3.00-4.75). All subjects were evaluated for dose-limiting toxicity (DLT); none occurred within the 7-day treatment period and no maximum tolerated dose was reached. A mixed-effects model used to analyze NRS scores showed that they tended to decrease as the number of days increased. Using a linear regression equation to analyze the relationship between NRS scores and number of days for each dose level showed the largest decrease in the 24.0g TID group in which the NRS score decreased by an average of 0.26 points for every additional day. The RP2D was identified as 24.0 g TID. Eight subjects experienced grade 1-2 treatment-related adverse events including anorexia (n=3), nausea (n=2), vomiting (n=2), and constipation (n=1).

Conclusion HSE combined with standard opioid analgesia was well tolerated and showed preliminary adjuvant analgesic activity in patients with refractory cancer pain.

PO-178

Transdermal fentanyl (TDF) vs immediate-release morphine tablets (IRMT) as opioid titration for opioid-naïve moderate cancer pain (ONMCP): a randomized, open-label, multi-site phase 3 trial

Liyu Su, Shen Zhao, Yingquan Ye, Rongbo Lin
Fujian Cancer Hospital

Purpose Oral IRMT titration is commonly used in ONMCP, but alternative routes are needed for some circumstances (e.g. Bowel obstruction). In China the lowest available dose of TDF is 25 µg/h, a relatively high initial titration dose. The newest patches allow fentanyl administration to 12.5 µg/h by cutting them in half. This study explored the efficacy and safety of TDF at 12.5 µg/h as initial titration dose.

Materials and methods A 28-day, open-label randomized trial was conducted at 4 cancer centers in China. ONMCP patients (NRS 4-6; 0=no pain and 10=excruciating pain), were randomly assigned to either TDF (Arm 1) or IRMT (Arm 2). Arm 1 consisted of a dose of 12.5 µg/h plus a single starting dose of IRMT 5 mg. Breakthrough cancer pain (BTcP) rescue was IRMT 5 mg at 1-hour intervals. TDF dosage was adjusted every 72 hours based on total IRMT rescue dose used in the past 24 hours (TDF in 2.1 mg increments per 30mg IRMT) with corresponding adjustments in rescue doses. Arm 2 was 5 mg orally every 4 hours, with BTcP management the same as Arm 1. Extended-release morphine was administered after 24 hours and adjusted daily based on total IRMT consumption, divided into 2 doses every 12 hours. The primary outcome was response defined as ≥20% reduction in NRS score at days 28 from baseline. A total of 209 patients were required for the non-inferiority test.

Results The trial terminated early due to slow enrollment amid COVID-19. As of July 31, 2022, 72 patients were enrolled, 34 (47.2%) in Arm 1 and 38 (52.8%) in Arm 2. Pain reduction outcomes are shown below. In the PPS population, the primary outcome was reached at day 28 (difference -0.03; 95% CI: -0.10-0.03; P=0.021). ESAS scores, patient satisfaction scores, and adverse effects were not significantly different between arms.

Conclusion Despite limitations, the study demonstrated that initiating opioid titration with at 12.5 µg/h is an acceptable and tolerable alternative in ONMCP patients.

HBV reactivation and its management in HBV-related hepatocellular carcinoma patients who underwent HAIC-targeted-immune-antiviral therapy: a multicenter study

Jiayun Liu¹, Bo Sun¹, Jiahua Zou², Xiaolin Zhang³, Haitao Li³, Hongyao Hu⁴, Hui Zhao⁴, Wei Lu⁵, Xun Ding⁵, Guilin Zhang¹, Ziqiao Lei¹, Chuansheng Zheng¹, Xuefeng Kan¹

1. Union Hospital, Tongji Medical College, Huazhong University of Science and Technology, Wuhan 430022, China

2. Department of Oncology, Huanggang Central Hospital, Huanggang 438000, China

3. Department of Radiology, Yichang Central People's Hospital, First College of Clinical Medical Science, China Three Gorges University, Yichang 443003, China

4. Department of Interventional Radiology, Renmin Hospital of Wuhan University, Wuhan 430060, China

5. Department of Interventional Diagnostic and Therapeutic Center, Zhongnan Hospital of Wuhan University, Wuhan 430071, China

Purpose Hepatitis B virus (HBV) reactivation may occur during hepatocellular carcinoma (HCC) treatments. This study aimed to assess HBV reactivation, its impact on prognosis, and its management in patients with HBV-related HCC, who received hepatic arterial infusion chemotherapy (HAIC) plus tyrosine kinase inhibitors (TKIs), immune checkpoint inhibitors (ICIs), and entecavir (HAIC+TKIs+ICIs+entecavir) treatments.

Materials and methods From January 2021 to December 2023, 307 patients in five centers with advanced HBV-related HCC, who received the quadruple treatment (HAIC+TKIs+ICIs+entecavir), were included. The HBV reactivation in these patients was observed. After HBV reactivation, one group patients continued the entecavir (HBV-R-E) treatment, the other group received the additional treatment of tenofovir alafenamide fumarate (HBV-R-E-T). Survivals of patients between different groups were compared.

Results The HBV reactivation was observed in 44 (14.3%) patients. Most patients (70.8%) in HBV-R-E-T group had a significant decrease of serum HBV-DNA level. The median progression-free survival and median overall survival (OS) in the HBV non-reactivation group were significantly longer than those of in the HBV reactivation group ($p < 0.001$, $p < 0.001$). The HBV-DNA level $\geq 1 \times 10^4$ IU/mL, positive HBeAg, and white blood cell count $< 4 \times 10^9$ /L were the independent risk factors of HBV reactivation. In addition, the median OS of patients in the HBV-R-E-T group was significantly longer than that of patients in the HBV-R-E group ($p < 0.001$).

Conclusion HBV reactivation could occur during the quadruple treatment (HAIC+TKIs+ICIs+entecavir), and it was associated with a poor prognosis. The additional treatment with tenofovir alafenamide fumarate can effectively manage the HBV reactivation and improve the survival of these HBV reactivation patients.

PO-180

Molecular mechanism and clinical translational study of remodeling immunosuppressive microenvironment in human lung adenocarcinoma by targeting CHCHD3-cGAS pathway

Zhang Mengzhe, Zhenfa Zhang

Tianjin medical university cancer institution and hospital

Purpose A significant proportion of lung adenocarcinoma (LUAD) patients exhibit poor response to neoadjuvant immunotherapy combined with chemotherapy, which adversely affects their prognosis. Identifying novel therapeutic targets and compounds to overcome this resistance is imperative.

Materials and methods We employed single-cell RNA sequencing (scRNA-seq) and spatial transcriptomics to identify potential biomarkers associated with poor prognosis in LUAD patients undergoing neoadjuvant immunotherapy combined with chemotherapy. Validation was performed using Tet-op-hEGFR-TD/CC10rtTA bitransgenic (EC) mouse models, NOD.Cg-PrkdcscidIL2rgtm1Wjl/SzJ (NSG) mouse models, humanized HSG mouse models, and patient-derived xenograft (PDX) models. Techniques included immunostaining, flow cytometry, in vivo tumorigenicity assays, RT-PCR, co-immunoprecipitation (Co-IP), drug screening, and luciferase reporter assays.

Results scRNA-seq and spatial transcriptomics revealed the significant role of the CHCHD3 gene in LUAD immunotherapy. Overexpression of CHCHD3 exhibited immunosuppressive effects in both PDX and EC mouse models. CHCHD3 directly interacts with cGAS, inhibiting the cGAS-STING pathway and reducing IFN- γ production. Conversely, CHCHD3 knockout upregulated CXCL5, enhancing the recruitment of CD8⁺ T cells, NK cells, and macrophages, thereby augmenting immunotherapy efficacy. Combining a CHCHD3 inhibitor with a PD-1 agonist significantly improved therapeutic outcomes in LUAD patients with high CHCHD3 expression.

Conclusion Our findings underscore the pivotal role of CHCHD3 in modulating the cGAS-STING pathway and suppressing CXCL5-mediated immune cell recruitment. Targeting CHCHD3 may enhance the sensitivity of LUAD to both chemotherapy and immunotherapy, offering a promising strategy for improving patient outcomes.

Survival Analysis and Nomogram for Postoperative Pulmonary Sarcomatoid Carcinoma Patients: SEER Database Analysis and External Validation

Chao Yi Jia, Wen Hao Zhao, Xin Li, Dian Ren, Hong Yu Liu, Jun Chen, Jia Cy
Tianjin Medical University General Hospital

Purpose Pulmonary sarcomatoid carcinoma (PSC) is a rare and deadly form of aggressive lung cancer. Surgery is considered one of the reliable treatment options for patients with PSC. This study aims to develop a nomogram to predict the overall survival (OS) of PSC patients undergoing surgery.

Materials and methods To develop the model, 481 PSC patients were extracted from the Surveillance, Epidemiology, and End Results (SEER) database as the training cohort. A total of 45 PSC patients who underwent surgery at Tianjin Medical University General Hospital were used as the external validation cohort. The discriminative capacity of the nomogram was rigorously assessed using time-dependent receiver operating characteristic (ROC) curves, represented by the area under the curve (AUC), the concordance index (C-index), and calibration curves. Decision curve analysis (DCA) was employed to comparatively evaluate the prognostic prediction performance between the nomogram and the 8th American Joint Committee on Cancer (AJCC) TNM staging system. Cox regression risk models were used to identify independent factors affecting patient prognosis. Kaplan-Meier survival analysis was performed for survival analysis based on risk stratification. Statistical significance was defined as $P < 0.05$, with all tests being two-sided.

Results After determining the relevant variables to include through Lasso and Cox regression analyses, we constructed a nomogram (Figure 1E). The concordance index (C-index) of the nomogram was 0.657 (95% CI, 0.638 to 0.676) in the training cohort and 0.716 (95% CI, 0.671 to 0.761) in the external validation cohort. In the training cohort, the AUC values for the 1-year, 3-year, and 5-year survival rates were 0.696, 0.710, and 0.663. In the external validation cohort, the AUC values for the 1-year, 3-year, and 5-year survival rates were 0.809, 0.765, and 0.785. Both the C-index and AUC indicate strong discriminatory ability of the nomogram. The calibration curve demonstrated a high degree of consistency between the predicted values and the actual data obtained from both the training and validation cohorts. DCA suggested that our nomogram outperforms the 8th AJCC-TNM staging system in predicting OS, indicating its potential clinical utility.

Conclusion In conclusion, we conducted survival analysis and developed a nomogram with robust C-index and AUC values. The calibration curves for the nomogram in both the training and external validation cohorts demonstrated excellent concordance between the predicted estimates and the actual observations. Additionally, the DCA curves indicated that the nomogram outperformed the 8th edition AJCC-TNM staging system in predicting OS, highlighting the clinical utility of the model. Using the nomogram to predict the 1-year, 3-year, and 5-year OS of PSC patients, this study aims to assist clinicians in stratifying surgically treated pulmonary sarcomatoid carcinoma patients and making informed, personalized treatment decisions.

PO-182

Analysis of the Efficacy of TACE Combined with Fuzhengxiao yao granules in the Treatment of Stage II Hepatitis B-Related Liver Cancer.

Xiaodong Li, Zhen Li

The First Affiliated Hospital of Zhengzhou University

Purpose To investigate the clinical efficacy of transarterial chemoembolization (TACE) combined with Fuzheng Xiaoyao granules in the treatment of hepatitis B-related primary liver cancer.

Materials and methods The clinical data of 56 patients with hepatitis B-related liver cancer who were prospectively enrolled were analyzed. Among them, 50 patients with stage II liver cancer achieved complete remission (CR) one month after TACE treatment. These patients were randomly divided into a control group and an experimental group, with 25 patients in each group. Both groups received symptomatic basic treatment. The experimental group was treated with TACE combined with Fuzheng Xiaoyao granules II (administered twice daily), while the control group received TACE combined with a placebo of Fuzheng Xiaoyao granules II. The clinical benefit rate, progression-free survival (PFS), T-cell subsets, and safety indicators such as liver and kidney function, platelet count (PLT), and prothrombin time (PT) were compared between the two groups.

Results The clinical benefit rates for the control and experimental groups were 39% and 61%, respectively, with a statistically significant difference ($P < 0.05$). The progression-free survival (PFS) was 9 months for the control group and 12 months for the experimental group, showing a statistically significant difference ($P < 0.05$). T-cell subset analysis revealed significant differences in CD3+, CD4+, CD8+, and CD4+/CD8+ ratios at 6 and 12 months post-treatment in the experimental group when compared to pre-treatment values. Furthermore, significant differences were observed between the experimental and control groups ($P < 0.05$). No significant differences in liver and kidney function, platelet count (PLT), prothrombin time (PT), or albumin (ALB) levels were found between the two groups ($P > 0.05$), indicating that Fuzheng Xiaoyao granules have good safety.

Conclusion Fuzheng Xiaoyao granules combined with TACE can improve the clinical benefit rate, prolong survival, and enhance prognosis in patients with stage II hepatitis B-related liver cancer.

PO-183

Highly elastic polyvinyl alcohol embolic microspheres for effective transarterial embolization

Li Liu¹, Xiangxian Xu³, Xiaoli Zhu⁴, Meng Dang², Yunming Zhang¹, Donghong Shi¹, Shenzhe Liu², Zhiwei Zhang², Jing Pan¹, Jing Zhong¹, Lin Ou-yang¹, Zhaogang Teng¹, Longjiang Zhang¹

1. Jinling Hospital of Nanjing University

2. Key Laboratory for Organic Electronics and Information Displays and Jiangsu Key Laboratory for Biosensors, Institute of Advanced Materials, Jiangsu National Synergetic Innovation Centre for Advanced Materials, Nanjing University of Posts and Telecommunications

3. Department of Radiology, Jiangsu Province Hospital of Chinese Medicine, Affiliated Hospital of Nanjing University of Chinese Medicine

4. Department of Interventional Radiology, The First Affiliated Hospital of Soochow University

Purpose Transarterial embolization therapy is a highly promising, minimally invasive interventional procedure for treating vascular and neoplastic diseases in the clinic. The use of highly elastic and deformable embolization microspheres is crucial for ensuring smooth delivery through the catheter and achieving complete endovascular embolization.

Materials and methods The results obtained from an in vitro embolization model demonstrated the good stability and elastic deformation ability of MegaSphere.

Results These properties allow these spheres to aggregate tightly and effectively embolize blood vessels at different levels. Furthermore, in a rabbit model, we achieved highly efficient renal embolization via MegaSphere. These microspheres could reach the distal vessels of the renal artery and effectively embolize small arteries within the renal cortex, resulting in complete terminal embolization. Substantial necrosis of the renal parenchyma was observed within seven days after embolization, indicating an excellent embolization effect. Moreover, in a rabbit model with liver VX2 transplant tumors, the use of drug-loaded MegaSphere-doxorubicin microspheres demonstrated strong efficacy in antitumor chemoembolization therapy. Through blockade of the tumor blood supply and increased local chemotherapy, effective inhibition of liver tumor progression was achieved within seven days following transcatheter arterial chemoembolization (TACE).

Conclusion In conclusion, this study highlights the promising potential of MegaSphere as an embolic agent with potential for clinical translational applications.

PO-184

Comparing the performance of ChatGPT and ERNIE Bot in answering questions regarding liver cancer interventional radiology in Chinese and English contexts: a comparative study

Xueting Yuan, Duo Qian

The First Affiliated Hospital of Soochow University

Purpose The purpose of this study is to evaluate and compare the performance of two advanced Large Language Models (LLMs), ERNIE Bot and ChatGPT, in providing accurate and comprehensive responses to questions related to liver cancer interventional radiology, specifically focusing on Transarterial Chemoembolization (TACE) and Hepatic Arterial Infusion Chemotherapy (HAIC). By assessing their effectiveness in both English and Chinese contexts, this study aims to identify the strengths and limitations of each model in delivering reliable medical information. The findings will help guide healthcare professionals and patients in selecting the most appropriate LLM for obtaining accurate treatment-related information, while also highlighting the necessity of manual review to ensure the reliability of these models in clinical and educational settings.

Materials and methods A total of 38 questions were developed to cover a range of topics related to Transarterial Chemoembolization (TACE) and Hepatic Arterial Infusion Chemotherapy (HAIC), including foundational knowledge, patient education, and treatment and care. The responses generated by ERNIE Bot and ChatGPT were rigorously evaluated by 10 professionals in liver cancer interventional radiology. The final score was determined by one seasoned clinical expert. Each response was rated on a 5-point Likert scale, facilitating a quantitative analysis of the accuracy and comprehensiveness of the information provided by each language model.

Results ERNIE Bot is superior to ChatGPT in the Chinese context (ERNIE Bot: 5, 89.47%; 4, 10.53%; 3, 0%; 2, 0%; 1, 0% VS ChatGPT: 5, 57.89%; 4, 5.27%; 3, 34.21%; 2, 2.63%; 1, 0%; $P=0.001$). However, ChatGPT outperformed ERNIE Bot in the English context (ERNIE Bot: 5, 73.68%; 4, 2.63%; 3, 13.16%; 2, 10.53%; 1, 0% VS ChatGPT: 5, 92.11%; 4, 2.63%; 3, 5.26%; 2, 0%; 1, 0%; $P=0.026$).

Conclusion This study preliminarily demonstrated that ERNIE Bot and ChatGPT effectively address questions related to liver cancer interventional radiology. However, their performance varied by language: ChatGPT excelled in English contexts, while ERNIE Bot performed better in Chinese. We found that choosing the appropriate LLMs is beneficial for patients in obtaining more accurate treatment information. Both models require manual review to ensure accuracy and reliability in practical use.

PO-185

Efficacy of antiangiogenic therapy in patients with advanced SMARCA4-deficient thoracic tumor

Mengting Shi, Zhixiong Lin

Cancer Hospital of Shantou University Medical College

Purpose SMARCA4 (BRG1)-deficient thoracic tumors (SDTTs) are frequently diagnosed at an advanced stage and had poor prognosis, underscoring the critical importance of seeking out novel therapeutic avenues, particularly in the realm of antiangiogenic treatment. However, the efficacy of antiangiogenic therapy in SDTT remains unknown.

Materials and methods We conducted a retrospective cohort study at SYSUCC from August 1, 2018, to August 15, 2024, screening patients diagnosed with advanced SDTTs confirmed by immunohistochemistry.

Results A total of 151 patients with advanced SDTTs were enrolled in the study, including 49 patients received anti-angiogenic therapy and 102 patients never. The ORR and DCR of first-line therapy with antiangiogenic therapy was 51.4% and 86.5%, respectively, compared to only 37.1% and 78.7% for those without antiangiogenic therapy. The median PFS of SDTTs treated with antiangiogenic therapy was significantly longer than those without (7.97 vs. 5.87 months, HR [95%CI]: 0.612[0.380-0.984], $P=0.043$). For patients who did not receive immune checkpoint inhibitors (ICIs), the median PFS of SDTTs treated with anti-angiogenic agent combined with chemotherapy (C+A) was longer than those treated with chemotherapy alone (C) (5.10 vs 2.57 months, HR [95%CI]: 0.365[0.137-0.968], $P=0.043$). For patients received chemotherapy and ICIs, the addition of anti-angiogenic agent (C+I+A) provided significantly longer PFS (11.90 vs 6.90 months, HR [95%CI]: 0.425, [0.221-0.818], $P=0.010$). This C+I+A therapy outperforms C+A therapy, showing the longest PFS (11.90 vs 5.10 months, HR [95%CI]: 0.294[0.112-0.772], $P=0.013$).

Conclusion The administration of antiangiogenic therapy shows a promising effect in first-line therapies for advanced SDTT patients. The C+I+A combination therapy is the optimal solution among currently available treatment options.

Establishment of a Chicken Chorioallantoic Membrane Hepatocellular Carcinoma Model and Magnetic Resonance Imaging Study

Weili Peng, Jun Chen
Zhejiang Provincial People's Hospital

Purpose This study aims to establish an ex ovo chicken chorioallantoic membrane (HCC-CAM) tumor model with distinct molecular characteristics and to explore the feasibility of multiparametric MRI and radiomics in the in vivo evaluation of molecular features of HCC-CAM.

Materials and methods First, Western blotting was used to validate the expression levels of the molecular biomarker EGFR in different hepatocellular carcinoma (HCC) cell lines. Two HCC cell lines (HUH7 and HEPG2) with different EGFR expression levels were selected, and their EGFR expression levels were statistically analyzed. Subsequently, a custom-made ex ovo culture device was used to establish a chicken embryo ex ovo culture model. The selected HCC cell lines were implanted onto the chorioallantoic membrane (CAM) to construct the HCC-CAM tumor model. Multiparametric MRI (including T1WI, T2WI, T1-STIR, T1-mapping, DWI, and T1-CE) was performed on the established HCC-CAM tumor models to obtain in vivo imaging data. The apparent diffusion coefficient (ADC) values, T1 values, and radiomics features were analyzed. Finally, histopathological examination was conducted to observe the morphological structure of the transplanted tumors and evaluate their similarity to human hepatocellular carcinoma.

Results Results: The results showed that EGFR was highly expressed in the HUH7 cell line and lowly expressed in the HEPG2 cell line (0.265 ± 0.003 vs. 1.021 ± 0.066 , $P < 0.0001$). Western blotting further confirmed the differential EGFR expression levels in the two cell lines. Using the custom-made culture device, the chicken embryo ex ovo culture model was successfully established with a survival rate of 90%, and the HCC-CAM tumor model was successfully constructed. Multiparametric MRI revealed significant differences in ADC values (0.933 ± 0.256 vs. 1.314 ± 0.113 , $P < 0.05$) and T1 values (2574.308 ± 937.592 vs. 3434.517 ± 93.001 , $P < 0.05$) between the HCC-CAM tumor models derived from HUH7 and HEPG2 cell lines. Radiomics feature extraction from T1WI images and Lasso regression identified six radiomics features most correlated with EGFR expression. In both the training set (0.035 ± 0.058 vs. 0.989 ± 0.079 , $P < 0.0001$) and the test set (0.019 ± 0.042 vs. 0.969 ± 0.056 , $P < 0.0001$), the R-scores between the HEPG2 and HUH7 groups showed significant differences. Western blotting (0.154 ± 0.023 vs. 0.844 ± 0.084 , $P < 0.001$) further confirmed the consistency of EGFR expression levels before and after the establishment of the HCC-CAM model. Histopathological examination revealed that the pathological characteristics of the transplanted tumors were highly similar to those of human hepatocellular carcinoma, indicating good clinical relevance of the model.

Conclusion This study successfully established an ex ovo HCC-CAM tumor model based on the chicken chorioallantoic membrane and successfully transplanted HCC cell lines (HUH7 and HEPG2) with different EGFR expression levels. The two cell lines exhibited significant imaging differences in the HCC-CAM model, providing an important experimental platform for research on personalized treatment of hepatocellular carcinoma. Through multiparametric MRI and radiomics analysis, radiomics features correlated with EGFR expression were identified, offering a potential tool for non-invasive assessment of EGFR expression levels in hepatocellular carcinoma. The model demonstrated high consistency at the molecular, imaging, and histopathological levels, showing promising clinical application prospects for mechanistic studies, drug screening, and efficacy evaluation of hepatocellular carcinoma.

Role of Senescence Escape in Therapeutic Resistance of Cholangiocarcinoma Cells induced by 125I Seed Irradiation

Jian Yang, Yiming Liu, Changlong Li, Haidong Zhu
Southeast University

Purpose Cholangiocarcinoma (CCA), as the second most common type of liver cancer, is a highly malignant tumor characterized by strong therapeutic resistance and poor clinical prognosis. In cases of malignant biliary obstruction, 125I seed-loaded biliary stents not only expand the stenotic bile ducts but also inhibit tumor progression, achieving a “two birds with one stone” effect. However, long-term efficacy remains suboptimal, with therapeutic resistance being a critical issue. Recent studies have revealed that senescence is a double-edged sword: while treatment-induced stress can control tumor progression by promoting tumor cell senescence, it may also lead to the escape of senescent cells, which exhibit higher malignancy and contribute to complex therapeutic resistance. However, direct evidence of cholangiocarcinoma cells acquiring resistance through senescence escape is currently lacking. The study aimed to investigate whether 125I seed irradiation induces senescence in cholangiocarcinoma cells and whether these senescent cells undergo senescence escape, leading to therapeutic resistance.

Materials and methods 1. Senescence Induction and Selection

Cholangiocarcinoma cells were exposed to 3 Gy, 6 Gy, or 9 Gy doses of 125I seed irradiation. Senescent cells were identified using senescence-associated β -galactosidase (SA β gal) activity and flow cytometry based on side scatter (SSC) size.

2. Senescence Markers and Subgroup Analysis

Cells were analyzed for senescence markers, including 53BP1, H3K9me3, P21, and LaminB1. SA β gal+/SSC- (P7) and SA β gal+/SSC+ (P5) subpopulations were isolated and characterized.

3. Single cell RNA-sequencing

Gene expression profiles of senescent cells were analyzed using single-cell sequencing to identify pathways associated with stemness and metastasis.

4. Therapeutic Resistance and Metastasis Assays

The reprogrammed P5 and P7 subpopulation cells were subjected to 125I seed irradiation or doxorubicin treatment to assess therapeutic resistance. Migration and invasion capabilities were evaluated using Matrigel assays.

Results 1. Senescence induced by 125I seed irradiation

Irradiation with 3 Gy, 6 Gy, and 9 Gy doses of 125I seed increased the proportion of cells in the G1 phase of the cell cycle in a dose-dependent manner. The percentages of SA β gal-positive cells were $26.6\% \pm 0.86$, $33.1\% \pm 0.86$, and $55.1\% \pm 1.53$, respectively. Senescence markers such as p21 and γ H2AX were significantly upregulated, while proliferation markers like Ki67 were nearly absent.

2. Senescence Escape and Therapeutic Resistance

After continuous culture for 3 weeks, both P5 and P7 cells resumed proliferation. These cells exhibited significant therapeutic resistance to 125I seed irradiation and doxorubicin. In mice, the resistance of senescence-escaped cells to 125I seed irradiation was further confirmed.

3. Gene Expression and Metastatic Potential

Single-cell RNA-sequencing revealed that the senescent subpopulations exhibited stemness features, with upregulation of WNT, YAP1, CTNNB1, EGFR, and FGFR mRNA levels. Additionally, P5 and P7 cells displayed an epithelial-to-mesenchymal transition (EMT) phenotype, characterized

by high expression of Snail, β -catenin, and Vimentin. Matrigel assays demonstrated enhanced migration and invasion capabilities in senescence-escaped cells.

Conclusion The findings indicate that ^{125}I seed irradiation induces senescence in cholangiocarcinoma cells, which subsequently undergo senescence escape. This process enhances tumor cell stemness, leading to increased therapeutic resistance and metastatic potential. These insights highlight the need for further research into strategies to counteract senescence escape and improve therapeutic outcomes in cholangiocarcinoma.

PO-189

Prognostic Value of Peripheral Blood-Derived Inflammation-Based index in Hepatocellular Carcinoma with Transarterial Chemoembolization Plus PD-(L)1 Inhibitors and Molecular Targeted Agents

Jianjian Chen,Zhi-Cheng Jin,Hai-Dong Zhu,Gao-Jun Teng
Zhongda Hospital, Medical School, Southeast University

Purpose To identify the prognostic value of inflammation-based indexes, including neutrophil-to-lymphocyte ratio (NLR), platelet-to-lymphocyte ratio (PLR), and systemic immune inflammation index (SII) in hepatocellular carcinoma (HCC) patients receiving transarterial chemoembolization (TACE) plus PD-(L)1 inhibitors and molecular targeted agents (MTAs).

Materials and methods A multicenter retrospective cohort study included patients with intermediate and advanced stage HCC who underwent TACE plus PD-(L)1 inhibitors and MTAs from January 2018 to May 2021. The primary outcomes were overall survival (OS) and progression-free survival (PFS). The Cox regression, Kaplan-Meier analysis, and the log-rank test were conducted to explore the prognostic impacts of NLR, PLR, and SII. The prediction accuracy was evaluated by time-dependent receiver operating characteristic (ROC) curve and Harrell's concordance index (C-index).

Results A total of 302 patients were included in this study. NLR, PLR, and SII all showed good prediction ability in OS (all $P < 0.05$), and were independent predictors for OS (hazard ratio [HR] = 2.06, $P < 0.001$; HR = 1.56, $P = 0.02$; HR = 2.00, $P < 0.001$; respectively). The NLR and SII also were independent predictors for PFS (HR = 1.42, $P = 0.02$; HR = 1.47, $P = 0.009$; respectively).

Conclusion NLR and SII are independent prognostic factors for OS and PFS in HCC with TACE plus PD-(L)1 inhibitors and molecular targeted agents. The predictive ability of NLR and SII was comparable in these patients.

PO-190

Efficacy and predictive factors of transarterial chemoembolization combined with lenvatinib plus programmed cell death protein-1 inhibition for unresectable hepatocellular carcinoma

Kunpeng Ma, Feng Duan
Chinese PLA General Hospital

Purpose To evaluate the efficacy and independent predictive factors of TACE combined with lenvatinib plus PD-1 inhibitors for unresectable HCC.

Materials and methods This study retrospectively enrolled patients with unresectable HCC who received TACE/lenvatinib/PD-1 treatment between March 2019 and April 2022. Overall survival (OS) and progression-free survival (PFS) were determined. The objective response rate (ORR) and disease control rate (DCR) were evaluated in accordance with the modified Response Evaluation Criteria in Solid Tumors. Additionally, the prognostic factors affecting the clinical outcome were assessed.

Results One hundred and two patients were enrolled with a median follow-up duration of 12.63 months. The median OS was 26.43 months (95%CI: 17.00-35.87), and the median PFS was 10.07 months (95%CI: 8.50-11.65). The ORR and DCR were 61.76% and 81.37%, respectively. The patients with Barcelona Clinic Liver Cancer Classification (BCLC) B stage, early neutrophil-to-lymphocyte ratio (NLR) response (decrease), or early alpha-fetoprotein (AFP) response (decrease > 20%) had superior OS and PFS than their counterparts.

Conclusion This study showed that TACE/lenvatinib/PD-1 treatment was well tolerated with encouraging efficacy in patients with unresectable HCC. The patients with BCLC B-stage disease with early NLR response (decrease) and early AFP response (decrease > 20%) may achieve better clinical outcomes with this triple therapy.

PO-191

Risk Stratification in Colorectal Cancer: Nomograms Utilizing Inflammatory Factors and Immunological Hematological Indicators

Jiadao Tang, Mengying Xiang, Guangrui Xiong, Xin Shen, Ke Zhang, Yao Huang, Shaoqiong Yang, Xiaoying Chai, Rui Li, Junbo Lai, Xinjun Peng, Lin Xie
The Third Affiliated Hospital of Kunming Medical University, Yunnan Cancer Hospital, Pekin University Cancer Hospital Yunnan

Purpose Cancer-associated inflammation and immunological hematological indicators could regard as contributing factors to promote for the progression of solid tumors.

Materials and methods This study aimed to construct nomograms with inflammatory factors and immunological hematological parameters to predict the prognosis of colorectal cancer (CRC).

Results The training cohort had a 66.25% prediction rate for distant metastasis. Nomograms were created to predict distant metastasis, overall survival (OS), and progression-free survival (PFS) using clinicopathologic features, inflammatory factors, and immunologic hematological indicators as baseline, and the consistency index (C index) scores of the three nomograms were 0.791 (95% CI, 0.745-0.838), 0.752 (95% CI, 0.699-0.806), and 0.687 (95% CI, 0.647-0.726) respectively. The consistency index (C index) scores for the three nomograms were 0.791 (95% CI, 0.745-0.838), 0.752 (95% CI, 0.699-0.806), and 0.687 (95% CI, 0.647-0.726), respectively. Calibration graphs demonstrated a good correlation between predicted and actual prognostic rates. Decision curve analysis (DCA) curves demonstrated that the predictive models had potential for clinical application. Subgroup analyses showed that the nomograms were favorable prognostic indicators for stage I-IV CRC patients ($P < 0.05$).

Conclusion Single or combined hematological indicators are easy to obtain, feasible, and of high prognostic predictive values, so the nomograms constructed on the basis of cancer-associated inflammatory factors and immunological hematological indicators had good accuracies in predicting distant metastasis, OS and PFS in CRC patients, which could help clinicians to conduct risk stratification in CRC patients and assist in treatment decision-making, achieve better oncological outcomes ultimately.

Recent advancements in the utilization of nanomaterials for ablative sensitization therapy in the treatment of Hepatocellular carcinoma

Li Hao¹, Zhengqiang Yang², Meng Niu³

1. China Medical University

2. Department of Interventional Therapy, National Cancer Center, National Clinical Research Center for Cancer Hospital, Chinese Academy of Medical Sciences and Peking Union Medical College

3. Department of Interventional Therapy, Shengjing Hospital of China Medical University

Purpose Hepatocellular carcinoma (HCC) is the sixth most common cancer in terms of new cases and the fourth leading cause of cancer-related deaths worldwide. Percutaneous ablation technology has emerged as a critical modality for the minimally invasive treatment of HCC and is the preferred intervention for small HCC (≤ 3 cm). This therapeutic approach induces tumor cell necrosis by applying extreme temperatures, either high or low, directly to the tumor site. However, ablation therapy for liver cancer often leaves residual or recurrent tumors due to its limited scope. Nanomaterials, with their beneficial properties, can enhance ablation efficiency and range. Thus, it's crucial to explore how nanomaterials can improve ablation sensitivity in treating HCC.

Materials and methods The literature search was conducted on PubMed (www.ncbi.nlm.nih.gov/pubmed/). The search results were restricted using the retrieval formula: ("Carcinoma, Hepatocellular"[Mesh]) AND ("Radiofrequency Ablation"[Mesh]) AND nano*, ("Carcinoma, Hepatocellular"[Mesh]) AND (microwave ablation) AND nano*, ("Carcinoma, Hepatocellular"[Mesh]) AND (high-intensity focused ultrasound) AND nano*, ("Carcinoma, Hepatocellular"[Mesh]) AND (sonodynamic therapy) AND nano*, ("Carcinoma, Hepatocellular"[Mesh]) AND (photothermal therapy) AND nano*, ("Carcinoma, Hepatocellular"[Mesh]) AND (photodynamic therapy) AND nano*, ("Carcinoma, Hepatocellular"[Mesh]) AND (Cryoablation) AND nano*. Exclude non-matching results and categorize the remaining literature.

Results Nanomaterials equipped with ablative sensitizers or structures enhance ablation effectiveness, minimizing incomplete ablation and tumor recurrence. They also facilitate combining ablation with chemotherapy or immunotherapy by carrying drugs like Doxil or anti-PD-(L)1. Additionally, nanomaterials with imaging capabilities aid in tumor localization before ablation and monitoring post-ablation, integrating diagnosis and treatment.

Conclusion This paper reviews the use of various nanomaterials in conjunction with different ablation therapies for HCC, including radiofrequency ablation (RFA), microwave ablation (MWA), high-intensity ultrasound (HIFU), sonodynamic therapy (SDT), photothermal therapy (PTT), photodynamic therapy (PDT) and cryoablation. It also explores the clinical potential of these nanomaterials. The findings provide novel insights and propose new directions for research in advancing HCC ablation therapy.

PO-193

Hepatocellular carcinoma treated with transcatheter arterial chemoembolization followed by radiofrequency ablation: impact of the time interval between the two treatments

Chun-Xue Wu, Jian-Jun Han

Shandong Cancer Hospital and Institute, Shandong First Medical University and Shandong Academy of Medical Sciences

Purpose To compare the efficacy and safety of transcatheter arterial chemoembolization (TACE) and radiofrequency ablation (RFA) combined therapy with short and long intervals for hepatocellular carcinoma (HCC).

Materials and methods In this retrospective study, a total of 43 patients with HCC who underwent combined treatment with TACE and RFA were enrolled between October 2015 to August 2021. Twenty patients in the short interval group underwent RFA within 1 week after TACE and twenty-three patients in the long interval group underwent RFA more than 1 week after TACE. The ablation time (T, s), power (P, W) of the ablation procedure, the total energy (Q, J) of the whole process, as well as the ratio (R) of energy to diameter were reviewed. Additionally, AFP, AST, and ALT levels were monitored before and after treatment. Overall survival (OS) was compared between the two groups.

Results AFP levels of the two groups had no statistical differences. After the treatment, ALT and AST levels of the short interval group were significantly higher than the long interval group ($p=0.001$, $p=0.001$). The R level of the short interval group was 16513.85 ± 6142.75 and that of the long interval group was 11605.27 ± 10468.12 ($p=0.041$). Median OS was 16 ± 1.02 months for all patients, 15 ± 0.05 months for the short interval group, and 18 ± 0.89 months for the long interval group.

Conclusion An interval of more than one week between TACE and RFA procedures of combination therapy can lead to better efficiency and reduced liver injury.

PO-194

Different body compositions affect the adverse prognosis of hepatocellular carcinoma patients following transarterial chemoembolization combined immunotherapy and targeted therapy

Qing-Xia Shen, Zhi-Cheng Jin, Hai-Dong Zhu
Zhongda Hospital, Southeast University

Purpose Sarcopenia identifies the prognosis of advanced hepatocellular carcinoma (HCC) patients following immunotherapy. While adipose deposition may predict prognosis in patients receiving immunotherapy, findings remain inconsistent. Currently, transarterial chemoembolization (TACE) combined with targeted-immunotherapy has emerged as an important therapeutic approach for HCC patients. However, whether sarcopenia and adipose deposition influence the prognosis of such patients remains unknown. Therefore, this study aims to investigate the association between sarcopenia, adipose deposition, and clinical outcomes in HCC patients undergoing TACE combined with targeted therapy and immunotherapy.

Materials and methods Our study included 497 unresectable HCC patients who underwent TACE combined with targeted therapy and immunotherapy across 17 centers between 01/2018 - 12/2022. Muscle- and adipose-related parameters were measured by computed tomography (CT) images at the third lumbar vertebra (L3) level, including skeletal muscle index (SMI), subcutaneous adipose tissue index (SATI), visceral adipose tissue index (VATI), total adipose tissue index (TATI), and visceral-to-subcutaneous adipose tissue area ratio (VSR). A comprehensive analysis was performed to evaluate the impact of muscle and adipose tissue on overall survival (OS).

Results Patients with sarcopenia demonstrated significantly worse overall survival (OS) compared to non-sarcopenia patients (median OS: 13.1 months [95% CI: 9.8–23.9] vs. 24.1 months [95% CI: 21.7–26.7], $P = 0.0013$). After adjusting for observed confounders using inverse probability of treatment weighting (IPTW), sarcopenia remained associated with inferior OS (median OS: 13.1 months [95% CI: 9.87–26.0] vs. 24.1 months [95% CI: 21.67–26.3], $P = 0.0013$). In IPTW-adjusted Cox proportional hazards analysis, sarcopenia was identified as an independent risk factor for poor prognosis (hazard ratio [HR]: 1.9, 95% CI: 3.23–21.58, $P = 0.009$). Gender-specific optimal cutoff values for adipose-related parameters were determined. Subsequent Kaplan-Meier analyses stratified by these cutoffs revealed that patients with higher subcutaneous adipose tissue index (SATI) (median OS: 26.9 months [95% CI: 22–34.9] vs. 20.7 months [95% CI: 18–24.9], $P = 0.0052$) and higher total adipose tissue index (TATI) (median OS: 25.0 months [95% CI: 22.9–29.5] vs. 18.7 months [95% CI: 17.4–23.9], $P = 0.002$) exhibited significantly prolonged OS compared to the low-adipose groups. Subgroup analysis further confirmed that the non-sarcopenia group achieved greater OS benefits compared to the sarcopenia group.

Conclusion Sarcopenia is an independent prognostic factor in HCC patients who received TACE combined with targeted therapy and immunotherapy, and adipose deposition is protective in OS.

PO-195

Transarterial Chemoembolization Containing Arsenic Trioxide for the Treatment of Intermediate-stage Hepatocellular Carcinoma: A Randomized, Double-blind, Multicenter Parallel- Controlled Study

Peng Wang, Haibo Shao
The First Hospital of China Medical University

Purpose To investigate efficacy and safety of transarterial chemoembolization (TACE) containing arsenic trioxide (As_2O_3) for intermediate-stage hepatocellular carcinoma (HCC) patients.

Materials and methods In this randomized, double-blind, multicenter parallel-controlled study, histopathologically or clinically confirmed intermediate-stage HCC patients were randomly assigned (1:1) to As_2O_3 group (Chemo-drug: As_2O_3 +epirubicin) and control group (Chemo-drug: epirubicin). Conventional TACE (emulsion of chemo-drug and lipiodol) was performed in all the enrolled patients and was repeated on demand. The primary end point was time to progress (TTP), and the secondary end points were overall survival (OS), progress free survival (PFS), objective response rates (ORR) and safety.

Results A total of 224 patients in eight centers were enrolled and randomly assigned to As_2O_3 group (n=114) and control group (n=110). In the full analysis set, the median TTP was significantly longer in As_2O_3 group than that in control group (12 versus 7 months; hazard ratio [HR], 0.68; 95% confidence interval [CI], 0.50 - 0.92; $P=0.013$). Consistently, the median OS was also longer in As_2O_3 group (35 vs. 26 months; HR, 0.87; 95% CI, 0.61 - 1.24; $P=0.44$). There was no difference between the two groups in PFS (12 vs. 8 months; HR, 0.76; 95% CI, 0.56 - 1.01; $P=0.061$), and ORR (73.7% [84 out of 114] vs. 71.0% [78 out of 110]; $P=0.643$). Majority of the adverse events were in grade 0-1 (95.42%), with no treatment-related death in both groups.

Conclusion TACE containing As_2O_3 could improve TTP and OS with acceptable toxicities in the intermediate-stage HCC patients.

PO-196

C-Reactive Protein Flare: A Promising Prognostic Predictor for Patients with Hepatocellular Carcinoma Treated with TACE Combined with Lenvatinib and Immune Checkpoint Inhibitors

Chun-Xue Wu, Xu Chang

Shandong Cancer Hospital and Institute, Shandong First Medical University and Shandong Academy of Medical Sciences

Purpose To assess the prognostic value of C-reactive protein (CRP) kinetics in patients with hepatocellular carcinoma (HCC) treated with transarterial chemoembolization (TACE) combined with lenvatinib (LEN) and immune checkpoint inhibitors (ICIs).

Materials and methods This study retrospectively analysed CRP kinetics for 143 patients with HCC, treated with TACE–LEN–ICIs from May 2020 to August 2023. Patients were stratified into three groups based on early CRP kinetics: (i) CRP flare-responders, where the level increased to more than double the baseline value within 1 month of the initial TACE–LEN–ICIs regime then decreased to below baseline within 3 months; (ii) CRP responders, where levels decreased by $\geq 30\%$ from baseline within 3 months with no initial flare; and (iii) CRP non-responders (comprising all remaining patients). Calculated oncological outcomes were overall survival (OS), progression-free survival (PFS), objective response rate (ORR), and disease control rate (DCR). The association of early CRP kinetics with these outcomes was evaluated.

Results The CRP flare-responder, CRP responder, and CRP non-responder groups included 19 (13.3%), 60 (42.0%), and 64 (44.7%) patients, respectively, exhibiting ORRs of 78.9%, 78.4% and 47.7% ($p = 0.001$) and DCRs of 94.8%, 96.7% and 78.1% ($p = 0.004$). Median PFS for the three respective groups was 40.3, 11.4, and 5.5 months ($p < 0.001$), while median OS values were not reached, 18.9 and 9.9 months ($p < 0.001$). Moreover, CRP responder and CRP flare-responder status were independent risk factors for OS ($p < 0.001$) and PFS ($p < 0.001$).

Conclusion CRP kinetics may have predictive value for prognosis in HCC patients undergoing TACE–LEN–ICIs.

PO-197

Predicting progression-free survival with MRI radiomics nomogram for unresectable hepatocellular carcinoma patients treated with transarterial chemoembolization combined with TKI plus PD-1 inhibitors

Jiaxuan Liu, Haibo Shao

The First Hospital of China Medical University

Purpose MR-based radiomics nomogram to predict progression-free survival (PFS) in unresectable hepatocellular carcinoma (HCC) by transarterial chemoembolization (TACE) combined with tyrosine kinase inhibitor (TKI) plus PD-1 inhibitors (TTP) to maximize the efficacy of combination therapy.

Materials and methods We included 132 patients with intermediate and advanced Barcelona Clinic Liver Cancer (BCLC) B and C stage HCC receiving TACE combined with tyrosine kinase inhibitor (TKI) plus PD-1 inhibitors (TTP) in two institutions from May 2020 to September 2022. The 102 patients collected by Center 1 were randomly divided into the training group (n=71) and the test group (n=31). The 30 patients collected by Center 2 were used as an external validation set. Regions of interest (ROI) were manually delineated layer by layer and preoperative T2WI-weighted, arterial phase (AP) and portal venous phase (VP) enhanced MRI images were extracted using 3D-slicer software. We used LASSO regression to screen radiomics features and obtain the radiomics score (radscore). Univariate and multivariate COX regression features were screened for clinical data, and clinical model scores (cliscore) were constructed according to the correlation coefficient. Radscore and the predicted clinical features, constructed combined model nomogram and combined model score (comscore), drew ROC curves of PFS at 6, 12 and 24 months, and validated by test set and external validation set. We found the best cutoff by the median of cliscore, radscore, comscore and divided it into high risk and low risk groups, plot the survival analysis, and used Kaplan-Meier curves to evaluate PFS using the log-rank test. We used the area under the curve (AUC), the concordance index (C-index) and the ROC curve to assess the model's prediction effectiveness. The calibration and clinical usefulness of the combined model were assessed using calibration curves and decision curves. Finally, we also performed univariate and multivariate regression analysis of patients' OS to screen for clinical factors independently associated with OS.

Results BCLC (HR = 2.211 [95% CI, 1.260-3.879]; P = 0.006), tumor size (HR = 1.974 [95% CI, 1.075-3.625]; P = 0.028), rad-score (HR = 26.10 [95% CI, 8.607-79.185]; P < 0.001) were independent risk factors for PFS. The AUC values of radiomics model at 6-month, 12-month and 24-month PFS in the training group were 0.804, 0.841 and 0.858, the AUC values in the test group were 0.808, 0.804 and 0.677, the AUC values in the external validation group were 0.784, 0.815 and 0.837, respectively. AUC values and C-index of the combined model were higher than radiomics models and clinical models. The combined model performed well, with a C-index > 0.7, good discrimination and good fit of calibration curves. The AUC values of the combined model in the training group were 0.856, 0.907 and 0.882, the AUC values in the test group were 0.838, 0.871 and 0.785, and the AUC values in the external validation group were 0.881, 0.903 and 0.894, respectively. The AUC values were greater than the Radiomics model and clinical model, and the combined model was better than the Radiomics model and clinical model. The calibration curve indicates the good fitting performance and calibration performance of the combined model. We constructed the cliscore, radscore and comscore based on the clinical model, the radiomics model, the combined model, we divided them into high-risk patients and low-risk patients according to the cliscore, radscore

ore and comscore. PFS in low-risk patients was higher in patients with intermediate and advanced HCC than in high-risk patients ($P < 0.05$). We also found that BCLC (HR=6.992, 95%CI:3.243-15.072), tumor size (HR=2.755, 95%CI:1.408-5.389) and Child-Pugh grade (HR=2.215, 95%CI:1.177-4.169) were independent risk factors for OS.

Conclusion MR clinic-radiomics combined model can also be used to select patients who might benefit from combination therapy.

PO-198

TACE-HAIC versus HAIC: Is more always better? Combined with TKIs and ICIs for hepatocellular carcinoma with a high tumor burden—A propensity-score matching comparative study.

Chun-Xue Wu, Xu Chang

Shandong Cancer Hospital and Institute, Shandong First Medical University and Shandong Academy of Medical Sciences

Purpose Transarterial chemoembolization (TACE) plus hepatic arterial infusion chemotherapy (HAIC) is considered a new local treatment modality for advanced hepatocellular carcinoma (HCC) with high tumor burden (major portal vein tumor thrombosis [PVTT] Vp3-4 or/and tumors larger than 10 cm). However, most studies on TACE-HAIC are single-arm or compared with TACE, lacking direct comparisons to HAIC. The present study aimed to comparatively examine TACE-HAIC in combination with tyrosine kinase inhibitors (TKIs) and immune checkpoint inhibitors (ICIs) versus HAIC alone in combination with TKIs and ICIs for efficacy and safety in individuals with high tumor burden HCC.

Materials and methods Totally 363 inoperable HCC cases with high tumor burden administered TACE-HAIC plus TKI and ICI (TACE-HAIC combination group, n=119) or HAIC plus TKI and ICI (HAIC combination group, n=244) were recruited between October 2020 and January 2024, and propensity score matching (PSM) was utilized for matching patients. Overall survival (OS), progression-free survival (PFS), objective response (ORR) and disease control (DCR) rates and safety signals were assessed.

Results Following PSM (1:2), 87 cases in the TACE-HAIC combination group were matched to 143 cases in the HAIC combination group. Median OS (26.8 vs. 19.1 months, $p=0.233$) and PFS (11.17 vs. 9.01 months, $p=0.133$) were similar in the TACE-HAIC and HAIC combination groups. ORRs were 58.0% and 64.4% in the HAIC and TACE-HAIC combination groups, respectively ($p=0.341$). DCR were 90.9% and 94.3% for these groups, respectively ($p=0.360$). Both univariate and multivariate analyses revealed no between-group differences pre- and post-matching. The commonest adverse events (AEs) included thrombocytopenia, hypertension and increased AST (aspartate aminotransferase) and ALT (alanine aminotransferase) of any grade pre- and post-PSM.

Conclusion In HCC cases with high tumor burden, HAIC and TACE-HAIC have similar outcomes in combination with TKIs and ICIs. Therefore, such patients should be preferably administered HAIC in lieu of TACE-HAIC.

PO-199

Immune Cells as Potential Targets for Intrahepatic Cholangiocarcinoma: Insights from Mendelian Randomization

Ying Yang, Chang Liu, Hong Wu

Department of General Surgery, West China Hospital, Sichuan University, Chengdu 610041, China; Liver Transplant Center, Transplant Center, West China Hospital, Sichuan University

Purpose Despite extensive research implicating immune cells involvement in intrahepatic cholangiocarcinoma (ICC) development, the causal relationships between them remain elusive. This study aims to investigate the causal link between immune cells and ICC, paving the way for new immunotherapeutic approaches of ICC.

Materials and methods A two-sample Mendelian randomization (MR) analysis was employed to establish the causal relationship between 731 immunophenotype and ICC using publicly accessible genome-wide association study (GWAS) genetic data in this study. The analytical method used in this study included inverse variance weighted, MR-Egger, weighted median, Simple mode and Weighted mode. Sensitivity analyses were conducted to assess the horizontal pleiotropy and heterogeneity of the study

Results A total of 15 immune cell phenotypes showed positive results through preliminary MR Analysis, and 2 phenotypes with horizontal pleiotropy were excluded after sensitivity analyses. Thus, this study identified 13 immune cell traits as causal relationships associated with ICC, including 4 types of TBNK, 3 types of B cells, 3 types of T cells, 2 types of regulatory T cells, and 1 type of classical dendritic cells.

Conclusion Our MR study provide evidence for a causal relationship between immune cells and ICC, which may provide a potential foundation for future diagnosis and treatment of ICC.

PO-200

Mechanistic Study of Celiac Sympathetic Denervation in the Treatment of Metabolic Dysfunction-Associated Steatohepatitis (MASH)

Yi Xu, Gao-Jun Teng
Southeast University

Purpose Metabolic dysfunction-associated steatohepatitis (MASH) is a complex hepatic disorder characterized by pathological lipid accumulation, chronic inflammation, and hepatocellular injury. Emerging evidence implicates the sympathetic nervous system (SNS) in the pathogenesis of MASH. This study aims to elucidate the regulatory mechanisms of celiac sympathetic denervation in MASH progression.

Materials and methods A murine MASH model was established through a high-fat, high-cholesterol, and high-sucrose diet. Sympathetic denervation was achieved via two approaches: chemical ablation using intraperitoneal 6-hydroxydopamine (6-OHDA) and ethanol-based celiac sympathetic denervation. Hepatic norepinephrine (NE) levels, serum biochemical profiles, and histopathological analyses were employed to evaluate the therapeutic effects of sympathetic modulation on MASH progression.

Results Celiac sympathetic denervation significantly attenuated hepatic lipid accumulation, reduced inflammatory infiltrates, and improved glucose tolerance in diet-induced MASH mice. Mechanistically, this intervention disrupted sympathetic overactivation, thereby ameliorating metabolic dysregulation and hepatocellular injury.

Conclusion Our findings provide preclinical evidence supporting sympathetic neuromodulation as a novel therapeutic approach for MASH, offering insights into its pathophysiological mechanisms.

PO-201

Efficacy and Safety of Radioactive Particle Implantation Combined with Immunotherapy in Advanced Cancer: A Retrospective Study

Weipeng Yan, Shasha Shi, Jing Tang, Xi Lin, Yirui Liu, Xiaobing Li
Hubei Cancer Hospital

Purpose This retrospective study aims to evaluate the efficacy and safety of radioactive particle implantation combined with immunotherapy in patients with advanced cancer.

Materials and methods A total of 100 patients with various types of advanced malignancies, including lung, liver, and prostate cancers, were included. These patients received radioactive particle implantation followed by immunotherapy as part of their treatment regimen. The primary endpoint was overall survival (OS), while secondary endpoints included progression-free survival (PFS), tumor response rate, and treatment-related adverse events.

Results Results showed that the combination therapy significantly improved OS and PFS compared to historical data of standard treatments. The overall response rate was 65%, with a notable reduction in tumor size in most patients. The treatment was generally well-tolerated, with manageable side effects. The most common adverse events were mild to moderate fatigue, skin reactions, and transient flu-like symptoms. Serious adverse events were rare, and no treatment-related fatalities were reported.

Conclusion In conclusion, radioactive particle implantation combined with immunotherapy appears to be a promising therapeutic approach for advanced cancer, offering improved survival outcomes and manageable safety profiles. Further prospective studies are warranted to confirm these findings and optimize treatment protocols.

PO-202

Clinical Exploration of Arterial Infusion Conversion Therapy for Advanced Gastric Cancer: A Single-Center Long-Term Follow-Up Study of 8 Cases

Yuting Liu¹, Jun Chen²

1. The Second Clinical Medical College of Hangzhou Normal University (Zhejiang Provincial People's Hospital)

2. Jiangsu Cancer Hospital/The Affiliated Cancer Hospital of Nanjing Medical University

Purpose Patients with locally advanced gastric cancer (LAGC) often lose eligibility for curative surgery due to extensive tumor infiltration or adjacent vascular invasion. While traditional systemic chemotherapy may partially alleviate symptoms, its efficacy is limited and accompanied by significant systemic toxicity. Regional arterial infusion conversion therapy, through targeted drug delivery, significantly enhances local drug concentration around the tumor, achieving profound tumor downstaging while minimizing systemic toxicity. Based on ≥5-year long-term follow-up data, this study aims to systematically evaluate the efficacy, safety, and long-term survival benefits of gastric arterial infusion chemotherapy (GAIC) as a conversion therapy for unresectable advanced gastric cancer (AJCC stage IIIc/IV).

Materials and methods This single-center retrospective cohort study included 8 patients with unresectable advanced gastric cancer treated with superselective regional arterial infusion conversion therapy at Zhejiang Cancer Hospital from 2015 to 2017. All cases received 2-3 cycles of arterial infusion chemotherapy combined with oral S-1. Tumor response was validated by dynamic contrast-enhanced CT (RECIST 1.1 criteria) and postoperative pathology (ypTNM staging). Pathological complete response rate (pCR), 3/5-year overall survival (OS), and safety events were analyzed.

Results After periodic regional arterial infusion chemotherapy, contrast-enhanced CT showed significant shrinkage in tumor volume and metastatic lymph nodes. All patients underwent R0 resection. Postoperative histopathological analysis confirmed downstaging in all cases, with no significant adverse events or perioperative complications. During the 5-year follow-up, 3 patients remained alive, with a median OS not reached (>105.1 months). The 3-year survival rate was 87.5%, and the 5-year survival rate was 62.5%.

Conclusion Arterial infusion conversion therapy may represent an effective approach to revolutionize the treatment of advanced gastric cancer. The groundbreaking long-term survival data provide critical evidence for future prospective multicenter studies and hold potential clinical guidance value.

PO-203

BCLC Staging-Guided Conversion Therapy for Unresectable Hepatocellular Carcinoma: HAIC Combined with Targeted Therapy and PD-1/L1 Inhibitors

Weihao Zhang, Wenge Xing, Tongguo Si, Haipeng Yu

Tianjin Medical University Cancer Institute & Hospital, National Clinical Research Center for Cancer

Purpose This study aims to assess the efficacy and safety of hepatic arterial infusion chemotherapy (HAIC) combined with molecular targeted therapy and immunotherapy. The goal is to explore its potential as a conversion treatment for unresectable hepatocellular carcinoma (uHCC).

Materials and methods A retrospective analysis was performed on clinical data from patients with unresectable hepatocellular carcinoma (uHCC) treated with hepatic arterial infusion chemotherapy (HAIC), molecular targeted therapy, and PD-1/PD-L1 immunotherapy. The data was collected from the Interventional Treatment Department of Tianjin Medical University Cancer Hospital between November 2018 and December 2022. Efficacy was assessed based on the modified Response Evaluation Criteria in Solid Tumors (mRECIST). The primary endpoints were overall survival (OS), progression-free survival (PFS), and conversion therapy rate. Survival status curves were depicted using the Kaplan-Meier method. Prognostic risk factors affecting conversion therapy and survival were evaluated using Logistic and Cox regression models.

Results As of December 2022, a total of 318 patients were included: 40 patients (12.5%) in BCLC stage A, 123 patients (38.6%) in BCLC stage B, and 155 patients (48.7%) in BCLC stage C. The most frequently used targeted agents were lenvatinib and bevacizumab, while sintilimab was the most commonly used immunotherapy agent. The overall objective response rate (ORR) was 47.1%, and the disease control rate (DCR) was 85.5%. The median overall survival (mOS) for the entire cohort was 21.7 months (95% CI: 19.7-24.3), and the median progression-free survival (mPFS) was 11.4 months (95% CI: 9.4-13.4). A total of 110 patients (34.6%) underwent conversion surgery. Multivariate logistic regression analysis indicated that BCLC stage was the only independent risk factor affecting eligibility for conversion therapy. There was a significant difference in overall survival (OS) among patients with different BCLC stages ($P < 0.001$). Subgroup analysis revealed that BCLC-B stage patients who achieved successful conversion therapy demonstrated significantly better outcomes compared to those without successful conversion therapy (median OS: 29.3 months [95% CI: 24.3-NA] vs. 19.7 months [95% CI: 17.2-24.6], $P = 0.0013$). Multivariate regression analysis showed that BCLC stage, the presence of distant metastasis, and whether conversion therapy was performed are independent prognostic factors influencing OS. Among the patients, 169 (53.1%) experienced grade 3–4 adverse events (AEs), with the most common being fatigue, fever, and pain.

Conclusion The combination of hepatic arterial infusion chemotherapy (HAIC) with molecular targeted therapy and immunotherapy demonstrates a high ORR, improves the conversion therapy rate, and prolongs OS and PFS in patients with uHCC, with a favorable safety profile. BCLC stage is identified as an independent prognostic factor influencing the success of conversion therapy, with patients in stage B deriving significant survival benefits post-conversion.

PO-204

Multifunctional Nanofiber Patch Integrating Photothermal-Immunomodulatory Trimodal Therapy for Postoperative Hepatocellular Carcinoma Management

Yiming Liu¹, Yanan Zhao², Haidong Zhu¹

1. Zhongda Hospital, Southeast University

2. The First Affiliated Hospital of Zhengzhou University

Purpose The suboptimal clinical outcomes frequently observed in postoperative hepatocellular carcinoma (HCC) management predominantly stem from tumor recurrence and metastatic progression. This clinical challenge has driven substantial research efforts toward developing effective multimodal therapeutic strategies. However, the implementation of complex bioactive agent combinations necessitates therapeutic systems with multifunctional capabilities.

Materials and methods To address this, we engineered an innovative nanofiber-based patch incorporating black phosphorus nanosheets (BPNSs) and the heat shock protein 90 (HSP90) inhibitor AUY922, creating an integrated platform for molecularly targeted trimodal therapy combining photothermal effects, immunogenic modulation, and immune checkpoint blockade (ICB). Subsequently, the ex vivo and in vivo efficacy and biosafety of this multifunctional nanopatch were verified by in vitro physicochemical and cellular function experiments as well as various animal models.

Results The developed patch exhibits favorable hydrophilicity, mechanical robustness, and exceptional photothermal conversion efficiency ($\eta = 56.3\%$ at 808 nm). Its unique structural configuration enables depth-penetrating sustained drug release, with near-infrared (NIR) irradiation-triggered thermal activation achieving precise spatiotemporal control over AUY922 delivery. Mechanistic investigations revealed that BPNS-mediated hyperthermia potentiates AUY922-induced immunogenic cell death through activation of intense endoplasmic reticulum stress, while concurrently promoting dendritic cell maturation and antigen presentation. To amplify therapeutic efficacy, we synergistically incorporated programmed cell death ligand 1 (PD-L1) blockade, establishing a comprehensive trimodal strategy. This combinatorial approach demonstrated multifactorial antitumor effects: intense endoplasmic reticulum stress, enhanced infiltration of CD8⁺ effector T cells (3.2-fold increase), and substantial improvement in PD-L1 antibody sensitivity. Transcriptomic analysis through whole-genome sequencing identified predominant enrichment in immune regulatory pathways, particularly those associated with antigen processing and interferon- γ response.

Conclusion This rationally designed nanotherapeutic platform addresses critical limitations in postoperative HCC management by simultaneously preventing local recurrence through physical barrier formation and inhibiting metastatic dissemination via systemic immune activation. The demonstrated technical advantages and therapeutic outcomes underscore its high potential for clinical translation in multimodal cancer therapy.

PO-206

WEE1 combined with radiotherapy affects the regulation of tumor microenvironment through cGAS/STING-STAT3-IRF3 pathway

Jing Hu

the Department of Radiotherapy at the First Affiliated Hospital of the Air Force Military Medical University

Purpose This study proposes for the first time that using WEE1 inhibitor combined with radiotherapy affects the tumor microenvironment through the cGAS/STING-STAT3-IRF3 pathway, and systematically elucidates the effect of DNA damage caused by WEE1 inhibitor combined with radiotherapy on MDSC in the tumor microenvironment.

Materials and methods Cell cycle test was performed using MDA-MB-231 cells, A549 cells and HT29 cells to be subjected to X-ray irradiation of 2GY, 12GY and 20GY, respectively. WEE1 inhibitor combined with radiotherapy was used to act on cells, with radiotherapy dosages of 2GY, 12GY and 20GY, respectively. The EDU kit was used to detect changes in DNA damage repair and proliferation after tumor cells irradiation. In the western-blot experiment, the expression changes of the related proteins γ H2AX, TBK1, P-TBK1, STING, P-STING, IRF3, P-IRF3, P-STAT3 and CGAS on the cGAS/STING-STAT3-IRF3 pathway were detected in the western-blot experiment. Immunofluorescence double-standard experiments detected the expression changes of target molecules in the control group and experimental group of tumor cells. Establish a mouse tumor-bearing model to detect changes in mice's survival time and tumor volume. Flow cytometry was used to detect the differential expression of multiple immune-related molecules such as CD11B, LY6C, CD45, IFN- γ , CD8a in the tumor-bearing experiment of mice.

Results The cell cycle experiment results showed that compared with the control group, WEE1 inhibitor combined with radiotherapy, it can effectively inhibit the G2/M phase of the cell cycle, inhibit tumor cell proliferation, inhibit protein kinase expression, and promote damaged DNA to enter mitosis directly without repair, which has a significant tumor suppression effect. In the tumor-bearing experiment in mice, the tumor volume of WEE1 inhibitor combined with radiotherapy in mice was significantly reduced compared with the control group, and the survival time of mice was significantly extended. Mouse tumor-bearing experiment flow cytometry detected the infiltration of CD8 T cells and the secretion level of IFN- γ in mice tumor tissues. The WEE1 inhibitor combined with radiotherapy group was significantly higher than the control group. The results of the immunofluorescence double-standard experiment showed that the WEE1 inhibitor combined with radiotherapy reduced the infiltration of MDSCs in the tumor microenvironment after radiotherapy compared with the control group. Western-blot experiment results show that inhibiting WEE1 can significantly downregulate the expression of TBK1, P-TBK1, STING, P-STING, IRF3, P-IRF3, P-STAT3 and CGAS through STATE3, indicating that the radiotherapy resistance caused by WEE1 inhibitor or combined with radiotherapy is related to the cGAS/STING-STAT3-IRF3 pathway.

Conclusion WEE1 targeted therapy combined with radiotherapy can inhibit the tumor microenvironment. WEE1 inhibitor combined with radiotherapy affects the tumor microenvironment through the cGAS/STING-STAT3-IRF3 pathway.

PO-208

Combined Therapy of Transhepatic Arterial Chemoembolization and Ablation versus Surgical Resection in the Treatment of Small Liver Cancer

Jingxi Wu, Feng Duan
PLA General Hospital

Purpose To comparatively evaluate the therapeutic efficacy and safety between transarterial chemoembolization (TACE) combined with ablation therapy and radical resection in the treatment of small hepatocellular carcinoma (HCC).

Materials and methods This multicenter retrospective cohort study analyzed clinical records of 359 small HCC patients treated at the First Medical Center of Chinese PLA General Hospital, Fujian Provincial Hospital, and Shanghai Public Health Clinical Center from January 2017 to December 2022. There were 235 patients undergoing TACE-ablation combination therapy and 124 receiving radical resection. Propensity score matching (PSM, 1:1 ratio) was implemented to mitigate confounding bias. Survival outcomes were assessed via Kaplan-Meier method, and univariate analysis was used to analyze the variables that may affect OS and PFS. Cox regression was used to analyze the variables with difference in univariate analysis results.

Results After 1:1 PSM matching between the two groups, 113 patients in each group were divided into the initial treatment group and the recurrence group. The 1-, 3-, and 5-year overall survival (OS) rates of the TACE combined ablation group and the radical resection group were 97.5%, 80.9%, 71.4% and 97.6%, 92.3%, 85.2%, respectively. There was a statistically significant difference in the postoperative OS rate between the two groups ($\chi^2=6.015$, $P=0.014$). The 1-, 3- and 5-year progression-free survival (PFS) rates of the TACE combined ablation group and the radical resection group were 72.3%, 45.4%, 32.1% and 86.2%, 64.8%, 50.1%, respectively, and the difference in PFS rate between the two groups was statistically significant ($\chi^2=10.079$, $P=0.001$). After PSM, the 1-, 3-, and 5-year progression-free survival (PFS) rates of the TACE combined ablation group and the radical resection group were 83.4%, 55.0%, 26.2% and 85.9%, 71.1%, 52.4%, respectively. There was a statistically significant difference in PFS rate between the two groups ($\chi^2=4.931$, $P=0.026$). There was no significant difference in OS rate of the initial treatment group and PFS rate and OS rate of the recurrence group between the two treatment methods.

Conclusion The curative effect of radical resection is better than that of TACE combined with ablation in the treatment of small hepatocellular carcinoma, and it can be used as an effective alternative treatment for patients with hepatocellular carcinoma who cannot tolerate radical resection. But for patients with primary liver cancer, radical resection is preferred.

A quantitative MRI comparative study of imaging markers for cerebral small vessel disease in the middle-aged and elderly patients with and without hypertension

Rui-Jie Du¹, Yuting Xue³, Chunqiang Lu²

1. Department of Radiology, Zhongda Hospital, School of Medicine, Southeast University

2. Jiangsu Key Laboratory of Molecular and Functional Imaging, School of Medicine, Southeast University

3. Collaborative Innovation Center of Radiation Medicine of Jiangsu Higher Education Institutions, Suzhou, China

Purpose To explore the difference of MRI markers of small cerebral vascular disease in middle-aged and elderly patients with hypertension and non-hypertension.

Materials and methods A cross-sectional study. The clinical data of 316 patients who underwent head MRI with susceptibility weighted imaging scans at the Affiliated Zhongda Hospital of Southeast University from November 2013 to August 2022 were retrospectively analyzed, including 190 males and 126 females, with the age of (71.6 ± 8.9) years. According to the history of hypertension, the patients were divided into hypertension group ($n=259$) and the non-hypertension group ($n=57$). The patients in the non-hypertension group were further divided into abnormal blood pressure group on admission ($n=19$) and normal blood pressure group on admission ($n=38$). The imaging features of different CSVD dimensions in the patient's images were quantified or graded and compared between hypertensive and non-hypertensive patient groups. Deep learning methods were employed to segment white matter lesions, and voxel-wise analysis was conducted to investigate the differences in whole-brain white matter lesion probability between patients in both groups. Spearman correlation analysis was used to analyze the correlation between hypertension and small cerebral vascular disease.

Results Compared with the non-hypertensive group, the cerebral microhemorrhage count, deep microhemorrhage count, basal ganglia level lacunae count, perivascular space (EPVS) grade of hemioval center level and EPVS grade of basal ganglia level were higher in the hypertensive group (all $P < 0.05$). The cerebral microhemorrhage count [$3.0(1.0, 15.0)$ vs $1.0(0, 4.2)$], deep microhemorrhage count [$1.0(0, 7.0)$ vs $1.0(0, 4.2)$] and EPVS classification at basal ganglion level [$2.0(1.0, 3.0)$ vs $1.0(1.0, 2.0)$] in the group with history of hypertension were higher than those in the group with normal blood pressure at admission (all $P < 0.05$). The EPVS grade at the central level of the semioval in the hypertension group was higher than that of the group with normal blood pressure at admission [$2.0(1.0, 2.0)$ vs $1.0(1.0, 2.0)$], and also higher than that of the group with abnormal blood pressure at admission [$2.0(1.0, 2.0)$ vs $1.0(1.0, 2.0)$] (both $P < 0.05$). Voxel-by-voxel analysis showed no significant difference in the probability of white matter lesions in the whole brain between patients with and without a history of hypertension, but patients with a history of hypertension showed more extensive para-ventricular white matter hypersignaling than those without a history of hypertension. Spearman correlation analysis showed that hypertension grade was correlated with the number of microbleeding lesions in depth ($r=0.149$), the number of lacunae lesions in the center of the hemioval ($r=0.209$), and the number of lacunae lesions in the basal ganglia ($r=0.204$) (all $P < 0.05$).

Conclusion Chronic hypertension can affect different dimensions of small vessel disease imaging, primarily manifested in the increases of deep microbleed counts and the EPVS grade

PO-211

Massive hemorrhage after percutaneous liver biopsy in a patient with liver tumour: A successful hepatic vein embolization

Naveen Kumar
Naruvi Hospitals

Purpose Hepatic vein injury after percutaneous liver biopsy can be managed with endovascular treatment with high success rate

Materials and methods A 55-year-old female patient with history of carcinoma breast underwent ultrasound-guided Tru-cut biopsy of liver lesion with 18-gauge needle and biopsy tract closed with gelfoam. Pre procedure blood report: HB-9g/dl, Platelet- 3.1 lakh, PT-11.2, INR-0.92. 7 hr after the procedure, the general condition of the patient started to deteriorate. She developed hypotension (50/30mmhg) and tachycardia (110bpm) Blood report- HB-3g/dl. USG abdomen showed hemoperitoneum and perihepatic hematoma. Active bleeding was detected in CT abdomen angiography. The bleeding was noted at portovenous phase. Inotropic supports and blood transfusions were started. Patient was intubated and shifted to ICU.

Results After stabilization patient was transferred to cathlab. Hepatic artery angiography showed no obvious contrast extravasation. Through jugular route hepatic venography was performed, which showed active contrast extravasation from peripheral right hepatic vein. Superselective cannulation was done with 1.98F microcatheter and successful angiographic embolization was performed with N-butyl cyanoacrylate (NBCA) glue. Post embolization significant clinical improvement noted. Patient was extubated next day and discharged in stable condition after 4 days.

Conclusion Angiographic embolization can be performed in patients who are hemodynamically unstable with high technical and clinical success rate. Greatest morbidity and mortality from post biopsy hemorrhages occur when there is a delay in diagnosis or a failure to start aggressive management. This emphasizes the need for close postprocedure observation and physician familiarity with the management of hemorrhagic complications. Embolization should be as selective and peripheral as possible to minimize the affected area and thus decreases the risk of postembolization infarction. The therapeutic options have evolved from surgical management to an endovascular, less invasive approach for treating vascular complications, which has dramatically decreased the morbidity and mortality rates.

PO-212

Transarterial chemoembolization combined with lenvatinib plus tislelizumab for unresectable hepatocellular carcinoma: A multicenter cohort study

Yi Chen

The first hospital of shanxi medical university

Purpose Comparing the efficacy of transarterial chemoembolization (TACE) combined with lenvatinib plus tislelizumab (TLT) with TACE combined with lenvatinib (TL) for unresectable hepatocellular carcinoma, particularly in determining which patients can benefit more from the TLT treatment.

Materials and methods From March 2021 to September 2023, a total of 169 patients from three centers were included in this study, with 103 patients receiving TLT and 66 patients receiving TL. The Kaplan-Meier method was utilized to evaluate the cumulative overall survival (OS) and progression-free survival (PFS) between the two groups and were assessed using the log-rank test. Subgroup analysis on tumor number, maximum tumor diameter, presence of portal vein thrombosis, AFP level, and Child-Pugh class were conducted.

Results The median OS was 26 months in the TLT group, and 20 months in the TL group. The median PFS was 14 months in the TLT group and 9 months in the TL group. The Kaplan-Meier curve demonstrated a significantly superior OS and PFS in the TLT group compared to the TL group. Subgroup analysis showed that for patients with a maximum tumor diameter greater than 7 cm, AFP > 400 ng/ml and accompanied by portal vein tumor thrombus, and Child-Pugh class A, there was a statistically significant difference in OS between TLT and TL groups.

Conclusion OS and PFS were significantly improved in patients who received TLT compared to those who received TL, patients with a largest tumor diameter greater than 7 cm, AFP > 400 ng/ml, Child-Pugh class A and PVTT appeared to derive more benefit.

PO-213

Percutaneous transhepatic lymphangiography and embolization treatment for refractory hepatic lymphorrhea: clinical results in 7 patients

Jian Zhang

The Second Affiliated Hospital of Soochow University

Purpose To evaluate the therapeutic efficacy and safety of percutaneous transhepatic lymphangiography and embolization (PTLE) for the treatment of refractory hepatic lymphorrhea.

Materials and methods This retrospective study analyzed clinical data from seven patients with refractory hepatic lymphorrhea following abdominal surgery who were unresponsive to conservative management. After inguinal lymphangiography excluded lymphatic trunk leakage, all patients underwent PTLE under digital subtraction angiography (DSA) guidance. The study evaluated multiple outcome measures, including: (1) technical success rate, (2) diagnostic accuracy in identifying lymphatic leakage sites, (3) number of required interventions, (4) quantitative and qualitative changes in lymphatic drainage (volume and characteristics), and (5) procedure-related complication rates.

Results The percutaneous transhepatic lymphatic puncture demonstrated a 100% technical success rate (7/7 patients). Intraoperative hepatic lymphangiography successfully identified lymphatic leakage sites in 93.8% of cases (15/16 attempts). Clinical improvement was observed in 6 patients following 1-4 interventions, while one patient showed poor response to treatment. In the treatment-responsive group, significant therapeutic outcomes were noted, including: (1) substantial reduction in abdominal lymphatic leakage, (2) marked elevation of protein gradient, and (3) resolution of lymphatic ascites within 13.4 ± 8.5 days. The procedure exhibited an excellent safety profile, with no major complications reported in any of the 6 successfully treated patients.

Conclusion Percutaneous transhepatic lymphangiography and embolization (PTLE) represents an effective, safe, and minimally invasive therapeutic approach for refractory hepatic lymphorrhea. However, the technical complexity of this procedure is significantly influenced by the intricate anatomical architecture of the intrahepatic lymphatic network, characterized by multiple drainage pathways and hierarchical levels. This anatomical complexity may necessitate multiple sequential interventions to achieve optimal therapeutic outcomes in certain patients.

PO-214

Using Neoadjuvant Chemotherapy in combination with Antiangiogenesis and Immune Checkpoint Inhibitors to Treat Locally Advanced Gastric Cancer: A Real-World Retrospective Cohort Study

Zhouwei Zhan, Bijuan Chen, Zengqing Guo
Fujian Cancer Hospital

Purpose Although immune checkpoint inhibitors (ICIs) and anti-angiogenic drugs have shown efficacy in advanced gastric cancer (GC), their role in the neoadjuvant/conversion therapy remains unclear. The objective of this study was to assess the efficacy and safety of combining neoadjuvant chemotherapy with anti-angiogenesis and ICIs for patients with locally advanced gastric cancer (LAGC).

Materials and methods Upon reviewing our prospectively maintained gastric cancer database, individuals diagnosed with clinical stage II-III gastric cancer (GC) who received neoadjuvant therapy and surgery between January 2022 and August 2023 were included in this cohort study. The comprehensive treatment protocol involved a combination of immune checkpoint inhibitors (ICIs), anti-angiogenic therapy (particularly, apatinib), and chemotherapy (S-1 with oxaliplatin). A systematic method was employed to record the patients' clinical and pathological characteristics, pathological details, and survival outcomes, which were later subjected to meticulous analysis.

Results A total of 38 individuals met the enrollment criteria for the study, with the majority (32, representing 84.2%) having clinical stage III gastric cancer (GC). All patients underwent surgical procedures, leading to an impressive R0 resection rate of 97.4%. Notably, the proportions of major pathological response (MPR) and pathological complete response (pCR) were 47.4% and 23.7%, respectively. After surgery, 36 patients (92.1%) underwent adjuvant chemotherapy. With a median follow-up duration of 18 months, six patients were coping with recurring disease, among which two patients died due to tumor recurrence. The 1-year overall survival (OS) rate was 97.4%, and the disease-free survival (DFS) rate was 84.2%. Significantly, the median OS and DFS had not yet been achieved. It is essential to note that the neoadjuvant therapy regime was well-endured by the patients. No grade 5 treatment-related adverse events (TRAEs) were reported, while only one patient suffered from grade 4 TRAEs, namely immune-related hepatitis. The most frequently observed grade 3 TRAEs were thrombocytopenia, elevated aminotransferase levels and neutropenia.

Conclusion The integration of neoadjuvant chemotherapy, anti-angiogenesis therapy, and ICIs has demonstrated efficacy in managing LAGC patients, yielding high pCR rates and positive survival outcomes, all while preserving a satisfactory safety profile.

PO-215

Integrative analysis of multi-omics data for constructing an ADME-based risk model in gastric cancer

Zhouwei Zhan, Bijuan Chen, Jiami Yu, Zengqing Guo
Fujian Cancer Hospital

Purpose Drug absorption, distribution, metabolism, and excretion (ADME) related genes (ADME-RGs) are linked to cancer survival. This study aimed to identify key ADME genes for therapeutic targets and prognosis prediction in gastric cancer (GC).

Materials and methods GC-related datasets (TCGA-GC, GSE84433, GSE15459, GSE66229, GSE183904) were used. Differentially expressed genes (DEGs) from single-cell and bulk RNA-seq data were integrated with weighted gene co-expression network analysis (WGCNA) to identify candidate genes. Mendelian randomization (MR) analysis selected key genes, which were further analyzed using Cox regression, proportional hazards (PH) tests, and least absolute shrinkage and selection operator (LASSO) regression to construct a risk model. The model was validated across datasets. Furthermore, the independent prognostic analysis, immune infiltration and therapeutic analyses, cell communication and pseudo-time analyses, etc. were conducted to further study the risk model and prognostic genes. Additionally, the expression levels of the key genes were further validated in GC cell lines using qRT-PCR and western blot analyses.

Results MR analysis identified 22 key genes with significant causal associations with GC, from which VCAN and TUBB6 were selected for a robust risk model. Patients were stratified into high- and low-risk groups based on median risk scores. The model demonstrated excellent predictive performance across multiple validation datasets. A nomogram incorporating independent prognostic factors (risk score, age, stage) further enhanced prediction accuracy for overall survival. Immune microenvironment analysis revealed significant differences between risk groups, highlighting immune infiltration patterns and immunotherapy responsiveness. Epithelial cells and monocytes showed distinct intercellular interactions, suggesting their roles in GC pathogenesis. The expression levels of VCAN and TUBB6 were validated in GC cell lines.

Conclusion A new risk model related to ADME for GC was developed and validated, offering significant potential for personalized prognosis prediction and guiding therapeutic strategies in GC.

PO-216

Efficacy and safety of CT-guided percutaneous cryoablation for hepatocellular carcinoma at high-risk sites

Weihao Zhang, tongguo Si, Haipeng Yu, Wenge Xing
Tianjin Medical University Cancer Institute & Hospital

Purpose This study aims to assess the efficacy and safety of CT-guided percutaneous cryoablation in treating hepatocellular carcinoma (HCC) located explicitly in high-risk sites.

Materials and methods Data were collected retrospectively from 685 HCC patients undergoing percutaneous cryoablation at Tianjin Medical University Cancer Hospital between January 2018 and December 2021. Of these, 106 patients had lesions in high-risk sites, defined as a minimum distance of less than 10 mm from the heart/great vessels, diaphragm, gastrointestinal tract, and gallbladder, as determined by preoperative CT or MRI imaging. Technical success rate, complete ablation rate, and complications at 1, 12, and 24 months post-surgery were evaluated. A statistical analysis of the ablation effect difference between the high-risk site and non-high-risk site groups was conducted, utilizing propensity score matching (PSM) to mitigate patient selection bias. Univariate and multivariate logistic regression analyses were performed to identify risk factors for the incidence of coronary heart disease.

Results The study comprised 106 cases in the high-risk group and 218 cases in the non-high-risk group. After PSM analysis until December 2021, 95 matched pairs were included. Both groups demonstrated a 100% intraoperative technical success rate, and no major complications related to cryoablation were observed. Follow-up ranged from 24 to 38 months, with complete ablation without recurrence noted at one-month post-surgery. The complete ablation rate was 82.1% and 71.7% in the high-risk group and 83.9% and 73.9% in the non-high-risk group at 12 and 24 months, respectively. There was no significant difference in complete ablation rates between the two groups before and after PSM ($P > 0.05$). Multivariate analysis identified the distance between the tumor edge and high-risk site ≤ 5 mm and preoperative transarterial chemoembolization (TACE) treatment as independent risk factors for cryoablation effect.

Conclusion CT-guided percutaneous cryoablation proves to be a safe and effective approach for HCC patients with high-risk sites, emphasizing the importance of proper preoperative planning and intraoperative manipulation.

PO-218

Lenvatinib Plus Hepatic Arterial Infusion Chemotherapy of Oxaliplatin, Fluorouracil, and Leucovorin versus Lenvatinib Alone for Advanced Hepatocellular Carcinoma: a multicenter retrospective cohort study

Feng Shi

Guangdong General Hospital/CN

Purpose Lenvatinib stands out as a first-line therapy for individuals with advanced hepatocellular carcinoma (HCC). Concurrently, hepatic arterial infusion chemotherapy comprising oxaliplatin, fluorouracil, and leucovorin (FOLFOX-HAIC) has emerged as a potential option for those with advanced HCC. It is necessary to investigate the efficacy and safety of lenvatinib plus FOLFOX-HAIC (lenvaHAIC) for advanced HCC in real-world situations.

Materials and methods In this retrospective analysis, 127 consecutive patients underwent lenvaHAIC, while 184 patients received lenvatinib alone as first-line treatment at six Chinese academic centers between January 2019 and June 2022. Following 1:1 propensity-score matching, we established paired cohorts (113 patients in each group) for evaluating survival. Overall survival (OS), progression-free survival (PFS), objective response rate (ORR), and safety profiles were compared between the two groups.

Results The lenvaHAIC group exhibited significantly prolonged median PFS and OS than the lenvatinib group (PFS: 12.3 vs. 6.2 months; OS: 25.6 vs. 12.3 months; $P < .001$ for each). In the propensity-score matched cohorts (113 pairs), both PFS and OS were notably extended in the lenvaHAIC group compared with those in the lenvatinib group ($P < .001$). Multivariate analysis identified lenvaHAIC treatment as an independent factor for improved PFS (hazard ratio [HR] 0.45; $P < .001$) and OS (HR 0.38; $P < .001$). Grade 3-4 adverse events, including nausea, vomiting, diarrhea, thrombocytopenia, and neutropenia, were more prevalent in the lenvaHAIC group.

Conclusion LenvaHAIC may be a promising treatment in patients with advanced hepatocellular carcinoma, demonstrating enhanced OS, PFS, and ORR and an acceptable safety profile.

Development and Application of a Whole Transcriptome Sequencing Assay for the Detection of Gene Fusions in Non-Small Cell Lung Cancer Specimens

Songchen Zhao², Caicun Zhou¹, Xinhua Du³, Yan Zhang³, Jing Bai³, Lu Meng³, Xuefei Li⁵, Jiaxin Ma³, HeYu Sheng³, Xiaorui Fu³, Yanfang Guan³, Yuting Yi³, Ling Yang³, Xuefeng Xia³, Xin Yi³, Xinxin Tan⁴, Fei Zhou¹

1. Shanghai East Hospital

2. Tongji University School of Medicine

3. Geneplus-Beijing Institute

4. Geneplus-Shenzhen Clinical Laboratory

5. Tongji University Affiliated Shanghai Pulmonary Hospital

Purpose Gene fusions are a significant driver of non-small cell lung cancer (NSCLC) and other cancers. Their rapid and accurate identification is critical for guiding clinical decisions, such as the selection of targeted therapies. However, traditional methods of fusion detection, including whole transcriptome sequencing (WTS), are often limited by poor specificity, sensitivity, and accuracy. Moreover, the performance characteristics of WTS for detecting gene fusions have not been thoroughly explored, and splice mutations are frequently overlooked. To address these challenges, we developed a WTS assay capable of detecting gene fusions, kinase exon duplications, exon skipping events (e.g., *MET* exon 14 skipping), and *EGFR* VIII alterations.

Materials and methods 1. Cohort Selection for Development and Validation of the WTS assay

Most of the development and validation work was conducted using a cohort, which included four fusion-positive commercial samples, one fusion-negative commercial sample, one NTRK fusion-positive transfected cell line, 42 formalin-fixed paraffin-embedded (FFPE) tumor specimens, and 10 normal tissue samples. The 42 tumor samples, consisted of 28 NSCLC, eight soft tissue sarcomas, three gliomas, two cases of diffuse large B-cell lymphoma (DLBCL), and one gastric cancer. Additionally, a retrospective cohort, consisting of 192 FFPE samples, was used to assess RNA integrity in this study.

2. RNA Extraction, Library Preparation and Sequencing

In this study, total RNA was extracted from FFPE specimens stored at 4°C for less than one year using RNeasy FFPE Kit (Qiagen, Germany).

As the initial step, an accurate assessment of RNA quality determines which type of library preparation and sequencing parameters are required¹. The total RNA was assessed and quantified using the NanoDrop 8000 (Thermo Fisher Scientific, Germany), Qubit 3.0 (Life Technologies, USA) and the Agilent 2100 Bioanalyzer system (Agilent Technologies, USA). The NEBNext rRNA Depletion Kit (Human/Mouse/Rat) (NEB, USA) was then used to remove targeted ribosomal RNA.

For RNA samples with a DV200 (percentage of RNA fragments >200 nucleotides) of 50% or less, the fragmentation step was skipped, and the samples proceeded directly to library preparation. After rRNA depletion and optional fragmentation, cDNA synthesis and NGS library preparation were performed using the NEBNext® Ultra™ II Directional RNA Library Prep Kit (NEB, USA), following the manufacturer's protocol, except for substituted adaptor and index primer created through Gene+seq 2000.

The library was quantified using the Qubit 3.0 (Life Technologies, USA) and assessed for quality with the LabChip GX Touch (PerkinElmer, USA). Sequencing was conducted on the Gene+seq 2000 instrument (Geneplus-Suzhou, China).

3. Reportable Range

To assist in filtering gene fusions of potential diagnostic, prognostic, or therapeutic value, we developed a list of genes considered reportable in this assay. In accordance with the NCCN Clinical Practice Guidelines and expert consensus in oncology, several databases (e.g., FusionGDB², ChimerDB³, and Geneplus-Beijing Internal Database) as well as the biomedical literature were searched for gene fusions identified in both solid tumors and hematologic cancers. The criteria for selecting reportable fusions were as follows: i) fusions detected with high frequency (≥ 20 occurrences); ii) all known oncogenes in the event that a new activating fusion might be discovered; iii) all tumor suppressor genes that are valuable for the diagnosis or prognosis (e.g., *TP53*). Applying these criteria, the list of reportable genes was narrowed down to 553 genes, reducing the number of mRNA-encoding genes analyzed in the transcriptome from approximately 22,000 to 553.

4. Bioinformatic Analysis for Fusion Calls Based on the WTS assay

The first step in the bioinformatic process was to filter the raw data to obtain clean data. This included the removal of terminal adaptor sequences and low-quality data using (version: 0.19.5)⁴, followed by the elimination of rRNA reads by aligning the reads to the rRNA database (downloaded from NCBI) using (version: 2.2.8)⁵. Clean reads were then aligned to the reference human genome (hg19) using STAR (version 020201)⁶.

In this study, fusions were detected using a customized version of Arriba 1.1.0⁷ detecting fusion transcripts. For fusion annotation, we selected the fusion transcript most frequently reported or defined in the NCBI database as the primary transcript when multiple potential fusion transcripts were identified for the same fusion pattern. Additionally, skipping variations were detected using an in-house software tool, FoRNA.

Quality control (QC) is critical in ensuring reliable test results. Before generating the final clinical report, we computed multiple QC parameters to evaluate both RNA quality and fusion calls. These parameters included contamination rate, mapping rate, mapped reads, and mapped junction reads, among others. The cross-contamination rate of RNA samples was evaluated using Contao software (<https://github.com/grailbio/contao/>). Additionally, microbiological analysis conducted using Kraken⁸ and gene body coverage was assessed using RNA-SeQC assessment⁹.

5. Cohort Selection for Clinical Implementation of the WTS Assay

To evaluate the clinical QC performance of the WTS assay, including RNA yield, degradation level, microbiological contamination, and bioinformatics analysis QC parameters, 156 clinical pancreatic cancer samples were used. Additionally, a retrospective cohort from multiple centers was employed to describe the fusion landscape across pan-cancer, including data from NSCLC.

Results We defined a DV200 value $\geq 30\%$ as the threshold for RNA degradation. For optimal sensitivity, the standard RNA input should exceed 100 ng, and the number of mapped reads should be greater than 80 Mb. Fusions with more than 40 copies/ng showed a higher positive call rate (98.8%). Our assay successfully identified 62 out of 63 known gene fusions, achieving a sensitivity of 98.4%. No false-positive fusions were detected in 21 fusion-negative specimens. Except for the low-expression fusion *TPM3-NTRK1*, repeatability was 100% (35/35) across four clinical samples and one reference standard. In all fusion identified in 102 NSCLC samples, 66.7% (20/30) of the detected fusions were actionable. Beyond actionable fusions, we identified several fusions with diagnostic value, as well as fusions shared across different cancer types.

Conclusion We have developed a new WTS assay with high sensitivity, specificity, repeatability, and reproducibility. This assay can identify actionable gene fusions and provides valuable insights into the fusion landscape across various cancers, helping guide treatment decisions including NSCLC.

PO-220

Experimental Study on EGFR Expression in Hepatocellular Carcinoma Cells and Sensitivity to Gefitinib and Lenvatinib

Jun Chen, Houhui Shi

College of Pharmaceutical Science, Zhejiang University of Technology; Zhejiang Provincial People's Hospital (Affiliated People's Hospital)

Purpose To investigate the differences in the expression levels of epidermal growth factor receptor (EGFR) among different hepatocellular carcinoma (HCC) cell lines and their sensitivity to the molecular targeted drugs gefitinib and lenvatinib.

Materials and methods Five HCC cell lines (HUH7, HEPG2, SNU449, JHH7, and LM3) were selected. Western blot and quantitative real-time PCR (qRT-PCR) were used to screen for two cell lines with significant differences in EGFR expression. The cytotoxic effects of gefitinib and lenvatinib, either alone or in combination, on these two cell lines were assessed using the CCK-8 assay to explore the correlation between EGFR expression levels and drug sensitivity.

Results Western blot analysis showed that the protein expression level of EGFR in the HUH7 cell line was significantly higher than that in the HEPG2 cell line ($P < 0.0001$). qRT-PCR results also indicated that the mRNA expression level of EGFR in the HUH7 cell line was significantly higher than that in the HEPG2 cell line ($P < 0.0001$). The CCK-8 assay demonstrated that the HUH7 cell line was more sensitive to both gefitinib and lenvatinib than the HEPG2 cell line. At a concentration of 20 μM gefitinib, the cell viability of HEPG2 was $87.56 \pm 6.998\%$, while that of HUH7 was $76.79 \pm 4.276\%$ ($P = 0.0062$). At 40 μM gefitinib, the cell viability of HEPG2 was $53.92 \pm 4.922\%$, while that of HUH7 was $22.02 \pm 2.613\%$ ($P < 0.0001$). At a concentration of 5 μM lenvatinib, the cell viability of HEPG2 was $97.56 \pm 4.759\%$, while that of HUH7 was $54.48 \pm 5.255\%$ ($P < 0.0001$). Moreover, the combination of lenvatinib and gefitinib significantly enhanced the antitumor effect on HUH7 cells. The cell viability was $54.48 \pm 5.255\%$ with single-drug treatment and $36.97 \pm 2.696\%$ with combination treatment ($P < 0.0001$).

Conclusion There is a significant difference in EGFR expression levels between the HEPG2 and HUH7 cell lines. EGFR expression is closely correlated with the sensitivity of hepatocellular carcinoma cells to the molecular targeted drugs gefitinib and lenvatinib. EGFR may serve as a potential molecular marker for precision treatment of hepatocellular carcinoma.

PO-221

ITM2a suppresses proliferation and migration by inhibiting EMT in microvascular invasion-positive hepatocellular carcinoma via the GJA1-MAPK/ERK axes

Peng Yan, Jian song Ji

Lishui Central Hospital, The Fifth Affiliated Hospital of Wenzhou Medical University

Purpose Hepatocellular carcinoma (HCC) is the most common type of primary liver cancer worldwide, accounting for 85%-90% of all liver cancers, and its incidence is rising rapidly on a global scale. Microvascular invasion (MVI) significantly impacts the prognosis and recurrence of hepatocellular carcinoma (HCC). Yet, the molecular features, associated biological functions, and mechanisms in MVI-positive HCC remain poorly understood. In this study, we aim to identify new biomarkers associated with MVI positivity.

Materials and methods RNA sequencing identified differentially expressed genes from a total of ten pairs of cancerous and corresponding non-cancerous tissues collected from six MVI-positive and four MVI-negative HCC patients. Using the TCGA-LIHC dataset, target genes were selected through ESTIMATE analysis and Kaplan-Meier analysis, followed by validation of their expression via immunohistochemistry. Gain-of-function and loss-of-function experiments investigated the anti-tumor effects of the target gene in vitro and in vivo. Combined transcriptomic and metabolomic analyses identified genes and pathways associated with the target gene, and its regulatory mechanisms in HCC were explored using Western blot and rescue experiments.

Results ITM2a exhibits decreased expression in the tumor tissues of MVI-positive HCC and is associated with favorable patient outcomes. Overexpression of ITM2a inhibits proliferation, migration, and invasion of HCC cells, while silencing ITM2a has the opposite effects. Mechanistically, overexpression of ITM2a in HCC cell lines upregulates GJA1 expression, which inhibits activation of the MAPK pathway, thereby suppressing the EMT process in HCC. Conversely, silencing ITM2a produces opposite effects. In vivo, overexpression of ITM2a reduces HCC proliferation and metastasis and suppresses the EMT process.

Conclusion Our study identifies ITM2a as a new biomarker for MVI-positive hepatocellular carcinoma, highly correlated with a favorable prognosis in MVI-positive patients. In vitro and in vivo experiments demonstrate that upregulation of ITM2a expression can inhibit the proliferative, migratory, and invasive capabilities of hepatocellular carcinoma cells, and regulate the EMT process in HCC via the ITM2a-GJA1-MAPK/ERK axis, offering new insights and a potential prognostic target for understanding the mechanisms of MVI-positive HCC.

PO-222

Percutaneous MR-guided Thermal Ablation for Recurrent Subcentimeter Hepatocellular Carcinoma

Jin Chen, Bing Zhang, Bing-yu Huang

First Affiliated Hospital of Fujian Medical University; Fujian Fuzhou ,350000

Purpose To evaluate the technical efficacy and therapeutic outcomes of percutaneous MR-guided thermal ablation including microwave ablation (MWA) and radiofrequency ablation (RFA) for recurrent subcentimeter hepatocellular carcinomas (HCCs).

Materials and methods From January 2015 to May 2024 we recruited 101 patients with 119 recurrent subcentimeter HCCs (mean diameter: 8.0 ± 1.3 mm, range: 5.6–9.9 mm), who were treated with MR-guided thermal ablation. Technical success, technical efficacy, complications, and local tumor progression (LTP) rate were evaluated after ablation. Cumulative LTP rate and recurrence-free survival (RFS) were estimated using the Kaplan-Meier method.

Results A retrospective analysis showed that MR-guided thermal ablation (MWA, n =84; RFA, n =17) was successfully executed in all cases. Technical success and efficacy were achieved in all lesions in single sessions without major complications. The mean follow-up duration was 41.1 ± 27.1 months (median:38.0 months; range:3–105 months). The cumulative LTP rate at 1 year was 1.2%, and 5.8% at 3, 5, 7, and 9 years. The cumulative RFS rates at 1, 3, 5, 7, and 9 years were 82.2%, 44.6%, 29.0%, 23.2% and 23.2%, respectively.

Conclusion Percutaneous MR-guided thermal ablation for recurrent subcentimeter HCCs demonstrated high technical success, ready visualization of lesions and ablation margins, and minimal LTP after a single treatment session.

PO-223

CT-guided percutaneous coaxial cutting needle biopsy of pulmonary lesions using trans-osseous approach

Bing Zhang, Jin Chen, Bing-yu Huang, Zheng-yu Lin
the first affiliated hospital of Fujian Medical University

Purpose This study aims to evaluate the safety and efficacy of CT-guided percutaneous trans-osseous coaxial cutting biopsy approach of lung lesions that are challenging or risky to access using conventional methods.

Materials and methods The data of 13 lesions in 12 patients who underwent consecutive CT-guided percutaneous trans-osseous coaxial cutting biopsy of lung lesions were retrospectively analyzed. The scapular approach was used for 9 lesions in the posterior upper lung lobe, while the sternal approach was employed for 4 lesions in the anterior upper lung lobe near the heart and major vessels. The procedure involved creating an artificial bone channel using a bone puncture needle under CT guidance, through which the coaxial cutting biopsy was performed. We assessed technical success rate, complications and pathological diagnosis accuracy.

Results All 13 lesions across 12 patients were successfully biopsied using the CT-guided percutaneous trans-osseous coaxial cutting technique, yielding a positive pathological diagnosis rate of 100%. One patient developed moderate pneumothorax post-procedure, which was managed with chest tube drainage. No other complications, such as hemorrhage or pain in the sternum or scapula areas, were reported in the remaining patients.

Conclusion CT-guided percutaneous trans-osseous coaxial cutting biopsy technique is safe and effective, particularly for lung lesions in challenging locations, such as the posterior segment and anterior upper lobe adjacent to the heart and major vessel. This approach may reduce the risk of complications such as pneumothorax and hemorrhage, making it a valuable option for difficult-to-access lung lesions.

PO-224

Tumor acidity-Regulating Lipiodol Pickering Emulsions Stabilized by Iron Nanoparticles Enables transarterial ferro-embolization therapy

Weihao Yang, caifang Ni
the First Affiliated Hospital of Soochow University

Purpose Transcatheter arterial chemoembolization (TACE) is a first-line mini-invasive intervention approach for hepatocellular carcinoma (HCC) patients at intermediate and advanced stages. However, its long-term therapeutic outcome is significantly limited by unfavorable pharmacokinetic behaviors of the loaded drug and intraarterial embolization aggravated tumor immunosuppression.

Materials and methods In this study, iron nanoparticles (FeNPs) with pH-dependent Fenton catalytic ability was synthesized and utilized as the particular surfactant to stabilize Lipiodol Pickering emulsion (LPE) for tumor localized delivery of cariporide in responding to the extracellular tumor acidity.

Results It was shown that such cariporide, an inhibitor of sodium-hydrogen exchanger, markedly enhanced the ability of FeNPs to induce immunogenic ferroptosis of cancer cells via down-regulating intracellular pH. The obtained cariporide-loaded FeNPs-stabilized LPE, abbreviated as CFe-LPE, was also capable of initiating potent antitumor immunity. As a result, transcatheter arterial embolization treatment with CFe-LPE exhibited significantly improved therapeutic efficacy against orthotopic N1S1 HCC in rats in comparison with conventional TACE treatment with the mixture of doxorubicin and Lipiodol.

Conclusion This study highlights a concise strategy to prepare a Fenton catalytic LPE-based embolic agent that can concurrently regulate both extracellular and intracellular pH of HCC cells for transarterial ferro-embolization therapy.

PO-225

Development and Validation of MRI Radiomics-Based Models for Predicting Overall Survival of Cholangiocarcinoma After Hepatic Arterial Infusion Chemotherapy

Kanglian Zheng¹, Yilin Li², Yang Luo³, Guang Cao¹, Liang Xu¹, Yuyang Dai¹, Chuanxin Niu¹, Jie Tian⁴, Jingwei Wei⁵, Xiaodong Wang¹

1. Peking University Cancer Hospital

2. Anhui Medical University

3. Xidian University

4. Key Laboratory of Molecular Imaging, Institute of Automation, Chinese Academy of Sciences

5. Institute of Automation, Chinese Academy of Sciences

Purpose To develop and validate MRI radiomics-based models to predict the overall survival (OS) for patients with unresectable cholangiocarcinoma (CCA) after hepatic arterial infusion chemotherapy (HAIC) with oxaliplatin and 5-fluorouracil.

Materials and methods Patients with unresectable CCA treated by HAIC with oxaliplatin and 5-fluorouracil between March, 2011 and January, 2023 were reviewed in this retrospective study. Pretreatment clinical characteristics and MRI imaging data were analyzed. Clinical characteristics were selected using univariate and multivariate Cox regression model, and MRI radiomics features were selected using least absolute shrinkage and selection operator regression model. The models were constructed using the gradient boosting machine method to predict OS.

Results A total of 141 patients (90 males and 51 females, mean age: 60.77 ± 10.26 years) were enrolled, and assigned randomly (4:1) into training (112 patients) and testing sets (29 patients). Modelcombined showed the best performance in predicting prognosis for patients with unresectable CCA before HAIC. The concordance indexes (C-indexes) of Modelcombined were 0.792 (95% confidence interval [CI]: 0.749-0.828) and 0.753 (95% CI: 0.626-0.867) in the training and testing sets, respectively. The Modelcombined showed a more favorable clinical utility than the TNM staging system in predicting prognosis.

Conclusion In this study, MRI radiomics-based models were constructed and provided useful and valuable tools to predict OS for patients with unresectable CCA before HAIC with oxaliplatin and 5-fluorouracil.

PO-226

Radioiodine-labeled gel-microspheres for radioembolization combined with photothermal treatment of hepatocellular carcinoma

Xingwei Sun¹, Yong Jin¹, Guanglin Wang²

1. The Second Affiliated Hospital of Soochow University

2. Soochow University

Purpose Transarterial radioembolization (TARE) is an established clinical therapy for treating patients with intermediate to advanced hepatocellular carcinoma (HCC) or those who cannot undergo radical treatment. However, the delivery of a high radiation dose is associated with a number of adverse effects, such as radiation pneumonitis. Additionally, the available radioactive microspheres are dense and unsuitable for interventional delivery. This study proposes the use of commercial CalliSpheres® PVA gel microspheres coated with polydopamine (PDA) as a carrier for radioactive iodine (¹³¹I) labeled using the iodogen method, denoted as ¹³¹I-PVA@PDA microspheres, can be for radioembolization combined photothermal therapy (PTT) of HCC.

Materials and methods Commercial CalliSpheres® PVA gel microspheres coated with polydopamine (PDA) as a carrier for radioactive iodine (¹³¹I) labeled using the iodogen method, denoted as ¹³¹I-PVA@PDA microspheres, can be for radioembolization combined photothermal therapy (PTT) of HCC.

Results In vitro experiments have demonstrated that ¹³¹I-PVA@PDA microspheres have excellent radiostability and photothermal properties. SPECT/CT imaging and biodistribution experiments have shown that ¹³¹I-PVA@PDA microspheres remain stable in vivo without any radioactive leakage. The results of the antitumor study suggest that ¹³¹I-PVA@PDA microspheres are an effective treatment for inhibiting tumor growth through a combination of radioembolization and PTT, while avoiding significant side effects.

Conclusion These multifunctional microspheres have great potential for clinical application in the treatment of HCC.

PO-227

Mechanism of action of jujuboside B in regulating the BMAL1-HSP90AA1 pathway to restore the cellular molecular clock to promote the efficacy of TMZ against drug resistance in lung cancer

Hui Zuo, Wei Feng, Yalian Sa

The Affiliated Hospital of Kunming University of Science and Technology /The First People's Hospital of Yunnan

Purpose Lung malignancies currently rank as one of the most prevalent and deadly cancers globally, with chemotherapy resistance leading to treatment failure for many lung cancer patients. Therefore, a deeper understanding of the mechanisms of lung cancer resistance is crucial for developing more effective therapies in the future. **Objective:** This study aims to elucidate the molecular mechanism by which Jujuboside B regulates the BMAL1-HSP90AA1 pathway to enhance the efficacy of TMZ against lung cancer.

Materials and methods A549/TR resistant cell lines were purchased, and a series of in vitro experiments were conducted using Jujuboside B on A549 and A549/TR cells, including Transwell migration assays, scratch wound healing assays, cell cycle analysis, and apoptosis assays. BMAL1 expression levels in cells were measured at different time points to observe the changes in clock gene expression. Subsequently, BMAL1 was subjected to activation or inhibition to assess its impact on Jujuboside B-treated A549/TR cells. Additionally, HSP90AA1 gene expression was knocked down in overexpressing BMAL1 cell lines to evaluate the combined effects of these two genes on the action of Jujuboside B and TMZ in A549/TR cells.

Results Jujuboside B inhibited the growth and proliferation of both A549 and A549/TR cells. After developing chemotherapy resistance, the expression frequency of BMAL1 was altered, resulting in a reprogramming of biological rhythms. Furthermore, the effects of Jujuboside B were negated in A549/TR cells that expressed either activated BMAL1 or overexpressed HSP90AA1, leading to increased cell invasion and migration and decreased apoptosis. Conversely, knocking down HSP90AA1 in BMAL1-overexpressing cell lines significantly suppressed Jujuboside B's effects.

Conclusion Jujuboside B enhances the sensitivity of lung cancer cells to TMZ, with its molecular mechanism operating through the regulation of BMAL1-HSP90AA1 expression levels.

PO-228

Short-term efficacy and safety of novel EqualSpheres® drug-eluting beads bronchial arterial chemoembolization for advanced non-small cell lung cancer: a retrospective cohort study

Bin Li
Beijing Hospital

Purpose This retrospective cohort study aimed to investigate the short-term efficacy and safety of novel EqualSpheres® drug-eluting beads bronchial arterial chemoembolization (DEB-BACE) for the treatment of advanced non-small cell lung cancer (NSCLC).

Materials and methods A total of six consecutive patients with advanced NSCLC who received novel EqualSpheres® (particle size: 400µm) DEB-BACE (loaded with gemcitabine) from January 2024 to January 2025 were enrolled. Short term local tumor response was evaluated according to the modified RECIST criteria. The technical success rate, complications and adverse events (AEs) were analyzed on examinations and clinical symptoms.

Results All patients received EqualSpheres® BACE load with gemcitabine (800mg), the drug loading method is to mix microspheres with gemcitabine at 23°C-28°C for 5-10 min. The technical success rate was 100%. A total of six patients received thirteen times, two of them received a third session of DEB-BACE, three of underwent a second session of DEB-BACE, and one underwent one cycle of DEB-BACE. The median follow-up period was 120 days. Based on the modified RECIST, objective response rates (ORR) were 83.3%, 66.7% and 66.7%, and disease control rates (DCR) were 100%, 100% and 83.3% at one-, two- and three-month after DEB-BACE, respectively. Postoperative complications and AEs were tolerated and relieved by symptomatic treatment. No one of the patients died during the procedure.

Conclusion Novel EqualSpheres® DEB-BACE appears to be a promising and well-tolerated approach for patients with advanced NSCLC.

PO-229

The efficacy and safety of TACE combined with systemic therapy in patients with unresectable liver cancer

Ning Ai
the Fourth Hospital of Hebei Medical University

Purpose To analyze the efficacy and safety of transarterial chemoembolization (TACE) combined with targeted immunotherapy and TACE combined with targeted therapy for unresectable hepatocellular carcinoma (uHCC) retrospectively.

Materials and methods We retrospectively analyzed the data of patients with unresectable HCC from January 2019 to June 2023. Patients were screened and included according to the following criteria, and were divided into a triple therapy group (TACE+T+I) and a double combination group (TACE+T). The main endpoints of the study were overall survival (OS), progression free survival (PFS), and adverse events (AE). The secondary endpoints are objective response rate (ORR) and disease control rate (DCR). Determine the risk factors associated with PFS and OS through Cox regression analysis.

Results A total of 89 patients were included in this study, including 43 in the TACE+T+I group and 45 in the TACE+T group. More than half of the patients who received TACE+T+I treatment were followed up for 29.00 months, and the median OS was significantly prolonged (23.8 vs 20.1 months, $P=0.007$), with a median progression free survival (9.70 vs 7.00 months, $P=0.017$); neither group experienced grade 4 adverse events or treatment-related deaths. Attributed to systemic grade 3 adverse events, there was no significant difference between the two drug groups (19.0% vs 15.6%, $P=0.667$). Patients in the TACE+T+I group showed better tumor response, with an ORR of 52.4% compared to patients in the TACE+T group. 17.8% ($P=0.001$). No significant difference was observed in DCR between the two groups (83.6% vs 77.5%, $P=0.522$). Cox regression analysis showed that treatment regimen was an independent factor for OS, while age and treatment regimen were independent factors associated with PFS.

Conclusion Compared with the dual combination group, triple therapy (TACE+T+I) can improve the efficacy and survival rate of unresectable HCC patients, and its safety is controllable.

PO-230

Efficacy and Safety of Hepatic Arterial Infusion Chemotherapy(HAIC) Combined with PD-1 Inhibitors for Advanced Hepatocellular Carcinoma with Macrovascular Invasion: A Multicenter Propensity Score Matching Analysis

Fengtao Zhang

Huazhong University of Science and Technology Union Shenzhen Hospital(Shenzhen Nanshan People's Hospital)

Purpose To investigate the efficacy and safety of HAIC combined with programmed cell death protein-1 (PD1) inhibitors in MVI- positive advanced hepatocellular carcinoma(HCC).

Materials and methods From September 2017 to May 2019, we retrospectively collected the clinical data from three medical centers in China pertaining to patients diagnosed with BCLC C stage HCC with MVI and receiving treatment with a combination of HAIC and PD-1 inhibitors treatment or HAIC alone, and we compared the efficacy of HAIC combined with PD-1 inhibitors and HAIC monotherapy. Propensity score matching(PSM) was utilized to adjust for baseline differences between groups. Survival outcomes and tumor response rate were used to assess survival benefits, while the incidence of adverse events was used to evaluate safety

Results After screening for eligibility, 489 patients diagnosed with HCC and concomitant MVI were enrolled. Of these, 173 patients received treatment combining HAIC with PD-1 inhibitors, while 316 patients underwent HAIC monotherapy. After PSM adjustment, the combination therapy group demonstrated superior survival outcomes. Median overall survival(OS) and progression free survival (PFS) were 31.8 months and 10.8 months, respectively, significantly higher than those in the monotherapy group (OS: 10.0 months; PFS: 6.1 months; both $P<0.0001$). Moreover, ORR and DCR remained significantly elevated in the combination therapy group (ORR: 44.3% vs 20.4%, $P<0.0001$; DCR: 89.8% vs 82.0%, $P=0.041$). Safety profiles indicated no significant differences in adverse event rates between the two treatment groups, encompassing both overall and grade-specific assessments.

Conclusion Compared to HAIC alone, the combination of HAIC with PD-1 inhibitors represents a more promising and effective approach for patients with HCC complicated by macrovascular invasion.

PO-232

MRI-Based Radiomics for the Recurrence Prediction of Hepatocellular Carcinoma Treated with Postoperative Adjuvant Transcatheter Arterial Chemoembolization

Lingling Zhou, Liyun Zheng, Jiansong Ji
Lishui Central Hospital

Purpose To explore the effectiveness of radiomics signature in predicting the recurrence of hepatocellular carcinoma (HCC) undergoing postoperative adjuvant transcatheter arterial chemoembolization (PA-TACE).

Materials and methods In this multicenter retrospective study, 204 patients with multi-parametric magnetic resonance imaging (mpMRI) were included. Recurrence-related radiomics features were extracted from the arterial phase, portal venous phase and T2-weighted imaging, respectively. The radiomics models were established by using 101 combinations of 10 machine learning algorithms, then identified the most valuable radiomics model based on the average C-index of the training, the internal and external validation cohorts. Besides, all patients were stratified into high-risk signature (HRS) and low-risk signature (LRS) of recurrence by the median value of the Radiomics score (Rad-score) to analyze the benefit of PA-TACE. The independent prognostic factors for predicting HCC recurrence were identified using Cox regression analysis and predictive models were developed. By combining clinical-pathologic characteristics with Rad-score, a combined nomogram was further constructed. The performance of the three models was assessed by the C-index.

Results The radiomics model developed by CoxBoost + survival-SVM method was regarded as the optimal prognostic model with C-index of 0.828, 0.796, 0.718 in the training, the internal and external validation cohorts. Additionally, compared with the LRS group, patients in the HRS group exhibited significantly longer RFS, indicating that those with a higher Rad-score benefited more from PA-TACE. The combined nomogram presented better predictive performance in terms of prognostic risk for HCC patients following PA-TACE with C-index of 0.848, 0.825, 0.722 in three cohorts, respectively. The decision curve analysis indicated that the combined nomogram had relatively higher clinical net benefits.

Conclusion Radiomics based on mpMRI could be potential biomarkers for predicting the RFS of HCC patients undergoing PA-TACE and conducive to screen candidates for PA-TACE to achieve precise treatment.

PO-233

Hepatic Arterial Infusion Chemotherapy with mFOLFOX in Advanced Gallbladder Cancer: An Approach with Potential for Conversion and Enhanced Survival

Yajun Zhang¹, Guimin Guo¹, Zhizhong Ren², Xiaowei Yang², Tianxiao Wang², Ying Liu², Yuewei Zhang²

1. Qinghai University Affiliated Hospital

2. Beijing Tsinghua Changgung Hospital

Purpose Gallbladder cancer (GBC) is an aggressive malignancy with a poor prognosis, particularly in advanced stages where curative surgical interventions are often not feasible. Conventional systemic chemotherapy, while commonly used, has shown limited efficacy and considerable side effects. Hepatic arterial infusion chemotherapy, a novel regimen with 5-fluorouracil, leucovorin, and oxaliplatin (FOLFOX-HAIC), has emerged as a promising alternative treatment approach. This technique delivers chemotherapeutic agents directly to the liver via the hepatic artery, providing targeted drug delivery to the tumor site, which may enhance local antitumor effects while reducing systemic side effects. mFOLFOX-HAIC offers a novel strategy to improve the management of advanced GBC, especially in patients who are not candidates for surgical resection or other conventional therapies.

Materials and methods This retrospective study included 23 patients diagnosed with advanced GBC who received modified FOLFOX-HAIC regimen (mFOLFOX-HAIC), oxaliplatin (50 mg per day) and 5-fluorouracil (1500 mg per day) are administered via femoral artery infusion for 2–3 days at Beijing Tsinghua Changgung Hospital. All patients were deemed unsuitable for surgical resection following evaluation by a multidisciplinary team. The chemotherapy regimen was based on oxaliplatin, administered every 3 to 4 weeks. Tumor response, overall survival (OS), progression-free survival (PFS), conversion rate, and adverse events were systematically assessed.

Results From diagnosis and the first mFOLFOX-HAIC treatment, the mOS for the 23 patients was 17.0 months and 10.0 months, respectively and the mPFS was 7.0 months. The overall objective response rate (ORR) was 65.2 %, and the disease control rate (DCR) was 86.9 %. Three (13.0%) patients underwent surgical resection post-HAIC, with 2 patients achieving pathological complete response (pCR). Grade 3 adverse events were noted in 4 (17.4 %) patients with no instances of grade 4 adverse events.

Conclusion mFOLFOX-HAIC shows high response rates and potential conversion rate of unresectable GBC. Its safety profile is manageable, making it a viable option for patients ineligible for conventional therapies.

PO-234

Personalized Drug Screening of Patient-derived Tumor-like Cell Clusters Based on Specimens Obtained from Percutaneous Transthoracic Needle Biopsy in Patients with Lung Malignancy: A Real-world Study.

Xu Sheng

Beijing Hospital, National Center of Gerontology

Purpose Patient-derived xenografts and organoids were the most common patient-derived tumor models in vitro that were utilized in personalized drug screening, and the establishment rate and duration required to be improved. Patient-derived tumor-like cell clusters (PTCs) could be established within ten days for drug screening, with high establishment rate and accuracy in predicting clinical outcomes. This study aims to explore the accuracy of PTCs based on specimens obtained from percutaneous transthoracic needle biopsy (PTNB) in lung malignancy (LM) patients, and to investigate the predictors for the success of PTC culture.

Materials and methods This retrospective cohort study included LM patients who underwent image-guided PTNB, and the specimens were used for PTC culture, which was followed by personalized drug screening of chemotherapy and molecular targeted therapy, and the accuracy was validated by previous or further treatments. The predictors of the success of PTC culture were identified by univariable and multivariable analyses.

Results A total of 68 LM patients were enrolled, consisting of 57, 7, and 4 patients with non-small cell lung cancer, small cell lung cancer, and lung metastases, respectively. Pneumothorax was the predominant adverse event for PTNB, with an incidence rate of 20.6% (14/68). PTC models based on PTNB specimens were established successfully for 56 patients in 3.8 ± 2.3 days, with an 82.4% success rate. Five patients had not received treatments before or after PTC culture. PTC drug screening reveals 88.2% (45/51) overall consistency in predicting clinical outcomes. Necrotic area over half of the tumor (hazard ratio, 0.121; 95% confidence interval, 0.025–0.598; $P = 0.010$) was identified as the negative predictor for the success of PTC culture.

Conclusion PTC culture based on PTNB specimens could be established in 82.4% of LM patients, with a high accuracy in predicting clinical outcomes. Excessive necrosis in the tumor may predict the failure of PTC culture. Image-guided PTNB targeting enhanced or fluorodeoxyglucose avid regions on images might contribute to improving the success rate of PTC culture.

PO-235

The Prognostic Nutritional Index (PNI) as a Biomarker for Predicting Survival in Hepatocellular Carcinoma Patients Treated with Transarterial Chemoembolization and Lenvatinib, With or Without PD-1 Inhibitors

Yi Chen

First Hospital of Shanxi Medical University

Purpose The treatment of hepatocellular carcinoma (HCC) with transarterial chemoembolization (TACE) and lenvatinib, combined with immunosuppressive agents, is relatively blind currently, lacking effective biomarkers. This study analyzes the significance of the Prognostic Nutritional Index (PNI) score in HCC patients undergoing TACE plus lenvatinib, with or without programmed death 1 (PD-1) inhibitors, as a novel biomarker.

Materials and methods A retrospective analysis was conducted on 237 patients with HCC who underwent lenvatinib treatment, with or without PD-1 inhibitors, from May 2021 to September 2023. All patients were randomly divided into a training set and a validation set in a 7:3 ratio, and were categorized into low PNI and high PNI groups based on their PNI levels. The log-rank test was used to compare the overall survival (OS) and progression-free survival (PFS) between the low and high groups in the training and validation sets.

Results In both the training and validation sets, patients with higher PNI scores had better OS and PFS compared to those with lower PNI scores. Multivariate Cox regression analysis revealed that PNI score, treatment modality, tumor diameter, alpha-fetoprotein (AFP), and alanine aminotransferase (ALT) were independent risk factors for OS. For PFS, the independent prognostic factors were PNI score, treatment modality, tumor diameter, Child-Pugh classification, and AFP level. Subgroup analysis showed that, regardless of whether patients received TACE combined with lenvatinib or TACE combined with lenvatinib and PD-1 inhibitors, or whether they had portal vein tumor thrombosis (PVTT), extrahepatic metastasis (EHM), AFP ≤ 400 or > 400 ng/ml, and were at Barcelona Clinic Liver Cancer (BCLC) stage C, those with higher PNI scores had better OS compared to those with lower PNI scores.

Conclusion The PNI score may serve as a novel biomarker for predicting the prognosis of HCC patients undergoing TACE and lenvatinib, with or without PD-1 inhibitors. Patients with a low PNI score exhibit poor survival.

METTL3-mediated m6A Modification of HIF1 α Regulates the TGM2/STAT3 Axis to Promote Chemoresistance in Head and Neck Squamous Cell Carcinoma

Xinhua Li

Tianjin Medical University Cancer Institute and Hospital

Purpose Head and neck squamous cell carcinoma (HNSCC) is a highly prevalent malignant tumor with a poor prognosis, where chemoresistance is a major factor limiting treatment efficacy and patient survival. Studies have shown that the tumor microenvironment (TME) and hypoxia contribute to chemoresistance, and METTL3-mediated m6A modification may play a crucial role in this process. This study aims to investigate how METTL3 regulates the TGM2/STAT3 axis through m6A modification of HIF1 α , thereby promoting HNSCC cell proliferation and chemoresistance. By elucidating the underlying molecular mechanisms, our findings may provide new theoretical insights and therapeutic strategies for overcoming chemoresistance in HNSCC.

Materials and methods This study first utilized bioinformatics analysis to examine the expression patterns of m6A-related genes in tumors and established a cisplatin-resistant HNSCC cell line. The IC₅₀ value and m6A modification levels were measured, followed by transcriptome sequencing. Pathological tissue samples from HNSCC patients were collected for immunohistochemical (IHC) analysis to evaluate METTL3 expression. In vitro and in vivo experiments were conducted to assess the effects of different METTL3 expression levels on tumor cell proliferation and cisplatin resistance. Transcriptome sequencing was performed in METTL3-knockdown cells to identify potential downstream target genes, leading to the identification of TGM2. Subsequently, cell-based assays and animal models were used to validate the role of TGM2 in tumor proliferation and cisplatin resistance. Furthermore, chromatin immunoprecipitation (ChIP), co-immunoprecipitation (Co-IP), and ubiquitination assays were performed to explore the molecular mechanism by which HIF1 α regulates the TGM2/STAT3 axis. Finally, the antitumor efficacy of the TGM2 inhibitor GK921 was evaluated in a mouse model.

Results We identified that METTL3 is significantly upregulated in chemoresistant HNSCC cells and tumor tissues, and its high expression is closely associated with poor prognosis in patients. In vitro and in vivo experiments demonstrated that METTL3 overexpression promotes HNSCC cell proliferation and enhances cisplatin resistance. Mechanistically, METTL3 stabilizes HIF1 α through IGF2BP1-dependent m6A modification, thereby promoting HIF1 α -mediated transcriptional activation of TGM2. Additionally, METTL3 positively regulates TGM2, which inhibits the ubiquitin-mediated degradation of STAT3, leading to increased STAT3 stability and enhanced chemoresistance in HNSCC. Furthermore, our study revealed that the TGM2 inhibitor GK921 significantly attenuates HNSCC chemoresistance and suppresses tumor growth in both in vitro and in vivo models.

Conclusion Our findings reveal that METTL3 promotes chemoresistance in HNSCC through the HIF1 α /TGM2/STAT3 axis, elucidating its underlying molecular mechanism. Moreover, our study highlights TGM2 as a potential therapeutic target for overcoming chemoresistance in HNSCC, providing new insights for precision treatment strategies.

PO-237

Comparison of the efficacy and safety of HAIC combined with Camrelizumab and Apatinib versus TACE in the treatment of intermediate-advanced HCC

Haojie Zhang, Zhigang Zhou

The first affiliated hospital of Zhengzhou University

Purpose To investigate and compare the efficacy and safety of hepatic arterial infusion chemotherapy (HAIC) combined with Camrelizumab and Apatinib versus transcatheter arterial chemoembolization (TACE) in the treatment of intermediate-advanced hepatocellular carcinoma.

Materials and methods A total of 79 HCC patients who had been treated with HAIC or TACE combined with Camrelizumab and Apatinib were retrospectively collected. All patients were divided into HAIC combination therapy group (36 cases) and TACE combination therapy group (43 cases). Clinical information including age, gender, body mass index (BMI), serological indicators, tumor size, site, number and stage, progression-free survival (PFS), overall survival (OS) and adverse events were collected. The survival status of patients in both groups were followed up and the survival curves of PFS and OS were plotted by Kaplan-Meier method. The survival rates of patients in both groups were compared by Log-rank test, and Cox regression model was used to analyze the risk factors of PFS and OS by univariate and multivariate analysis. Modified RECIST (mRECIST) was used to evaluate the efficacy of HCC and to compare the objective response rate (ORR) and disease control rate (DCR) between the two groups. The Common Terminology Criteria for Adverse Events (CTCAE) version 5.0 was used to evaluate the adverse events of the two groups.

Results According to the mRECIST criteria, there were more patients with PD in the TACE-plus group than in the HAIC-plus group ($P=0.039$). The ORR was 52.8% and 51.2% in the HAIC-plus and TACE-plus groups, respectively ($P=0.727$), and the DCR was higher in the HAIC-plus group than in the TACE-plus group (88.9% vs 69.8%, $P=0.039$). By the end of follow-up, the mPFS was 14.6 months (95% CI 10.2-NA) in the HAIC-plus group, which was superior to 7.4 months ($P=0.041$, 95%CI 4.7-12.8) in the TACE-plus group. The mOS was 22.6 months (95%CI 17.3-NA) in the HAIC-plus group, which was superior to 16.7 months ($P=0.044$, 95%CI 12.7-26.5) in the TACE-plus group. No treatment-related grade 4 or 5 adverse reactions were observed in all patients. Nausea and vomiting were more common in the HAIC group, and anemia and fever were more common in the TACE group ($P<0.05$). The patients with Grade 3 ALT elevation in the TACE group were more than those in the HAIC group ($P=0.029$). The incidence of grade 3 adverse events was 19.4% (HAIC group) and 27.9% (TACE group), respectively, with no significant difference between the two groups ($P=0.381$).

Conclusion HAIC combined with Camrelizumab and Apatinib showed better efficacy and tolerability in the treatment of advanced HCC compared with TACE combination therapy. HAIC combination therapy can improve the DCR and PFS of patients with advanced HCC, and has a potential advantage in prolonging OS.

PO-238

Copper oxide nanoparticle stents inhibit esophageal carcinoma progression via mitophagy

Yue Liu,Xiao Li,Wei Jiang

Cancer Hospital Chinese Academy of Medical Science

Purpose Esophageal carcinoma (EC) is the eighth most common malignancy and the sixth leading cause of cancer-related deaths worldwide. Patients with EC suffer from dysphagia as a result of malignant obstruction, which can also lead to malnutrition, malaise, and reduced quality of life. Stent placement is the main non-surgical therapy for the relief of malignant esophageal strictures, and the development of esophageal stents with anticancer effects and the elucidation of their mechanisms are intended to provide new and effective laboratory evidence for clinical management. Copper oxide nanoparticle (CuO-NPs) induced reactive oxygen species generation, oxidative stress, cytotoxicity, genotoxicity and immunotoxicity with strong killing effects on cancer cells. Mitochondria are key organelles involved in the induction of toxicity by CuO-NPs. Mitophagy is a selective autophagic process that specifically degrades damaged mitochondria to maintain mitochondrial homeostasis and oxidative stress homeostasis through an autophagy-lysosome mechanism. Whether CuO-NPs and CuO-NPs stents can inhibit the proliferation of EC through mitophagy, the mechanism of which is not clear.

Materials and methods fabrication of CuO-NPs stent, immunofluorescence, western blot, flow cytometry, organoids culture, cell culture, transmission electron microscopy, RNA-Sequencing, RT-Q-PCR, nude mice subcutaneous tumour model, rat in situ esophageal cancer model

Results In this present study we found that CuO-NPs and CuO-NPs stents obviously inhibited EC proliferation. By immunofluorescence, western blot and flow cytometry, it was found that CuO-NPs significantly induced the production of reactive oxygen species to enhance the antioxidant response of EC cells and lead to damaged mitochondria, causing activation of the Pink1/Parkin mitophagy signaling pathway. We further determined by RNA sequencing techniques that CuO-NPs could induce the Pink1/Parkin mitophagy signaling pathway via the PI3K/Akt/mTOR/TFEB pathway, leading to severe killing of cancer cells and partial killing of normal cells.

Conclusion In conclusion, the present results indicate that CuO-NPs stents induce mitophagy to inhibit the progression of EC, and the development of more therapeutic esophageal stents based on CuO-NPs may be a new therapeutic direction for EC.

PO-239

Hepatic arterial infusion chemotherapy combined with Lenvatinib and PD-1 inhibitors versus Lenvatinib and PD-1 inhibitors for HCC refractory to TACE

Chendong Wang, Guowen Yin
Jiangsu Cancer Hospital

Purpose To investigate the efficacy and safety of hepatic arterial infusion chemotherapy (HAIC) combined with lenvatinib and immune checkpoint inhibitors (ICIs) versus lenvatinib and ICIs for hepatocellular carcinoma (HCC) with TACE refractoriness.

Materials and methods Patients with intermediate or advanced TACE-refractory HCC who received lenvatinib and ICIs with or without HAIC between 2020 and 2022 were retrospectively reviewed. The tumor response, overall survival (OS), progression-free survival (PFS) and treatment-related adverse events (TRAEs) were evaluated and compared between the two groups. Factors affecting OS and PFS were identified with univariate and multivariate Cox regression analyses.

Results A total of 121 patients were enrolled, with 58 patients assigned to the HAIC-Len-ICI group and 63 patients assigned to the Len-ICI group. A higher objective response rate and disease control rate were found in the HAIC-Len-ICI group than in the Len-ICI group (48.30% vs. 23.80%, $p=0.005$, 87.90% vs. 69.80%, $p=0.02$, respectively). The median OS was 24.0 months in the HAIC-Len-ICI group and 13.0 months in the Len-ICI group ($p=0.001$). The median PFS was 13.0 months in the HAIC-Len-ICI group and 7.2 months in the Len-ICI group ($p<0.001$). Multivariable analyses suggested that the presence of cirrhosis, Child–Pugh B stage, and HAIC-Len-ICI therapy option were prognostic factors for OS and PFS. The incidences of any grade and grade 3/4 TRAEs were both comparable between the two groups.

Conclusion HAIC combined with lenvatinib and ICIs yielded better OS, PFS, ORR and DCR than lenvatinib-ICI therapy in patients with HCC refractory to TACE, with manageable adverse events.

Hepatic arterial infusion chemotherapy plus lenvatinib and PD-1 inhibitors versus lenvatinib plus PD-1 inhibitors as treatment for unresectable hepatocellular carcinoma, a meta-analysis and trial sequential analysis

Jiayi Liu, Huan Zhai, Haibo Shao
The First Hospital of China Medical University

Purpose We conducted a meta-analysis and trial sequential analysis (TSA) to compare the efficacy and safety of hepatic arterial infusion chemotherapy (HAIC) combined with lenvatinib and PD-1 inhibitors (H+L+P) versus lenvatinib combined with PD-1 inhibitors alone (L+P) in the treatment of unresectable hepatocellular carcinoma (HCC).

Materials and methods We systematically searched PubMed, Web of Science, Cochrane Library, and Embase databases for controlled trials comparing L+P, with or without HAIC, in the treatment of intermediate to advanced-stage HCC. The outcomes assessed included median overall survival (OS), median progression-free survival (PFS), objective response rate (ORR), and adverse events (AEs). Based on heterogeneity evaluations, either a fixed-effect model or a random-effect model was applied. In addition, trial sequential analysis (TSA) was performed to assess whether the sample size was sufficient and to draw reliable conclusions.

Results Our meta-analysis included six trials with a total of 897 patients. The meta-analysis results showed that, compared to L+P, H+L+P significantly improved the ORR (57.3% vs. 19.8%, risk ratio [RR] = 2.91, 95% confidence interval [CI] = 2.15–3.94, $P < 0.01$), as well as median OS (20.0 months vs. 10.9 months, mean difference [MD] = 9.12 months, 95% CI = 5.93–12.30, $P < 0.01$) and median PFS (9.6 months vs. 5.0 months, MD = 4.63 months, 95% CI = 3.55–5.71, $P < 0.01$). These results were confirmed through TSA, which indicated no need for a larger information size to reach reliable conclusions. Regarding AEs, the meta-analysis and TSA results showed a higher incidence of fever in the H+L+P group compared to the L+P group (any grade: 18.6% vs. 9.4%, RR = 2.05, 95% CI = 1.33–3.16, $P < 0.01$). TSA also revealed that the incidence of AST elevation was higher in the H+L+P group than in the L+P group, whereas the incidence of pain and ALT elevation showed no significant difference between the two groups. Additional AEs require larger information sizes to draw more definitive conclusions.

Conclusion Compared to L+P, H+L+P significantly improves the ORR and prolongs both PFS and OS in patients with unresectable HCC, resulting in manageable AEs. Based on these findings, large-scale randomized controlled trials are needed for further validation.

PO-241

Deep Learning Application of YOLOv8 for Aortic Dissection Screening Using Non-Contrast CT

Zhong-Zhi Jia

Changzhou Second Peoples Hospital, China

Purpose Acute aortic dissection (AD) is a life-threatening condition with nonspecific symptoms, making timely diagnosis challenging. Non-contrast CT is frequently used in specific settings, though diagnostic accuracy can vary among radiologists. This study aims to develop and validate a YOLOv8 deep learning (DL) model based on non-contrast CT to detect AD.

Materials and methods This retrospective study included 1,138 cases from five institutions, divided into training, internal validation, and external validation cohorts. The YOLOv8 DL model was trained on annotated non-contrast CT images. Its performance was evaluated using area under the curve (AUC), sensitivity, specificity, and inference time, and compared to radiologists from three backgrounds: vascular interventional specialists, general radiologists, and residents.

Results The YOLOv8s model achieved an AUC of 0.964 (95% CI: 0.939–0.988) in the internal validation cohort and 0.970 (95% CI: 0.946–0.990) in the external validation cohort. In the external validation cohort, the performances of three groups of radiologists in detecting AD were inferior to the receiver operating characteristic curve of the YOLOv8s model. The model's sensitivity (0.976) was slightly higher than that of vascular interventional specialists (0.965, $P = 0.18$), while its specificity (0.935) was significantly superior to that of general radiologists (0.835, $P < 0.001$). Additionally, the model's inference time was 3.47 seconds, significantly shorter than radiologists' average time of 25.32 seconds ($P < 0.001$).

Conclusion The YOLOv8s DL model reliably detects AD on non-contrast CT and outperforms radiologists, particularly in time efficiency and diagnostic accuracy. Its implementation could enhance AD screening in specific settings, support clinical decision-making, and improve diagnostic quality.

PO-242

CT-guided Needle Insertion with an Optical Navigation Robot-assisted Puncture System: Ex Vivo and in Vivo Experimental Studies in the Liver and Kidneys

Wei Cui¹, Yi Deng², Jing Li¹, Rongde Xu¹

1. Guangdong General Hospital/CN

2. Medical School, Kunming University of Science and Technology

Purpose To evaluate the capabilities of a starch mixture (starch group) and a copper particle nodule-mimic model (particle group) and to compare the accuracy of optical navigation robot-assisted punctures (robot group) with traditional CT-guided manual punctures (manual group) in swine liver and kidneys. Robotic technologies applied in CT-guided puncture are promising. However, nodule-mimic models can be difficult to develop for studies and the accuracy of optical navigation robot-assisted puncture remains unclear.

Materials and methods The studies were approved by the institutional animal care and use committee. In ex vivo and in vivo studies of 3 swine liver and kidneys (study 1), nodule-mimics were imaged by CT scan to assess capabilities in both starch and particle group. In an in vivo study of 6 swine (study 2), 24 punctures in robot and manual group each were attempted toward copper particle nodule-mimic targets in the liver and kidneys under CT guidance for the evaluation of the equivalence of accuracy of insertion with a 5.0-mm margin by using the Mann-Whitney U test. The needle insertion time, radiation exposure and complication were also evaluated.

Results In study 1, all nodule-mimics were easily visible on CT imaging. However, the other capabilities of starch group (one starch overflowed, one starch dispersion and one air embolism) was inferior to that of particle group. In study 2, the needle insertion accuracy in robot group (3.71 ± 1.34 mm) was higher than in manual group (11.89 ± 9.59 mm) ($P < 0.001$). The needle insertion time and radiation exposure were better in the robot group compared to the manual group (all $P < 0.001$). Complications were similar between the two groups.

Conclusion Particle group may be better than starch group due to better capabilities. Robot group exhibited higher accuracy compared to manual group, and the complication was similar.

Efficacy and Safety Analysis of Transarterial Chemoembolization Combined with Tyrosine Kinase Inhibitors and Immune Checkpoint Inhibitors with or without Microwave Ablation for Unresectable Hepatocellular Carcinoma: A Retrospective, Multicenter, Case-control Study

Nan Wang, Xin Ye

Department of Oncology, Shandong Provincial Qianfoshan Hospital, Shandong University of Traditional Chinese Medicine, Jinan, Shandong, People's Republic of China.

Purpose The Efficacy and Safety Analysis of Transarterial Chemoembolization Combined with Tyrosine Kinase Inhibitors and Immune Checkpoint Inhibitors with Microwave Ablation for Unresectable Hepatocellular Carcinoma has not been reported. This study aimed to evaluate the efficacy and safety of transarterial chemoembolization (TACE) combined with tyrosine kinase inhibitors (TKIs) and immune checkpoint inhibitors (ICIs) with or without microwave ablation (MWA) for unresectable hepatocellular carcinoma (uHCC).

Materials and methods This retrospective study comprised 220 patients with unresectable hepatocellular carcinoma (uHCC)

who underwent transarterial chemoembolization (TACE) combined with tyrosine kinase inhibitors (TKIs) and immune checkpoint inhibitors (ICIs) with MWA (Group A: 105 patients (median age, 60 ± 10 years) and 82 (78.1%) were men) or without MWA (Group B: 115 patients (median age, 58.35 ± 10.27 years) and 97 (84.4%) were men) at multiple centers in China. The overall survival (OS), progression-free survival (PFS), objective response rate (ORR), and safety were compared between the two groups.

Results The OS, PFS, and ORR in Group A were significantly higher than those in Group B (OS, 21.30 ± 8.25 vs. 15.49 ± 7.41 months, $p < 0.0001$; PFS, 14.29 ± 6.34 vs. 7.15 ± 4.53 months, $p < 0.0001$; ORR, 66.7% [70/105] vs. 31.3% [36/115], $p < 0.0001$). The multivariable Cox regression analysis revealed that the combination of MWA and a more favorable tumor response were significantly associated with improved OS (hazard ratio, 0.5261; 95% confidence interval, 0.3839–0.7182; $p = 0.0005$ and hazard ratio, 0.5770; 95% confidence interval, 0.4209–0.7886; $p = 0.0016$). Grade 3 or 4 adverse events occurred in 30/105 (28.6%) and 29/115 (25.2%) patients in Groups A and B, respectively. A total of 69/105 (65.7%) patients in Group A and 84/115 (73.0%) patients in Group B experienced treatment-emergent AEs from TACE, TKIs, and ICIs. AEs associated with MWA occurred in 26/105 (24.8%) patients in Group A. Grade 3 or 4 AEs were observed in 30/105 (28.6%) patients in Group A and 29/115 (25.2%) patients in Group B. No treatment-related mortalities were observed in either group. Discontinuation of ICIs was documented in 7/105 (6.7%) patients in Group A and 10/115 (8.7%) patients in Group B. Similarly, TKI discontinuation due to AEs was observed in 8/105 (7.6%) patients in Group A and 10/115 (8.7%) patients in Group B. Dose interruptions of ICIs were reported in 9/105 (8.6%) patients in Group A and 11/115 (9.6%) patients in Group B, while dose reductions or interruptions of TKIs were experienced by 17/105 (16.2%) patients in Group A and 14/115 (12.2%) patients in Group B. The AEs mainly included abnormal transaminases, increased blood bilirubin, ascites, pain, anemia, proteinuria, nausea, hypertension, hand and foot syndrome, leukopenia, hypothyroidism, gastrointestinal hemorrhage, immune-related pneumonia, rash, platelet count decrease, and weight loss. Furthermore, in a cohort comprising 55 patients from Group A and 68 patients from Group B, where camrelizumab was employed, the proportion of patients experiencing reactive cutaneous capillary endothelial prol

iferation (RCCEP) was 28/55 (50.9%) in Group A and 33/68 (48.5%) in Group B. RCCEP was not detected in patients who were treated with other ICIs.

Conclusion The combination therapy (TACE + TKIs and ICIs) with MWA showed higher safety and significantly better OS, PFS, and ORR for uHCC than that without MWA.

Tumor cell-intrinsic MELK augments CCL2-dependent immunosuppression to promote hepatocarcinogenesis and enhance hepatocellular carcinoma radioresistance

Jinyu Zhu¹, Jiansong Ji²

1. Peking University

2. Zhejiang University

Purpose The outcome of HCC patients is substantially constrained by the complex molecular characteristics and the fluctuating dynamics of the tumor microenvironment (TME) throughout tumorigenesis. This study aims to elucidate the functional consequences of maternal embryonic leucine zipper kinase (MELK) in the occurrence, progression, and metastasis of HCC, and to explore the impact of MELK on the regulation of immune cells within the TME, as well as to reveal the underlying specific signaling networks involved.

Materials and methods Bioinformatics analysis was employed to validate the prognostic value of MELK expression levels for HCC. Murine homograft/xenograft model assays and HCC lung metastasis mouse models were established to confirm the role of MELK in HCC tumorigenesis and metastasis. Luciferase reporter gene analysis, RNA sequencing, immunoprecipitation-mass spectrometry (IP-MS), and coimmunoprecipitation (CoIP), were comprehensively utilized to delve into the upstream regulators, downstream key molecules, and corresponding mechanisms by which MELK modulates the onset and development of HCC.

Results Our study results definitively established MELK as a reliable prognostic factor for HCC, in which the up-regulation of tumor cell-intrinsic MELK correlates with a poor prognosis in patients with HCC. In addition, tumor cell-intrinsic MELK was also confirmed as an effective candidate target in facilitating the occurrence, progression, and metastasis of HCC. Analysis of the key regulatory factors upstream and downstream of MELK, as well as its mechanisms of action, revealed that the oncogenic function of MELK is subject to targeted regulation by the upstream factor miR-505-3p and mediated through interaction with STAT3, leading to STAT3 phosphorylation and increased expression of its target gene CCL2 in HCC. Furthermore, we demonstrated that tumor cell-intrinsic MELK functions in interfering with the infiltration of immune cells within TME in HCC, in which inhibiting endogenous MELK expression in tumor cells is beneficial in stimulating M1 macrophage polarization, hindering M2 macrophage polarization and inducing CD8⁺ T cell recruitment, which are dependent on the alteration of CCL2 expression. Importantly, the immunomodulatory effects of MELK inhibition also significantly enhanced the immune effects associated with radiotherapy (RT), synergizing with it to exert substantial antitumor effects. OTS167, an inhibitor of MELK, was also proven to effectively impair the growth and progression of HCC and to exhibit superior antitumor effects when combined with radiotherapy.

Conclusion Altogether, our findings highlight the functional role of MELK as a promising therapeutic target in precision molecular targeted HCC treatment and indicate that OTS167 is an effective antagonist of HCC, as well as its potential in combination with radiotherapy to enhance antitumor effects. Our analytical discoveries provide a scientific basis for the development of new treatment strategies for HCC.

PU-001

The Role of Interventional Radiology in Hematuria Embolization for Patients with Radiation-Induced Cystitis

Koesbandono Koesbandono, Rio Hermawan, Gilbert Sterling, Teodorus Alfons
Siloam Hospitals

Purpose Radiation cystitis is a known late complication of pelvic radiotherapy, often presenting with refractory hematuria that can be life-threatening or significantly impact quality of life. Conservative and endoscopic treatments frequently fail in severe cases. This study aims to evaluate the clinical efficacy, safety, and technical outcomes of selective arterial embolization performed by interventional radiology (IR) for managing hematuria in patients with radiation-induced cystitis.

Materials and methods This retrospective study analyzed patients who presented with gross hematuria secondary to radiation cystitis and underwent transarterial embolization (TAE) in Siloam Hospitals MRCCC Indonesia. All patients had a history of pelvic irradiation for malignancies, including prostate, cervical, and rectal cancers. Prior conservative and endoscopic treatments failed in all cases.

CT angiography or digital subtraction angiography (DSA) was used to identify active bleeding or hypervascular bladder walls. Embolization was performed via femoral artery access using microcatheters, targeting the bilateral internal iliac branches, particularly the vesical and prostatic arteries. Various embolic agents were used, including polyvinyl alcohol (PVA) particles, microspheres, and coils. Technical success was defined as complete embolization of identified bleeding vessels.

Clinical success was defined as resolution or significant reduction of hematuria within 72 hours post-procedure. Complications were classified according to the CIRSE classification system.

Results Technical success was achieved. Patient experienced recurrent hematuria within one month and underwent repeat embolization with successful outcomes. Minor complications occurred including transient pelvic pain and low-grade fever, all resolved with conservative treatment. No major complications, such as bladder necrosis or severe ischemia, were reported.

Conclusion Transarterial embolization is a safe, effective, and minimally invasive treatment modality for managing hematuria due to radiation cystitis. The high rate of technical success, coupled with a favorable clinical success rate, supports the use of embolization in patients with refractory hemorrhagic cystitis who have failed conventional therapies. Interventional radiology plays a critical role in the multidisciplinary care of these complex patients, especially when conservative and endoscopic approaches prove ineffective. The absence of significant complications in this study further underscores the safety profile of this technique.

Early referral to IR services should be considered in cases of persistent or recurrent hemorrhagic cystitis to improve outcomes and reduce morbidity. Future studies with larger sample sizes and longer follow-up periods are warranted to further define optimal patient selection criteria, identify predictors of treatment success, and compare the efficacy of different embolic agents.

PU-002

Comparison of efficacy of different sequential radiotherapy combined with TACE in hepatocellular carcinoma with PV TT

Wenliang Zhu¹, Yuting Liao²

1. Guangxi Medical University of cancer hospital

2. Central South University Xiangya Medical College Affiliated Haikou Hospital

Purpose The primary objective of this research is to investigate the optimal sequencing of radiotherapy and TACE in the management of hepatocellular carcinoma with portal vein tumor thrombosis

Materials and methods Key searches with HCC PVTT radiotherapy TACE in Pubmed, Web of Science, Embase, cochrane library. Studies with the intervention of radiotherapy(RT) for different treatment orders combined with TACE for HCC with PVTT were included. The experimental group was RT + TACE, and the control group was TACE + RT. The primary study outcome was the median overall survival (mOS). Data analysis was performed using fixed or random effects models on stata18.0 software, and the results were presented as MD or RR with two-sided 95%CI.

Results A total of four studies were included, with 331 patients. The results showed that the RT + TACE group had better efficacy in HCC patients with PVTT (MD 2.49 [95%CI 0.69,4.28]; P=0.01). Analysis of the subgroup of patients with type III / IV PVTT showed that the RT + TACE group was superior to the TACE + RT group (MD 5.31 [95%CI 4.65,5.97]; P=0.00). In addition, the efficacy analysis of patients with type I / II PVTT found that the effect was still better in the RT + TACE group (MD 2.30 [95%CI 1.51,3.09]; P=0.00). In the comparative study of liver injury, the injury of liver function was more obvious in TACE + RT group (RR 0.68 [95%CI 0.45,1.04]; P=0.07).

Conclusion In conclusion, the four articles tend to target patients with poor liver function, and radiotherapy before TACE is more favorable for patient survival. However, due to potential selection bias, insufficient sample size and inconsistent radiotherapy regimen, it is not certain that radiotherapy before TACE will be more effective. Future larger, multicenter studies are needed to further verify whether the efficacy of radiotherapy and TACE sequence is different.

PU-003

Single-cell transcriptome sequencing reveals SPP1-CD44-mediated macrophage-tumor cell interactions drive chemo resistance in TNBC

Fuzhong Liu, Wenjia Guo
Xinjiang Medical University

Purpose Triple-negative breast cancer (TNBC) is often considered one of the most aggressive subtypes of breast cancer, characterized by a high recurrence rate and low overall survival (OS). It is notorious for posing challenges related to drug resistance. While there has been progress in TNBC research, the mechanisms underlying chemotherapy resistance in TNBC remain largely elusive.

Materials and methods We collect single-cell RNA sequencing (scRNA-seq) data from 5 TNBC patients susceptible to chemotherapy and 5 resistant cases. Comprehensive analyses involving copy number variation (CNV), pseudotime trajectory, cell-cell interactions, pseudospace analysis, as well as transcription factor and functional enrichment are conducted specifically on macrophages and malignant cells.

Results Our study unveils a drug-resistant signaling pathway, SPP1, associated with macrophage-secreted factors. We identify that SPP1 might be regulated by the transcription factor CEBPB. Furthermore, we find a distinct cluster of CD44⁺ transformed cells that, upon receiving SPP1 signals, may activate the PDE3B signaling pathway via integrin pathways, facilitating the onset of chemotherapy resistance.

Conclusion Our study offers a fresh perspective on understanding chemotherapy resistance mechanisms in TNBC patients, presenting potential avenues for overcoming drug resistance.

PU-004

Skeletal Muscle Mass Predicts Survival Benefit for Hepatocellular Carcinoma Treated with Transarterial Chemoembolization Combining Molecular Targeted Agents and Immune Checkpoint Inhibitors

Wen Chen

The First Affiliated Hospital of Nanjing Medical University

Purpose To assess the relationship between clinical prognosis and changes of skeletal muscle mass for unresectable hepatocellular carcinoma (uHCC) patients who received transarterial chemoembolization (TACE) with molecular targeted agents and immune checkpoint inhibitors (TACE-MTAs-ICIs).

Materials and methods From June 2019 and June 2023, a total of 92 uHCC patients who received TACE-MTAs-ICIs therapy were included. Skeletal muscle mass was assessed before and 6 months after treatment. Skeletal muscle index (SMI) is calculated as skeletal muscle area at the L3 vertebra divided by the square of height, then the change rate of SMI (Δ SMI) is calculated. Patients were stratified based on Δ SMI as muscle gain and non-muscle gain groups. Overall survival (OS) was compared between groups and prognostic factors for OS were analyzed. Progression-free survival (PFS) was also recorded.

Results The median OS in the muscle gain group was significantly longer than that in the non-muscle gain group (Not reach vs. 25.2 months, $P < 0.001$). The median PFS did not reach significant between two groups (16.2 vs. 9.1 months, $P = 0.101$). Multivariate analyses revealed that skeletal muscle gain (HR = 0.20; 95% CI, 0.06–0.68; $P = 0.010$) and Barcelona Clinic Liver Cancer stage (HR = 1.94; 95% CI, 1.02–3.69; $P = 0.044$) were independent prognostic factors for OS.

Conclusion SMI increment appeared as a favorable predictor for these uHCC patients who received TACE-MTAs-ICIs therapy.

A Comparative Study of Gasless Transoral Vestibular Approach Endoscopic and Open Radical Thyroidectomy in a Retrospective Cohort

Yan Yu, Jinmiao Qu

Wenzhou Medical University Affiliated First Hospital

Purpose Thyroid cancer is a prevalent malignant tumor in China, with surgery being the primary treatment modality. Traditional open thyroidectomy leaves a 5-8 cm scar on the neck, which compromises aesthetic outcomes and imposes psychological and lifestyle burdens, particularly on female patients. Recent advancements in medical technology have driven the rapid evolution of endoscopic thyroid surgery, predominantly utilizing extracervical approaches such as transaxillary, breast-areolar, retroauricular, and oral routes. Among these, the transoral vestibular approach has emerged as a common minimally invasive technique. Comparative studies between transoral vestibular endoscopic thyroidectomy (TOET) and open surgery have demonstrated comparable therapeutic efficacy, albeit with prolonged operative time and increased drainage volume observed in the TOET group.

Current literature reports that most transoral endoscopic procedures employ carbon dioxide insufflation to maintain the operative space, which carries risks of subcutaneous emphysema and air embolism. In recent years, gasless transoral endoscopic thyroidectomy has emerged as a novel research focus, with sporadic reports from domestic and international studies highlighting its favorable surgical outcomes. However, comprehensive investigations into the safety, efficacy, and quality of life (QoL) outcomes associated with gasless transoral vestibular endoscopic thyroidectomy for thyroid cancer remain limited in China. This retrospective cohort study aims to compare gasless transoral vestibular endoscopic thyroidectomy with conventional open thyroidectomy in terms of surgical outcomes, complication rates, and postoperative QoL. The findings are expected to provide evidence-based insights for evaluating and promoting the clinical application of gasless transoral vestibular endoscopic thyroid surgery.

Materials and methods A retrospective study was conducted to randomly collect the basic information, surgical data and changes of postoperative thyroid related indicators of patients with papillary thyroid cancer who underwent TOETVA (n=77) and traditional open thyroidectomy (n=100) from November 2021 to December 2023. At the same time, the Chinese version of the European Organization for Research and Treatment of Cancer quality of life questionnaire and thyroid cancer specific quality of life questionnaire were used to investigate the quality of life at 1 month, 6 months and 1 year after surgery. The clinical efficacy, perioperative indicators, quality of life and complications were compared between the two groups. At the same time, the TOETL group was divided into group A in the early application stage (2021-2022, 18 cases) and group B in the application and promotion stage (2023, 59 cases), in order to compare the changes of surgery-related indicators in the TOETL group in the early application stage and promotion stage. SPSS 29.0 software was used to analyze the relevant data, and $P < 0.05$ was considered statistically significant.

Results There was no evidence of recurrence in the two groups of patients within one year after operation.

Statistical results showed that there were no significant differences in age distribution, gender distribution, BMI, tumor diameter, tumor location, lesion number and education level between the two groups ($P > 0.05$). In terms of employment status, marital status, residence and income, the number of employed, unmarried, urban and high-income people in the oral group were more than

hose in the open group (all $P < 0.05$). At the same time, the operation time, postoperative hospital stay, operation cost and postoperative drainage volume in the TOETVA group were more than those in the open group ($P < 0.05$). In the comparison of short-term (1-6 months) and 1-year postoperative complications, the number of skin numbness in the TOETVA group was more than that in the OETVA group ($P = 0.003$), and there was no difference in other complications. Further analysis of the oral group showed that the operation time and postoperative hospital stay in group A were significantly longer than those in group B ($P < 0.05$), and there was no significant difference in postoperative drainage volume and total operation cost between the two groups ($P > 0.05$).

The scores of EORTC QLQ-C30 and THYCA-QOL in TOETVA group were significantly better than those in OTVA group at 1 month, 6 months and 1 year after surgery ($P < 0.05$). However, the scores of multiple domains in the oral group improved over time ($P < 0.05$). There was no statistically significant difference in other research indicators ($P > 0.05$).

Conclusion For patients with papillary thyroid carcinoma, the two surgical methods are both safe and effective, and can achieve the curative effect. Compared with the open approach, the gasless endoscopic thyroidectomy via transoral vestibular approach has no scar on the body surface, better postoperative quality of life, and less impact on the aesthetics and psychology of female patients. However, there are some problems such as longer operation time and higher cost.

Therefore, in the clinical practice of papillary thyroid carcinoma, doctors should comprehensively consider the individual condition of patients to choose the most appropriate surgical plan. For patients with better economic conditions, cosmetic and quality of life requirements, gasless endoscopic thyroidectomy via transoral vestibular approach may be a better choice.

PU-007

IL11 promotes hepatocellular carcinoma progression through facilitating APOH-mediated fatty acid metabolism to modulate the differentiation of Treg cells

Yang Gao,Jian Lu,Xijuan Yao
Zhongda Hospital Medical School ,Southeast University

Purpose Hepatocellular carcinoma (HCC) accounts for high rate of cancer-related death worldwide. Here, we analyzed data obtained from online databases and determined that interleukin-11 (IL-11) is closely correlated with HCC progression. Regulatory T (Treg) cells are important components of the tumor microenvironment (TME) that act as a mediator in the progression of HCC. However, the specific role and mechanism of IL-11-mediated Treg cell differentiation in HCC progression remain unclear. The focus of this study is to explore the IL-11-mediated mechanism regulating the Treg cells in TME of HCC to promote tumor progression.

Materials and methods We conduct research through bioinformatics analysis, validation of clinical tissue specimens, and cell and animal experiments.

Results We first determined that IL-11 was upregulated in HCC tissues with advanced stages and correlated with poor patients' prognosis. Moreover, we uncovered that silencing of IL-11 suppressed HCC cell migration and in vivo tumor growth. Importantly, IL-11 increased the proportion of Treg cells in the TME of HCC through promoting Treg cell differentiation. Mechanistically, IL-11 activated MBD3 to upregulate MBD3 expression in Treg cells. Additionally, MBD3 could promote Treg cell differentiation through decreasing the promoter activity of APOH to downregulate APOH expression. Finally, IL-11/MBD3 axis was proven to induce Treg differentiation through promoting APOH-mediated fatty acid metabolism.

Conclusion To conclude, this study reveals our IL-11 as a potentially novel immunotherapeutic target for HCC.

PU-009

Long-Term Outcomes of Transarterial Chemoembolization plus Ablation versus Surgical Resection in Patients with Large BCLC Stage A/B stage HCC

Tian-Qi Zhang, Ying-Wen Hou, Zhi-Mei Huang, Jin-Hua Huang
Sun Yat-sen University Cancer center

Purpose Large hepatocellular carcinoma (HCC) tumors exhibit heterogeneous morphologies and varied responses to treatment. We evaluated outcomes of patients with different large HCC morphologies receiving transarterial chemoembolization plus ablation (TA) or surgical resection (SR).

Materials and methods Patients with HCC ≥ 5 cm receiving SR or TA between May 2016 and December 2020 were analyzed retrospectively and with propensity score matching (PSM). Overall survival (OS) and progression-free survival (PFS) of the 2 treatment groups were compared. Prognostic factors for survival were analyzed using multivariate Cox regression. Tumors were classified according to imaging morphology and gross pathology: Type I, simple nodular; Type II, simple nodular with extranodular growth or confluent multinodular; Type III, infiltrative.

Results Of 644 patients, 374 met the inclusion criteria (300 received SR and 74 received TA). After PSM, each group consisted of 46 patients, with no significant differences in baseline characteristics. Before PSM, median follow-up was 51.2 (IQR 29.6-65.3) months, and the SR group had longer OS (HR 2.13, 95% CI 1.44-3.15, $p < 0.001$) and PFS (HR 2.31, 95% CI 1.66-3.20, $p < 0.001$) than the TA group; after PSM these differences were not significant. Infiltrative HCC (Type III) was an independent negative prognostic factor for OS and PFS. Tumor diameter ≥ 10 cm and multiple tumors were independent negative prognostic factors for PFS. Within both treatment groups, patients with infiltrative HCC had shorter OS and PFS than patients with non-infiltrative HCC (Types I and II) (all $p < 0.001$).

Conclusion For patients with HCC ≥ 5 cm, tumor morphology is an important prognostic factor. In patients with non-infiltrative HCC, TA and SR had comparable OS and PFS after PSM. For patients with infiltrative HCC, TA and SR had limited efficacy.

PU-010

Analysis of key genes and signaling pathways shared by liver cancer and interventional liver cancer based on bioinformatics methods

Pengfei Lu, Diwen Zhu, Xiaomei Lu, Hua Zhang, Rui Mao, Weixin Ren
The First Affiliated Hospital of Xinjiang Medical University

Purpose To explore the common gene characteristics and pathogenic mechanisms of liver cancer and interventional liver cancer using bioinformatics methods.

Materials and methods Download the liver cancer and adjacent cancer dataset (GSE89377) and interventional liver cancer and adjacent cancer dataset (GSE60502) from the GEO (Gene Expression Omnibus) database, perform differential analysis using the R language package, and obtain common differentially expressed genes (DEGs) using Venn maps. Perform GO (gene ontology) and KEGG (Kyoto Encyclopedia of genes and genomes) enrichment analysis on DEGs, and obtain key modules and core genes in the PPI (protein protein interaction) network using Cytoscape software. Perform network interaction analysis of genes, transcription factors, and mi RNA in the NetworkAnalyst database. DGIdb database is used for gene drug interaction analysis.

Results A total of 71 DEGs were screened, and GO analysis and KEGG analysis showed that these DEGs are mainly located in the extracellular region and organelles bound to the cell membrane. They participate in oxidoreductase activity, zinc ion binding, and iron ion binding, thereby regulating exogenous biological metabolic processes, negative growth regulation, cell response to cadmium ions, detoxification of copper ions, etc. Further weight analysis was conducted on 71 DEGs, and a total of 7 core genes (CYP1A2, CYP2E1, CYP3A4, CYP2C9, SLC10A1, SLCO1B3, SLC22A1) were screened.

Conclusion These DEGs may be potential targets that affect the efficacy of interventional therapy for liver cancer.

PU-011

MNX1-AS1 reduces chemosensitivity by promoting the PI3K/AKT pathway in breast cancer

Y S, Yuan Peng

National Cancer Centre/National Clinical Research Center for Cancer/Cancer Hospital, Chinese Academy of Medical Sciences and Peking Union Medical College

Purpose Long noncoding RNAs (lncRNAs) are involved in tumorigenesis and chemosensitivity. However, the roles and underlying mechanisms of lncRNAs in breast cancer (BC) are still unknown.

Materials and methods

In this work, we used bioinformatics analysis and in situ hybridization (ISH) assays to detect MNX1-AS1 expression in BC samples. The role of MNX1-AS1 was detected by in vitro functional assays and analysis of in vivo xenograft tumour models. The mechanism of MNX1-AS1 was clarified using subcellular fractionation, FISH, RNA sequencing, RIP and ChIP assays. We encapsulated MNX1-AS1 siRNA into nanoparticles and evaluated the superiority of these nanoparticles over free siRNA in systemic drug delivery.

Results

MNX1-AS1 is highly expressed in BC, promotes paclitaxel resistance via the PI3K/AKT pathway, and is associated with a poor prognosis in BC patients. Thus, MNX1-AS1 activates the PI3K/AKT pathway. Additionally, lipid nanoparticles were used to effectively deliver MNX1-AS1 siRNA to tumour-bearing mice, and exhibited significantly antitumor effects.

Conclusion These findings indicate that lncRNA MNX1-AS1-mediated activation of the PI3K/AKT pathway promotes BC progression and chemoresistance and that targeting of MNX1-AS1 may be a new therapeutic approach to increase the efficacy of chemotherapy against BC.

PU-012

2024 Guangzhou consensus of Minimally Invasive and Multidisciplinary Comprehensive Treatment for Hepatocellular Carcinoma

Qi-Feng Chen, Pei-Hong Wu
Sun Yat-sen University Cancer Center

Purpose Hepatocellular carcinoma (HCC) ranks as the fourth most common cancer globally and the third most prevalent cancer in China, where the incidence of chronic hepatitis B infection remains high.

Materials and methods Pathologically, HCC is characterized by a rich blood supply, multicentric origins, early vascular invasion, and intrahepatic metastasis. As a result, HCC should be considered a systemic disease from its onset rather than a localized disease. Consequently, a comprehensive treatment approach is essential for managing HCC, incorporating local treatments (such as surgical resection and ablation), organ-level treatments (such as transcatheter arterial therapy), and systemic treatments (such as immunotherapy, molecular targeted therapy, and antiviral therapy).

Results Experts from the fields of hepatology, oncology, surgery, radiology, and radiation oncology, under the Chinese Anti-Cancer Association, have revised the 2020 Guangzhou consensus and developed new recommendations, 2024 Guangzhou consensus, that integrate the latest research findings and expert opinions.

Conclusion These guidelines offer valuable information and guidance for clinicians, trainees, and researchers involved in the diagnosis and treatment of HCC.

PU-014

Treatment strategy for patients with aortic aneurysm complicated with malignant tumors

WENTAO ZHENG

Chongqing University Cancer Hospital

Purpose To explore the treatment strategy for patients with aortic aneurysm complicated with malignant tumors.

Materials and methods The clinical data of 32 patients with aortic aneurysm complicated with malignant tumors from June 2018 to December 2023 were retrospectively analyzed. There were 29 males (90.6%) and 3 females (9.4%), with an age range of 45-84 years, and the average age was (65.50 ± 9.26) years. All patients were diagnosed with malignant tumors by pathological biopsy or multiple imaging methods, and aortic aneurysms were diagnosed by thoracic and abdominal CTA, among whom 32 patients were treated with endovascular exclusion. Among the patients with endovascular exclusion, there were 9 cases (28.1%) of thoracic aortic aneurysm, 23 cases (71.9%) of abdominal aortic aneurysm, and 5 cases (21.7%) of abdominal aortic aneurysm combined with iliac aneurysm. Among the malignant tumors, there were 4 cases (1:3, thoracic and abdominal aortic aneurysm patients, 12.5%), 7 cases (1:6, 21.9%) of colorectal cancer, 4 cases (1:3, 12.5%) of liver cancer, 10 cases (4:6, 31.3%) of lung cancer, 4 cases (2:2, 12.5%) of retroperitoneal tumor, and 1 case of gastric cancer, nasopharyngeal cancer, and endometrial cancer combined with abdominal aortic aneurysm. After endovascular exclusion, 8 patients (2:6, 25%) underwent surgical radical resection combined with multiple treatments, 7 patients (2:5, 21.9%) underwent chemotherapy, 9 patients (3:6, 28.1%) underwent chemotherapy combined with targeted and immunotherapy, 4 patients (1:3, 12.5%) underwent transcatheter arterial chemoembolization, and 3 patients (1:2, 9.4%) underwent palliative treatment.

Results 32 cases of aortic aneurysm patients with malignant tumors were successfully treated with endovascular graft exclusion and stenting, with a successful rate of 100%. After the operation, 29 (90.6%) patients with malignant tumors were effectively treated.

Conclusion Endovascular graft exclusion is safe and effective for the treatment of aortic aneurysm patients with malignant tumors. After endovascular graft exclusion, patients can be treated with surgical treatment, chemotherapy, immunotherapy, targeted therapy and other treatments.

PU-015

Efficacy and Safety of hydromorphone Patient-controlled Analgesia (PCIA) for analgesia after adjunctive uterine artery embolization in patients with scarred pregnancies

Jing Shi

Fuyang Municipal People's Hospital

Purpose Objective To evaluate the efficacy and safety of patients-controlled intravenous analgesia (PCIA) for postoperative analgesia after assisted uterine artery embolization (UAE) in patients with scarred pregnancies.

Materials and methods 116 patients with scarred pregnancies undergoing UAE-assisted treatment from January 2021 to September 2022 in Fuyang People's Hospital were selected. According to the different intravenous self-controlled analgesic drugs after UAE, they were randomly divided into an observation group and a control group, each group was 58 cases. Hydrocodone 2 mg (observation group) and sufentanil 2 µg (control group) were injected 10 min before the start of surgery, and the patient-controlled intravenous analgesia pump was connected. Observation group: hydrocodone 10 mg + flurbiprofen ester 100 mg + 0.9% sodium chloride injection 100 ml was configured to the analgesic pump; control group: sufentanil 2 µg/kg + flurbiprofen 100 mg + 0.9% sodium chloride injection 100 ml was configured; the patient-controlled analgesia pump was connected to the patient-controlled intravenous analgesia pump. percent, sodium chloride injection of 100 ml was configured into the analgesic pump. Visual analog scale (VAS) scores, Bruggmann comfort scale (BCS) scores, the number of analgesic pump presses, and the number of analgesic drugs used in the two groups were recorded at 0.5h, 4h, 8h, 12h, 24h, and 48h after UAE, Adverse reactions and the incidence of postoperative complications.

Results 116 patients with scarred pregnancies undergoing UAE-assisted treatment from January 2021 to September 2022 in Fuyang People's Hospital were selected. According to the different intravenous self-controlled analgesic drugs after UAE, they were randomly divided into an observation group and a control group, each group was 58 cases. Hydrocodone 2 mg (observation group) and sufentanil 2 µg (control group) were injected 10 min before the start of surgery, and the patient-controlled intravenous analgesia pump was connected. Observation group: hydrocodone 10 mg + flurbiprofen ester 100 mg + 0.9% sodium chloride injection 100 ml was configured to the analgesic pump; control group: sufentanil 2 µg/kg + flurbiprofen 100 mg + 0.9% sodium chloride injection 100 ml was configured; the patient-controlled analgesia pump was connected to the patient-controlled intravenous analgesia pump. percent, sodium chloride injection of 100 ml was configured into the analgesic pump. Visual analog scale (VAS) scores, Bruggmann comfort scale (BCS) scores, the number of analgesic pump presses, and the number of analgesic drugs used in the two groups were recorded at 0.5h, 4h, 8h, 12h, 24h, and 48h after UAE, Adverse reactions and the incidence of postoperative complications.

Conclusion Hydrocodone and sufentanil PCIA help to relieve postoperative pain after uterine artery embolization in scarred pregnancy, but hydrocodone compared with sufentanil can significantly reduce the postoperative VAS score, improve the postoperative BCS score, reduce the number of postoperative analgesic pump presses and the dosage of analgesic drugs in the 48h postoperative period, and the incidence of adverse reactions is low, which has a certain value of promotion.

PU-017

Application of Percutaneous Transhepatic Cholangioscopy in Diagnosis of Postoperative Biliary Strictures of cholangiocarcinoma patients

Tao Li

Shandong Provincial Hospital Affiliated to Shandong First Medical University

Purpose The differentiation between benign and malignant conditions following the occurrence of cholangioenteric anastomotic strictures is of utmost importance as it significantly impacts subsequent treatment plans and patient prognosis[1]. The purpose of this study was to evaluate the use of percutaneous transhepatic cholangioscopy with the EYEMAX biliary sub - scope followed by liver biopsy in patients with cholangiocarcinoma for biopsy and in diagnosing the benign or malignant nature of post - operative biliary strictures in cholangiocarcinoma patients.

Materials and methods After successful biliary puncture, dilation was performed successively through 6F, 9F, and 10F sheaths. The EYEMAX biliary sub - scope was inserted through the 10F sheath for direct visualization of the nature of the lesions. Biopsies could be carried out under direct vision for pathological diagnosis.

Results We successfully conducted a percutaneous transhepatic cholangioscopy in a patient with post - operative biliary stricture following cholangiocarcinoma surgery. Prior to this, enhanced abdominal CT highly suspected a recurrence of cholangiocarcinoma. During the operation, we clearly observed the stricture of the cholangioenteric anastomosis and the hyperplastic mucosa, which was considered to be an inflammatory stricture. The pathology showed chronic inflammation of the mucosa and fibrous tissue hyperplasia at the cholangioenteric anastomosis. Consequently, we performed balloon dilation and placed a 10F internal - external biliary drainage tube. Currently, the patient has recovered well. A subsequent abdominal imaging examination shows no signs of tumor recurrence, thus avoiding unnecessary chemotherapy and the incorrect placement of a bare metal stent.

Conclusion Percutaneous transhepatic cholangioscopy with the EYEMAX biliary sub - scope is a feasible method for obtaining biopsies and diagnosing the nature of biliary lesions in cholangiocarcinoma patients and their post - operative biliary strictures. It provides a valuable option for accurate diagnosis in relevant clinical scenarios. Conventional methods like EUS - guided fine - needle aspiration biopsy or ERCP have been helpful in diagnosing cholangioenteric anastomotic strictures. However, they have limitations. The accuracy of these methods is sub - optimal, and ERCP is not only technically challenging but also time - consuming and may cause severe complications such as intestinal perforation. In contrast, our proposed method is time - efficient and safe. With the continuous improvement and miniaturization of the biliary sub - scope, it is anticipated that more patients with such conditions will benefit from this approach in the future.

PU-019

Experimental Study on Drug Delivery System Based on Reprogrammed Macrophages for Hepatocellular Carcinoma Treatment

Yilin Zeng, Run Lin

The First Affiliated Hospital, Sun Yat-sen University

Purpose Hepatocellular carcinoma (HCC) is a leading cause of cancer-related mortality, with limited efficacy of current therapies like immune-checkpoint inhibitors (ICIs) due to the immunosuppressive tumor microenvironment (TME). M2 tumor-associated macrophages (TAMs) dominate the TME and correlate with poor prognosis, while M1 macrophages enhance antitumor immunity. This study aims to develop a drug delivery system based on reprogrammed macrophages to convert M2 to M1 phenotypes, thereby reversing immunosuppression and improving HCC treatment outcomes.

Materials and methods (1) RNA-seq data from 373 TCGA-LIHC cases were analyzed using CIBERSORT to evaluate immune cell infiltration and Kaplan-Meier survival curves were generated based on M2 macrophage infiltration and M2/M1 ratios. (2) In vitro, PTX/R848-induced M2 repolarization was confirmed by qPCR, flow cytometry, morphological analysis, and cytokine analysis. (3) A PTX/R848-loaded hydrogel (PTX/R848@Gel) was synthesized for localized drug delivery. (4) A subcutaneous Hepa 1-6 mouse model was established, and therapeutic efficacy was assessed via tumor growth curves and survival analysis. (5) Tumor tissues were collected for immune profiling to evaluate TME remodeling.

Results The results showed: (1) M2 macrophages are the predominant subtype in HCC and are negatively associated with overall survival. (2) PTX/R848 effectively reprograms M2 to M1-like macrophages, upregulating M1 markers (e.g., CD80) and pro-inflammatory cytokines (e.g., IL-12, TNF- α) at both mRNA and protein levels. (3) PTX/R848@Gel was successfully synthesized, with favorable biodegradability. (4) In vivo, the PTX/R848 group achieved a complete response rate (CRR) of 87.5% and prolonged median survival. (5) PTX/R848@Gel reprograms macrophages and remodels the immunosuppressive TME, thereby achieving effective antitumor immunotherapy.

Conclusion In this study, we confirmed the capacity of PTX and R848 for macrophage modulation in vitro and successfully developed a dual-drug depot composed of PTX and R848 encapsulated within a thermosensitive hydrogel (PTX/R848@Gel). The incorporated PTX and R848 were gradually released from the gel, serving as an in situ vaccine to stimulate antitumor immune responses. PTX/R848@Gel effectively reprogrammed M2 TAMs into M1-like macrophages and reversed the immunosuppressive TME, resulting in significant antitumor efficacy in a subcutaneous HCC model. Based on these results, we propose PTX/R848@Gel as a potential therapeutic strategy for HCC treatment.

PU-021

Efficacy of Atezolizumab Plus Bevacizumab Combined with Transarterial Chemoembolization for Unresectable Hepatocellular Carcinoma: A Real-World Study

Xiao Shen, Qing-Quan Zu, Hai-Bin Shi, Sheng Liu
The First Affiliated Hospital with Nanjing Medical University,

Purpose Transarterial chemoembolization (TACE), when used in combination with immunotherapy and antiangiogenic therapy, has been shown to have synergistic anticancer effects. The aim of this study was to further assess the efficacy and safety of TACE combined with atezolizumab and bevacizumab in the treatment of unresectable hepatocellular carcinoma (HCC) in the real world.

Materials and methods Between August 2021 and September 2023, clinical information was collected from consecutive HCC patients who received treatment via TACE-Atezo/Bev at four tertiary institutions. This study evaluated the objective response rate (ORR), overall survival (OS), and progression-free survival (PFS) as outcomes. Predictors for OS and PFS were also analyzed. Treatment-related adverse events (TRAEs) were recorded and assessed.

Results Ninety-two patients were enrolled in this study, with a median follow-up duration of 14.1 months. The ORRs based on the modified Response Evaluation Criteria in Solid Tumors (RECIST) and RECIST 1.1 criteria were 54.3% and 41.3%, respectively. The median OS and PFS of the patients were 15.9 months [95% confidence interval (CI), 14.5–17.2 months] and 9.1 months (95% CI, 7.4–10.8 months), respectively. Multivariate analyses revealed that the Eastern Cooperative Oncology Group score and neutrophil–lymphocyte ratio were independent risk factors for OS, whereas tumor size and extrahepatic metastasis were independent risk factors for PFS. Grade 3/4 TRAEs occurred in 16.3% (15/92) of the patients and were controlled conservatively.

Conclusion The combination of Atezo/Bev with TACE demonstrated acceptable synergistic therapeutic effects and manageable safety profiles in patients with unresectable HCC.

PU-022

Efficacy and safety of 100-300um and 300-500um drug eluting beads in the treatment of colorectal cancer liver metastasis by TACE

Rujian Wang,Zhongfeng Sheng,Yutian Jiang,Tao Wang
The Affiliated Yantai Yuhuangding Hospital of Qingdao University

Purpose To compare the efficacy and safety of 100-300um and 300-500um drug eluting beads in the treatment of colorectal cancer liver metastasis by TACE.

Materials and methods A total of 65 patients with unresectable colorectal cancer liver metastasis (CRC-LM) diagnosed in Yantai Yuhuangding Hospital from November 2020 to November 2022 were enrolled and randomly divided into small size group (n=33) and large size group (n=32). The small particle size group was treated with 100-300um drug-loaded microspheres, and the large particle size group was treated with 300-500um drug-loaded microspheres. The primary endpoints were objective response rate (ORR) and disease control rate (DCR); The secondary endpoints were progression-free survival (PFS), overall survival (OS) and safety of the two groups, and the Kaplan-Meie method was used to depict the survival curve. COX regression model was used to analyze the influencing factors of PFS and OS in patients.

Results A total of 5 patients were lost to follow-up during the treatment process, and 30 patients in each group could be evaluated and compared. There was no significant difference in ORR and DCR between the two groups at 1, 3, 6 and 12 months after surgery, and the ORR in the small size group (50.0%) was better than that of the large size group (26.7%) at 3 months after surgery ($p=0.063$). The mPFS and mOS in the small size group were 15.0 months and 26 months, respectively, which in the large size group were 13.8 months and 21.5 months, respectively, and there was no significant difference between the two groups ($p>0.05$). There was no significant difference in the adverse reactions between the two groups ($P>0.05$), and there was no death-induced by treatment. CHILD-PUGH Grade, ECOG score, and number of metastases were independent factors for PFS and OS in this study.

Conclusion The treatment of 100-300um and 300-500um drug eluting beads in colorectal cancer liver metastasis is efficacious and safe.

PU-023

Optimizing Imaging Diagnosis Based on Anatomical Complexity of the Inferior Pulmonary Ligament: Dynamic 3D Reconstruction and Interventional-Surgical Decision Support

Xichun Gao
Liwan Central Hospital

Purpose The inferior pulmonary ligament (IPL), a thin fold of pleura connecting the lower lobe to the diaphragm and mediastinum, presents unique challenges in preoperative assessment due to its anatomical proximity to critical structures like the pulmonary vessels, bronchi, and phrenic nerve. Conventional 2D imaging often fails to quantify tumor invasiveness accurately, leading to misdiagnosis rates as high as 34% in reported literature. This study aims to develop a multimodal radiomics-driven dynamic 3D reconstruction framework to address these limitations and enhance interdisciplinary decision-making for IPL tumors.

Materials and methods Literature-Driven Anatomical Analysis: A systematic review of PubMed and CNKI (2019–2024) identified 12 studies highlighting IPL tumor diagnostic pitfalls, including vascular invasion underestimation (28–40% cases) and diaphragmatic adhesion misclassification. Technical Development: Multimodal Image Fusion: A deep learning-based non-rigid registration algorithm (3D CNN) aligned high-resolution CT (0.6-mm slices), MRI-DWI/ADC (soft-tissue contrast), and PET-CT (metabolic activity), achieving a registration error of 0.8 ± 0.3 mm. Dynamic 3D Reconstruction: Using U-Net semi-automatic segmentation, interactive 3D models of tumors and adjacent structures (e.g., pulmonary arteries, bronchi) were generated, with real-time visualization via mixed-reality headsets. Radiomics Analysis: PyRadiomics extracted 1,309 features (morphological, textural, wavelet), refined by LASSO regression to 12 invasiveness predictors. A random forest classifier was trained on open-source TCIA datasets ($n=210$ thoracic tumors). Prospective Clinical Validation: 15 suspected IPL tumor cases (Liwan Central Hospital, 2023–2024) underwent 3D-guided assessment, compared with traditional CT evaluations by two senior radiologists. **Results** Technical Performance: The registration algorithm reduced processing time by 40% (18.2 ± 3.1 vs. 30.5 ± 5.4 minutes, $P < 0.001$) compared to manual methods. 3D models demonstrated high concordance with intraoperative findings ($\text{ICC} = 0.87$, 95% CI: 0.82–0.91), particularly in delineating vascular encasement. Diagnostic Accuracy: The radiomics model outperformed conventional CT: sensitivity 94.1% vs. 73.5% ($P = 0.003$), specificity 88.6% vs. 67.2% ($P = 0.011$), AUC 0.93 (95% CI: 0.88–0.97) vs. 0.76. Key predictors included CT arterial-phase texture entropy (importance=0.34), ADC heterogeneity (0.29), and PET metabolic tumor volume (0.25). Clinical Impact: 3D navigation altered surgical plans in 4/15 cases (26.7%): two shifted from lobectomy to diaphragm-sparing resection, and two underwent preoperative targeted embolization. The 3D-guided group showed reduced intraoperative blood loss (220 ± 45 mL vs. 350 ± 68 mL, $P < 0.001$) and shorter hospitalization (6.2 ± 1.5 vs. 8.7 ± 2.1 days, $P = 0.002$).

Conclusion This study establishes a novel imaging framework that integrates dynamic 3D reconstruction and radiomics to overcome the anatomical complexity of IPL tumors. By providing quantifiable invasiveness parameters and real-time surgical navigation, the technology bridges interdisciplinary gaps between radiology, interventional oncology, and thoracic surgery. Future work will focus on open-source algorithm sharing (code available on GitHub) and multicenter validation to standardize IPL tumor assessment protocols.

PU-024

Preoperative T2 MRI radiomics signature in predicting the short - term efficacy of interventional therapy for adenomyosis: a clinical study

Dongcun Yuan
Anhui women and child health center

Purpose To explore the predictive value of radiomics based on pre-interventional MR imaging for the therapeutic effect of uterine adenomyosis treated by interventional therapy.

Materials and methods A retrospective analysis was conducted on 140 patients with uterine adenomyosis who underwent vascular interventional therapy. MRI examinations were performed within one week before the intervention, and pelvic MRI follow-ups were conducted at 6 months and 1 year after the intervention. The therapeutic effect after interventional therapy was evaluated according to the criteria for the relief of uterine adenomyosis. Stratified sampling was used to divide the patients into a training set ($n = 98$) and a test set ($n = 42$) at a ratio of 7:3. The patients were divided into an effective group (39 cases) and an ineffective group (101 cases) based on the treatment response. Lesion regions were delineated on preoperative T2WI images using ITK-SNAP software, and radiomics features were extracted. Univariate analysis and the least absolute shrinkage and selection operator were used to screen radiomics features and establish a radiomics model. The predictive efficacy of the radiomics model for ineffective treatment after UAE in uterine adenomyosis was evaluated using the receiver operating characteristic curve (ROC), and the area under the curve (AUC) was calculated. The clinical practical value of the model was evaluated using decision curve analysis.

Results Nine most valuable radiomics features were included in the predictive model. The AUC of the radiomics model for predicting ineffective treatment after UAE in uterine adenomyosis was 0.838 (95% CI 0.751 - 0.924) in the training set and 0.817 (95% CI 0.677 - 0.954) in the test set. Decision curve analysis showed that the radiomics model had a high clinical net benefit.

Conclusion The radiomics model based on T2WI can effectively predict the therapeutic effect of UAE in patients with uterine adenomyosis, assisting clinicians in early identification of ineffective risks and timely adjustment of treatment strategies.

PU-025

Value and satisfaction analysis of humanistic care combined with narrative nursing in patients with advanced malignant tumors

Wang Hongyan
Chongqing University Cancer Hospital

Purpose In the nursing intervention of patients with advanced malignant tumors, the practical effect of humanistic care, narrative nursing combined nursing and patient satisfaction were analyzed and studied.

Materials and methods From October 2022 to October 2024, 72 patients admitted to our department were selected to carry out this study. They were divided into two groups, the conventional group and the research group, with 36 patients in each group. Narrative nursing intervention was carried out in the conventional group, while narrative nursing and humanistic nursing intervention was carried out in the study group. The specific observation and analysis indicators are as follows: the improvement effect of depression and anxiety and nursing satisfaction of patients in the two groups.

Results Data analysis showed that the improvement effect of depression and anxiety in the study group was significantly better than that in the conventional group ($P < 0.05$), and the satisfaction was higher than that in the conventional group ($P < 0.05$).

Conclusion For patients with advanced malignant tumors with clinical nursing intervention, the use of narrative nursing intervention and humanistic care combined form of nursing is of significant value, the main role is to effectively improve patients' depression, anxiety and other adverse emotions, but also to improve patients' nursing satisfaction rate, suggesting clinical practice application and reference.

Sustained release hypoxia-activated prodrug-loaded BSA nanoparticles enhance transarterial chemoembolization against hepatocellular carcinoma

Yinghong Hao¹, Wenzhi Zhu¹, Jie Li², Ruirui Lin², Wenting Huang², Qurat Ul Ain², Kaikai Liu², Ning Wei¹, Delei Cheng², Yi Wu², Weifu Lv²

1. Anhui University of Chinese Medicine

2. The First Affiliated Hospital of USTC, University of Science and Technology of China

Purpose Transarterial chemoembolization (TACE) is the standard of care for patients with advanced hepatocellular carcinoma (HCC), but facing the problem of low therapeutic effect. Conventional TACE formulations contain Lipiodol (LP) and chemotherapeutic agents characterized by burst release due to the unstable emulsion. Herein, we developed a novel TACE system by inducing bovine serum albumin (BSA) loaded hypoxia-activated prodrug (tirapazamine, TPZ) nanoparticle (BSATPZ) for sustained drug release. In the rabbit VX2 liver cancer model, TACE treatment induced a long-term hypoxic tumor microenvironment as demonstrated by increased expression of HIF-1 α in the tumor. BSATPZ nanoparticles combined with LP greatly enhanced the anti-tumor effects of the TACE treatment. Compared to conventional TACE treatment, BSATPZ nanoparticle-based TACE therapy more significantly delayed tumor progression and inhibited the metastases in the lungs. The effects could be partially mediated by the rebuilt immune responses, as BSATPZ nanoparticle can serve as an immunogenic cell death (ICD) inducer. Collectively, our results suggest that BSATPZ nanoparticle-based TACE therapy could be a promising strategy to improve clinical outcomes for patients with HCC and provide a preclinical rationale for evaluating TPZ therapy in clinical studies.

Materials and methods In this study, we developed BSA nanoparticles as a TPZ drug delivery vehicle aiming to achieve high localized TPZ concentrations and sustained release of TPZ in tumors to kill HCC cells and enhance the therapeutic efficacy of TACE against HCC by exploiting the secondary hypoxic microenvironment. We prepared BSA nanoparticles and loaded them with the hypoxia-activated prodrug, TPZ, which we designated BSATPZ. We also constructed a rabbit VX2 liver tumor model to observe the anti-tumor effects of BSATPZ in different conditions. Together, our novel drug delivery system and animal model enabled us to (1) use TACE to deliver BSA TPZ locally to liver tumors via catheter to achieve localized, high drug concentrations and reduce systemic toxicity; (2) achieve sustained, slow release of TPZ owing to the properties of the BSA nanoparticle delivery system; and (3) block the arterial blood supply to liver tumors and create a hypoxic environment to stimulate TPZ activation (Scheme 1). We found that TACE combined with BSATPZ (BSATPZ/LP) had an improved therapeutic effect in the treatment of liver tumors, increased immune cell infiltration in tumor tissue, as well as a synergistic effect in the prevention of lung metastases. Our results suggest that TACE with BSATPZ/LP could be a promising strategy to improve clinical outcomes for patients with HCC and provide a preclinical rationale for evaluating TPZ therapy in clinical studies.

Results In this study, we observed that the combination of lipiodol (LP) and BSATPZ nanoparticles after TACE treatment effectively prolonged embolization and induced a hypoxic tumor microenvironment. MRI and digital subtraction angiography (DSA) analyses demonstrated that TACE treatment successfully blocked the blood supply to the tumor site, with the hypoxic environment persisting post-treatment. Immunofluorescence analysis revealed a significant increase in the expression of hypoxia-inducible factor 1- α (HIF-1 α), further confirming the establishment of the hypoxic microenvironment. Moreover, BSATPZ nanoparticles exhibited good stability, sustained re

lease properties, and cytotoxicity in vitro, particularly demonstrating strong anti-tumor effects under hypoxic conditions. In pharmacokinetic experiments, BSATPZ/LP showed high drug concentrations at the tumor site, with prolonged retention, effectively reducing systemic toxicity. This strategy enhanced the anti-tumor effect by prolonging drug release and activating the prodrug in the hypoxic tumor microenvironment (TME). The results indicated that TACE combined with BSATPZ/LP not only efficiently embolized the tumor blood supply and induced sustained tumor hypoxia, but also reshaped the immune microenvironment, significantly enhancing immune cell infiltration, especially CD4⁺ and CD8⁺ T cells and regulatory T cells (Tregs). Additionally, BSATPZ under hypoxic conditions induced immunogenic cell death (ICD) by releasing damage-associated molecular patterns (DAMPs) such as calreticulin (CRT) and high-mobility group box 1 (HMGB1), thereby activating the immune system to target the tumor. In vivo experiments demonstrated that BSATPZ/LP treatment effectively suppressed primary tumor growth and, through enhanced immune responses, synergistically inhibited lung metastasis, highlighting the potential of this strategy in improving clinical outcomes for patients with advanced hepatocellular carcinoma.

Conclusion Our study demonstrated the effectiveness of the novel TACE system, which combines LP with BSA nanoparticles loaded with TPZ. This new system achieved a controlled and sustained drug release directly at the tumor site, thus activating the prodrug in the hypoxic TME. Consequently, it led to improved anti-tumor efficacy at the primary tumor site, coupled with synergistic benefits against lung metastases. In addition, we found that a rejuvenated immune response may partially mediate the anti-tumor efficacy of the new TACE system. This strategy provided an effective approach to address the issue of burst drug release during TACE while also leveraging the secondary hypoxic TME induced by TACE therapy to achieve sustained tumor cell eradication. Specifically, the new TACE system encompassed the following aspects: 1) TPZ-loaded BSA nanoparticles are delivered to the local tumor through the catheter, enabling the sustained drug release; 2) LP embolization of tumor blood vessels resulted in a sufficient hypoxic environment for drug activation and tumor cell destruction; 3) BSATPZ/LP, serving as a great ICD inducer, has great potential to rebuild the liver immune tumor microenvironment and enhance the antitumor response. Our results suggested that TACE therapy with BSATPZ/LP could not only serve as a promising strategy for improving clinical outcomes in patients with advanced HCC, but also provided a preclinical basis for further development of TPZ-based interventional therapies.

PU-027

Lenvatinib Ameliorates the Immunosuppressive Microenvironment of Hepatocellular Carcinoma after Transarterial Chemoembolization

Shen Zhang, Xiao Li Zhu

First Affiliated Hospital of Soochow University

Purpose To explore the effects of transarterial chemoembolization (TACE) and TACE combined with lenvatinib on microenvironment of hepatocellular carcinoma.

Materials and methods An in situ HCC rat model was established via laparotomy, confirmed by magnetic resonance imaging (MRI). Rats underwent TACE or sham (normal saline) via tail artery under DSA guidance. The combined therapy group received lenvatinib post-TACE. Tumor response was monitored via serial MRI. On day 8, rats were euthanized for pathological assessment, focusing on immune-cell alterations in HCC tissues. Statistical significance ($P < 0.05$) was determined using one-way ANOVA.

Results MRI exhibited a pronounced reduction in tumor volume in the combined treatment group versus TACE and sham groups on day 7 post embolization ($P < 0.001$), accompanied by significantly increased HCC necrosis ($P = 0.008$). After embolization, the number of CD8+T cells declined compared to the sham group ($P < 0.001$), yet lenvatinib enhanced CD8+T cell infiltration after TACE ($P = 0.004$). The combined group also significantly elevated the number of Granzyme B+ cells ($P = 0.001$). Notably, CD68+CD163+ monocytes increased after TACE ($P < 0.001$), but declined after the administration of lenvatinib ($P = 0.155$). Similarly, CD25+Foxp3+T lymphocytes surged after TACE ($P < 0.001$) and subsided slightly with the treatment of lenvatinib ($P = 0.286$).

Conclusion Lenvatinib ameliorated the immunosuppressive milieu in residual HCC tissue following TACE.

PU-028

Prognostic Prediction of Immune Indicator Changing Trend in Unresectable Hepatocellular Carcinoma Undergoing TACE plus ICIs and Anti-VEGF Antibodies/TKIs

Xiaoyang Xu

the First Affiliated Hospital of Soochow University, Jiangsu 215000

Purpose To explore changing trends in circulating immune indicators of hepatocellular carcinoma (HCC) undergoing TACE plus immune checkpoint inhibitors (ICIs) and anti-VEGF antibodies/TKIs and to elucidate the relationship between immune response and tumor prognosis.

Materials and methods This single-center retrospective study included patients with unresectable HCC undergoing TACE plus ICIs and anti-VEGF antibodies/TKIs from March 11, 2019, to February 15, 2024. Peripheral blood samples, including blood cell count and immune indicators, were collected at baseline and every cycle. The primary outcomes were objective response rate (ORR) at the first evaluation. According to the first evaluation based on mRECIST, patients were classified into PD, SD and OR groups for analysis. Further subgroup analysis was performed on the OR group based on whether experiencing progression after the first evaluation. Lymphocyte subsets were measured by flow cytometry. Immunoglobulins were measured by the immune turbidimetric method. Neutrophil-to-lymphocyte ratio (NLR) was measured by the complete blood count. Simple linear regression was employed to examine the dynamic trends.

Results A total of 63 patients were enrolled, with an ORR of 55.6% and a disease control rate (DCR) of 87.3% at the first evaluation. The median overall survival (mOS) was 27.5 months (95% CI: 22.5-32.5 months). In the OR group (n=35), more active immune responses, expressed in a decrease in CD3-CD19⁺ (p=0.004), CFB (p=0.027), NLR (p<0.001) and an increase in Ig λ (p=0.010), Ig κ (p=0.037), Ig A (p=0.005), Ig G (p=0.006), were related to better prognosis, while similar patterns seen in the OR-nPD subgroup. Concurrently, no significant differences were noted in the PD group (n=8).

Conclusion The combination therapy may modify the tumor microenvironment of HCC. Changing trends in circulating immune indicators and NLR can serve as potential biomarkers for predicting tumor response and guiding clinical treatment.

PU-029

Evaluation of the Radiation Protection Efficacy of a Novel Domestic Lead-Free Protective Glove in a Simulated Direct X-ray Beam

Mingming Li, Caifang Ni

The First Affiliated Hospital of Soochow University

Purpose To assess the radiation protection efficacy of the novel domestic lead-free protective glove in a simulated direct X-ray beam under two fluoroscopy modes (automatic exposure control and manual fixed parameter modes) and to investigate the impact of phantom thickness on glove performance, fluoroscopic radiation parameters, and operator radiation dose in the automatic exposure control mode.

Materials and methods Thermoluminescent detectors were fixed inside and outside the glove at the same marked position on the palm area of hand-shaped phantoms. The experiment was divided into three groups based on the exposure level of the gloves: (1) R0 group, no glove exposure; (2) R1 group, exposure of one glove; and (3) R2 group, exposure of two gloves. A standard Virtual Water phantom with a thickness of 20 cm was used to simulate the patient. Dose measurements for the gloves were conducted under automatic exposure control and manual fixed parameter modes. Additionally, dose measurements were performed using three different phantom thicknesses (15 cm, 20 cm, 25 cm) in the automatic exposure control mode. Operator radiation dose (lens of the eye, neck, and chest areas) was measured using a human phantom. Fluoroscopic radiation parameters were recorded to analyze the impact of glove exposure level on the dose field.

Results The dose reduction performance of the novel domestic glove was similar under both fluoroscopy modes, with a reduction rate of 72.9-81.4%. In manual fixed mode, the dose optimization rate was 76.6-81.1%, while in automatic exposure control mode, the optimization rate decreased to 51.3-57% as glove exposure level increased ($P < 0.05$). The increase in phantom thickness did not significantly affect the attenuation performance of the gloves but did reduce hand dose in the direct X-ray beam. However, increasing phantom thickness and glove exposure levels led to an increase in the operator phantom's radiation dose, with the highest dose observed in the chest area closest to the X-ray tube and primary beam and the lowest dose in the lens of the eye. The entrance dose rate was basically unchanged in the manual fixed mode but increased with the increasing thickness of the phantom and the higher exposure level of the gloves in automatic exposure control mode.

Conclusion The novel domestic lead-free protective glove demonstrated stable dose reduction performance in the simulated direct X-ray beam. The gloves performed better in manual fixed mode, with stable entrance dose rate. However, in automatic exposure control mode, increasing phantom thickness and glove exposure levels led to increased entrance dose rate and operator radiation dose. These findings suggest that operators can perform effective hand protection without increasing the radiation risk to patients and operators by choosing manual fixed fluoroscopy mode when performing necessary hand exposures.

PU-030

Radiation dose reduction with modified fluoroscopy during totally implantable venous access port

Zonghong Han, Qi Wang
The First People's Hospital of Changzhou

Purpose We aimed to evaluate the effect on the radiation dose to the patient during totally implantable venous access port by modified fluoroscopy.

Materials and methods Radiation dose data were retrospectively analyzed 6 months before (Standard group) and after modified fluoroscopy (Modified group). Patient demographics, effective dose, dose-area product and the number of fluoroscopy during the procedure were determined. Mann-Whitney U test and compared with an unpaired t-test analysis. A P value of less than .05 indicated a significant difference.

Results A total of 2235 patients were evaluated, aged 61 ± 8.3 years, with 885 males and 1350 females. The DAP ($10.33 \pm 2.35 \mu\text{Gy}/\text{m}^2$ VS $34.47 \pm 8.25 \mu\text{Gy}/\text{m}^2$, $p < 0.001$) and ED ($0.51 \pm 0.12 \text{ Sv}$ VS $1.03 \pm 0.41 \text{ Sv}$, $p < 0.05$) of patients in the improved fluoroscopy group were significantly lower than those in the traditional fluoroscopy group, and the right side was significantly lower than the left side. Due to the fact that doctors do not need to wear lead coats, their radiation dose is significantly reduced.

Conclusion The modified fluoroscopy technique significantly reduces the radiation dose of patients and is worthy of further promotion and application.

PU-031

Paradoxical embolism caused by totally implantable venous access port: A case report and literature review

Zonghong Han, Qi Wang
The First People's Hospital of Changzhou

Purpose Totally implantable venous access ports (TIVAPs) are commonly used for patients undergoing chemotherapy and long-term repeated infusions. The incidence of thrombosis is low and rarely leads to serious complications.

Materials and methods We report a case of right atrial thrombosis and paradoxical embolism in a 58-year-old male with atrial fibrillation (AF) and patent foramen ovale (PFO) 28 months after TIVAP implantation.

Results The patient presented with dizziness and left limb weakness, subsequent diagnostic imaging revealed right temporal lobe infarction and a mass in the right atrium, who eventually recovered and was discharged after cardiac surgery and anticoagulation.

Conclusion This case highlights the rare but severe complication of right atrial thrombosis associated with TIVAP, particularly in patients with AF and PFO. Proper placement and timely removal of totally implantable venous access ports are crucial to minimize complications. Further research is needed to determine the necessity of anti-coagulation and PFO screening in patients with AF receiving central venous catheters.

Intravenous thrombolytic therapy for pancreatic cancer during chemotherapy: a case report and literature review

Wanhua Li
Chongqing University Cancer Hospital

Purpose This paper reports a case of pancreatic cancer complicated with deep vein thrombosis, acute pulmonary embolism (PE) and intravenous thrombolysis during AG chemotherapy.

Materials and methods The patient was a 53 year old male who was definitely diagnosed as pancreatic cancer with liver metastasis and had no indication for radical surgery. The first choice was AG regimen (gemcitabine 1500mg+albumin bound paclitaxel 200mg) for systemic intravenous chemotherapy. The patient experienced sudden chest tightness and swelling in the right lower limb during the 5th course of d8 chemotherapy, with an increase in D-dimer levels compared to before (8.17mg/L FEU). Pulmonary artery CTA showed multiple pulmonary artery branch embolism in both lungs. Lower limb deep vein ultrasound indicates thrombus formation in the middle and lower segments of the right superficial femoral vein and beyond. The patient was diagnosed with malignant tumor and had a high risk of pulmonary embolism due to recurrent thrombus detachment during subsequent chemotherapy. There were no contraindications for anticoagulation or thrombolysis, so a retrievable inferior vena cava filter was placed in the emergency department, and intraoperative thrombolysis and thrombectomy were performed to reduce thrombus burden. Based on the patient's recent chemotherapy and previous chemotherapy induced bone marrow suppression, a reduced dose injection of urokinase (400000 units) was administered via popliteal vein catheterization for thrombolysis after surgery. Low molecular weight heparin standard anticoagulation was also used during hospitalization.

Results After 24 hours of thrombolysis, the patient's symptoms improved and there were no adverse reactions such as bleeding during thrombolysis treatment. The right lower limb popliteal vein and superficial femoral vein showed unobstructed blood flow through popliteal vein catheterization. After discharge, the patient was orally administered rivaroxaban tablets and diosmin tablets. Blood routine and coagulation tests were dynamically followed up, and the dosage of rivaroxaban was adjusted according to the bone marrow suppression after chemotherapy. After one month of follow-up, the patient had no recurrence or aggravation of thrombosis, and lower limb swelling had subsided.

Conclusion Literature review shows that the incidence of venous thrombosis in pancreatic cancer patients is 5% -25%, which is related to the enhancement of tumor procoagulant activity, chemotherapy drugs (such as gemcitabine) and the reduction of activity. Mechanical thrombus clearance and thrombolytic therapy can quickly relieve thrombus burden, but strict screening of indications is required. Before thrombolytic therapy, it is necessary to strictly evaluate whether there are contraindications. In addition, patients with pancreatic cancer often suffer from malnutrition or abnormal liver function, so the dosage of anticoagulant drugs should be adjusted individually. For example, warfarin requires regular monitoring of INR, while the safety of direct oral anticoagulants (DOACs) in advanced tumors remains controversial. This case suggests that the hypercoagulability of pancreatic cancer during chemotherapy needs multidisciplinary collaborative management. Thrombolytic therapy is safe and effective under strict monitoring, but it is necessary to be alert to the potential increased risk of neurotoxicity of chemotherapy drugs (such as paclitaxel).

PU-033

Early tumor shrinkage is a prognostic factor for unresectable HCC receiving TACE combined with immune checkpoint inhibitors plus molecular targeted therapies

Jintao Huang

The First Affiliated Hospital of Soochow University

Purpose To evaluate the prognostic role of early tumor shrinkage (ETS) in unresectable hepatocellular carcinoma (HCC) receiving transarterial chemoembolization (TACE) combined with immune checkpoint inhibitors (ICIs) plus molecular targeted therapies (MTT).

Materials and methods The multicentric retrospective study screened unresectable HCC receiving TACE combined with ICIs plus MTT between January 2019 and December 2022 at three centers. The primary outcome was the relationship between ETS and overall survival (OS). The secondary outcomes were the influence of ETS on progression-free survival (PFS) and the comparison of ETS and radiological response according to the modified response evaluation criteria in solid tumors (mRECIST).

Results A total of 332 patients were enrolled in the study. Patients who had $ETS \geq 10\%$ experienced notably superior OS than those with $ETS < 10\%$ (median, 34.5 vs. 17.3 months, $p < 0.001$), as well as superior PFS (median, 16.4 vs. 9.1 months, $p < 0.001$). Besides tumor distribution, Barcelona Clinic Liver Cancer (BCLC) stage, and albumin-bilirubin grade, ETS remained an independent prognostic factor for OS in multivariate analysis. In addition, ETS demonstrated better prognostic capability in contrast to the mRECIST criteria during initial follow-up.

Conclusion ETS could effectively predict the prognosis for unresectable HCC receiving TACE combined with ICIs plus MTT and potentially improve clinical decision-making.

PU-034

Clinical Observation of Focused Ultrasound Ablation for Aggressive Fibroma

Baorang Zhu, Wuwei Yang

Associate Chief Physician of the Department of Oncology, Fifth Medical Center of the PLA General Hospital

Purpose To evaluate the safety and efficacy of high intensity focused ultrasound (HIFU) in the treatment of Aggressive Fibromatosis (AF).

Materials and methods Retrospective analysis of our hospital from January 2010 to February 2020, the application of JC type high intensity focused ultrasound system, ablation treatment of invasive fibroma patients, a total of 51 patients with AF confirmed by histology, using HIFU ablation treatment. The severity of adverse reactions was evaluated according to the SIR classification (International Society for Interventional Radiotherapy Complication Scale, Sacks D et al. JVIR. 2003) until 3 months after treatment. Incidence of non-perfused areas within the treated tumor, non-perfused volume ratio (NPVR), and tumor volume reduction were assessed using contrast-enhanced MRI before surgery and 1 and 3 months after surgery.

Results Enrolled patients (18 men, 22 women, median age 25 years; median maximum diameter: 7.6 cm, range: 3.5-15.3 cm) underwent 74 HIFU ablations, with a mean of 1.8 ablations per patient (range 1-4). In the majority of cases (70/74, 94.6%), no serious adverse events were observed. There was no significant difference in the incidence of adverse events between patients who received a single treatment and those who received multiple treatments. Non-perfused areas were observed in each treated tumor, with a median NPVR of 76.9% (range, 35-100%). After 3 months of treatment, the remission rate of symptoms was 80%, and the tumor volume reduction rate was $35.2 \pm 4.6\%$.

Conclusion HIFU ablation is a non-invasive and easily repeatable local treatment, which is a promising treatment for AF.

PU-035

Focused ultrasound ablation combined with programmed death receptor-1 monoclonal antibody Analysis of Curative Effect on Advanced Pancreatic Cancer

Baorang Zhu, Wuwei Yang

Associate Chief Physician of the Department of Oncology, Fifth Medical Center of the PLA General Hospital

Purpose To evaluate the efficacy and safety of focused ultrasound ablation (FUA) combined with programmed death receptor-1 (PD-1) monoclonal antibody in the treatment of advanced pancreatic cancer.

Materials and methods From January 2019 to July 2022, 51 patients with advanced pancreatic cancer treated with FUA alone or FUA combined with PD-1 were retrospectively analyzed. The local efficacy, survival time, adverse reactions and T cell subsets before and after treatment were recorded, and the differences in prognosis and factors affecting overall survival were analyzed.

Results There were 24 cases in the combined group and 27 cases in the FUA group. The median progression-free survival (PFS) was 8.9 and 6.5 months, and the median survival time (OS) was 11 and 9.4 months, respectively. The PFS and OS of the combination group were significantly better than those of the FUA group ($p < 0.05$). Kaplan-Meier survival analysis and multivariate analysis showed that general anesthesia and ablation efficacy were the independent factors affecting the survival time of patients in the combined group ($p < 0.05$). Spearman correlation analysis showed that the proportions of CD4⁺, Treg, CD4⁺ naive T and CD4⁺ memory T cells were positively correlated with OS in the combined group before treatment, and the proportions of CD8⁺ cells were negatively correlated with OS in the combined group before treatment ($p < 0.05$).

Conclusion Compared with FUA alone, FUA combined with PD-1 can prolong the survival time of patients with advanced pancreatic cancer, and has less adverse reactions. The results of lymphocyte subsets detection before FUA combined with PD-1 may be related to the prognosis of patients with pancreatic cancer.

PU-036

Short-term efficacy of argon-helium cryoablation for liver metastases Analysis of clinical influencing factors

Baorang Zhu, Wuwei Yang

Associate Chief Physician of the Department of Oncology, Fifth Medical Center of the PLA General Hospital

Purpose Objective To evaluate the short-term efficacy, safety and influencing factors of percutaneous cryoablation for liver metastases

Materials and methods From January 2013 to December 2017, the clinical data of patients with liver metastases treated by percutaneous cryoablation were retrospectively analyzed, the efficacy and complications of local ablation were evaluated, the local recurrence-free survival rate was counted, and the main influencing factors of complete ablation and local recurrence were analyzed.

Results a total of 119 lesions in 65 patients were treated with single therapy, CR was 56.9% (37/65), PR was 29.2% (19/65), and 13.9% (9/65) were lost to follow-up. Complications occurred in 152 cases, with the highest incidence of 95.4% (62/65) of liver function injury, 89.5% (136/152) of which were mild. There were no permanent sequelae and treatment-related deaths. The overall 1-, 2-, and 3-year recurrence-free survival rates were 47.75%, 36.8%, and 36.8%, respectively, and the median time to recurrence was 7.9 months. Univariate and multivariate analysis showed that the influencing factors of local recurrence were tumor number and tumor size ($P < 0.05$).

Conclusion Argon-helium cryoablation for liver metastases has a high short-term effective rate, and the complications can be controlled, but the long-term efficacy needs further observation, which is worth further study.

PU-037

Efficacy evaluation and predictive factors analysis of uterine artery embolization in the treatment of adenomyosis

Hao Zhang

The Second Affiliated Hospital of Soochow University.

Purpose The aim of this study was to evaluate the efficacy of uterine artery embolization (UAE) for the treatment of adenomyosis and to explore predictive factors for its therapeutic outcome.

Materials and methods This retrospective analysis reviewed the medical records of 44 patients with adenomyosis who underwent UAE treatment at our hospital from January 2020 to August 2022. The study investigated factors predictive of the efficacy of UAE treatment for adenomyosis, including MRI findings, serum CA125 levels, and follow-up dysmenorrhea scores.

Results All 44 patients with adenomyosis received a single UAE treatment. MRI follow-up at 12 months postoperatively showed a mean reduction in uterine volume from $299.60 \pm 182.42 \text{ cm}^3$ preoperatively to $173.14 \pm 104.00 \text{ cm}^3$ postoperatively, a decrease of 36.64% ($P < 0.05$). The dysmenorrhea score decreased from 7.70 ± 2.60 to 2.20 ± 2.37 , with a relief rate of 88.64% ($P < 0.05$), and no severe adverse reactions occurred. Enhanced MRI indicated complete necrosis of the lesions in 30 patients (68.18%). The preoperative serum CA125 levels (101.97 ± 60.30) and mean apparent diffusion coefficient (ADC) values (1.012 ± 0.271) in patients with completely necrotic lesions were significantly lower than those in patients with incompletely necrotic lesions ($P < 0.05$). The mean T2 signal ratio (T2SR) value (0.582 ± 0.198) in patients with completely necrotic lesions was significantly higher than that in patients with incompletely necrotic lesions ($P < 0.05$). Analysis based on the receiver operating characteristic (ROC) curve showed that the area under the curve (AUC), sensitivity, and specificity for preoperative CA125 were 0.844, 60%, and 80%, respectively; for preoperative ADC values, the AUC, sensitivity, and specificity were 0.760, 80%, and 65%, respectively; and for preoperative T2SR values, the AUC, sensitivity, and specificity were 0.760, 80%, and 70%, respectively. It was indicated that an $\text{ADC} \geq 1.116 \times 10^{-3} \text{ mm}^2/\text{s}$, a $\text{T2SR} \leq 0.479$, and a $\text{CA125} \geq 109.10$ can serve as strong predictive factors for the efficacy of UAE treatment for adenomyosis.

Conclusion UAE treatment for adenomyosis can effectively alleviate dysmenorrhea symptoms in patients and is considered safe and effective. ADC, T2SR, and CA125 can serve as strong predictive factors for the efficacy of UAE treatment for adenomyosis, which are of significant value in predicting lesion response and can aid in guiding the selection of treatment plans for patients.

PU-038

Clinical efficacy of hepatic arterial infusion chemotherapy (HAIC) in advanced hepatocellular carcinoma complicated with portal vein cancer thrombus

Jian Jing

Radiology, the second affiliated hospital of the Soochow University

Purpose To investigate the clinical efficacy of hepatic artery infusion chemotherapy (HAIC) with FOLFOX regimen applied to advanced hepatocellular carcinoma (HCC) with combined portal vein tumor thrombosis (PVTT).

Materials and methods Clinical data of 32 patients with advanced hepatocellular carcinoma treated by HAIC from August 2020 to June 2022 were retrospectively analyzed. FOLFOX4 (Oxaliplatin (OXA)+ calcium leucovorin (CF)+ 5-fluorouracil (5-FU)) regimen was used for arterial infusion: OXA 85mg/m², arterial pumped, 2 hours; CF 200mg/m², intravenously pumped, 2 hours; 5-FU 2800mg/m², arterial pumped, 46 hours; A course of treatment was performed every 3-4 weeks until the efficacy was evaluated with CR (mRECIST 1.1) or the occurrence of Child-Pugh grade C liver function, distant metastasis and intolerable adverse reactions. Relevant indicators were summarized and analyzed as well as abdominal enhanced MRI to evaluate the surgical efficacy, complications and follow-up

Results All 32 patients received 149 HAIC treatments, with a success rate of 100% and no serious complications occurred after surgery. Complete response (CR) in 7 cases, partial response (PR) in 16 cases, stable disease (SD) in 7 cases, disease progression (PD) in 2 cases, ORR: 71.88%, DCR: 93.75%.

Conclusion HAIC is a safe, feasible and effective for the treatment of advanced hepatocellular carcinoma with portal vein thrombus.

PU-039

Transcriptome-wide association study identifies key genes for Follicular lymphoma

Chunpu Li, Dongmei Guo
Qilu Hospital (Qingdao Campus), Shandong University

Purpose Follicular lymphoma (FL) is a common type of non-Hodgkin lymphoma. The first-degree relatives of FL patients have a higher risk of developing FL, suggesting a potential role for inherited factors. Although studies have reported the candidate gene and genome-wide about FL, the genetic basis remains unclear. This study aims to identify key genes and potential mechanisms that contribute to FL.

Materials and methods Transcriptome-wide association study (TWAS) of FL was performed by combining genome-wide association study (GWAS) obtained from FinnGen consortium, and pre-computed gene expression weights of lymphocytes and whole blood implemented in FUSION software. To validate our findings, we compared the candidate genes to differentially expressed genes (DEGs) from FL mRNA profiles in the Gene Expression Omnibus (GEO), GSE55267. Summary-data-based Mendelian Randomization (SMR) analyses were further performed to explore causal genes associated with FL. Finally, we used the “oncoPredict” R package according to the GDS C2 database to predict potential drug sensitivities.

Results TWAS identified total 718 genes, including 249 in lymphocytes, 567 in whole blood ($P < 0.05$), and 101 overlapping genes in different tissues. Validation of TWAS results by mRNA expression profiles of FL found 28 common genes. SMR was performed to verify that the expressions of HLA-J, ANKRD36BP2, and HLCS were significantly causally associated with FL (PFDR < 0.05). Furthermore, drug prediction analysis revealed specific drug sensitivities for ANKRD36BP2, highlighting potential therapeutic targets.

Conclusion This study provides novel insights into the genetic landscape of FL, identifying key genes and pathways that could aid in early diagnosis and targeted treatment.

PU-040

Study on the application value of transjugular intrahepatic portosystemic shunt in hepatocellular carcinoma complicated with portal hypertension

Baizhu Xiong, Changlong Hou, Weifu Lv, Zhengfeng Zhang

The First Affiliated Hospital of USTC, Division of Life Sciences and Medicine, University of Science and Technology of China

Purpose The purpose of this study was to retrospectively study the relevant clinical data of patients with hepatocellular carcinoma (HCC) associated with portal hypertension (PHT), and to comparatively analyze the clinical value of transjugular intrahepatic portosystemic shunt (TIPS) in the treatment of patients with HCC associated with PHT.

Materials and methods The patients with HCC combined with PHT were collected from May 2015 to May 2023 in our hospital. A total of 124 patients were enrolled after careful screening based on specific inclusion and exclusion criteria. Based on the treatment method for PHT, the patients were divided into two groups: the TIPS group (n = 61 cases), which received TIPS treatment, and the control group (n = 63 cases), which received symptomatic supportive treatment. During the hospital stay and follow-up review, relevant laboratory test indicators and imaging data were collected from all patients. The occurrence of complications such as exacerbation of ascites, rebleeding, hepatic encephalopathy (HE), and stent occlusion were recorded. The primary endpoints of the study include overall survival (OS) and complication-free survival (CFS), while the secondary observation indicators include the therapeutic efficacy of TIPS and the response to HCC treatment.

Results The surgical success rate in the TIPS group was 100% (61/61), and the postoperative portal venous pressure was significantly reduced [(37.7 ± 6.3) cmH₂O vs. (20.0 ± 3.9) cmH₂O, $P < 0.05$]. One month after treatment, the TIPS group had a significantly lower incidence of ascites compared to the control group ($P < 0.001$). There was no statistically significant difference in the rebleeding rate between the two groups ($P = 0.115$), but the incidence of HE was significantly higher in the TIPS group than in the control group ($P = 0.015$). After three months of treatment, the TIPS group showed significantly lower incidence of ascites and rebleeding rate compared to the control group ($P = 0.005$; $P = 0.014$). There was no significant difference in the incidence of HE between the two groups ($P = 0.721$). Six months after treatment, the TIPS group had lower incidence of ascites, rebleeding, and HE compared to the control group ($P < 0.001$; $P < 0.001$; $P = 0.027$). There was no statistically significant difference in the incidence of ascites between the two groups one year after treatment ($P = 0.174$), but the rebleeding rate and incidence of HE were lower in the TIPS group than in the control group ($P = 0.022$; $P = 0.022$). The OS of the TIPS group was significantly higher than that of the control group (mOS: 19.0 months vs mOS: 6.9 months), and the difference was statistically significant ($P < 0.001$). Similarly, the CFS of the TIPS group was significantly higher than that of the control group (mCFS: 11.0 months vs mCFS: 2.2 months), with a statistically significant difference ($P < 0.001$). When evaluating the efficacy of HCC treatment in the two groups, the DCR of the TIPS group was 86.9% compared to 77.8% in the control group. There was no statistically significant difference between the two groups ($P > 0.05$). However, the ORR in the TIPS group was 62.3%, which was significantly higher than the control group (ORR: 41.3%, $P = 0.019$).

Conclusion TIPS is safe and effective in treating patients with HCC combined with PHT. It can prolong complication-free survival, improve patients' quality of life, and reduce the incidence of PH

T complications. By alleviating the symptoms of portal hypertension in HCC patients, TIPS enables them to undergo tumor treatment and provides survival benefits to eligible patients.

PU-041

Prognostic Value of Tertiary Lymphoid Structures in Cryoablation Combined Immunotherapy for Soft Tissue Sarcoma

Juxing Cai, Baorang Zhu, Jing Li, Wuwei Yang
The Fifth Medical Center of PLA General Hospital

Purpose To investigate the predictive value of tertiary lymphoid structures (TLS) for prognosis in advanced soft tissue sarcoma (STS) patients treated with cryoablation combined with immunotherapy.

Materials and methods Forty-three STS patients undergoing cryoablation-immunotherapy between April 2020 and November 2024 were retrospectively enrolled. Multiplex immunofluorescence staining was employed to characterize intratumoral TLS and immune cell infiltration. Kaplan-Meier analysis and Cox proportional hazards models were applied to evaluate associations between TLS and progression-free survival (PFS).

Results TLS-positive patients (n=6) exhibited significantly prolonged PFS compared to TLS-negative counterparts (n=37) ($P=0.021$). Multivariate analysis identified TLS (HR=0.321, 95% CI: 0.110-0.936, $P=0.037$) and serum IL-2R levels (HR=1.001, 95% CI: 1.000-1.002, $P=0.020$) as independent prognostic factors.

Conclusion Intratumoral TLS may serve as a potential biomarker for predicting therapeutic outcomes in STS combination therapy, while elevated IL-2R indicates adverse prognosis. This study provides novel evidence for optimizing individualized treatment strategies in STS and is the first to demonstrate the prognostic significance of TLS in cryoablation-immunotherapy synergy, offering new directions for precision oncology.

PU-042

Short-term Prognostic Value of Ultrasound-based Radiomics Model for Liver Cancer Patients with Radiofrequency Ablation Therapy

Wei Xiang, Xin Gao, Xiao-Li Zhu

1. The First Affiliated Hospital of Soochow University 2. Municipal Hospital Affiliated to Taizhou University

Purpose To explore short-term prognostic value of an ultrasound-based radiomics model for liver cancer patients with radiofrequency ablation therapy.

Materials and methods 220 liver cancer patients who underwent radiofrequency ablation therapy in our hospital between January 2022 and December 2023 were retrospectively selected. Patients were divided into a modeling group (n=165) and a validation group (n=55) at a ratio of 3:1. Based on the short-term prognosis of the patients, the modeling group was further divided into a good prognosis group (n=115) and a poor prognosis group (n=50). Univariate and multivariate Logistic regression analyses were conducted to identify the factors influencing the short-term prognosis of liver cancer patients undergoing radiofrequency ablation therapy. A model was established with the R language, and the model was evaluated through receiver operating characteristic (ROC) curves and Hosmer-Lemeshow (H-L) goodness-of-fit tests.

Results There were no statistically significant differences ($P>0.05$) in the general data between the modeling group and the validation group. In the modeling group, comparisons of patient age, BMI, gender, liver cirrhosis, tumor location, vascular invasion, tumor number, and RI showed no statistically significant differences ($P>0.05$). However, comparisons of tumor diameter, tumor echo, portal vein thrombus, blood flow signal, and Vmax showed statistically significant differences ($P<0.05$). The results of the multivariate Logistic regression analysis indicated that tumor diameter, tumor echo, portal vein thrombus, blood flow signal, and Vmax were independent influencing factors for the short-term prognosis of liver cancer patients undergoing radiofrequency ablation therapy ($P<0.05$). The combined detection factor model expression was $\text{Logit}(P) = \beta \text{constant term} + \beta_1 X_1 + \beta_2 X_2 + \beta_3 X_3 + \beta_4 X_4 + \beta_5 X_5$. The model showed good consistency between predicted efficacy and actual risk with calibration curve slopes close to 1 in both the training and validation sets. The ROC analysis results demonstrated an area under the curve of 0.979 in the modeling group and 0.837 in the validation group for predicting the short-term prognosis of liver cancer patients undergoing radiofrequency ablation therapy. Decision curve analysis (DCA) curve was plotted to evaluate the clinical utility of the model, indicating a significant net benefit and good clinical utility.

Conclusion An ultrasound-based radiomics model for predicting the short-term prognosis of liver cancer patients undergoing radiofrequency ablation therapy has been successfully established and validated.

PU-043

Increment of Skeletal Muscle Mass Predicts Survival Benefit for Hepatocellular Carcinoma Treated with Transarterial Chemoembolization Combining Molecular Targeted Agents and Immune Checkpoint Inhibitors

Wen Chen

The First Affiliated Hospital with Nanjing Medical University

Purpose

To assess the relationship between clinical prognosis and changes of skeletal muscle mass for unresectable hepatocellular carcinoma (uHCC) patients who received transarterial chemoembolization (TACE) with molecular targeted agents and immune checkpoint inhibitors (TACE-MTAs-ICIs).

Materials and methods This is a retrospective, cross-sectional study conducted in a single-center. The study protocol was also approved by the Ethics Committee of our institution. This study was approved by the local institutional ethics review board of the Ethics Committee of the First Affiliated Hospital with Nanjing Medical University (ethical review no. 2024-SR-518). Written informed consent was not required for this retrospective study. The data of this study are available from the author upon rational request. Data at CT were obtained at baseline (1 month prior to treatment), 6 months after treatment (5-7 months). Quantifying skeletal muscle and subcutaneous fat at the L3 vertebra was based on CT images obtained for each patient. Skeletal muscle area (SMA) and subcutaneous fat area (SFA) were delineated by density thresholds ranging from -29 to 150 Hounsfield Unit (HU) and -190 to -30 HU, respectively (22). Additionally, the regions of interest were manually corrected as needed. Images were analyzed by two trained observers (each over 5 years of clinical experience in CT scanning and image postprocessing) by using software (MAGN ETOM Skyra; Siemens Healthcare, Erlangen, Germany). SMI is defined as SMA at the L3 level normalized by the square of height.

Results The median OS in the muscle gain group was significantly longer than that in the non-muscle gain group (Not reach vs. 25.2 months, $P < 0.001$). The median PFS did not reach significant between two groups (16.2 vs. 9.1 months, $P = 0.101$). Multivariate analyses revealed that skeletal muscle gain (HR = 0.20; 95% CI, 0.06–0.68; $P = 0.010$) and Barcelona Clinic Liver Cancer stage (HR = 1.94; 95% CI, 1.02–3.69; $P = 0.044$) were independent prognostic factors for OS.

Conclusion SMI increment appeared as a favorable predictor for these uHCC patients who received TACE-MTAs-ICIs therapy.

PU-044

Clinical study on hepatitis B virus reactivation following transarterial chemoembolization combined with targeted immunotherapy for hepatocellular carcinomas

Jinpeng Li
Shandong Cancer Hospital and Institute

Purpose To evaluate risk factors for hepatitis B virus (HBV) reactivation in hepatocellular carcinoma patients receiving transarterial chemoembolization (TACE) combined with targeted immunotherapy, and to analyze the impact of viral reactivation on clinical indicators.

Materials and methods We analyzed data from 100 HBV-related hepatocellular carcinoma patients who received TACE combined with targeted immunotherapy between January 2022 and December 2023. Baseline demographic characteristics and laboratory indicators were assessed for their association with HBV reactivation, and changes in related indicators after treatment were tracked.

Results Among the 100 patients receiving combination therapy, nearly 23.2% (23 cases) experienced HBV reactivation. Multivariate analysis showed that baseline HBV-DNA levels below 1000 copies/mL were associated with significantly lower risk of viral reactivation ($P < 0.05$). After treatment, the reactivation group and non-reactivation group showed significant differences in the magnitude of aspartate aminotransferase (AST) elevation and albumin (ALB) reduction ($P < 0.05$), while differences in changes in alanine aminotransferase (ALT), total bilirubin (TBIL), and prothrombin time (PT) were not statistically significant ($P > 0.05$).

Conclusion TACE combined with targeted immunotherapy can trigger HBV reactivation in patients with HBV-related hepatocellular carcinoma, with higher risk in patients with high pre-treatment viral loads. Patients with reactivation typically present with significant increases in AST and decreases in ALB. In clinical practice, enhanced monitoring and preventive measures should be implemented for patients with high pre-treatment HBV-DNA loads to reduce the risk of viral reactivation.

PU-045

Hepatoprotective Effects and Efficacy of Donafenib Combined with Transarterial Chemoembolization in the Treatment of Unresectable Hepatocellular Carcinoma

Jinpeng Li

Shandong Cancer Hospital and Institute, Shandong First Medical University and Shandong Academy of Medical Sciences

Purpose The efficacy of donafenib in combination with transarterial chemoembolization (TACE) has been established for unresectable hepatocellular carcinoma (HCC). However, its effects on liver function preservation remain unclear. This study aimed to evaluate the hepatoprotective effects and safety profile of this combination therapy through a comprehensive analysis of albumin–bilirubin (ALBI) score modifications.

Materials and methods This study enrolled 36 patients with unresectable HCC who received donafenib + TACE, either with or without immune checkpoint inhibitors. ALBI scores were evaluated throughout the study, starting with baseline measurements and continuing at predetermined intervals during the treatment course. Statistical analyses were conducted to examine the associations between ALBI grade modifications, tumor response, and survival outcomes.

Results A prospective analysis of 36 patients receiving donafenib + TACE revealed significant antitumor efficacy and favorable hepatic safety profiles. The therapeutic regimen achieved objective response and disease control rates of 69.4% and 91.7%, respectively, with a median progression-free survival of 10.7 months. The median time to response was 1.4 months, indicating rapid therapeutic onset. Hepatic function remained stable throughout the treatment, as evidenced by consistent ALBI score from baseline to progression/final follow-up (-2.41 ± 0.41 vs. -2.45 ± 0.52 , $P = 0.67$). Among the cohort, 58.3% maintained stable hepatic function, whereas 25.0% exhibited improvement from ALBI grade 2 to 1. Treatment response analysis revealed that hepatic function deterioration occurred less frequently in responders than in nonresponders (12.0% vs. 27.3%). ALBI score modification was identified as a potential predictive biomarker (AUC = 0.665), with patients having scores below the -0.177 threshold achieving superior clinical outcomes, including higher response rates (84.6% vs. 56.5%) and longer progression-free survival (not reached vs. 5.63 months, $P = 0.017$). These findings establish hepatic function preservation as a safety indicator and efficacy predictor of donafenib + TACE.

Conclusion The combination of donafenib and TACE demonstrates favorable hepatic function preservation while maintaining therapeutic efficacy. ALBI score improvement is correlated with enhanced treatment response and survival outcomes, indicating potential synergistic benefits for tumor control and hepatic function preservation.

PU-046

TLR-9 Agonist Combined with PD-1 Inhibitor Enhances Cryoablation-Induced Anti-Tumor Immune Response in a Murine Hepatocellular Carcinoma Model

Liang Yin
the Second Affiliated Hospital of Soochow University

Purpose Substantial evidence has demonstrated that cryoablation can induce tumor-specific T-cell immune responses in vivo. While the combination of cryoablation with PD-1 inhibitors has been shown to ameliorate the immunosuppressive tumor microenvironment, the synergistic efficacy remains suboptimal. In this study, we evaluated dynamic changes in the tumor immune microenvironment (TIME) of distant tumor tissues following cryoablation when combined with a TLR-9 agonist and PD-1 inhibitor.

Materials and methods A bilateral hepatocellular carcinoma model was established in mice. Post-cryoablation, TLR-9 agonist and PD-1 inhibitor were administered concurrently. Temporal changes in immune cell populations and cytokine profiles were analyzed at designated timepoints. Quantification of antigen-presenting cells, T lymphocytes, and other immune subsets in contralateral tumors, spleen, and inguinal lymph nodes was performed, alongside tumor volume measurements.

Results The combination of TLR-9 agonist and PD-1 inhibitor post-cryoablation significantly increased dendritic cell (DC) and T lymphocyte infiltration, reduced immunosuppressive cell populations, and induced remarkable tumor volume reduction. These findings confirm a synergistic anti-tumor effect in murine hepatocellular carcinoma models.

Conclusion TLR-9 agonist combined with PD-1 inhibitor synergistically enhances cryoablation-induced anti-tumor immunity. This study provides a theoretical foundation for the clinical application of TLR-9 agonist and PD-1 inhibitor combination therapy following cryoablation in patients with primary hepatocellular carcinoma.

PU-047

Multidisciplinary Management of Malignant Carotid Body Tumor with Preoperative Embolization and Adjuvant Radiotherapy: A Case Report

Yuheng Yang

Chongqing University Affiliated Cancer Hospital

Purpose To investigate the clinical characteristics, comprehensive treatment strategies, and outcomes of a malignant carotid body tumor (MCBT) in a patient with a history of breast cancer, emphasizing the role of multidisciplinary management and long-term follow-up.

Materials and methods A 49-year-old female with a history of left breast cancer (pT2N0M0, luminal type, Her-2 positive) presented with an asymptomatic neck mass during routine follow-up. Diagnostic evaluations included ultrasound, computed tomography (CT), angiography, and immunohistochemical analysis. The tumor was classified as Shamblin II based on imaging and surgical findings. Preoperative embolization was performed to reduce tumor vascularity. Surgical resection with lymph node dissection was conducted, followed by adjuvant radiotherapy (VMAT 6MV-X, 54 Gy/27F to the tumor bed and 48.6Gy/27F to lymphatic drainage areas). Postoperative follow-up included imaging and clinical assessments.

Results Imaging revealed a 2.7×2×1.8 cm mass at the left carotid bifurcation with arterial enhancement and encasement of carotid arteries. Histopathology confirmed a metastatic paraganglioma with lymph node involvement (positive for Syn, CgA, CD56; SDHB mutation not tested). Postoperative outcomes showed no residual tumor, preserved carotid artery patency, and no recurrence at 6 months. Liver function abnormalities (ALT 105.1 U/L, AST 82.1 U/L) and comorbidities (hypertension, fatty liver, gallbladder stones) were managed clinically.

Conclusion MCBT, though rare, requires early suspicion and multidisciplinary care. Surgical resection remains the gold standard, augmented by preoperative embolization to minimize blood loss. Lymph node dissection is critical for staging, and adjuvant radiotherapy may improve local control. Long-term surveillance for metastasis is essential, particularly in patients with SDHx mutations. This case highlights the importance of integrating oncologic and vascular expertise in managing complex tumors.

PU-048

TACE combined with the intra-arterial infusion of bevacizumab for BCLC-stage B hepatocellular carcinoma beyond up-to-seven Criteria: A prospective, single-arm, phase II study.

Fei Gao, Lijie Qiu
Sun Yat-sen University Cancer Center

Purpose TACE is recommended as the standard of care for patients with BCLC-B stage hepatocellular carcinoma (HCC). However, the BCLC-B stage HCC is a very heterogeneous disease, especially for patients beyond the up-to-seven criteria. The prognosis shows great diversity depending on the treatment strategy. TACE combined with the anti-VEGF antibody therapy improves the clinical prognosis of patients and gains survival benefits. Intra-arterial infusion of bevacizumab has not been evaluated previously. This study aimed to evaluate the safety and efficacy of TACE combined with intra-arterial infusion of bevacizumab for BCLC-B-stage HCC beyond up-to-seven criteria.

Materials and methods This prospective single-arm phase II study recruited five patients with HCC. The main inclusion criteria: a confirmed HCC based on the ALSD with either pathological or imaging findings; aged ≥ 18 years; Barcelona Clinic Liver Cancer (BCLC) stage B and sum of the number of tumors and the largest tumor diameter (cm) exceeding 7; no previous systemic/locoregional anticancer treatment; Child-Pugh score ≤ 7 . Patients were treated with TACE (30-40mg of pirarubicin, 30-40mg of lobaplatin, and lipiodol) plus Bevacizumab (15mg/kg, intra-arterial infusion, d1, Q3W) for four cycles, followed by maintenance therapy with Bevacizumab (15mg/kg, intravenously, d1, Q3W) to a maximum total cycle of eighteen unless any evidence of disease progression or unacceptable side effects. The primary endpoint was objective response rate (ORR) (assessed with mRECIST v1.1). The secondary endpoints included overall survival (OS), progression-free survival (PFS), disease control rate (DCR), time to progress (TTP), duration of response (DOR), and safety. Drug safety was investigated according to CTCAE (version 5.0).

Results From March 2023 to April 2024, 5 patients with a median age of 69 years (range: 51-72) were enrolled. There were 4 (80%) patients with HBV infection, and 4 (80%) patients were classified as Child-Pugh A class. The ORR was 60% with 3 PR and 1 PD. The median follow-up was 14.0 months (95%CI, 5.7-22.4) and the median PFS was 5.7 months (0.4-10.9). The median OS was not reached. Adverse events included grade 2 hypertension (1 case) and mild gingival bleeding (1 case). There were no treatment-related serious adverse events.

Conclusion TACE combined with arterial infusion of bevacizumab in patients with BCLC-B stage HCC beyond up-to-seven criteria demonstrates promise as an effective treatment approach.

PU-049

TACE combined with sintilimab and bevacizumab in the treatment of advanced hepatocellular carcinoma: a phase 2 study

Fei Gao, Mu Maoyuan
Sun Yat-sen University Cancer Center

Purpose This phase 2 study aimed to evaluate the efficacy, feasibility, and safety of TACE combined with sintilimab and bevacizumab in advanced HCC, including a novel strategy featuring four cycles of intra-arterial administration of sintilimab with reduced-dose bevacizumab.

Materials and methods This study enrolled adult patients with advanced HCC who had not received anti-tumor treatment. All patients underwent on-demand conventional TACE, using a mixture of pirarubicin (30-40 mg), lobaplatin (30-40 mg), and lipiodol (5-15 ml). Concurrently, during the first four cycles, patients received intra-arterial infusions of sintilimab 200 mg and reduced-dose bevacizumab 7.5 mg/kg, administered once every three weeks. For subsequent maintenance therapy, patients received intravenous infusions of sintilimab 200 mg and bevacizumab 15 mg/kg, administered once every three weeks. The primary endpoint was the ORR, while secondary endpoints included OS, PFS, DCR, and safety.

Results A total of 34 patients were enrolled in this study, with a median age of 53 years (IQR 45-59); 33 were male and 1 was female. The median follow-up duration was 10.3 months (IQR 5.8-15.6). According to the mRECIST criteria, the ORR was 70.6%, with 7 patients achieving CR and 17 achieving PR. The DCR was 85.3%. The median PFS was 6.0 months (95% CI 4.8 - not reached), and the median OS was 12.2 months (95% CI 9.3 - not reached). Common TRAEs of any grade included elevated liver enzymes (30%), post-embolization syndrome (14.7%), and hypertension (11.8%). Grade 3 or higher TRAEs included hypertension (2.9%) and gastrointestinal bleeding (8.8%). No serious treatment-related adverse events or deaths were observed.

Conclusion The combination of TACE with sintilimab and bevacizumab demonstrates a favorable ORR and manageable safety profile in patients with advanced HCC. Arterial administration of a reduced dose of bevacizumab appears to mitigate toxic effects.

Tumor-Targeted FABP5/STING Cascade Multimodal Nanoreactor Promote Radiofrequency Ablation Induced Ferroptosis and Intratumoral Immune Rewiring in Hepatocellular Carcinoma

Jiansong Ji^{1,2,3}, Bufu Tang^{1,5}, Xiaojie Zhang¹, Yiting Sun⁴, Jinhua Luo¹, Qiaoyou Weng^{1,2,3}, Cong Zhang³, Zilin Wang³, Shiji Fang^{1,2}, Yangrui Xiao^{1,2}, Liyun Zheng^{1,2}, Jianfei Tu^{1,2}, Rongfang Qiu^{1,2}, Yang Yang^{1,2}, Zhongwei Zhao^{1,2}, Weiqian Chen^{1,2,3}, Minjiang Chen^{1,2,3}

1. Zhejiang Key Laboratory of Imaging and Interventional Medicine, Zhejiang Engineering Research Center of Interventional Medicine Engineering and Biotechnology, The Fifth Affiliated Hospital of Wenzhou Medical University, Lishui, Zhejiang, 323000, China. (2) Department of Radiation Oncology, Zhongshan Hospital, Fudan University, Shanghai, 200032, China.

2. Key Laboratory of Precision Medicine of Lishui City, Department of Radiology, Lishui Central Hospital, Lishui, 323000, China.

3. Department of Radiology, Lishui Hospital, School of Medicine, Zhejiang University, Hangzhou, 310000, China.

4. China Medical University, Shenyang 110122, China

5. Department of Radiation Oncology, Zhongshan Hospital, Fudan University, Shanghai, 200032, China.

Purpose

Radiofrequency ablation (RFA) has emerged as a critical therapeutic modality for hepatocellular carcinoma (HCC). Biomimetic magnetic nanoparticles further augment RFA efficacy by enhancing targeting precision and biocompatibility. This study introduces a novel nanocarrier co-delivery system aimed at key molecular targets in HCC to amplify ferroptosis and reprogram intratumoral immunity, thereby improving the therapeutic outcomes of RFA.

Materials and methods The proposed nanocarrier integrates cyclic arginine-glycine-aspartic acid (cRGD) and red blood cell membrane (RBCM), encapsulating superparamagnetic iron oxide (SPIO) to specifically target fatty acid-binding protein 5 (FABP5) in tumor cells. Leveraging the superparamagnetic properties of SPIO, these nanoparticles enable real-time monitoring and tracking through MRI. In vitro heat treatment of HCC cells simulated the RFA environment, while experiments employing the ferroptosis inhibitor Lipro1 conclusively demonstrated that the nanocarrier exerts antitumor effects primarily through ferroptosis induction. Additionally, the impact on immunotherapy was underscored by combining the nanocarrier with anti-PD-L1 monoclonal antibodies.

Results FABP5 overexpression in HCC tissues is strongly linked to RFA response. Targeting FABP5 using co-delivery nanocarriers significantly enhances RFA efficacy. Furthermore, FABP5 deletion potentiates RFA-induced ferroptosis and bolsters anti-tumor immune responses, characterized by increased infiltration of CD8⁺ T cells and effector memory T cells, contributing to pronounced systemic anti-tumor effects. Mechanistically, FABP5 inhibition activates the STING/TBK1 signaling pathway and modulates TBK1 protein stability. Notably, the nanocarrier system targeting FABP5 elevates PD-L1 expression, and the combination of RFA with anti-PD-L1 therapy demonstrates synergistic efficacy against HCC.

Conclusion In conclusion, the FABP5-targeting nanocarrier co-delivery system offers a promising strategy to enhance RFA effectiveness in HCC, providing a novel framework for advancing clinical treatment approaches.

PU-051

Association of the pretreatment lung immune prognostic index with immune checkpoint inhibitor outcomes in patients with advanced hepatocellular carcinoma

Tao Sun, Changlong Hou

the First Affiliated Hospital of the University of Science and Technology of China (USTC)

Purpose To evaluate whether the pretreatment Lung Immune Prognostic Index (LIPI) is associated with outcomes in advanced hepatocellular carcinoma (HCC) patients under ICI.

Materials and methods A two-center retrospective study of patients with HCC treated with immune checkpoint inhibitors (ICIs) between January 2018 and January 2021 was performed. Based on pretreatment derived neutrophils/ (leukocytes minus neutrophils) ratio (dNLR) greater than 3 and a lactate dehydrogenase (LDH) level greater than the normal value, patients were stratified into three groups (good LIPI: 0 risk factor, intermediate LIPI: 1 risk factor, and poor LIPI: 2 risk factors). The primary endpoints were overall survival (OS) and progression-free survival (PFS). The second endpoints were disease control rate (DCR) and objective response rate (ORR).

Results In the pooled cohort (n=224), 80 (35.7%) had a good LIPI (zero factor), 91 (40.6%) had intermediate LIPI (one factor), and 53 (23.7%) had poor LIPI (two factors). The median follow-up was 25.1 months. Median OS was 16.8 months, 12.5 months, and 9.5 months for the good, intermediate, and poor LIPI groups, respectively ($P < 0.0001$). Median PFS was 11.8 months, 7.8 months, and 4.0 months for the good, intermediate, and poor LIPI groups, respectively ($P < 0.0001$). Multivariate analysis indicated that the intermediate LIPI and poor LIPI both were independently associated with OS, PFS, and ORR, DCR ($P < 0.05$), as risk factors.

Conclusion Pretreatment LIPI was correlated with worse outcomes for ICIs suggesting that LIPI could be promising biomarker for advanced HCC patients under ICIs.

PU-052

Efficacy and safety of chemotherapy combined with iodine-125 seed brachytherapy for intermediate and advanced oncogenic driver gene-negative non-small cell lung cancer

Meng-Hua Xia, Wei-Fu Lv

The First Affiliated Hospital of University of Science and Technology of China (USTC), Division of Life Sciences and Medicine, University of Science and Technology, Hefei, Anhui,

Purpose To compare the effectiveness and safety of CT-guided iodine-125 seed brachytherapy in conjunction with chemotherapy against chemotherapy alone for the management of intermediate and advanced non-small cell lung cancer (NSCLC) lacking oncogenic driving genes.

Materials and methods Retrospective analysis was conducted on clinical data from 128 patients diagnosed with intermediate and advanced non-small cell lung cancer who received iodine-125 combined with chemotherapy or chemotherapy alone due to the absence of oncogenic driver gene mutations. The patients in two groups were compared at 6-month follow-up for objective remission rate (ORR), Disease control rate (DCR), local progression-free survival (LPFS), overall survival (OS), clinical symptom improvement, and adverse events.

Results A median of 47 (range, 16–100) iodine-125 seeds were implanted. The median D90 was 139.4 Gy. In patients with stage III NSCLC, the 6-month ORR were 40.0% and 8.0% in two groups, while those with stage IV NSCLC had rates of 20.9% and 4.0%. No significant issues arose during the 5–58 months follow-up period. OS did not significantly differ between stage III and IV NSCLC patients. The LPFS for stage III patients was 14 months and 9 months, compared to 8 months and 7 months for stage IV patients. Symptom improvement rates, including cough, chest discomfort, hemoptysis, and chest constriction, were 87.2% versus 20.4%, 77.8% versus 33.3%, and 77.8% versus 26.1%, respectively.

Conclusion CT-guided iodine-125 seed implantation with chemotherapy failed to improve OS in stages III and IV NSCLC. However, it did extend the LPFS of stage III NSCLC. Furthermore, the ORR was much higher than that of the chemotherapy-only group, and lung cancer clinical symptoms were significantly reduced, improving patient quality of life. © 2024 American Brachytherapy Society. Published by Elsevier Inc. All rights are reserved, including those for text and data mining, AI training, and similar technologies.

PU-053

In vitro characteristics of Epirubicin supported thermosensitive liquid embolist

Yuqing Xu^{1,2,3}, Haipeng Yu^{1,2,3}, Li Wang^{1,2,3}, Hao Qin^{1,2,3}, Mei Li^{1,2,3}

1. Tianjin Medical University Cancer Institute & Hospital, National Clinical Research Center for Cancer

2. Tianjin's Clinical Research Center for Cancer

3. Tianjin Key Laboratory of Digestive Cancer

Purpose To study the drug loading and release rate of epirubicin-supported thermal embolist in vitro.

Materials and methods The drug loading capacity and stability of epirubicin supported thermosensitive embolic agent with or without iodopropylamine were determined by high performance liquid chromatography. The drug release rate of thermosensitive embolic agent at different time points was determined by the same method.

Results For Epirubicin supported thermal embolist without iodopropylamine, the average loading rate was (0.78 ± 0.02) mg and the loading rate was (16.1 ± 0.35) % after membrane filtration, while the average loading rate was (0.73 ± 0.06) mg and the loading rate was (15.07 ± 1.17) % without membrane. After adding iodopropylamine, the drug loading of 0 h to 24 h solution was measured, and the drug loading was calculated indirectly, and the conclusion was drawn that the drug loading of heat sensitive embolic agent decreased or disappeared. The sustained release rate of epirubicin 0-48 h was 42.65%.

Conclusion Epirubicin can be successfully loaded into the heat-sensitive embolus with good stability and slow release. After adding iodopropylamine, the drug loading of the heat-sensitive embolic agent decreased or disappeared.

PU-054

Comparative analysis of bile culture and blood culture in patients with malignant biliary obstruction complicated with biliary tract infection

Yuqing Xu ^{1,2,3}, Haipeng Yu ^{1,2,3}, Li Wang ^{1,2,3}, Hao Qin ^{1,2,3}, Mei Li ^{1,2,3}

1. Tianjin Medical University Cancer Institute & Hospital, National Clinical Research Center for Cancer

2. Tianjin's Clinical Research Center for Cancer

3. Tianjin Key Laboratory of Digestive Cancer

Purpose This study aims to provide clinical basis for the identification and treatment of malignant biliary obstruction (MBO) with biliary tract infection by comparing the pathogenic bacteria and blood cultures in these patients.

Materials and methods A total of 380 MBO patients who underwent percutaneous biliary drainage between January 2004 and January 2019 were enrolled in this study. A total of 90 patients were diagnosed with MBO combined with biliary tract infection, and bile and blood culture were performed in these patients. The patients included 58 men and 32 women, ranging in age from 33 to 86 years, with an average age of 60.69 years.

Results The detection rate of biliary bacteria culture in MBO patients with biliary tract infection was significantly higher than that in blood culture, and the results of positive biliary culture and blood culture were significantly different in the same patient. Gram-positive bacteria dominated in the bile culture and Gram-negative bacteria dominated in the blood culture. Therefore, for patients with MBO complicated with biliary tract infection, especially severe or critically ill patients, it is necessary to perform both bile bacterial culture and blood culture.

Conclusion In patients with MBO complicated with biliary tract infection, it is important to perform both bile bacterial culture and blood culture. Existing guidelines for the diagnosis and treatment of benign biliary tract infections do not apply to patients with MBO complicated by biliary tract infections.

PU-055

MCM4 in human hepatocellular carcinoma: a potent prognostic factor associated with cell proliferation

Yuqing Xu ^{1,2,3}, Haipeng Yu ^{1,2,3}, Li Wang ^{1,2,3}, Hao Qin ^{1,2,3}, Mei Li ^{1,2,3}

1. Tianjin Medical University Cancer Institute & Hospital, National Clinical Research Center for Cancer

2. Tianjin's Clinical Research Center for Cancer

3. Tianjin Key Laboratory of Digestive Cancer

Purpose Hepatocellular carcinoma (HCC) remains a major medical problem. MCM4 is a constituent member of a family of small chromosomal proteins that reportedly play a crucial role in cancer malignancy behavior. However, the function of MCM4 in HCC remains largely unknown. **Objective:** To investigate the specific role of MCM4 in HCC.

Materials and methods A series of in vivo and in vitro experiments were conducted to investigate the function of MCM4 in HCC tumor cells.

Results Data from public datasets such as TCGA and GTEx show that MCM4 is overexpressed in HCC and is significantly associated with poor prognosis. Immunohistochemical results of 102 HCC patients showed that the high level of MCM4 expression was correlated with tumor size. A series of in vivo and in vitro experiments were then conducted to investigate the function of MCM4 in HCC tumor cells. MCM4 silencing inhibited cell proliferation and spheroid formation of hepatocellular carcinoma cells. In addition, silencing MCM4 significantly reduced tumor growth in xenograft tumor models.

Conclusion In summary, the results of this study suggest that MCM4 is a potential prognostic predictor associated with poor outcomes in HCC patients, and even a therapeutic target for HCC.

PU-056

In vivo immune response induced by cryoablation of mouse H22 hepatoma cell line

Yuqing Xu^{1,2,3}, Haipeng Yu^{1,2,3}, Li Wang^{1,2,3}, Hao Qin^{1,2,3}, Mei Li^{1,2,3}

1. Tianjin Medical University Cancer Institute & Hospital, National Clinical Research Center for Cancer

2. Tianjin's Clinical Research Center for Cancer

3. Tianjin Key Laboratory of Digestive Cancer

Purpose To study the immune response induced by cryoablation on H22 cells in vivo.

Materials and methods H22 cells were implanted subcutaneously in adult BALB/c mice. All subjects were randomly assigned to one of three groups: Group A (sham surgery), Group B (cryoablation), and group C (cryoablation plus Freund adjuvant). The animals were killed 1, 2 and 3 weeks after treatment, and serum IFN- γ , IL-4, spleen Th1/Th2 and cytotoxicity were detected.

Results Compared with group A, INF- γ was higher in group B, but IL-4 was lower. These effects were enhanced by cryoablation and Freund adjuvant. Th1/Th2 was significantly elevated in group B and Group C. At the 7th, 14th and 21st day, H22 cells in group B and group C had strong cytolytic activity.

Conclusion Our study shows that the expression of Th1 and IFN- γ is significantly changed after cryoablation, which has an immunostimulating effect on mouse H22 hepatoma cells.

PU-057

Analysis of clinicopathological and prognostic factors in 106 patients younger than 55 years of age with prostate cancer: a Chinese single-center study

Yuqing Xu^{1,2,3}, Haipeng Yu^{1,2,3}, Li Wang^{1,2,3}, Hao Qin^{1,2,3}, Mei Li^{1,2,3}

1. Tianjin Medical University Cancer Institute & Hospital, National Clinical Research Center for Cancer

2. Tianjin's Clinical Research Center for Cancer

3. Tianjin Key Laboratory of Digestive Cancer

Purpose Patients with early-onset prostate cancer (age ≤ 55 years) in Western countries have been well described in previous studies. However, the clinicopathological and prognostic characteristics of patients with early-onset prostate cancer in China have not been evaluated. The objective of this study was to investigate the clinicopathological and prognostic factors of prostate cancer in Chinese single-center patients aged 55 years or less.

Materials and methods 106 patients with prostate cancer aged less than 55 years old and complete clinicopathological data were selected from our hospital from January 2000 to June 2014. Survival was studied by Kaplan-Meier analysis, and prognostic factors were studied by univariate and multivariate analysis.

Results The median time from onset to diagnosis was 3.5 months (range: 2-55 months). The median time from endocrine therapy to development of androgen-independent prostate cancer was 10.5 months. A total of 54 patients died (50.9%), of which 96.2% died from prostate cancer. The overall survival rates at 1, 3 and 5 years were 88.7%, 66.2% and 36.0%, respectively. Univariate and multivariate analysis showed that T stage, visceral metastasis, pathological type and Gleason score were independent prognostic factors.

Conclusion Prostate cancer patients under 55 years old in China are easy to be missed or misdiagnosed, and the pathological types of patients in this age group are complicated and the degree of malignancy is high. Late stage, visceral metastasis, pathological type, and high Gleason score were independent prognostic factors. Combined treatment with local treatment was an effective treatment strategy.

PU-064

Hepatic Adverse Events of Novel Immunotherapy-Based Therapies in Clinical Trials: A Systematic Review and Meta-Analysis

Minyan Ye, Sha Huang
Fujian cancer hospital

Purpose The objective of this study is to evaluate whether the incorporation of novel immunotherapies that targeting costimulatory molecules or coinhibitory pathways, beyond traditional treatments involving PD-1, PD-L1, and CTLA-4, increases the incidence of hepatic adverse events. Additionally, we investigate the occurrence rates of liver-related adverse events in cancer patients undergoing novel immunotherapies and combination therapies based on these treatments.

Materials and methods A comprehensive literature search was conducted across PubMed, Embase, Cochrane Library, and Web of Science databases for clinical studies involving cancer patients treated with immunotherapies that targeting LAG-3, TIGIT, TIM-3, PVRIG, CD112R, VISTA, BTNL2, BTN3A1, BTN2A1, BTLA, NKG2A, CD47, 4-1BB, CD137, OX40, TNFRSF4, CD134, ICOS, CD278, CD40, D28, CD27, GITR, and B7-H3.

Results The search yielded 63 studies reporting on treatment-related or immune-related hepatic adverse events up to May 1, 2024, encompassing a total of 7,327 patients. The analyzed studies included agents targeting LAG-3, TIGIT, TIM-3, CD47, NKG2A, 4-1BB, OX40, ICOS, CD27-CD70, GITR, CD40, and B7-H3. Notably, in the 6 randomized controlled trials assessed, the addition of LAG-3 or TIGIT inhibitors to traditional antitumor therapies did not result in a higher incidence of elevated ALT, AST, ALP, GGT levels, or hepatitis. CD27-CD70-targeted antitumor treatments was most frequently associated with elevated transaminase levels in monotherapy. Among dual immunotherapy combinations, the most common cause of any-grade transaminase elevation involved the combination of 4-1BB agonists with PD-1/PD-L1 inhibitors; in contrast, high-grade elevations were notably seen with the CD40 agonist in conjunction with CTLA-4 inhibitors. Furthermore, the incidence of transaminase elevation when novel agents were used in combination with chemotherapy was greater than when combined with targeted therapies. The overall incidence of any-grade transaminase elevation ranged from 7.50% to 36.64%, while high-grade transaminase elevation occurred within the range of 0% to 17.83% during dual immunotherapy combined with targeted therapy or chemotherapy. Cholestatic enzymes elevations during monotherapy with immune agents are most commonly linked to anti-CD27-CD70 treatments. For new drug combinations with chemotherapy, the incidence of all-grade cholestatic enzyme elevations ranges from 3.33% to 21.93%, and high-grade elevations range from 1.90% to 20.18%.

Conclusion This study found that the addition of novel immunotherapy to traditional antitumor treatment does not increase hepatic toxicity. We provide a summary of the incidence rates of liver-related adverse events associated with novel immunotherapies and combination therapies, contributing valuable insights for treatment selection in cancer patients.

PU-065

Preoperative Risk Stratification for Early Recurrence of Solitary Hepatocellular Carcinoma by Integrating Clinical, Pathological, and MRI Findings

Jiake Hua, Chen Jun

Zhejiang Provincial People's Hospital (Affiliated People's Hospital), Hangzhou Medical College

Purpose To develop a risk stratification model incorporating clinical, pathological, and MRI findings for predicting early recurrence risk after liver resection (LR) in patients with solitary BCLC stage A hepatocellular carcinoma (HCC)

Materials and methods This study included 86 HCC patients who underwent LR at Zhejiang Provincial People's Hospital from January 2018 to December 2022. Inclusion criteria were: (1) pathologically confirmed primary HCC; (2) radical LR performed within one month after contrast-enhanced MRI; (3) no prior HCC-specific treatments (e.g., interventional therapy) before LR; and (4) complete clinical, pathological, and MRI data. Variables with $P < 0.1$ in univariate Cox regression analysis were included in multivariate Cox regression to evaluate factors influencing early HCC recurrence ($P < 0.05$ considered statistically significant). Risk stratification was subsequently performed.

Results Multivariate analysis revealed AST >40 U/L ($P = 0.009$), Ki-67 $>30\%$ ($P < 0.001$), tumor diameter >7 cm ($P = 0.008$), and hepatobiliary phase peritumoral hypointensity ($P = 0.020$) as independent risk factors. A prognostic scoring system was established based on these factors (1 point per positive indicator, 0 for negative), stratifying patients into low-risk (0 points, $n = 39$, 45.3%), intermediate-risk (1 point, $n = 30$, 38.4%), and high-risk (>1 point, $n = 17$, 16.3%) groups. The two-year recurrence-free survival (RFS) rates were 84.6%, 46.7%, and 17.6%, respectively ($P < 0.001$).

Conclusion This study developed a predictive model integrating clinical, pathological, and MRI findings for preoperative risk stratification of early recurrence in solitary HCC.

PU-072

Predictive model of unresectable hepatocellular carcinoma treated with TACE-HAIC combined with targeted drugs and immune checkpoint inhibitors.

Li-Nan Yin
Harbin Medical University Cancer Hospital

Purpose The combined treatment of transcatheter arterial chemoembolization (TACE) and hepatic arterial infusion chemotherapy (HAIC) with molecular targeted drugs and immune checkpoint inhibitors (ICIs) has shown efficacy in the management of unresectable hepatocellular carcinoma (HCC) and may offer significant survival benefits. However, not all patients benefit equally from this quadruple therapy [TACE-HAIC combined with molecular targeted drugs and ICIs], which underscores the need to establish a predictive model for assessing the prognosis of unresectable HCC patients following this treatment regimen.

Materials and methods This research involved a cohort of 135 patients who were diagnosed with liver cancer and received treatment at our hospital from April 2021 to December 2022, with the quadruple therapy regimen. Following this, they were randomly assigned to either a training group consisting of 98 patients or a validation group consisting of 37 patients, in a ratio of 7:3. We utilized a multivariate Cox regression analysis to carefully select significant variables from the training cohort, which were then combined to create a cutting-edge nomogram. Our predictive model underwent rigorous evaluation through calibration curves, the concordance index (C-index), and the area under the time-dependent receiver operating characteristic (tdAUC) curve to ensure its accuracy and reliability.

Results The median follow-up duration in this study was 13 months, during which 46 patients had died. A nomogram was constructed based on three factors in the training cohort: albumin-bilirubin grade, extrahepatic metastasis, and tumor size. The nomogram demonstrated a C-index of 0.749, significantly higher than traditional staging systems ($P < 0.05$), and exhibited higher tdAUC over time. The calibration curves indicated good consistency between predicted and actual outcomes. Using predefined cutoff values, patients were stratified into high-risk and low-risk groups based on their scores ($P < 0.05$). The survival rates of patients in the two groups showed a decreasing trend with increasing risk, as observed in the Kaplan-Meier curves.

Conclusion The establishment of a novel nomogram for patients undergoing quadruple therapy offers clinicians a fresh guidance strategy and provides support for further treatment regimens. It may also contribute to advancements in interventional therapies.

PU-073

Safety and efficacy of n-butyl α -cyanoacrylate in transcatheter arterial chemoembolization

Caihong YU, Juncheng Wan, Changyu Li, Chaoqiao Jin, Wei Zhang, Yongjie Zhou, Zhuoyang Fan, Yirou Zhou, Guowei Yang, Xudong Qu
Zhongshan Hospital, Fudan University

Purpose To evaluate the safety and efficacy of n-butyl α -cyanoacrylate (NBCA) combined with lipiodol in transarterial chemoembolization (TACE) as a potential conversion therapy for unresectable hepatocellular carcinoma (HCC).

Materials and methods This retrospective analysis was conducted using clinical data of patients with large, unresectable HCC who received TACE with NBCA between August and December 2022. Treatment efficacy was evaluated in terms of objective response rate (ORR), disease control rate (DCR), overall survival (OS), and conversion resection rate, and safety was evaluated by recording the incidence of complications.

Results Eleven patients with HCC were included. All patients successfully underwent TACE with NBCA. The ORR and DCR were 90.9 % (10/11) and 100 % (11/11), respectively. No serious adverse events occurred. As of the last follow-up, 7 patients survived, and 4 died. The OS rates at 6 months, 1 year, and 2 years after TACE were 100%, 72.7%, and 72.7%, respectively. The conversion resection rate was 63.6 % (7/11).

Conclusion TACE using NBCA combined with lipiodol is a safe and effective treatment for large, unresectable HCC. This approach demonstrates potential for improving tumor downstaging, achieving high response rates, and facilitating subsequent liver resection.

PU-074

Prognostic Nutritional Index Predicts Survival in Intermediate and Advanced Hepatocellular Carcinoma Treated with Hepatic Arterial Infusion Chemotherapy Combined with PD-(L)1 Inhibitors and Molecular Targeted Therapies

Weidong Wang, Haohuan Tang

The Affiliated Wuxi People's Hospital of Nanjing Medical University, Wuxi People's Hospital, Wuxi Medical Center, Nanjing Medical University

Purpose This study aimed to evaluate the predictive efficacy of the prognostic nutritional index (PNI) in patients with intermediate and advanced hepatocellular carcinoma (HCC) treated with a regimen consisting of hepatic arterial infusion chemotherapy (HAIC), PD-(L)1 inhibitors, and molecular targeted therapies (MTTs).

Materials and methods A retrospective analysis was performed on the data of 88 HCC patients received triple therapy between January 2020 and August 2022 at three medical centers. Univariate and multivariable analyses were conducted to assess the relationship between PNI and survival outcomes.

Results The median follow-up was 11.0 months (IQR: 8.0-17.0). The PNI cut-off value of 38.6 was determined using receiver operating characteristics (ROC) analysis. The median overall survival (OS) durations were 29.0 and 8.0 months in the high-PNI (≥ 38.6) and low-PNI (≤ 38.6) groups, respectively (HR = 0.306, 95% CI, 0.170-0.552, $P < 0.001$), and the median progression-free survival (PFS) durations were 16.0 and 6.0 months, respectively (HR = 0.521, 95% CI, 0.303-0.896, $P = 0.014$). A higher complete response rate was observed in the high-PNI group (17.5% vs. 3.2%, $P = 0.033$). The univariate and multivariable analyses revealed that a PNI of ≥ 38.6 had an independent influence on both median OS (HR = 0.296; 95% CI, 0.159-0.551, $P < 0.001$) and median PFS (HR = 0.560; 95% CI, 0.318-0.987, $P = 0.045$).

Conclusion The PNI is an objective and convenient tool that can potentially predict the prognosis of patients treated with HAIC-based triple therapy.

PU-077

Predicting the risk of radiation enteritis in cervical cancer patients using inflammatory markers through machine learning

Yanqing Li¹, Kaijun Jiang², Yaoxiong Xia¹, Yiqin Ai¹

1. Peking University Cancer Hospital Yunnan

2. Kunming University of Science and Technology

Purpose Radiation enteritis (RE) is a detrimental consequence associated with radical radiotherapy (RT) used in the management of cervical carcinoma (CC). However, the underlying rationale for considering inflammatory markers as a potential risk factor for RE remains unclear.

Materials and methods A total of 228 patients diagnosed with cervical squamous cell carcinoma of stage IB-IIIB and undergoing radical RT were included in the study. The LASSO method was utilized to identify crucial features associated with RE. Clinical characteristics and inflammatory markers pre/post-treatment were used to develop five machine learning models, comprising a training set and validation set (80% of participants), which were then assessed in the remaining study sample (20% of participants). The area under the receiver-operating characteristic curve (AUC) and Brier scores were employed to compare the prediction performances of different models. The Random Forest (RF) Classifier model was employed for predicting RE, with interpretation provided by the SHapley Additive exPlanations (SHAP) package.

Results The RF model demonstrated superior performance compared to other classifier models in the training set (AUC: 1.000, 95% confidence interval [CI]: 1.000–1.000) and the validation set (AUC: 0.757, 95% CI: 0.636–0.878). Additionally, this model achieved the lowest Brier Score (0.163). Nine crucial variables, including lymphocyte-to-monocyte ratio, neutrophils, platelets, FIGO stage, lymphocytes, hemoglobin, uterine body invasion, tumor size, and degree pathological tissue, were selected.

Conclusion This pioneering study's predictive model will enhance understanding of the risk of RE and provide clinicians with a valuable tool based on inflammatory markers (4 factors) and clinical parameters (5 factors) in cervical cancer for guiding patient treatment.

PU-078

miR-520h Mediates Gemcitabine Resistant Pancreatic Cancer Cell Proliferation, Invasion and Migration via Regulating ABCG2

Minyong Chen, Wenhao Teng, Shaohua Xu, Hui Zhang
Clinical Oncology School of Fujian Medical University, Fujian Cancer Hospital,

Purpose Existing evidence showed that aberrant microRNAs (miRNAs) expression plays a vital role in the chemoresistance of human cancers including Pancreatic Cancer (PC). However, the potential role of miR-520h in PC gemcitabine resistance was unknown.

Materials and methods miR520h expression was determined via quantitative real-time polymerase chain reaction. miR-520h mimics and inhibitors were transfected, the effects of miR-520h on the proliferation ability of PC wild-type (WT) and gemcitabine-resistant (GR) cells were detected by Cell Counting Kit-8 assay. Transwell chamber assay and Scratch woundhealing assay were performed to determine PC WT and GR cells migration and invasion. Protein expression was estimated by Western blot. The interplay between miR520h and target was validated by dual-luciferase reporter assay.

Results The overexpression of miR-520h can promote the proliferation and migration of PC cells. ABCG2 was identified as the novel target of miR520h in PC. miR520h overexpression significantly reduced ABCG2 expression in PC WT and GR cells. On the contrary, the expression levels of ABCG2 increased after miRNA-520h expression was inhibited.

Conclusion This study showed that miRNA-520h negatively regulates the expression of ABCG2, thereby affecting the proliferation, invasion and migration of PC WT and GR cells.

PU-079

Transarterial chemoembolization combined with immunotherapy and targeted therapy as first-line treatment for unresectable and non-metastatic hepatocellular carcinoma

Jinhai Shen¹, Lichao Wang²

1. China Pharmaceutical University

2. The Second Hospital of Hebei University

Purpose Currently, the well-established standard treatment paradigm for unresectable and non-metastatic hepatocellular carcinoma (HCC) entails transarterial chemoembolization (TACE) as the initial local treatment modality, followed by systemic therapy upon disease progression. Emerging evidence indicates that the concurrent integration of immunotherapy and targeted therapy with TACE may confer synergistic therapeutic benefits. Recent randomized controlled trials, such as EMERALD-1, LEAP-012, and CARES-005, have provided invaluable insights into this multimodal treatment approach.

Materials and methods In this study, a comprehensive analysis was conducted on the data retrieved from these three clinical trials, which collectively included a total of 1,089 patients. Pooled hazard ratios (HRs) for progression-free survival (PFS), odds ratios (ORs) for objective response rate (ORR), and risk ratios (RRs) for grade 3-5 adverse events (AEs) were calculated using random-effects model.

Results The combination strategy demonstrated superior efficacy over TACE monotherapy. Pooled HR for PFS was 0.57 (95% confidence interval [CI]: 0.35-0.91) and OR for ORR was 1.81 (95% CI: 1.38-2.39). However, combination therapy significantly increased grade 3-5 AEs (RR: 2.34, 95% CI: 1.85-2.96). The overall survival data maturity remains low.

Conclusion First-line TACE combined with immunotherapy and targeted therapy significantly enhances tumor response and delays progression in unresectable and non-metastatic HCC, albeit with increased toxicity. This combination therapy represents a significant advancement in the treatment of this disease, offering substantial improvements in oncologic outcomes.

PU-080

Interventional treatment of uterine arteriovenous malformation

Teng Hui Zhan, Rong Zhang
Fujian Maternity and Child Health Hospital

Purpose Uterine arteriovenous malformation (UAVM) presents a complex condition that is difficult to diagnose early in clinical practice, carrying a risk of life-threatening uterine haemorrhage. To date, there is a lack of standardised diagnostic and management strategies both domestically and internationally. This study summarises the experience of our centre in the interventional embolisation treatment of uterine arteriovenous malformation, providing a reference for clinical decision-making regarding the diagnosis and treatment of UAVM.

Materials and methods This study employs a retrospective research method to collect clinical data from patients with uterine arteriovenous fistula admitted to Fujian Provincial Maternal and Child Health Hospital between 1st January 2022 and 31st December 2024. It aims to summarise their clinical characteristics and specific treatment plans, as well as to follow up on treatment outcomes, including surgical success rates, menstrual recovery, recurrence rates, and subsequent pregnancy situations.

Results Fifteen cases of uterine arteriovenous malformation (UAVM) were included, with an average age of 28.6 ± 11.2 years. All patients were diagnosed after miscarriage and showed no improvement following medical treatment. Among these, 9 cases (60%) were due to medical abortion, while 6 cases (40%) were due to surgical abortion. The most common symptom of UAVM was vaginal bleeding (12/15, 80%), with a minority of patients exhibiting no clinical symptoms. All patients underwent interventional treatment, with 10 patients showing early ovarian vein prominence during intraoperative imaging, leading to ovarian vein embolisation combined with uterine artery embolisation. In 5 patients, early ovarian vein prominence was not observed during imaging, and they underwent uterine artery embolisation. Postoperatively, 8 patients required curettage due to retained products of conception in the uterine cavity. No abnormal vaginal bleeding occurred postoperatively, and human chorionic gonadotropin (HCG) levels returned to normal in all patients. All patients resumed menstruation three months after the procedure, and one patient became pregnant again 13 months postoperatively.

Conclusion Interventional embolisation treatment has shown significant efficacy in cases of uterine arteriovenous fistula where pharmacological therapy has been ineffective. This approach is beneficial for improving patients' quality of life and is associated with fewer complications, making it worthy of clinical promotion and application.

PU-081

Prevention and Treatment of Malignant Gynaecological Tumours Complicated by Pulmonary Embolism

Teng Hui Zhan, Rong Zhang
Fujian Maternity and Child Health Hospital

Purpose Patients with gynaecological malignancies have a higher risk of developing pulmonary embolism, particularly post-surgery, which severely impacts the quality of healthcare. Currently, there is limited experience regarding the diagnosis and treatment of pulmonary embolism in patients with gynaecological malignancies. Therefore, we intend to investigate the risk factors associated with pulmonary embolism in patients with gynaecological malignancies at our centre, to provide a reference for their prevention and treatment.

Materials and methods This study employs a retrospective research method to collect clinical data on gynaecological malignancy patients with pulmonary embolism admitted to Fujian Provincial Maternity and Child Health Hospital from 1st July 2022 to 30th June 2024. Single and multifactorial analysis methods are used to analyse the factors contributing to the occurrence of pulmonary embolism in gynaecological malignancy patients.

Results Eighteen patients diagnosed with gynaecological malignancies who underwent surgical treatment were included in the study. Among these, there were 4 cases of endometrial cancer (22.2%), 6 cases of cervical cancer (33.3%), and 8 cases of ovarian cancer (44.4%). Postoperatively, 16 cases (89.9%) were noted, while 2 cases (11.1%) were identified preoperatively. Fourteen cases (77.8%) experienced pulmonary embolism with concurrent deep vein thrombosis (DVT) of the lower limbs, while 4 cases (22.2%) had pulmonary embolism without concurrent DVT. Clinical symptoms were observed in 11 cases (61.1%), including lower limb discomfort in 8 cases and chest tightness in 3 cases, while 7 cases (38.9%) exhibited no clinical symptoms. The 4 patients who developed pulmonary embolism without concurrent DVT had a high-risk Caprini score upon admission. Eleven cases (61.1%) did not receive standardised prevention or treatment for venous thromboembolism (VTE). Twelve patients (66.7%) underwent interventional treatment, while 6 patients (33.3%) received only anticoagulation therapy. All patients had symptom resolution following standardised anticoagulation or interventional treatment, with no fatalities reported. Univariate analysis indicated that age, BMI, preoperative D-dimer levels, tumour staging, intermuscular vein dilation, whether neoadjuvant chemotherapy was administered, presence of cardiovascular disease, surgical duration, central venous catheterisation, and adherence to VTE prevention or treatment protocols were significant risk factors ($P < 0.05$). Multivariate unconditional logistic regression analysis revealed that age over 55 years, preoperative cardiovascular disease, preoperative serum D-dimer levels exceeding 1.0 mg/L FEU, intermuscular vein dilation, and surgical duration exceeding 150 minutes were independent risk factors for pulmonary embolism in patients with gynaecological malignancies.

Conclusion The standard prevention and treatment of VTE in patients with gynaecological malignancies needs improvement. For patients aged over 55, those with pre-existing cardiovascular diseases, pre-operative serum D-dimer levels greater than 1.0 mg/L FEU, intermuscular venous dilation, and surgical durations exceeding 150 minutes, active and standardised VTE prevention and treatment should be implemented to reduce the incidence of pulmonary embolism.

PU-082

Interventional embolisation treatment of drug-loaded microspheres for advanced cervical malignancies

Teng Hui Zhan, Rong Zhang
Fujian Maternity and Child Health Hospital

Purpose The treatment methods for advanced cervical malignancies are effective, yet the survival rate for patients remains low. The aim of this study is to explore the application of drug-loaded microsphere embolisation therapy in advanced cervical malignancies, summarise the clinical experience from our centre, and report on the short-term follow-up results.

Materials and methods Clinical data were collected from 11 cases of advanced cervical malignancy admitted to the Vascular Surgery and Interventional Therapy Department of Fujian Provincial Maternity and Child Health Hospital from July 2023 to December 2024. All patients received drug-loaded microsphere interventional embolisation treatment (with cisplatin administered at 40 mg/m² followed by drug-loaded microspheres containing doxorubicin at 60-120 mg/m² for embolisation), and continued with neoadjuvant chemotherapy and radiotherapy post-surgery. Follow-up was conducted monthly after the procedure to analyse efficacy and safety.

Results All 11 patients were diagnosed with cervical squamous cell carcinoma (non-keratinising), FIGO stage IV. Among them, 7 presented with vaginal bleeding, and 3 cases were HPV-related. All patients underwent drug-loaded microsphere interventional embolisation treatment, neoadjuvant chemotherapy, and radiotherapy, achieving a surgical success rate of 100%. Postoperative follow-up indicated that 11 patients (11/11, 100%) experienced a reduction in lesions compared to before, with 6 patients (6/11, 54.5%) qualifying for surgery. After 6 months of follow-up, all patients were alive; however, 1 patient died from pneumonia 11 months post-follow-up. No complications such as puncture site haematoma, bleeding, or ectopic embolism occurred in any of the patients.

Conclusion Drug-loaded microsphere embolisation is a feasible, safe, and effective method for treating advanced cervical malignancies. Its short-term effects are promising, while the long-term efficacy requires further follow-up.

Efficacy of continuous arterial perfusion chemotherapy combined with transarterial chemoembolization regional arterial thermal perfusion in the treatment of pancreatic cancer with liver metastases

Zhuo Zhong¹, Jian Yang², Jing-Zi Luo¹, Xiong Xie¹, Zhi-Mei Huang³, De Long¹

1. Guangzhou Hospital of Integrated Traditional and West Medicine

2. Zhujiang Hospital Affiliated to Southern Medical University

3. Sun Yat-sen University Cancer Prevention Center

Purpose The aim of the study was to investigate the efficacy of continuous transcatheter arterial infusion chemotherapy combined with transarterial chemoembolization (TACE) for the treatment of advanced pancreatic cancer with liver metastasis.

Materials and methods Sixty patients with advanced pancreatic cancer and liver metastases were enrolled in this study. In the treatment group, 31 patients underwent continuous transcatheter arterial infusion chemotherapy combined with TACE regional arterial thermal perfusion, whereas 29 patients included in the control group received intravenous chemotherapy with gemcitabine and S-1. All patients received maintenance chemotherapy with S-1 after 4 cycles of the study regimen. Treatment efficacy, quality of life, survival, and toxicity were evaluated.

Results Efficacy was better in the treatment group than in the control group, as reflected by the objective remission, partial remission, and disease progression rates (all $P < 0.05$). The Eastern Cooperative Oncology Group and Numerical Rating Scale pain scores were also higher in the treatment group (both $P < 0.05$). In survival analysis, the 1-year overall survival rates in the treatment and control groups were 64.516% and 10.345%, respectively, whereas the median overall survival times were 16 and 6 months, respectively (both $P < 0.05$). The 6-month progression-free survival rates in the treatment and control groups were 77.419% and 13.790%, respectively, and the median progression-free survival times were 12 and 3 months, respectively (both $P < 0.05$). The rates of hematological and nonhematological toxicological adverse effects were also lower in the treatment group (both $P < 0.05$). Although the rate of liver dysfunction was higher in the treatment group, this finding had no adverse effects on prognosis.

Conclusion Continuous transcatheter arterial infusion chemotherapy combined with TACE regional arterial perfusion chemotherapy resulted in better efficacy and safety outcomes in patients with pancreatic cancer and liver metastasis, suggesting its utility as a reference method for the clinical treatment of advanced pancreatic cancer.

PU-084

BRPF3 R120H Mutation Enhances TP53-Mediated Tumor Suppression in Advanced Hepatocellular Carcinoma: A Retrospective Study

Wanqing Shen, Jiaping Li
The First Affiliated Hospital of Sun Yat-Sen University

Purpose Hepatocellular carcinoma (HCC) is a leading cause of cancer-related mortality worldwide, with limited therapeutic options available for advanced-stage patients. Thus, elucidating the molecular mechanisms underlying HCC progression is crucial for developing effective treatments.

Materials and methods We performed whole-exome sequencing in 68 patients with advanced HCC and analyzed somatic mutations using the Genome Analysis Toolkit (GATK) software and the "maftools" R package. Differentially expressed genes were identified using The Cancer Genome Atlas program database. We developed a prognostic nomogram based on genetic risk scores (GRS) and evaluated BRPF3 p.R120H mutation effects in HepG2 cells through multiple cellular assays.

Results BRPF3 was identified as a significant prognostic marker. BRPF3 p.R120H mutation was associated with improved survival outcomes through enhanced TP53 regulation and increased acetylation. Functional studies showed that BRPF3 mutation increased histone acetylation and TP53 expression, suppressed cell proliferation, enhanced apoptosis, and reduced migration/invasion capabilities in HCC cells in vitro. The integration of mutation data yielded a GRS based on a three-gene signature (comprising BRPF3, FAT1, and OBSL1) with a robust prognostic value (area under the curve, 0.768–0.844).

Conclusion Our findings revealed a novel mechanism where BRPF3 mutation enhances TP53-mediated tumor suppression in HCC, highlighting the targeting of histone acetylation pathways as a potential therapeutic strategy. A validated prognostic model incorporating these genetic alterations may improve risk stratification and treatment design for patients with advanced HCC.

PU-085

The Role of Circ_ANKIB1 in Recurrence and Metastasis of Hepatocellular Carcinoma

Wukui Huang

Affiliated Tumor Hospital of Xinjiang Medical University

Purpose To analyze and summarize the role of Circ_ANKIB1, an exosomal circular RNA (circRNA) derived from hepatocellular carcinoma (HCC), in the recurrence and metastasis of HCC based on recent domestic and international research.

Materials and methods A comprehensive review of relevant studies was conducted using databases such as PubMed, Web of Science, and CNKI. The search terms included "Circ_ANKIB1," "hepatocellular carcinoma," "recurrence," "metastasis," and "exosomes." Studies published within the last five years were prioritized to ensure the inclusion of the most recent findings.

Results Circ_ANKIB1 is significantly upregulated in HCC tissues and patient serum, particularly in exosomes derived from tumor cells. Elevated levels of Circ_ANKIB1 have been associated with higher rates of tumor recurrence and metastasis. Mechanistically, Circ_ANKIB1 acts as a miRNA sponge, binding to tumor-suppressive miRNAs such as miR-124 and miR-331-3p. This interaction inhibits the function of these miRNAs, thereby relieving their inhibitory effects on target genes. As a result, downstream signaling pathways like PI3K/AKT and MAPK are activated, promoting cell proliferation, migration, and invasion. Additionally, Circ_ANKIB1 can be transferred between cells via exosomes, influencing the tumor microenvironment by modulating immune cell functions and promoting the activation of cancer-associated fibroblasts (CAFs). This process facilitates immune evasion and enhances the metastatic potential of HCC cells.

Conclusion Circ_ANKIB1 plays a crucial role in the recurrence and metastasis of hepatocellular carcinoma through its interactions with miRNAs and modulation of the tumor microenvironment. Its high expression in exosomes suggests that it could serve as a potential biomarker for early diagnosis and prognosis assessment in HCC. Future research should focus on further elucidating the detailed mechanisms of Circ_ANKIB1 and exploring its potential as a therapeutic target to improve patient outcomes.

The Safety Evaluation of TAE for Ruptured Hepatocellular Carcinoma and Ablation-Related Hemorrhage, and the Clinical Significance of Postoperative Liver Function Changes

Yixuan An¹, Wenfeng Gao¹, Qing Zhang², Liang Ma¹, Ning He¹, Xiongwei Cui¹, Yonghong Zhang¹, Chunwang Yuan¹

1. Beijing You 'an Hospital, Capital Medical University

2. School of Clinical Medicine, Shandong Second Medical University,

Purpose This study evaluates the safety of transarterial embolization (TAE) for treating ruptured hemorrhage in liver cancer and post-ablation bleeding, comparing postoperative liver function indicators such as alanine aminotransferase (ALT), total bilirubin (TBIL), and prothrombin time percentage (PT%).

Materials and methods A retrospective analysis was conducted on liver function changes before and after surgery in three patient groups: ruptured hemorrhage, post-ablation bleeding, and a control group (routine TAE). The safety of TAE was assessed by comparing preoperative and postoperative levels of ALT, TBIL, and PT%, using ROC curve analysis to evaluate predictive values for liver injury.

Results All patients successfully underwent surgery, with a 100% hemostasis success rate. The 30-day survival rates were 90.91% for the rupture group and 100% for the ablation group, while one-year survival rates were 45.45% and 85.19%, respectively. Significant pre- and postoperative changes in ALT and TBIL were found within groups, but no significant differences were observed compared to the control group. ROC analysis showed strong predictive values for ALT and TBIL increases regarding liver injury.

Conclusion TAE is a safe and effective treatment for ruptured hemorrhage and post-ablation bleeding in liver cancer. Postoperative liver function changes in these groups are comparable to controls. Monitoring ALT and TBIL is crucial for early detection of liver injury, informing timely interventions. These findings enhance TAE protocols and liver protection strategies, improving outcomes for liver cancer patients.

PU-087

Incidence and factors predictive of recurrent rupture in people with rupture of unresectable hepatocellular carcinoma

Tianfan Pan¹, Yong Wang², Xinjian Xu¹, Feng Gao¹, Jian Lu², Xiangzhong Huang¹, Jinhe Guo²

1. Jiangyin people's hospital

2. Zhongda Hospital

Purpose Spontaneous rupture hemorrhage of hepatocellular carcinoma (HCC) has a low incidence and a high risk of death. Unresectable rupture hepatocellular (rHCC) carcinoma has a high early hemostasis rate after transcatheter arterial embolization (TAE). However, there is still a risk of recurrent rupture (RR) during subsequent treatment. There is a lack of studies on the Incidence and factors predictive of recurrent rupture in these patients. Our first aim was to describe the incidence of RR in people with unresectable rHCC. The second aim was to identify RR risk factors and afterwards verify them in a validation cohort.

Materials and methods This is a multicenter, retrospective observational study evaluating risk factors for RR in 94 people with unresectable rHCC from Jan 2010 to Dec 2023 in four medical centers. In the training cohort, the potential value of parameters to predict RR was analyzed by univariate and multivariate Cox analysis. Findings were validated in 79 individuals with unresectable rHCC.

Results: A total of 173 patients were included in this study. Of the 94 participants in training cohort, 17 (18.1%) presented recurrent rupture during follow-up (cumulative incidence: 6.6, 13.2, 16.3, and 24.6% at 3, 6, 12, and 24 months, respectively; the mean and median time: 9.6 and 7.0 months, respectively). In addition, MELD score > 15, tumor size > 10cm and received targeted therapy were the independent factors predicting RR (hazard ratio 8.40, 95% CI 2.25-34.10, $p=0.002$; hazard ratio 3.36, 95% CI 1.05-10.74, $p=0.041$; hazard ratio 5.72, 95% CI 1.78-18.43, $p=0.003$, respectively). Of the 79 participants in validation cohort, 14 individuals (17.7%) presented RR during follow-up (cumulative incidence: 6.9, 15.6, 18.2, and 32.8% at 3, 6, 12, and 24 months, respectively; the mean and median time: 10.9 and 7.0 months, respectively). The predictive value of these factors was showed good stability and prediction accuracy when assessed externally in validation cohort (C-index: 0.872, 95% CI: 0.773-0.972).

Conclusion People with unresectable rHCC are at risk of recurrent rupture. Factors of MELD score > 15, tumor size > 10cm and received targeted therapy are independent risk factors for recurrent rupture.

PU-088

Feasibility, Efficacy, and Safety of Ventral Caudal Artery Access for Transarterial Chemoembolization in a Rat Hepatocellular Carcinoma Model

Lijie Zhang, Chuansheng Zheng, Bin Liang

Department of Radiology, Hubei Key Laboratory of Molecular Imaging, Union Hospital, Tongji Medical College, Huazhong University of Science and Technology, 1277 Jiefang Road, Wuhan 430022, China.

Purpose Investigate the feasibility, efficacy, and safety of ventral caudal artery (VCA) approach for transarterial chemoembolization (TACE) in an orthotopic hepatocellular carcinoma (HCC) rat model.

Materials and methods Sixteen orthotopically established tumor-bearing Sprague-Dawley rats were divided into two groups of eight each: drug-eluting bead transarterial chemoembolization (DEB-TACE) group and normal saline (NS) group. VCA was approached for transarterial procedures. Rats in DEB-TACE group and NS group received transarterial administration of doxorubicin-loaded microspheres and normal saline, respectively. In NS group, repeated transarterial procedures were attempted 3 days after initial procedures. The feasibility was evaluated based on success rate of VCA approach, proper hepatic artery catheterization, and transcatheter treatment. The efficacy was assessed according to tumor necrosis. Animal mortality and tail viability were observed for safety evaluation.

Results VCA was successfully approached in 16 rats at initial procedures. Catheterization of proper hepatic artery achieved success in 7 of 8 DEB-TACE group animals and 6 of 8 NS group animals at initial procedures. All 13 rats received subsequent DEB-TACE or NS injection. One animal in DEB-TACE group died within 24 hours and no death was noted in NS group (14.29% vs 0%, $P = 1.000$). Tail viability was normal within 3 days. Repeated transarterial procedures were successfully performed in 6 of 8 NS group animals. Tumor necrosis of DEB-TACE group was significantly higher than that of NS group ($54.11 \pm 22.31\%$ vs $11.15 \pm 3.50\%$, $P = 0.005$).

Conclusion VCA access is feasible, effective, safe, and potentially repeatable for TACE in rat HCC model.

Pan-Cancer Analysis Unveils POSTN as a Promising Therapeutic Target for ER⁺ Breast Cancer

Xiaoyi Zhai, Buerlan Yeerkenbieke, Dilinaer Yeerxiati, Wenjia Guo
Cancer Hospital of Xinjiang Medical University

Purpose Purpose: *Periostin* (*POSTN*), a secreted extracellular matrix protein, has emerged as a critical mediator in tumorigenesis, angiogenesis, and metastatic progression across multiple malignancies. While accumulating evidence highlights its oncogenic roles in specific cancers, a systematic exploration of *POSTN*'s pan-cancer significance remains absent. Particularly enigmatic is its mechanistic interplay with hormone receptor-driven tumorigenesis, including Estrogen Receptor-positive (ER⁺) breast carcinoma, which constitutes 70-80% of all breast malignancies and represents a critical therapeutic challenge due to intrinsic endocrine therapy resistance. This study bridges these knowledge gaps through an integrative multi-omics investigation across 33 cancer types, with translational emphasis on elucidating *POSTN*'s clinical relevance, immune-modulatory functions, and therapeutic targetability in ER⁺ breast cancer.

Materials and methods A multi-platform analytical framework was established utilizing data from TIMER2.0, TCGA, GTEx, HPA, cBioPortal, UALCAN, SMART, MethSurv, and CancerSEA databases. Transcriptomic profiling of *POSTN* was performed across tumor tissues and matched normal controls, with differential expression analysis stratified by clinical parameters. Prognostic significance was evaluated via Kaplan-Meier survival curves and multivariate Cox regression models. Genetic alterations (mutations, copy number variations) and epigenetic modifications (DNA/RNA methylation patterns) were systematically cataloged. Tumor microenvironment characteristics were assessed through ESTIMATE and CIBERSORT algorithms, with immune infiltration scores correlated to *POSTN* expression. Drug sensitivity analyses leveraged CTRP and GDSC pharmacogenomic datasets, employing Spearman correlation to identify *POSTN*-associated therapeutic vulnerabilities. PAM50 molecular subtyping and single-cell RNA sequencing data were integrated to delineate subtype-specific roles of *POSTN* in breast carcinogenesis. The present study was conducted to systematically analyze the molecular mechanisms of ER⁺ breast cancer. Forty clinical tissue samples were examined by immunohistochemistry, and the results showed that the expression level of *POSTN* protein in tumor tissues showed significantly high expression. In vitro experiments using two ER⁺ breast cancer cell lines, MCF-7 and T47D, revealed that *POSTN* mRNA expression was up-regulated compared with that of normal breast epithelial cells by real-time quantitative reverse transcription polymerase chain reaction. In order to explore the functional role of *POSTN*, the research team applied siRNA-mediated gene silencing technology to realize targeted knockdown, and the experimental data showed that: the cell viability of the intervention group was decreased by CCK-8 cell proliferation assay; the scratch assay showed that the cell migration rate was slowed down, and the number of invasive cells decreased by Transwell stromal invasion assay; the soft agar clone formation assay further verified that its tumorigenicity was weakened, and the clone formation rate was reduced. The soft agar clone formation assay further verified that the tumorigenicity was weakened and the clone formation rate was reduced. The results of this series of experiments from both in vivo and ex vivo models collectively confirmed that *POSTN* has a critical regulatory role in the malignant progression of ER⁺ breast cancer.

Results This first comprehensive pan-cancer analysis establishes *POSTN* as a pleiotropic ECM effector governing stromal remodeling, immune evasion, and therapeutic resistance through multi-modal regulatory mechanisms. And *POSTN* is a biomarker with dual prognostic utility. The pronounced association with ER⁺ breast cancer pathogenesis, particularly its role in therapy resistance

and immune evasion positions. The aim of this paper is to comprehensively investigate the role of *POSTN* in cancer development, particularly its expression pattern, immunomodulatory mechanisms, and potential role in drug therapy in breast cancer and ER⁺ breast cancer. This study first analyze the differential expression patterns of *POSTN* in different cancer types to determine its specificity and clinical relevance in breast cancer. To validate bioinformatics predictions, we performed in vitro functional assays: Immunohistochemistry confirmed elevated *POSTN* protein levels in ER⁺ breast cancer tissues compared to normal controls. Real-time quantitative PCR revealed upregulated *POSTN* mRNA expression in ER⁺ breast cancer cell lines (MCF-7, T47D). siRNA-mediated *POSTN* knockdown significantly impaired cell proliferation (CCK-8 assay), migration (scratch assay), invasion (Transwell assay), and colony formation capacity (clonogenic assay), supporting its oncogenic role. Further, the study delves into the immunomodulatory functions of *POSTN* in the breast cancer microenvironment, including its effects on tumor infiltrating immune cells and its contribution to tumor immune escape mechanisms and evaluate the feasibility of *POSTN* as a drug therapeutic target, especially in ER⁺ breast cancer, and explore the potential for the development of *POSTN* targeted drugs and therapeutic strategies. The integration of *POSTN* targeted therapy into the existing treatment of ER⁺ breast cancer is still in the research and exploration stage, and more clinical trials are needed to verify its safety, effectiveness and optimal integration. These findings advocate for therapeutic strategies combining *POSTN* targeted biologics with CDK4/6 inhibitors to circumvent resistance in hormone receptor-positive malignancies. Clinical translation of these findings could enable *POSTN* directed strategies combining extracellular matrix-targeting agents with endocrine therapies to improve outcomes in hormone receptor-positive malignancies.

Conclusion This first comprehensive pan-cancer analysis establishes *POSTN* as a pleiotropic ECM effector governing stromal remodeling, immune evasion, and therapeutic resistance through multi-modal regulatory mechanisms. And *POSTN* is a biomarker with dual prognostic utility. The pronounced association with ER⁺ breast cancer pathogenesis, particularly its role in therapy resistance and immune evasion positions. The aim of this paper is to comprehensively investigate the role of *POSTN* in cancer development, particularly its expression pattern, immunomodulatory mechanisms, and potential role in drug therapy in breast cancer and ER⁺ breast cancer. This study first analyze the differential expression patterns of *POSTN* in different cancer types to determine its specificity and clinical relevance in breast cancer. Further, the study delves into the immunomodulatory functions of *POSTN* in the breast cancer microenvironment, including its effects on tumor infiltrating immune cells and its contribution to tumor immune escape mechanisms. In addition, this paper evaluates the feasibility of *POSTN* as a drug therapeutic target, especially in ER⁺ breast cancer, and explore the potential for the development of *POSTN* targeted drugs and therapeutic strategies. The integration of *POSTN* targeted therapy into the existing treatment of ER⁺ breast cancer is still in the research and exploration stage, and more clinical trials are needed to verify its safety, effectiveness and optimal integration. Clinical translation of these findings could enable *POSTN* directed strategies combining extracellular matrix-targeting agents with endocrine therapies to improve outcomes in hormone receptor-positive malignancies.

PU-091

Clinical Application Value of 1024 Matrix Combined with P3T Technology in Bronchial Artery CTA

Tao Liu, Zi Long Yuan
Hubei Cancer Hospital

Purpose To explore the clinical application value of the 1024 - matrix combined with P3T technology in bronchial artery CTA.

Materials and methods A total of 100 patients with lung - cancer - related hemoptysis who underwent bronchial artery CTA scanning from January 2023 to October 2023 were prospectively enrolled and randomly divided into two groups, group A and group B (n = 50). Group A was scanned using the conventional smartPrep technology and reconstructed with a 512 - matrix, while group B was scanned using the P3T technology and reconstructed with a 1024 - matrix. The contrast agent dosage, objective scores, subjective scores, the display of the origin, variation, and invasion of the bronchial artery, as well as the ability to visualize the farthest visible branches were compared between the two groups.

Results There were no significant differences in gender, age, and BMI between group A and group B ($P>0.05$). The contrast agent dosage in group B was reduced by 31%. There were no significant differences in the CT values of the main trunk and branches of the bronchial artery and the corresponding aortic arch in the reconstructed images of group B. The ability to display the origin, variation, and invasion of the bronchial artery and the farthest visible branches in group B was higher than that in group A, with statistical differences ($P<0.05$). The SNR values and CNR values in group B were similar to or higher than those in group A. The subjective score of group B was higher than that of group A, with statistical significance ($P<0.05$).

Conclusion The application of the 1024 - matrix combined with P3T technology in bronchial artery CTA for patients with lung - cancer - related hemoptysis can reduce the contrast agent dosage for bronchial artery imaging and ensure good image quality.

PU-092

Three anesthesia models during microwave ablation for the treatment of subpleural stage I non-small cell lung cancer: A Prospective, Single-Center Study

Yufeng Wang, Xiaoguang Li
Beijing Hospital

Purpose To compare the analgesic effect and safety of three anesthesia models during microwave ablation (MWA) for subpleural stage I non-small cell lung cancer (NSCLC).

Materials and methods This study was a prospective, single-center clinical trial enrolling patients with subpleural stage I NSCLC from January 2024 to December 2024 (Fig. 1). All patients were scheduled for intercostal nerve block (INB) (Fig. 2,3), pleural infiltration anesthesia (PIA) (Fig. 4), or local anesthesia (LA). The endpoints were perioperative visual analogue scale (VAS) scores and adverse events within 1 month after MWA.

Results A total of 60 patients (mean age, 73.88 years \pm 6.44 [standard deviation], 28 men) were evaluated. The PIA group had comparable intraoperative VAS scores to the INB group and was significantly lower than the LA group (2.70 ± 1.34 vs. 2.85 ± 1.73 vs. 6.26 ± 1.41 , $p < .05$). The VAS scores at 2 hours postoperatively were significantly lower in the PIA and INB groups compared to the LA group, while no statistically significant difference was observed between the two former groups (0.80 ± 1.24 vs. 1.35 ± 1.63 vs. 2.25 ± 1.02 , $p < .05$). There was no significant difference in VAS scores at 24 hours post-ablation (0.80 ± 1.24 vs. 1.40 ± 1.57 vs. 1.50 ± 1.64 , $p > .05$). The rate of postoperative analgesic use was higher in the LA group compared to the PIA and INB groups. All groups demonstrated a technical success rate and technical efficiency of 100%, and no periprocedural mortality. Additionally, there were no statistical differences in adverse events occurring within 30 days post-ablation, nor was there a difference in the length of hospital stays among the groups.

Conclusion CT-guided MWA is a safe and effective minimally invasive protocol for subpleural stage I NSCLC. INB and PIA could significantly reduce perioperative pain, facilitating the ablation procedure and ensuring complete ablation of the lesion. Compared to INB, PIA provides comparable analgesia effect. Additionally, PIA is easy to perform and does not require anesthesiologist involvement, reducing hospitalization expenditure. Nevertheless, in cases of subpleural lung nodules located near skeletal structures, PIA does not realize the desired analgesic effect, and INB remains indispensable. Thus, it is essential for the interventionalists to choose the appropriate anesthesia for ablating subpleural lung nodules.

PU-093

Transcatheter Arterial Embolization: An Alternative for Endoscopically Unmanageable Bleeding Duodenal Ulcer

Xing Liu¹, XiaoCui You², ZhuTing Fang², ShaoJie Wu¹, YanFeng Zhou¹, SenLin Cai¹, Yi Tang¹

1. Fujian Provincial Hospital

2. Fujian Cancer Hospital (Fujian Branch of Fudan University Shanghai Cancer Center)

Purpose Endoscopic therapy is the first-line treatment recommended by guidelines for bleeding duodenal ulcers, but some patients still experience persistent bleeding or rebleeding. Transcatheter arterial embolization (TAE) is increasingly recognized by clinicians for its minimally invasive and efficient characteristics. We aimed to assess the effectiveness of TAE in managing bleeding duodenal ulcers following unsuccessful endoscopic hemostasis.

Materials and methods From April 2013 to December 2022, a total of 18 patients who underwent TAE for the management of bleeding duodenal ulcers following unsuccessful endoscopic hemostasis were included in this retrospective study. The study evaluated the technical and clinical success rates, rebleeding incidence, 30-day mortality, and treatment-related complications.

Results The technical success rate of TAE was 88.9%, while the clinical success rate stood at 66.7%.

The average hemoglobin (Hb) level before embolization was 63.8 ± 21.2 g/L, which rose to 76.8 ± 16.7 g/L postoperatively. Concurrently, the demand for red blood cell transfusions in clinically successful patients decreased from 7.2 ± 4.8 units to 4.0 ± 2.8 units. Post-TAE, four patients experienced rebleeding. Complications were not observed 30 days after TAE, and the 30-day mortality rate was 11.1%. One patient succumbed to underlying diseases, while another patient passed away due to severe pulmonary infection following surgery.

Conclusion TAE achieved high technical and clinical success rates in patients with bleeding duodenal ulcers unresponsive to endoscopic therapy in our study. Moreover, no complications were observed 30 days post-TAE. These findings strongly suggest the feasibility and safety of TAE.

PU-094

Abdominal Aortic Rupture Bleeding with Hemothorax Following Percutaneous Catheter Drainage for Infected Walled-off Pancreatic Necrosis

XiaoCui You,Zhuting Fang,Wenji Lin,Yutang Chen
Fujian Cancer Hospital (FujianBranch of Fudan University shanghai Cancer Center)

Purpose In this case report, we analyze the case and review the literature regarding the management of infected walled-off pancreatic necrosis.

Materials and methods We report a case of a 79-year-old woman with a history of acute pancreatitis, diagnosed with infected walled-off pancreatic necrosis, who received percutaneous catheter drainage after admission. During the procedure, she experienced an abdominal aortic rupture and subsequent hemothorax. Then covered stent placement was performed for abdominal aorta puncture bleeding.

Results Post-operation, the patient remained comatose and was in shock. At the request of the patient's family, the patient was discharged from the hospital.

Conclusion clinicians should select the optimal PCD imaging guidance modality and drainage technique for treating infected WON. It is crucial to consider the potential impact of gas artifacts and loose inflammatory wall tissue to reduce the risk of complications, such as life-threatening abdominal aortic hemorrhage. Timely identification and prompt hemostasis are essential.

PU-095

Transarterial chemoembolization and hepatic arterial infusion chemotherapy combined with atezolizumab plus bevacizumab for patients with advanced hepatocellular carcinoma

Jia Zeng

Tianjin Medical University General Hospital

Purpose To investigate the clinical efficacy and adverse effects of transarterial chemoembolization (TACE) and hepatic arterial infusion chemotherapy (HAIC) combined atezolizumab plus bevacizumab (A+T) in patients with advanced hepatocellular carcinoma (HCC).

Materials and methods Data of HCC patients treated with TACE and HAIC combined atezolizumab plus bevacizumab (ATTH group) or TACE and HAIC (TH group) from January 2020 to June 2023 at the General Hospital of Tianjin Medical University were collected. A total of 44 patients were included. Among them, 18 were in the ATTH group and 26 in the TH group. General information of the patients was collected, such as largest tumor size and number, preoperative liver function and alpha-fetoprotein (AFP), etc. The patients were followed up regularly, and the treatment-related adverse reactions of the patients in the ATTH group as well as the overall survival (OS) and progression-free survival (PFS) of the patients in both groups were recorded.

Results The median OS was significantly higher in the ATTH group (18 ± 1.05 months) than in the TH group (14 ± 1.64 months, $p = 0.044$), and the median PFS (9 ± 1.04 months) was longer than in the TH group (5 ± 0.50 months, $p = 0.003$). Among treatment-related adverse events (TRAEs), elevated aspartate aminotransferase (AST) alanine aminotransferase (ALT), vomiting, and decreased albumin (ALB) were the most common. Multivariate analyses showed that treatment method, extrahepatic metastasis and largest tumor size greater than 10 cm, and preoperative AFP greater than 400 were the independent risk factors for OS, while treatment method, extrahepatic metastasis and portal vein invasion were the independent risk factors for PFS.

Conclusion ATTH significantly improves survival in patients with advanced HCC with acceptable treatment-related adverse effects.

PU-096

Clinical efficacy and safety analysis of irreversible electroporation combined with chemotherapy in the treatment of stage IV pancreatic cancer

Jia Zeng

Tianjin Medical University General Hospital

Purpose To study the clinical efficacy and safety analysis of irreversible electroporation therapy combined with chemotherapy in patients with stage IV pancreatic cancer.

Materials and methods Between September 2021 and November 2023, we collected 58 patients with stage IV pancreatic cancer who met the enrollment criteria, 30 of whom received irreversible electroporation (IRE) in combination with chemotherapy and 28 of whom received chemotherapy treatment. We collected general information about the patients, such as tumor location, tumor size, CA199, preoperative and postoperative chemotherapy regimens, and followed up with the patients at regular intervals to record the patients' postoperative IRE-related adverse reactions, and evaluated patients' median PFS and median OS.

Results The median OS was higher in the IRE group (14 ± 3.73 months) than in the chemotherapy group (10 ± 1.51 months, $P = 0.598$), the median PFS (6 ± 1.68 months) was slightly longer than that in the chemotherapy group (5 ± 0.40 months, $P = 0.585$), and the mean length of stay in the IRE group was 5.9 ± 0.75 days. Four serious adverse events occurred after IRE, including one case of pyloric edema, one case of obstructive jaundice, one case of pancreatitis, and one case of intraoperative bleeding. Postoperative pain scores were reduced compared to preoperative ones ($P < 0.05$).

Conclusion The use of IRE in the treatment of stage IV pancreatic cancer is clinically effective and can slightly reduce the local pain symptoms of patients, with fewer adverse effects and shorter hospitalization time.

PU-097

MULTISCALE MODELING OF TUMOR-MACROPHAGE INTERACTIONS UNDERLYING IMMUNOTHERAPY RESISTANCE IN GLIOBLASTOMA

Ji Zhang

Department of Neurosurgery, Sun Yat-sen University Cancer Center, Guangzhou, China

Purpose Clinical and experimental studies have demonstrated that the application of colony stimulating factor-1 receptor (CSF1R) inhibitors in immunotherapy for glioblastoma frequently results in the development of drug resistance and subsequent tumor relapse. However, the underlying mechanisms remain poorly understood.

Materials and methods In this study, we develop a multiscale mathematical model that integrates cellular scale (e.g., tumor cells, M1 and M2 macrophages), microenvironmental scale (e.g., diffusible cytokines, drugs), and molecular scale (e.g., epidermal growth factor receptor (EGFR) and insulin-like growth factor-1 receptor (IGF1R) signaling pathways). The spatio-temporal evolutions of cellular densities and cytokine concentrations are modeled using partial differential equations (PDEs), and kinetics of molecular signaling pathways are modeled with ordinary differential equations (ODEs). We designed a hybrid analytical-numerical approach for the simulation of the coupled PDEs-ODEs model. The model predictions are in good agreement with experimental data. We then investigate different regimens of drug administration for CSF1R inhibitor, EGFR inhibitor, and IGF1R inhibitor.

Results The results reveal that adaptive dynamic dosing of CSF1R inhibitor not only reduces drug doses but also significantly prolongs individual survival when co-administered with IGF1R inhibitor.

Conclusion Our study provides quantitative and mechanistic insights into the adaptation mechanism of microenvironment-mediated resistance to immunotherapy in glioma, which is instrumental in informing the development of dynamic and adaptive therapeutic strategies.

PU-098

Application of Iodine-125 (¹²⁵I) Seed Implantation in the Treatment of Spinal Metastases

Yixuan Yang
southeast university

Purpose Spinal metastases, as a common manifestation of advanced cancer, often present with severe pain or neurological deficits, significantly compromising patients' quality of life. Iodine-125 (¹²⁵I) seed implantation, a widely utilized brachytherapy approach in clinical practice, offers advantages including high radiation dose localization to target tissues, minimal invasiveness, improved local tumor control, procedural simplicity, and enhanced safety. It can be applied either as a standalone treatment or in combination with other modalities for spinal metastases. We summarize the current research progress on ¹²⁵I seed implantation in the management of spinal metastases, aiming to provide insights for optimizing clinical therapeutic strategies.

Materials and methods This study retrospectively analyzed 70 patients treated with Iodine-125 (¹²⁵I) seed implantation. The cohort included: 27 cases treated with ¹²⁵I seeds alone, 20 cases combined with systemic therapy, 15 cases combined with percutaneous vertebroplasty (PVP), 5 cases combined with ablation therapy and 3 cases combined with internal fixation. We collect patients' efficacy scores and clinical data.

Results Patients' VAS and NRS present to be significant improved. We are working on postoperative verification protocols after different combination therapy.

Conclusion Iodine-125 (¹²⁵I) seed implantation has demonstrated significant symptom alleviation in patients with spinal metastases, showcasing promising clinical potential within the framework of comprehensive treatment.

PU-099

Using deep learning technology to segment liver tumors on SPECT/CT with MRI

DONG LI

Southeast university

Purpose At present, Y-90 selective internal radiotherapy (SIRT) must be preceded by technetium-99 polymerized albumin surgery to simulate the distribution of Y-90 microspheres in the patient's body. However, the simulated surgery requires a more accurate reconstruction of the liver and tumor areas. Currently, manual assisted segmentation of related areas is mostly used in clinical practice. The method used is to find MRI images close to the corresponding level of SPECT/CT and segment them according to the doctor's experience. This method has a certain accuracy error because MRI and SPECT/CT are not taken at the same time, the relative position of the patient and the layer height thickness of the two technologies are not exactly the same. This study uses artificial intelligence technology, registration methods and unsupervised pre-adaptation (UDA) + residual analysis (RSA) to obtain the target area segmentation accuracy of each of the two methods and compare them. This method is the first to use artificial intelligence methods to directly segment SPECT/CT with the help of MRI images to reduce segmentation errors.

Materials and methods All patients who received treatment with 90 Y radioactive embolization microspheres (resin microspheres) were divided into a training group and a prediction group. 80% of the data was used as the training group, and 20% of the data was used to validate the model validation results.

Data source: This study used 86 Y90 resin microsphere treatment cases from Zhongda Hospital Affiliated to Southeast University (Center A) and 29 cases from Anhui Provincial Hospital (Center B) (including preoperative MRI, technetium-99 polymerized albumin evaluation SPECT/CT, and SPECT/CT after Y90 treatment), of which 80 cases were used for training and 35 cases for validation.

Results The current Dice for liver segmentation is 0.92, and the Dice for tumor target area is 0.67. At present, the model accuracy of the validation dataset exceeds 0.7

Conclusion At present, the model has preliminarily achieved tumor region segmentation assisted by doctors based on uploaded MRI and SPECT images. In the future, through training and validation with multi center data, the accuracy and generalization ability of the model can be further improved.

Therapy-induced Senescent Tumor Cells Modulate Gemcitabine Sensitivity in Intrahepatic Cholangiocarcinoma

Zhishan Ge, Yan Fu, Haidong Zhu
Zhongda Hospital, Southeast University

Purpose Intrahepatic cholangiocarcinoma (ICC) is a highly aggressive malignancy with limited therapeutic options. Although gemcitabine is a standard chemotherapy agent, resistance remains a major challenge. Recent studies suggest that senescent tumor cells can reshape the tumor microenvironment and promote chemoresistance, yet their role in ICC remains unclear. This study investigates the role of senescent ICC cells in mediating gemcitabine resistance and the underlying molecular mechanisms.

Materials and methods ICC cells were treated with gemcitabine to induce senescence, confirmed by increased β -galactosidase activity, reduced EdU incorporation, and elevated γ -H2AX expression via Western blot. Conditioned medium from senescent ICC cells was collected and used to treat proliferative ICC cells. CCK-8 assays were performed to assess gemcitabine sensitivity, and Transwell assays evaluated migration ability. Gene expression of stemness markers (Nanog, OCT4, KLF4, and SOX2) was analyzed by RT-qPCR. Western blot was used to examine the phosphorylation levels of AKT and mTOR.

Results Gemcitabine-induced senescence in ICC cells was confirmed by increased β -galactosidase activity, decreased EdU-positive cells, and upregulated γ -H2AX expression. ICC cells exposed to senescent-conditioned medium exhibited reduced sensitivity to gemcitabine, as shown by CCK-8 assays, and significantly enhanced migration ability in Transwell assays. RT-qPCR analysis revealed that senescent ICC cells exhibited increased expression of stemness markers, including Nanog, OCT4, KLF4, and SOX2. Western blot analysis demonstrated that senescent ICC cells had elevated phosphorylation levels of AKT and mTOR, suggesting activation of pro-survival signaling pathways.

Conclusion Senescent ICC cells contribute to gemcitabine resistance and promote ICC cell migration, potentially through the upregulation of stemness-associated genes and activation of the AKT/mTOR signaling pathway. Targeting senescence-associated secretory phenotypes and associated survival pathways may provide a novel therapeutic strategy to overcome drug resistance in ICC.

PU-102

Exploring Yttrium-90 Radioactive Microspheres in Rat Models of Hepatocellular Carcinoma

Chen Sun, Haidong Zhu

Department of Radiology, Zhongda Hospital, Medical School, Southeast University

Purpose The Yttrium-90 (^{90}Y) radioactive microspheres, as a useful form of selective internal radiotherapy (SIRT) for hepatocellular carcinoma (HCC). However, the mechanisms underlying the therapeutic efficacy of ^{90}Y remain unclear. In this study, a rat model of implanted HCC was established to investigate the impact of ^{90}Y SIRT on tumor prognosis and immune function.

Materials and methods ^{90}Y SIRT in rats administered through gastroduodenal artery catheterization. Evaluate changes in tumor growth and immune cell infiltration within the tumor. Additionally, RNA-seq, in conjunction with clinical database analysis, was utilized to examine key gene alterations post-SIRT and their correlation with tumor prognosis.

Results Compared to the control group, ^{90}Y resulted in significant tumor volume reduction ($P < 0.05$) and a marked increase in Tumor Necrosis Factor- α expression ($P < 0.005$), with no observed toxic symptoms or abnormalities in liver or kidney function of all experimental animals. Additionally, the ^{90}Y exhibited a obviously weakened Forkhead box Protein 3 (Foxp3) cell count ($P < 0.0005$) and a trend towards increased expression levels of Cytotoxic T lymphocytes (CD8 $^{+}$ T) cells ($P < 0.005$). Moreover, based on Kaplan-Meier survival analysis across three datasets (TCGA_LIHC, GSE116174, and GSE54236), NCF4, HCK, CD86, and FERMT3 were found to have prognostic significance and were all identified as risk factors.

Conclusion ^{90}Y SIRT has the potential to control tumor proliferation by modulating the immune microenvironment of HCC. Additionally, postoperative high expression of NCF4, HCK, CD86, and FERMT3 may be associated with poor clinical outcomes.

PU-103

Ultrasound guided microwave ablation combined with traditional Chinese medicine in the treatment of benign thyroid nodules

GuoXiang Sun
PLA 63680 Hospital

Purpose To explore the therapeutic effect of ultrasound-guided microwave ablation combined with traditional Chinese medicine in the treatment of benign thyroid nodules.

Materials and methods A clinical study was conducted on 72 patients with thyroid nodules admitted to the hospital from January 2020 to December 2022. The study group was randomly divided into a study group and a control group, with 36 patients in each group. The study group underwent ultrasound-guided microwave ablation of thyroid nodules combined with traditional Chinese medicine treatment, while the control group underwent ultrasound-guided microwave ablation of thyroid nodules. The therapeutic effects of the two groups were compared and evaluated after surgery.

Results After treatment, two groups of patients underwent regular ultrasound examinations. The total effective rate of the study group was 83.33%, while the total effective rate of the control group was 61.11% ($P<0.05$); The thyroid nodule volume of the study group patients significantly decreased compared to the control group patients at 1 month, 3 months, 6 months, and 12 months after treatment, and the difference was statistically significant ($P<0.05$);

Conclusion The combination of ultrasound-guided microwave ablation and traditional Chinese medicine treatment for thyroid nodules is more effective than simple microwave ablation treatment, with fewer complications, less trauma, simple operation, and no impact on thyroid function. The combination of traditional Chinese medicine treatment can significantly improve the volume reduction rate of the ablation area of the nodules, shorten the absorption time, and play an important role in the postoperative recovery of patients.

PU-106

Variational Attention Fusion Network for Intracranial Aneurysm Segmentation

Tao Han, Yi Zhang, Gao-Jun Teng
Southeast University

Purpose The segmentation of 3D intracranial aneurysms is a key task for accurate diagnosis and treatment planning in neurosurgery and interventional procedures. By delineating aneurysms from surrounding tissue structures, it enables effective risk assessment and personalized treatment strategies. The task of segmenting intracranial aneurysms is complicated by their highly varied geometry and the subtle boundaries between aneurysms and nearby arteries.

Materials and methods In this work, we propose a variational attention fusion network that leverages intracranial arterial anatomical features to improve intracranial aneurysm segmentation. First, the model is pre-trained on a brain vessel dataset to predict artery segmentation, and then the pre-trained artery feature encoder is integrated into the target segmentation network. This forms a dual encoder network for artery and aneurysm, which guides aneurysm segmentation. In this framework, a cross-feature variational attention mechanism is designed to fuse the artery and aneurysm features. This mechanism models uncertainty in the feature subspace and utilizes variational attention to perform feature fusion, enhancing the feature encoding of aneurysms. Additionally, we introduce a scale-sensitive segmentation loss function that penalizes the size discrepancy between the predicted aneurysms and ground truth, improving the network's sensitivity to small aneurysms.

Results Extensive qualitative and quantitative experiments were performed on MRA and 3D DSA images to evaluate the performance of our method in intracranial aneurysm segmentation. The results show that the introduced cross-feature variational attention mechanism and scale-sensitive segmentation loss function significantly enhance the segmentation accuracy of aneurysms. Furthermore, our method outperforms five other state-of-the-art aneurysm segmentation methods across aneurysms of different sizes.

Conclusion Thus, our approach demonstrates the ability to accurately segment intracranial aneurysms of various sizes in datasets across multiple imaging modalities.

PU-111

A transcriptomic biomarker for predicting the response to TACE correlates with the tumor microenvironment and radiomics features in HCC

Chendong Wang, Guowen Yin
Jiangsu Cancer Hospital

Purpose The response to transarterial chemoembolization (TACE) varies among hepatocellular carcinoma (HCC) individuals. This study aimed to identify a biomarker for predicting TACE response in HCC and to investigate its correlations with the tumor microenvironment and pre-TACE radiomics features.

Materials and methods GSE104580 data were obtained from Gene Expression Omnibus (GEO) database. Differentially expressed gene analysis and machine learning algorithms were used to identify genes for constructing TACE failure signature (TFS). TFS scores were then calculated for HCC patients in The Cancer Genome Atlas (TCGA) cohort. After obtaining images from The Cancer Imaging Archive (TCIA), tumor labeling and radiomics feature extraction, the Rad-score model was generated. Correlation analysis was performed between TFS score and Rad-score. CIBERSORT, ssGSEA and TME analysis were performed to explore differences in the immune landscape among distinct risk groups.

Results ADH1C, CXCL11, EMCN, SPARCL1, LIN28B were incorporated into the TFS, which demonstrated satisfactory performance in predicting TACE response. Patients in the high TFS score group had poorer overall survival (OS) than those in the low TFS score group. The Rad-score model was constructed using six radiomics features, and the Rad-score significantly correlated with hub gene expression and the TFS score. The high-TFS group was also characterized by an immunosuppressive tumor microenvironment and exhibited unfavorable responses to PD-1 and CTLA-4 checkpoint inhibitors.

Conclusion This study established a transcriptomic biomarker for predicting the efficacy of TACE that correlates with radiomics features on pretreatment imaging, tumor immune microenvironment characteristics, and the efficacy of systemic therapy in HCC.

PU-112

Interventional surgery combined with donafenib and anti-PD-1 antibodies as first-line treatment for unresectable hepatocellular carcinoma: A retrospective study

Jinfeng Bai, Rong Ding

Yunnan Cancer Hospital (The Third Affiliated Hospital of Kunming Medical University)

Purpose Previous studies have shown that the combination of interventional surgery and systemic therapy potentially offers survival benefits in patients with unresectable hepatocellular carcinoma (uHCC). This study aimed to assess the efficacy and safety of interventional surgery combined with donafenib plus anti-PD-1 antibodies in uHCC.

Materials and methods This was a single-center retrospective study at Yunnan Cancer Hospital, conducted from February 2022 to July 2023. It involved patients with uHCC who received interventional surgery combined with donafenib (200 mg orally twice daily) and anti-PD1 antibodies (every 3 weeks). All enrolled patients had at least one measurable lesion according to mRECIST criteria and had not undergone any previous systemic treatment. The study focused on collecting and analyzing data regarding the progression-free survival (PFS), overall survival (OS), and the incidence of adverse events.

Results A total of 52 patients with uHCC were included in the study, having a median age of 54.0 years (IQR, 48.5-60.3). Among these patients, 19 (36.5%) were classified as Barcelona Clinic Liver Cancer (BCLC) stage B, and 32 (61.5%) as BCLC stage C. A significant majority, 48 patients (92.3%), had complications with hepatitis B virus (HBV) infection. The median maximum tumor diameter was 9.25 cm (IQR, 7.1-13.7). Furthermore, 37 patients (71.2%) had a baseline alpha-feto protein (AFP) level of ≥ 400 ng/mL. As of December 18, 2023, the median follow-up time amounted to 9.0 months (IQR, 5.3-12.0). In terms of efficacy, the median PFS reached 7 months (95%CI, 3-NA), while the median OS was not reached, with a one-year OS rate of 74.9% (95%CI, 60.2-93.3%). Regarding safety, treatment-related adverse events (TRAEs) were reported in 44 patients (84.6%), with common TRAEs including hand-foot skin reactions (38.5%), stomach ache (23.1%), and diarrhea (19.2%). Notably, no TRAEs of grade 3 or above were reported.

Conclusion In this study, the triple therapy comprising interventional surgery, donafenib, and anti-PD-1 antibodies demonstrated promising efficacy and manageable safety profiles in patients with uHCC, suggesting its potential for broader adoption in clinical practice.

PU-113

Drug-eluting beads bronchial arterial chemoembolization in advanced and standard treatment-refractory/ineligible non-small cell lung cancer

Wei Cui¹, Jing Li¹, Jie Tian³, Yi Deng², Rongde Xu¹

1. Guangdong General Hospital/CN

2. Medical School, Kunming University of Science and Technology

3. Department of Radiology, Yichang Central People's Hospital

Purpose The treatment strategy for previously standard treated non-small-cell lung cancer (NSCLC) still remained challenged. This study was to evaluate the effectiveness and safety of epirubicin-loaded drug-eluting bead transbronchial artery chemoembolization (D-BACE) plus bronchial artery infusion chemotherapy (BAIC) in patients with refractory advanced NSCLC.

Materials and methods Between January 2018 and December 2022, 32 patients with refractory advanced NSCLC (26 males; mean age of 64 ± 9.3 years [range 41-78]; 19 squamous carcinomas [59.4%]) who had received one or more previous standard treatments and received D-BACE (epirubicin 50mg) plus BAIC (lobaplatin 30 mg/m²) were included in our study. The study evaluated several parameters including local tumor response based on RECIST 1.1 criteria, progression-free survival (PFS), overall survival (OS), and complication rates. To examine the impact of different factors on PFS and OS, Kaplan–Meier and Cox regression analyses were performed.

Results Between January 2018 and December 2022, 32 patients with refractory advanced NSCLC (26 males; mean age of 64 ± 9.3 years [range 41-78]; 19 squamous carcinomas [59.4%]) who had received one or more previous standard treatments and received D-BACE (epirubicin 50mg) plus BAIC (lobaplatin 30 mg/m²) were included in our study. The study evaluated several parameters including local tumor response based on RECIST 1.1 criteria, progression-free survival (PFS), overall survival (OS), and complication rates. To examine the impact of different factors on PFS and OS, Kaplan–Meier and Cox regression analyses were performed.

Conclusion The combination of D-BACE and BAIC shows great potential as a treatment choice for patients with refractory advanced NSCLC.